

Transition-Metal Catalyzed C-C Bond Activation of Cyclopropenones and C-H Bond Activation of Phenoxyacetamides

by

Tanmayee Nanda

CHEM11201704031

**National Institute of Science Education and Research,
Bhubaneswar, Odisha**

*A thesis submitted to the
Board of Studies in Chemical Sciences
In partial fulfillment of requirements
for the Degree of*

**DOCTOR OF PHILOSOPHY
of
HOMI BHABHA NATIONAL INSTITUTE**

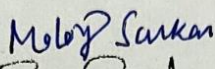
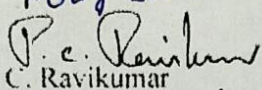
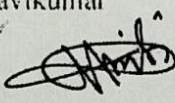
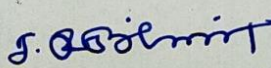
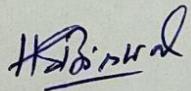



Dec, 2022

Homi Bhabha National Institute¹

Recommendations of the Viva Voce Committee

As members of the Viva Voce Committee, we certify that we have read the dissertation prepared by **Tanmayee Nanda** entitled "**Transition-Metal Catalyzed C-C Bond Activation of Cyclopropanones and C-H Bond Activation of Phenoxyacetamides**" and recommend that it may be accepted as fulfilling the thesis requirement for the award of Degree of Doctor of Philosophy.

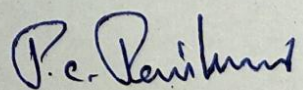
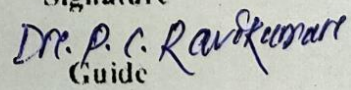
Chairman - Dr. Moloy Sarkar		Date: 22.03.23
Guide / Convener - Dr. Ponneri C. Ravikumar		Date: 22/03/2023
Examiner - Prof. Debabrata Maiti		Date: 22/03/2023
Member 1- Dr. S. Peruncheralathan		Date: 22.03.2023
Member 2- Dr. Himanshu Sekhar Biswal		Date: 22/03/2023
Member 3- Dr. Shantanu Pal		Date: 22/03/23

Final approval and acceptance of this thesis is contingent upon the candidate's submission of the final copies of the thesis to HBNI.

I/We hereby certify that I/we have read this thesis prepared under my/our direction and recommend that it may be accepted as fulfilling the thesis requirement.

Date: 22/03/2023

Place: NISER, Bhubaneswar


Signature

Guide

¹ This page is to be included only for final submission after successful completion of viva voce.

STATEMENT BY AUTHOR

This dissertation has been submitted in partial fulfillment of requirements for an advanced degree at Homi Bhabha National Institute (HBNI) and is deposited in the library to be made available to borrowers under rules of the HBNI.

Brief quotations from this dissertation are allowable without special permission, provided that accurate acknowledgement of source is made. Requests for permission for extended quotation from or reproduction of this manuscript in whole or in part may be granted by the Competent Authority of HBNI when in his or her judgment the proposed use of the material is in the interests of scholarship. In all other instances, however, permission must be obtained from the author.



Tanmayee Nanda

DECLARATION

I, hereby declare that the investigation presented in the thesis has been carried out by me. The work is original and has not been submitted earlier as a whole or in part for a degree/diploma at this or any other Institution / University.



Tanmayee Nanda

List of Publications

(A) Published Research Paper (# pertaining to thesis):

- #1) **Tanmayee Nanda**, and Ponneri C. Ravikumar. A Palladium-Catalyzed Cascade C–C Activation of Cyclopropanone and Carbonylative Amination: Easy Access to Highly Functionalized Maleimide Derivatives. *Org. Lett.*, **2020**, 22, 1368-1374. (**Highlighted in the organic chemistry portal**).
- #2) **Tanmayee Nanda**, Pragati Biswal, Bedadyuti Vedvyas Pati, Shyam Kumar Banjare, and Ponneri C. Ravikumar. Palladium-Catalyzed C–C Bond Activation of Cyclopropanone: Modular Access to Trisubstituted α,β -Unsaturated Esters and Amides, *J. Org. Chem.*, **2021**, 86, 2682-2695.
- #3) **Tanmayee Nanda**, Shyam Kumar Banjare, Wang-Yeuk Kong, Wentao Guo, Pragati Biswal, Lokesh Gupta, Astha Linda, Bedadyuti Vedvyas Pati, Smruti Ranjan Mohanty, Dean J. Tantillo, and Ponneri C. Ravikumar. Breaking the Monotony: Cobalt and Maleimide as an Entrant to the Olefin-Mediated *Ortho* C–H Functionalization. *ACS Catal.* **2022**, 12, 11651–11659.
- #4) **Tanmayee Nanda**, Shubham Kumar Dhal, Gopal Krushna Das Adhikari, Namrata Prusty, and Ponneri C. Ravikumar. Carboamination and Olefination: Revealing Two different Pathways in *ortho* C-H Functionalization of Phenol. (*Manuscript submitted*)

(B) Review:

- 5) **Tanmayee Nanda**,[#] Muhammed Fastheem,[#] Astha Linda, Bedadyuti Vedvyas Pati, Shyam Kumar Banjare, Pragati Biswal, and Ponneri C. Ravikumar. Advancement in Palladium-Catalyzed C-C bond Activation of Strained Ring Systems: Three and four-membered carbocycles as prominent C3/C4 building blocks. *ACS Catal.* **2022**, 12, 13247–13281. ([#]*equally contributed*).

(C) Book Chapter:

- 6) **Tanmayee Nanda**, Smruti Ranjan Mohanty, and Ponneri C. Ravikumar. Book Chapter: Recent advances in Multicomponent reaction through C-H bond functionalization. Handbook of CH Functionalizations (CHF), Wiley-VCH Publishers, **2022**.
<https://doi.org/10.1002/9783527834242.chf0218>

(D) Other Research Publications:

- 7) Shyam Kumar Banjare, [#] **Tanmayee Nanda**, [#] Bedadyuti Vedvyas Pati, Gopal Krushna Das Adhikari, Ponneri C. Ravikumar. Breaking the Trend: Insight into Unforeseen Reactivity of Alkynes in Cobalt-Catalyzed Weak Chelation-Assisted Regioselective C(4)–H Functionalization of 3-Pivaloyl Indole. *ACS Catal.* **2021**, *11*, 11579–11587. ([#]*equally contributed*).
- 8) Pragati Biswal, [#] **Tanmayee Nanda**, [#] Shyam Kumar Banjare, Smruti Ranjan Mohanty, Ranjit Mishra, and Ponneri C. Ravikumar. *N*-allylbenzimidazole as a Strategic Surrogate in the Rh-catalyzed Stereoselective trans-propenylation of Aryl C(*sp*²)-H Bonds. *Chem. Commun.*, **2023**, *59*, 199–202. (*just accepted*) ([#]*equally contributed*).
- 9) **Tanmayee Nanda**, Ashish Dharmendra Shukla, Muhammed Fastheem, Bedadyuti Vedvyas Pati, and Ponneri C. Ravikumar. NHC-catalyzed base assisted C-C bond cleavage of cyclopropanone: an approach towards the synthesis of azetidinone and benzoxazepines. (*Manuscript under preparation*)
- 10) **Tanmayee Nanda**, Muhammed Fastheem, Shyam Kumar Banjare, and Ponneri C. Ravikumar. Palladium-Catalyzed Cascade C–C Bond Activation of Cyclopropanone: A strategic approach towards the synthesis of pyrrolo-quinolinedione and anticancer drug mitomycin skeleton. (*Manuscript under preparation*).

- 11) Shyam Kumar Banjare, **Tanmayee Nanda**, Ponneri C. Ravikumar. Cobalt-Catalyzed Regioselective Direct C-4 Alkenylation of 3-Acetylindole with Michael Acceptors Using a Weakly Coordinating Functional Group. *Org. Lett.* **2019**, *21*, 8138–8143.
- 12) Shyam Kumar Banjare, **Tanmayee Nanda**, Bedadyuti Vedvyas Pati, Pragati Biswal, Ponneri C. Ravikumar. O-Directed C-H Functionalization via Cobaltacycles: A Sustainable Approach for C-C and C-Heteroatom Bond Formations. *Chem. Commun.* **2021**, *57*, 3630–3647.
- 13) Shyam Kumar Banjare, Pranav Shridhar Mahulkar, **Tanmayee Nanda**, Bedadyuti Vedvyas Pati, Lamphiza O Najjar and Ponneri C. Ravikumar. Diverse reactivity of alkynes in C-H activation reactions. *Chem Commun.*, **2022**, *58*, 10262-10289.
- 14) Gopal Krushna Das Adhikari, Bedadyuti Vedvyas Pati, **Tanmayee Nanda**, Pragati Biswal, Shyam Kumar Banjare and Ponneri C. Ravikumar Co(II)-Catalyzed C–H/N–H Annulation of Cyclic Alkenes with Indole-2-carboxamides at Room Temperature: One-Step Access to β -Carboline-1-one Derivatives. *J. Org. Chem.* **2022**, *87*, 4438-4448.
- 15) Smruti Ranjan Mohanty, Namrata Prusty, **Tanmayee Nanda**, Shyam Kumar Banjare and Ponneri C. Ravikumar. Pyridone Directed Ru-Catalyzed Olefination of sp^2 (C–H) Bond Using Michael Acceptors: Creation of Drug Analogues. *J. Org. Chem.*, **2022**, *87*, *9*, 6189-6201.
- 16) Namrata Prusty,[#] Shyam Kumar Banjare,[#] Smruti Ranjan Mohanty, **Tanmayee Nanda**, Komal Yadav, and Ponneri C. Ravikumar. Synthesis and Photophysical Study of Heteropolycyclic and Carbazole Motif: Nickel-Catalyzed Chelate-Assisted Cascade C–H Activations/Annulations. *Org. Lett.* **2021**, *23*, 9041-9046. ([#]*equally contributed*).
- 17) Bedadyuti Vedvyas Pati, Shyam Kumar Banjare, Gopal Krushna Das Adhikari, **Tanmayee Nanda**, and Ponneri C. Ravikumar. Rhodium-Catalyzed Selective C(sp^2)–H Activation/Annulation of tert-Butyl Benzoyloxycarbamates with 1,3-Diynes: A One

Step Access to Alkynylated Isocoumarins and Bis-Isocoumarins. *Org. Lett.* **2022**, *24*, 5651-5656.

- 18) Namrata Prusty, Smruti Ranjan Mohanty, Shyam Kumar Banjare, **Tanmayee Nanda**, and Ponneri C. Ravikumar. Switching the Reactivity of the Nickel-Catalyzed Reaction of 2-Pyridones with Alkynes: Easy Access to Polyaryl/Polyalkyl Quinolinones. *Org. Lett.* **2022**, *24*, 6122-6127.
- 19) Smruti Ranjan Mohanty, Namrata Prusty, Shyam Kumar Banjare, **Tanmayee Nanda**, and Ponneri C. Ravikumar. Overcoming the Challenges toward Selective C(6)-H Functionalization of 2-Pyridone with Maleimide through Mn(I)-Catalyst: Easy Access to All-Carbon Quaternary Center. *Org. Lett.* **2022**, *24*, 848-852.
- 20) Pragati Biswal, **Tanmayee Nanda**, Namrata Prusty, Smruti Ranjan Mohanty, Ponneri C. Ravikumar. Rhodium-Catalyzed Oxidative Annulation of Aniline with N-allylbenzimidazole: Synthesis of 2-Methylindoles via C-N bond Cleavage. (*Communicated*)
- 21) Bedadyuti Vedvyas Pati, N. N. Puthalath, Shyam Kumar Banjare, **Tanmayee Nanda**, and Ponneri C. Ravikumar. Transition Metal-catalyzed C-H /C-C Activation and Coupling with 1, 3-diyne. *Org. Biomol. Chem.*, **2023**, Accepted Manuscript DOI: <https://doi.org/10.1039/D3OB00238A>
- 22) Bedadyuti Vedvyas Pati, Smruti Ranjan Mohanty, Subhrakant Jena, **Tanmayee Nanda**, and Ponneri C. Ravikumar. Overcoming the Limitation of Strong Chelation in C-H Bond Activation – A Rh Catalyzed Chemo-selective Synthesis of Isocoumarin. (*Manuscript under preparation*)
- 23) Shyam Kumar Banjare, Saista Afreen, Wang-Yeuk Kong, Wentao Guo, **Tanmayee Nanda**, Gopal Krushna Das Adhikari, Nuapada Preeyanka, Dean J. Tantillo, and Ponneri C. Ravikumar. Cobalt catalyzed decarbonylative ipso-C-C bond functionalization:

Synthesis of Indole C-3 functionalized acyloins using 1,2-diketone. DOI 10.26434/chemrxiv-2022-4kckr. (*Communicated*)

- 24) S. K. Banjare, A. Saxsena, **T. Nanda**, N. Prusty, and Ponneri. C. Ravikumar. Weak-chelation assisted regioselective *ortho*-(*sp*²)-H ethynylation of *N*-aryl γ -lactam utilizing cobalt (III)-catalyst. *Org. Lett.* **2022**, ASAP.

Conferences:

1. 'A Palladium-Catalyzed Cascade C- C Activation of Cyclopropenone and Carbonylative Amination: Easy Access to Highly Functionalized Maleimide Derivatives' **Tanmayee Nanda**, and Ponneri. C. Ravikumar*; Presented at National Conference on Organic Synthesis (**N-COS-2020**), Organized by PG Department of Chemistry, Berhampur University, Odisha. during 02-03 March 2020. (**In-person poster and Short oral presentation**).
2. 'Palladium-Catalyzed C-C bond Activation: Harnessing the strain of Cyclopropenone'; **Tanmayee Nanda**, and Ponneri. C. Ravikumar*; Presented at the 1st Satellite Meeting, India – ACS Fall 2021, 25 & 26 August 2021.
3. 'Palladium-Catalyzed C-C bond Activation: Harnessing the strain of Cyclopropenone' **Tanmayee Nanda**, and Ponneri. C. Ravikumar*; Presented in ACS Fall 2021-Virtual, 25 & 26 August 2021 (held in Atlanta GA, USA).
4. 'Palladium-Catalyzed Cascade C-C Activation of Cyclopropenone and Carbonylative Amination: Easy Access to Highly Functionalized Maleimide Derivatives' **Tanmayee Nanda**, Pragati Biswal, Bedadyuti Vedvyas Pati, Shyam Kumar Banjare, and Ponneri. C. Ravikumar*; Presented in National Conference on Recent Advances in Heterocyclic Chemistry (RAHC-2022), Ravenshaw University, Cuttack, Odisha (**online**).
5. 'Palladium-Catalyzed C-C bond Activation: Harnessing the strain of Cyclopropenone' **Tanmayee Nanda**, Pragati Biswal, Bedadyuti Vedvyas Pati, Shyam Kumar Banjare,

and Ponneri. C. Ravikumar*; Presented in “Chemical Research Society of India 28th National Symposium in Chemistry (CRSI NSC-28), India during 4-6 February 2022”
(In-person poster presentation).



Tanmayee Nanda

Dedicated to
My Grandmother
Late. Labangalata Nanda
&
My Parents (Sri. Debadatta Nanda and Smt.
Pankaja Kumari Rath)

ACKNOWLEDGEMENTS

First and foremost, I am extremely grateful to my supervisor, **Dr. Ponneri C. Ravikumar** for his invaluable advice, continuous support, and patience during my Ph.D. study. His immense knowledge and ample experience have encouraged me throughout my academic and daily life.

I take this opportunity to thank my doctoral committee members, **Dr. Moloy Sarkar, Dr. S. Peruncheralathan, Dr. Himansu S. Biswal, and Dr. Shantanu Pal** (IIT, Bhubaneswar) for their valuable suggestions. I am grateful to all the faculties of school of chemical sciences, NISER.

I would like to acknowledge NISER for giving the laboratory facilities and DAE for financial support. I am also thankful to **Dr. S. Nembenna, and Dr. Rudresh Acharya**, school of biological sciences NISER, for sharing their laboratory facilities.

I would like to extend my gratitude to my coursework instructors, **Dr. S. Peruncheralathan, Dr. C. Gunanathan, Dr. Nagendra K. Sharma, Prof. A. Srinivasan, Dr. Moloy Sarkar, Dr. U. Lourderaj** as well.

I am also thankful to all the non-teaching staff of school of chemical sciences

I am grateful to my labmates **Dr. Pragati, Shyam, Dr. Smruti, Vedavyas, Dr. Gopal, Namrata, Dr. Rajesh, Dr. Laxman, Dr. Asit, Rohit, Gaji, Lokesh, Saista, Shubham, Abhipsa, Annapurna, Sofaya, Fastheem, Nitha, Astha, Lipsa, Ashish, Pranav, & Lam**. Besides being lab mates, I also found good friends who are there in both good and bad times. Thus, I would like to extend my sincere gratitude to **Dr. Pragati, Shyam, and Rohit** for being excellent advisors, **Namrata** for taking care of me, **Saista, Shubham, and Abhipsa** for creating beautiful memories and being happy about my success. I had a great time working with master's students and guiding them.

I made excellent friends during these five years, who never failed to help me in my critical situations. I want to take this opportunity and thank **Kiran, Sudip, and Anwasha** for their help and support. I thank **Amita and Pragyn** for providing emotional support.

I would like to thank **Dr. Kasturi Sahu, Dr. Narayan Ch. Jana, Dr. Syamasrit Dash, Dr. Subhayan Chakraborty, Dr. Bibhuti Bhusana Palai, and Ms. Sagarika Meher** for their timely help during my research work.

This journey would not be complete without the constant lifting up by my two friends, **Subhangi** and **Niroja**, when I was at my lowest.

I would like to thank my sister **Ms. Anmayee Nanda**, brother-in-law **Mr. Aditya Narayan Dash**, nephew **Adyanmaya Dash** and brother **Mr. Debasish Nanda**, for supporting me in every situation.

I sincerely thank my grandparents, **Pandit Fakir Mohan Nanda** and **Smt. Labanga Lata Nanda**, for their love, and blessings. I cannot be thankful enough to my parents, **Sri. Debadatta Nanda** and **Smt. Pankaja Kumari Rath** for giving me morals of high value. Their constant motivation and unconditional love keep me going.

Finally, I would like to thank the Almighty for blessing me and showing me the right path.



Tanmayee Nanda

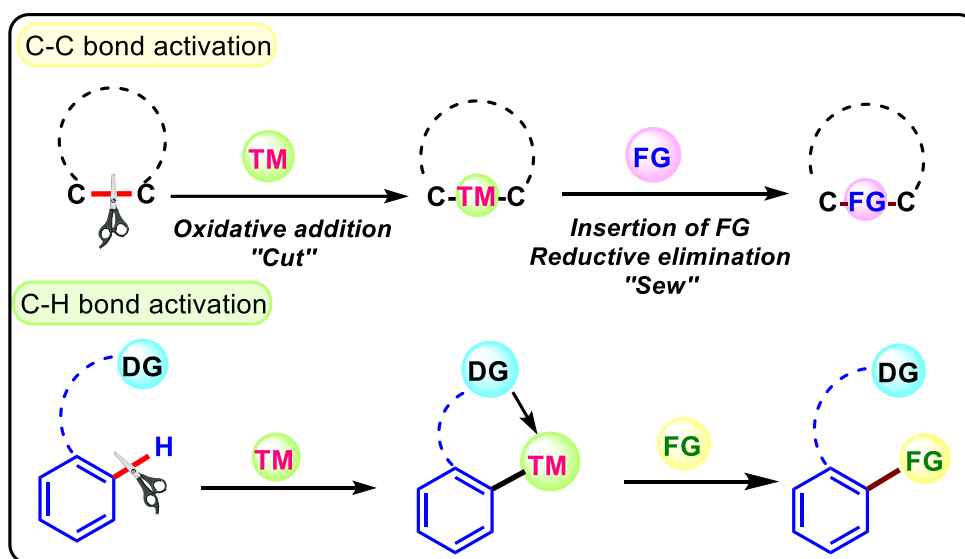
CONTENTS

	Page No.
Thesis title	i
Recommendations of the <i>viva-voce</i> committee	ii
Statement by author	iii
Declaration	iv
List of publications	v
Dedications	xi
Acknowledgments	xii
Contents	xiv
Synopsis	xv
List of Figures	xix
List of Schemes	xxi
List of Tables	xxiv
List of Abbreviations	xxv
Chapter 1A: Introduction To C-C Bond Activation of Three-membered Strained Systems	1
Chapter 1B: Introduction To C-H Bond Activation	29
Chapter 2: A Palladium-Catalyzed Cascade C-C Activation of Cyclopropanone and Carbonylative Amination: Easy Access to Highly Functionalized Maleimide Derivatives	45
Chapter 3: Palladium-Catalyzed C-C Bond Activation of Cyclopropanone: Modular Access to Trisubstituted α,β -Unsaturated Esters and Amides	85
Chapter 4: Breaking the Monotony: Cobalt and Maleimide as an Entrant to the Olefin Mediated <i>ortho</i> C-H Functionalization	143
Chapter 5: Carboamination and Olefination: Revealing Two Different Pathways in <i>Ortho</i> C-H Functionalization of Phenoxy-acetamide	195
Summary	259
About The Author	261

SYNOPSIS

Chapter 1: Brief introduction to transition metal-catalyzed C-C and C-H bond activation processes (**Scheme 1**).

Abstract: The transition metal-catalyzed reaction brought great success to both organic and organometallic chemists. Since the development of this field, numerous transformations have been achieved in step and atom economical fashion. In transition metal-catalyzed reactions, the inert bond activation strategy has taken a center stage and grabbed the attention of scientists worldwide. Among the various type of inert bond, C-C and C-H bond activation is of particular interest as this constitutes the basic backbone of all the organic molecular skeletons.

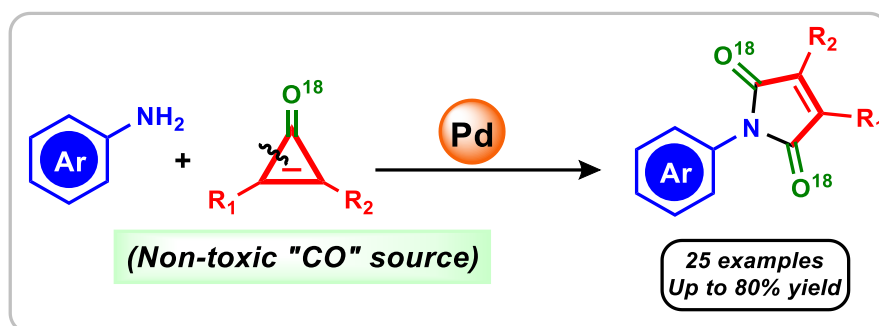


Scheme 1: Transition-metal catalyzed C-C and C-H bond activation.

But features like high bond dissociation energy, (BDE of C-C bond is 347 kJ/mol and C-H bond is 413 kJ/mol) and its non-polar nature makes it particularly challenging to break such bonds. The selectivity between the cleavage of C-C and C-H bonds is another additional challenge, as the later bond is statistically more abundant and more exposed to interact with the metal orbitals. In contrast, the C-C bond is sterically encumbered, and thus the kinetic, and thermodynamics favor C-H bond activation over the C-C bond activation. Most of the C-C bond cleavage process has been achieved by taking the help of chelation assistance provided by the directing group, strain release, and aromatization. In addition, C-H bond activation is generally governed by the presence of the directing group in the proximal or distal position.

Chapter 2. Palladium-catalyzed C-C bond activation of cyclopropenone: Synthesis of highly functionalized maleimide derivatives.

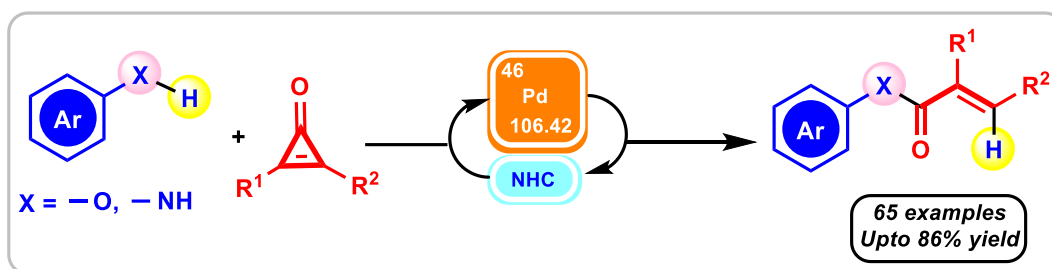
Abstract: We described the first report on palladium-catalyzed C-C bond activation of cyclopropenone and concomitant carbonylative amination to produce maleimides (**Scheme 2**). The interesting aspect of this reaction is that the sacrificial elimination of carbon monoxide from the substrate and recapture by one of the intermediates in the catalytic cycle to form maleimides. ^{18}O isotopic studies confirmed that the source of carbon monoxide is cyclopropenone. A wide range of substrates delivered the desired product in moderate to good yield. A cheaper catalytic condition comprised of palladium metal as the catalyst has been developed compared to the popularly used costly rhodium-catalyzed conditions. The detailed mechanistic study is an attractive part of the whole protocol, as it explains the role of each reagent used in the reaction and validates the mechanism.



Scheme 2: Synthesis of maleimides through palladium-catalyzed C-C bond activation of cyclopropenone.

Chapter 3. Palladium-catalyzed C-C bond activation of cyclopropenone: Synthesis of tri-substituted α,β -unsaturated acrylates, and acrylamides.

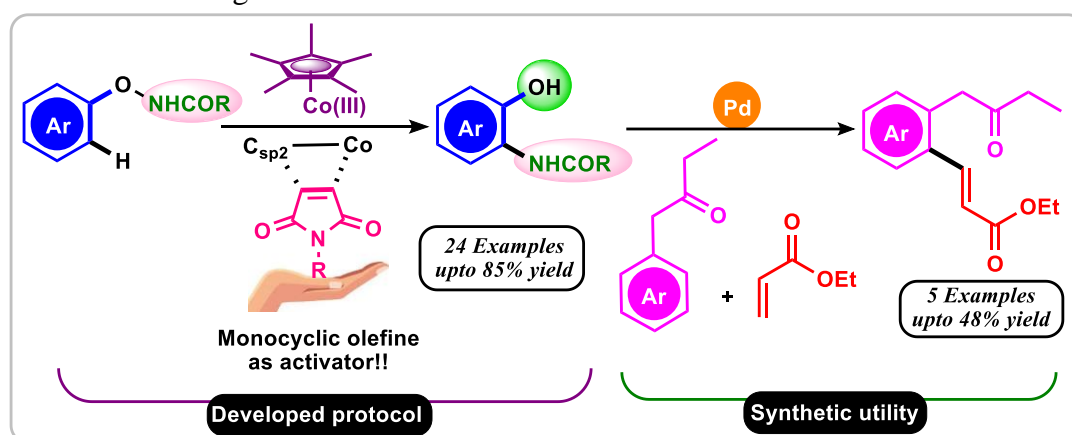
Abstract: Strain-driven palladium/*N*-heterocyclic carbene catalyzed C-C bond activation of diphenylcyclopropenone (DPC) has been explored for the one-step access to tri-substituted α,β -unsaturated esters, and amides (**Scheme 3**). The designed transformation works under mild conditions, and a wide range of α,β -unsaturated esters and amides have been synthesized. Mechanistic studies support the oxidative addition of the C-C bond of cyclopropenone to *in situ* generated Pd(0) intermediate. We have proved that vinylic hydrogen in the product comes from phenol/aniline through deuterium labeling studies. Late-stage functionalization of bioactive molecules such as procaine, estrone, and hymecromone demonstrates the robustness of this protocol.



Scheme 3: α,β -Unsaturated acrylates, and acrylamides through palladium-catalyzed C-C bond activation of cyclopropanone.

Chapter 4. Cobalt and maleimide as an entrant to the olefin-mediated *ortho* C-H functionalization.

Abstract: A catalytic system is discovered for the intramolecular C-H amidation of *N*-phenoxy acetamide derivatives (**Scheme 4**). A cobalt catalyst has been employed for the olefin-mediated *ortho* C-H functionalization. Moreover, a monocyclic olefin, maleimide, has been used as a transient mediator instead of well-established bicyclic norbornenes. Maleimide promotes a Co(III) intermediate to undergo oxidative addition into the O–N bond to form a Co(V) nitrene species and subsequently directs nitrene addition to the *ortho* position. A wide range of maleimide has been demonstrated as an olefin mediator.

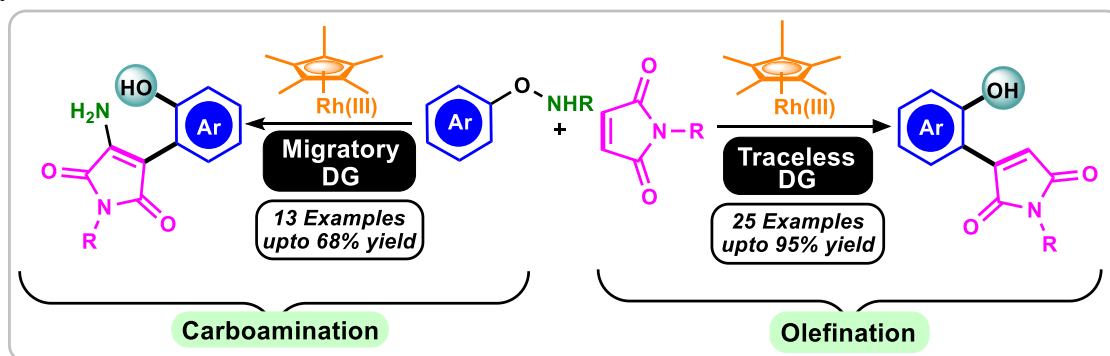


Scheme 4: Cobalt and maleimide co-catalyzed *ortho*-amidation of phenols.

Chapter 5. Carboamination and Olefination: Revealing two different pathways in *ortho* C-H functionalization of phenoxyacetamide.

Abstract: Herein, we have demonstrated a rhodium-catalyzed carboamination of olefin with the double bond intact and *ortho*-olefination of phenoxyacetamide (**Scheme 5**). For the first time, deacylative carboamination of the maleimide has been achieved wherein phenoxyacetamide was behaved as the aminating source. The rhodium nitrenoid species adding to the double bond of maleimide to form aziridine is an interesting aspect of this methodology. In addition, the cleavage of amide C–N bond through hydrolysis by in situ generated water has been proved from ^{19}F NMR analysis. The key intermediate involved

has been well characterized through the HRMS study and validates the proposed catalytic cycle. In addition to carboamination, we have disclosed the C-H olefination protocol where the maleimide group has been installed successfully in the *ortho*-position of phenoxyacetamide. In this protocol, phenoxy acetamide behaved as a traceless directing group with the in-situ release of acetamide. The base-assisted E2-elimination is the key to the success of this reaction. A wide range of phenoxy acetamide and maleimide underwent reaction under our standard condition to deliver the desired product in good to excellent yield.



Scheme 5: Olefination of phenol and carboamination of maleimide.

List of figures

1	Figure 1A.1	Thermodynamic factor	4
2	Figure 1A.2	Orbital overlapping	5
3	Figure 1A.3	Steric and statistical factor	5
4	Figure 1A.4	Strain energies of cycloalkanes	6
5	Figure 1A.5	Modes of C-C bond activation in 3 and 4-membered strained systems	6
6	Figure 1A.6	Trend of palladium-catalyzed C-C bond activation in the past 11 years	8
7	Figure 1A.7	Synthetic utility of cyclopropenone	18
8	Figure 1B.1	Traditional organic synthesis	31
9	Figure 1B.2	Factor determining the inertness of C-H bond	32
10	Figure 1B.3	Non-directed C-H bond functionalization	33
11	Figure 1B.4	General catalytic cycle for directed C-H functionalization	35
12	Figure 1B.5	Redox-neutral directing group	37
13	Figure 2.1	ORTEP diagram of 3ad with 50% ellipsoid probability	76
14	Figure 3.1	ORTEP diagram of 3aw with 50% ellipsoid probability	135
15	Figure 3.2	ORTEP diagram of 5aq with 50% ellipsoid probability	136
16	Figure 4.1	Computed (PBE0-D4/Def2-TZVPP//SMD(TFE)-PBE0-D3(BJ)/Def2-SVP) reaction profiles for Cp*Co(OAc) ₂ -catalyzed rearrangement of <i>N</i> -(<i>p</i> -tolylloxy)acetamide mediated by <i>N</i> -ethylmaleimide	158
17	Figure 4.2	Computed (PBE0-D4/Def2-TZVPP//SMD(TFE)-PBE0-D3(BJ)/Def2-SVP) reaction profiles for Cp*Co(OAc) ₂ -catalyzed rearrangement of 2j mediated by <i>N</i> -ethylmaleimide	159

18	Figure 4.3	ESI-MS spectra of intermediate 3b₅ '	169
19	Figure 4.4	ESI-MS spectra of intermediate 3h₅ '	170
20	Figure 4.5	ORTEP diagram of 5 with 50% ellipsoid probability	187
21	Figure 5.1	Overview on transition metal catalyzed carboamination and C-H olefination	199
22	Figure 5.2	Previous challenges and our approach	200
23	Figure 5.3	Mass analysis for reaction of 1b with 2c	224
24	Figure 5.4	Mass analysis for reaction of 1b with 3be	227
25	Figure 5.5	ORTEP diagram of 3be with 50% ellipsoid probability	252
26	Figure 5.6	ORTEP diagram of 4ac with 50% ellipsoid probability	253
27	Figure 5.7	ORTEP diagram of 6 with 50% ellipsoid probability	254

List of schemes

1	Scheme 1A.1	Pd-catalyzed regioselective activation of gem-difluorinated cyclopropanes	9
2	Scheme 1A.2	Pd-catalyzed regioselective activation of gem-difluorinated cyclopropanes	9
3	Scheme 1A.3	Application of the methodology	10
4	Scheme 1A.4	Pd-catalyzed ring-opening cross-coupling of cyclopropenes with aryl iodides	11
5	Scheme 1A.5	Catalytic cycle	12
6	Scheme 1A.6	Scope of the Pd-Catalyzed (3C + 2C) Cycloaddition	13
7	Scheme 1A.7	Scope of the Enantioselective Pd-Catalyzed (4 + 3) Cycloaddition	14
8	Scheme 1A.8	Pd-catalyzed dearomatization of anthranils with vinyl cyclopropanes by (4+3) cyclization reaction	15
9	Scheme 1A.9	Palladium-catalyzed selective C–C bond cleavage and stereoselective alkenylation between cyclopropanol and 1,3-diyne	17
10	Scheme 1A.10	Modes of ring opening in cyclopropenones	19
11	Scheme 1A.11	Palladium-Catalyzed Ring-Opening Alkynylation of Cyclopropenones	20
12	Scheme 1A.12	Intermolecular σ -bond cross-exchange reaction between cyclopropenones and (benzo)silacyclobutanes	21
13	Scheme 1B.1	Non-directed C-H bond functionalization	33
14	Scheme 1B.2	Schematic representation of directed C-H bond activations	35
15	Scheme 1B.3	Carboamination of alkynes	37

16	Scheme 1B.4	Reports on phenoxyacetamide as a directing group and aminating agent	38
17	Scheme 2.1	Transition metal catalyzed synthesis of the maleimide and our presumptions	48
18	Scheme 2.2	Scope with respect to aniline	53
19	Scheme 2.3	Scope with respect to diarylcyclopropenone	54
20	Scheme 2.4	Application	55
21	Scheme 2.5-2.7	Mechanistic studies	56-58
22	Scheme 2.8	Catalytic cycle	59
23	Scheme 3.1	Literature survey and our approach	89
24	Scheme 3.2	Scope of phenols for the synthesis of acrylate derivatives	93
25	Scheme 3.3	Scope of Anilines for the synthesis of Acrylamide derivatives	95
26	Scheme 3.4	Synthetic application	96
27	Scheme 3.5-3.8	Mechanistic studies	98-100
28	Scheme 3.9	Catalytic cycle	101
29	Scheme 4.1	Palladium/NBE catalyzed Catellani reaction	146
30	Scheme 4.2	Traditional olefin-mediator and metal used in C-H functionalization reaction	147
31	Scheme 4.3	Reactivity comparison between NBE and maleimide and our approach	148
32	Scheme 4.4	Substrate Scope	153
33	Scheme 4.5-4.6	Mechanistic studies	155-156
34	Scheme 4.7	Catalytic cycle	160
35	Scheme 4.8	Diversification of Natural Products and Applications	161
36	Scheme 4.9	Application <i>o</i> -hydroxy acetamidate as ligand	162

37	Scheme 5.1	Scope of various substrates and maleimide towards <i>ortho</i> -olefination	206
38	Scheme 5.2	Scope of various substrates and maleimide towards carboamination product	207
39	Scheme 5.3-5.4	Mechanistic studies	208-209
40	Scheme 5.5	Catalytic cycle for olefination reaction	211
41	Scheme 5.6	Catalytic cycle for carboamination reaction	212
42	Scheme 5.7	Synthetic utility	213

List of tables

1	Table 2.1	Optimization of the Reaction Condition	50
2	Table 3.1	Optimization of Reaction Conditions (ligand screening)	90
3	Table 3.2	Optimization of Reaction Conditions (other parameters)	91
4	Table 4.1	Optimization of Reaction Conditions	150
5	Table 4.2	Investigation of Monocyclic Maleimides in the Cp*Co Catalyzed C(<i>sp</i> ²)-H <i>o</i> -Amidation	152
6	Table 5.1	Optimization of Reaction Condition for <i>ortho</i> C-H Olefination with Maleimide	202
7	Table 5.2	Screening of Various Direction Groups	204
8	Table 5.3	Optimization Table for Cp*Rh Catalyzed Carboamination of Maleimide 2	218

List of Abbreviations

AcOH	Acetic acid
CH ₃ CN	Acetonitrile
<i>S_EAr</i>	Aromatic electrophilic substitution
BHT	Butylated hydroxytoluene
¹³ C NMR	Carbon nuclear magnetic resonance
Cp*CoCOI ₂	Carbonyl(pentamethylcyclopentadienyl)cobalt Diiodide
Cu(OAc) ₂	Copper(II) acetate
CHCl ₃	Chloroform
CDCl ₃	Chloroform-d
CMD	Concerted metalation deprotonation
DCE	1,2-dichloroethane
DCM/CH ₂ Cl ₂	Dichloromethane
DMSO	Dimethyl sulfoxide
DMF	Dimethylformamide
DPC	Diphenylcyclopropenone
DEPT-135	Distortionless enhancement by polarization transfer
DG	Directing group
EtOAc	Ethyl acetate
FG	Functional group
GC	Gas chromatography
HMBC	¹ H- ¹³ C Heteronuclear Multiple Bond Correlation Spectroscopy
HFIP	1,1,1,3,3,3-Hexafluoro isopropanol
HRMS	High resolution mass spectrometry
IR	Infrared
KIE	Kinetic Isotope Effect
MeOH	Methanol
NHC	<i>N</i> -heterocyclic carbene
CD ₃ OD	d ₄ -Methanol
OLED	Organic light emitting diode
PAHs	Polycyclic aromatic hydrocarbons

$\text{Pd}(\text{OAc})_2$	Palladium acetate
$(\text{Cp}^*\text{RhCl}_2)_2$	Pentamethylcyclopentadienylrhodium(III) chloride dimer
K_2CO_3	Potassium carbonate
DG^{OX}	Redox neutral directing group
AgOAc	Silver acetate
AgTFA	Silver trifluoroacetate
AgBF_4	Silver tetrafluoroborate
Ag_2SO_4	Silver sulphate
NaH	Sodium hydride
Na_2SO_4	Sodium sulphate
THF	Tetrahydrofuran
TEMPO	(2,2,6,6-Tetramethylpiperidin-1-yl)oxyl
TFA	Trifluoroacetic acid
TFE	Trifluoroethanol
TM	Transition metal
$\text{Zn}(\text{OAc})_2$	Zinc acetate

Chapter 1A

Introduction To C-C Bond Activation of Three-membered Strained Systems

1A.1 Introduction

1A.2 Thermodynamic and Kinetic factors

1A.3 Three-membered strained systems and palladium catalysis

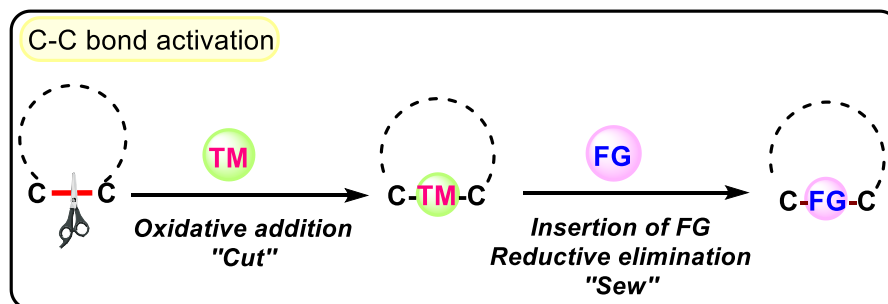
1A.4 Cyclopropanone as 3C building block

1A.5 Conclusion

1A.6 References

Chapter 1A

Introduction To C-C Bond Activation of Three-membered Strained Systems



1A.1 INTRODUCTION

The transition metal-catalyzed reaction brought great success to both organic and organometallic chemists. Since the development of this field, numerous transformations have been achieved in step and atom economical fashion. In transition metal-catalyzed reactions, the inert bond activation strategy has taken center stage and grabbed the attention of scientists worldwide. The C-C and C-H bond activation is of particular interest among the various inert bonds, as this constitutes the basic backbone of all the organic molecular skeletons.

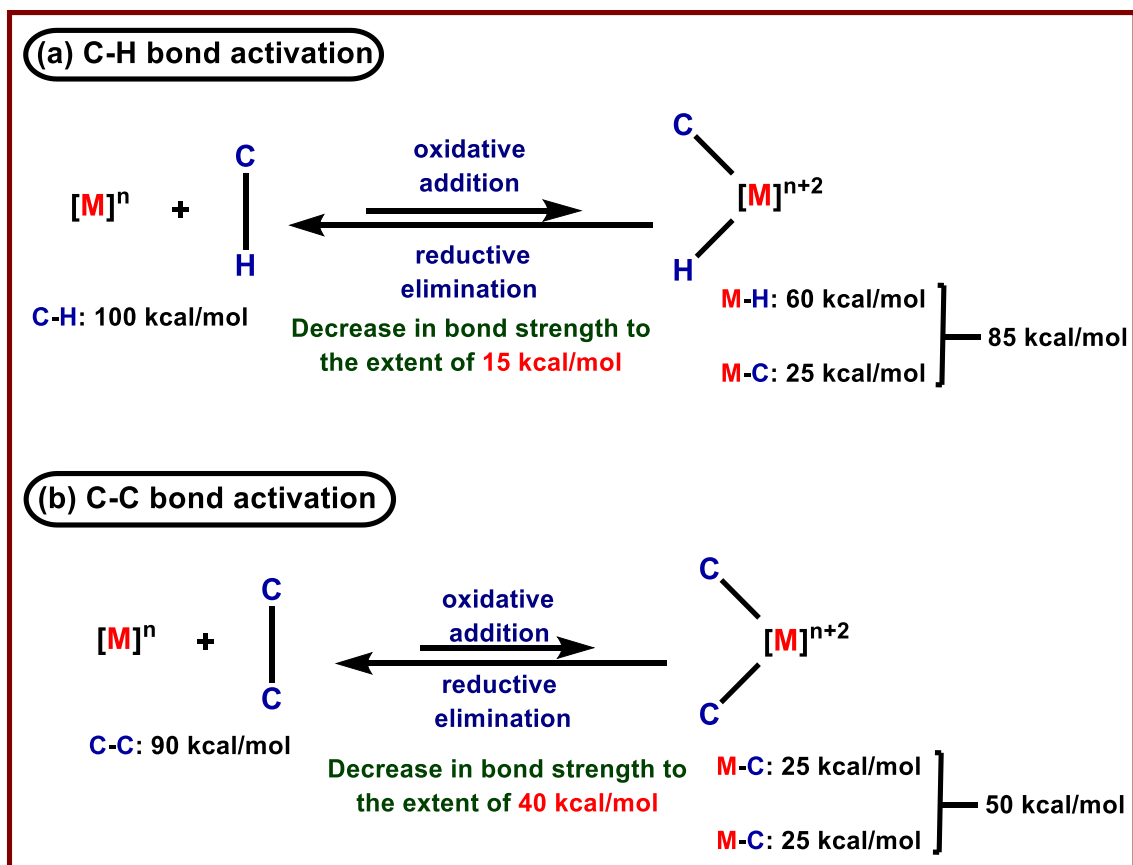
In recent years, transition metal-catalyzed strong C-C bond activation has significantly attracted the attention of synthetic chemists. This protocol enables the simultaneous and direct functionalization of two different M-C bonds. Strain-driven C-C bond activation has resulted in various otherwise difficult transformations among different C-C bond activation strategies. The cleavage and formation of these C-C bonds are incredibly significant in organic synthesis. While C-C bond-forming reactions are heavily exploited for making a variety of artificial substances, including medicines, pesticides, fertilizers, and plastics.¹

1A.2 THERMODYNAMIC AND KINETIC FACTORS

Selective C-C bond cleavage reactions are usually regarded as very difficult due to their

(i) high thermodynamic stability, (ii) orbital directionality, and (ii) steric hindrance around the C-C bond.²

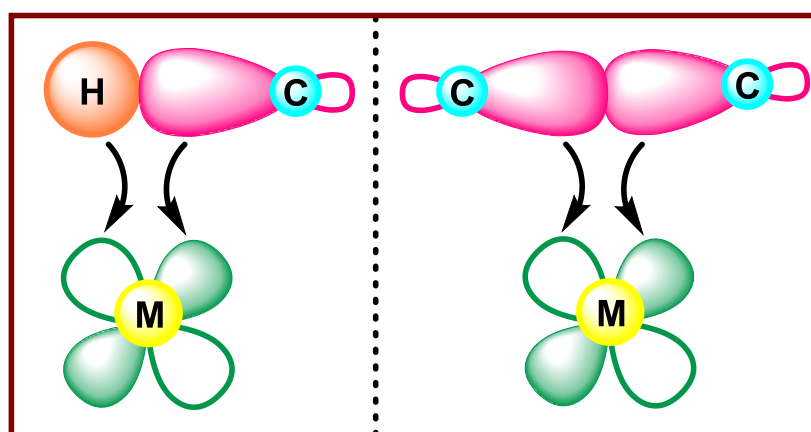
Figure 1A.1 Thermodynamic factor



The high bond dissociation energy of the C-H and C-C bond makes it stable and inert in most chemical reactions. As shown in figure 1A.1, the oxidative addition of metal to the C-H bond to form the C-M-H bond leads to the release of 25 kcal/mol of energy which can be easily attained at room temperature. In this case, a strong M-H bond, and a relatively weaker M-C bond are formed. On the contrary, the oxidative addition of the metal to the C-C bond results in two weak M-C bonds, which amount to a total loss of 50 kcal/mol of energy, making the process relatively very difficult.

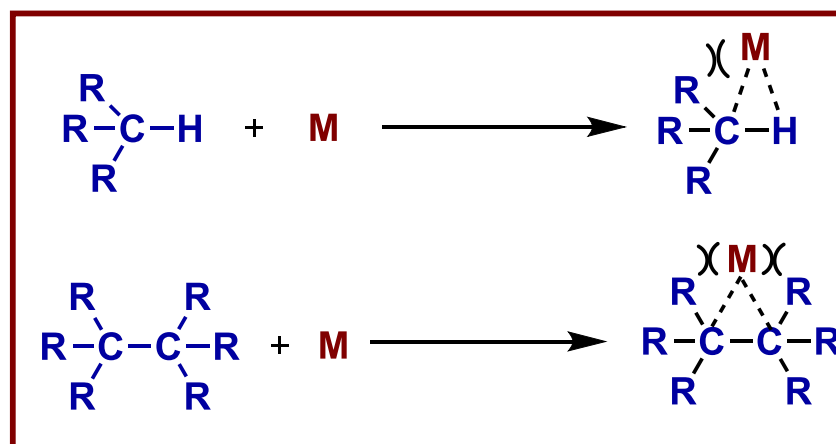
In addition to the thermodynamic factor, orbital overlapping and statistical factors make the C-C bond activation process challenging. The directional nature of the sp^3 -orbital of the C-C bond does not allow an effective overlap with the metal orbitals (Figure 1A.2). Whereas in the case of the C-H bond, the metal orbitals can favorably interact with the spherically symmetrical 1s orbital of the hydrogen atom, facilitating the oxidative addition process. Thus, transition metal-catalyzed C-H bond activation is relatively easier than C-C bond activation.

Figure 1A.2 Orbital overlapping



Further, the number of C-H bonds present in most of the organic molecules is more in number as compared to the C-C bond. Therefore, from a statistical point of view, C-H bond activation is more favorable than C-C bond activation.

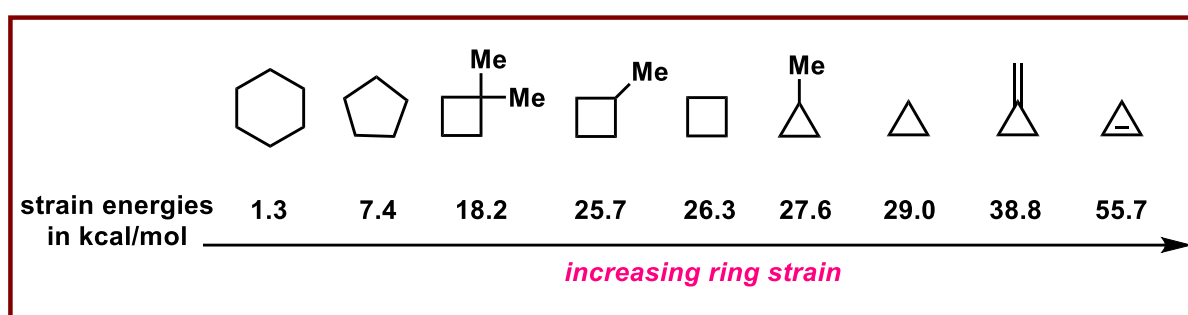
Figure 1A.3 Steric and statistical factor



In general C-C bonds are crowded by the presence of other atoms attached to these carbon atoms. Therefore, the approach of metal toward the C-C bond is sterically less favorable (Figure 1A.3).

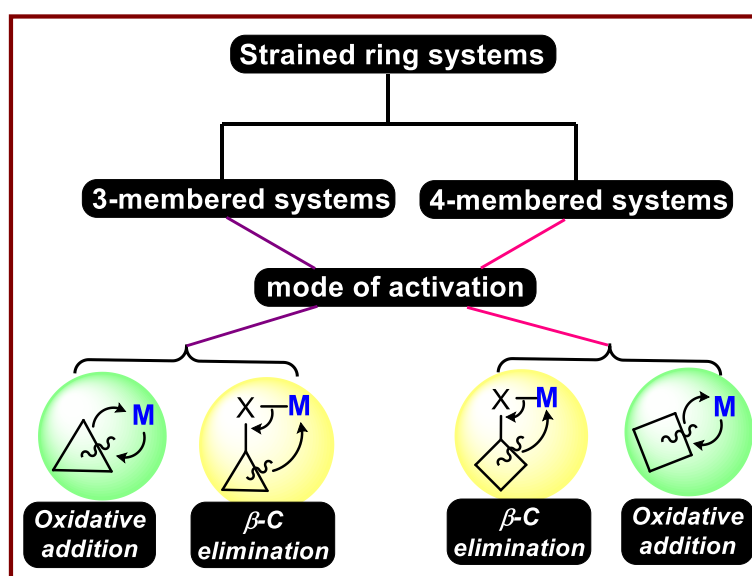
Despite these challenges, many organic molecules, including complex natural products, have been synthesized through the transition metal-catalyzed C-C bond cleavage/activation process.³

Figure 1A.4 Strain energies of cycloalkanes



Metal-catalyzed C-C bond activation typically proceeds through one of the following three pathways^{2,4} (i) chelation assistance (ii) driven by aromaticity, and (iii) strain release. Among them, strain-driven C-C bond activation gained particular importance in recent years.

Figure 1A.5 Modes of C-C bond activation in 3 and 4-membered strained systems



Three and four-membered strained ring systems such as cyclopropanes, and cyclobutanes are good candidates for C-C bond activation processes. The inherent strain in such systems largely offsets the thermodynamic barrier for the C-C bond cleavage process (Figure 1A.4). Hence, a wide range of interesting organic skeletons can be synthesized. Activation of the C-C bond, or the addition of C-C bonds to the metal (oxidative addition), can be accomplished in both the directed and non-directed pathways. The directed path can frequently improve reaction rates and provide enhanced regiocontrol. Further, the C-C bond activation process occurs in two pathways (i) oxidative addition of C-C bonds to the transition metal and (ii) β -carbon elimination (Figure 1A.5).

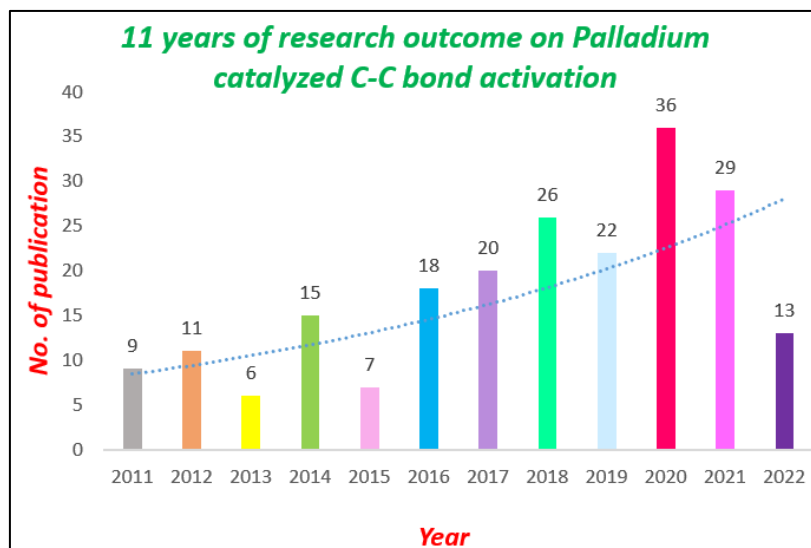
1A.3 THREE-MEMBERED STRAINED SYSTEMS AND PALLADIUM CATALYSIS

Cyclopropane and its derivatives are highly strained three-membered carbocycles that have been used as an important 3C surrogate to synthesize various value-added scaffolds. The cyclopropane derivatives include difluorocyclopropane, cyclopropene, alkylidene cyclopropane, vinyl cyclopropane, cyclopropyl amine, and cyclopropanol have been extensively studied.⁵ Apart from the strained starting material, an efficient, cost-effective metal catalyst is also necessary. In this context, the C-C bond activation reaction in the presence of a simple palladium catalyst will be more valuable and cost-effective than the costly rhodium-catalyzed conditions.

The scientific community has extensively used Palladium as a catalyst to synthesize various drugs, natural products, and bioactive scaffolds.⁶ Its practical utility as a catalyst has been exploited in various C-X bond activation strategies. Among them, using a simple palladium catalyst in the C-C bond activation of strained cycloalkanes is a booming area. Compared to the C-H bond activation reaction, C-C bond activation reactions have not been extensively explored.⁷ But this trend is changing very fast, as many groups are actively

involved in the C-C bond activation of strained ring systems. This is reflected in the number of publications over the last eleven years (figure 1A.6).

Figure 1A.6 Trend of palladium-catalyzed C-C bond activation in the past 11 years

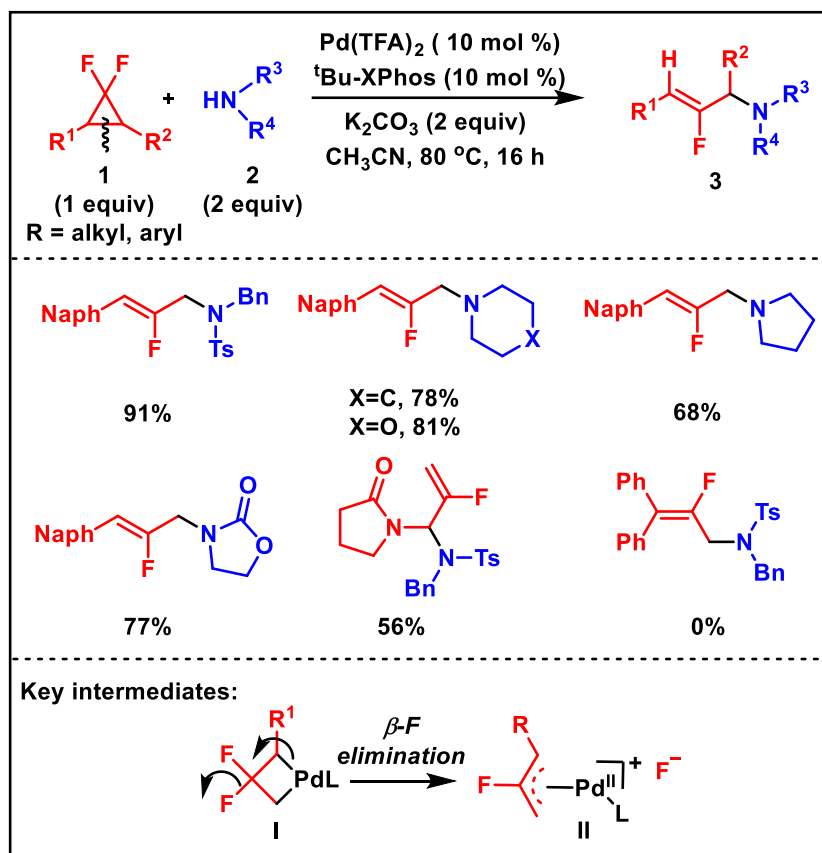


Here are some of the selected recent examples on palladium-catalyzed C-C bond activation of various three-membered strained systems.

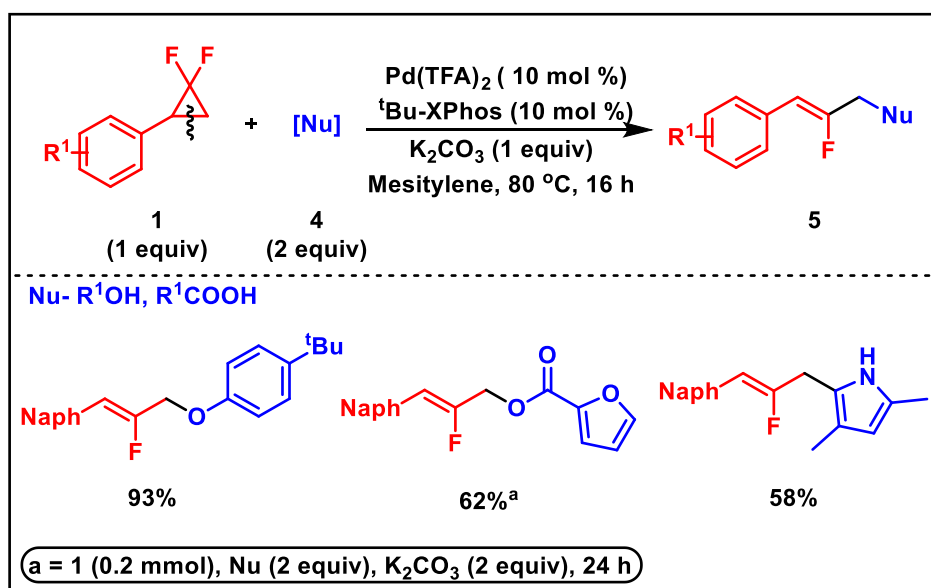
1A.31 Cyclopropane:

Fu and co-workers unraveled the first report on Pd-catalyzed regioselective activation of gem-difluorinated cyclopropanes in 2015. The C-C bond cleavage followed by simultaneous β -F elimination of gem difluorinated cyclopropanes **1** and coupling with a wide range of nucleophiles **2/4** delivered 2-fluoroallylic amines **3**, ethers, esters, and alkylation products **5** with high *Z*-selectivity (Scheme 1A.1 and 1A.2).⁸ This procedure is operationally simple and utilizes readily available substrates compared to the earlier methods⁹ providing the product in good yields with high *Z*-selectivity. The N, C, and O nucleophiles used in the reaction provide a distinct and important synthetic building blocks for synthesizing a range of 2-fluorinated allylic products. The *N*-nucleophiles (mono-protected benzylamines, protected aromatic amines, secondary amines) mainly gave a major linear product with high *Z*-selectivity.

Scheme 1A.1 Pd-catalyzed regioselective activation of gem-difluorinated cyclopropanes

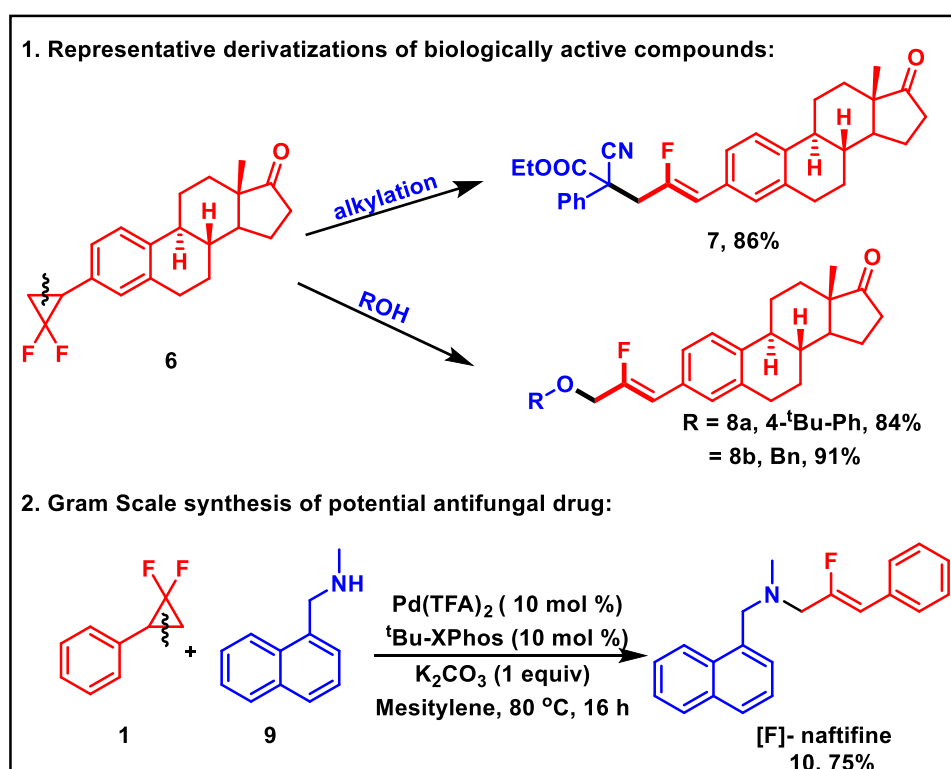


Scheme 1A.2 Pd-catalyzed regioselective activation of gem-difluorinated cyclopropanes



When 1-(2,2-difluorocyclopropyl)pyrrolidin-2-one was used as a substrate, it resulted in a branched product with a moderate yield. The substrate with terminal substituents did not yield the product even at higher temperatures. With some modification in the reaction condition, other nucleophiles such as phenols, alcohols, and carboxylate salts delivered the corresponding 2-fluoro allylic ether, ester, and alkylation product in excellent to moderate yields. The synthetic protocol has been employed on steroid-derived difluoro cyclopropane **6**, delivering products **7** and **8** in excellent yields and selectivity (Scheme 1A.3). This reaction can also be done on a gram scale to deliver [F]-naftifine **10**, a potential antifungal drug, giving promising hope for its future use in industrial applications.

Scheme 1A.3 Application of the methodology



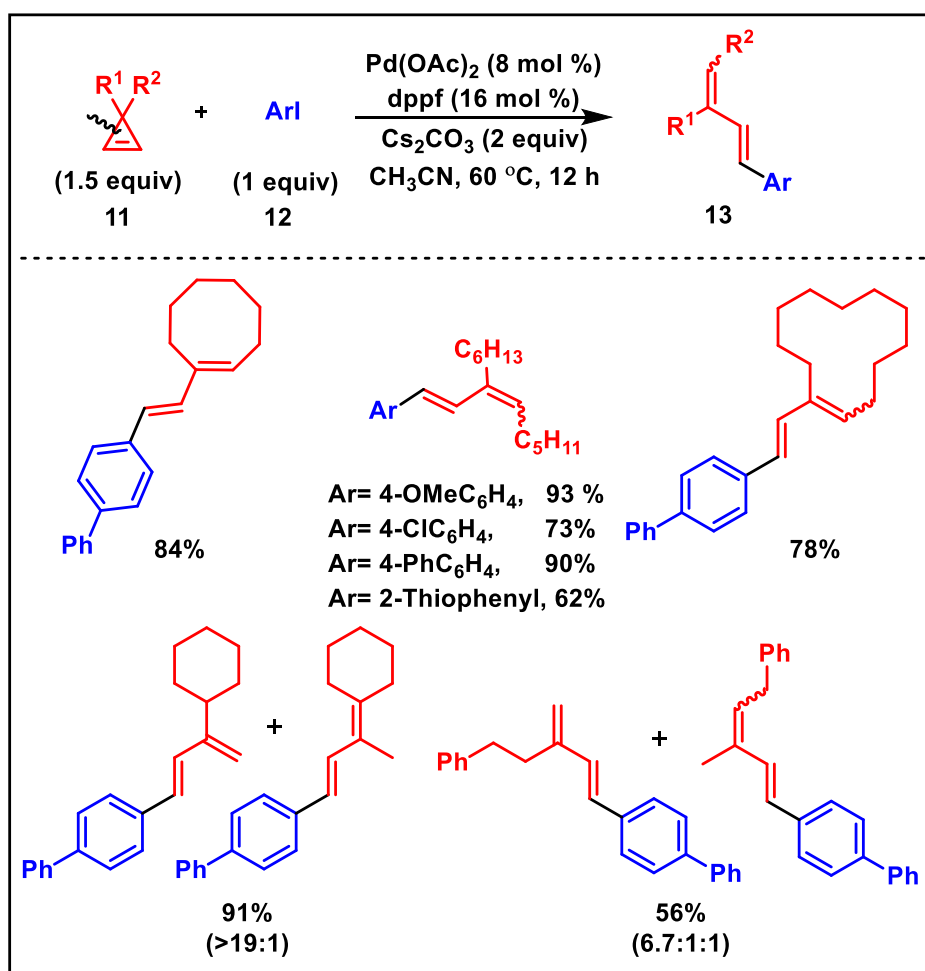
The preliminary DFT study suggested that the oxidative addition of Pd(0) to the C-C bond is energetically more facile with an energy barrier of +7.9 kcal/mol than oxidative addition to the C-F bond with an energy barrier of +46.5 kcal/mol. Thus, **I** undergo β -F elimination to give **II**, which undergoes a subsequent nucleophilic attack to provide the desired product

(Scheme 1A.1). The overall energy barrier is 29.4 kcal/mol, which is consistent with the reaction temperature.

1.32 Cyclopropene:

Cyclopropene is another class of three-membered strained systems used widely as a 3C synthon and an active coupling partner in different value-added transformations. Under the catalytic condition, the double bond of cyclopropene interacts with metal to undergo various efficient transformations.

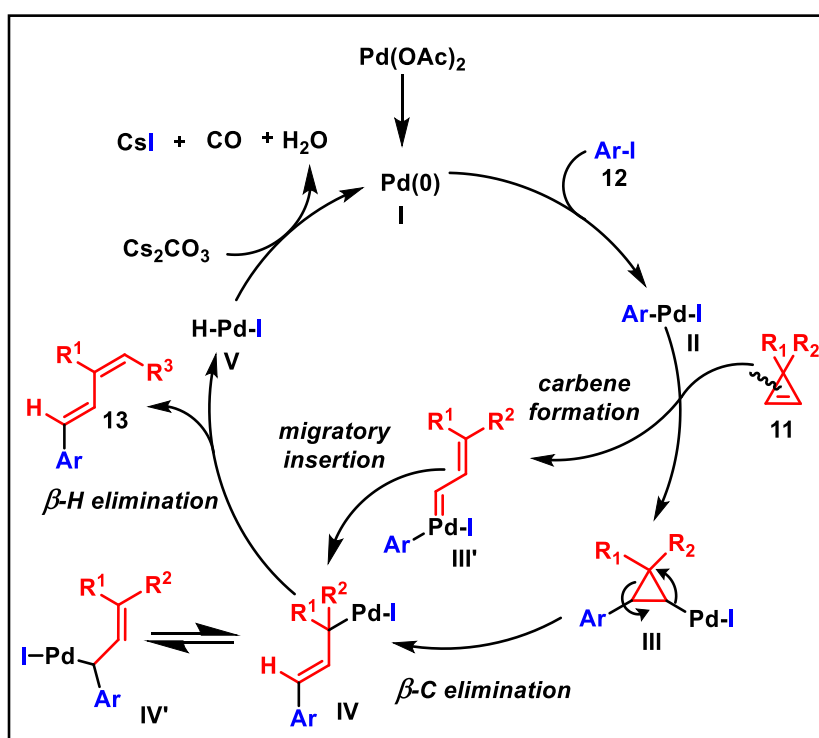
Scheme 1A.4 Pd-catalyzed ring-opening cross-coupling of cyclopropenes with aryl iodides



In 2014, Wang and co-workers developed stereoselective Pd(0) catalyzed ring opening cross-coupling of cyclopropene **11** with aryl iodide **12** that delivered 1,3-butadiene

derivatives **13** (Scheme 1A.4).¹⁰ The generality of the reaction condition has been tested by varying substituents on cyclopropene and aryl iodide. As observed, the electron-donating substituent on aryl iodides gave a better yield at a lower temperature than the electron-withdrawing group. Aryl iodides with two aliphatic chains resulted in a mixture of *E* and *Z*-isomers. Cyclopropene and 4-iodobiphenyls produced regioisomers due to two different substituents on the cyclopropene ring, which can undergo β -H elimination.

Scheme 1A.5. Catalytic cycle



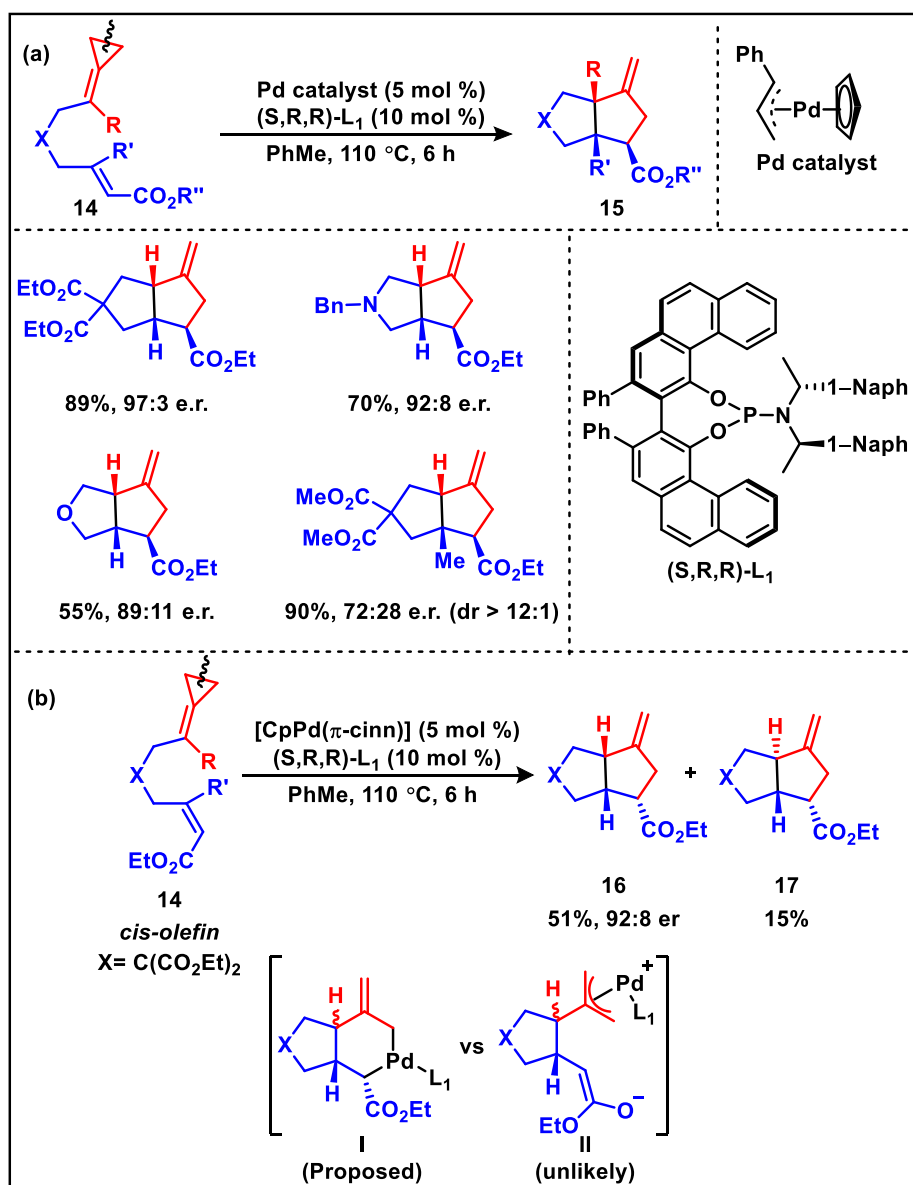
They have proposed a plausible catalytic cycle for the above transformation (Scheme 1A.5). The cyclopropene is activated by the Pd(II) aryl iodide intermediate in two different pathways. In one pathway, insertion of the C-C bond of cyclopropane **11** in the metal alkyl bond **II** afforded cyclopropyl palladium species **III**, which on β -carbon elimination leads to the opening of the strained ring to give the intermediate **IV**. Subsequent β -H elimination from intermediate **IV** afforded 1,3-diene product **13**. However, in another pathway, it may also proceed via the formation of palladium carbene species **III'** followed by the migration of the aryl group to deliver the intermediate **IV**. Intermediate **IV** on the subsequent β -H

elimination delivered the desired product **13**, with the generation of active palladium (II) species. The active Pd(0) species regenerate from intermediate **V** in the presence of Cs₂CO₃ for the next catalytic cycle.

1.33 Alkylidene cyclopropane (ACP):

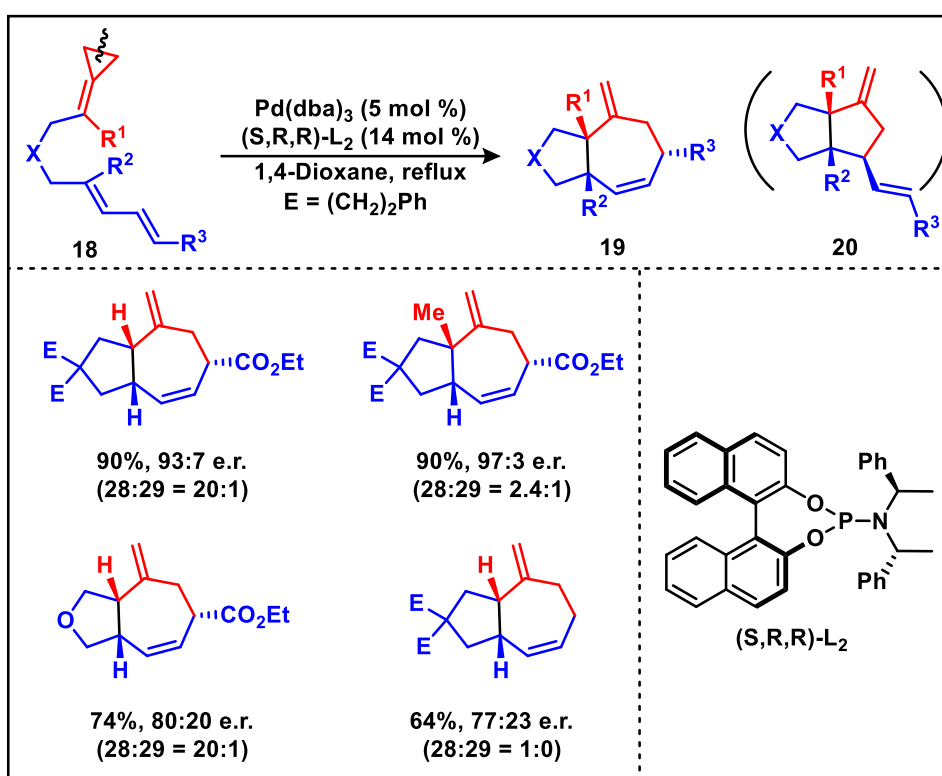
Alkylidene cyclopropane (ACPs) is a class of three-membered strained systems that have been heavily exploited in the palladium-catalyzed C-C bond activation.¹¹ ACPs are primarily used as active 3C synthons in the cycloaddition reaction to synthesize various value-added products.

Scheme 1A.6. Scope of the Pd-Catalyzed (3C + 2C) Cycloaddition



In 2018, Lopez and co-workers discovered that alkylidenecyclopropanes (ACPs) **14** and alkenes could undergo a highly enantioselective (3C + 2C) intramolecular cycloaddition (Scheme 1A.6a).¹² The best result was obtained when chiral phosphoramidite ligand **L**₁ was used in the reaction. According to the observed stereospecificity and control experiment, the reaction is suggested to go through the proposed key intermediate **I** rather than intermediate **II**, where the stereochemistry is inverse (Scheme 1A.6b).

Scheme 1A.7. Scope of the Enantioselective Pd-Catalyzed (4 + 3) Cycloaddition

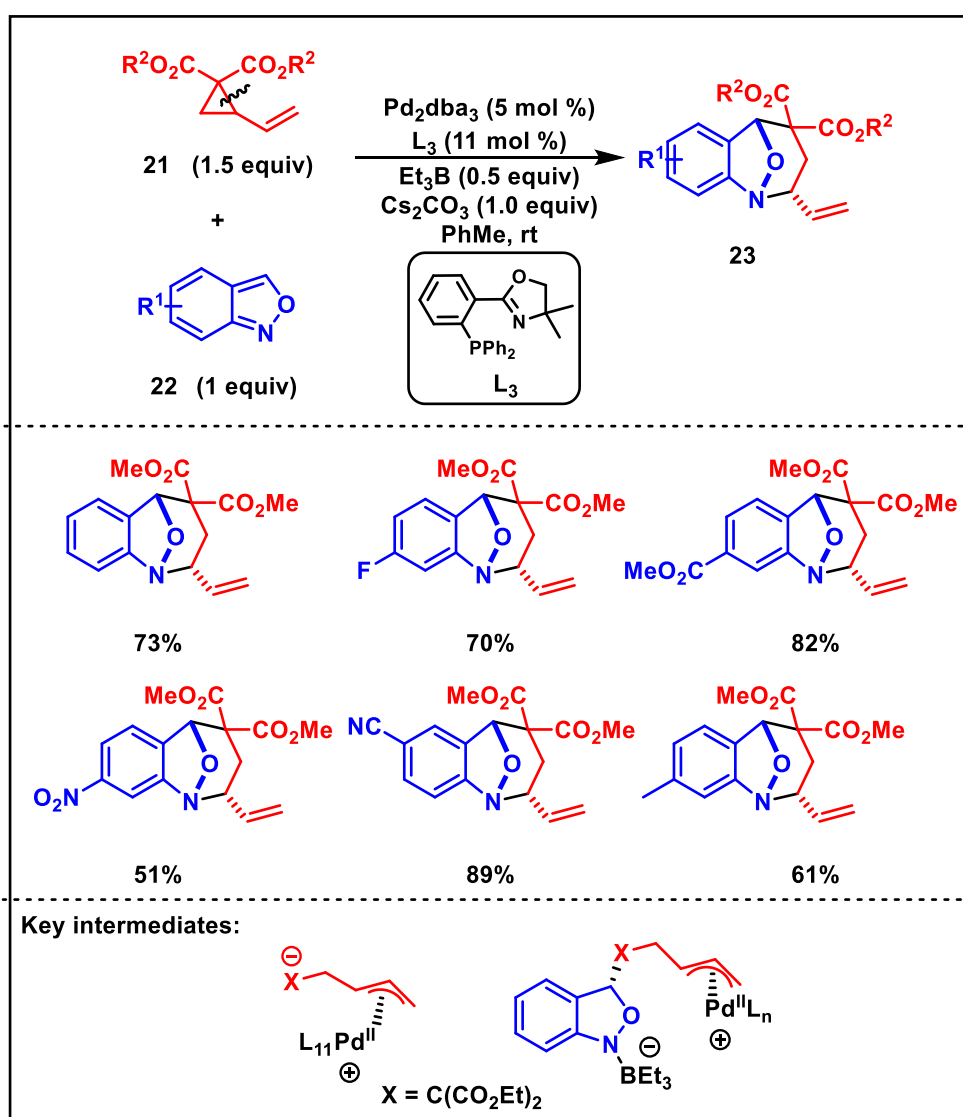


Furthermore, they showed that when dienes **18** (in place of alkenes), are used as reaction partners, extremely efficient (4C + 3C) cycloadditions can be done with the help of analogous but less bulky phosphoramidites **L**₂ (Scheme 1A.7). These reactions offer a practical, straightforward, and selective route to optically active and synthetically attractive 5,5- and 5,7-bicyclic compounds.

1.34 Vinyl Cyclopropane (VCP):

Lately, vinyl cyclopropanes (VCPs) containing electron-withdrawing groups have gained much attention as a new group of "three-carbon-atom" precursors for asymmetric cycloaddition reactions. They can generate 1,3-dipolar equivalents in the presence of Pd(0) catalysts and then trap a dipolarophile to form diverse substituted five-membered rings.^{13,14}

Scheme 1A.8. Pd-catalyzed dearomatization of anthranils with vinyl cyclopropanes by (4+3) cyclization reaction



In 2019, You and co-workers developed Pd-catalyzed dearomative (4+3) cyclization reactions of anthranils **22** with VCPs **21** (Scheme 1A.8).¹⁵ They discovered that triethyl borane is an effective anthranil activator and that dearomative (4+3) cyclization of

anthranils with VCPs can be accomplished using Pd-catalysis. At room temperature, the reaction performed with good yield and excellent diastereoselectivity using a widely accessible Pd catalyst and a catalytic quantity of borane as an activator. The reactions were carried out with high enantioselectivity after adding a chiral PHOX ligand **L**₃.

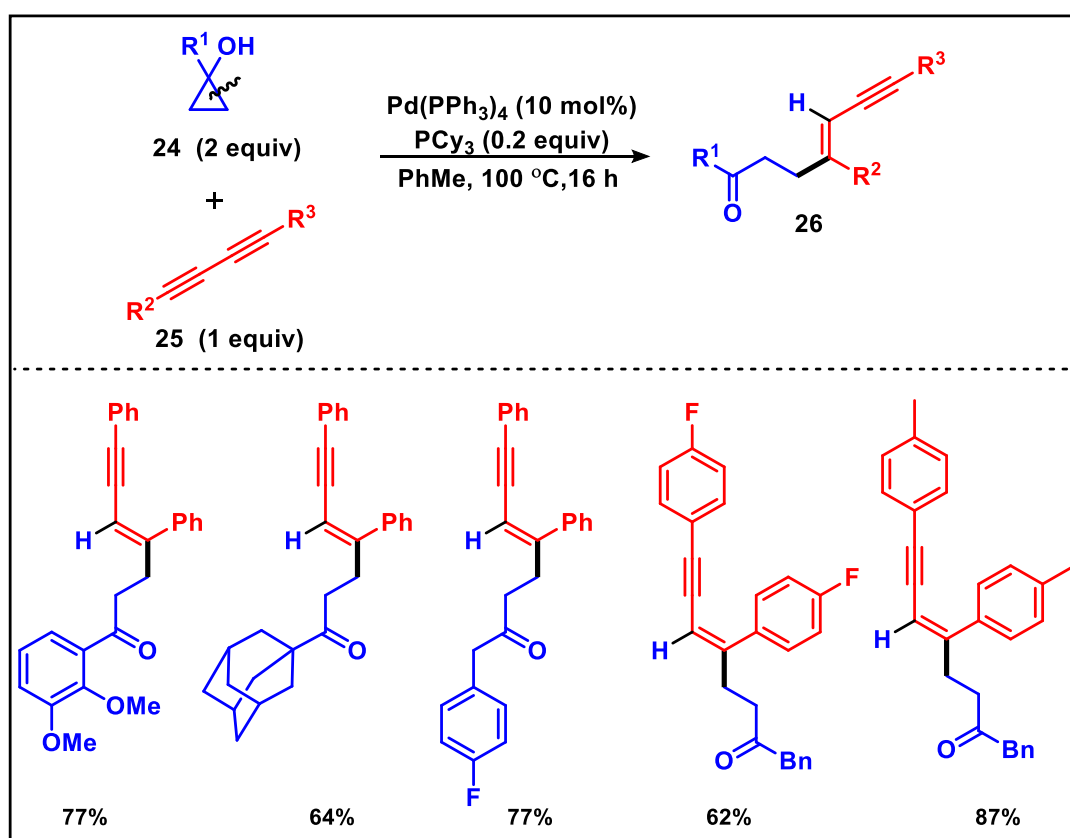
The newly developed approach made it simple to access a variety of bridged cyclic molecules, which were shown to undergo various transformations. Borane is important for this transformation because it forms a borane–anthranil complex, which has been validated by NMR experiments. In ¹H NMR, the chemical shift of anthranil downshifted when Et₃B was added, demonstrating Et₃B coordination with anthranil. The key intermediate involved in the reaction has been shown in scheme 1A.8. The generality of the reaction has been demonstrated using a variety of substrates. The electron-withdrawing groups in the substrates, such as ester, trifluoromethyl, cyanide, and even nitro, reacted with VCP to provide the bridged cyclic products in high to excellent yields. Moreover, the electron-donating methyl group was also compatible in this reaction, as the product was produced in 61% yield.

1.35 Cyclopropanol:

Cyclopropanols are the smallest cyclic alcohols, first studied by Cottle and co-workers in 1942 as a three-carbon synthetic precursor.¹⁶ Recently, there has been a surge of popularity in the use of cyclopropanols because of its facile synthetic procedure, namely Kulinkovich's reaction and unique reactivity.¹⁷ Out of several pathways through which ring opening of cyclopropanol is possible, the C-C bond activation pathway catalyzed by transition metal recently gained immense attention. In the presence of a metal catalyst, the cyclopropanol ring opens mainly through the β -carbon elimination pathway rather than the oxidative addition of the C-C bond to the metal.

With the growing interest in cyclopropanol as 3C synthon, its utility has been recently explored by Ravikumar, Lourderaj, and co-workers. 1,3-enynes are very important skeletons because of their usefulness in material and pharmaceutical chemistry.¹⁸ With the target of providing a one-step synthetic protocol for synthesizing 1,3-enynes **26**, Ravikumar and co-workers have demonstrated the palladium-catalyzed stereoselective alkenylation between cyclopropanol **24** and 1,3-diynes **25** (Scheme 1A.9).¹⁹ Thus, 10 mol % of $\text{Pd}(\text{PPh}_3)_4$, and 20 mol % of PCy_3 , in toluene solvent at 100 °C, were the optimal condition for the desired transformation. Various cyclopropanol and 1,3-dialkyne derivatives were compatible under the optimized reaction condition and successfully delivered a wide range of 1,3-enyne products.

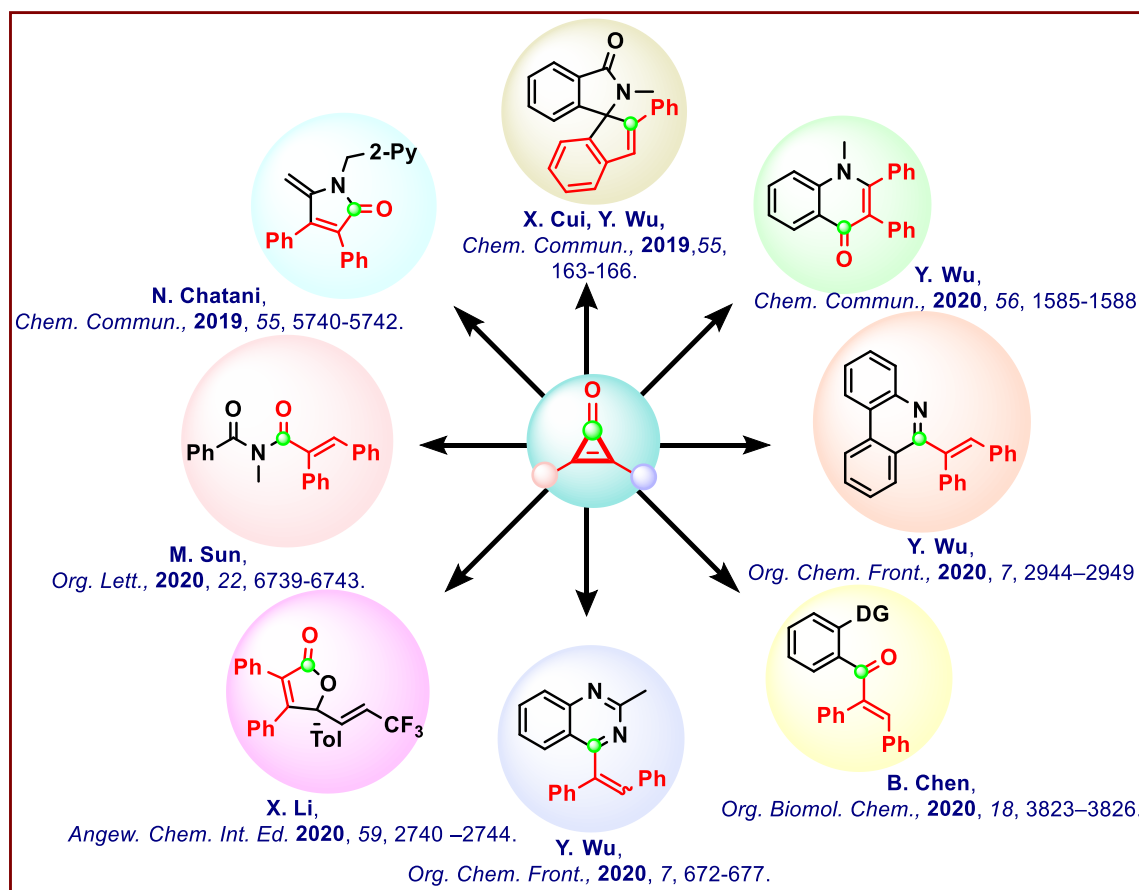
Scheme 1A.9 Palladium-catalyzed selective C–C bond cleavage and stereoselective alkenylation between cyclopropanol and 1,3-diyne



1A.4 CYCLOPROPENONE AS 3C BUILDING BLOCK

Cyclopropenones were first synthesized by Berslow then Volpin and his co-workers in 1959.²⁰ Cyclopropenone having an enormous synthetic interest serves as a versatile building block. Because of basic unsaturation and ring strain, cyclopropenone derivatives are important molecules for both theoretical and experimental chemists. Recently, the chemistry of strained ring systems is gaining immense attention due to their ability to provide molecular complexity and diversity to the final product.

Figure 1A.7 Synthetic utility of cyclopropenone

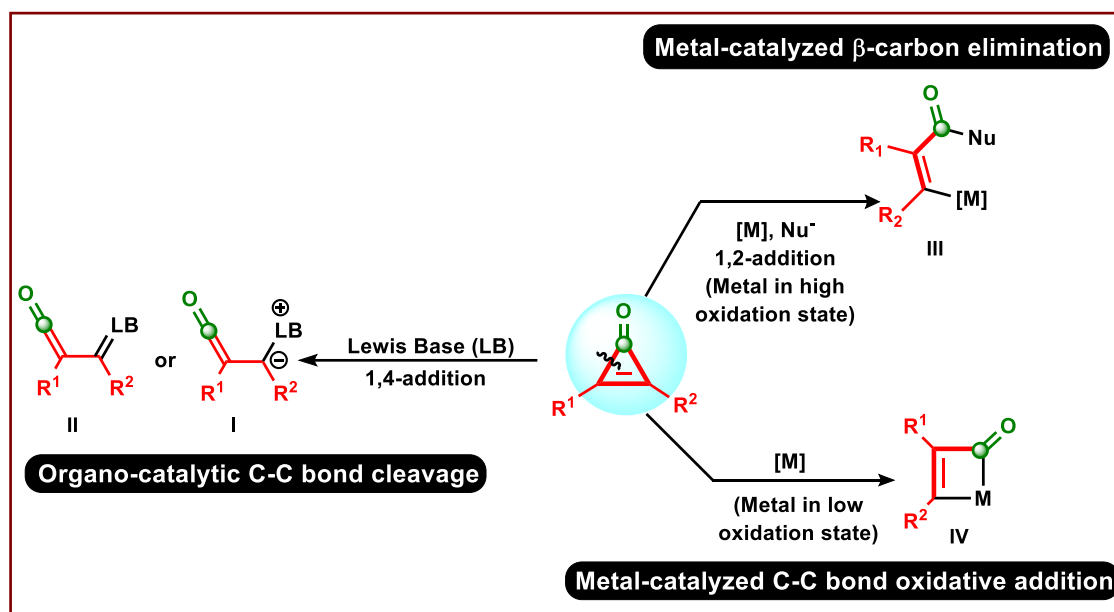


Among the three-membered ring systems, cyclopropenone is the Hückel-aromatic compound which undergoes C-C bond cleavage in the presence of transition metal catalyst and organo-catalyst and serves as an important 3C synthon (Figure 1A.7).²¹ The ring opening of cyclopropenone depends on the nature of the catalyst used in a particular

reaction. Three modes of ring opening are possible, as depicted in scheme 1A.10. In the presence of a Lewis base, cyclopropenone ring opening occurs via 1,4-addition to deliver a ketene intermediate **I** and **II** having an electrophilic center. Thus, it can undergo valuable transformations in the presence of an appropriate nucleophile.

Further, there are two modes of transition metal-catalyzed ring opening of cyclopropenone. In one case, metal with a high oxidation state behaves as a Lewis acid and coordinates with the cyclopropenone's oxygen atom, facilitating the β -carbon elimination in the presence of a nucleophile to generate intermediate **III**. In another case, metals with low oxidation states undergo oxidative addition between C-C bonds to generate intermediate **IV**. Among these three pathways, the metal-catalyzed C-C bond oxidative addition pathway is less explored and limited to a few examples that have been discussed in the coming paragraphs.

Scheme 1A.10 Modes of ring opening in cyclopropenones

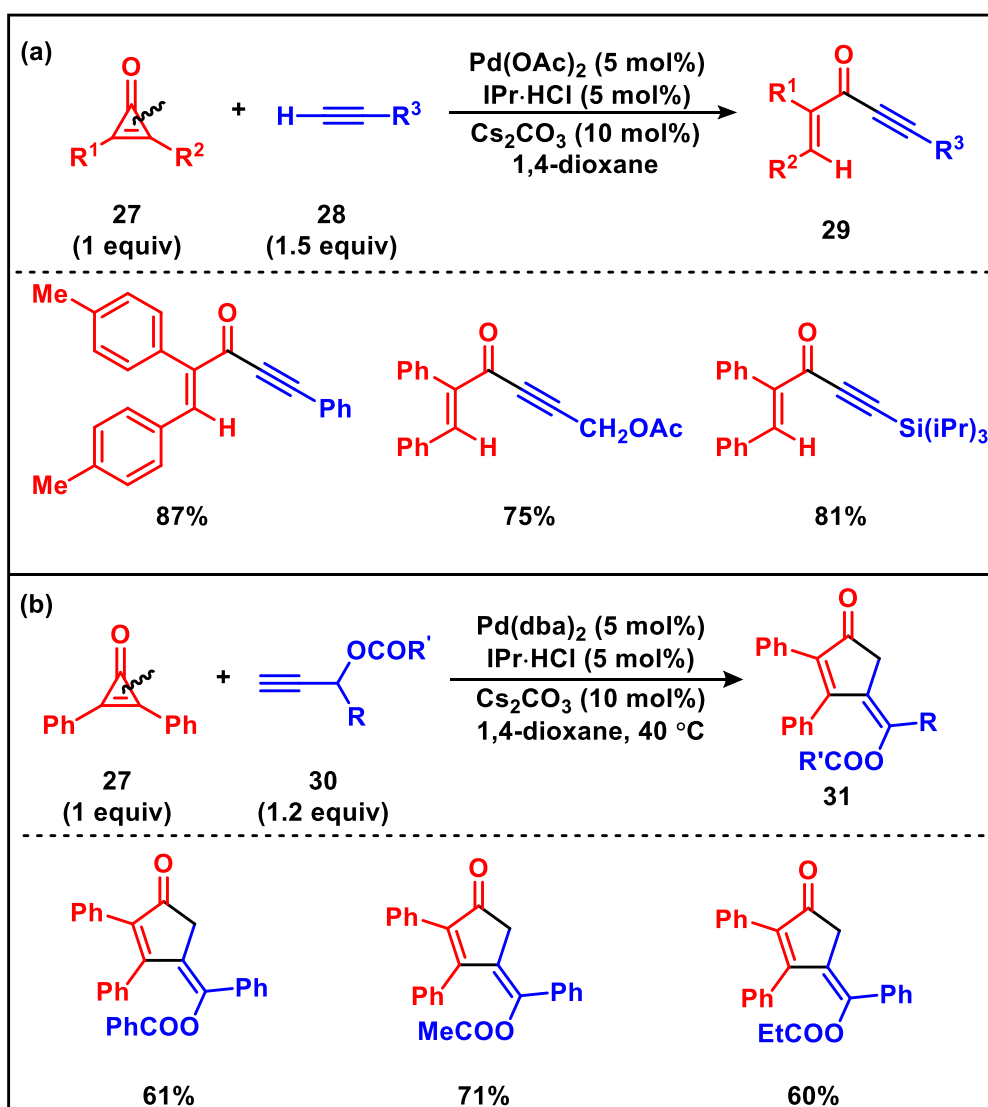


Cyclopropenone underwent various valuable transformations under palladium-catalyzed conditions. In 2013, Matsuda and co-workers reported a palladium-NHC-complex catalyzed ring-opening alkynylation process of cyclopropenones **27** (Scheme 1A.11a).²² In

this reaction, alkenyl alkynyl ketones **29** were produced in good yields. Additionally, they described a (3+2) annulation process where mono-substituted propargylic esters **30** are chosen as the model substrate that results in cyclopentenones **31**.

The reaction was found to give best yield in the presence of Pd(OAc)₂ (5.0 mol %), IPr·HCl (5.0 mol %), Cs₂CO₃ (10 mol %), in 1,4-dioxane (1.0 mL).

Scheme 1A.11 Palladium-Catalyzed Ring-Opening Alkynylation of Cyclopropenones



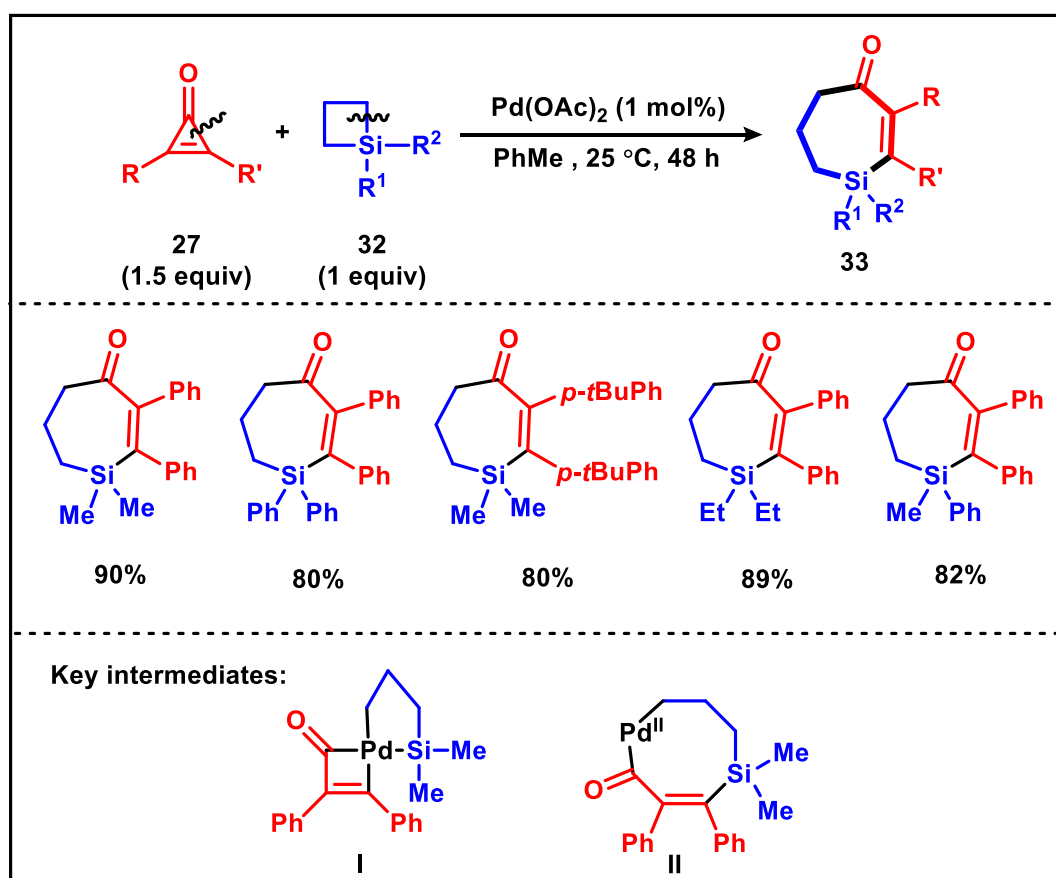
A wide range of substrates was subjected to the standard reaction condition. 4-Methylphenyl cyclopropenone gave the desired ketones in excellent yield. Then, they investigated the substrate scope by varying different terminal alkynes. Here, alkyl- and

silyl-acetylenes gave the corresponding product in good yield. Moreover, tertiary propargylic alcohol also reacted with diphenylcyclopropenone to provide a good yield of the corresponding product.

In addition to the above findings, secondary propargylic esters with an aryl or alkenyl substituent at the propargylic position **30** led to unexpected (3+2) annulation (Scheme 1A.11b). In this case, Pd(dba)₂ was used as a catalyst instead of Pd(OAc)₂.

In 2018, Zhao and co-workers developed a unique σ -bond cross exchange of cyclopropenone **27** with (benzo)silacyclobutanes **32** that directly creates sila-(benzo)suberones **33** under mild reaction conditions (Scheme 1A.12).²³

Scheme 1A.12 Intermolecular σ -bond cross-exchange reaction between cyclopropenones and (benzo)silacyclobutanes



This was the first intermolecular σ -bond cross-metathesis reaction between the C-Si bond of (benzo)silacyclobutanes **32** and the C-C bond of cyclopropenones **27**. This reaction is significant because it would lead to the development of new drug-like candidates bearing sila-(benzo)suberones.

Moreover, this reaction is carried out using a 1 mol% palladium catalyst. Different di-aryl cyclopropenones with substituents in the *para*- or *meta*-position proceeded smoothly to produce the required sila-benzosuberones in good yields. Additionally, silacyclobutanes containing various substituents on silicon, including ethyl, butyl, and phenyl groups, were also amenable substrates for this intermolecular σ -bond exchange process. The key intermediate involved in the reaction was depicted in scheme 1A.12.

1A.5 CONCLUSION

In this chapter, we have discussed the C-C bond activation, the key determining factor, and the strategies involved in this process. The strain-driven C-C bond activation strategy is the most popular among the various strategies. Three-membered strained systems are good candidates for undergoing C-C bond activation by virtue of the release of ring strain. The significant pathways involved are (i) oxidative addition and, (ii) β -carbon elimination in the presence of the metal catalyst. Further, palladium-catalyzed C-C bond activation of a three-membered strained system enabled the synthesis of a wide range of complex molecular architectures, thus grabbing a lot of attention among the synthetic community. Difluorocyclopropanes, cyclopropenes, alkylidene cyclopropanes, vinyl cyclopropanes, and cyclopropanols are the most pursued strained systems that have been studied under palladium catalysis. However, the limited reports with cyclopropenone as an important 3C building block, makes it an exciting chemical space to explore further.

1A.6 REFERENCES

1. For related reviews see; (a) Luh, T.-Y.; Leung, M.-K.; Wong, K.-T. Transition Metal-Catalyzed Activation of Aliphatic C–X Bonds in Carbon–Carbon Bond Formation. *Chem. Rev.* **2000**, *100*, 3187–3204. (b) Tsuji, J. *Transition Metal Reagents and Catalysts: Innovations in Organic Synthesis*; Wiley: Chichester, 2000; pp 1–456. (c) Dubbaka, S. R.; Vogel, P. Organosulfur Compounds: Electrophilic Reagents in Transition-Metal-Catalyzed Carbon–Carbon Bond-Forming Reactions. *Angew. Chem., Int. Ed.* **2005**, *44*, 7674–7684. (d) Kakiuchi, F.; Kochi, T. Transition-Metal-Catalyzed Carbon–Carbon Bond Formation via Carbon–Hydrogen Bond Cleavage. *Synthesis* **2008**, *2008*, 3013–3039. (e) Magano, J.; Dunetz, J. R. Large-Scale Applications of Transition Metal-Catalyzed Couplings for the Synthesis of Pharmaceuticals. *Chem. Rev.* **2011**, *111*, 2177–2250. (f) Choi, J.; Fu, G. C. Transition metal-catalyzed alkyl-alkyl bond formation: Another dimension in cross-coupling chemistry. *Science* **2017**, *356*, eaaf7230.
2. For discussions on the orbital interactions, see: (a) Rybtchinski, B.; Milstein, D. Metal Insertion into C–C Bonds in Solution. *Angew. Chem., Int. Ed.* **1999**, *38*, 870–883. (b) *Cleavage of Carbon–Carbon Single Bonds by Transition Metals*; Murakami, M., Chatani, N., Eds.; Wiley-VCH: Weinheim, Germany, 2015. (c) For discussions on the thermodynamic and kinetic difficulties in C–C bond cleavage, see: Murakami, M.; Ishida, N. Potential of Metal Catalyzed C–C Single Bond Cleavage for Organic Synthesis. *J. Am. Chem. Soc.* **2016**, *138*, 13759–13769.
3. (a) Jun, C.-H. Transition Metal-Catalyzed Carbon–Carbon Bond Activation. *Chem. Soc. Rev.* **2004**, *33*, 610–618. (b) *C–C Bond Activation: Topics in current chemistry*; Dong, G., Ed.; Springer: Berlin, 2014; Vol. 346. (c) Souillart, L.; Cramer, N. Catalytic C–C Bond Activations via Oxidative Addition to Transition Metals. *Chem. Rev.* **2015**, *115*, 9410–9464. (d) Fumagalli, G.; Stanton, S.; Bower, J. F. Recent Methodologies That Exploit C–C Single-Bond Cleavage of Strained Ring Systems by Transition Metal Complexes. *Chem. Rev.* **2017**, *117*, 9404–9432. (e) Kim, D.-S.; Park, W.-J.; Jun, C.-H. Metal–Organic Cooperative Catalysis in C–H and C–C Bond Activation. *Chem. Rev.* **2017**, *117*, 8977–9015. (f) Kerschgens, I.; Rovira, A. R.; Sarpong, R. Total Synthesis of (–)-Xishacorene B from (R)-Carvone Using a C–C Activation Strategy. *J. Am. Chem. Soc.* **2018**, *140*, 9810–9813. (g) Deng, L.; Dong, G. Carbon–Carbon Bond Activation of Ketones. *Trends Chem.* **2020**, *2*, 183–198. (h) Nakao, Y. Metal mediated C–CN Bond Activation in Organic Synthesis. *Chem. Rev.* **2021**, *121*, 327–344. (i) Lu, H.; Yu, T.-Y.; Xu, P.-F.; Wei, H. Selective Decarbonylation via Transition-Metal-Catalyzed Carbon–Carbon Bond Cleavage. *Chem. Rev.* **2021**, *121*, 365–411. (j) Lusi, R. F.; Perea, M. A.; Sarpong, R. C–C Bond Cleavage of α -Pinene Derivatives Prepared from Carvone as a General Strategy for Complex Molecule Synthesis. *Acc. Chem. Res.* **2022**, *55*, 746–758.
4. (a) Dreis, A. M.; Douglas, C. J. Catalytic Carbon–Carbon σ Bond Activation: An Intramolecular Carbo-Acylation Reaction with Acylquinolines. *J. Am. Chem. Soc.* **2009**, *131*, 412–413. (b) Ruhland, K. Transition Metal-Mediated Cleavage and Activation of C–C Single Bonds. *Eur. J. Org. Chem.* **2012**, *14*, 2683–2706. (c) Wang, J.; Chen, W.; Zuo, S.; Liu, L.; Zhang, X.; Wang, J. Direct Exchange of a Ketone Methyl or Aryl Group to Another Aryl Group through C–C Bond Activation Assisted by Rhodium Chelation. *Angew. Chem., Int. Ed.* **2012**, *51*, 12334–12338. (d) Dennis, J. M.; Compagner, C. T.; Dorn, S. K.; Johnson, J. B. Rhodium-Catalyzed Interconversion of Quinolinyl Ketones with Boronic Acids via C–C Bond

- Activation. *Org. Lett.* **2016**, *18*, 3334–3337. (e) Xia, Y.; Lu, G.; Liu, P.; Dong, G. Catalytic activation of carbon-carbon bonds in cyclopentanones. *Nature* **2016**, *539*, 546–550.
5. Nanda, T.;[#] Fastheem, M.;[#] Linda, A.; Pati, B. V.; Banjare, S. K.; Biswal, P.; Ravikumar, P. C. Advancement in Palladium-Catalyzed C-C bond Activation of Strained Ring Systems: Three and four-membered carbocycles as prominent C3/C4 building blocks. *ACS Catal.* **2022**, *12*, 13247–13281. ([#]*equally contributed*).
 6. (a) Mikami, K.; Hatano, M.; Akiyama, K. Active Pd(II) Complexes as Either Lewis Acid Catalysts or Transition Metal Catalysts. *Top. Organomet. Chem.* **2005**, *14*, 279–321. (b) Doucet, H.; Hiero, J.-C. Palladium coupling catalysts for pharmaceutical applications. *Curr. Opin. Drug Discovery Dev.* **2007**, *10*, 672–690. (c) Catellani, M.; Motti, E.; Della Ca', N. Catalytic Sequential Reactions Involving Palladacycle-Directed Aryl Coupling Steps. *Acc. Chem. Res.* **2008**, *41*, 1512–1522. (d) Chen, X.; Engle, K. M.; Wang, D. H.; Yu, J. Q. Palladium(II)-Catalyzed C-H Activation/C-C Cross-Coupling Reactions: Versatility and Practicality. *Angew. Chem., Int. Ed.* **2009**, *48*, 5094–5115. (e) Gunay, M. E.; Ilyashenko, G.; Richards, C. J. Models for the basis of enantioselection in palladium mediated C-H activation reactions. *Tetrahedron: Asymmetry*, **2010**, *21*, 2782–2787. (f) Tietze, L. F.; Dufert, A. Multiple Pd-catalyzed reactions in the synthesis of natural products, drugs, and materials. *Pure Appl. Chem.* **2010**, *82*, 1375–1392. (g) Adrio, L. A.; Hii, K. K. Palladium-Catalyzed Heterofunctionalization of C-H, C=C and C≡C Bonds. *Curr. Org. Chem.* **2011**, *15*, 3337–3361. (h) Chinchilla, R.; Nájera, C. Chemicals from Alkynes with Palladium Catalysts. *Chem. Rev.* **2014**, *114*, 1783–1826. (i) Della Ca', N.; Fontana, M.; Motti, E.; Catellani, M. Pd/ Norbornene: A Winning Combination for Selective Aromatic Functionalization via C–H Bond Activation. *Acc. Chem. Res.* **2016**, *49*, 1389–1400. (j) Jones, D. J.; Lautens, M.; McGlacken, G. P. The Emergence of Pd-Mediated Reversible Oxidative Addition in Cross Coupling, Carbohalogenation and Carbonylation Reactions. *Nat. Catal.* **2019**, *2*, 843–851. (k) Marchese, A. D.; Larin, E. M.; Mirabi, B.; Lautens, M. Metal Catalyzed Approaches toward the Oxindole Core. *Acc. Chem. Res.* **2020**, *53*, 1605–1619. (l) Thombal, R. S.; Rubio, P. Y. M.; Lee, D.; Maiti, D.; Lee, Y. R. Modern Palladium-Catalyzed Transformations Involving C–H Activation and Subsequent Annulation. *ACS Catal.* **2022**, *12*, 5217–5230.
 7. For recent reviews on C-H functionalization, see: a) Lyons, T. W.; Sanford, M. S. Palladium-Catalyzed Ligand-Directed C–H Functionalization Reactions. *Chem. Rev.* **2010**, *110*, 1147–1169. b) Ackermann, L. Carboxylate-assisted transition-metal-catalyzed C–H bond functionalizations: mechanism and scope. *Chem. Rev.* **2011**, *111*, 1315–1345. c) Daugulis, O.; Roane, J.; Tran, L. D. Bidentate, Monoanionic Auxiliary-Directed Functionalization of Carbon–Hydrogen Bonds. *Acc. Chem. Res.* **2015**, *48*, 1053–1064. d) He, J.; Wasa, M.; Chan, K. S. L.; Shao, Q.; Yu, J.-Q. Palladium-Catalyzed Transformations of Alkyl C–H Bonds. *Chem. Rev.* **2017**, *117*, 8754–8786. e) Lam, N. Y. S.; Wu, K.; Yu, J. Q. Advancing the Logic of Chemical Synthesis: C–H Activation as Strategic and Tactical Disconnections for C–C Bond Construction. *Angew. Chem., Int. Ed.* **2021**, in press, DOI: 10.1002/anie.202011901.
 8. (a) Xu, J.; Ahmed, E. A.; Xiao, B.; Lu, Q. Q.; Wang, Y. L.; Yu, C. G.; Fu, Y. Pd-Catalyzed Regioselective Activation of gem-Difluorinated Cyclopropanes: A Highly Efficient Approach to 2-Fluorinated Allylic Scaffolds. *Angew. Chem., Int. Ed.* **2015**, *54*, 8231–8235.

9. Nihei, T.; Hoshino, T.; Konno, T. Unusual Reaction Behavior of gem-Difluoro cyclopropane Derivatives: Stereoselective Synthesis of β -Mono fluoroallylic Alcohols, Ethers, Esters, and Amide. *Org. Lett.* **2014**, *16*, 4170–4173.
10. Zhang, H.; Wang, B.; Wang, K.; Xie, G.; Li, C.; Zhang, Y.; Wang, J. Pd-Catalyzed Ring-Opening Cross-Coupling of Cyclopropenes with Aryl Iodides. *Chem. Commun.* **2014**, *50*, 8050–8052.
11. (a) Delgado, A.; Rodríguez, J. R.; Castedo, L.; Mascareñas, J. L. Palladium-Catalyzed [3 + 2] Intramolecular Cycloaddition of Alk-5-ynylidenecyclopropanes: A Rapid, Practical Approach to Bicyclo[3.3.0]octenes. *J. Am. Chem. Soc.* **2003**, *125*, 9282–9283. (b) López, F.; Delgado, A.; Rodríguez, J. R.; Castedo, L.; Mascareñas, J. L. Ruthenium-Catalyzed [3 + 2] Intramolecular Cycloaddition of Alk-5-ynylidenecyclopropanes Promoted by the “First-Generation” Grubbs Carbene Complex. *J. Am. Chem. Soc.* **2004**, *126*, 10262–10263. (c) Duran, J.; Gulías, M.; Castedo, L.; Mascareñas, J. L. Ligand-Induced Acceleration of the Intramolecular [3 + 2] Cycloaddition between Alkynes and Alkylidenecyclopropanes. *Org. Lett.* **2005**, *7*, 5693–5696. (d) Gulías, M.; García, R.; Delgado, A.; Castedo, L.; Mascareñas, J. L. Palladium-Catalyzed [3 + 2] Intramolecular Cycloaddition of Alk-5-ynylidenecyclopropanes. *J. Am. Chem. Soc.* **2006**, *128*, 384–385. (e) García-Fandiño, R.; Gulías, M.; Castedo, L.; Granja, J. R.; Mascareñas, J. L.; Cardenas, D. J. Palladium-Catalyzed [3 + 2] Cycloaddition of Alk-5-ynylidenecyclopropanes to Alkynes: A Mechanistic DFT Study. *Chem. Eur. J.* **2008**, *14*, 272–281. (f) Garcia-Fandino, R.; Gulias, M.; Mascarenas, J. L.; Cardenas, D. J. Mechanistic Study on the Palladium-Catalyzed (3 + 2) Intramolecular Cycloaddition of Alk-5-ynylidenecyclopropanes. *Dalton Trans.* **2012**, *41*, 9468–9481.
12. Verdugo, F.; Villarino, L.; Durán, J.; Gulías, M.; Mascareñas, J. L.; López, F. Enantioselective Palladium-Catalyzed [3C + 2C] and [4C + 3C] Intramolecular Cycloadditions of Alkylidenecyclopropanes. *ACS Catal.* **2018**, *8*, 6100–6105.
13. (a) Morizawa, Y.; Oshima, K.; Nozaki, H. Pd (0) promoted rearrangement of 2-(1, 3-butadienyl) cyclopropane-1, 1-dicarboxylate esters to 2-alkenyl-3-cyclopentene-1, 1-dicarboxylate esters. *Tetrahedron Lett.* **1982**, *23*, 2871–2874. (b) Shimizu, I.; Ohashi, Y.; Tsuji, J. Palladium-catalyzed [3+ 2] cycloaddition reaction of vinylcyclopropanes with α , β -unsaturated esters or ketones. *Tetrahedron Lett.* **1985**, *26*, 3825–3828. (c) Hudlicky, T.; Kutchan, T. M.; Naqvi, S. M. The vinylcyclopropane–cyclopentene rearrangement. *Org. React.* **1985**, *33*, 247–335. (d) Burgess, K. Regioselective and stereoselective nucleophilic addition to electrophilic vinylcyclopropanes. *J. Org. Chem.* **1987**, *52*, 2046–2051. (e) Goldschmidt, Z.; Crammer, B. Vinylcyclopropane rearrangements. *Chem. Soc. Rev.* **1988**, *17*, 229–267. (f) Hiroi, K.; Yamada, A. Transition metal-catalyzed asymmetric cycloaddition reactions of a chiral (β -sulfinyl)vinylcyclopropane derivative: asymmetric synthesis of a cyclopentane derivative using a chiral sulfinyl functionality as the chiral source. *Tetrahedron: Asymmetry* **2000**, *11*, 1835–1841.
14. (a) Shimizu, I.; Ohashi, Y.; Tsuji, J. Palladium (0)-catalyzed cycloaddition of activated vinylcyclopropanes with aryl isocyanates. *Chem. Lett.* **1987**, *6*, 1157–1158. (b) Parsons, A. T.; Campbell, M. J.; Johnson, J. S. Diastereoselective synthesis of tetrahydrofurans via palladium (0)-catalyzed [3+ 2] cycloaddition of vinylcyclopropanes and aldehydes. *Org. Lett.* **2008**, *10*, 2541–2544. (c) Parsons, A. T.; Johnson, J. S. Diastereoselective synthesis of tetrahydrofurans via a palladium (0)-catalyzed [3+ 2] cycloaddition of vinylcyclopropanes and aldehydes. *J. Am. Chem. Soc.* **2009**, *131*, 3122–3123. (d) Parsons, A. T.; Smith, A. G.; Neel, A. J.;

- Johnson, J. S. Dynamic kinetic asymmetric synthesis of substituted pyrrolidines from racemic cyclopropanes and aldimines: reaction development and mechanistic insights. *J. Am. Chem. Soc.* **2010**, *132*, 9688–9692.
15. Cheng, Q.; Xie, J. H.; Weng, Y. C.; You, S. L. Pd-Catalyzed Dearomatization of Anthranils with Vinylcyclopropanes by [4 + 3] Cyclization Reaction. *Angew. Chem., Int. Ed.* **2019**, *58*, 5739–5743.
 16. (a) Magrane, J. K.; Cottle, D. L. The Reaction of Epichlorohydrin with the Grignard Reagent. *J. Am. Chem. Soc.* **1942**, *64*, 484–487. (b) Stahl, G. W.; Cottle, D. L. The Reaction of Epichlorohydrin with the Grignard Reagent. Some Derivatives of Cyclopropanol. *J. Am. Chem. Soc.* **1943**, *65*, 1782–1783.
 17. Kulinkovich, O. G. The Chemistry of Cyclopropanols. *Chem. Rev.* **2003**, *103*, 2597–2632.
 18. (a) Rudi, A.; Schleyer, M.; Kashman, Y. Clathculins A and B, Two Novel Nitrogen-Containing Metabolites from the Sponge *Clathrina* aff. *Reticulum*. *J. Nat. Prod.* **2000**, *63*, 1434–1436. (b) Iverson, S. L.; Uetrecht, J. P. Identification of a reactive metabolite of terbinafine: insights into terbinafine-induced hepatotoxicity. *Chem. Res. Toxicol.* **2001**, *14*, 175–181. (c) El-Jaber, N.; Estevez-Braun, A.; Ravelo, A. G.; Muñoz- Muñoz, O.; Rodriguez-Afonso, A.; Murguía, J. R. Acetylenic Acids from the Aerial Parts of *Nanodea muscosa*. *J. Nat. Prod.* **2003**, *66*, 722–724. (d) Furstner, A.; Turet, L. Concise and Practical Synthesis of Latrunculin A by Ring-Closing Enyne–Yne Metathesis. *Angew. Chem., Int. Ed.* **2005**, *44*, 3462–3466.
 19. Pati, B. V.; Ghosh, A.; Yadav, K.; Banjare, S. K.; Pandey, S.; Lourderaj, U.; Ravikumar, P.C. Palladium-catalyzed selective C–C bond cleavage and stereoselective alkenylation between cyclopropanol and 1,3-diyne: one-step synthesis of diverse conjugated enynes. *Chem. Sci.*, **2022**, *13*, 2692–2700.
 20. (a) R. Breslow, R. R. Haynie and J. Mirra, THE SYNTHESIS OF DIPHENYLCYCLOPROPENONE. *J. Am. Chem. Soc.*, **1959**, *81*, 247–248. (b) Vol'pin, M.E.; Koreshkov, Y.D.; Kursanov, D.N.; Diphenylcyclopropenone, a three-membered analog of tropone.. *Russ Chem Bull*, **1959**, *8*, 535–536.
 21. (a) Yuan, T.; Pi, C.; You, C.; Cui, X.; Du, S.; Wan, T.; Wu, Y. Rapid assembly of cyclopentene spiroisoidolinones via a rhodium-catalysed redox-neutral cascade reaction *Chem. Commun.* **2019**, *55*, 163–166. (b) Haito, A.; Chatani, N. Rh (I)-Catalyzed [3 + 2] annulation reactions of cyclopropenones with amides. *Chem. Commun.* **2019**, *55*, 5740–5742. (c) Xu, J.-L.; Tian, H.; Kang, J.-H.; Kang, W.-X.; Sun, W.; Sun, R.; Li, Y.-M.; Sun, M. Ag(I)-Catalyzed Addition of Cyclopropenones and Nitrones to Access Imides. *Org. Lett.* **2020**, *22*, 6739–6743. (d) Bai, D.; Yu, Y.; Guo, H.; Chang, J.; Li, X. Nickel(0)-Catalyzed Enantioselective [3 + 2] Annulation of Cyclopropenones and α,β -Unsaturated Ketones/Imines. *Angew. Chem., Int. Ed.* **2020**, *59*, 2740–2744. (e) Xing, H.; Chen, J.; Shi, Y.; Huang, T.; Hai, L.; Wu, Y. Synthesis of 4-Ethenyl Quinazolines via Rhodium(III)-Catalyzed [5 + 1] Annulation Reaction of N-Arylamidines with Cyclopropenones. *Org. Chem. Front.* **2020**, *7*, 672–677. (f) Liu, Y. F.; Tian, Y.; Su, K. X.; Guo, X.; Chen, B. H. RhodiumCatalyzed ortho-Acrylation of Aryl Ketone O-Methyl Oximes with Cyclopropenones. *Org. Biomol. Chem.* **2020**, *18*, 3823–3826. (g) Chen, J.; Tang, B.; Liu, X.; Lv, G.; Shi, Y.; Huang, T.; Xing, H.; Guo, X.; Hai, L.; Wu, Y. Ruthenium(ii)-catalyzed [5 + 1] annulation reaction: a facile and efficient approach to construct 6- ethenyl phenanthridines utilizing a primary amine as a directing group. *Org. Chem. Front.* **2020**, *7*, 2944–2949. (h) Shi, Y. S.; Xing, H. M.; Huang, T. L.; Liu, X. X.; Chen, J.; Guo, X. Y.; Li, G. B.; Wu, Y. Divergent C-H activation

- synthesis of chalcones, quinolones and indoles. *Chem. Commun.* **2020**, 56, 1585–1588.
22. Matsuda, T.; Sakurai, Y. Palladium-Catalyzed Ring-Opening Alkynylation of Cyclopropenones. *Eur. J. Org. Chem.* **2013**, 2013, 4219–4222.
23. Zhao, W.-T.; Gao, F.; Zhao, D. Intermolecular σ -Bond CrossExchange Reaction between Cyclopropenones and (Benzo)- silacyclobutanes: Straightforward Access towards Sila(benzo)- cycloheptenones. *Angew. Chem., Int. Ed.* **2018**, 57, 6329–6332.

Chapter 1B

Introduction To C-H Bond Activation

1B.1 Introduction

1B.2 Non-directed and Directed C-H bond activation

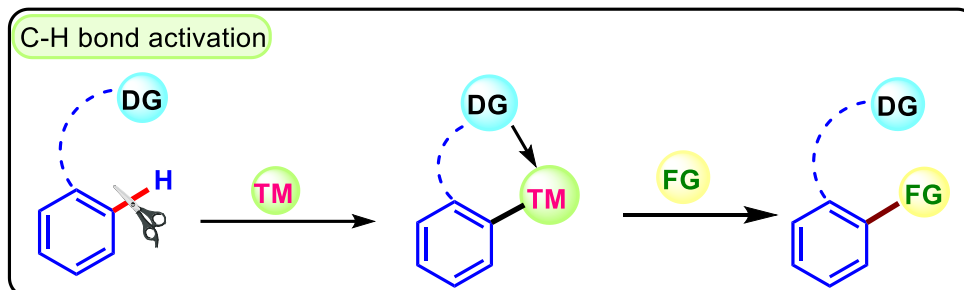
1B.3 Redox-neutral Directing group

1B.5 Conclusion

1B.6 References

Chapter 1B

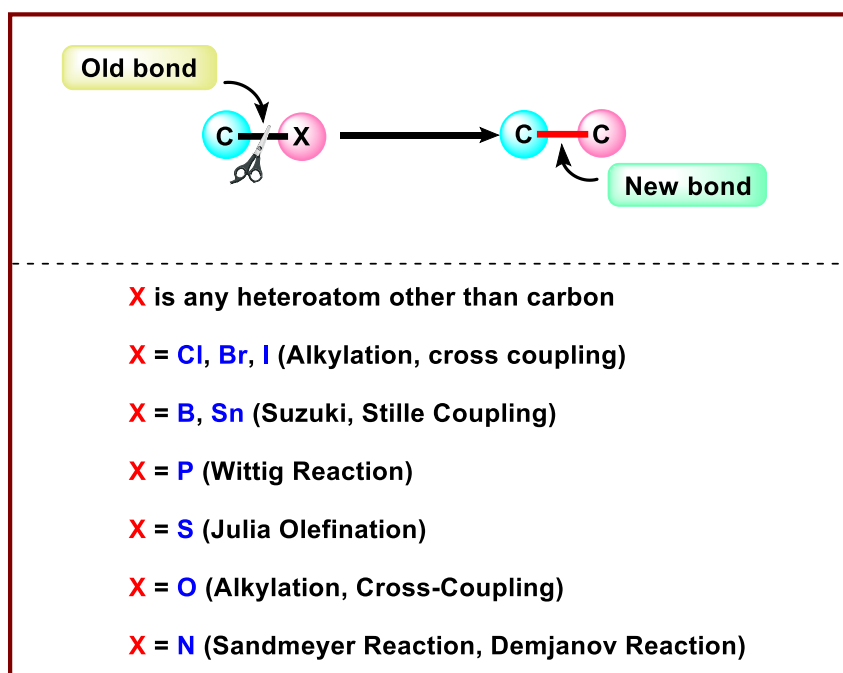
Introduction To C-H Bond Activation



1B.1 INTRODUCTION

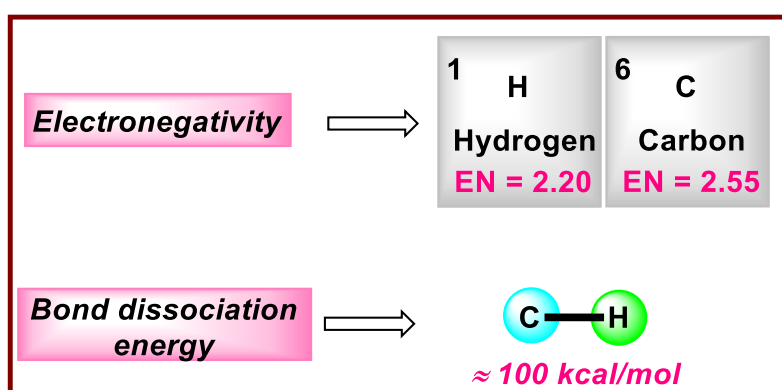
In traditional organic synthesis, functional group modification of arene ring relies on the prefunctionalization. It necessitates the presence of a modifiable functional group such as halo (alkylation and cross coupling), boron (Suzuki coupling), tin (Stille coupling), sulphur (Julia olefination), phosphorous (Wittig reaction), oxygen (alkylation and cross coupling), and nitrogen (Sandmeyer and Demjanov reaction) (Figure 1B.1).¹

Figure 1B.1 Traditional organic synthesis



However, direct C-H functionalization of the arene ring is restricted due to the high bond dissociation energy of 100 kcal/mol and its non-polar nature (Figure 1B.2). Regioselectivity and chemoselectivity are other added challenges to direct C-H functionalization of the arene ring. The similar nature of the C-H bonds makes them chemically non-distinguishable. Thus, selectivity is the major issue.

Figure 1B.2 Factor determining the inertness of C-H bond

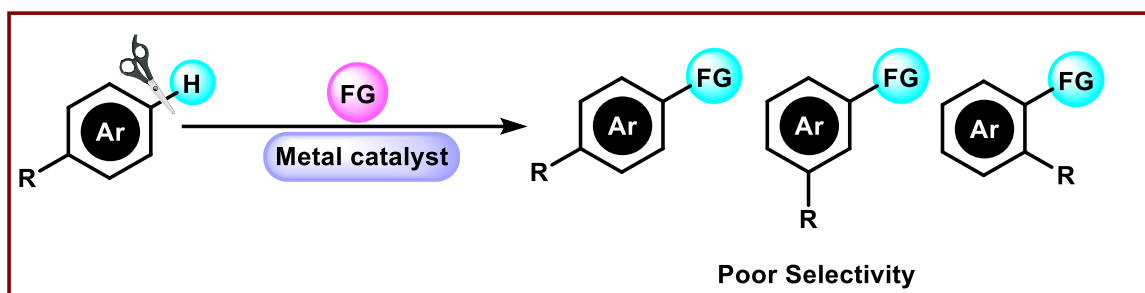


In the past few decades, the transition-metal catalyzed C-H bond activation methods have evolved as a path-breaking finding that enables the selective C-H functionalization with a high step and atom economy, also unbiased of the inherent electronics of the molecule. The selectivity has been achieved using an appropriate directing group,² ligand,³ and weak chelation interaction.⁴ In the early stage, the reports were heavily crowded with costly and toxic 4d and 5d transition metals. However, the scientific community later paid close attention to sustainable synthesis by increasing the use of 3d transition metal. The 3d transition metals were considered sustainable because of their availability in the earth crust and low toxicity in the ppm level.⁵ With all these advancements, the C-H bond activation method has evolved as an alternative, greener, and more sustainable approach than the earlier classical synthesis. The C-H bond activation can follow two pathways (i) non-directed and (ii) directed.

1B.2 NON-DIRECTED AND DIRECTED C-H BOND ACTIVATION

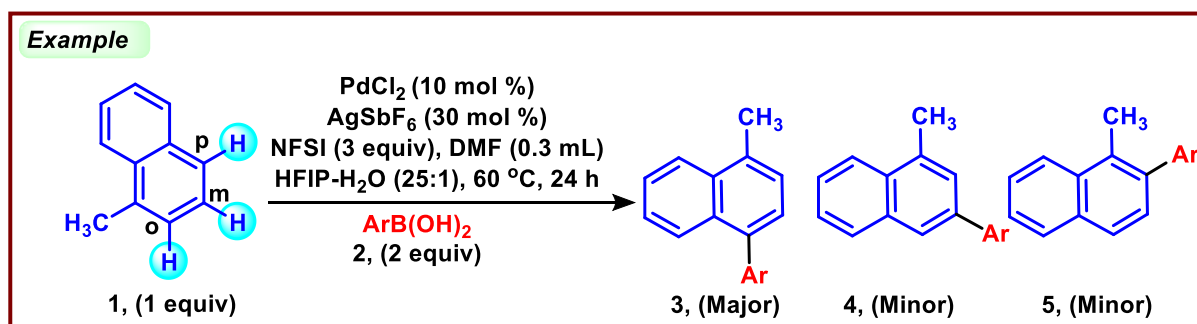
Non-directed C-H bond activation strategy involves the direct functionalization of arene C-H bond in the presence of a metal catalyst. However, the chemically equivalent C-H bond in the arene motif makes it challenging to obtain the desired product with high selectivity (Figure 1B.3).

Figure 1B.3 Non-directed C-H bond functionalization



In 2017, Ye and coworkers demonstrated the non-directed C-H arylation of arene **1**, resulting in the mixture of *ortho*, *meta*, and *para*-arylated products. Though a mixture of regioisomers was observed, the *para*-arylated product **3** is the major one (Scheme 1B.1).⁶ Palladium chloride 10 mol % was used as the catalyst, AgSbF₆ (30 mol %) as a halide scavenger, *N*-fluorobenzenesulfonimide (NFSI, 3 equiv) as a strong oxidant. Dimethyl formamide was used as the ligand for this transformation. This example represents a typical non-directed C-H bond arylation protocol with the limitation of selectivity. However, there are many other examples by Yu, Fernandez-Ibanez, Ritter, and Gemmermen group.⁷

Scheme 1B.1 Non-directed C-H bond functionalization



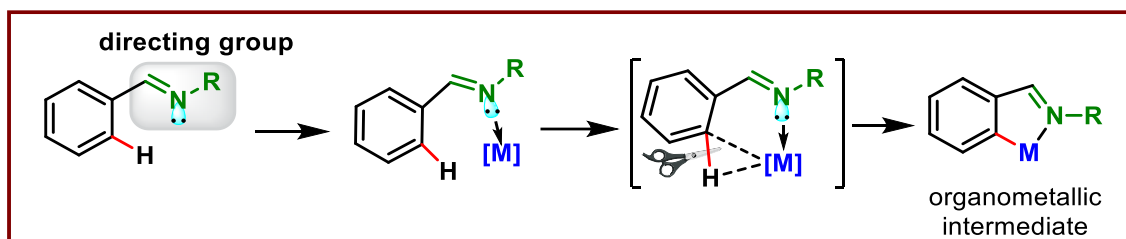
Limitations of non-directed C-H functionalizations: Even though there are many reports on non-directed functionalization of inert C-H bonds, these reports are associated with common limitations such as follows:

- (i) Functionalizations are highly biased toward the electronics
- (ii) Regioselectivity is entirely controlled by the nature of the substituent/functional group present
- (iii) Very poor regioselectivity (mainly when electron donating group is present in the arene ring)

As a solution to the above-mentioned issues, directed C-H bond activation has evolved as an emerging methodology, providing highly regioselective functionalizations of the inert C-H bond.⁸

Functional groups, such as imine, amine, amide, and carbonyl, present in the substrates can coordinate with the transition metals. The coordinating atom present in the above-mentioned functional group (N, O, S, P) chelates the transition metal by donating its free lone pair of electrons to the empty *d*-orbitals of the metal (Scheme 1B.2). Hence, the substrate now directs the metal towards the proximal C-H bond which enables agostic interaction and results in a 3c-2e transition state. This agostic interaction arises from the σ -donation by the C-H bond to the empty metal *d*-orbital and back bonding by the metal orbital occurring synergistically. This interaction weakens the inert C-H bond and leads to forming an organometallic intermediate, carbon-metal bond. This process is called as directed C-H bond activation. This organometallic species is nucleophilic and can be coupled with a suitable coupling partner for forming C-C and C-hetero (halide, N, O, S, B) bonds.

Scheme 1B.2 Schematic representation of directed C-H bond activations

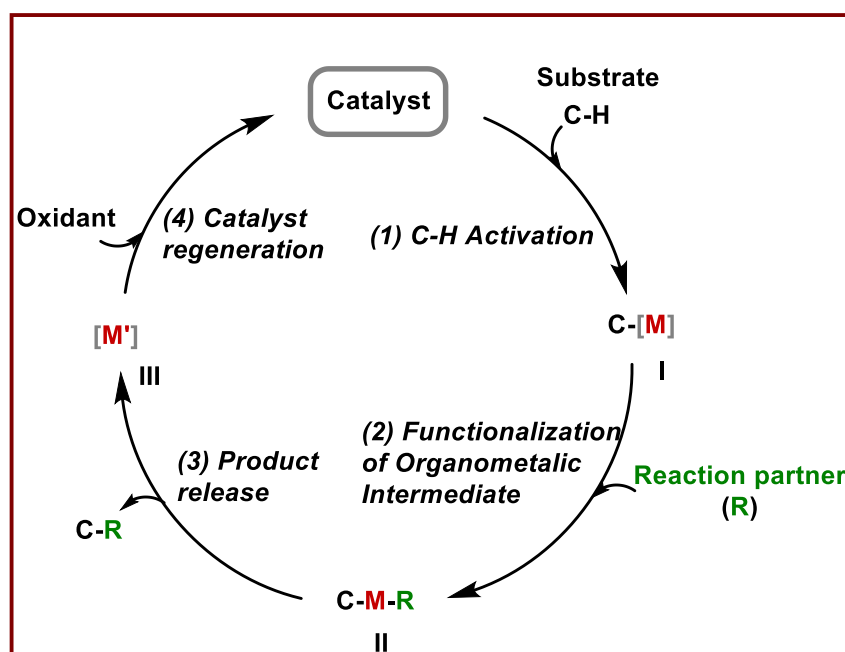


The overall process of directed C-H functionalization can be understood from a general catalytic cycle that proceeds through four stages (Figure 1B.4).

Stage 1: At first, the active transition metal catalyst chelate with the σ -donor atom of the directing group, which through agostic interaction with the proximal C-H bond (C-H activation process), gives an organometallic intermediate **I** {C-[M]}.

Stage 2: The intermediate **I** is functionalized with a secondary substrate (coupling partner), forming intermediate **II**, where both substrate and the coupling partner are bonded with the metal catalyst [C-M-R].

Figure 1B.4: General catalytic cycle for directed C-H functionalization



Stage 3: Both the substrate and the coupling partner couple, delivering the final product (C-R) and the reduced metal catalyst [M'].

Stage 4: Involves catalyst regeneration from the reduced catalyst by copper salts/silver salts/molecular oxygen/organic oxidants.

1B.3 REDOX NEUTRAL DIRECTING GROUP

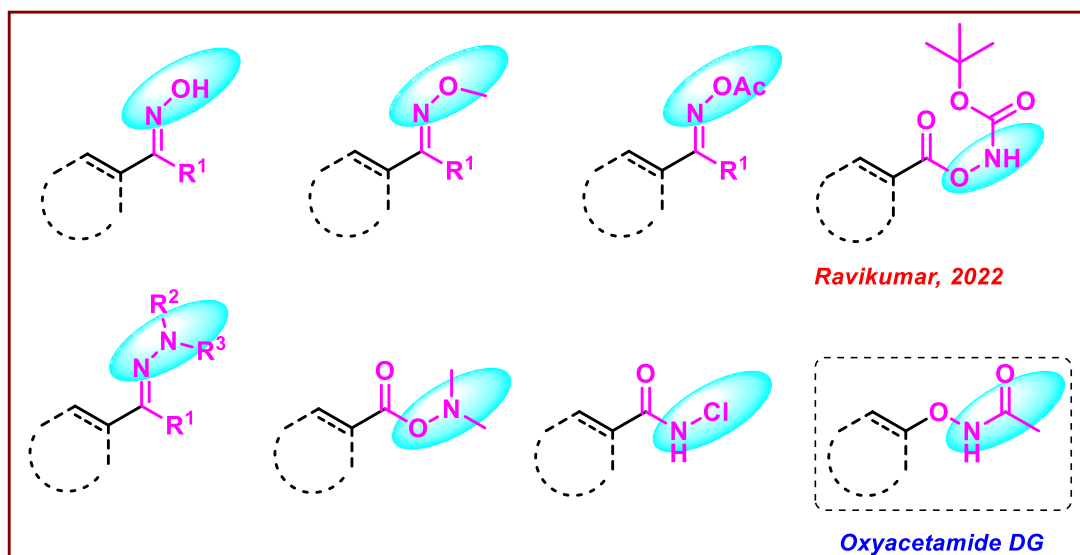
In chelation-assisted C-H functionalization methodology, different functional groups have been used as directing groups (**DG**). Based on the number of chelation sites and reactivities, the directing groups could be classified into five categories.² These are: (i) monodentate directing groups, (ii) bidentate directing groups, (iii) transient directing groups (TDGs), (iv) Traceless directing groups, and (v) Redox-neutral directing groups. The scientific community has witnessed much progress toward developing directing groups. Among all the directing groups, the redox-neutral directing group grabbed our focus as it precludes external oxidants in the stoichiometric amount. In the catalytic cycle, during the reoxidation of metal, the redox-neutral directing group behaved as an internal oxidant and oxidized the metal to the active form.

These directing groups generally have a weak polarizable bond like N-O/N-N/N-Cl/N-S/S-Cl/Si-H, to which metal gets oxidatively added to regain its oxidation state.^{9a,b} Therefore, chemists are using the directing group with these weak bonds, and such directing groups are known as redox-neutral directing groups (DG^{ox}). In the last two decades, many redox-neutral directing groups have been used for valuable transformations.^{9c} The commonly used redox-neutral directing groups are shown in figure 1B.5. Recently, we have also developed a unique redox-neutral directing group to demonstrate the synthesis of isocoumarine and bis-isocoumarine derivatives.¹⁰

Nowadays, versatile substrates having a multifunctional directing group are increasingly popular. In this context, phenoxyacetamide emerged as one of the most versatile substrates that have been used as (i) internal oxidant, (ii) directing group, and (iii) electrophilic aminating agent. Due to the presence of a cleavable -NHAc group, this is

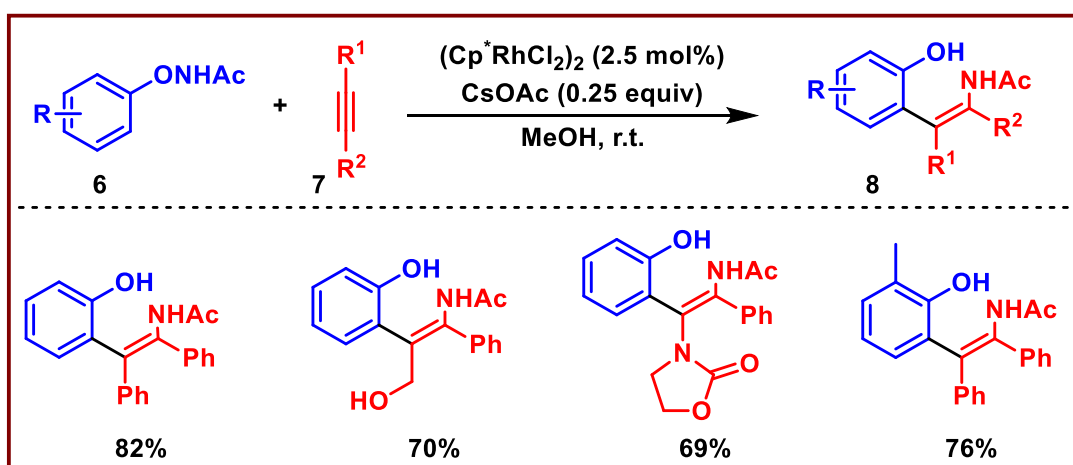
generally referred as an auto-cleavable directing group. For the first time, Lu and Liu, in 2013, introduced phenoxyacetamide as a redox-neutral directing group in the rhodium-catalyzed carboamination of alkynes (Scheme 1B.3).¹¹

Figure 1B.5 Redox-neutral directing group

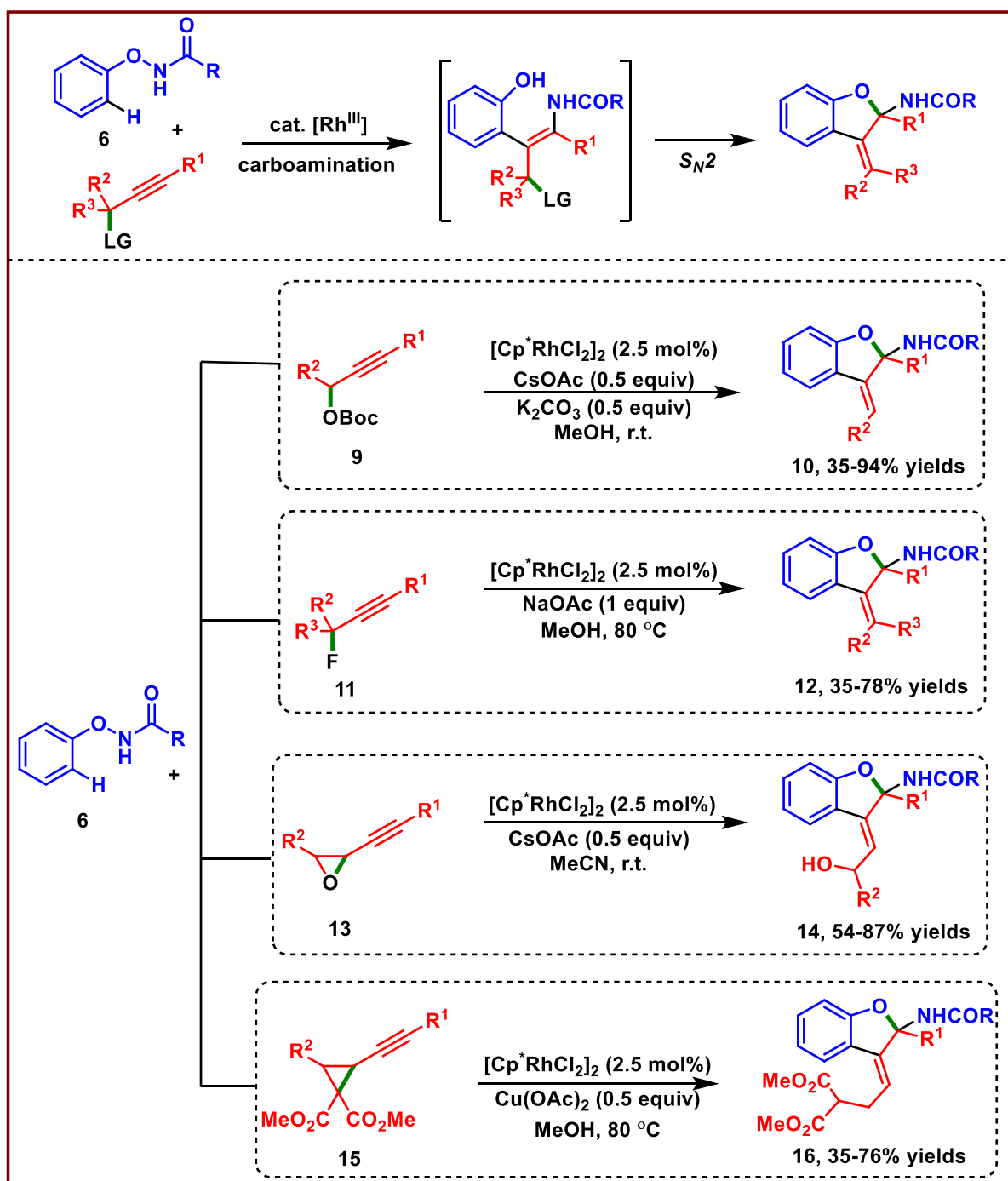


The demonstrated protocol is widely applied to biaryl and aryl alkyl disubstituted alkynes, propiolates, and ynamides. Methanol and ethylene glycol was crucial for the carboamination event, whereas ^tBuOH, CH₂Cl₂, and toluene favored the benzofuran formation with the departure of the acetamido group, confirmed from the solvent screening.

Scheme 1B.3 Carboamination of alkynes



Scheme 1B.4 Reports on phenoxyacetamide as a directing group and aminating agent



When a suitable leaving group was preinstalled at the propargylic position, an S_N2 -type substitution could be expected due to the good nucleophilic ability of the phenol unit in the enamide intermediate (Scheme 1B.4). Lu, Liu, *et al.* first disclosed this hypothesis by employing tert-butyl carbonate (OBoc) as a leaving group for synthesizing 3-alkylidene dihydro benzofuran derivatives **10**.¹² Such a protocol was applied to both primary and

secondary propargylic carbonates but failed with the tertiary series due to steric hindrance. This limitation could be overcome by using the fluoride as an alternative leaving group, in which the $[H \cdots F]$ bonding-assisted intramolecular S_N2 -type substitution process might be involved by utilizing the fluorine atom as a feasible leaving group with less steric hindrance.¹³ In addition, the introduction of an epoxide¹⁴ or cyclopropane¹⁵ at the propargylic position enabled similar intramolecular S_N2 ring-opening processes, thus illustrating the good compatibility of this strategy in constructing benzofuran skeletons. Of note, these conversions all favored the stereoselective formation of an (*E*)-exocyclic C–C double bond. The above schemes sum up the role of phenoxyacetamide as both directing group and an electrophilic aminating agent.

1B.5 CONCLUSION

In this chapter, we have discussed the classical C–H functionalization methods and the limitation associated with it. The major limitations such as regioselectivity, chemoselectivity, step, and atom economy associated with the classical C–H functionalization method can be overcome by transition metal catalyzed C–H bond activation. The need for preactivated starting led to the discovery of non-directed C–H functionalizations, which worked well in many transformations. Even though non-directed C–H functionalization is more eco-friendly, it is also associated with major issues like (i) reactivity is highly biased with electronically rich arenes and (ii) very poor regioselectivity. This gave rise to a directed C–H bond activation functionalization strategy, free from these limitations. Amidst the directing group, studying the reactivity of the redox-neutral directing group is interesting as it precludes the use of stoichiometric amounts of metal oxidant. Phenoxyacetamide has grabbed a lot of attention because of its versatility as (i) a redox-neutral directing group and (ii) an electrophilic aminating agent. Further exploration

with this substrate to explore new reactivity is a desirable and this inspired us to explore its potential in metal catalyzed C-H activation reactions.

1B.6 REFERENCES

1. (a) de Meijere, A.; Meyer, F. E. Fine feathers make fine birds: The Heck reaction in modern garb. *Angew. Chem., Int. Ed. Engl.* **1994**, *33*, 2379-2411. (b) Beletskaya, I. P.; Cheprakov, A. V. The Heck reaction as a sharpening stone of palladium catalysis. *Chem. Rev.* **2000**, *100*, 3009-3066. (c) Stille, K. J. The Palladium-Catalyzed Cross-Coupling Reactions of Organotin Reagents with Organic Electrophiles. *Angew. Chem., Int. Ed. Engl.* **1986**, *25*, 508-524. (d) Farina, V.; Krishnamurthy, V.; Scott, W. The stille reaction. *J. Org. React.* **1997**, *50*, 1. (e) Miyaura, N.; Suzuki, A. Palladium-catalyzed cross-coupling reactions of organoboron compounds. *Chem. Rev.* **1995**, *95*, 2457-2483. (f) Suzuki, A. Recent advances in the cross-coupling reactions of organoboron derivatives with organic electrophiles, 1995-1998. *J. Organomet. Chem.* **1999**, *576*, 147-168. (g) Sonogashira, K. In *Comprehensive Organic Synthesis*; Trost, B. M., Ed.; Pergamon: New York, **1991**; pp 521-549. (h) Hatanaka, Y.; Hiyama, T. Highly selective cross-coupling reactions of organosilicon compounds mediated by fluoride ion and a palladium catalyst. *Synlett* **1991**, 845-853. (i) Hiyama, T. Palladium-catalyzed cross-coupling reaction of organometalloids through activation with fluoride ion. *Pure Appl. Chem.* **1994**, *66*, 1471-1478. (j) Kotani, R. Demjanov Rearrangement of 1-Methylcyclohexanemethylamine *J. Org. Chem.* **1965**, *30*, 350-354.
2. (a) Lyons, T. W.; Sanford, M. S. Palladium-Catalyzed Ligand Directed C-H Functionalization Reactions. *Chem. Rev.* **2010**, *110*, 1147-1169. (b) Gutekunst, W. R.; Baran, P. S. C-H Functionalization Logic in Total Synthesis. *Chem. Soc. Rev.* **2011**, *40*, 1976-1991. (c) Hartwig, J. F. Evolution of C-H Bond Functionalization from Methane to Methodology. *J. Am. Chem. Soc.* **2016**, *138*, 2-24. (d) Gensch, T.; Hopkinson, M. N.; Glorius, F.; Wencel-Delord, J. Mild Metal-Catalyzed C-H Activation: Examples and Concepts. *Chem. Soc. Rev.* **2016**, *45*, 2900-2936. (e) Rej, S.; Ano, Y.; Chatani, N. Bidentate Directing Groups: An Efficient Tool in C-H Bond Functionalization Chemistry for the Expedient Construction of C-C Bonds. *Chem. Rev.* **2020**, *120*, 1788-1887. (f) Lam, N. Y. S.; Wu, K.; Yu, J.-Q. Advancing the Logic of Chemical Synthesis: C-H Activation as Strategic and Tactical Disconnections for C-C Bond Construction. *Angew. Chem., Int. Ed.* **2021**, *60*, 15767-15790.
3. (a) Halder, C.; Bisht, R.; Chaturvedi, J.; Guria, S.; Hassan, M. M. M.; Ram, B.; Chattopadhyay, B. Ligand- and Substrate-Controlled para C-H Borylation of Anilines at Room Temperature. *Org. Lett.* **2022**, *24*, 8147-8152. (b) Das, S. K.; Das, S.; Ghosh, S.; Roy, S.; Pareek, M.; Roy, B.; Sunoj, R. B.; Chattopadhyay, B. An Iron(II)-Based Metalloradical System for Intramolecular Amination of C(sp²)-H and C(sp³)-H Bonds: Synthetic Applications and Mechanistic Studies. *Chemical Science* **2022**, *13*, 11817-11828. (c) Bisht, R.; Halder, C.; Hassan, M. M. M.; Hoque, E. M.; Chaturvedi, J.; Chattopadhyay, B. Metal-Catalysed C-H Bond Activation and Borylation. *Chem. Soc. Rev.* **2022**, *51*, 5042-5100. (d) Hoque, E. M.; Bisht, R.; Unnikrishnan, A.; Dey, S.; Hassan, M. M. M.; Guria, S.; Rai, R. N.; Sunoj, R. B.; Chattopadhyay, B. Iridium-Catalyzed Ligand-Controlled Remote para-Selective C-H Activation and Borylation of Twisted Aromatic Amides. *Angew. Chem. Int. Ed.* **2022**, *61*, e202203539.
4. (a) Banjare, S. K.; Nanda, T.; Pati, B. V.; Biswal, P.; Ravikumar, P. C. O-Directed C-H functionalization via cobaltacycles: a sustainable approach for C-C and

- C–heteroatom bond formations. *Chem. Commun.* **2021**, 57, 3630–3647. (b) Zhang, J.; Lu, X.; Shen, C.; Xu, L.; Ding, L.; Zhong, G. Recent advances in chelation-assisted site- and stereoselective alkenyl C–H functionalization. *Chem. Soc. Rev.* **2021**, 50, 3263–3314.
5. (a) Gandeepan, P.; Müller, T.; Zell, D.; Cera, G.; Warratz, S.; Ackermann, L. 3d Transition Metals for C–H Activation. *Chem. Rev.* **2019**, 119, 2192–2452. (b) Dalton, T.; Faber, T.; Glorius, F. C–H Activation: Toward Sustainability and Applications. *ACS Cent. Sci.* **2021**, 7, 245–261.
 6. Luan, Y.-X.; Zhang, T.; Yao, W.-W.; Lu, K.; Kong, L.-Y.; Lin, Y.-T.; Ye, M. Amide-Ligand-Controlled Highly para-Selective Arylation of Monosubstituted Simple Arenes with Arylboronic Acids. *J. Am. Chem. Soc.* **2017**, 139, 1786–1789.
 7. (a) Wang, P.; Verma, P.; Xia, G.; Shi, J.; Qiao, J. X.; Tao, S.; Cheng, P. T. W.; Poss, M. A.; Farmer, M. E.; Yeung, K.-S.; et al. Ligand-Accelerated Non-Directed C–H Functionalization of Arenes. *Nature* **2017**, 551, 489–493. (b) Naksomboon, K.; Valderas, C.; Gómez-Martínez, M.; ÁlvarezCasao, Y.; Fernández-Ibáñez, M. Á. S. O-Ligand-Promoted PalladiumCatalyzed C–H Functionalization Reactions of Nondirected Arenes. *ACS Catal.* **2017**, 7, 6342–6346. (c) Liu, L.-Y.; Yeung, K.-S.; Yu, J.-Q. Ligand-Promoted NonDirected C–H Cyanation of Arenes. *Chem. - Eur. J.* **2019**, 25, 2199–2202. (d) Zhao, D.; Xu, P.; Ritter, T. Palladium-Catalyzed Late-Stage Direct Arene Cyanation. *Chem.* **2019**, 5, 97–107. (e) Farizyan, M.; Mondal, A.; Mal, S.; Deufel, F.; van Gemmeren, M. Palladium-Catalyzed Nondirected Late-Stage C–H Deuteration of Arenes. *J. Am. Chem. Soc.* **2021**, 143, 16370–16376.
 8. (a) Godula, K.; Sames, D. C–H Bond Functionalization in Complex Organic Synthesis. *Science* **2006**, 312, 67–72. (b) Yamaguchi, J.; Yamaguchi, A. D.; Itami, K. C–H Bond Functionalization: Emerging Synthetic Tools for Natural Products and Pharmaceuticals. *Angew. Chem., Int. Ed.* **2012**, 51, 8960–9009. (c) McMurray, L.; O'Hara, F.; Gaunt, M. J. Recent Developments in Natural Product Synthesis Using Metal-Catalysed C–H Bond Functionalisation. *Chem. Soc. Rev.* **2011**, 40, 1885. (d) He, R.; Huang, Z.-T.; Zheng, Q.-Y.; Wang, C. Isoquinoline Skeleton Synthesis via Chelation-Assisted C–H Activation. *Tetrahedron Lett.* **2014**, 55, 5705–5713.
 9. (a) Huang, H.; Ji, X.; Wu, W.; Jiang, H. Transition metal-catalyzed C–H functionalization of N-oxygenamine internal oxidants *Chem. Soc. Rev.* **2015**, 44, 1155. (b) Yu, X.-L.; Chen, K.-H.; Guo, S.; Shi, P.-F.; Song, C.; Zhu, J. Direct access to cobaltacycles via C–H activation: N-chloroamide-enabled room-temperature synthesis of heterocycles. *Org. Lett.* **2017**, 19, 5348–5351. (c) Mo, J.; Wang, L.; Liu, Y.; Cui, X. Transition-Metal-Catalyzed Direct C–H Functionalization under External-Oxidant-Free Conditions *Synthesis* **2015**, 47, 439–459. (d) Guimond, N.; Fagnou, K. Isoquinoline Synthesis via Rhodium-Catalyzed Oxidative Cross-Coupling/Cyclization of Aryl Aldimines and Alkynes. *J. Am. Chem. Soc.* **2009**, 131, 12050–12051. (e) Too, P. C.; Wang, Y.-F.; Chiba, S. Rhodium (III)-Catalyzed Synthesis of Isoquinolines from Aryl Ketone O-Acyloxime Derivatives and Internal Alkynes. *Org. Lett.* **2010**, 12, 5688–5691. (f) Kiran Chinnagolla, R.; Pimparkar, S.; Jeganmohan, M. Ruthenium-Catalyzed Highly Regioselective Cyclization of Ketoximes with Alkynes by C–H Bond Activation: A Practical Route to Synthesize Substituted Isoquinolines. *Org. Lett.* **2012**, 14, 3032–3035. (g) Sen, M.; Kalsi, D.; Sundararaju, B. Cobalt (III)-Catalyzed Dehydrative [4+2] Annulation of Oxime with Alkyne by C–H and N–OH Activation. *Chem. - Eur. J.*, **2015**, 21, 15529–15533.
 10. Pati, B. V.; Banjare, S. K.; Adhikari, G. K. D.; Nanda, T.; Ravikumar, P. C. Rhodium-Catalyzed Selective C(sp²)–H Activation/Annulation of tert-Butyl Benzoyloxycarbamates with 1,3-Diynes: A One Step Access to Alkynylated

- Isocoumarins and Bis-Isocoumarins. *Org. Lett.* **2022**, *31*, 5651–5656.
11. Liu, G.; Shen, Y.; Zhou, Z.; Lu, X. Rhodium(III)-Catalyzed Redox-Neutral Coupling of N-Phenoxyacetamides and Alkynes with Tunable Selectivity. *Angew. Chem., Int. Ed.* **2013**, *52*, 6033–6037.
 12. Zhou, Z.; Liu, G.; Chen, Y.; Lu, X. Cascade Synthesis of 3- Alkylidene Dihydrobenzofuran Derivatives via Rhodium(III)-Catalyzed Redox-Neutral C-H Functionalization/Cyclization. *Org. Lett.* **2015**, *17*, 5874–5877.
 13. Zhong, X.; Lin, S.; Gao, H.; Liu, F.-X.; Zhou, Z.; Yi, W. Rh(III)- Catalyzed Redox-Neutral C-H Activation/[3 + 2] Annulation of NPhenoxy Amides with Propargylic Monofluoroalkynes. *Org. Lett.* **2021**, *23*, 2285–2291.
 14. Li, Y.; Shi, D.; Tang, Y.; He, X.; Xu, S. Rhodium(III)-Catalyzed Redox-Neutral C-H Activation/Annulation of N-Aryloxyacetamides with Alkynyloxiranes: Synthesis of Highly Functionalized 2,3- Dihydrobenzofurans. *J. Org. Chem.* **2018**, *83*, 9464–9470.
 15. Li, Y.; Shi, D.; He, X.; Wang, Y.; Tang, Y.; Zhang, J.; Xu, S. RedoxNeutral Annulation of Alkynylcyclopropanes with N-Aryloxyamides via Rhodium(III)-Catalyzed Sequential C-H/C-C Activation. *J. Org. Chem.* **2019**, *84*, 1588–1595.

Chapter 2

A Palladium-Catalyzed Cascade C-C Bond Activation of Cyclopropenone and Carbonylative Amination: Easy Access to Highly Functionalized Maleimide Derivatives

2.1 Abstract

2.2 Introduction

2.3 Results and Discussions

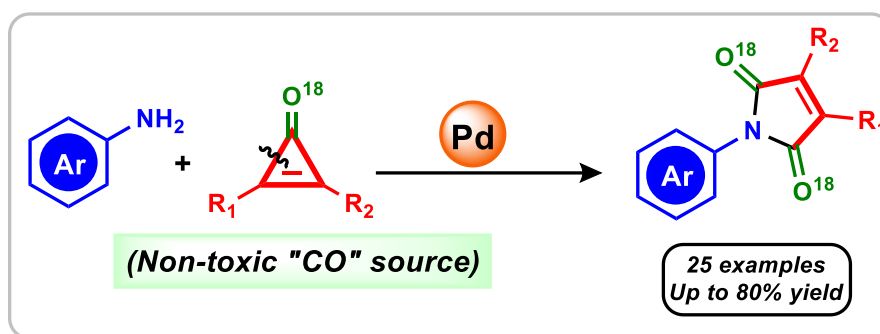
2.4 Conclusion

2.5 Experimental Section

2.6 References

Chapter 2

A Palladium-Catalyzed Cascade C-C Bond Activation of Cyclopropenone and Carbonylative Amination: Easy Access to Highly Functionalized Maleimide Derivatives



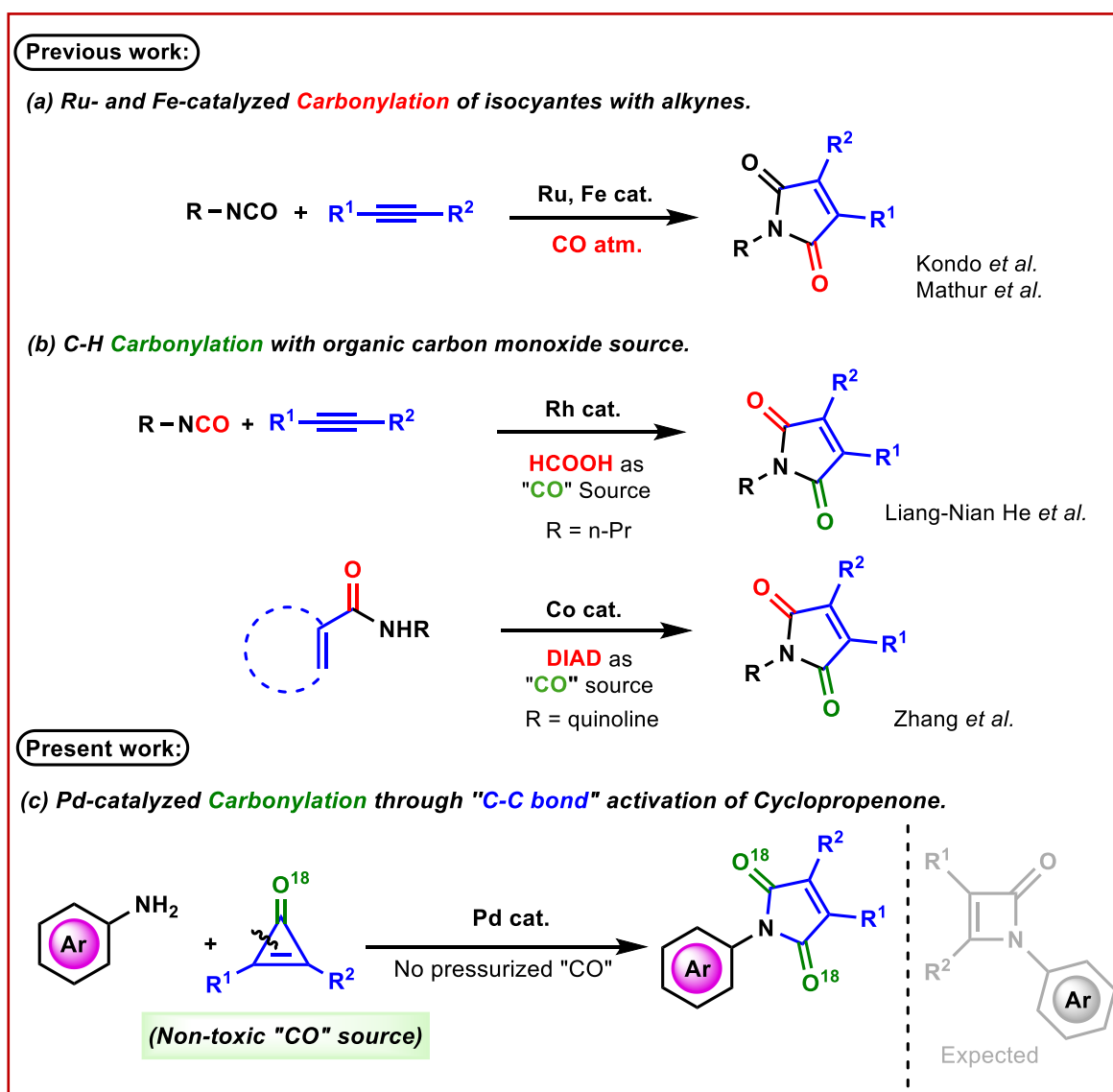
2.1 ABSTRACT: We describe herein the first report on palladium-catalyzed C–C bond activation of cyclopropenone and concomitant carbonylative amination to produce maleimides. The interesting aspect of this reaction is that the sacrificial elimination of carbon monoxide from the substrate which is efficiently recaptured by one of the intermediates in the catalytic cycle for the formation of maleimides. ¹⁸O isotopic studies confirmed that the source of carbon monoxide is from cyclopropenone.

2.2 INTRODUCTION

Progressive developments in transition metal catalysis have enabled activation of functionally inert C–H and C–C bonds and their applications in the synthesis of complex organic scaffolds.¹ While C–H bond activation has been extensively studied, a complementary and more useful C–C bond activation is relatively less explored.² In general C–C bond activation is a thermodynamically unfavorable process.³ Stoichiometric C–C bond activation has been known for over 60 years in organometallic chemistry;⁴ however, catalytic C–C bond activation is a recent development. The C–C bond activation proceeds

through two pathways: oxidative addition of transition metal into the C–C bonds and β -carbon elimination. In recent decades, selective C–C bond activation has been achieved by employing the strategies of chelation assistance, aromatization, and ring strain release.⁵ In a strained system such as cyclopropane or cyclobutane, the release of strain through the oxidative addition of metal renders the C–C bond activation process favorable. Numerous architecturally complex organic molecules have been synthesized through the catalytic C–C bond activation process by pioneering groups such as Dong,⁶ Jun,⁷ Bower,⁸ Marek,⁹ Yu,¹⁰ and Loh.¹¹

Scheme 2.1 Transition metal catalyzed synthesis of the maleimide and our presumptions



Three-membered strained systems such as vinyl cyclopropanes,¹² alkylidenecyclopropanes,¹³ cyclopropyl ketones,¹⁴ carboxamide,¹⁵ and imines¹⁶ have been extensively studied. However, the use of cyclopropenones, the smallest Huckel aromatic compound, remains less explored.¹⁷ Hence, we decided to diversify the scope of C–C activation on cyclopropenone and explore this underexplored chemical space. Literature precedence revealed that cyclopropenone is known to form metallacyclobutenone with metals like nickel,^{17a} platinum,¹⁸ and rhodium,^{17h,19} wherein rhodacyclopentenone is known to decompose at high temperature to form respective alkyne and carbon monoxide.¹⁹ Taking these concepts and limitations into account we planned to develop a new methodology for one-step access to azetone derivatives.

With this goal in mind, we subjected cyclopropenone with aniline in the presence of a palladium catalyst. To our surprise and delight, we obtained a highly functionalized maleimide motif which suggested that release and recapturing of carbon monoxide is happening in situ. In recent years, the development of methodologies to synthesize biaryl-maleimides is gaining much attention from synthetic communities because of their potential applications for optoelectronic devices.²⁰ Moreover, maleimide scaffolds are present in various natural products that shows excellent biological and pharmaceutical properties.²¹ According to the literature reports, various approaches have already been disclosed for the synthesis of maleimides. The Kondo^{22a} and Mathur^{22b} groups reported the [2 + 2 + 1] co-cyclization of isocyanate and alkyne in the presence of pressurized CO gas to synthesize highly functionalized maleimide using Ru and Fe, respectively (Scheme 2.1a). Later, the use of toxic CO gas has been avoided by taking advantage of formic acid²³ and DIAD²⁴ as organic CO sources (Scheme 2.1b). The currently developed protocol involves palladium-catalyzed C–C activation of cyclopropenone followed by carbonylation amination to form the *N*-heterocyclic maleimide scaffolds. During this process, 0.5 equiv

of the substrate is used up for the *in situ* generations of carbon monoxide. This reaction involves the elimination and insertion of CO into another palladacycle which is very unique and the first of its kind in the C–C bond activation process. Herein for the first time, cyclopropenone has been used as a nontoxic CO source in the presence of a palladium catalyst and can act as a sole carbon monoxide source which is further confirmed by ^{18}O isotope studies.

2.3 RESULTS AND DISCUSSIONS

As mentioned earlier our goal was to synthesize azetones through a C–C bond activation pathway; accordingly, we chose diphenylcyclopropenone **1a** and aniline **2a** as the model substrates. Initially, the reaction was carried out in the presence of palladium acetate as the catalyst, tetrabutylammonium bromide as an additive, and sodium acetate as the base at 120 °C for 12 h in DMF (0.25 M). Surprisingly, we obtained the maleimide product **3aa** in 55% yield instead of azetone (Table 2.1, entry 1).

Table 2.1 Optimization of the Reaction Condition^a

$\text{1a (1 equiv)} + \text{2a (2.5 equiv)} \xrightarrow[\text{DMF (0.25 M), 1h, 120 }^\circ\text{C}]{\text{Pd(OAc)}_2 \text{ (15 mol \%), base (4 equiv), Bu}_4\text{NBr (1 equiv), additive (1.5 equiv)}} \text{3aa}$

entry	base	additives	yield (%) ^b
1	NaOAc	---	55% ^c
2	NaOAc	K ₂ S ₂ O ₈	63%
3	NaOAc	Ag ₂ CO ₃	22% ^c
4	NaOAc	Ag ₂ O	28% ^c
5	NaOAc	Cu(OAc) ₂	7% ^c
6	NaOAc	BQ	45% ^c
7	NaOAc	Na ₂ S ₂ O ₈	60% ^c

8	LiOAc	K ₂ S ₂ O ₈	73%
9	KOAc	K ₂ S ₂ O ₈	75%
10	CsOAc	K ₂ S ₂ O ₈	58%
11	Li ₂ CO ₃	K ₂ S ₂ O ₈	50%
12	K ₂ CO ₃	K ₂ S ₂ O ₈	49%
13	Cs ₂ CO ₃	K ₂ S ₂ O ₈	28%
14	NaHCO ₃	K ₂ S ₂ O ₈	48%
15	KHCO ₃	K ₂ S ₂ O ₈	44%
16	CsOPiv	K ₂ S ₂ O ₈	61%
17	K ₂ HPO ₄	K ₂ S ₂ O ₈	63%
18	KOAc	K ₂ S ₂ O ₈ , without Bu ₄ NBr	<5% ^d
19	----	K ₂ S ₂ O ₈	7% ^d
20	KOAc	K ₂ S ₂ O ₈ , without Pd(OAc) ₂	nd

^aConditions: **1a** (1 equiv), **2a** (2.5 equiv), Pd(OAc)₂ (15 mol %), Bu₄NBr (1 equiv), base (4 equiv) additive (1.5 equiv), DMF as a solvent. ^bIsolated yields, ^cReaction time 12 h, ^dGC yield (dodecane was taken as an internal standard for GC).

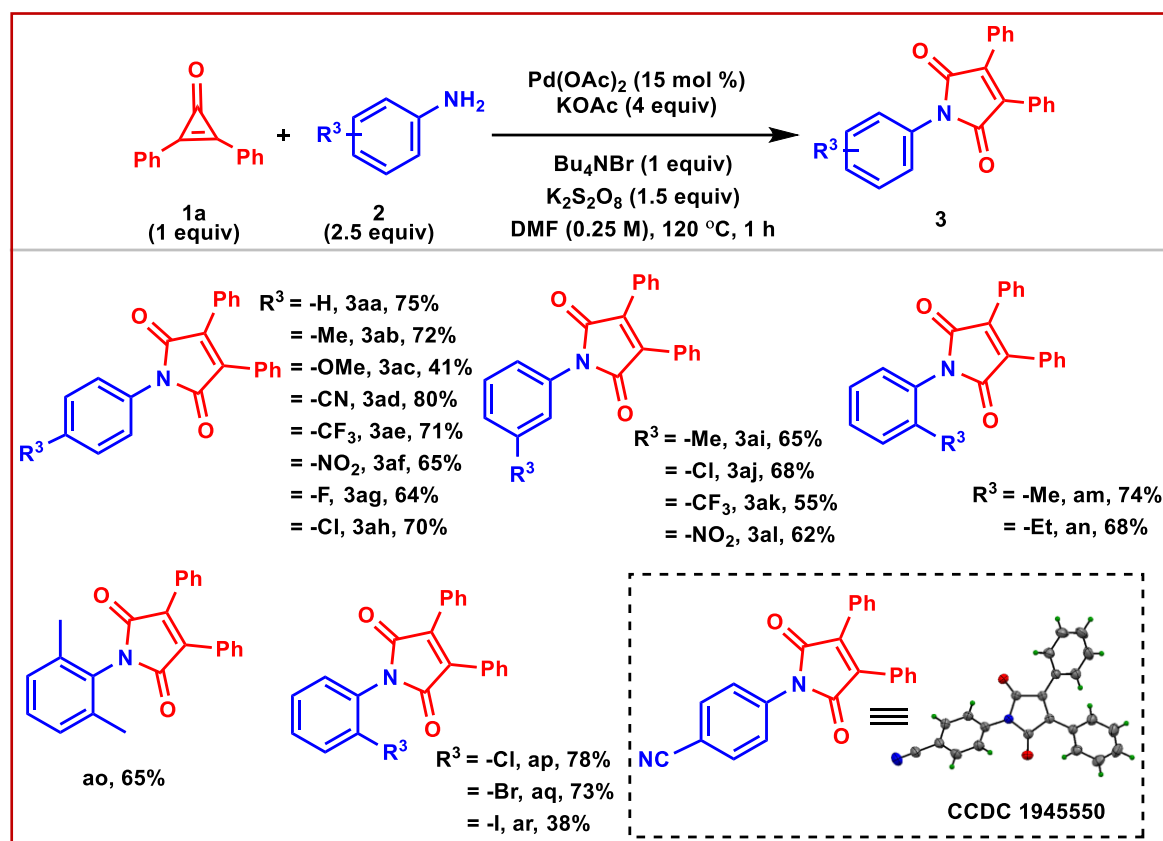
As maleimides are also biologically important molecules we decided to optimize the conditions further to obtain a good yield of maleimide **3aa**. Interestingly, under the same reaction conditions, the addition of K₂S₂O₈ further improved the yield of the desired product to 63% within a short reaction time (Table 2.1, entry 2). Encouraged by this intriguing observation, several other additives were screened out of which K₂S₂O₈ was found to be the most effective additive increasing the catalytic efficiency of the reaction (Table 2.1, entry 3-7). Aiming to enhance the product yield further, we screened various other acetate bases. Fruitful results were observed in the case of LiOAc and KOAc which gave 73% and 75% of **3aa**, respectively (Table 2.1, entries 8-9), whereas cesium acetate decreased the yield of **3aa** to 58% (Table 2.1, entry 10). Likewise, carbonate and bicarbonate bases failed to enhance the yield of the C–C activated product (Table 2.1, entries 11–15). To confirm the importance of the base we performed analogous experiments with CsOPiv and K₂HPO₄ (Table 2.1, entries 16-17). In both these cases, no

increment in the product yield was observed. Thus, KOAc was found to be the best base producing a 75% yield of the desired product which implies that optimum basicity is required for this pathway. Then we performed the control experiments in the absence of tetrabutylammonium bromide (TBAB), base (KOAc) and observed an insignificant GC yield (Table 2.1, entries 18-19) which implies that both TBAB and KOAc are required for the reaction to proceed catalytically. Also, it has been reported in the literature that TBAB helps in the reduction of Pd(II) to Pd(0).²⁵ Besides, to understand the influence of the palladium acetate on the titled reaction, we carried out the reaction in the absence of the catalyst which failed to give the product **3aa** (Table 2.1, entry 20).

After establishing the optimal reaction conditions, we evaluated the substrate scope of this Pd-catalyzed cascade C–C activation and carbonylative amination reaction. At first, we treated diphenylcyclopropenone **1a** with a variety of *para*-substituted anilines. We found that with the gradual increase or decrease in the electron density of the substituent in the *para* position, the yields tend toward the lower side. While, *p*-toluidine gave a 72% yield of the corresponding maleimide product (Scheme 2.2, **3ab**), relatively more electron-rich *p*-OMe aniline delivered only 41% of the desired product (Scheme 2.2, **3ac**). Similarly, while *p*-NO₂ aniline gave a moderate yield (65%) of the corresponding product (Scheme 2.2, **3ad**), relatively less electron-withdrawing substrates such *p*-CN and *p*-CF₃ anilines gave better yields, 80%, and 71%, respectively (Scheme 2.2, **3ae-3af**). Between *p*-Cl and *p*-F aniline, the *p*-Cl aniline worked well giving a 70% yield (Scheme 2.2, **3ag**) whereas *p*-F aniline gave only 64% of the corresponding adduct (Scheme 2.2, **3ah**). Further, we subjected *meta*-substituted anilines to our reaction conditions and obtained the desired product in 55%-68% yield (Scheme 2.2, **3ai-3al**). Furthermore, the compatibility of the *ortho*-substituted anilines has also been tested. A series of mono- and dialkyl substituted substrates were found to be compatible indicating the robustness of the reaction toward

steric hindrance (Scheme 2.2, **3am-3ao**). Substrates bearing a halo group at the *ortho* position also gave the desired products (Scheme 2.2, **3ap-3ar**), thus offering the potential for further functionalization. The single crystal X-ray analysis further confirmed the structure of the highly functionalized maleimide **3ad** (Scheme 2.2).

Scheme 2.2 Scope with respect to aniline^a

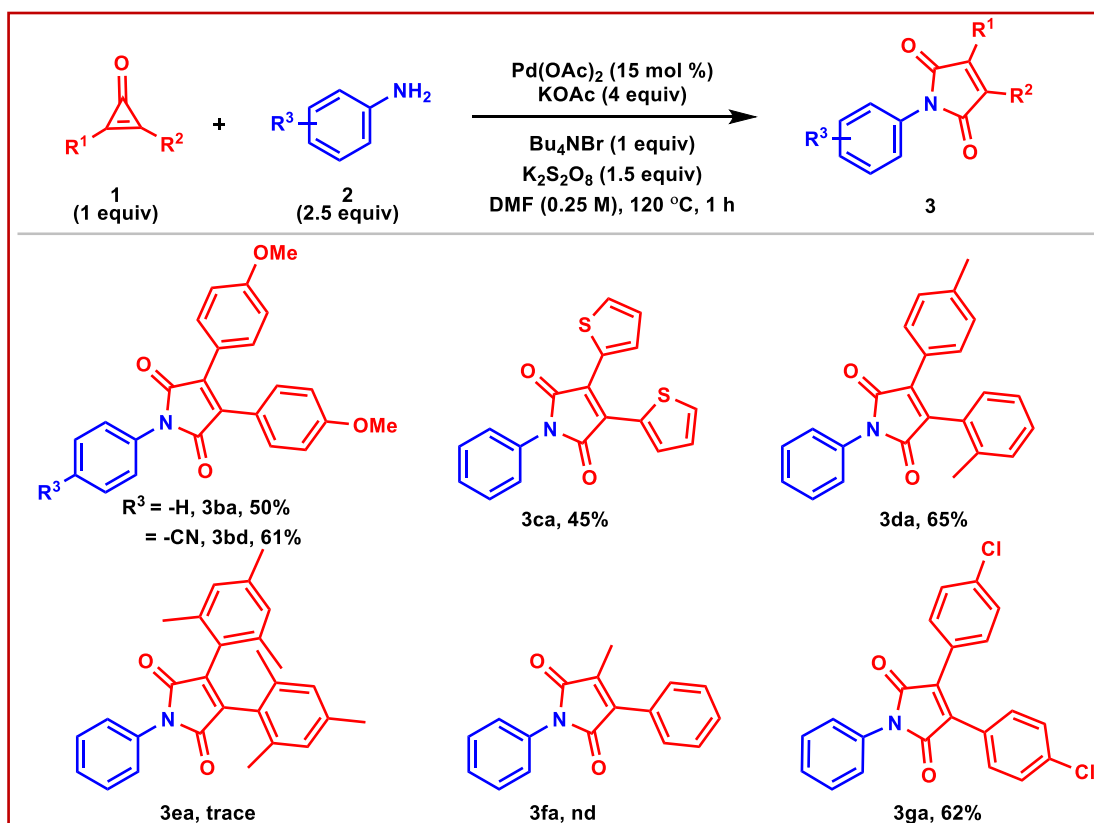


^aConditions: **1a** (1 equiv), **2a** (2.5 equiv), Pd(OAc)₂ (15 mol %), Bu₄NBr (1 equiv), KOAc (4 equiv), K₂S₂O₈ (1.5 equiv), DMF (0.25 M), 120 °C, 1 h, under N₂; isolated yields are shown. ^bReaction time 2 h.

Next, we examined the scope of diarylcyclopropanone by varying substituents on the aryl ring system. As shown in Scheme 2.3, a series of maleimides were synthesized in moderate to good yields. Depending on the nature and position of the substituent in the aryl ring, the reactivity changed. Simple aniline when treated with *p*-methoxy diphenylcyclopropanone resulted in only 50% of the desired product (Scheme 2.3, **3ba**), whereas *p*-CN aniline showed some improvement in the reactivity giving a 61% yield (Scheme 2.3, **3bd**) of the

highly functionalized maleimide. Thiophene-substituted cyclopropenone gave the desired product in 45% yield (Scheme 2.3, **3ca**). With unsymmetrical diaryl substituted cyclopropenone, the desired product was obtained in 65% yield (Scheme 2.3, **3da**). Next, when sterically crowded dimesitylene cyclopropenone was utilized as the substrate, the reaction failed to give any isolable yield of the product. However, the product was detected in HRMS (Scheme 2.3, **3ea**), thus, indicating that the steric hindrance on the aryl group of the cyclopropenone plays a key role in determining the reactivity. Furthermore, unsymmetrical phenyl methyl cyclopropenone failed to give the desired product (Scheme 2.3, **3fa**). Whereas *para*-chloro substituted diphenyl cyclopropenone gave 62% of the desired product (Scheme 2.3, **3ga**). Altogether, these results highlighted the importance and utility of this new protocol.

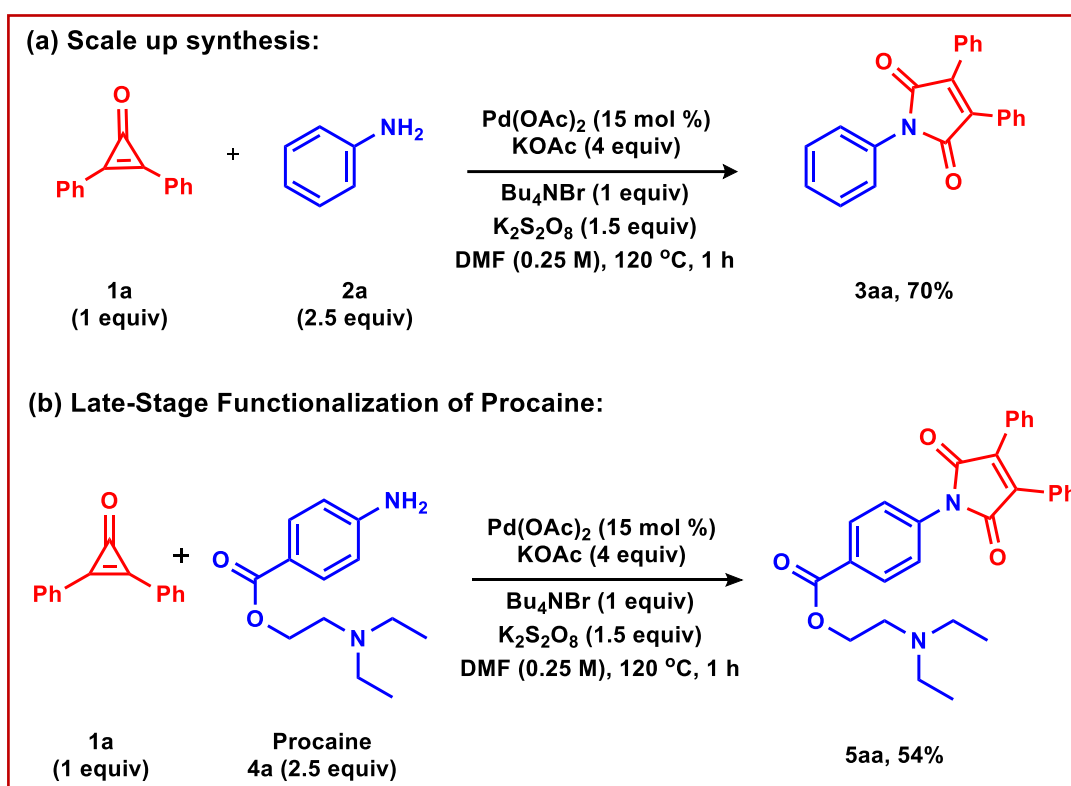
Scheme 2.3 Scope with respect to diarylcyclopropenone^a



^aConditions: **1a** (1 equiv), **2a** (2.5 equiv), $\text{Pd}(\text{OAc})_2$ (15 mol %), Bu_4NBr (1 equiv), KOAc (4 equiv), $\text{K}_2\text{S}_2\text{O}_8$ (1.5 equiv), DMF (0.25 M), 120°C , 1 h, under N_2 ; isolated yields are shown.

To check the feasibility of the transformation on large scale, we also performed the reaction in 1 mmol scale and obtained a 70% yield of product **3aa** (Scheme 2.4a). As the biarylated maleimide skeleton is prominently present in various drugs molecules,²¹ it would be very beneficial to directly construct this backbone on the bioactive compounds. For instance, it could be directly appended onto procaine **4a**, a drug that was used as a local anesthetic (Scheme 2.4b). We obtained a 54% yield of the corresponding functionalized product **5aa**.

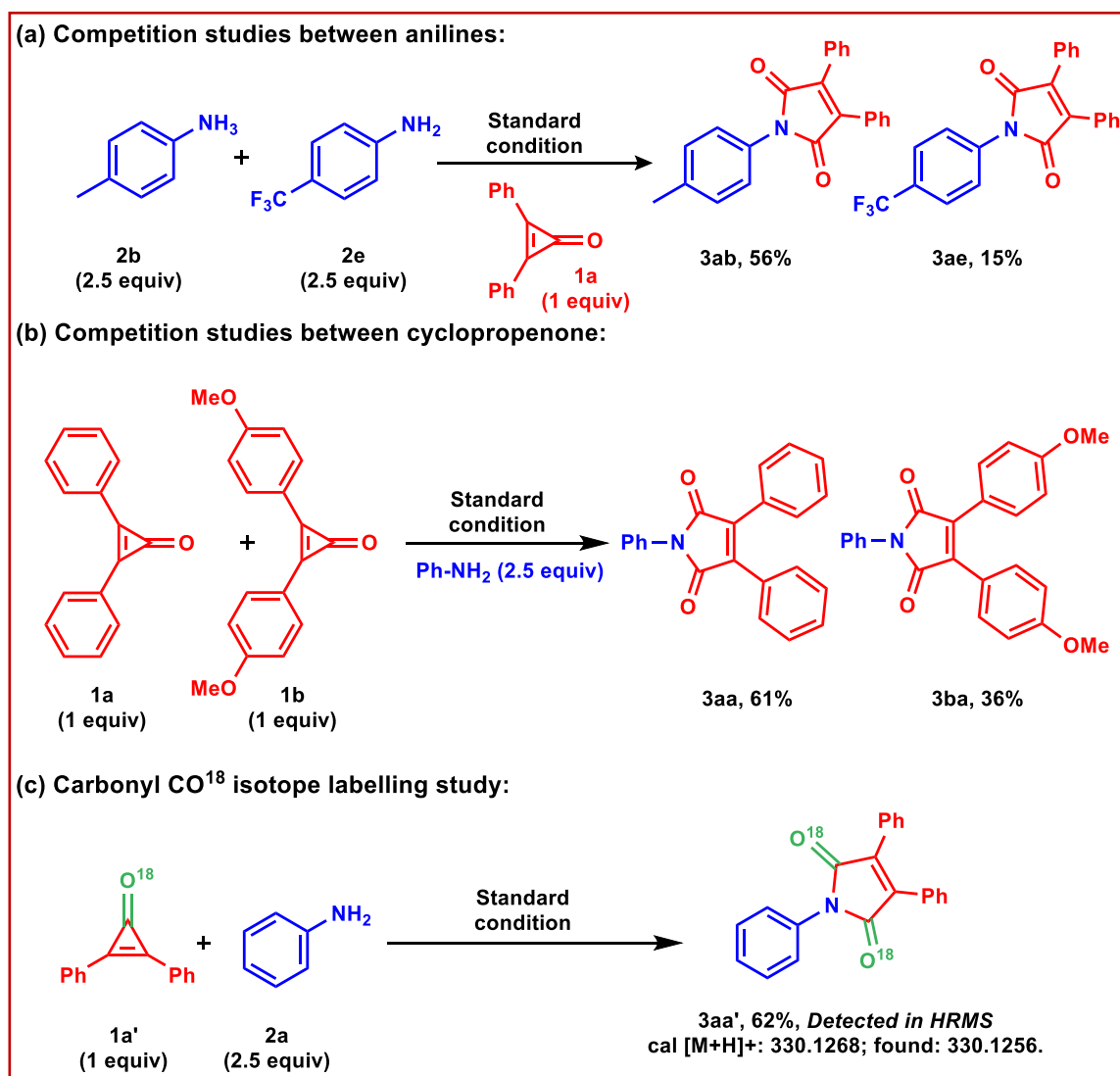
Scheme 2.4 Application



To understand the effect of the substituent in both chosen starting materials, we performed the control experiment between electron-rich and electron-poor substrates. When the intermolecular competition reaction was conducted between *p*-toluidine and *p*-trifluoromethyl aniline, *p*-toluidine reacted faster giving a 56% yield of the respective product (Scheme 2.5a). Analogously, when we performed a competition experiment between electron-neutral and electron-rich cyclopropanone, lesser reactivity was observed for electron-rich cyclopropanone delivering only 36% of the maleimide adduct (Scheme

2.5b). To further prove that cyclopropenone is acting as the source of carbon monoxide, ^{18}O -labeled cyclopropenone **1a'** and the aniline **2a** were subjected to the standard reaction conditions, and the respective ^{18}O -labeled maleimide product **3aa'** was detected by HRMS (Scheme 2.5c). This experiment confirmed that the other carbonyl group in the product is coming from cyclopropenone. Furthermore, to understand whether the reaction proceeds through a radical

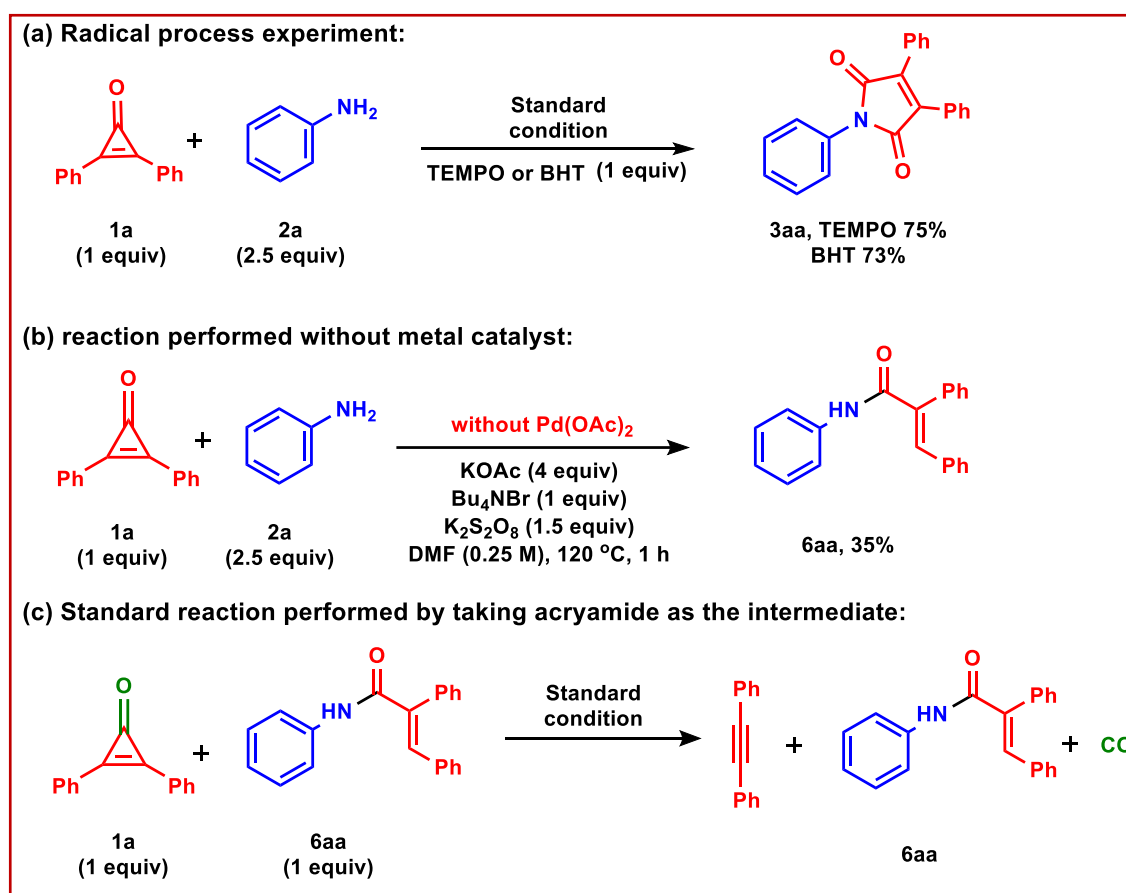
Scheme 2.5 Mechanistic studies



or ionic mechanism, we performed the reaction in the presence of a stoichiometric amount of a radical scavenger (TEMPO and BHT). The reaction did not quench under these conditions giving 75% and 73% yields of the desired C–C activated product, respectively

(Scheme 2.6a). To gain more insight into the Pd(0) catalyzed C–C bond activation of cyclopropenone, we performed the reaction without Pd(OAc)₂ and isolated acrylamide **6aa** as one of the products in 35% yield (Scheme 2.6b) without any trace of diphenylacetylene or product **3aa** (confirmed by HPLC). To confirm whether this acrylamide is an active intermediate in this transformation or not, we have taken the acrylamide **6aa** and subjected it to the standard reaction conditions (Scheme 2.6c). Surprisingly, we did not observe any trace of maleimide

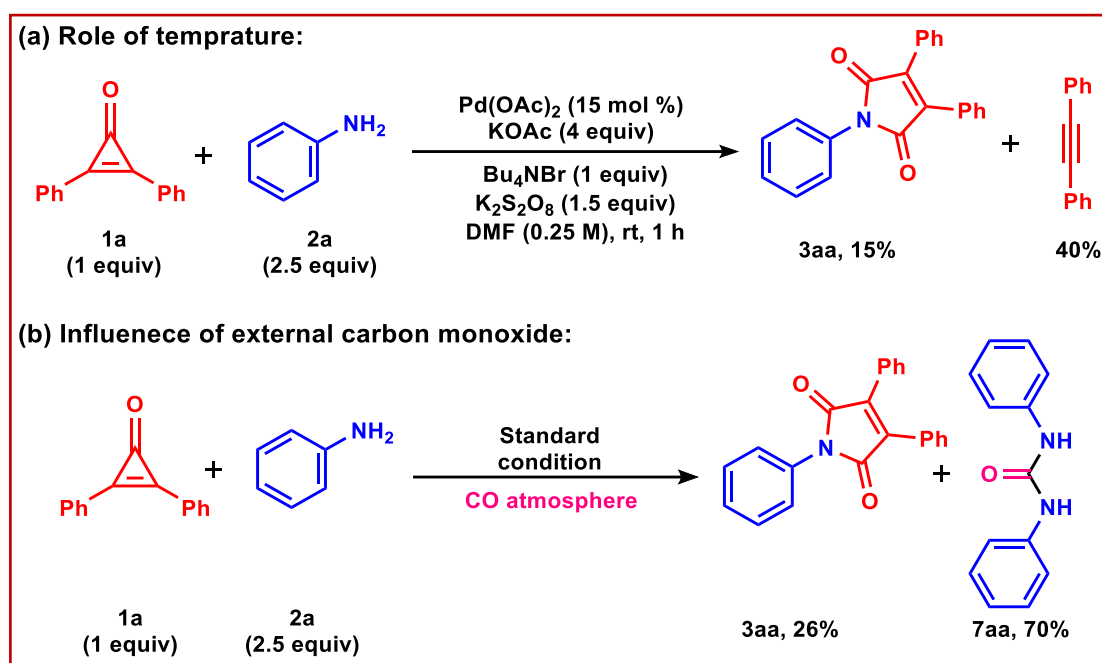
Scheme 2.6 Mechanistic studies



3aa (confirmed by HPLC) which proves that acrylamide **6aa** is not an active intermediate in this reaction. Interestingly all of the cyclopropenone was converted to diphenyl acetylene in the presence of Pd(OAc)₂, which is indirect evidence that the palladium catalyst was involved in the decarbonylation process of cyclopropenone. To further ensure that the decarbonylation of cyclopropenone was not a pyrolytic process, we performed the reaction

at room temperature and observed the product maleimide **3aa** in 15% yield along with diphenylacetylene **3a'** in 40% yield (Scheme 2.7a). This experiment further confirms unambiguously that the extrusion of CO is not a pyrolytic process but a metal-catalyzed process. We performed an experiment (Scheme 2.7b) with external CO to check the influence on the yield. Contrary to our expectation the product **3aa** yield decreased to 26%, interestingly we obtained side product diphenyl urea **7aa** as the major product in 70% yield (Scheme 2.7b).

Scheme 2.7 Mechanistic studies

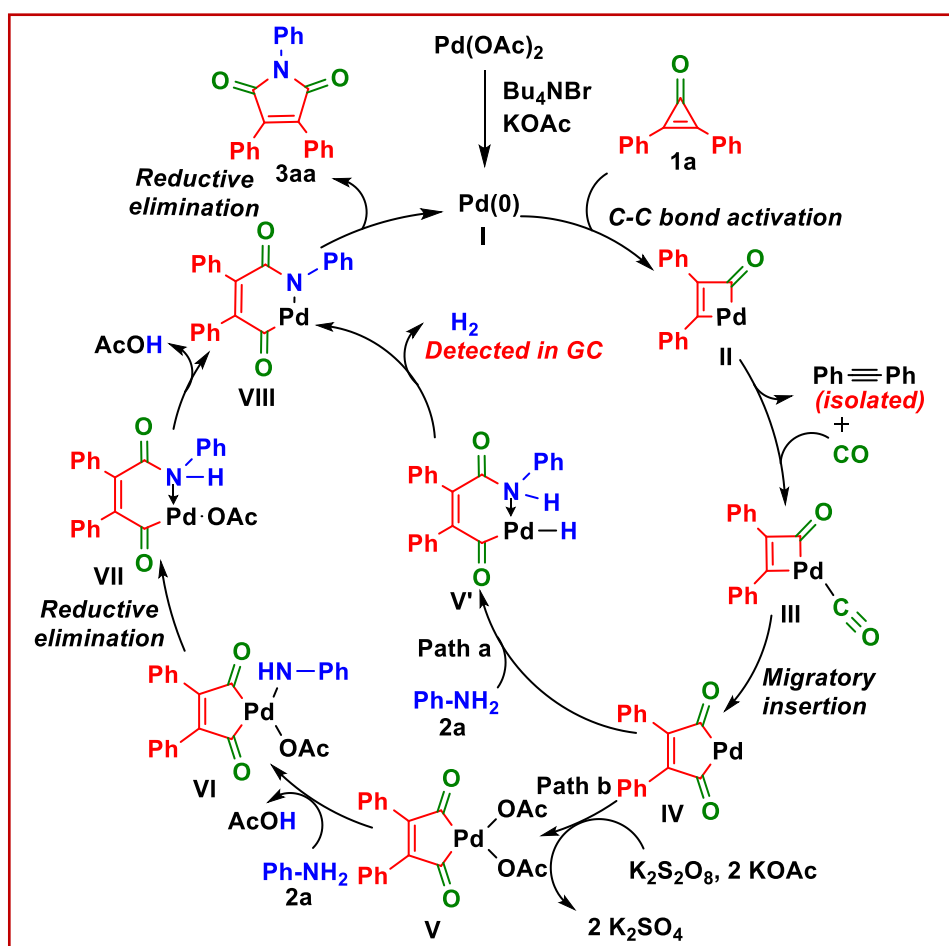


This implies that in the presence of external CO the reaction pathway leading to the formation of diphenyl urea **7aa** is predominant.

Based on the above experiments along with literature precedents,^{17,26} a plausible mechanism has been proposed (Scheme 2.8). First, Pd(OAc)₂ is converted to Pd(0) in situ in the presence of Bu₄NBr and KOAc.²⁵ Then, oxidative addition of Pd(0) to the C–C bond of cyclopropenone results in the intermediate **II** which upon the recapture of CO (detected in GC) leads to **III**. The migratory insertion of CO forms intermediate **IV** which can take part in two probable pathways. In path **a** intermediate **IV** undergoes nucleophilic addition

with aniline **2a** followed by subsequent H₂ elimination (confirmed through GC) to give intermediate **VIII**. While in path **b**, in the presence of K₂S₂O₈ intermediate **IV** undergoes oxidation to give intermediate **V**. Intermediate **V** undergoes ligand exchange in the presence of aniline **2a** followed by elimination of AcOH resulting in intermediate **VI**. Further reductive elimination along with AcOH elimination leads to intermediate **VII**. Then, intermediate **VII** undergoes reductive elimination to generate Pd(0) along with the desired product **3aa** completing the catalytic cycle.

Scheme 2.8 Catalytic cycle



2.4 CONCLUSION

In summary, we have developed a palladium-catalyzed cascade C-C bond activation and carbonylative amination of substituted cyclopropanone with various anilines. An ¹⁸O isotope labeling study proved that the source of the extra carbonyl is from the starting

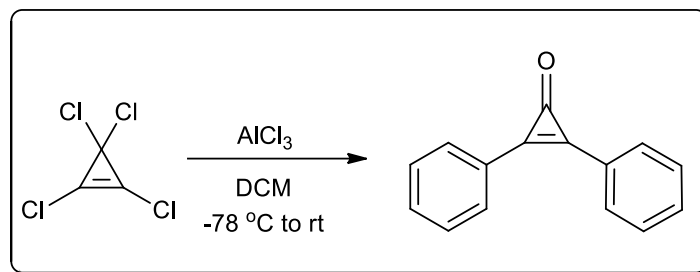
material cyclopropenone. To the best of our knowledge, this type of cyclization reaction is the first of its kind wherein the extruded CO which is efficiently recaptured for the next step cyclization reaction. We have also shown an application of this protocol by late-stage functionalization of marketed drug procaine. Thus, the established methodology has the potential to trigger the development of new drug-like candidates bearing maleimide as the core unit.

2.5 EXPERIMENTAL SECTION

Reactions were performed using a borosil-sealed tube vial under an N₂ atmosphere. Column chromatography was done by using 100-200 & 230-400 mesh size silica gel of Merck Company. Gradient elution was performed by using distilled petroleum ether and ethyl acetate. TLC plates were detected under UV light at 254 nm. ¹H NMR, ¹³C NMR, recorded on Bruker AV 400, 700 MHz NMR spectrometer using CDCl₃ as internal standards the residual CHCl₃ for ¹H NMR (δ = 7.26 ppm) and the deuterated solvent signal for ¹³C NMR (δ = 77.36 ppm) is used on reference.²⁷ Multiplicity (s = single, d = doublet, t = triplet, q = quartet, m = multiplet, dd = double doublet), integration, and coupling constants (J) in hertz (Hz). HRMS signal analysis was performed using a micro TOF Q-II mass spectrometer and X-ray diffraction analysis was performed using RIGAKU-XRD at SCS, NISER. Reagents and starting materials were purchased from Sigma Aldrich, Alfa Aesar, TCI, Avra, Spectrochem, and other commercially available sources, and used without further purification unless otherwise noted.

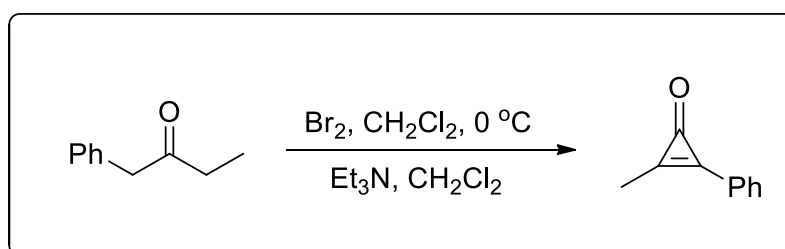
Representative Procedures:

(a) General procedure for synthesis of cyclopropenones:^{28,29}



To a suspension of tetrachlorocyclopropene (0.64 mmol) and anhydrous AlCl_3 (1.35 mmol) in CH_2Cl_2 (10 mL) was added dropwise, a solution of benzene (1.28 mmol) in CH_2Cl_2 (1 mL) at $-78\text{ }^\circ\text{C}$. The mixture was stirred for 2 h then warmed up to room temperature and stirred for another 2 h. After completion of the reaction as monitored by TLC analysis, the resulting mixture was quenched with water, diluted with CH_2Cl_2 , and washed with water ($2 \times 50\text{ mL}$) and brine ($2 \times 50\text{ mL}$). The organic layers were dried over anhydrous Na_2SO_4 , filtered, and concentrated under reduced pressure to yield the crude residue as an orange oil. The crude residue was then purified by flash column chromatography on silica gel (20% EtOAc in hexanes) to afford diarylcyclopropenone (85% yield) as a white solid.

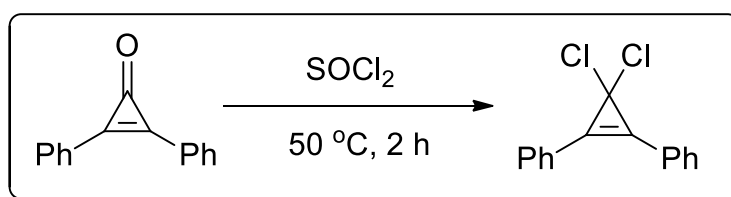
(b) Procedure for the synthesis of methyl phenyl cyclopropenone:³⁰



1-phenyl-2-butanone (8.9 mmol) and dichloromethane (0.5 M) were added to an oven-dried flask with a stir bar under nitrogen. The solution was cooled to $0\text{ }^\circ\text{C}$ and neat bromine (22.3 mmol) was added dropwise via syringe over 5 minutes. After the addition was completed, the reaction was stirred at room temperature for another 30 minutes. The reaction was

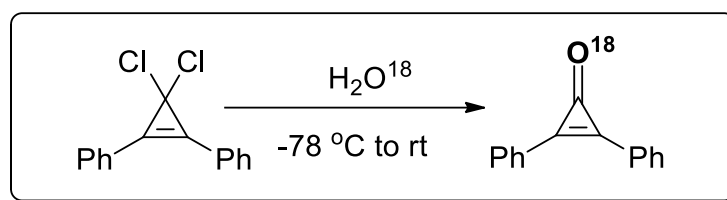
poured into a separatory funnel containing 20 mL sat. aq. $\text{Na}_2\text{S}_2\text{O}_3$. The layers were separated, and the aqueous layer was extracted with ether (2 x 15 mL). The combined organics were washed with sat. aq. NaHCO_3 (20 mL) and brine (20 mL), were dried with anhydrous MgSO_4 , filtered, and concentrated in vacuum. The yellowish oil was dissolved in dichloromethane (0.5 M) and triethylamine (9 mL) and stirred at room temperature for 8 hours under nitrogen. The reaction was then diluted with ether (100 mL). The organics were washed with sat. aq. CuSO_4 and brine (100 mL each), were dried over anhydrous Na_2SO_4 , filtered, and concentrated in vacuum. Further purification was accomplished by flash column chromatography eluting with ether. Product-containing fractions were concentrated to give a light-brown solid (45%).

(c) **1,1-Dichloro-2,3-diphenylcyclopropene:**



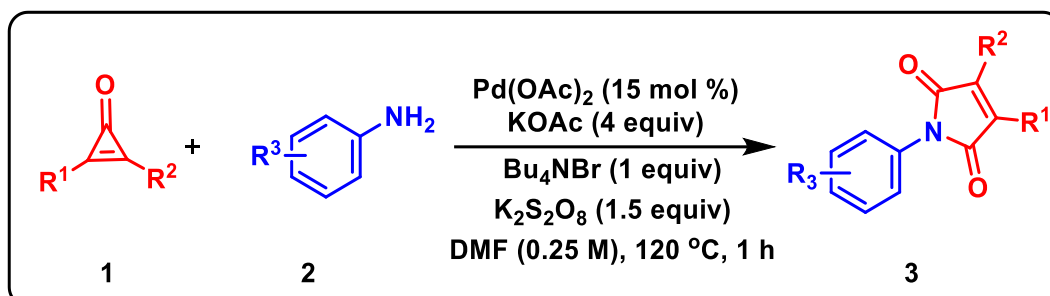
Following the method of Perkins,³¹ 2,3-diphenylcyclopropenone (19.4 mmol) was added to a 100-mL round-bottomed flask fitted with a reflux condenser. To this, was added neat thionyl chloride (550 mmol) and solution was heated to 50 °C for 2 h. After 2 h, the reaction was cooled to 23 °C and concentrated under vacuum to yield a light-yellow solid. The solid was recrystallized from hexanes to afford a white solid (87% yield). ^1H NMR (400 MHz, CD_3CN) δ 8.18-8.16 (m, 4H, ArH), 7.77-7.73 (m, 2H, ArH), 7.71-7.67 (m, 4H, ArH). ^{13}C NMR (100 MHz, CDCl_3) δ 131.3, 130.2, 129.3, 125.8, 123.9.

(d) **2,3-diphenyl cyclopropenone-¹⁸O:**³²



Solid 1,1-dichloro-2,3-diphenylcyclopropene (0.2 mmol) was treated with H₂¹⁸O (50 μ l, 97 atom % ¹⁸O) at -78 °C and the mixture was subsequently warmed to ambient temperature. Evolved HCl was removed in vacuo from time to time during this period. After stirring the mixture overnight and removal of the volatile components in vacuo, the residual moisture adherent to the remaining solid was removed by azeotropic distillation with C₆H₆. The ¹⁸O-enrichment in the white solid product (yield quantitative) was determined by mass spectroscopy to be about 75%

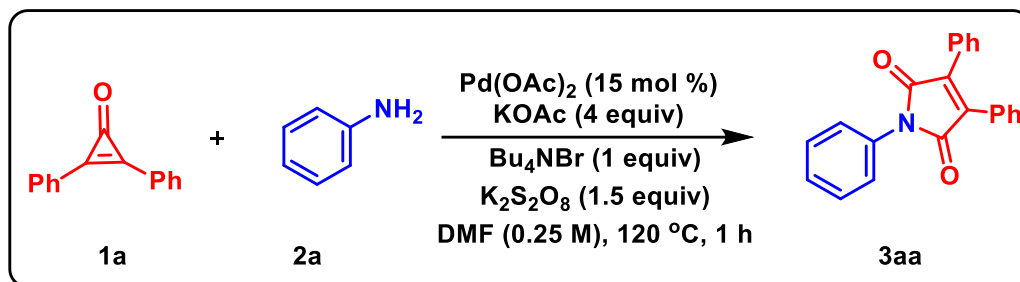
(e) **General procedure for synthesis of highly substituted maleimide:**



To a solution of diarylcyclopropenone **1** (0.096 mmol) in DMF (0.25 M), under N₂ atmosphere was added, Pd(OAc)₂ (15 mol %), n-Bu₄NBr (0.096 mmol), KOAc (0.38 mmol), K₂S₂O₈ (0.14 mmol) aniline **2** (0.24 mmol) and stirred vigorously (750 rpm) in a preheated aluminum block at 120 °C for 1 h. After completion of the reaction (in 1 h) as monitored by TLC analysis, the solvent was evaporated under reduced pressure and the residue was purified by column chromatography on silica gel (elute: EtOAc/hexane) to give the pure product **3**.

(KOAc was taken first inside the 25ml seal tube and heated under vacuum to make the reaction moisture free)

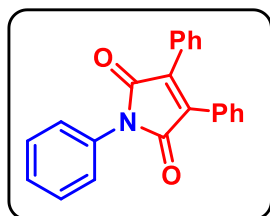
(f) General procedure for synthesis of highly substituted maleimide in 1 mmol scale:



To a solution of diphenyl cyclopropenone **1a** (1 mmol) in DMF (0.25 M), under N₂ atmosphere was added, Pd(OAc)₂ (15 mol %), n-Bu₄NBr (1 mmol), KOAc (4 mmol), K₂S₂O₈ (1.5 mmol), and aniline **2a** (2.5 mmol) stirred vigorously (750 rpm) in a preheated aluminum block at 120 °C for 1 h. After completion of the reaction (in 1 h) as monitored by TLC analysis, the solvent was evaporated under reduced pressure and the residue was purified by column chromatography on silica gel (elute: EtOAc/hexane) to give the pure product light yellow solid (112 mg, 70% yield) **R_f**: 0.5 (in 10% EtOAc/hexane).

(KOAc was taken first inside the 25ml seal tube and heated under vacuum to make the reaction moisture free.)

Experimental characterization data of products:

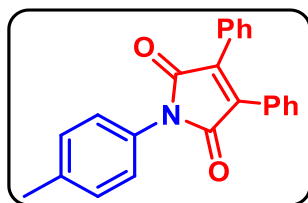


1,3,4-triphenyl-1H-pyrrole-2,5-dione (3aa):

Physical State: light yellow solid (12 mg, 75% yield). **R_f**= 0.5 (in 10% EtOAc/hexane). **¹H NMR (CDCl₃, 400 MHz):** δ 7.52-7.46 (m, 8H), 7.38-7.34 (m, 7H). **¹³C{¹H} NMR (CDCl₃, 100 MHz):**

δ 169.8, 136.5, 132.1, 130.3 (2C), 129.3, 128.9, 128.7, 128.0, 126.4. **IR (KBr, cm⁻¹):** 1710,

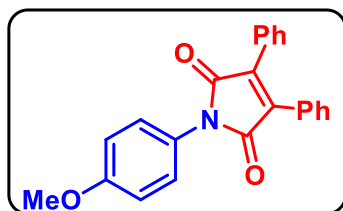
1636, 1401. **HRMS (ESI) m/z:** $[M+Na]^+$ calcd for $C_{22}H_{15}NO_2Na$: 348.0995; found: 348.1011.



3,4-diphenyl-1-(p-tolyl)-1H-pyrrole-2,5-dione (3ab):

Physical State: dark yellow solid (11.5 mg, 72% yield), R_f = 0.7 (in 10% EtOAc/hexane). **1H NMR ($CDCl_3$, 400 MHz):** δ

7.53–7.51 (brd, J = 6.4 Hz, 4H), 7.42 – 7.28 (m, 10H), 2.40 (s, 3H). **$^{13}C\{^1H\}$ NMR ($CDCl_3$, 100 MHz):** δ 170.0, 138.1, 136.7, 130.4, 130.2, 130.0, 129.6, 129.0, 128.9, 126.4, 21.3. **IR (KBr, cm^{-1}):** 1712, 1401. **HRMS (ESI) m/z:** $[M+H]^+$ calcd for $C_{23}H_{18}NO_2$: 340.1332; found: 340.1333.

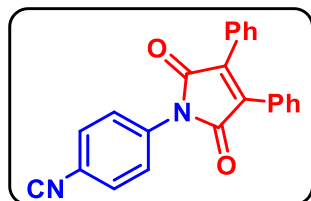


1-(4-methoxyphenyl)-3,4-diphenyl-1H-pyrrole-2,5-dione (3ac):

Physical State: light yellow solid (7 mg, 41% yield), R_f =

0.35 (in 10% EtOAc/hexane). **1H NMR ($CDCl_3$, 400 MHz):** δ 7.53–7.51 (m, 4H), 7.42–7.33 (m, 8H), 7.01 (d, J = 8.8 Hz, 2H), 3.85 (s, 3H). **$^{13}C\{^1H\}$ NMR ($CDCl_3$, 100 MHz):** δ 170.2, 159.3, 136.5, 130.3 (2C), 128.9, 128.8, 127.9, 124.7, 114.7, 55.8. **IR (KBr, cm^{-1}):** 1711, 1402. **HRMS (ESI) m/z:** $[M+Na]^+$ calcd for $C_{23}H_{17}NO_3Na$: 378.1101; found: 378.1119.

4-(2,5-dioxo-3,4-diphenyl-2,5-dihydro-1H-pyrrol-1-yl) benzonitrile (3ad):



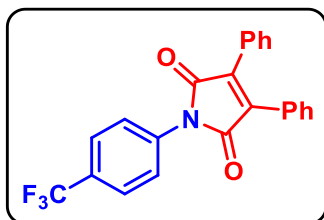
Physical State: dark yellow solid (13.5 mg, 80% yield), R_f = 0.25 (in 10% EtOAc/hexane). **1H NMR ($CDCl_3$, 400 MHz):** δ

7.79 (d, J = 8.8 Hz, 2H), 7.72 (d, J = 8.8 Hz, 2H), 7.51 (brd, J = 7.2 Hz, 4H), 7.45–7.36 (m, 6H). **$^{13}C\{^1H\}$ NMR ($CDCl_3$, 100 MHz):** δ 169.1, 136.9, 136.3,

133.2, 130.7, 130.3, 129.0, 128.3, 126.1, 118.6, 111.2. **IR** (KBr, cm^{-1}): 2229, 1716, 1386.

HRMS (ESI) m/z: $[\text{M}+\text{H}]^+$ calcd for $\text{C}_{23}\text{H}_{15}\text{N}_2\text{O}_2$: 351.1128; found: 351.1139.

3,4-diphenyl-1-(4-(trifluoromethyl)phenyl)-1H-pyrrole-2,5-dione (3ae):



Physical State: yellow solid (13 mg, 71% yield), $R_f = 0.7$

(in 10% EtOAc/hexane). **^1H NMR (CDCl_3 , 400 MHz):** δ

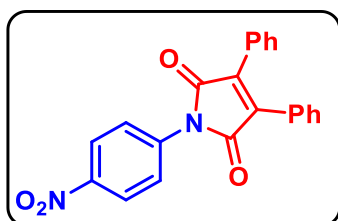
7.76 (d, $J = 8.4$ Hz, 2H), 7.67 (d, $J = 8.4$ Hz, 2H), 7.52 (brd,

$J = 6.8$ Hz, 4H), 7.44-7.36 (m, 6H). **$^{13}\text{C}\{^1\text{H}\}$ NMR (CDCl_3 , 175 MHz):** δ 169.4, 136.8,

135.3, 130.6, 130.3, 129.9, 129.7, 129.0, 128.5, 126.5 (q, $J = 3.5$ Hz), 126.2. **^{19}F NMR**

(CDCl_3 , 376 MHz): δ -62.5. **IR (KBr, cm^{-1}):** 1714, 1398. **HRMS (ESI) m/z:** $[\text{M}+\text{H}]^+$

calcd for $\text{C}_{23}\text{H}_{15}\text{F}_3\text{NO}_2$: 394.1049; found: 394.1052.



1-(4-nitrophenyl)-3,4-diphenyl-1H-pyrrole-2,5-dione

(3af):

Physical State: yellow solid (11 mg, 65% yield), $R_f = 0.5$

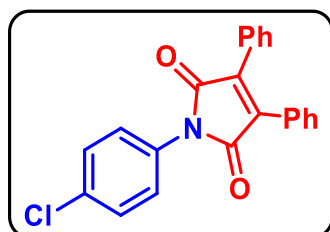
(in 10% EtOAc/hexane). **^1H NMR (CDCl_3 , 400 MHz):** δ

8.39 (d, $J = 8.8$ Hz, 2H), 7.82 (d, $J = 8.8$ Hz, 2H), 7.54 (brd, $J = 6.8$ Hz, 4H), 7.48-7.40 (m,

6H). **$^{13}\text{C}\{^1\text{H}\}$ NMR (CDCl_3 , 100 MHz):** δ 169.1, 146.4, 138.0, 137.1, 130.7, 130.3, 129.1,

128.3, 126.0, 124.7. **IR (KBr, cm^{-1}):** 1709, 1514, 1499. **HRMS (ESI) m/z:** $[\text{M}+\text{H}]^+$ calcd

for $\text{C}_{22}\text{H}_{15}\text{N}_2\text{O}_4$: 371.1032; found: 371.1031.



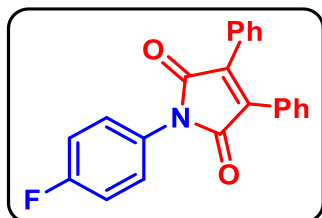
1-(4-chlorophenyl)-3,4-diphenyl-1H-pyrrole-2,5-dione

(3ag):

Physical State: yellow oily liquid (12 mg, 70% yield), $R_f =$

0.7 (in 15% EtOAc/hexane). **^1H NMR (CDCl_3 , 400 MHz):** δ

7.51 (brd, $J = 6.8$ Hz, 4H), 7.45-7.36 (m, 10H). $^{13}\text{C}\{^1\text{H}\}$ NMR (CDCl_3 , 100 MHz): δ 169.6, 136.7, 133.7, 130.7, 130.4, 130.3, 129.6, 129.0, 128.6, 127.5. IR (KBr, cm^{-1}): 1709, 1400. HRMS (ESI) m/z : $[\text{M}+\text{H}]^+$ calcd for $\text{C}_{22}\text{H}_{15}\text{ClNO}_2$: 360.0786; found: 360.0781.

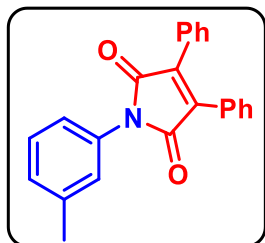


1-(4-fluorophenyl)-3,4-diphenyl-1H-pyrrole-2,5-dione

(3ah):

Physical State: yellow solid (10.5 mg, 64% yield), $R_f = 0.7$ (in

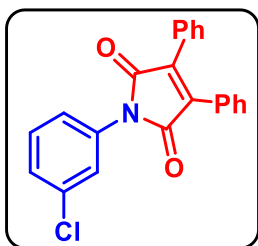
10% EtOAc/hexane). ^1H NMR (CDCl_3 , 400 MHz): δ 7.52-7.50 (m, 4H), 7.46-7.36 (m, 8H), 7.18 (t, $J = 8.8$ Hz, 2H). $^{13}\text{C}\{^1\text{H}\}$ NMR (CDCl_3 , 100 MHz): δ 169.8, 162.1 (d, $J = 246$ Hz), 136.6, 130.4, 130.3, 129.0, 128.7, 128.3 (d, $J = 8$ Hz), 128.0 (d, $J = 3$ Hz), 116.4 (d, $J = 23$ Hz). ^{19}F NMR (CDCl_3 , 376 MHz): δ -113.4. IR (KBr, cm^{-1}): 1711, 1443, 1400. HRMS (ESI) m/z : $[\text{M}+\text{H}]^+$ calcd for $\text{C}_{22}\text{H}_{15}\text{FNO}_2$: 344.1081; found: 344.1086.



3,4-diphenyl-1-(m-tolyl)-1H-pyrrole-2,5-dione (3ai):

Physical State: yellow solid (10.5 mg, 65% yield), $R_f = 0.25$ (in 10% EtOAc/hexane). ^1H NMR (CDCl_3 , 400 MHz): δ 7.52 (brd, $J = 6.8$ Hz, 4H), 7.42-7.35 (m, 7H), 7.27-7.24 (m, 2H),

7.19 (d, $J = 7.6$ Hz, 1H), 2.41 (s, 3H). $^{13}\text{C}\{^1\text{H}\}$ NMR (CDCl_3 , 100 MHz): δ 170.0, 139.3, 136.7, 132.1, 130.4, 130.31, 129.2, 129.0, 128.9 (2C), 127.2, 123.7, 21.7. IR (KBr, cm^{-1}): 1710, 1492, 1383. HRMS (ESI) m/z : $[\text{M}+\text{H}]^+$ calcd for $\text{C}_{23}\text{H}_{18}\text{NO}_2$: 340.1332; found: 340.1344.

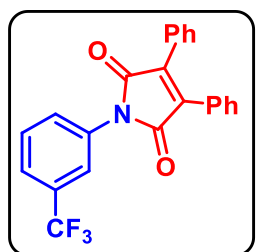


1-(3-chlorophenyl)-3,4-diphenyl-1H-pyrrole-2,5-dione (3aj):

Physical State: yellow solid (11.5 mg, 68% yield), $R_f = 0.6$ (in 10% EtOAc/hexane). $^1\text{H NMR}$ (CDCl_3 , 700 MHz): δ 7.53-7.51 (m, 5H), 7.43-7.35 (m, 9H). $^{13}\text{C}\{^1\text{H}\}$ NMR (CDCl_3 , 175 MHz):

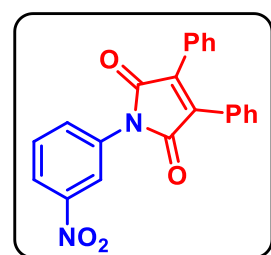
δ 169.5, 136.7, 134.9, 133.2, 130.5, 130.3 (2C), 129.0, 128.6, 128.2, 126.5, 124.4. **IR** (KBr, cm^{-1}): 1714, 1434, 1393. **HRMS** (ESI) m/z : $[\text{M}+\text{H}]^+$ calcd for $\text{C}_{22}\text{H}_{15}\text{ClNO}_2$: 360.0791; found: 360.0790.

3,4-diphenyl-1-(3-(trifluoromethyl)phenyl)-1H-pyrrole-2,5-dione (3ak):



Physical State: yellow oily liquid (10.5 mg, 55% yield), $R_f = 0.8$ (in 15% EtOAc/hexane). $^1\text{H NMR}$ (CDCl_3 , 400 MHz): δ 7.82 (s, 1H), 7.72-7.62 (m, 3H), 7.53-7.51 (m, 4H), 7.44-7.36 (m, 6H). $^{13}\text{C}\{^1\text{H}\}$ NMR (CDCl_3 , 175 MHz): δ 169.4, 136.8, 132.7, 132.0,

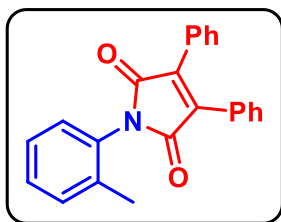
131.8, 130.5, 130.3, 129.9, 129.4, 129.0, 128.5, 124.6 (q, $J = 3.5$ Hz), 123.2 (q, $J = 3.5$ Hz). $^{19}\text{F NMR}$ (CDCl_3 , 376 MHz): δ -62.6. **IR** (KBr, cm^{-1}): 1714, 1455, 1396. **HRMS** (ESI) m/z : $[\text{M}+\text{H}]^+$ calcd for $\text{C}_{23}\text{H}_{15}\text{F}_3\text{NO}_2$: 394.1049; found: 394.1067.



1-(3-nitrophenyl)-3,4-diphenyl-1H-pyrrole-2,5-dione (3al):

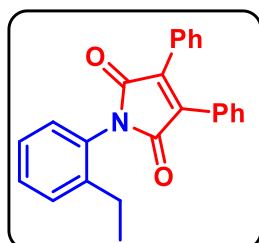
Physical State: yellow solid (10.5 mg, 62% yield) $R_f = 0.25$ (in 10% EtOAc/hexane). $^1\text{H NMR}$ (CDCl_3 , 400 MHz): δ 8.47 (s, 1H), 8.24 (d, $J = 8.0$ Hz, 1H), 7.91 (d, $J = 8.0$ Hz, 1H), 7.68 (t, $J = 8.0$

Hz, 1H), 7.53 (brd, $J = 7.2$ Hz, 4H), 7.45-7.38 (m, 6H). $^{13}\text{C}\{^1\text{H}\}$ NMR (CDCl_3 , 100 MHz): δ 169.3, 148.8, 136.9, 133.3, 131.7, 130.7, 130.3, 130.1, 129.0, 128.3, 122.5, 121.2. **IR** (KBr, cm^{-1}): 1714, 1527, 1400. **HRMS** (ESI) m/z : $[\text{M}+\text{H}]^+$ calcd for $\text{C}_{22}\text{H}_{15}\text{N}_2\text{O}_4$: 371.1026; found: 371.1030.



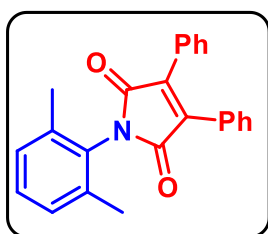
3,4-diphenyl-1-(o-tolyl)-1H-pyrrole-2,5-dione (3am):

Physical State: White solid (17mg, 53% yield). $R_f = 0.6$ (20% EtOAc/hexane). $^1\text{H NMR}$ (CDCl_3 , 700 MHz): δ 7.54 (brd, $J = 7.0$ Hz, 4H), 7.41-7.30 (m, 9H), 7.23 (d, $J = 7.0$ Hz, 1H), 2.26 (s, 3H). $^{13}\text{C}\{^1\text{H}\}$ NMR (CDCl_3 , 175 MHz): δ 169.9, 136.9, 136.7, 131.5, 131.0, 130.3 (2C), 129.6, 129.1, 128.9 (2C), 127.1, 18.5. **IR** (KBr, cm^{-1}): 1707, 1636, 1401. **HRMS** (ESI) m/z : $[\text{M}+\text{H}]^+$ calcd for $\text{C}_{23}\text{H}_{18}\text{NO}_2$: 340.1338; found: 340.1342.



1-(2-ethylphenyl)-3,4-diphenyl-1H-pyrrole-2,5-dione (3an):

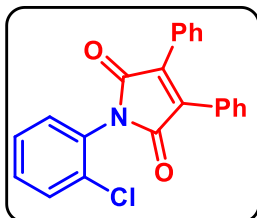
Physical State: yellow solid (11.5 mg, 68% yield), $R_f = 0.6$ (in 10% EtOAc/hexane). $^1\text{H NMR}$ (CDCl_3 , 400 MHz): δ 7.55-7.53 (m, 4H), 7.44 – 7.30 (m, 9H), 7.21 (d, $J = 7.6$ Hz, 1H), 2.58 (q, $J = 7.6$ Hz, 2H), 1.22 (t, $J = 7.6$ Hz, 3H). $^{13}\text{C}\{^1\text{H}\}$ NMR (CDCl_3 , 100 MHz): δ 170.3, 142.8, 136.6, 130.4 (2C), 130.3, 129.9, 129.5, 129.4, 128.9 (2C), 127.1, 24.5, 14.5. **IR** (KBr, cm^{-1}): 1710, 1399. **HRMS** (ESI) m/z : $[\text{M}+\text{H}]^+$ calcd for $\text{C}_{24}\text{H}_{20}\text{NO}_2$: 354.1489; found: 354.1488.



1-(2,6-dimethylphenyl)-3,4-diphenyl-1H-pyrrole-2,5-dione (3ao):

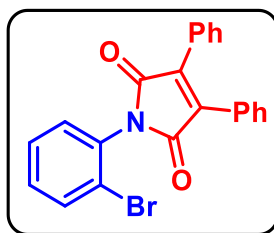
Physical State: yellow solid (10.5 mg, 65% yield), $R_f = 0.6$ (in 10% EtOAc/hexane). $^1\text{H NMR}$ (CDCl_3 , 700 MHz): δ 7.56-7.55 (m, 4H), 7.42 – 7.36 (m, 6H), 7.25 (t, $J = 7.7$ Hz, 2H), 7.17 (d, $J = 7.7$ Hz, 2H), 2.22 (s, 3H). $^{13}\text{C}\{^1\text{H}\}$ NMR (CDCl_3 , 175 MHz): δ 169.8, 137.3, 136.5, 130.4, 130.3, 130.2, 129.6,

128.9 (2C), 128.8, 18.5. **IR (KBr, cm⁻¹):** 1709, 1480, 1372. **HRMS (ESI) m/z:** [M+H]⁺ calcd for C₂₄H₂₀NO₂: 354.1489; found: 354.1494.



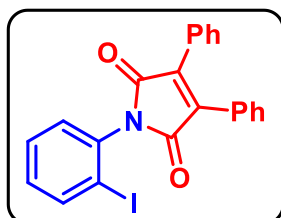
1-(2-chlorophenyl)-3,4-diphenyl-1H-pyrrole-2,5-dione (3ap):

Physical State: yellow solid (14 mg, 78% yield), **R_f** = 0.4 (in 10% EtOAc/hexane). **¹H NMR (CDCl₃, 400 MHz):** δ 7.54 (brd, *J* = 6.4 Hz, 4H), 7.42-7.36 (m, 10H). **¹³C{¹H} NMR (CDCl₃, 175 MHz):** δ 169.2, 136.9, 133.6, 131.0, 130.8, 130.7, 130.4, 130.3, 130.0, 128.9, 128.7, 128.0. **IR (KBr, cm⁻¹):** 1714, 1482. **HRMS (ESI) m/z:** [M+Na]⁺ calcd for C₂₂H₁₄ClNO₂Na: 382.0605; found: 382.0603.



1-(2-bromophenyl)-3,4-diphenyl-1H-pyrrole-2,5-dione (3aq):

Physical State: pale-yellow solid (14 mg, 73% yield), **R_f** = 0.4 (in 10% EtOAc/hexane). **¹H NMR (CDCl₃, 400 MHz):** δ 7.74 (d, *J* = 8.0 Hz, 1H), 7.55 (brd, *J* = 6.4 Hz, 4H), 7.46 (t, *J* = 7.6 Hz, 1H), 7.41-7.33 (m, 8H). **¹³C{¹H} NMR (CDCl₃, 100 MHz):** δ 169.2, 136.8, 133.9, 131.8, 131.2, 131.1, 130.4, 130.3, 128.9, 128.7 (2C), 123.7. **IR (KBr, cm⁻¹):** 1716, 1401. **HRMS (ESI) m/z:** [M+Na]⁺ calcd for C₂₂H₁₄BrNO₂Na: 426.0100; found: 426.0131.



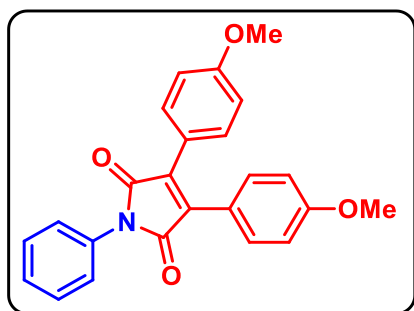
1-(2-iodophenyl)-3,4-diphenyl-1H-pyrrole-2,5-dione (3ar):

Physical State: brown liquid (8 mg, 38% yield), **R_f** = 0.5 (in 10% EtOAc/hexane). **¹H NMR (CDCl₃, 700 MHz):** δ 7.97 (d, *J* = 8.4 Hz, 1H), 7.56-7.55 (m, 3H), 7.49 (t, *J* = 7.7 Hz, 1H), 7.42 – 7.34 (m, 8H), 7.19 (t, *J* = 7.7 Hz, 1H). **¹³C{¹H} NMR (CDCl₃, 175 MHz):** δ 169.1, 140.2, 136.9,

135.6, 131.2, 130.7, 130.4 (2C), 129.6, 128.9, 128.7, 99.3. **IR (KBr, cm⁻¹):** 1714, 1400.

HRMS (ESI) m/z: [M+H]⁺ calcd for C₂₂H₁₅INO₂: 452.0147; found: 452.0148.

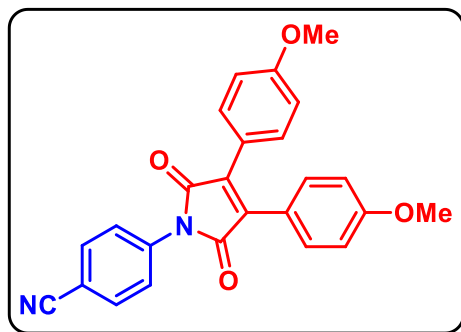
3,4-bis(4-methoxyphenyl)-1-phenyl-1H-pyrrole-2,5-dione (3ba):



Physical State: orange solid (9 mg, 50% yield), **R_f** = 0.4 (in 10% EtOAc/hexane). **¹H NMR (CDCl₃, 700 MHz):** δ 7.53 (d, *J* = 9.1 Hz, 4H), 7.48 (t, *J* = 8.4 Hz, 2H), 7.44 (d, *J* = 7.7 Hz, 2H), 7.36 (t, *J* = 7.7 Hz, 1H), 6.90 (d, *J* = 9.1 Hz, 4H), 3.84 (s, 3H). **¹³C{¹H} NMR**

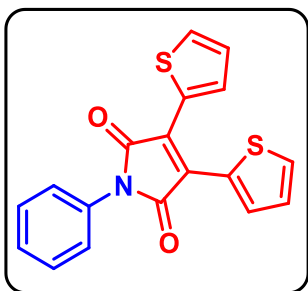
(CDCl₃, 175 MHz): δ 170.4, 161.1, 134.5, 132.3, 131.9, 129.3, 127.9, 126.5, 121.5, 114.5, 55.6. **IR (KBr, cm⁻¹):** 1711, 1633, 1401. **HRMS (ESI) m/z:** [M+Na]⁺ calcd for C₂₄H₁₉NO₄Na: 408.1206; found: 408.1207.

4-(3,4-bis(4-methoxyphenyl)-2,5-dioxo-2,5-dihydro-1H-pyrrol-1-yl) benzonitrile (3bd):



Physical State: orange solid (12 mg, 61% yield), **R_f** = 0.3 (in 20% EtOAc/hexane). **¹H NMR (CDCl₃, 700 MHz):** δ 7.77 (d, *J* = 8.4 Hz, 2H), 7.70 (d, *J* = 8.4 Hz, 2H), 7.52 (d, *J* = 9.1 Hz, 4H), 6.91 (d, *J* = 9.1 Hz, 4H), 3.85 (s, 3H). **¹³C{¹H} NMR**

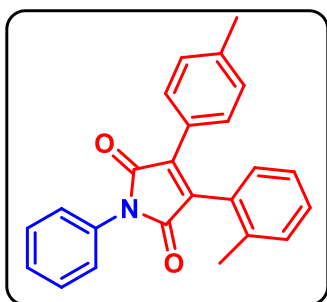
(CDCl₃, 175 MHz): δ 169.6, 161.4, 136.5, 134.8, 133.2, 131.9, 131.4, 126.1, 121.0, 114.6, 111.0, 55.7. **IR (KBr, cm⁻¹):** 2222, 1710, 1401. **HRMS (ESI) m/z:** [M+H]⁺ calcd for C₂₅H₁₉N₂O₄: 411.1345; found: 411.1345.



1-phenyl-3,4-di(thiophen-2-yl)-1H-pyrrole-2,5-dione (3ca):

Physical State: orange solid (7.5 mg, 45% yield), R_f = 0.7 (in 20% EtOAc/hexane). **^1H NMR (CDCl_3 , 400 MHz):** δ 7.88 (d, J = 3.6 Hz, 2H), 7.61 (d, J = 5.2 Hz, 2H), 7.51-7.36 (m, 5H), 7.16 (t, J = 4.0 Hz, 2H). **$^{13}\text{C}\{^1\text{H}\}$ NMR (CDCl_3 , 100**

MHz): δ 169.3, 131.9 (2C), 131.6, 129.8, 129.4, 128.6, 128.2, 128.0, 126.5. **IR (KBr, cm^{-1}):** 1709, 1401. **HRMS (ESI) m/z :** $[\text{M}+\text{H}]^+$ calcd for $\text{C}_{18}\text{H}_{12}\text{NO}_2\text{S}_2$: 338.0304; found: 338.0313.

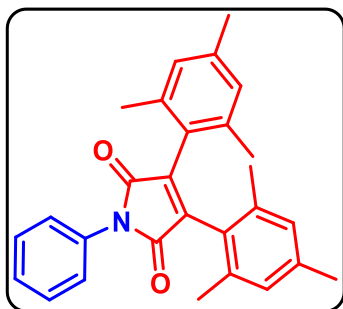


1-phenyl-3-(o-tolyl)-4-(p-tolyl)-1H-pyrrole-2,5-dione

(3da):

Physical State: orange solid (11 mg, 65% yield), R_f = 0.7 (in 10% EtOAc/hexane). **^1H NMR (CDCl_3 , 400 MHz):** δ 7.49-7.48 (m, 4H), 7.42-7.27 (m, 7H), 7.11 (d, J = 8.0 Hz, 2H),

2.33 (s, 3H), 2.10 (s, 3H). **$^{13}\text{C}\{^1\text{H}\}$ NMR (CDCl_3 , 100 MHz):** δ 170.0, 169.8, 141.0, 137.7, 137.1, 132.2, 131.2, 131.1, 130.1, 130.0, 129.9, 129.7, 129.3, 129.2, 128.6, 128.0, 126.5, 126.4, 21.8, 20.5. **IR (KBr, cm^{-1}):** 1711, 1491. **HRMS (ESI) m/z :** $[\text{M}+\text{Na}]^+$ calcd for $\text{C}_{24}\text{H}_{19}\text{NO}_2\text{Na}$: 376.1308; found: 376.1323.

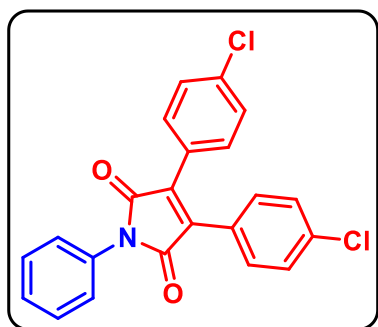


3,4-dimesityl-1-phenyl-1H-pyrrole-2,5-dione (3ea):

Trace product detected in HRMS.

HRMS (ESI) m/z : $[\text{M}+\text{H}]^+$ calcd for $\text{C}_{28}\text{H}_{28}\text{NO}_2$: 410.2120; found: 410.2148.

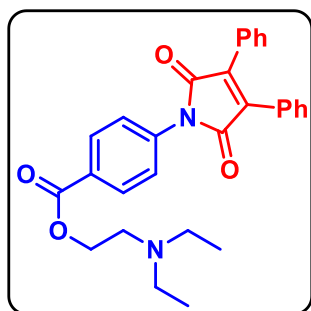
3,4-bis(4-chlorophenyl)-1-phenyl-1H-pyrrole-2,5-dione (3ga):



Physical State: yellow solid (12 mg, 62% yield), R_f = 0.6 (in 10% EtOAc/hexane). **^1H NMR** (CDCl_3 , 400 MHz): δ 7.52-7.41 (m, 9H), 7.38 (d, J = 7.6 Hz, 4H). **$^{13}\text{C}\{^1\text{H}\}$ NMR** (CDCl_3 , 100 MHz): δ 169.4, 136.9, 135.6, 131.8, 131.6, 129.5 (2C), 128.3, 126.9, 126.5.

IR (KBr, cm^{-1}): 1709, 1485, 1390. **HRMS (ESI) m/z :** $[\text{M}+\text{H}]^+$ calcd for $\text{C}_{22}\text{H}_{14}\text{NO}_2\text{Cl}_2$: 394.0396; found: 394.0379.

2-(diethylamino)ethyl-4-(2,5-dioxo-3,4-diphenyl-2,5-dihydro-1H-pyrrol-1-yl)benzoate (5aa):

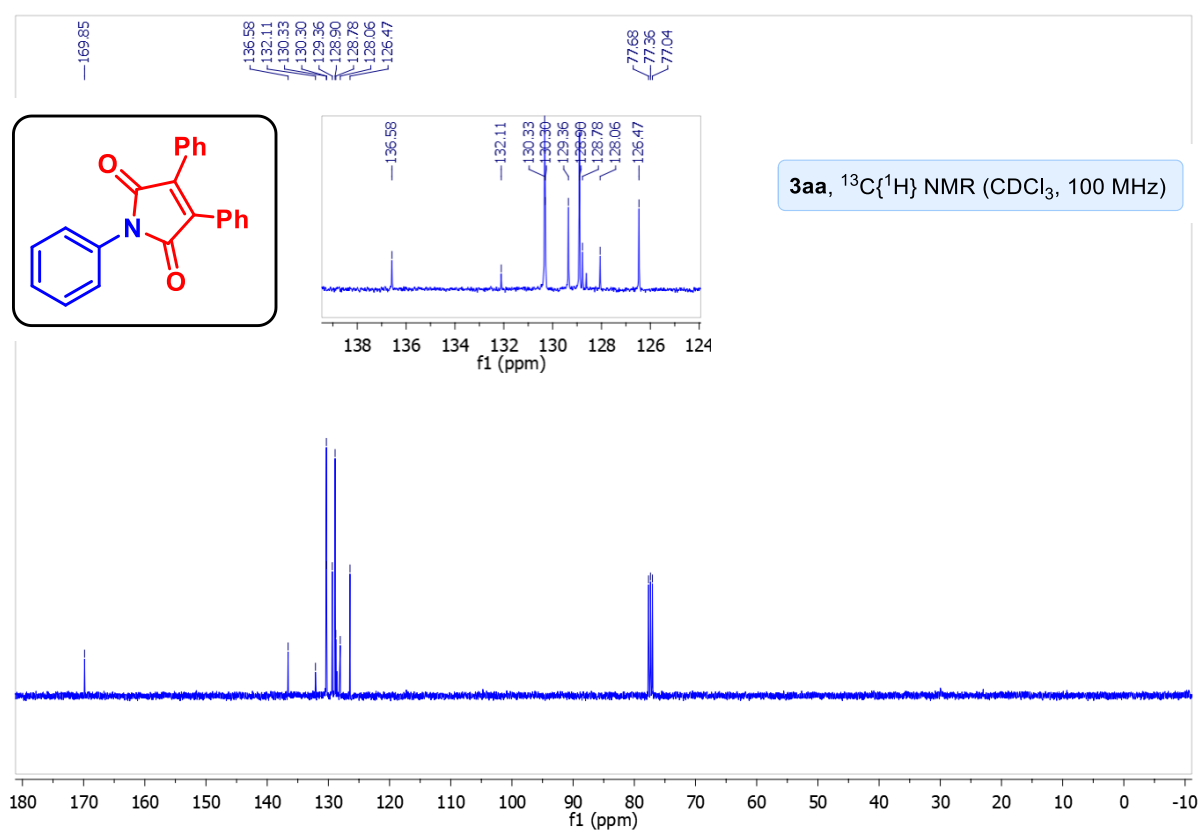
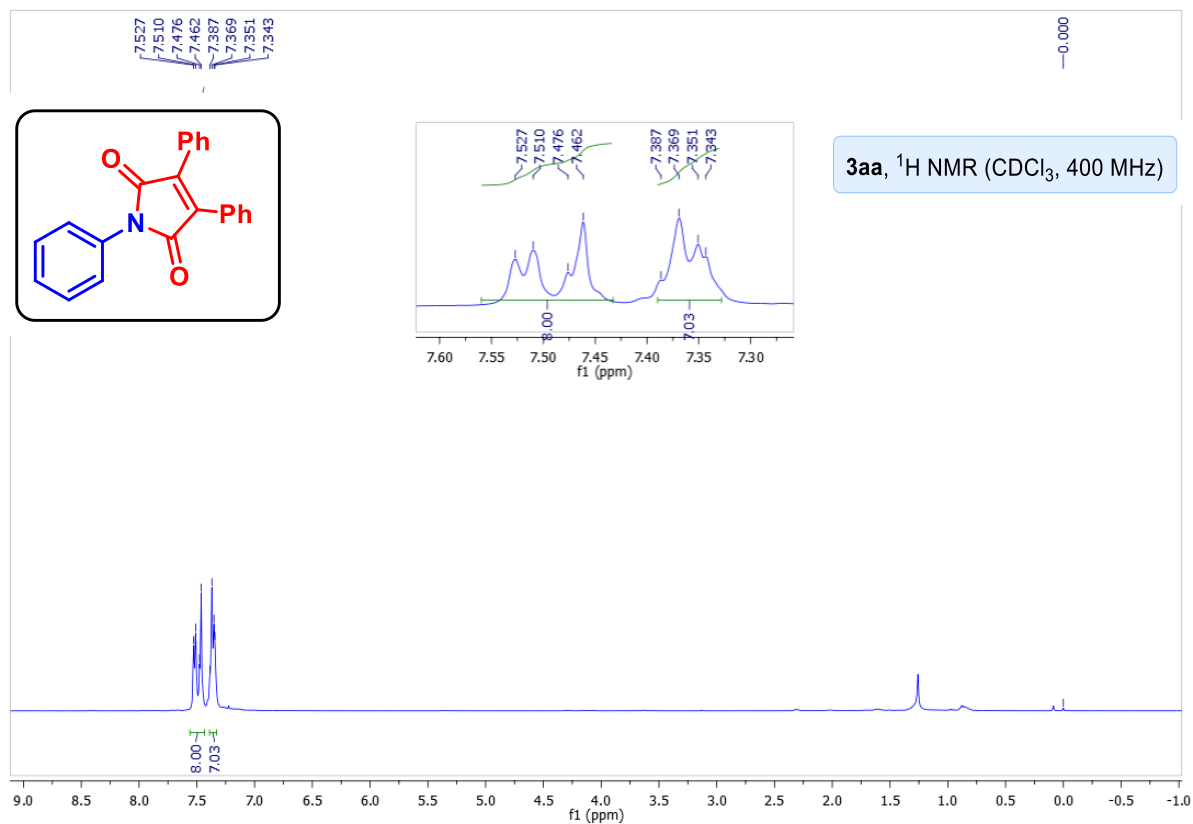


(5aa):

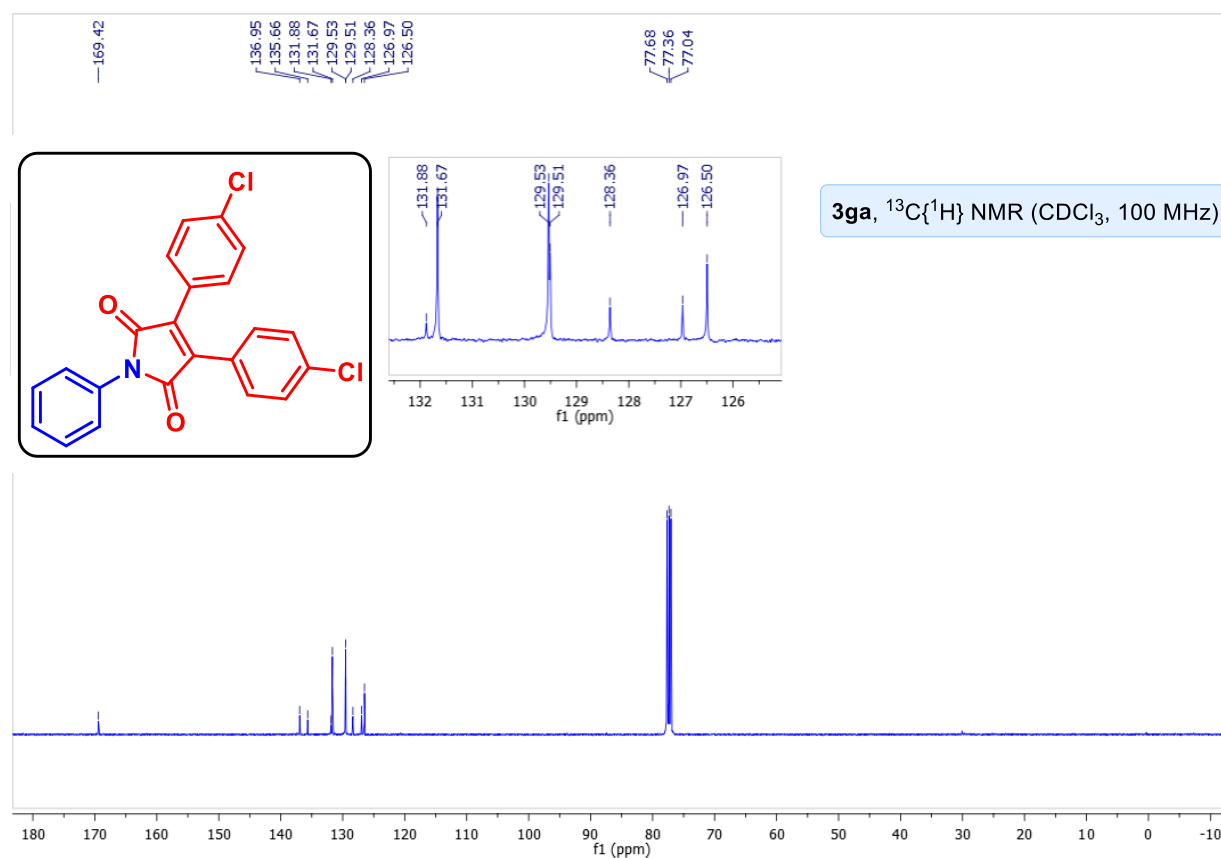
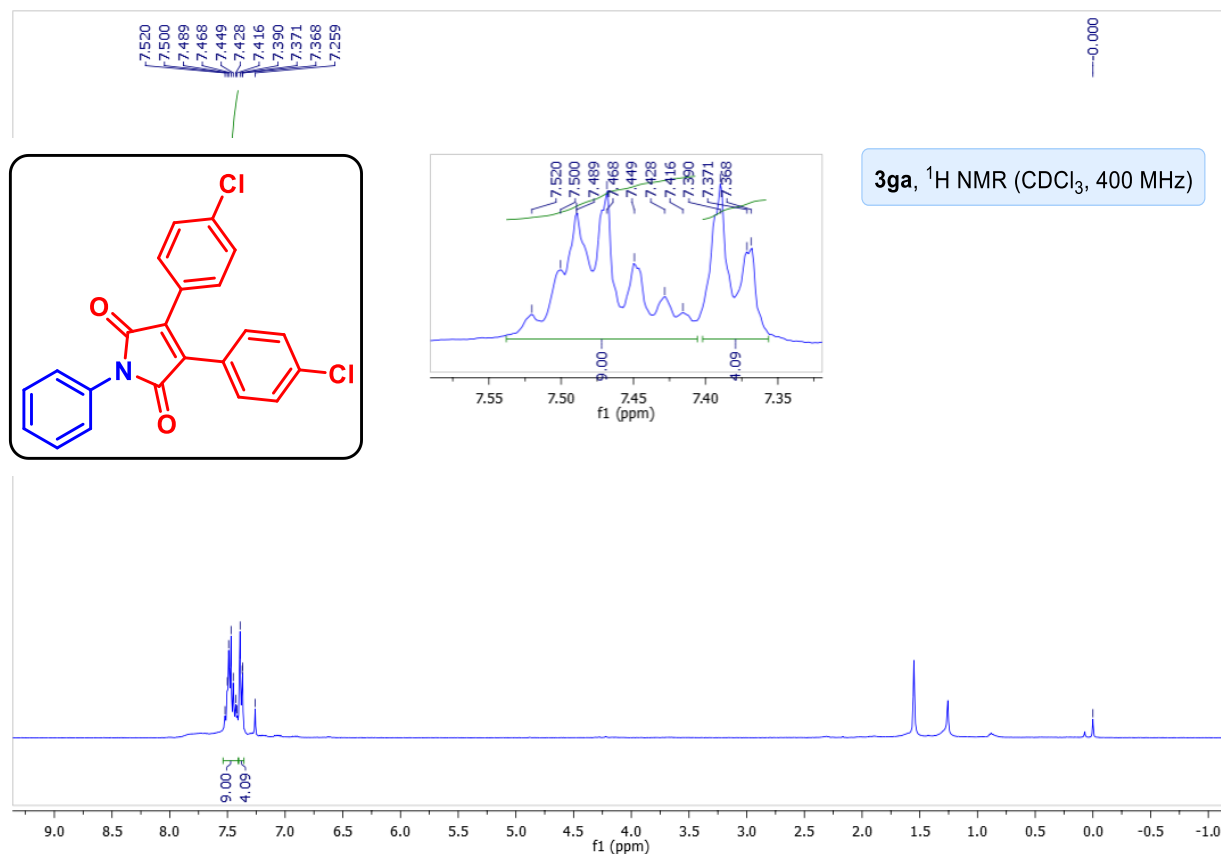
Physical State: yellow liquid (27 mg, 54% yield), R_f = 0.6 (in 10% EtOAc/hexane). **^1H NMR** (CDCl_3 , 400 MHz): δ 8.16 (d, J = 8.8 Hz, 1H), 7.62 (d, J = 8.8 Hz, 7H), 7.53-7.51 (m, 2H), 7.42-7.36 (m, 3H), 4.48 (t, J = 6 Hz, 1H), 2.98 (t, J

= 6 Hz, 1H), 2.75 (q, J = 7.2 Hz, 2H), 1.12 (t, J = 7.2 Hz, 1H). **$^{13}\text{C}\{^1\text{H}\}$ NMR** (CDCl_3 , 100 MHz): δ 169.4, 166.1, 136.8, 136.3, 130.7, 130.5, 130.3, 129.2, 129.0, 128.5, 125.7, 63.0, 50.8, 47.6, 11.5. **IR** (KBr, cm^{-1}): 1774, 1711, 1399. **HRMS (ESI) m/z :** $[\text{M}+\text{H}]^+$ calcd for $\text{C}_{29}\text{H}_{29}\text{N}_2\text{O}_4$: 469.2122; found: 469.2130.

NMR spectra of 1,3,4-triphenyl-1H-pyrrole-2,5-dione (3aa):



NMR spectra of 3,4-bis(4-chlorophenyl)-1-phenyl-1H-pyrrole-2,5-dione (3ga):



X-ray data of 4-(2,5-dioxo-3,4-diphenyl-2,5-dihydro-1H-pyrrol-1-yl)benzonitrile

(3ad): Crystals of the compound 4-(2,5-dioxo-3,4-diphenyl-2,5-dihydro-1H-pyrrol-1-yl)benzonitrile (**3ad**) were obtained after slow evaporation of ethyl acetate. Crystals suited for single crystal X-Ray diffraction measurements were mounted on a glass fiber. Geometry and intensity data were collected with a Rigaku Smartlab X-ray diffractometer equipped with graphite-monochromated Mo-K α radiation ($\lambda = 0.71073$ Å, multilayer optics). Temperature was controlled using an Oxford Cryostream 700 instrument. Intensities were integrated with SAINT and SMART software packages and corrected for absorption with SADABS. The structure was solved by direct methods and refined on F² with SHELXL-97 using Olex-2 software.

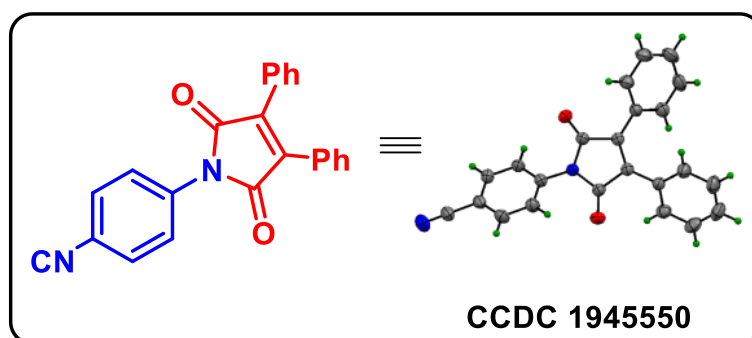
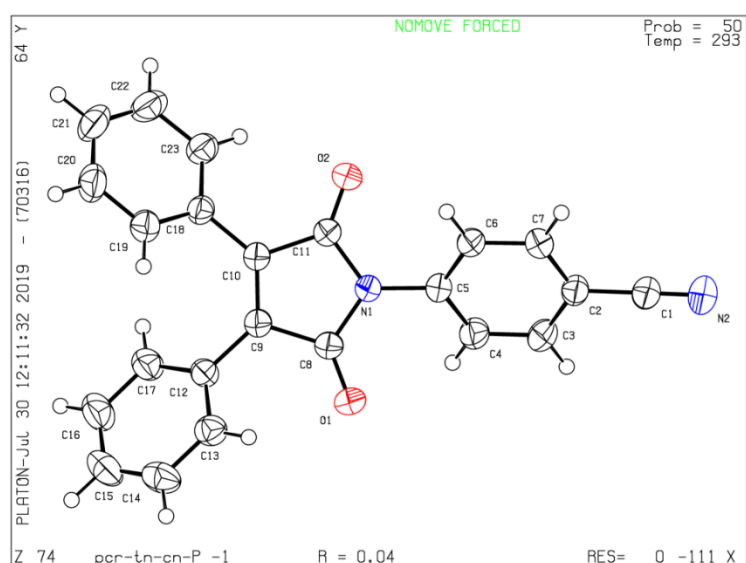


Figure 2.1 ORTEP diagram of **3ad** with 50% ellipsoid probability



2.6 REFERENCES

1. Jones, W. D. The Fall of the C-C Bond. *Nature* **1993**, *364*, 676–677. (b) Dyker, G. Transition Metal Catalyzed Coupling Reactions under C-H Activation. *Angew. Chem., Int. Ed.* **1999**, *38*, 1698–1712. (c) Kakiuchi, F.; Murai, S. Activation of C-H Bonds: Catalytic Reactions. In *Activation of Unreactive Bonds and Organic Synthesis*; Murai, S., Alper, H., Gossage, R. A., Grushin, V. V., Hidai, M., Ito, Y., Jones, W. D., Kakiuchi, F., van Koten, G., Lin, Y. S., et al., Eds.; Springer: Berlin, Heidelberg, 1999; pp 47–79. (d) Ritleng, V.; Sirlin, C.; Pfeffer, M. Ru, Rh, and Pd-Catalyzed C-C Bond Formation Involving C-H Activation and Addition on Unsaturated Substrates: Reactions and Mechanistic Aspects. *Chem. Rev.* **2002**, *102*, 1731–1770. (e) Jun, C.-H.; Moon, C. W.; Lee, H.; Lee, D.Y. Chelation-Assisted Carbon-Carbon Bond Activation by Rh (I) Catalysts. *J. Mol. Catal. A: Chem.* **2002**, *189*, 145–156. (f) Godula, K.; Sames, D. C-H Bond Functionalization in Complex Organic Synthesis. *Science* **2006**, *312*, 67–72. (g) Kakiuchi, F. Catalytic Addition of C-H Bonds to C-C Multiple Bonds. In *Directed Metallation*; Chatani, N., Ed.; Springer: Berlin, Heidelberg, 2007; pp 1–33. (h) Jun, C.-H.; Park, J.-W. Directed C-C Bond Activation by Transition Metal Complexes. In *Directed Metallation*; Chatani, N., Ed.; Springer: Berlin, Heidelberg, 2007; pp 117–143. (i) Noisier, A. F. M.; Brimble, M. A. C-H Functionalization in the Synthesis of Amino Acids and Peptides. *Chem. Rev.* **2014**, *114*, 8775–8806.
2. (a) Seiser, T.; Saget, T.; Tran, D. N.; Cramer, N. Cyclobutanes in Catalysis. *Angew. Chem., Int. Ed.* **2011**, *50*, 7740–7752. (b) Murakami, M.; Matsuda, T. Metal-Catalysed Cleavage of Carbon-Carbon Bonds. *Chem. Commun.* **2011**, *47*, 1100–1105. (c) Ruhland, K. Transition Metal-Mediated Cleavage and Activation of C-C Single Bonds. *Eur. J. Org. Chem.* **2012**, *14*, 2683–2706. (d) Chen, F.; Wang, T.; Jiao, N. Recent Advances in Transition Metal-Catalyzed Functionalization of Unstrained Carbon-Carbon Bonds. *Chem. Rev.* **2014**, *114*, 8613–8661. (e) Souillart, L.; Cramer, N. Catalytic C-C Bond Activations via Oxidative Addition to Transition Metals. *Chem. Rev.* **2015**, *115*, 9410–9464.
3. Jun, C.-H. Transition Metal-Catalyzed Carbon-Carbon Bond Activation. *Chem. Soc. Rev.* **2004**, *33*, 610–618.
4. C. F. H. Tipper, Some Platinous-Cyclopropane Complexes *J. Chem. Soc.* **1955**, 2045–2046.
5. (a) Dreis, A. M.; Douglas, C. J. Catalytic Carbon-Carbon σ Bond Activation: An Intramolecular Carbo-Acylation Reaction with Acylquinolines. *J. Am. Chem. Soc.* **2009**, *131*, 412–413. (b) Wang, J.; Chen, W.; Zuo, S.; Liu, L.; Zhang, X.; Wang, J. Direct Exchange of a Ketone Methyl or Aryl Group to Another Aryl Group through C-C Bond Activation Assisted by Rhodium Chelation. *Angew. Chem., Int. Ed.* **2012**, *51*, 12334–12338. (c) Dennis, J. M.; Compagner, C. T.; Dorn, S. K.; Johnson, J. B. Rhodium-Catalyzed Interconversion of Quinoliny Ketones with Boronic Acids via C-C Bond Activation. *Org. Lett.* **2016**, *18*, 3334–3337. (d) Xia, Y.; Lu, G.; Liu, P.; Dong, G. Catalytic activation of carbon-carbon bonds in cyclopentanones. *Nature* **2016**, *539*, 546–550. (e) Kim, D.-S.; Park, W.-J.; Jun, C.-H. Metal-Organic Cooperative Catalysis in C-H and C-C Bond Activation. *Chem. Rev.* **2017**, *117*, 8977–9015. (f) Fumagalli, G.; Stanton, S.; Bower, J. F. Recent Methodologies That Exploit C-C Single-Bond Cleavage of Strained Ring Systems by Transition Metal Complexes. *Chem. Rev.* **2017**, *117*, 9404–9432. (g) Xia, Y.; Wang, J.; Dong, G. Suzuki-Miyaura Coupling of Simple Ketones via Activation of Unstrained

- Carbon-Carbon Bonds. *J. Am. Chem. Soc.* **2018**, *140*, 5347–5351. (h) Xu, Y.; Qi, X.; Zheng, P.; Berti, C. C.; Liu, P.; Dong, G. Deacylative transformations of ketones via aromatization-promoted C–C bond activation. *Nature* **2019**, *567*, 373–378.
6. (a) C–C Bond Activation; Dong, G., Ed.; Springer: Berlin, 2014; Topics in Current Chemistry 346. (b) Chen, P.; Billett, B. A.; Tsukamoto, T.; Dong, G. Cut and Sew” Transformations via Transition Metal-Catalyzed Carbon-Carbon Bond Activation. *ACS Catal.* **2017**, *7*, 1340–1360. (c) Deng, L.; Chen, M.; Dong, G. Concise Synthesis of (–)-Cycloclavine and (–)-5-epi-Cycloclavine via Asymmetric C–C Activation. *J. Am. Chem. Soc.* **2018**, *140*, 9652–9658.
 7. (a) Suggs, J. W.; Jun, C.-H. Directed Cleavage of Carbon-Carbon Bonds by Transition Metals: the α -Bonds of Ketones. *J. Am. Chem. Soc.* **1984**, *106*, 3054–3056. (b) Suggs, J. W.; Jun, C.-H. Metal-Catalyzed Alkyl Ketone to Ethyl Ketone Conversions in Chelating Ketones via Carbon-Carbon Bond Cleavage. *J. Chem. Soc., Chem. Commun.* **1985**, 92–93. (c) Suggs, J. W.; Jun, C.-H. Synthesis of a Chiral Rhodium Alkyl via Metal Insertion into an Unstrained C–C bond and Use of the Rate of Racemization at Carbon to Obtain a Rhodium-Carbon Bond Dissociation Energy. *J. Am. Chem. Soc.* **1986**, *108*, 4679–4681. (d) Jun, C.-H.; Lee, H. Catalytic Carbon-Carbon Bond Activation of Unstrained Ketone by Soluble Transition-Metal Complex. *J. Am. Chem. Soc.* **1999**, *121*, 880–881. (e) Jun, C.-H.; Lee, D.-Y.; Lee, H.; Hong, J.-B. A Highly Active Catalyst System for Intermolecular Hydroacylation. *Angew. Chem., Int. Ed.* **2000**, *39*, 3070–3072. (f) Jun, C.-H.; Lee, H.; Lim, S.-G. The C–C Bond Activation and Skeletal Rearrangement of Cycloalkanone Imine by Rh (I) Catalysts. *J. Am. Chem. Soc.* **2001**, *123*, 751–752. (g) Jun, C.-H.; Lee, H.; Moon, C. W.; Hong, H.-S. Cleavage of Carbon-Carbon Triple Bond of Alkyne via Hydroiminoacylation by Rh (I) catalyst. *J. Am. Chem. Soc.* **2001**, *123*, 8600–8601.
 8. (a) Shaw, M. H.; Melikhova, E. Y.; Kloer, D. P.; Whittingham, W. G.; Bower, J. F. Directing Group Enhanced Carbonylative Ring Expansions of Amino-Substituted Cyclopropanes: Rhodium-Catalyzed Multicomponent Synthesis of N-Heterobicyclic Enones. *J. Am. Chem. Soc.* **2013**, *135*, 4992–4995. (b) Shaw, M. H.; McCreanor, N. G.; Whittingham, W. G.; Bower, J. F. Reversible C–C Bond Activation Enables Stereocontrol in Rh-Catalyzed Carbonylative Cycloadditions of Aminocyclopropanes. *J. Am. Chem. Soc.* **2015**, *137*, 463–468. (c) Shaw, M. H.; Croft, R. A.; Whittingham, W. G.; Bower, J. F. Modular Access to Substituted Azocanes via a Rhodium-Catalyzed Cycloaddition–Fragmentation Strategy. *J. Am. Chem. Soc.* **2015**, *137*, 8054–8057. (d) McCreanor, N. G.; Stanton, S.; Bower, J. F. Capture–Collapse Heterocyclization: 1,3-Diazepanes by C–N Reductive Elimination from Rhodacyclopentanones. *J. Am. Chem. Soc.* **2016**, *138*, 11465–11468. (e) Wang, G.-W.; Bower, J. F. Modular Access to Azepines by Directed Carbonylative C–C Bond Activation of Aminocyclopropanes. *J. Am. Chem. Soc.* **2018**, *140*, 2743–2747. (f) Dalling, A. G.; Yamauchi, T.; McCreanor, N. G.; Cox, L.; Bower, J. F. Carbonylative C–C Bond Activation of Electron-Poor Cyclopropanes: Rhodium-Catalyzed (3 + 1 + 2) Cycloadditions of Cyclopropylamides. *Angew. Chem., Int. Ed.* **2019**, *58*, 221–225 (g) Ma, X. F.; Hazelden, I. R.; Langer, T.; Munday, R. H.; Bower, J. F. Enantioselective aza-heck cyclizations of N-(tosyloxy)carbamates: Synthesis of pyrrolidines and piperidines. *J. Am. Chem. Soc.* **2019**, *141*, 3356–3360.
 9. (a) Vasseur, A.; Marek, I. Merging allylic C–H bond activation and C–C bond cleavage *en route* to the formation of a quaternary carbon stereocenter in acyclic systems. *Nat. Protoc.* **2017**, *12*, 74–87. (b) Nairoukh, Z.; Cormier, M.; Marek, I. Merging C–H and C–C bond cleavage in organic synthesis. *Nature Rev. Chem.* **2017**, *1*, 74–87. (c) Bruffaerts, J.; Vasseur, A.; Singh, S.; Masarwa, A.; Didier, D.; Oskar, L.;

- Perrin, L.; Eisenstein, O.; Marek, I. Zirconocene-Mediated Selective C-C Bond Cleavage of Strained Carbocycles: Scope and Mechanism. *J. Org. Chem.* **2018**, *83*, 3497–3515.
10. Jiao, L.; Yuan, C.; Yu, Z.-X. Tandem Rh (I)-Catalyzed [(5 + 2)+1] Cycloaddition/Aldol Reaction for the Construction of Linear Triquinane Skeleton: Total Syntheses of (±)-Hirsutene and (±)-1- Desoxyhypnophilin. *J. Am. Chem. Soc.* **2008**, *130*, 4421–4430.
 11. Li, S.; Shi, P.; Liu, R.-H.; Hu, X.-H.; Loh, T.-P. Cobalt-Catalyzed N–O and C–C Bond Cleavage in 1,2-Oxazetidines: Solvent-Controlled C–H Aminomethylation and Hydroxymethylation of Heteroarenes. *Org. Lett.* **2019**, *21*, 1602–1606.
 12. For selected recent reports, see: (a) Wender, P. A.; Fournogerakis, D. N.; Jeffreys, M. S.; Quiroz, R. V.; Inagaki, F.; Pfaffenbach, M. Structural Complexity through Multicomponent Cycloaddition Cascades Enabled by Dual-Purpose, Reactivity Regenerating 1,2,3-Triene Equivalents. *Nat. Chem.* **2014**, *6*, 448–452. (b) Hong, X.; Stevens, M. C.; Liu, P.; Wender, P. A.; Houk, K. N. Reactivity and Chemoselectivity of Allenes in Rh(I)-Catalyzed Intermolecular (5 + 2) Cycloadditions with Vinylcyclopropanes: Allene-Mediated Rhodacycle Formation Can Poison Rh(I)-Catalyzed Cycloadditions. *J. Am. Chem. Soc.* **2014**, *136*, 17273–17283. (c) Liu, C.-H.; Yu, Z.-X.; Rhodium (I)-Catalyzed Bridged [5 + 2] Cycloaddition of cis-Allene-vinylcyclopropanes to Synthesize the Bicyclo[4.3.1]decane Skeleton. *Angew. Chem., Int. Ed.* **2017**, *56*, 8667–8671. (d) Yang, J.; Xu, W.; Cui, Q.; Fan, X.; Wang, L.-N.; Yu, Z.-X. Asymmetric Total Synthesis of (–)-Clovan-2,9-dione Using Rh(I)-Catalyzed [3 + 2 + 1] Cycloaddition of 1-Yne-vinylcyclopropane and CO. *Org. Lett.* **2017**, *19*, 6040–6043.
 13. For selected recent reports, see: (a) Chen, K.; Zhu, Z.-Z.; Zhang, Y.-S.; Tang, X.-Y.; Shi, M. Rhodium (II)-Catalyzed Intramolecular Cycloisomerizations of Methylenecyclopropanes with N-Sulfonyl 1,2,3-Triazoles. *Angew. Chem., Int. Ed.* **2014**, *53*, 6645–6649. (b) Evans, P. A.; Negru, D. E.; Shang, D. Rhodium-Catalyzed [(3 + 2) + 2] Carbocyclization of Alkynylidenecyclopropanes with Substituted Allenes: Stereoselective Construction of Tri- and Tetrasubstituted Exocyclic Olefins. *Angew. Chem., Int. Ed.* **2015**, *54*, 4768–4772. (c) Yang, S.; Rui, K.-H.; Tang, X.-Y.; Xu, Q.; Shi, M. Rhodium/Silver Synergistic Catalysis in Highly Enantioselective Cycloisomerization/Cross Coupling of KetoVinylidenecyclopropanes with Terminal Alkynes. *J. Am. Chem. Soc.* **2017**, *139*, 5957–5964. (d) Su, Y.; Inglesby, P. A.; Evans, P. A. Intramolecular Thioether Migration in the Rhodium-Catalyzed Ene-Cycloisomerization of Alkenylidenecyclopropanes by a Metal-Mediated β-Sulfide Elimination. *Angew. Chem., Int. Ed.* **2018**, *57*, 673–677. (e) Verdugo, F.; Villarino, L.; Duran, J.; Gullías, M.; Mascareñas, J. L.; Lopez, F. Enantioselective Palladium-Catalyzed [3C + 2C] and [4C + 3C] Intramolecular Cycloadditions of Alkylidenecyclopropanes. *ACS Catal.* **2018**, *8*, 6100–6105.
 14. (a) Liu, L.; Montgomery, J. Dimerization of Cyclopropyl Ketones and Crossed Reactions of Cyclopropyl Ketones with Enones as an Entry to Five-Membered Rings. *J. Am. Chem. Soc.* **2006**, *128*, 5348–5349. (b) Ogoshi, S.; Nagata, M.; Kurosawa, H. Formation of Nickeladihydropyran by Oxidative Addition of Cyclopropyl Ketone. Key Intermediate in Nickel-Catalyzed Cycloaddition. *J. Am. Chem. Soc.* **2006**, *128*, 5350–5351. (c) Sumida, Y.; Yorimitsu, H.; Oshima, K. Palladium-Catalyzed Preparation of Silyl Enolates from α,β-Unsaturated Ketones or Cyclopropyl Ketones with Hydrosilanes. *J. Org. Chem.* **2009**, *74*, 7986–7989. (d) Sumida, Y.; Yorimitsu, H.; Oshima, K. Nickel-Catalyzed Borylation of Aryl Cyclopropyl Ketones with Bis(pinacolato)diboron to Synthesize 4-Oxoalkylboronates. *J. Org. Chem.* **2009**, *74*,

- 3196-3198. (e) Tamaki, T.; Ohashi, M.; Ogoshi, S. [3 + 2] Cycloaddition Reaction of Cyclopropyl Ketones with Alkynes Catalyzed by Nickel/Dimethylaluminum Chloride. *Angew. Chem., Int. Ed.* **2011**, *50*, 12067–12070.
15. (a) Liu, Q.-S.; Wang, D.-Y.; Yang, Z.-J.; Luan, Y.-X.; Yang, J.-F.; Li, J.-F.; Pu, Y.-G.; Ye, M. Ni–Al Bimetallic Catalyzed Enantioselective Cycloaddition of Cyclopropyl Carboxamide with Alkyne. *J. Am. Chem. Soc.* **2017**, *139*, 18150–18153. (b) Wang, Y.-X.; Ye, M. Recent Advances in Ni–Al Bimetallic Catalysis for Unreactive Bond Transformation. *Sci. China: Chem.* **2018**, *61*, 1004–1013.
16. (a) Kamitani, A.; Chatani, N.; Morimoto, T.; Murai, S. Carbonylative [5 + 1] Cycloaddition of Cyclopropyl Imines Catalyzed by Ruthenium Carbonyl Complex. *J. Org. Chem.* **2000**, *65*, 9230–9233. (b) Wender, P. A.; Pedersen, T. M.; Scanio, M. J. C. Transition Metal-Catalyzed Hetero-[5 + 2] Cycloadditions of Cyclopropyl Imines and Alkynes: Dihydroazepines from Simple, Readily Available Starting Materials. *J. Am. Chem. Soc.* **2002**, *124*, 15154–15155. (c) Liu, L.; Montgomery, J. [3 + 2] Cycloaddition Reactions of Cyclopropyl Imines and Enones. *Org. Lett.* **2007**, *9*, 3885–3887. (d) Tamaki, T.; Ohashi, M.; Ogoshi, S. Formation of Six-membered Aza-nickelacycles by Oxidative Addition of Cyclopropyl Imines to Nickel (0). *Chem. Lett.* **2011**, *40*, 248–249. (e) Chen, G.-Q.; Zhang, X.-N.; Wei, Y.; Tang, X.-Y.; Shi, M. Catalyst-Dependent Divergent Synthesis of Pyrroles from 3-Alkynyl Imine Derivatives: A Noncarbonylative and Carbonylative Approach. *Angew. Chem., Int. Ed.* **2014**, *53*, 8492–8497.
17. (a) Baba, A.; Ohshiro, Y.; Agawa, T. Reactions of diphenylcyclopropenone with ketenes in the presence of nickel tetracarbonyl. *J. Organomet. Chem.* **1976**, *110*, 121–127. (b) Wender, P. A.; Paxton, T. J.; Williams, T. J. Cyclopentadienone Synthesis by Rhodium(I)-Catalyzed [3 + 2] Cycloaddition Reactions of Cyclopropenones and Alkynes. *J. Am. Chem. Soc.* **2006**, *128*, 14814–14815. (c) Matsuda, T.; Sakurai, Y. Palladium-Catalyzed Ring-Opening Alkynylation of Cyclopropenones. *Eur. J. Org. Chem.* **2013**, *2013*, 4219–4222. (d) Xu, J.; Cao, J.; Fang, C.; Lu, T.; Du, D. Organocatalytic C–C Bond Activation of Cyclopropenones for the Ring-Opening Formal [3+2] Cycloaddition with Isatins. *Org. Chem. Front.* **2017**, *4*, 560–564. (e) Kong, L. H.; Zhou, X.-K.; Xu, Y.-W.; Li, X.-W. Rhodium (III) Catalyzed Acylation of C (sp³)-H Bonds with Cyclopropenones. *Org. Lett.* **2017**, *19*, 3644–3647. (f) Ren, J.-T.; Wang, J.-X.; Tian, H.; Xu, J.-L.; Hu, H.; Aslam, M.; Sun, M. Ag(I)-Catalyzed [3 + 2]-Annulation of Cyclopropenones and Formamides via C–C Bond Cleavage. *Org. Lett.* **2018**, *20*, 6636–6639. (g) Zhao, W.-T.; Gao, F.; Zhao, D.; Intermolecular σ -Bond Cross Exchange Reaction between Cyclopropenones and (Benzo)silacyclobutanes: Straightforward Access towards Sila-(benzo)cycloheptenones. *Angew. Chem.* **2018**, *130*, 6437–6440. (h) While preparation of this work Chatani group recently published metal catalyzed ring opening reaction of cyclopropenone. Haito, A.; Chatani, N.; Rh (I)-Catalyzed [3+2] annulation reactions of cyclopropenones with amides. *Chem. Commun.*, **2019**, *55*, 5740–5742. (i) Deng, L.; Dong, G. Carbon–Carbon Bond Activation of Ketones. *Trends in Chemistry*. Cell Press **2020**. <https://doi.org/10.1016/j.trechm.2019.12.002>.
18. Wong, W.; Singer, S. J.; Pitts, W. D.; Watkins, S. F.; Baddley, W. H. Preparation and X-ray Crystallographic Determination of the Structure of the Platinacyclobutenone [(C₆H₅)₃P]₂Pt[OC₃(C₆H₅)₂]. *J. Chem. Soc., Chem. Commun.* **1972**, 672–673.
19. Song, L.; Arif, A. M.; Stang, P. J. Interaction of Rhodium(I) with Cyclopropenones: Decarbonylation and Formation of 1-Rhodacyclopentene-2,5-diones and Cationic Oxygen σ -Bound Cyclopropenone Complexes. X-ray Crystal Structure of trans-Carbonylbis(triphenylphosphine)(di-tert-

- butylcyclopropenone)rhodiumTrifluoromethane sulfonate. *Organometallics*, **1990**, *9*, 2792-2797.
20. (a) Wu, W.-C.; Yeh, H.-C.; Chan, L.-H.; Chen, C.-T.; Red Organic Light-Emitting Diodes with a Non-doping Amorphous Red Emitter. *Adv. Mater.* **2002**, *14*, 1072-1075. (b) Jang, M. E.; Yasuda, T.; Lee, J.; Lee, S. Y.; Adachi, C. Organic Light-Emitting Diodes Based on Donor-Substituted Phthalimide and Maleimide Fluorophores. *Chem. Lett.* **2015**, *44*, 1248–1250.
 21. (a) Coghlan, M.; Culbert, A.; Cross, D.; Corcoran, S.; Yates, J.; Pearce, N.; Rausch, O.; Murphy, G.; Carter, P.; Cox, L.; Mills, D.; Brown, M.; Haigh, D.; Ward, R.; Smith, D.; Murray, K.; Reith, A.; Holder, J.; Selective small molecule inhibitors of glycogen synthase kinase-3 modulate glycogen metabolism and gene transcription. *Chem. Biol.* **2000**, *7*, 793-803. (b) Cheng, C.-F.; Lai, Z.-C.; Lee, Y.-J.; Total synthesis of (±)-camphorataimides and (±)-himanimides by NaBH₄/Ni(OAc)₂ or Zn/AcOH stereoselective reduction. *Tetrahedron* **2008**, *64*, 4347-4353. (c) Doi, I.; Tsuji, G.; Kawakami, K.; Nakagawa, O.; Taniguchi Y.; Sasaki, S.; The Spermine–Bisaryl Conjugate as a Potent Inducer of B- to Z-DNA Transition. *Chem. Eur. J.* **2010**, *16*, 11993-11999. (d) Sortino, M.; Garibotto, F.; Filho, V. C.; Gupta, M.; Enriz, R.; Zacchino, S.; Antifungal, cytotoxic and SAR studies of a series of N-alkyl, N-aryl and N-alkylphenyl-1,4-pyrrolediones and related compounds. *Bioorg. Med. Chem.* **2011**, *19*, 2823-2834. (e) Nirogi, R.; Dwarampudi, A.; Kambhampati, R.; Bhatta, V.; Kota, L.; Shinde, A.; Badange, R.; Jayarajan, P.; Bhyrapuneni, G.; Dubey, P. K.; Rigidized 1-aryl sulfonyl tryptamines: Synthesis and pharmacological evaluation as 5-HT₆ receptor ligands. *Bioorg. Med. Chem. Lett.* **2011**, *21*, 4577-4580.
 22. (a) Kondo, T.; Nomura, M.; Ura, Y.; Wada, K.; Mitsudo, T.-A. Ruthenium-catalyzed [2+ 2+ 1] cocyclization of isocyanates, alkynes, and CO enables the rapid synthesis of polysubstituted maleimides. *J. Am. Chem. Soc.* **2006**, *128*, 14816-14817. (b) Mathur, P.; Joshi, R. K.; Rai, D. K.; Jha, B.; Mobin, S. M. One Pot Synthesis of Maleimide and Hydantoin by Fe(CO)₅ Catalyzed [2 + 2 + 1] Co-Cyclization of Acetylene, Isocyanate and CO. *Dalton Trans.* **2012**, *41*, 5045–5054.
 23. (a) Hou, J.; Xie, J.; Zhou, Q.; Palladium-Catalyzed Hydrocarboxylation of Alkynes with Formic Acid. *Angew. Chem., Int. Ed.* **2015**, *54*, 6302-6305. (b) Qi, X.; Li, H.-P.; W, F.-X.; Palladium-Catalyzed One-Pot Carbonylative Sonogashira Reaction Employing Formic acid as the CO Source. *Chem. Asian J.* **2016**, *11*, 2453 – 2457. (c) Fu, M.; Shang, R.; Cheng, W.; Fu, Y. Nickel-Catalyzed RegioAnd Stereoselective Hydrocarboxylation of Alkynes with Formic Acid through Catalytic CO Recycling. *ACS Catal.* **2016**, *6*, 2501–2505. (d) Hou, J.; Yuan, M.; Xie, J.; Zhou, Q. Nickel-Catalyzed Hydrocarboxylation of Alkynes with Formic Acid. *Green Chem.* **2016**, *18*, 2981–2984. (e) Wu, F.- P.; Peng, J.-B.; Qi, X.; Wu, X.-F. Palladium-catalyzed Carbonylative Transformation of Organic Halides with Formic Acid as the Coupling Partner and CO Source: Synthesis of Carboxylic Acids. *J. Org. Chem.* **2017**, *82*, 9710–9714.
 24. (a) Ni, J.; Li, J.; Fan, Z.; Zhang, A. Cobalt-Catalyzed Carbonylation of C(sp²)–H Bonds with Azodicarboxylate as the Carbonyl Source. *Org. Lett.* **2016**, *18*, 5960–5963. (b) Usman, M.; Zhang, X.-W.; Wu, D.; Guan, Z.-H.; Liu, W.-B.; Application of dialkyl azodicarboxylate frameworks featuring multi-functional properties. *Org. Chem. Front.* **2019**, *6*, 1905–1928.
 25. (a) Jeffery, T.; Galland, J.-C. *Tetrahedron Lett.* **1994**, *35*, 4103-4106. (b) Pryjomska-Ray, I.; Trzeciak, A. M.; Ziolkowski, J. J. *J. Mol. Catal. A: Chem.* **2006**, *257*, 3-8.
 26. (a) Hartwig, J.-F.; Bergman, R.-G.; Andersen R.-A.; Insertion Reactions of CO and CO₂ with Ruthenium Benzyl, Arylamido, and Aryloxide Complexes: A Comparison

- of the Reactivity of Ruthenium-Carbon, Ruthenium-Nitrogen, and Ruthenium-Oxygen Bonds. *J. Am. Chem. Soc.* **1991**, *113*, 6499-6508. (b) Hanna, T. A.; Baranger, A. M.; Bergman, R. G.; Reactivity of Zirconocene Azametallacyclobutenes: Insertion of Aldehydes, Carbon Monoxide, and Formation of α,β -Unsaturated Imines. Formation and Trapping of $[\text{Cp}_2\text{Zr}=\text{O}]$ in a $[4 + 2]$ Retrocycloaddition *J. Org. Chem.* **1996**, *61*, 4532–4541. (c) Kim, M.; Mishra, N. K.; Park, J.; Han, S.; Shin, Y.; Sharma, S.; Lee, Y.; Lee, E.-K.; Kwak, J. H.; Kim, I. S. Decarboxylative acylation of indolines with α -keto acids under palladium catalysis: a facile strategy for the synthesis of 7-substituted indoles. *Chem. Commun.* **2014**, *50*, 14249–14252. (d) Mandal, S.; Bera, T.; Dubey, G.; Saha, J.; Laha, J. K. Uses of $\text{K}_2\text{S}_2\text{O}_8$ in Metal-Catalyzed and Metal-Free Oxidative Transformations. *ACS Catal.* **2018**, *8*, 5085-5144. (e) Luo, Y.; Shan, C.; Liu, S.; Zhang, T.; Zhu, L.; Zhong, K.; Bai, R.; Lan, Y. Oxidative Addition Promoted C-C Bond Cleavage in Rh-Mediated Cyclopropanone Activation: A DFT Study. *ACS Catal.* **2019**, *9*, 10876–10886.
27. Gottlieb, H. E.; Kotlyar, V.; Nudelman, A. NMR chemical shifts of common laboratory solvents as trace impurities. *J. Org. Chem.* **1997**, *62*, 7512.
 28. Yuan, Y. C.; Kamaraj, R.; Bruneau, C.; Labasque, T.; Roisnel, T.; Gramage-Doria, R. Unmasking Amides: Ruthenium-Catalyzed Protodecarbonylation of N-Substituted Phthalimide Derivatives. *Org. Lett.* **2017**, *19*, 6404–6407.
 29. Li, B.; Lan, J.; Wu, D.; You, J. Rhodium(III)-Catalyzed orthoHeteroarylation of Phenols through Internal Oxidative C–H Activation: Rapid Screening of Single-Molecular White-Light-Emitting Materials. *Angew. Chem., Int. Ed.* **2015**, *54*, 14008–14012.
 30. Bernardes, G. J. L.; Chalker, J. M.; Errey, J. C.; Davis, B. G. Facile Conversion of Cysteine and Alkyl Cysteines to Dehydroalanine on Protein Surfaces: Versatile and Switchable Access to Functionalized Proteins. *J. Am. Chem. Soc.* **2008**, *130*, 5052-5053.
 31. Liu, G.; Shen, Y.; Zhou, Z.; Lu, X. Rhodium(III)-Catalyzed Redox-Neutral Coupling of N-Phenoxyacetamides and Alkynes with Tunable Selectivity. *Angew. Chem., Int. Ed.* **2013**, *52*, 6033-6037.
 32. Li, B.; Lan, J.; Wu, D.; You, J. Rhodium(III)-Catalyzed ortho Heteroarylation of Phenols through Internal Oxidative C–H Activation: Rapid Screening of Single-Molecular White-Light-Emitting Materials. *Angew. Chem., Int. Ed.* **2015**, *54*, 14008–14012.

Chapter 3

Palladium-Catalyzed C-C Bond Activation of Cyclopropenone: Modular Access to Trisubstituted α,β -Unsaturated Esters and Amides

3.1 Abstract

3.2 Introduction

3.3 Results and Discussions

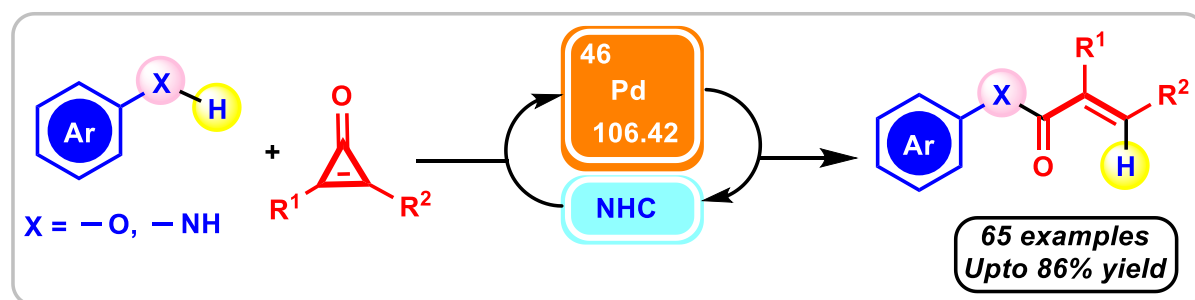
3.4 Conclusions

3.5 Experimental Section

3.6 References

Chapter 3

Palladium-Catalyzed C-C Bond Activation of Cyclopropenone: Modular Access to Trisubstituted α,β -Unsaturated Esters and Amides



3.1 ABSTRACT: Strain driven palladium/*N*-heterocyclic carbene catalyzed C-C bond activation of diphenylcyclopropenone (DPC) has been explored for the one-step access to tri-substituted α,β -unsaturated esters and amides. The designed transformation works under mild conditions providing exclusive single stereoisomer. Mechanistic studies support the oxidative addition of the C-C bond of cyclopropenone to in situ generated Pd(0) intermediate. We have proved that vinylic hydrogen in the product is coming from phenol/aniline through deuterium labeling studies. Late-stage functionalization of bioactive molecules such as procaine, estrone, and hymecromone demonstrates the robustness of this protocol.

3.2 INTRODUCTION

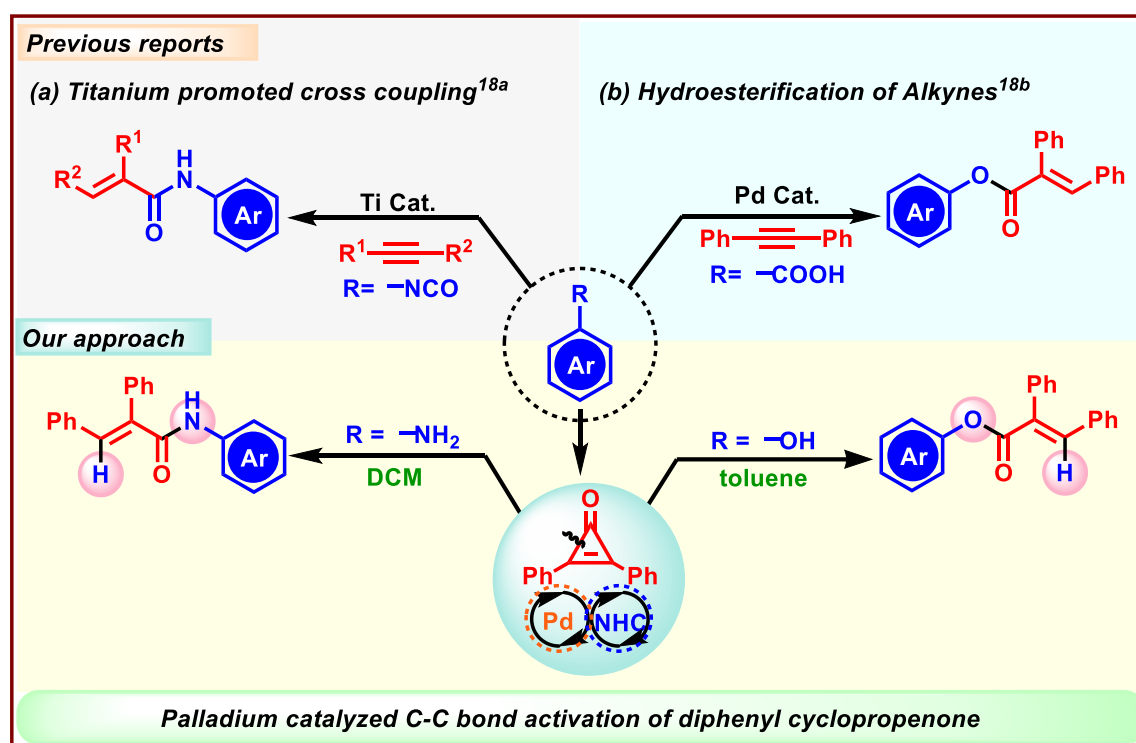
Transition metal-catalyzed carbon-carbon (C-C) bond activation has attracted the attention of both organometallic chemists and organic chemists due to its fundamental scientific importance and potential utility in organic synthesis.¹ Owing to the C-C bond's statistical abundance and inertness, selective activation of the C-C bond is quite challenging and

remains underdeveloped.² Over the last few years, significant breakthroughs have been achieved by Murakami *et al.*,³ Dong *et al.*⁴ and Bower *et al.*⁵ among others⁶, and these reports mainly focused on C-C bond activation of strained ring system due to thermodynamic advantage in breaking of strained systems. Thus, the C-C bond activation arena driven by ring strain of three and four-membered carbocycles has undergone dramatic expansion over the years, resulting in a straightforward route to construct complex value-added scaffolds.⁷ There are two primary modes of C-C bond activation pathways (i) oxidative addition of C-C bonds to transition metals and (ii) β -carbon elimination. Recently, through the β -carbon elimination pathway, we have demonstrated C-C bond activation of cyclopropanol to achieve 1,6-diketone derivatives.⁸ In this vein, the smallest Huckel aromatic system cyclopropenone is less investigated.⁹ Although, Rh, Pt, and Ni catalyzed ring opening of cyclopropenone was reported before,⁹ limited scope and lack of mechanistic evidence offers a multitude of scope to explore the C-C bond activation of cyclopropenone.

α,β -Unsaturated esters and amides are common structural motifs present in drugs and natural products. For instance, these molecules show antifungal, 17 β -HSDCl inhibitory activity, analgesic, antioxidant, anti-inflammatory, antitumor, antiviral, and MMP-2/9 inhibitory activity.^{10,11} Thus, ester and amide bond forming reactions are considered as one of the most important transformation in the pharmaceutical industry. However, only limited methods are known to synthesize these molecules like aldol condensation,¹² Wittig reaction,¹³ Horner-Wadsworth-Emmons reactions,¹⁴ and nucleophilic substitution of activated carboxylic acid derivatives, respectively.¹⁵ Nevertheless, some starting materials are not easy to access, and sensitive functional groups are not tolerated. Moreover, to synthesize highly substituted conjugated esters and amides, strategies like hydroxy-carbonylation,¹⁶ and amino-carbonylation¹⁷ of alkynes have been employed. Furthermore,

Rahaim and coworkers have synthesized conjugated amides by coupling alkynes with Weinreb amides^{18a}, and Tsuji *et al.* have reported the synthesis of conjugated esters by hydro esterification of carboxylic acid derivatives^{18b} (Scheme 3.1). While these new approaches have enabled the synthesis of trisubstituted conjugated esters and amides, stereoselectivity challenges and tedious operational conditions necessitates the development of modified methods. Thus, it's an important objective to construct α,β -unsaturated esters, and amides directly and selectively.

Scheme 3.1 Literature survey and our approach



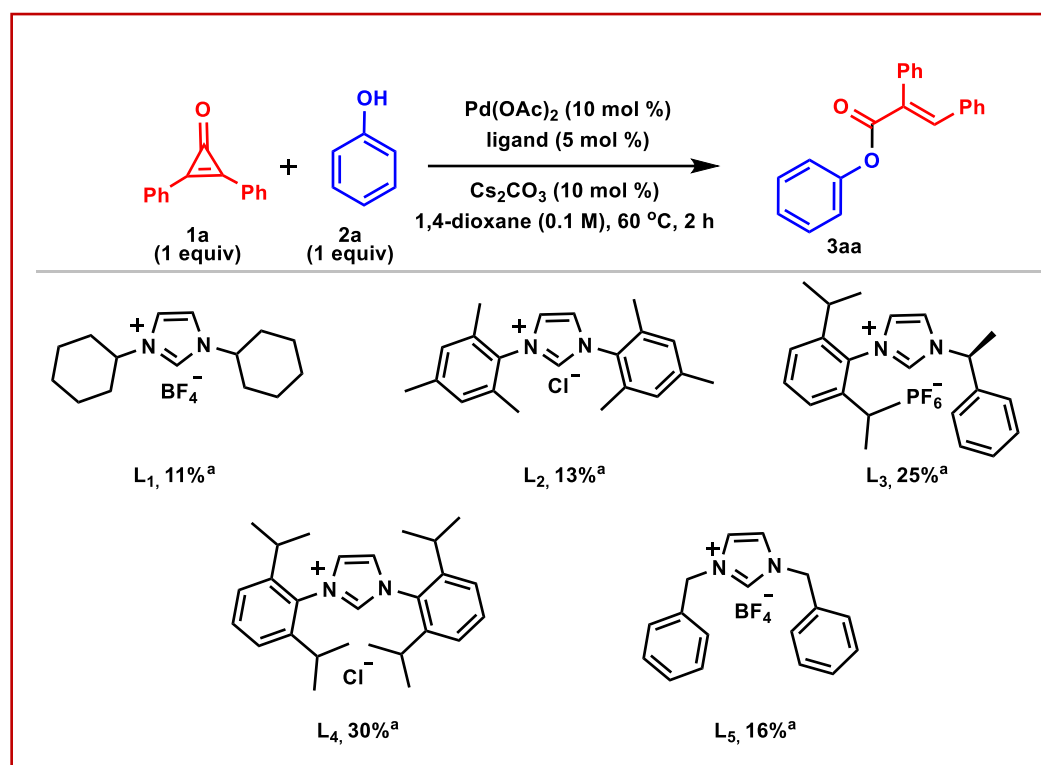
We have recently illustrated the catalytic C-C bond activation of cyclopropenone in the presence of a palladium catalyst resulting in highly functionalized maleimide wherein cyclopropenone was shown to behave as carbon monoxide surrogate.¹⁹ Thus, the above successful approach and our continuous interest encouraged us to explore an expeditious strategy to prepare conjugated esters and amides through Pd(0) catalyzed C-C bond activation of diphenylcyclopropenone in the presence of commercially available phenol

and aniline moiety. In this protocol, NHC ligand plays a vital role in generating Pd(0) catalyst in the presence of a catalytic amount of base. Notable features of our strategy include (i) palladium-catalyzed C-C bond activation of cyclopropanone, (ii) high stereoselectivity, (iii) wide range of functional group tolerance, (iv) short reaction time and, (v) late-stage functionalization of bioactive molecules and drugs like umbelliferon, estrone and procaine, respectively. Herein we have disclosed palladium-catalyzed ligand-controlled C-C bond activation of cyclopropanone to give unsaturated esters and amides in a stereoselective manner.

3.3 RESULTS AND DISCUSSIONS

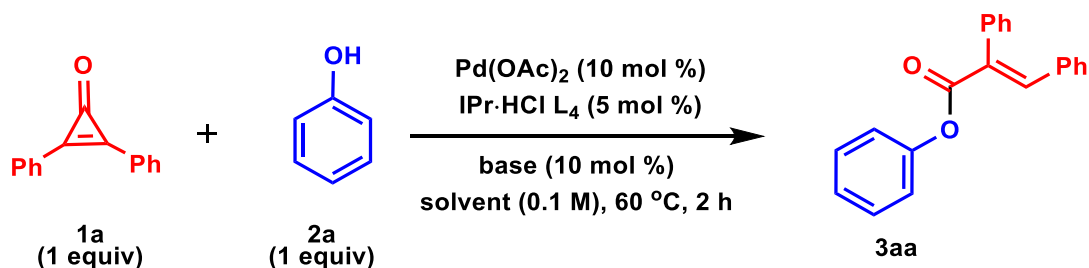
We began our investigation by examining various parameters for the reaction of diphenylcyclopropanone **1a** with phenol **2a** in the presence of Pd(OAc)₂ as a catalyst. First, we have screened different N-heterocyclic carbene ligand using Cs₂CO₃ as a base in 1,4-dioxane solvent, as they are known to generate Pd(0) catalyst *in situ*.²⁰

Table 3.1 Optimization of Reaction Conditions (ligand screening)



^aGC yield (dodecane was taken as internal standard for GC).

Table 3.2 Optimization of Reaction Conditions (other parameters)



entry	base	additives	yield (%) ^b
1	THF	Cs_2CO_3	23% ^c
2	benzene	Cs_2CO_3	25% ^c
3	cyclohexane	Cs_2CO_3	38% ^c
4	toluene	Cs_2CO_3	78% ^c
5	toluene	Li_2CO_3	37% ^c
6	toluene	Na_2CO_3	78% ^c
7	toluene	K_2CO_3	85%^c (83%)
8	toluene	NaHCO_3	38% ^c
9	toluene	LiOAc	13% ^c
10	toluene	NaOAc	<10% ^c
11	toluene	KOAc	6% ^c
12	toluene	K_2CO_3 , without metal	nd
13	toluene	K_2CO_3 , without ligand	nd

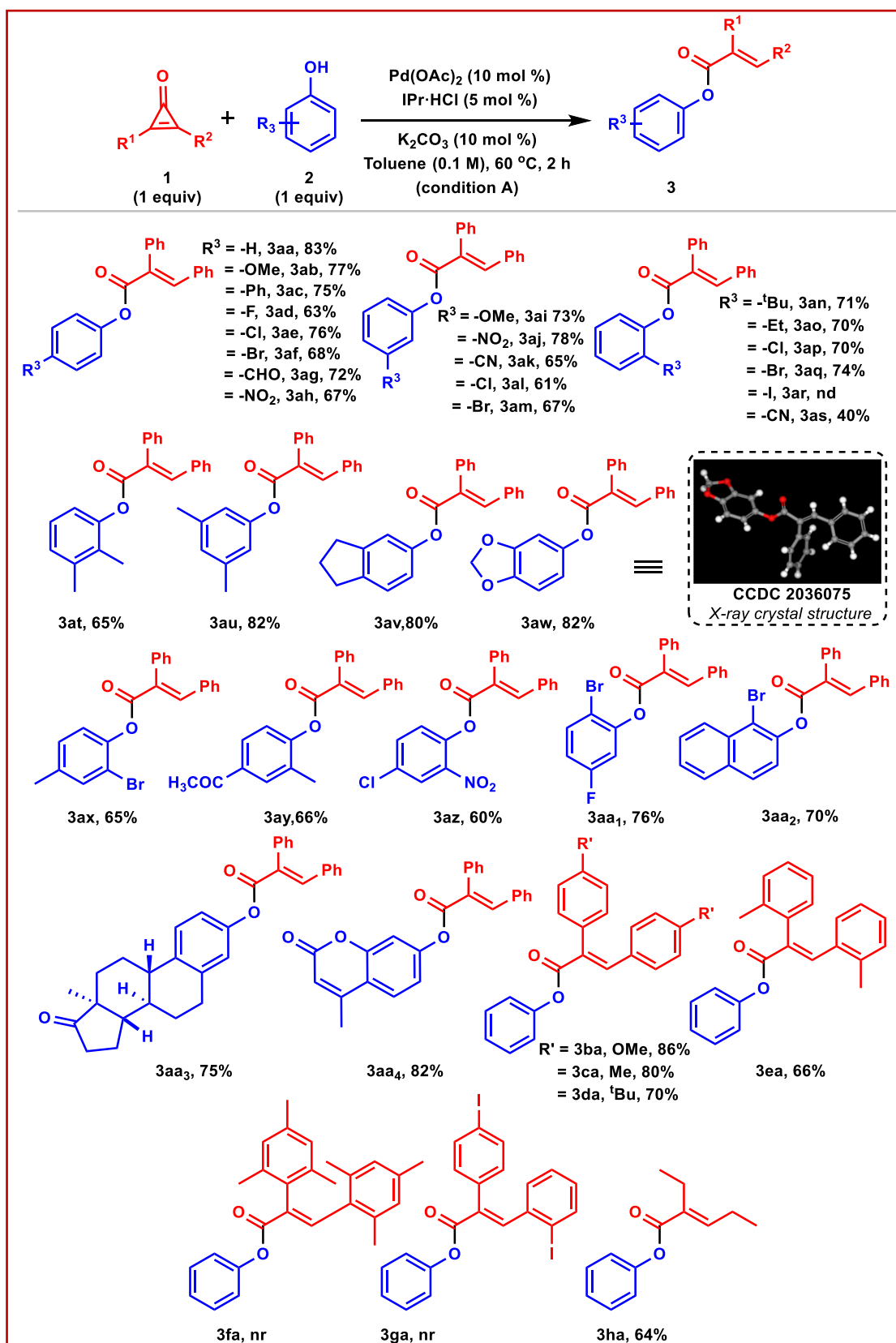
^aConditions: **1a** (1 equiv), **2a** (1 equiv), $\text{Pd}(\text{OAc})_2$ (10 mol %), base (10 mol %), ligand (5 mol %), solvent (0.1 M), temperature (60 °C). ^bIsolated yields, ^cGC yield (dodecane was taken as internal standard for GC).

The screening started with less sterically hindered imidazolium salts $\text{ICy}\cdot\text{HBF}_4$ (**L**₁) as ligand and 11% yield of the respective α,β -unsaturated ester was observed (Table 3.1, **L**₁). Further, to explore the steric effect of the ligand, other NHC ligand were screened. By increasing sterics in the ligand, the yield enhanced to 30% (Table 3.1, **L**₂-**L**₄), and decreasing the sterics further led to inferior result (Table 3.1, **L**₅) which implies that, $\text{IPr}\cdot\text{HCl}$ (**L**₄) is providing the optimal stereo-electronics for the entitled transformation. Intrigued by this result, we screened different nonpolar solvents. Interestingly, after the extensive screening of various solvents, it was found that performing the reaction in toluene

led to an improved yield of α,β -unsaturated ester (Table 3.2, entry 1-4). Aiming to further improve the yield, we performed the reaction with different bases. As Cs_2CO_3 has positive impact on the reaction, various carbonates such as Li_2CO_3 , Na_2CO_3 , and K_2CO_3 (Table 3.2, entry 5-7) were screened. Among them, K_2CO_3 enhanced the desired product's yield to 83% (Table 3.2, entry 7). Furthermore, changing the base to bicarbonate and acetates didn't show any fruitful results (Table 3.2, entry 8-11). Besides, when the reaction was performed in the absence of ligand and catalyst, no product was obtained (Table 3.2, entry 12-13). This implies that the ligand and catalyst were working synergistically for the above transformation.

After establishing the condition, we initiated our studies to explore the scope of the reaction. As expected, a variety of substituted phenol could participate in the current C-C activation reaction regardless of the electronic nature of substituents incorporated in the phenyl ring. A series of electron-donating, aryl, and electron-withdrawing *para*-substituted phenols was subjected to the reaction, which gave 67-77% (Scheme 3.2, **3ab-3ah**) yield. Further, *meta* substituted phenol delivered the unsaturated ester in good yields (Scheme 3.2, **3ai-3am**). In this case, *m*-nitro substituted phenol showed superior reactivity giving 78% yield of the respective product (Scheme 3.2, **3aj**). Switching the substituent position from *meta* to *ortho* didn't change the reactivity much. The compatibility of *ortho* *t*-Bu and ethyl phenol suggests that the reaction is relatively robust towards steric hindrance (Scheme 3.2, **3an-3ao**). When *o*-Cl and *o*-Br phenol were subjected to the standard condition, 78% and 74% yield (Scheme 3.2, **3ap-3aq**) of corresponding esters were obtained, respectively. The tolerance of halo substituted phenols under palladium-catalyzed reaction conditions provides an excellent opportunity to do various late-stage functionalization with the product esters.

Scheme 3.2 Scope of phenols for the synthesis of acrylate derivatives^a

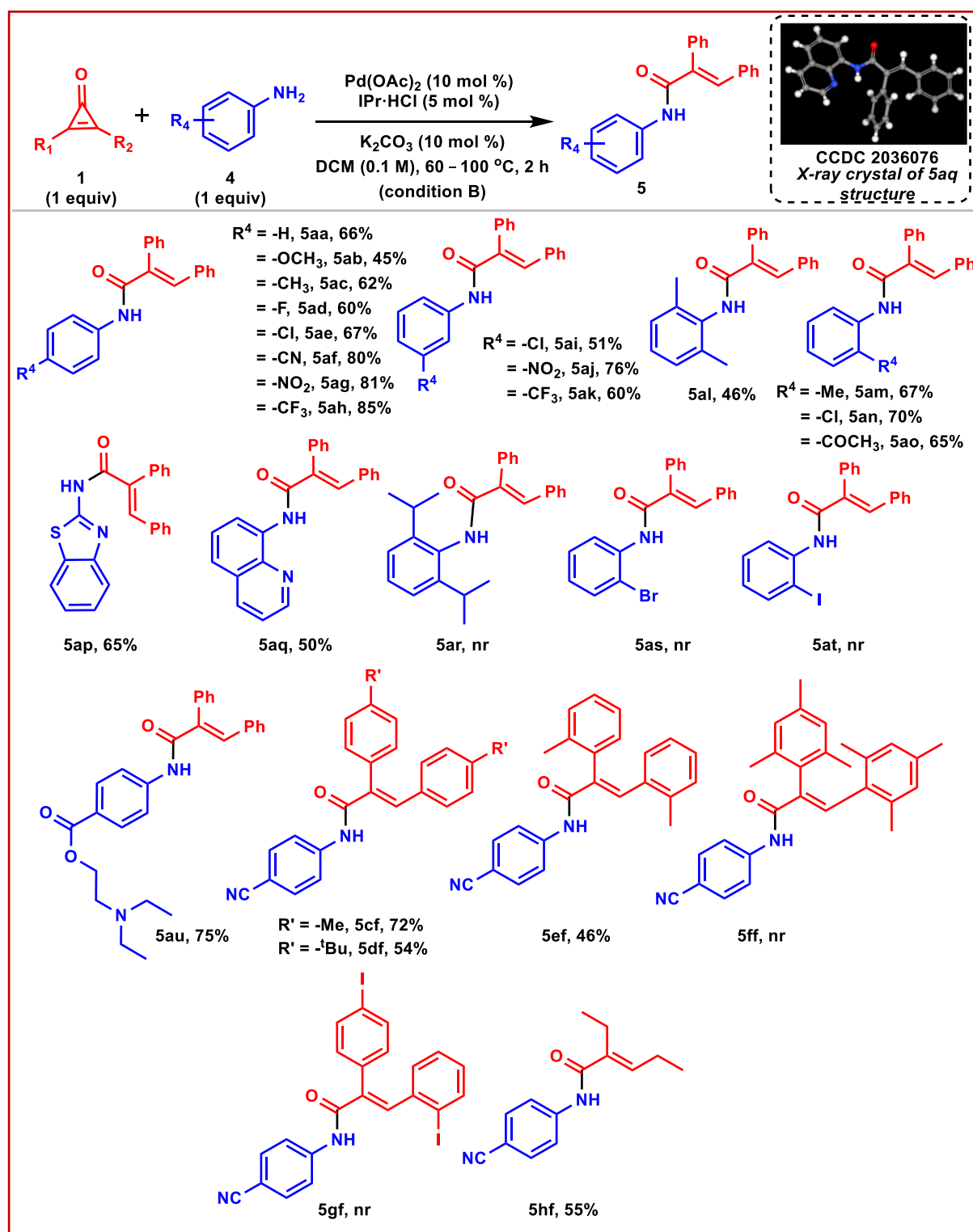


^aConditions: **1a** (1 equiv), **2a** (1 equiv), Pd(OAc)_2 (10 mol %), K_2CO_3 (10 mol %), $\text{IPr}\cdot\text{HCl}$ (5 mol %), toluene (0.1 M), 60 $^\circ\text{C}$, 2 h.

But *o*-iodophenol failed to give the desired unsaturated ester leading to several uncharacterizable products (Scheme 3.2, **3ar**). Furthermore, *o*-CN phenol also provided the desired product **3as** in 40% yield. The variation concerning phenol was not limited to only mono-substituted derivatives. To check the viability of the developed methodology, we chose di-substituted phenol, giving rise to a highly substituted benzene system in the product moiety (Scheme 3.2, **3at-3aa₁**). In addition to this, 2-bromo naphthol shows good reactivity giving a 70% yield of the desired product (Scheme 3.2, **3aa₂**). The construction of a biologically important skeleton around another bioactive molecule assumes significance. With this thought, we have chosen estrone **2a₃**, 4-Methylumbelliferone **2a₄** (commonly known as hymecromone, which is used as a drug in bile therapy) and the respective derivatized unsaturated ester was synthesized in good yields (Scheme 3.2, **3aa₃-3aa₄**). Further, the scope of the reaction was extended to different aryl, and alkyl-substituted cyclopropenone (Scheme 3.2, **3ba-3ha**). While various electron-rich aryl substituents in cyclopropenone ring gave the desired product in very good yield (Scheme 3.2, **3ba-3da**), sterically hindered substrates showed retarded reactivity resulting in lower yield or even no reaction (Scheme 3.2, **3ea-3ga**). Furthermore, di-alkyl substituted cyclopropenone was also subjected to the standard condition giving 64% yield of the desired unsaturated ester **3ha**.

As the current methodology is compatible with a series of phenol moieties, aniline was chosen as the substrate to show the developed protocol's diversity. As α,β -unsaturated amide is present in several biologically active molecules, developing a one-step protocol is essential. With this motivation, when condition **A** was directly applied to the reaction of aniline **4a** with diphenyl cyclopropenone **1a**, we got only a 45% yield of the desired product **5aa**. After several solvent optimizations, delightfully, we found DCM was found to be working well, giving 66% (Scheme 3.3, **5aa**) yield of the unsaturated amide.

Scheme 3.3 Scope of Anilines for the synthesis of Acrylamide derivatives^a

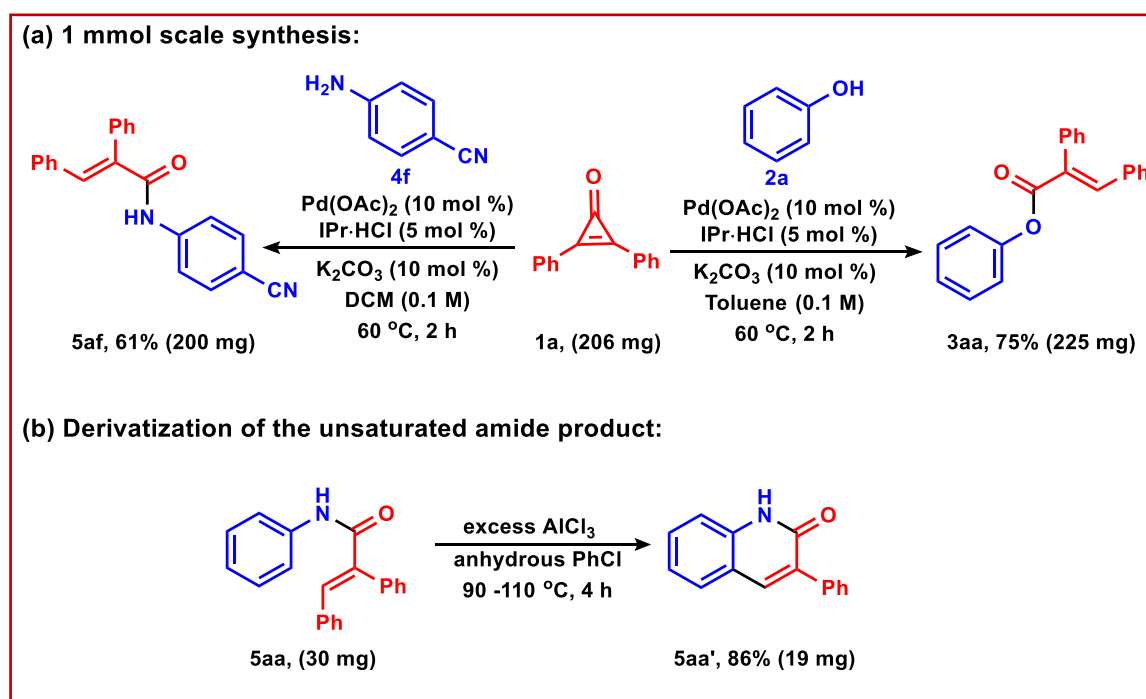


^aConditions: **1a** (1 equiv), **4a** (1 equiv), $\text{Pd}(\text{OAc})_2$ (10 mol %), K_2CO_3 (10 mol %), $\text{IPr}\cdot\text{HCl}$ (5 mol %), DCM (0.1 M), 60 °C.

A wide variety of substituted anilines were next evaluated under the optimized reaction conditions, as demonstrated in Scheme 3.3. The substitution of aniline in the *para* position

with electron-releasing groups such as methoxy and methyl was found compatible giving 45% and 62% yield, respectively (Scheme 3.3, **5ab-5ac**). Further, modifiable halo substituents in the *para* position of aniline worked well, giving good yields of the desired unsaturated amides (Scheme 3.3, **5ad-5ae**). The enhanced yield was observed in the case of electron-withdrawing groups like -CN, -NO₂, and -CF₃ substituted aniline delivering 80-85% yields of the desired product (Scheme 3.3, **5af-5ah**). Further, the reaction of *meta*-substituted aniline resulted in good yields of unsaturated amides (Scheme 3.3, **5ai-5ak**).

Scheme 3.4 Synthetic application



When *ortho*-2,6-dimethyl aniline (Scheme 3.3, **5al**) was taken as the substrate detrimental effect on the reaction yield was observed, otherwise *o*-Me, *o*-Cl, and *o*-acetyl anilines delivered a quantitative amount of the desired products (Scheme 3.3, **5am-5ao**). Furthermore, when 2-aminobenzothiazole and 8-aminoquinoline were taken as the substrate, the desired unsaturated amide was obtained in 65% and 50% yield, respectively (Scheme 3.3, **5ap-5aq**). However, *ortho*-substituted diisopropyl, bromo, and iodo aniline failed to give their respective products (Scheme 3.3, **5ar-5at**) which implies, steric bulk in the substrate might be retarding the reaction. While screening electronically divergent

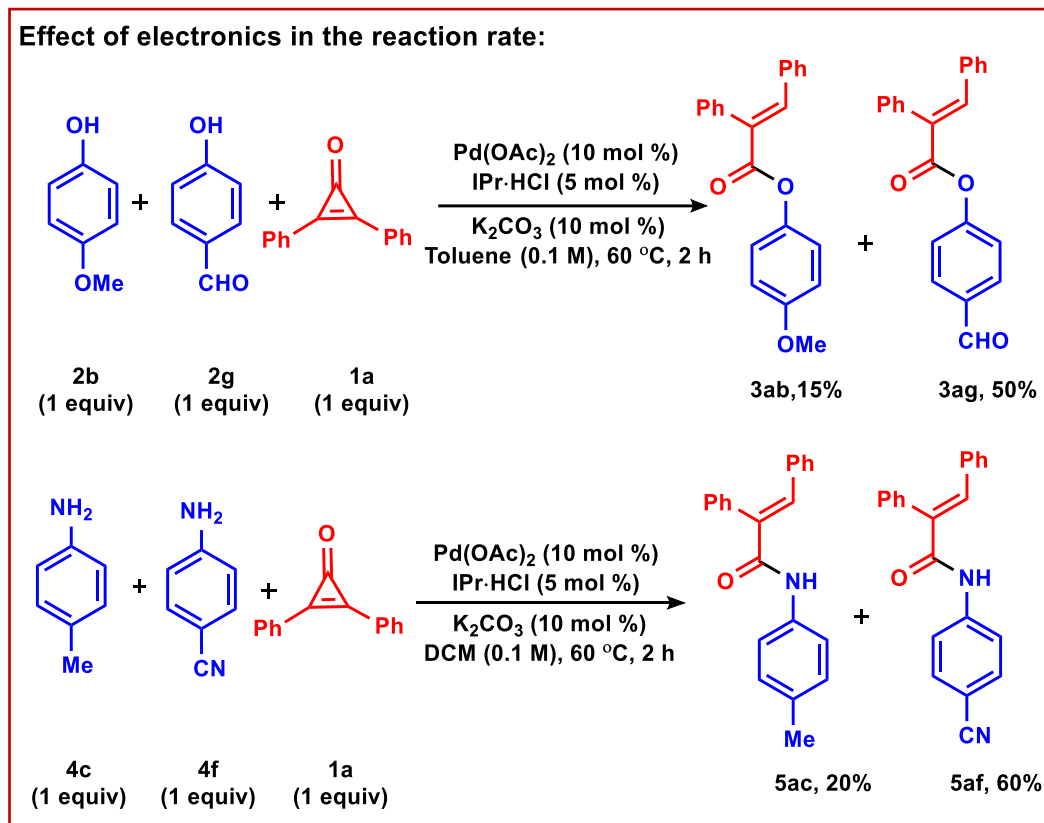
anilines, procaine **4u** (local anesthetic) was also subjected to the standard reaction condition, it was found compatible delivering a 75% yield of the desired unsaturated amide **5au**. In essence, the developed methodology provides a rapid and modular approach to accessing several bioactive compounds.

Furthermore, the scope of α,β -unsaturated amide was expanded to different di-aryl substituted cyclopropenone, delivering the desired product in good to moderate yield (Scheme 3.3, **5cf-5ef**). Sterically hindered di-aryl cyclopropenone failed to give any product, leaving unreacted starting materials (Scheme 3.3, **5ff-5gf**). We have also screened di-ethyl substituted cyclopropenone, it gave the respective unsaturated amide **5hf** in 55% yield. The X-ray data of **3aw** and **5aq** unambiguously justify the structure of demonstrated products. Moreover, the survival of a wide range of sensitive functional groups under the reaction condition without interference indicates notable innate chemoselectivity.

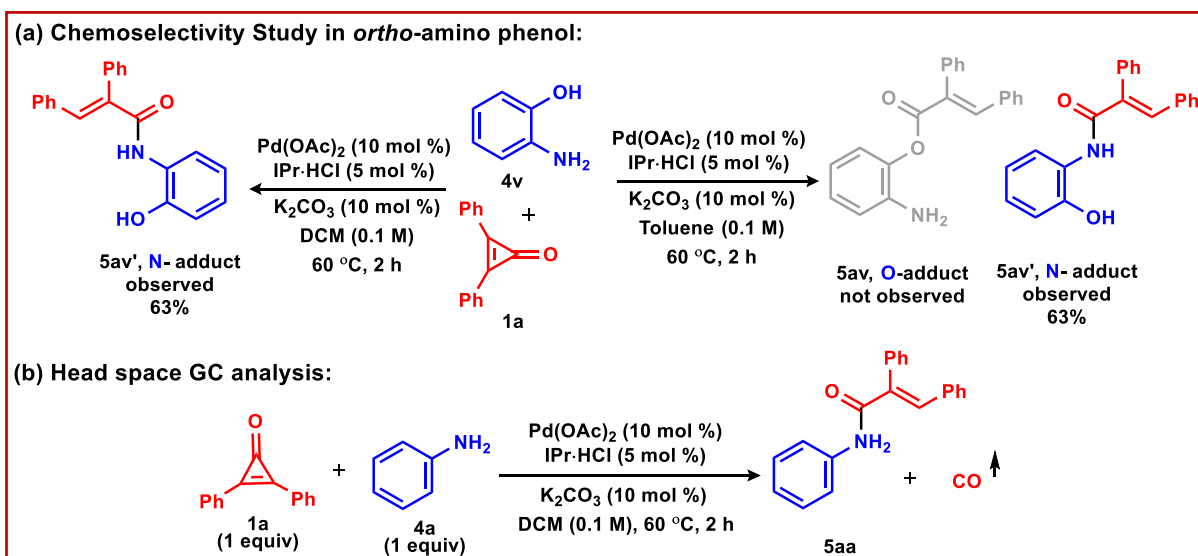
The scale-up experiment and synthetic transformation reactions were carried out to explore the efficiency and practical utility of this method. When a 1 mmol scale reaction was conducted, α,β -unsaturated ester **3aa**, and amide **5af** were isolated in 75% and 61% yield, respectively (Scheme 3.4a). Along with that, product applicability was shown in scheme 3.4b, where substrate **5aa** was subjected to Lewis acid-catalyzed condition.²⁰ In the presence of excess AlCl_3 , we have isolated 3-phenyl carbostyryl **5aa'** as the product in 86% yield (Scheme 3.4b). In this process one phenyl ring got eliminated, which was supported by the result disclosed by Ramakrishnan *et al.*^{20a} Next, we examined the effect of electronics on the reaction rate. When a competition reaction was carried out between electron-rich and deficient substrates, the rate of the reaction was found to be accelerated by the electron-deficient substrates (Scheme 3.5). When *o*-aminophenol **4v** was subjected to the optimized reaction conditions **A** and **B**, we observed that amide formation is highly selective though another reactive phenolic site was available. This suggests that the reaction

is highly chemoselective (Scheme 3.6a). For a better understanding of this reaction, several control experiments were conducted.

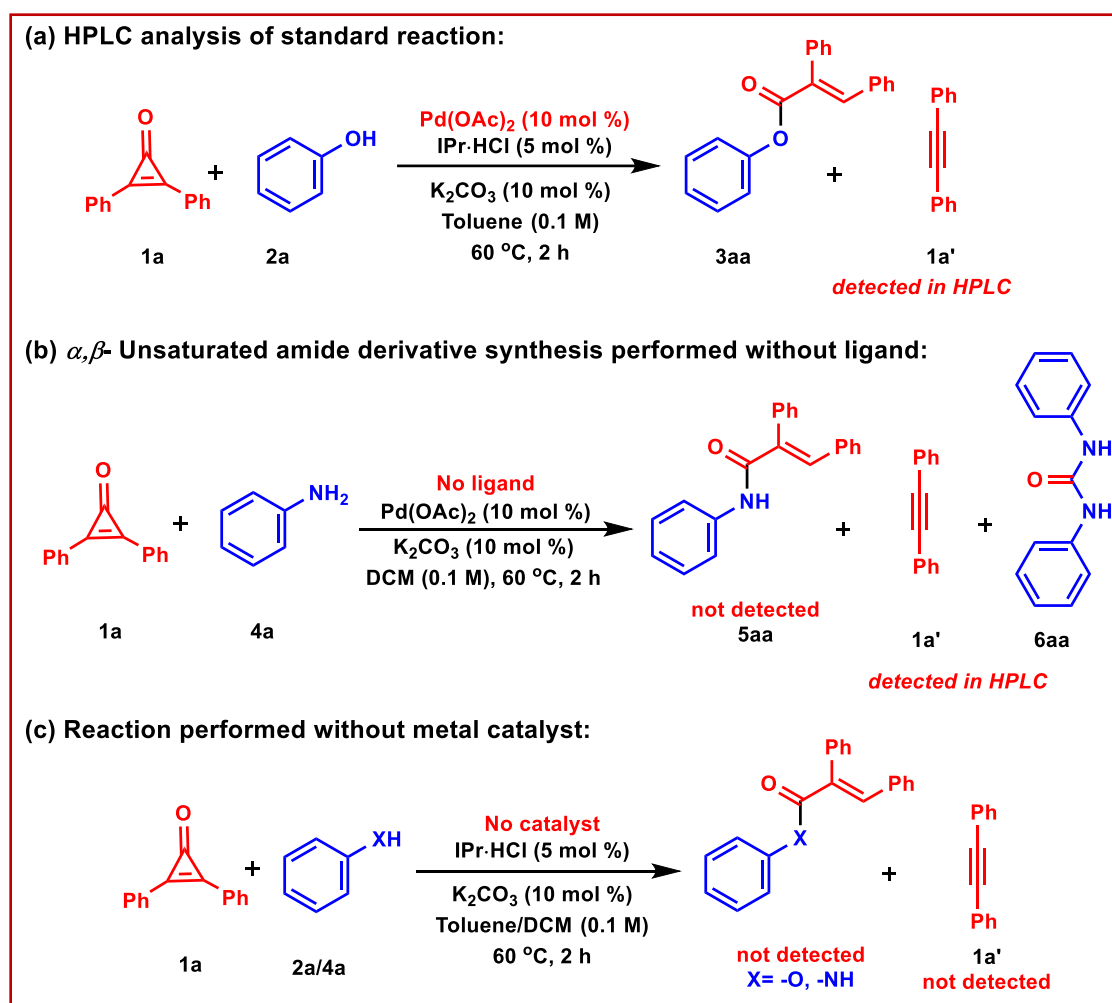
Scheme 3.5 Mechanistic studies



Scheme 3.6 Mechanistic studies



Scheme 3.7 Mechanistic studies

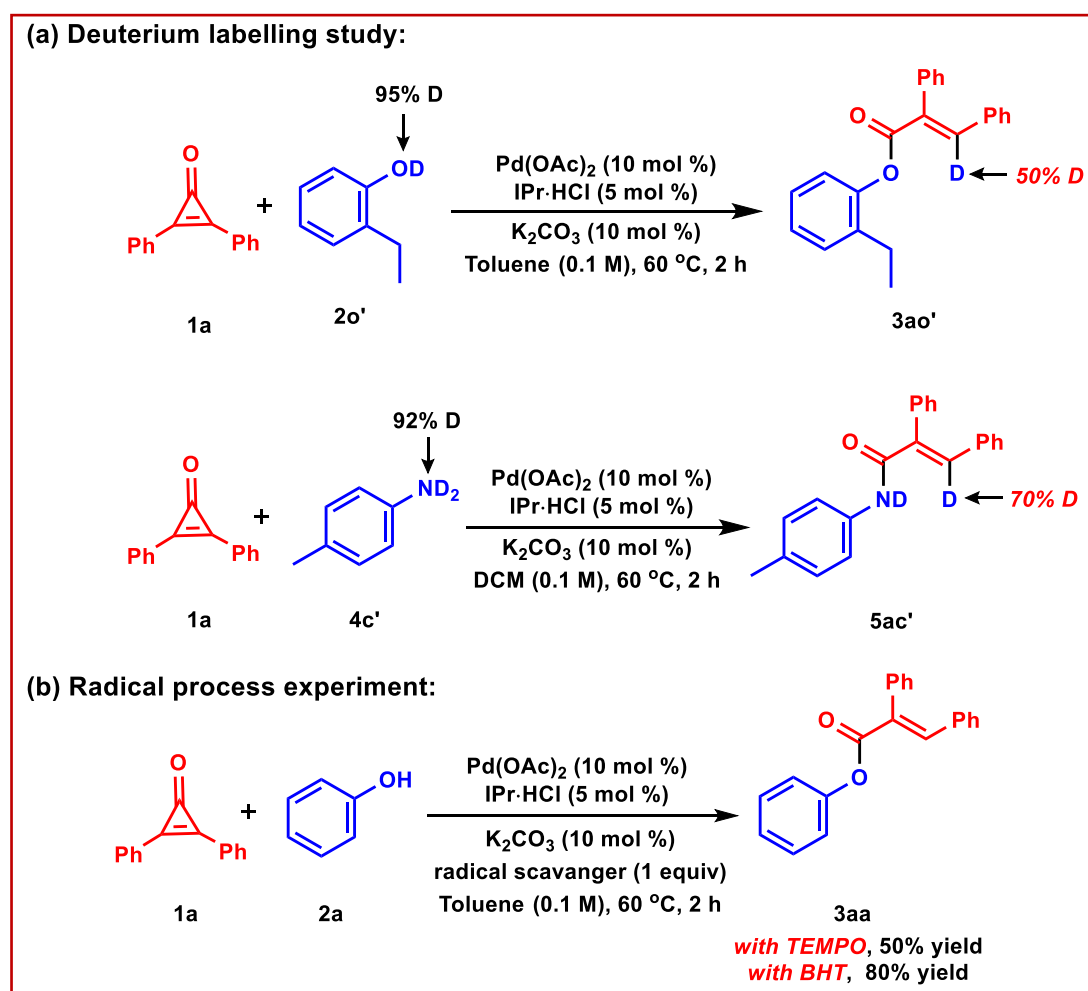


When the reaction was monitored in gas chromatography, we observed a carbon monoxide (CO) peak in the GC (Scheme 3.6b). Under the standard reaction condition, diphenylacetylene was formed as a side product (Scheme 3.7a) (confirmed through HPLC). The fact that in presence of a metal catalyst, diphenyl acetylene is forming along with the extrusion of carbon monoxide signifies the presence of a four-membered palladacycle intermediate in the catalytic cycle as described in our previous report.¹⁹ Thus, to substantiate the formation of a four-membered palladacycle from which diphenylacetylene **1a'** and CO is forming, the reaction was carried out without ligand where no product was observed, but tolane **1a'** (diphenylacetylene) was detected as the by-product along with diphenyl urea **6aa** (Scheme 3.7b) (confirmed through HPLC). Along with that, when a

standard reaction was performed without a metal catalyst there was no reaction (Scheme 3.7c) (confirmed through crude NMR).

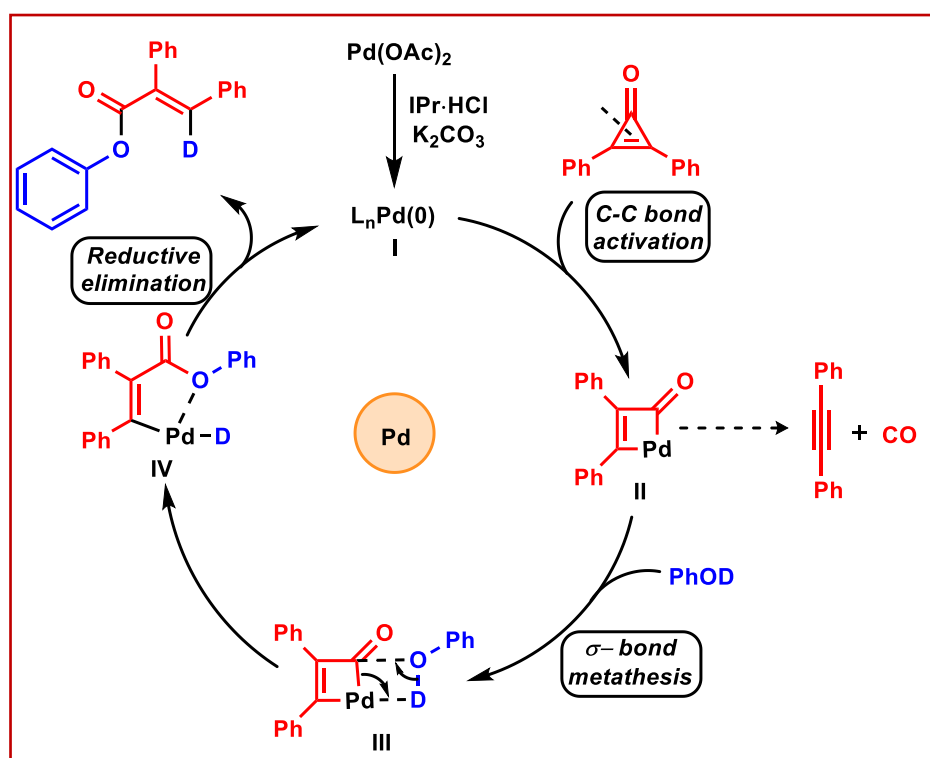
Furthermore, to get additional information about the origin of vinylic hydrogen in the product, we performed a deuterium exchange experiment. The deuterated phenol **2o'** (95% D) and aniline **4c'** (92% D) were subjected to the optimized reaction conditions giving **3ao'** and **5ac'** in 50% and 70% deuterium exchanged products respectively (Scheme 3.8a). To check the nature of the intermediate, a radical process experiment has been performed. In presence of 1 equivalent of radical scavengers like TEMPO and BHT, we observed decent reactivity giving 50% and 80% of the desired product **3aa** (Scheme 3.8b) indicating that the reaction was proceeding through a non-radical pathway.

Scheme 3.8 Mechanistic studies



Based on the above experiments and literature precedence's,²⁰ a plausible catalytic cycle has been proposed (Scheme 3.9). The formation of Pd(0) in presence of imidazolinium salt and catalytic amount of base was well explored.²⁰ Taking this into account, we presumed the formation of Pd(0) intermediate **I** which is undergoing oxidative addition with the C-C bond of diphenyl cyclopropanone to give intermediate **II**. Intermediate **II** undergoes σ -bond metathesis with phenol-D, across C-Pd bond to form intermediate **IV** (supported by experiments in Schemes 3.5 and 3.8a). Then, intermediate **IV** undergoes reductive elimination to deliver the desired product **3aa'** regenerating the active Pd(0) catalyst for the next catalytic cycle.

Scheme 3.9 Catalytic cycle



3.4 CONCLUSION

In summary, we have established a palladium catalyzed C-C bond activation strategy of smallest Huckel aromatic system for the synthesis of α,β -unsaturated esters and amides in highly stereo and chemo selective manner. The current protocol is quite general, covers a broad range of substrate. Further, we have demonstrated this strategy's general application

for the late-stage functionalization of bioactive molecules. In addition, The conversion of the α,β -unsaturated amide in to biologically important quinolone motif, provides a unique opportunity to extend the developed protocol.

3.5 EXPERIMENTAL SECTION

General Information:²¹

Reactions were performed using borosil schlenk tube vial under N₂ atmosphere. Column chromatography was done by using 100-200 & 230-400 mesh size silica gel of Acme Chemicals. A gradient elution was performed by using distilled petroleum ether and ethyl acetate. TLC plates detected under UV light at 254 nm. ¹H NMR and ¹³C NMR were recorded on Bruker AV 400, 700 MHz spectrometer using CDCl₃ as internal standards the residual CHCl₃ for ¹H NMR (δ = 7.26 ppm) and the deuterated solvent signal for ¹³C NMR (δ = 77.36 ppm) is used as reference.^{21b} Multiplicity (s = single, d = doublet, t = triplet, q = quartet, m = multiplet, dd = double doublet), integration, and coupling constants (*J*) in hertz (Hz). HRMS signal analysis was performed using micro TOF Q-II mass spectrometer. X-ray analysis was conducted using Rigaku Smartlab X-ray diffractometer at SCS, NISER. Reagents and starting materials were purchased from Sigma Aldrich, Alfa Aesar, TCI, Avra, Spectrochem and other commercially available sources and used without further purification unless otherwise noted. *N*-heterocyclic carbene ligand were prepared according to the literature report.^{21a,b}

1. (a) General procedure for synthesis of cyclopropenones (method A):^{19, 22} To a suspension of tetrachlorocyclopropene (0.64 mmol, 1 equiv) and anhydrous AlCl₃ (1.35 mmol, 1.05 equiv) in CH₂Cl₂ (0.06 M, 10 mL) was added dropwise, a solution of benzene (1.28 mmol, 2 equiv) in CH₂Cl₂ (1.2 M, 1 mL) at -78 °C. The mixture was stirred for 2 h then warmed up to room temperature and stirred for another 2 h. After completion of the reaction as monitored by TLC analysis, the resulting mixture was quenched with water,

diluted with CH_2Cl_2 , washed with water ($2 \times 50 \text{ mL}$) and brine ($2 \times 50 \text{ mL}$). The organic layers were dried over anhydrous Na_2SO_4 , filtered and concentrated under reduced pressure to yield the crude residue as an orange oil. The crude residue was then purified by flash column chromatography on silica gel (20% EtOAc in hexanes) to afford diarylcyclopropenone (175 mg, 85% yield) as a white solid.

1. (b) General procedure for synthesis of cyclopropenones (method B):²² n-Butyllithium (2.2 mmol, 2.2 equiv) was added dropwise over a period of 60 min to a stirring solution of chloroform (0.20 ml, 2.5 mmol) and alkyne (1.0 mmol, 1 equiv) in THF (20 ml, 0.05 M) under N_2 atm at -78°C . The resulting mixture was stirred for an additional 4 h at -78°C before conc. hydrochloric acid (1 ml, 1 M) was added dropwise over 10 min. The cooling bath was removed, and the mixture was stirred for 10 min. without external cooling, before water (20 ml) was added. The mixture was extracted with dichloromethane (5 x 20 ml) and the combined organic extracts were dried (MgSO_4) and evaporated in vacuo. The products were isolated by flash chromatography.

2. General procedure for synthesis of highly substituted acrylates 3 (condition A): To a 25 ml schlenk tube under N_2 atmosphere, diphenyl cyclopropenone **1a** (0.1 mmol, 1 equiv) in toluene 1 ml (0.1 M) was added, $\text{Pd}(\text{OAc})_2$ (10 mol %, 0.1 equiv), $\text{IPr}\cdot\text{HCl}$ (5 mol %, 0.05 equiv), K_2CO_3 (10 mol %, 0.1 equiv), phenol **2** (0.1 mmol, 1 equiv) and stirred vigorously (750 rpm) in a preheated aluminum block at 60°C for 2 h. After completion of the reaction (in 2 h) as monitored by TLC analysis, the solvent was evaporated under reduced pressure and the residue was purified by column chromatography on silica gel (elute: EtOAc/hexane) to give the pure product **3**.

(Caution: use mask while using $\text{IPr}\cdot\text{HCl}$)

3. General procedure for synthesis of highly substituted acrylate 3aa in 1 mmol scale:

To a 25 ml schlenk tube under N_2 atmosphere, diphenyl cyclopropenone **1a** (1 mmol, 1

equiv) in toluene (0.1 M, 10 ml) was added, Pd(OAc)₂ (10 mol %, 0.1 equiv), IPr·HCl (5 mol %, 0.05 equiv), K₂CO₃ (10 mol %, 0.1 equiv), phenol **2a** (1 mmol, 1 equiv) and stirred vigorously (750 rpm) in a preheated aluminum block at 60 °C for 2 h. After completion of the reaction (in 2 h) as monitored by TLC analysis, the solvent was evaporated under reduced pressure and the residue was purified by column chromatography on silica gel (elute: EtOAc/hexane) to give the pure product **3aa**. white solid (225 mg, 75% yield) *R_f* = 0.7 (in 10% EtOAc/hexane).

4. General procedure for synthesis of highly substituted acrylamide 5 (condition B):

To a 25 ml schlenk tube under N₂ atmosphere, diphenyl cyclopropenone **1a** (0.1 mmol, 1 equiv) in DCM (0.1 M, 1 ml) was added, Pd(OAc)₂ (10 mol %, 0.1 equiv), IPr·HCl (5 mol %, 0.05 equiv), K₂CO₃ (10 mol %, 0.1 equiv), aniline **4** (0.1 mmol, 1 equiv) and stirred vigorously (750 rpm) in a preheated aluminum block at 60 °C for 2 h. After completion of the reaction (in 2 h) as monitored by TLC analysis, the solvent was evaporated under reduced pressure and the residue was purified by column chromatography on silica gel (elute: EtOAc/hexane) to give the pure product **5**.

5. General procedure for synthesis of highly substituted acrylamide 5af in 1 mmol scale: To a 25 ml schlenk tube under N₂ atmosphere, diphenyl cyclopropenone **1a** (1 mmol, 1 equiv) in DCM (0.1 M, 10 ml) was added, Pd(OAc)₂ (10 mol %, 0.1 equiv), IPr·HCl (5 mol %, 0.05 equiv), K₂CO₃ (10 mol %, 0.1 equiv), aniline **4f** (1 mmol, 1 equiv) and stirred vigorously (750 rpm) in a preheated aluminum block at 60 °C for 2 h. After completion of the reaction (in 2 h) as monitored by TLC analysis, the solvent was evaporated under reduced pressure and the residue was purified by column chromatography on silica gel (elute: EtOAc/hexane) to give the pure product **5af**. white solid (200 mg, 61% yield) *R_f* = 0.4 (in 10% EtOAc/hexane).

6. General procedure for competition reaction between phenols: To a 25 ml schlenk tube under N₂ atmosphere, diphenyl cyclopropenone **1a** (0.1 mmol, 1 equiv) in toluene (0.1 M, 1 ml) was added, Pd(OAc)₂ (10 mol %, 0.1 equiv), IPr·HCl (5 mol %, 0.05 equiv), K₂CO₃ (10 mol %, 0.1 equiv), 4-methoxyphenol **2b** (0.1 mmol, 1 equiv), 4-hydroxybenzaldehyde **2g** (0.1 mmol, 1 equiv) and stirred vigorously (750 rpm) in a preheated aluminum block at 60 °C for 2 h. After completion of the reaction (in 2 h) as monitored by TLC analysis, the solvent was evaporated under reduced pressure and the residue was purified by column chromatography on silica gel (elute: EtOAc/hexane) to give **3ab** in 15% yield and **3ag** in 50% yield respectively.

7. General procedure for competition reaction between anilines: To a 25 ml schlenk tube under N₂ atmosphere, diphenyl cyclopropenone **1a** (0.1 mmol, 1 equiv) in DCM (0.1 M, 1 ml) was added, Pd(OAc)₂ (10 mol %, 0.1 equiv), IPr·HCl (5 mol %, 0.05 equiv), K₂CO₃ (10 mol %, 0.1 equiv), 4-methylaniline **4c** (0.1 mmol, 1 equiv), 4-aminobenzonitrile **4f** (0.1 mmol, 1 equiv) and stirred vigorously (750 rpm) in a preheated aluminum block at 60 °C for 2 h. After completion of the reaction (in 2 h) as monitored by TLC analysis, the solvent was evaporated under reduced pressure and the residue was purified by column chromatography on silica gel (elute: EtOAc/hexane) to give **5ac** in 20% yield and **5af** in 60% yield respectively.

8. General procedure for radical process experiment:

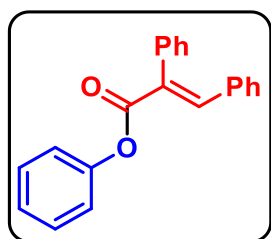
To a 25 ml schlenk tube under N₂ atmosphere, diphenyl cyclopropenone **1a** (0.1 mmol, 1 equiv) in toluene (0.1 M, 1 ml) was added, Pd(OAc)₂ (10 mol %, 0.1 equiv), IPr·HCl (5 mol %, 0.05 equiv), K₂CO₃ (10 mol %, 0.1 equiv), phenol **2a** (0.1 mmol, 1 equiv), radical scavenger (0.1 mmol, 1 equiv) and purged with nitrogen more than three times. The reaction mixture was stirred vigorously (750 rpm) in a preheated aluminum block at 60 °C for 2 h. After completion of the reaction (in 2 h) as monitored by TLC analysis, the solvent

was evaporated under reduced pressure and the residue was purified by column chromatography on silica gel (elute: EtOAc/hexane) gave the pure product **3aa** in 50% and 80% yield in presence of TEMPO and BHT respectively.

9. General procedure for the synthesis of 2-quinolone:^{20g}

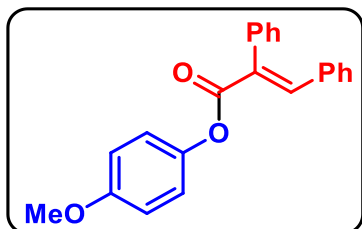
To a solution of **5aa** (0.1 mmol, 1 equiv) in anhydrous chlorobenzene (260 μ L, 0.5 M) was added AlCl_3 (0.5 mmol, 5 equiv) portion wise at room temperature. The reaction mixture was stirred at 90 $^\circ\text{C}$ for 3 h and then at 110 $^\circ\text{C}$ for 1 h. After 4 h, the reaction was quenched with NaHCO_3 and then the solvent was evaporated in *vacuo*. The crude mixture was purified by column chromatography on silica gel (elute: EtOAc/hexane) gave the pure product **5aa'** in 86% (19 mg) yield.

Experimental characterization data of products:



(E)-phenyl 2,3-diphenylacrylate (3aa):^{18b}

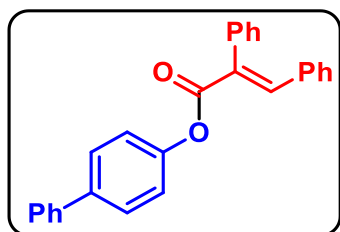
Physical State: white solid (25 mg, 83%), $R_f = 0.8$ (10% EtOAc/hexane), **mp** = 133-135 $^\circ\text{C}$. ^1H NMR (CDCl_3 , 400 MHz): δ 8.04 (s, 1H), 7.41-7.32 (m, 7H), 7.25-7.09 (m, 8H). $^{13}\text{C}\{^1\text{H}\}$ NMR (CDCl_3 , 100 MHz): δ 166.4, 151.1, 142.0, 135.5, 134.4, 131.9, 130.8, 129.8, 129.4, 129.3, 128.7, 128.3, 128.0, 125.7, 121.6. **IR** (KBr, cm^{-1}): 3129, 1723, 1400, 1151. **HRMS** (ESI) **m/z**: $[\text{M}+\text{Na}]^+$ Calcd for $\text{C}_{21}\text{H}_{16}\text{O}_2\text{Na}$: 323.1043; Found 323.1042.



(E)-4-methoxyphenyl 2,3-diphenylacrylate (3ab):^{18b}

Physical State: white solid (25 mg, 77% yield), $R_f = 0.6$ (10% EtOAc/hexane), **mp** = 130-132 $^\circ\text{C}$. ^1H NMR (CDCl_3 , 400 MHz): δ 7.94 (s, 1H), 7.32-7.24 (m, 5H), 7.18-7.09 (m, 3H), 7.03-6.98 (m, 4H), 6.81 (d, $J = 8.0$ Hz, 2H), 3.72 (s, 3H). $^{13}\text{C}\{^1\text{H}\}$ NMR (CDCl_3 , 100 MHz): δ 167.0, 157.5, 144.9, 142.1, 135.8, 134.8, 132.3, 131.1, 130.2, 129.6, 129.0, 128.6,

128.3, 122.6, 114.7, 55.9. **IR (KBr, cm⁻¹):** 3135, 1719, 1400, 1149. **HRMS (ESI) m/z:** [M+Na]⁺ Calcd for C₂₂H₁₈O₃Na 353.1148; Found: 353.1154.



(E)-[1,1'-biphenyl]-4-yl 2,3-diphenylacrylate (3ac):^{18b}

Physical State: white solid (28 mg 75%), **R_f** = 0.8 (10%

EtOAc/hexane), **mp** = 130-132 °C. **¹H NMR (CDCl₃, 400**

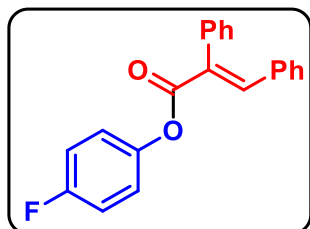
MHz): δ 8.06 (s, 1H), 7.58 (t, *J* = 8.0 Hz, 4H), 7.45–7.34 (m,

8H), 7.25–7.18 (m, 5H), 7.12 (d, *J* = 8.0 Hz, 2H). **¹³C{¹H} NMR (CDCl₃, 100 MHz):** δ

166.7, 150.9, 142.4, 140.7, 139.2, 135.8, 135.2, 134.7, 132.2, 131.1, 130.2, 129.7, 129.1

(2C), 128.6, 128.4, 127.6, 127.4, 122.2. **IR (KBr, cm⁻¹):** 3141, 1720, 1401, 1151. **HRMS**

(ESI) m/z: [M+H]⁺ Calcd for C₂₇H₂₁O₂: 377.1536; Found: 377.1508.



(E)-4-fluorophenyl 2,3-diphenylacrylate (3ad):

Physical State: white solid (20 mg, 63%), **R_f** = 0.7 (10%

EtOAc/hexane), **mp** = 124-126 °C. **¹H NMR (CDCl₃, 400**

MHz): δ 8.03 (s, 1H), 7.43-7.37 (m, 3H), 7.33-7.31 (m, 2H),

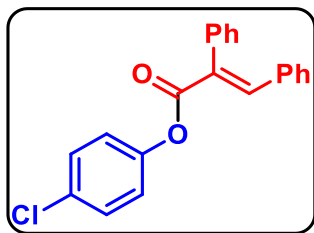
7.26-7.17 (m, 3H), 7.12-7.03 (m, 6H). **¹³C{¹H} NMR (CDCl₃, 100 MHz):** δ 166.7, 160.5

(d, *J*_{C-F} = 242.0 Hz), 147.2 (d, *J*_{C-F} = 3.0 Hz), 142.6, 135.7, 134.6, 132.0, 131.1, 130.1,

129.8, 129.1, 128.6, 128.4, 123.3 (d, *J*_{C-F} = 9.0 Hz), 116.3 (d, *J*_{C-F} = 24.0 Hz). **¹⁹F NMR**

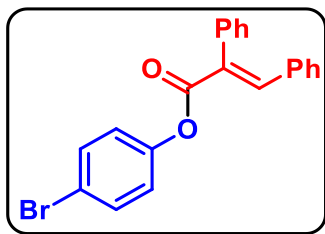
(CDCl₃, 376 MHz): δ -117.2. **IR (KBr, cm⁻¹):** 3141, 1720, 1502, 1401, 1142. **HRMS (ESI)**

m/z: [M+H]⁺ Calcd for C₂₁H₁₆FO₂: 319.1129; Found: 319.1127.



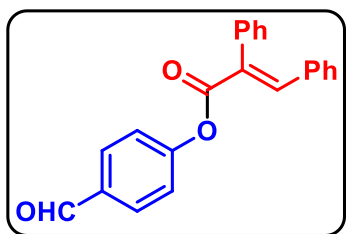
***(E)*-4-chlorophenyl 2,3-diphenylacrylate (3ae):**^{18b}

Physical State: white solid (25 mg, 76%), $R_f = 0.7$ (10% EtOAc/hexane), **mp** = 140-142 °C. **¹H NMR (CDCl₃, 400 MHz):** δ 8.02 (s, 1H), 7.43-7.30 (m, 7H), 7.26-7.17 (m, 3H), 7.10-7.08 (m, 4H). **¹³C{¹H} NMR (CDCl₃, 100 MHz):** δ 166.4, 149.9, 142.7, 135.6, 134.6, 131.9, 131.4, 131.1, 130.1, 129.9, 129.7, 129.1, 128.6, 128.4, 123.3. **IR (KBr, cm⁻¹):** 3141, 1721, 1486, 1149. **HRMS (ESI) m/z:** [M+Na]⁺ Calcd for C₂₁H₁₅ClO₂Na: 357.0658; Found: 357.0650.



***(E)*-4-bromophenyl 2,3-diphenylacrylate (3af):**

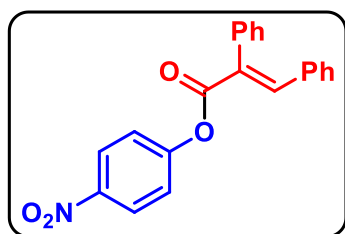
Physical State: white solid (26 mg, 68%), $R_f = 0.8$ (10% EtOAc/hexane), **mp** = 156-158 °C. **¹H NMR (CDCl₃, 400 MHz):** δ 8.02 (s, 1H), 7.49 (d, $J = 8.0$ Hz, 2H), 7.40-7.38 (m, 3H), 7.32-7.30 (m, 2H), 7.26-7.17 (m, 3H), 7.09 (br-, $J = 4.0$ Hz, 2H), 7.04 (d, $J = 8.0$ Hz, 2H). **¹³C{¹H} NMR (CDCl₃, 100 MHz):** δ 166.3, 150.5, 142.8, 135.6, 134.6, 132.7, 131.9, 131.1, 130.1, 129.9, 129.1, 128.6, 128.4, 123.7, 119.1. **IR (KBr, cm⁻¹):** 3140, 1721, 1400, 1148. **HRMS (ESI) m/z:** [M+H]⁺ Calcd for C₂₁H₁₆BrO₂: 379.0328; Found: 379.0301.



***(E)*-4-formylphenyl 2,3-diphenylacrylate (3ag):**

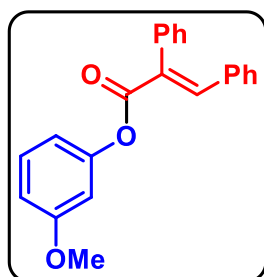
Physical State: white solid (23 mg, 72%), $R_f = 0.3$ (10% EtOAc/hexane), **mp** = 127-130 °C. **¹H NMR (CDCl₃, 400 MHz):** δ 9.99 (s, 1H), 8.06 (s, 1H), 7.92 (d, $J = 8.0$ Hz, 2H), 7.44-7.39 (m, 3H), 7.35-7.32 (m, 4H), 7.26-7.18 (m, 3H), 7.11 (d, $J = 8.0$ Hz, 2H). **¹³C{¹H} NMR (CDCl₃, 100 MHz):** δ 191.3, 166.0, 156.2, 143.2, 135.4, 134.5, 134.2, 131.6, 131.4,

131.2, 130.1, 130.0, 129.2, 128.7, 128.5, 122.7. **IR (KBr, cm⁻¹):** 3136, 1720, 1704, 1401, 1146. **HRMS (ESI) m/z:** [M+K]⁺ Calcd for C₂₂H₁₆O₃K: 367.0737; Found: 367.0730.



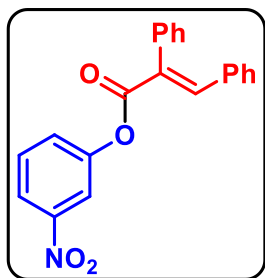
(E)-4-nitrophenyl 2,3-diphenylacrylate (3ah):

Physical State: white crystalline solid (23 mg, 67%), R_f = 0.5 (10% EtOAc/hexane), **mp** = 167-170 °C. **¹H NMR (CDCl₃, 400 MHz):** δ 8.27 (s, 1H), 8.06 (s, 1H), 7.45-7.40 (m, 3H), 7.35-7.31 (m, 4H), 7.27-7.18 (m, 3H), 7.11 (d, J = 8.0 Hz, 2H). **¹³C{¹H} NMR (CDCl₃, 100 MHz):** δ 165.7, 156.2, 145.6, 143.7, 135.3, 134.3, 131.3, 130.2, 130.0, 129.2, 128.7, 128.6, 125.4, 122.8, 122.0. **IR (KBr, cm⁻¹):** 3114, 1723, 1517, 1155. **HRMS (ESI) m/z:** [M+K]⁺ Calcd for C₂₁H₁₅NO₄K: 384.0638; Found: 384.0633.



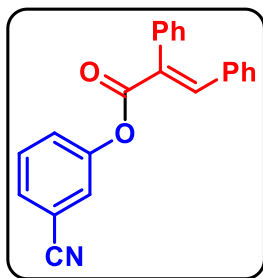
(E)-3-methoxyphenyl 2,3-diphenylacrylate (3ai):

Physical State: white solid (24 mg, 73%), R_f = 0.6 (10% EtOAc/hexane), **mp** = 104-106 °C. **¹H NMR (CDCl₃, 400 MHz):** δ 8.03 (s, 1H), 7.42-7.16 (m, 9H), 7.10 (d, J = 8.0 Hz, 2H), 6.79-6.69 (m, 3H), 3.79 (s, 3H). **¹³C{¹H} NMR (CDCl₃, 100 MHz):** δ 166.6, 160.7, 152.4, 142.3, 135.7, 134.7, 132.2, 131.1, 130.1, 130.0, 129.7, 129.0, 128.6, 128.3, 114.1, 112.1, 107.8, 55.7. **IR (KBr, cm⁻¹):** 3141, 1725, 1489, 1075. **HRMS (ESI) m/z:** [M+Na]⁺ Calcd for C₂₂H₁₈O₃Na: 353.1148 ; Found: 353.1175.



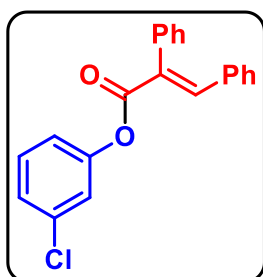
(E)-3-nitrophenyl 2,3-diphenylacrylate (3aj):

Physical State: pale white solid (27 mg, 78%), $R_f = 0.5$ (10% EtOAc/hexane), **mp** = 120-122 °C. ^1H NMR (CDCl_3 , 400 MHz): δ 8.11 (d, $J = 8.0$ Hz, 1H), 8.07 (s, 1H), 8.05 (s, 1H), 7.58-7.50 (m, 2H), 7.43-7.40 (m, 3H), 7.34-7.25 (m, 3H), 7.20 (t, $J = 8.0$ Hz, 2H), 7.11 (d, $J = 8.0$ Hz, 2H). $^{13}\text{C}\{^1\text{H}\}$ NMR (CDCl_3 , 100 MHz): δ 166.0, 151.7, 149.1, 143.6, 135.3, 134.4, 131.3, 130.2, 130.1 (2C), 129.2, 128.7, 128.6, 128.5, 128.4, 121.0, 117.8. **IR** (KBr , cm^{-1}): 3123, 1720, 1401, 1155. **HRMS** (ESI) m/z : $[\text{M}+\text{Na}]^+$ Calcd for $\text{C}_{21}\text{H}_{15}\text{NO}_4\text{Na}$: 368.0893; Found: 368.0879.



(E)-3-cyanophenyl 2,3-diphenylacrylate (3ak):

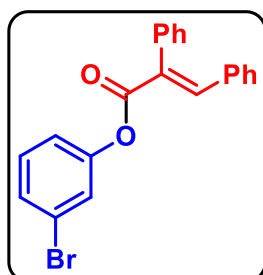
Physical State: white solid (21 mg, 65%), $R_f = 0.4$ (10% EtOAc/hexane), **mp** = 146-148 °C. ^1H NMR (CDCl_3 , 400 MHz): δ 8.05 (s, 1H), 7.54-7.47 (m, 3H), 7.45-7.40 (m, 4H), 7.33-7.31 (m, 2H), 7.26-7.25 (m, 1H), 7.20 (t, $J = 8.0$ Hz, 2H) 7.11 (d, $J = 8.0$ Hz, 2H). $^{13}\text{C}\{^1\text{H}\}$ NMR (CDCl_3 , 100 MHz): δ 166.0, 151.5, 143.4, 135.3, 134.4, 131.3, 131.2, 130.6, 130.1, 130.0, 129.7, 129.2, 128.7, 128.6, 127.0, 125.8, 118.2, 113.7. **IR** (KBr , cm^{-1}): 3132, 2230, 1725, 1401, 1148. **HRMS** (ESI) m/z : $[\text{M}+\text{K}]^+$ Calcd for $\text{C}_{22}\text{H}_{15}\text{NO}_2\text{K}$: 364.0740; Found: 364.0739.



(E)-3-chlorophenyl 2,3-diphenylacrylate (3al):

Physical State: white solid (20 mg, 61%), $R_f = 0.7$ (10% EtOAc/hexane), **mp** = 103-105 °C. ^1H NMR (CDCl_3 , 400 MHz): δ 8.03 (s, 1H), 7.41-7.38 (m, 3H), 7.32-7.17 (m, 8H), 7.11-7.05 (m, 3H). $^{13}\text{C}\{^1\text{H}\}$ NMR (CDCl_3 , 100 MHz): δ 166.3, 151.9, 142.8, 135.6, 134.9, 134.6, 131.8, 131.2, 130.3, 130.1, 129.9, 129.1, 128.6, 128.4, 126.3, 122.6,

120.4. **IR (KBr, cm⁻¹):** 3140, 1723, 1401, 1148. **HRMS (ESI) m/z:** [M+Na]⁺ Calcd for C₂₁H₁₅ClO₂Na: 357.0653; Found: 357.0638.



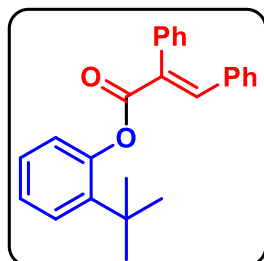
(E)-3-bromophenyl 2,3-diphenylacrylate (3am):

Physical State: pale-yellow solid (25 mg, 67%), **mp** = 102-104 °C, **R_f** = 0.8 (10% EtOAc/hexane). **¹H NMR (CDCl₃, 400 MHz):** δ 8.02 (s, 1H), 7.41-7.30 (m, 7H), 7.26-7.17 (m, 4H), 7.12-7.09 (m, 3H).

¹³C{¹H} NMR (CDCl₃, 100 MHz): δ 166.3, 151.9, 142.8, 135.5,

134.5, 131.8, 131.2, 130.7, 130.1, 129.9, 129.2, 129.1, 128.6, 128.4, 125.4, 122.6, 120.8.

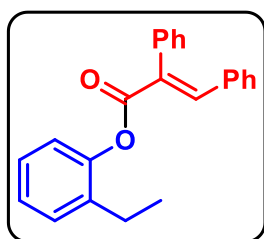
IR (KBr, cm⁻¹): 3141, 1723, 1401, 1148. **HRMS (ESI) m/z:** [M+Na]⁺ Calcd for C₂₁H₁₅BrO₂Na: 401.0148; Found: 401.0118.



(E)-2-(tert-butyl)phenyl 2,3-diphenylacrylate (3an):

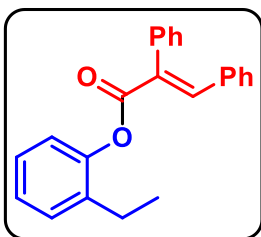
Physical State: colourless liquid (25 mg, 71%), **R_f** = 0.7 (10% EtOAc/hexane). **¹H NMR (CDCl₃, 400 MHz):** δ 8.06 (s, 1H), 7.43-7.33 (m, 6H), 7.26-7.07 (m, 8H), 1.20 (s, 9H). **¹³C{¹H} NMR**

(CDCl₃, 100 MHz): δ 166.9, 149.9, 142.5, 141.4, 135.9, 134.7, 132.7, 131.2, 130.2, 129.8, 129.1, 128.6, 128.3, 127.4, 127.1, 125.9, 124.2, 34.6, 30.2. **IR (KBr, cm⁻¹):** 3053, 1731, 1421. **HRMS (ESI) m/z:** [M+Na]⁺ Calcd for C₂₅H₂₄O₂Na: 379.1669; Found: 379.1680.



(E)-2-ethylphenyl 2,3-diphenylacrylate (3ao):

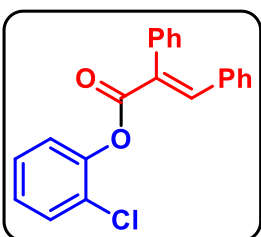
Physical State: pale-yellow solid (23 mg, 70%), **R_f** = 0.7 (10% EtOAc/hexane), **mp** = 88-90 °C. **¹H NMR (CDCl₃, 400 MHz):** δ 8.04 (s, 1H), 7.43-7.33 (m, 5H), 7.24-7.15 (m, 6H), 7.11 (d, *J* = 8.0



Hz, 3H), 2.50 (q, $J = 8.0$ Hz, 2H), 1.10 (t, $J = 8.0$ Hz, 3H). $^{13}\text{C}\{^1\text{H}\}$

NMR (CDCl_3 , 100 MHz): δ 166.6, 149.5, 142.2, 136.1 (2C), 136.0, 134.7, 132.3, 131.2, 130.0, 129.7, 129.1, 128.6, 128.3, 127.0, 126.3, 122.4, 23.8, 14.6. **IR (KBr, cm^{-1}):** 3143, 1724, 1487.

HRMS (ESI) m/z : $[\text{M}+\text{H}]^+$ Calcd for $\text{C}_{23}\text{H}_{21}\text{O}_2$: 329.1536; Found: 329.1534.



(E)-2-chlorophenyl 2,3-diphenylacrylate (3ap):

Physical State: white crystalline solid (26 mg, 78%), $R_f = 0.7$

(10% EtOAc/hexane), **mp** = 128-130 °C. ^1H **NMR (CDCl_3 , 400**

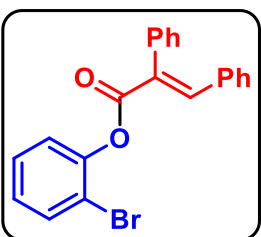
MHz): δ 8.09 (s, 1H), 7.45-7.37 (m, 6H), 7.29-7.15 (m, 6H), 7.12

(d, $J = 8.0$ Hz, 2H). $^{13}\text{C}\{^1\text{H}\}$ **NMR (CDCl_3 , 100 MHz):** δ 165.8, 147.8, 143.0, 135.6, 134.6,

131.6, 131.2, 130.6, 130.2, 129.8, 129.0, 128.6, 128.4, 127.9, 127.3, 127.2, 124.1. **IR (KBr,**

cm^{-1}): 3140, 1724, 1476, 1150. **HRMS (ESI) m/z :** $[\text{M}+\text{Na}]^+$ Calcd for $\text{C}_{21}\text{H}_{15}\text{ClO}_2\text{Na}$:

357.0653; Found: 357.0654.



(E)-2-bromophenyl 2,3-diphenylacrylate (3aq):

Physical State: pale-yellow solid (28 mg, 74%), $R_f = 0.7$ (10%

EtOAc/hexane), **mp** = 100-102 °C. ^1H **NMR (CDCl_3 , 400 MHz):**

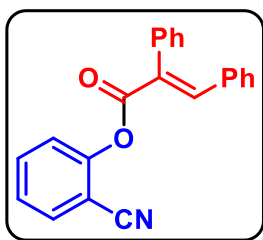
δ 8.10 (s, 1H), 7.60 (d, $J = 8.0$ Hz, 1H), 7.43-7.37 (m, 5H), 7.34-

7.30 (m, 1H), 7.26-7.17 (m, 4H), 7.12 (d, $J = 8.0$ Hz, 3H). $^{13}\text{C}\{^1\text{H}\}$ **NMR (CDCl_3 , 100**

MHz): δ 165.8, 149.0, 143.1, 135.6, 134.6, 133.6, 131.6, 131.2, 130.3, 129.9, 129.0, 128.7,

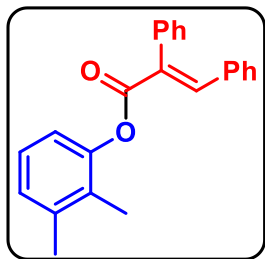
128.6, 128.4, 127.5, 124.2, 116.5. **IR (KBr, cm^{-1}):** 3141, 1724, 1491, 1150. **HRMS (ESI)**

m/z : $[\text{M}+\text{Na}]^+$ Calcd for $\text{C}_{21}\text{H}_{15}\text{BrO}_2\text{Na}$: 401.0148; Found: 401.0149.



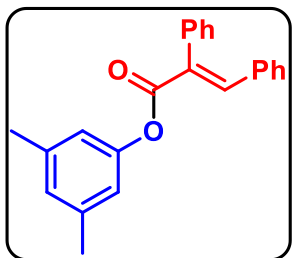
(E)-2-cyanophenyl 2,3-diphenylacrylate (3as):

Physical State: colourless liquid (13 mg, 40%), $R_f = 0.5$ (10% EtOAc/hexane). $^1\text{H NMR}$ (CDCl_3 , 400 MHz): δ 8.13 (s, 1H), 7.68 (d, $J = 8$ Hz, 1H), 7.63 (t, $J = 8$ Hz, 2H), 7.42-7.30 (m, 7H), 7.20 (t, $J = 8$ Hz, 2H), 7.13 (d, $J = 8$ Hz, 2H). $^{13}\text{C}\{^1\text{H}\}$ NMR (CDCl_3 , 100 MHz): δ 165.6, 153.3, 144.0, 135.2, 134.3, 134.2, 133.5, 131.4, 130.2, 130.1, 129.2, 128.6 (2C), 126.6, 126.4, 123.6, 115.6, 107.4. **IR** (KBr, cm^{-1}): 3131, 2238, 1772, 1729, 1401, 1141. **HRMS** (ESI) m/z : $[\text{M}+\text{Na}]^+$ Calcd for $\text{C}_{22}\text{H}_{15}\text{NO}_2\text{Na}$: 348.0995; Found: 348.0991.



(E)-2,3-dimethylphenyl 2,3-diphenylacrylate (3at):

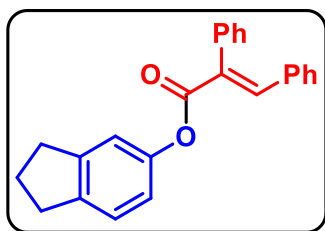
Physical State: white solid (21 mg, 65%), $R_f = 0.7$ (10% EtOAc/hexane), $\text{mp} = 108\text{-}110$ °C. $^1\text{H NMR}$ (CDCl_3 , 400 MHz): δ 8.04 (s, 1H), 7.43-7.34 (m, 5H), 7.24-7.17 (m, 3H), 7.12-7.08 (m, 3H), 7.02 (d, $J = 8.0$ Hz, 1H), 6.93 (d, $J = 8.0$ Hz, 1H), 2.28 (s, 3H), 2.06 (s, 3H). $^{13}\text{C}\{^1\text{H}\}$ NMR (CDCl_3 , 100 MHz): δ 166.6, 149.9, 142.1, 138.7, 136.0, 134.8, 132.3, 131.1, 130.1, 129.7, 129.1, 129.0, 128.6, 128.3, 127.6, 126.3, 119.7, 20.4, 12.8. **IR** (KBr, cm^{-1}): 3145, 1723, 1467, 1156. **HRMS** (ESI) m/z : $[\text{M}+\text{Na}]^+$ Calcd for $\text{C}_{23}\text{H}_{20}\text{O}_2\text{Na}$: 351.1356; Found: 351.1351.



(E)-3,5-dimethylphenyl 2,3-diphenylacrylate (3au):

Physical State: white solid (27 mg, 82%), $R_f = 0.8$ (10% EtOAc/hexane), $\text{mp} = 108\text{-}110$ °C. $^1\text{H NMR}$ (CDCl_3 , 400 MHz): δ 8.01 (s, 1H), 7.39-7.31 (m, 5H), 7.24-7.16 (m, 3H), 7.10-7.09 (br, $J = 4.0$ Hz, 2H), 6.85 (s, 1H), 6.76 (s, 2H), 2.30 (s, 6H). $^{13}\text{C}\{^1\text{H}\}$ NMR (CDCl_3 , 100 MHz): δ 166.9, 151.3, 142.1, 139.5, 135.9, 134.8, 132.4, 131.1, 130.1, 129.6,

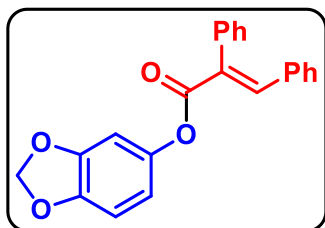
129.0, 128.5, 128.2, 127.7, 119.4, 21.5. **IR (KBr, cm⁻¹):** 3133, 1725, 1401, 1155. **HRMS (ESI) m/z:** [M+Na]⁺ Calcd for C₂₃H₂₀O₂Na: 351.1356; Found: 351.1344.



(E)-2,3-dihydro-1H-inden-5-yl 2,3-diphenylacrylate (3av):

Physical State: pale-yellow solid (27 mg, 80%), **R_f** = 0.8 (10% EtOAc/hexane), **mp** = 102-105 °C. **¹H NMR (CDCl₃, 400 MHz):** δ 8.01 (s, 1H), 7.41-7.31 (m, 5H), 7.23-7.16 (m,

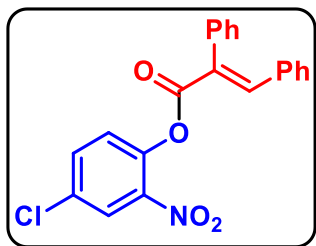
4H), 7.10 (d, *J* = 8.0 Hz, 2H), 6.99 (s, 1H), 6.87 (dd, *J* = 8.0, 4.0 Hz, 1H), 2.89 (q, *J* = 8.0 Hz, 4H), 2.09 (pent, *J* = 8.0 Hz, 2H). **¹³C{¹H} NMR (CDCl₃, 100 MHz):** δ 167.1, 149.9, 145.9, 142.0, 141.9, 135.9, 134.8, 132.5, 131.1, 130.2, 129.6, 129.0, 128.5, 128.2, 125.0, 119.4, 117.9, 33.2, 32.6, 26.1. **IR (KBr, cm⁻¹):** 3141, 1726, 1401, 1159. **HRMS (ESI) m/z:** [M+Na]⁺ Calcd for C₂₄H₂₀O₂Na: 363.1356; Found: 363.1353.



(E)-benzo[d][1,3]dioxol-5-yl 2,3-diphenylacrylate (3aw):

Physical State: amorphous solid (28 mg, 82%), **R_f** = 0.5 (10% EtOAc/hexane), **mp** = 153-155 °C. **¹H NMR (CDCl₃, 400 MHz):** δ 8.00 (s, 1H), 7.42-7.36 (m, 3H), 7.32-7.30 (m, 2H),

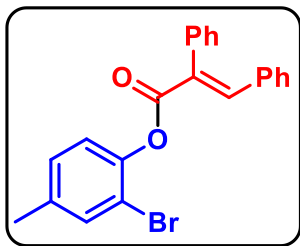
7.23-7.16 (m, 3H), 7.09 (d, *J* = 8.0 Hz, 2H), 6.77 (d, *J* = 8.0 Hz, 1H), 6.67 (br, 1H), 6.57 (dd, *J* = 8.0, 4.0 Hz, 1H), 5.97 (s, 2H). **¹³C{¹H} NMR (CDCl₃, 100 MHz):** δ 167.0, 148.2, 145.7, 145.6, 142.3, 135.7, 134.7, 132.1, 131.1, 130.1, 129.7, 129.0, 128.6, 128.3, 114.2, 108.2, 104.1, 101.9. **IR (KBr, cm⁻¹):** 3140, 1721, 1400, 1171. **HRMS (ESI) m/z:** [M+Na]⁺ Calcd for C₂₂H₁₆O₄Na: 367.094; Found: 367.0941.



(E)-4-chloro-2-nitrophenyl 2,3-diphenylacrylate (3ax):

Physical State: pale-yellow liquid (23 mg, 60%), $R_f = 0.6$ (10% EtOAc/hexane). $^1\text{H NMR}$ (CDCl_3 , 400 MHz): δ 8.10 (d, 1H), 8.06 (s, 1H), 7.60 (dd, $J = 8.0, 4.0$ Hz, 1H), 7.42-7.35

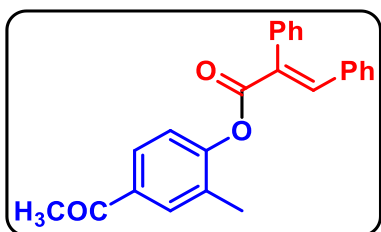
(m, 5H), 7.26-7.17 (m, 4H), 7.10 (br, $J = 4.0$ Hz, 2H). $^{13}\text{C}\{^1\text{H}\}$ NMR (CDCl_3 , 100 MHz): δ 165.7, 144.4, 143.6, 135.2, 135.0, 134.8, 134.3, 132.2, 131.4, 130.8, 130.2, 129.2, 128.7, 128.6, 126.9, 126.8, 126.1. **IR** (KBr , cm^{-1}): 3140, 1777, 1721, 1400, 1107. **HRMS** (ESI) m/z : $[\text{M}+\text{Na}]^+$ Calcd for $\text{C}_{21}\text{H}_{14}\text{ClNO}_4\text{Na}$: 402.0504; Found: 402.0500.



(E)-2-bromo-4-methylphenyl 2,3-diphenylacrylate (3ay):

Physical State: pale-yellow solid (26 mg, 65%), $R_f = 0.7$ (10% EtOAc/hexane), $\text{mp} = 80\text{-}83$ °C. $^1\text{H NMR}$ (CDCl_3 , 400 MHz): δ 8.09 (s, 1H), 7.42-7.37 (m, 6H), 7.25-7.16 (m, 3H), 7.11 (d, $J = 8.0$ Hz, 3H), 7.06 (d, $J = 8.0$ Hz, 1H), 2.32 (s, 3H). $^{13}\text{C}\{^1\text{H}\}$ NMR (CDCl_3 , 100 MHz):

δ 166.0, 146.7, 142.9, 137.6, 135.6, 134.7, 133.9, 131.7, 131.2, 130.3, 129.8, 129.3, 129.0, 128.6, 128.4, 123.6, 116.0, 20.9. **IR** (KBr , cm^{-1}): 3155, 1721, 1401, 1148. **HRMS** (ESI) m/z : $[\text{M}+\text{Na}]^+$ Calcd for $\text{C}_{22}\text{H}_{17}\text{BrO}_2\text{Na}$: 415.0304; Found: 415.0303.

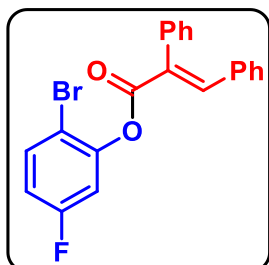


(E)-4-acetyl-2-methylphenyl 2,3-diphenylacrylate (3az):

Physical State: pale white solid (23 mg, 66%), $R_f = 0.2$ (10% EtOAc/hexane), $\text{mp} = 130\text{-}131$ °C. $^1\text{H NMR}$ (CDCl_3 , 400 MHz): δ 8.05 (s, 1H), 7.84-7.81 (m, 2H),

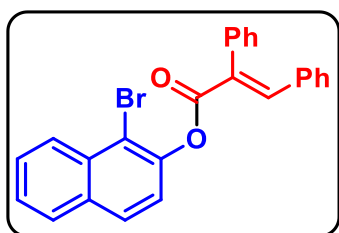
7.43-7.39 (m, 3H), 7.35-7.33 (m, 2H), 7.24-7.18 (m, 4H), 7.11 (d, $J = 8.0$ Hz, 2H), 2.58 (s, 3H), 2.21 (s, 3H). $^{13}\text{C}\{^1\text{H}\}$ NMR (CDCl_3 , 100 MHz): δ 197.6, 165.9, 153.9, 142.9, 135.7, 135.1, 134.5, 131.7, 131.6, 131.2, 131.0, 130.0 (2C), 129.2, 128.7, 128.5, 127.7, 122.4,

26.9, 16.7. **IR (KBr, cm⁻¹):** 3133, 1719, 1685, 1401, 1152. **HRMS (ESI) m/z:** [M+Na]⁺
Calcd for C₂₄H₂₀O₃Na: 379.1305; Found: 379.1297.



(E)-2-bromo-5-fluorophenyl 2,3-diphenylacrylate (3aa1):

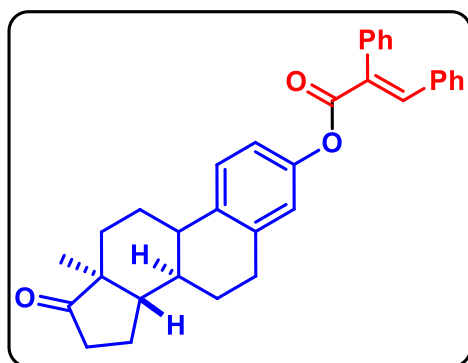
Physical State: pale-yellow solid (30 mg, 76%), **R_f** = 0.8 (10% EtOAc/hexane), **mp** = 115-118 °C. **¹H NMR (CDCl₃, 400 MHz):** δ 8.10 (s, 1H), 7.57-7.53 (m, 1H), 7.42-7.38 (m, 5H), 7.27-7.24 (m, 1H), 7.19 (t, *J* = 8.0 Hz, 2H), 7.12 (d, *J* = 8.0 Hz, 2H), 7.00 (dd, *J* = 8.0, 4.0 Hz, 1H), 6.87 (td, *J* = 8.0 Hz, 4.0 Hz, 1H). **¹³C{¹H} NMR (CDCl₃, 100 MHz):** δ 165.3, 162.2 (d, *J*_{C-F} = 247.0 Hz), 149.7 (d, *J*_{C-F} = 11.0 Hz), 143.6, 135.3, 134.5, 133.9 (d, *J*_{C-F} = 9.0 Hz), 131.3, 131.2, 130.2, 130.0, 129.1, 128.6, 128.5, 114.8 (d, *J*_{C-F} = 22.0 Hz), 112.3 (d, *J*_{C-F} = 25.0 Hz), 111.1 (d, *J*_{C-F} = 4.0 Hz). **¹⁹F NMR (CDCl₃, 376 MHz):** δ -112.1. **IR (KBr, cm⁻¹):** 3141, 1736, 1401, 1147. **HRMS (ESI) m/z:** [M+Na]⁺ Calcd for C₂₁H₁₄BrFO₂Na: 419.0053; Found: 419.0029.



(E)-1-bromonaphthalen-2-yl 2,3-diphenylacrylate (3aa2):

Physical State: white solid (30 mg, 70%), **R_f** = 0.7 (10% EtOAc/hexane), **mp** = 166-168 °C. **¹H NMR (CDCl₃, 400 MHz):** δ 8.26 (d, *J* = 8.0 Hz, 1H), 8.16 (s, 1H), 7.81 (dd, *J* = 8.0, 4.0 Hz, 2H), 7.59 (t, *J* = 8.0 Hz, 1H), 7.50 (t, *J* = 8.0 Hz, 1H), 7.44-7.38 (m, 5H), 7.32 (d, *J* = 8.0 Hz, 1H), 7.24 (d, *J* = 8.0 Hz, 1H), 7.19 (t, *J* = 8.0 Hz, 2H), 7.14 (d, *J* = 8.0 Hz, 2H). **¹³C{¹H} NMR (CDCl₃, 100 MHz):** δ 165.9, 147.2, 143.1, 135.6, 134.7, 133.0, 132.7, 131.7, 131.2, 130.3, 129.9, 129.1, 129.0, 128.6, 128.5 (2C), 128.0, 127.3, 126.6, 122.3, 115.4. **IR (KBr, cm⁻¹):** 3142, 1719, 1401, 1151. **HRMS (ESI) m/z:** [M+H]⁺ Calcd for C₂₅H₁₈BrO₂: 429.0485; Found: 429.0442.

(E)-(8R,13S,14S)-13-methyl-17-oxo-7,8,9,11,12,13,14,15,16,17-decahydro-6H-



cyclopenta[a]phenanthren-3-yl

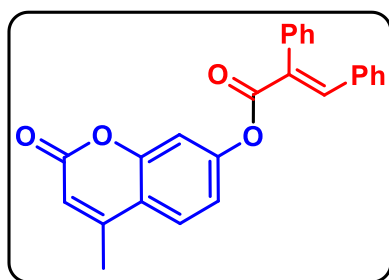
2,3-

diphenylacrylate (3aa3):

Physical State: pale white solid (35 mg, 75%), R_f = 0.2 (10% EtOAc/hexane), **mp** = 148-150 °C. ^1H

NMR (CDCl₃, 400 MHz): δ 8.01 (s, 1H), 7.39-

7.36 (m, 3H), 7.33-7.16 (m, 6H), 7.10 (d, J = 8.0 Hz, 2H), 6.91 (dd, J = 8.0, 4.0 Hz, 1H), 6.87 (br, J = 4.0 Hz, 1H), 2.90 (t, J = 4.0 Hz, 2H), 2.50 (dd, J = 8.0, 4.0 Hz, 1H), 2.39 (s, 1H), 2.17-1.94 (m, 5H), 1.66-1.62 (m, 1H), 1.59-1.45 (m, 7H), 0.91 (s, 3H). $^{13}\text{C}\{^1\text{H}\}$ **NMR (CDCl₃, 100 MHz):** δ 170.1, 166.9, 149.3, 142.1, 138.2, 137.5, 135.8, 134.8, 132.3, 131.1, 130.2, 129.6, 129.0, 128.6, 128.3, 126.6, 121.8, 119.0, 50.7, 48.2, 44.4, 38.3, 36.1, 31.8, 29.7, 26.6, 26.1, 21.9, 14.1. **IR (KBr, cm⁻¹):** 3139, 1724, 1633, 1401, 1160. **HRMS (ESI) m/z:** $[\text{M}+\text{H}]^+$ Calcd for C₃₃H₃₃O₃: 477.2424; found: 477.2419.



(E)-4-methyl-2-oxo-2H-chromen-7-yl

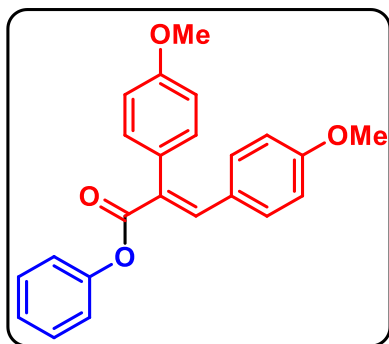
2,3-

diphenylacrylate (3aa4):

Physical State: white solid (31 mg, 82%), R_f = 0.3 (10% EtOAc/hexane), **mp** = 200-203 °C. ^1H **NMR (CDCl₃, 400**

MHz): δ 8.06 (s, 1H), 7.60 (d, J = 8.0 Hz, 1H), 7.44-7.39

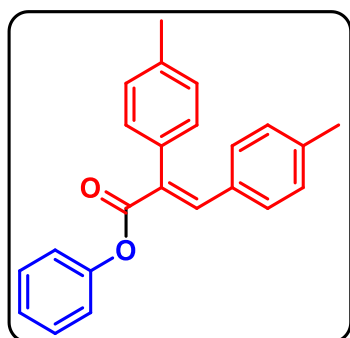
(m, 3H), 7.35-7.32 (m, 2H), 7.28-7.10 (m, 7H), 6.26 (s, 1H), 2.43 (s, 3H). $^{13}\text{C}\{^1\text{H}\}$ **NMR (CDCl₃, 100 MHz):** δ 166.0, 160.8, 154.5, 153.9, 152.2, 143.3, 135.4, 134.4, 131.5, 131.2, 130.1, 130.0, 129.2, 128.6, 128.5, 125.5, 118.5, 118.1, 114.8, 110.8, 19.0. **IR (KBr, cm⁻¹):** 3143, 1726, 1624, 1401, 1142. **HRMS (ESI) m/z:** $[\text{M}+\text{H}]^+$ Calcd for C₂₅H₁₉O₄: 383.1278; Found: 383.1266.



(E)-phenyl 2,3-bis(4-methoxyphenyl)acrylate (3ba):

Physical State: pale white solid (31 mg, 86%), R_f = 0.5 (10% EtOAc/hexane), **mp** = 120-121 °C. ^1H NMR (CDCl_3 , 400 MHz): δ 7.95 (s, 1H), 7.37 (t, J = 7.6 Hz, 2H), 7.25 (t, J = 4.4 Hz, 2H), 7.20 (t, J = 7.2 Hz, 1H),

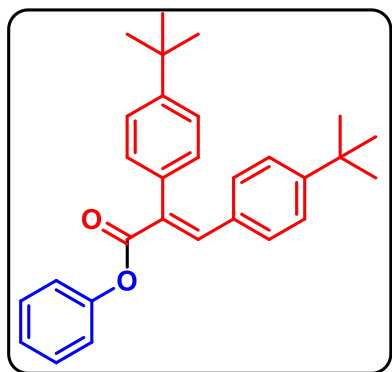
7.13 (d, J = 8.4 Hz, 2H), 7.09 (d, J = 8.8 Hz, 2H), 6.94 (d, J = 8.8 Hz, 2H), 6.72 (d, J = 9.2 Hz, 2H), 3.84 (s, 3H), 3.77 (s, 3H). $^{13}\text{C}\{^1\text{H}\}$ NMR (CDCl_3 , 100 MHz): δ 167.2, 160.8, 159.5, 151.6, 141.8, 132.9, 131.4, 129.6, 129.3, 128.3, 127.6, 125.9, 122.0, 114.6, 114.1, 55.5. **IR (KBr, cm^{-1}):** 3129, 1716, 1401. **HRMS (ESI) m/z :** $[\text{M}+\text{H}]^+$ Calcd for $\text{C}_{23}\text{H}_{21}\text{O}_4$: 361.1434; found: 361.1428.



(E)-phenyl 2,3-di-p-tolylacrylate (3ca):^{18b}

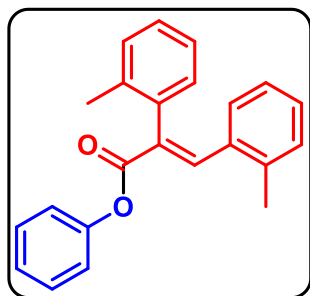
Physical State: pale brown solid (26 mg, 80%), R_f = 0.5 (5% EtOAc/hexane), **mp** = 133-134 °C. ^1H NMR (CDCl_3 , 400 MHz): δ 7.98 (s, 1H), 7.37 (t, J = 7.6 Hz, 2H), 7.22-7.19 (m, 5H), 7.13 (d, J = 8.0 Hz, 2H), 7.03-6.99 (m, 4H), 2.39 (s,

3H), 2.29 (s, 3H). $^{13}\text{C}\{^1\text{H}\}$ NMR (CDCl_3 , 100 MHz): δ 167.0, 151.5, 142.1, 140.0, 138.0, 132.9, 132.0, 131.1, 130.0, 129.8, 129.6, 129.3, 125.9 (2C), 122.0, 21.7 (2C). **IR (KBr, cm^{-1}):** 3134, 1717, 1603, 1399. **HRMS (ESI) m/z :** $[\text{M}+\text{Na}]^+$ Calcd for $\text{C}_{23}\text{H}_{20}\text{O}_2\text{Na}$: 351.1356; found: 351.1331.



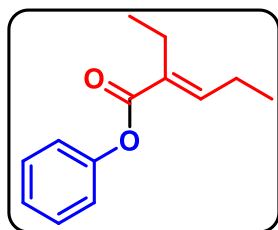
(E)-phenyl 2,3-bis(4-(tert-butyl)phenyl)acrylate (3da):

Physical State: yellow solid (29 mg, 70%), $R_f = 0.6$ (5% EtOAc/hexane), **mp** = 122-123 °C. **^1H NMR (CDCl_3 , 400 MHz):** δ 7.98 (s, 1H), 7.42 (d, $J = 8.8$ Hz, 2H), 7.36 (t, $J = 7.6$ Hz, 3H), 7.26 (d, $J = 8.4$ Hz, 2H), 7.22-7.18 (m, 3H), 7.14 (d, $J = 8.4$ Hz, 2H), 7.05 (d, $J = 8.4$ Hz, 2H), 1.36 (s, 9H), 1.26 (s, 9H). **$^{13}\text{C}\{^1\text{H}\}$ NMR (CDCl_3 , 100 MHz):** δ 167.1, 153.2, 151.6, 151.2, 142.0, 133.0, 132.0, 131.1, 129.7, 129.6, 126.0, 125.9, 125.6 (2C), 122.0, 35.1, 35.0, 31.7, 31.4. **IR (KBr, cm^{-1}):** 3134, 1720, 1605, 1398, 1195. **HRMS (ESI) m/z :** $[\text{M}+\text{H}]^+$ Calcd for $\text{C}_{29}\text{H}_{33}\text{O}_2$: 413.2475; found: 413.2469.



(E)-phenyl 2,3-di-o-tolylacrylate (3ea):

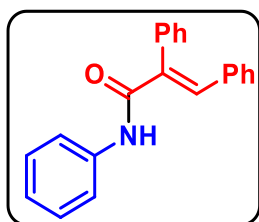
Physical State: white solid (22 mg, 66%), $R_f = 0.6$ (10% EtOAc/hexane), **mp** = 132-133 °C. **^1H NMR (CDCl_3 , 400 MHz):** δ 8.26 (s, 1H), 7.37-7.35 (m, 2H), 7.23-7.19 (m, 3H), 7.17-7.09 (m, 6H), 6.83 (t, $J = 7.6$ Hz, 1H), 6.69 (d, $J = 7.6$ Hz, 1H), 2.46 (s, 3H), 2.24 (s, 3H). **$^{13}\text{C}\{^1\text{H}\}$ NMR (CDCl_3 , 100 MHz):** δ 166.8, 151.5, 140.9, 138.4, 137.0, 135.4, 133.9, 132.3, 130.5 (2C), 130.4, 129.6, 129.4, 129.3, 128.4, 126.3, 126.0, 125.8, 121.9, 20.4, 20.0. **IR (KBr, cm^{-1}):** 3131, 1722, 1615, 1401, 1189. **HRMS (ESI) m/z :** $[\text{M}+\text{Na}]^+$ Calcd for $\text{C}_{23}\text{H}_{20}\text{O}_2\text{Na}$: 351.1356; found: 351.1343.



(E)-phenyl 2-ethylpent-2-enoate (3ha):

Physical State: colourless liquid (13 mg, 64%), $R_f = 0.8$ (5% EtOAc/hexane). **^1H NMR (CDCl_3 , 400 MHz):** δ 7.40-7.36 (m, 2H), 7.23-7.19 (m, 1H), 7.12-7.09 (m, 2H), 6.96 (t, $J = 7.2$ Hz, 1H), 2.42 (q, $J = 7.6$ Hz,

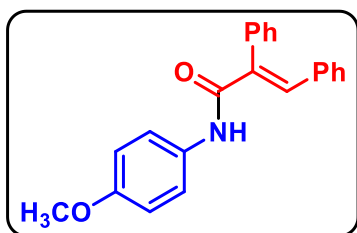
2H), 2.28 (pent, $J = 7.6$ Hz, 2H), 1.10 (m, 6H). $^{13}\text{C}\{^1\text{H}\}$ NMR (CDCl_3 , 100 MHz): δ 166.7, 151.5, 146.1, 133.3, 129.6, 125.8, 122.1, 22.2, 20.4, 14.3, 13.7. IR (KBr, cm^{-1}): 3146, 1728, 1643, 1401, 1197. HRMS (ESI) m/z : $[\text{M}+\text{H}]^+$ Calcd for $\text{C}_{13}\text{H}_{17}\text{O}_2$: 205.1223; found: 205.1223.



(E)-N-2,3-triphenylacrylamide (5aa):^{23a}

Physical State: yellow solid (20 mg, 66%), $R_f = 0.5$ (10% EtOAc/hexane), **mp** = 143-145 °C; ^1H NMR (CDCl_3 , 400 MHz): δ 7.94 (s, 1H), 7.52-7.47 (m, 3H), 7.42 (d, $J = 8.0$ Hz, 2H), 7.36

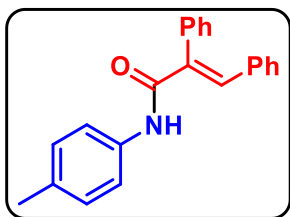
(dd, $J = 8.0, 1.6$ Hz, 2H), 7.28-7.24 (m, 2H), 7.17-7.11 (m, 4H), 7.05 (t, $J = 8.0$ Hz, 1H), 7.01 (d, $J = 8.0$ Hz, 2H). $^{13}\text{C}\{^1\text{H}\}$ NMR (CDCl_3 , 100 MHz): δ 165.3, 138.6, 138.1, 136.1, 135.1, 134.9, 130.8, 130.4, 130.2, 129.2 (2C), 129.1, 128.5, 124.7, 120.2. IR (KBr, cm^{-1}): 3406, 1677, 1597, 1264.



(E)-N-(4-methoxyphenyl)-2,3-diphenylacrylamide (5ab):^{23c}

Physical State: pale-yellow solid (14 mg, 45%), $R_f = 0.7$ (20% EtOAc/hexane), **mp** = 136-138 °C. ^1H NMR (CDCl_3 ,

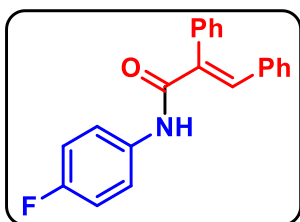
400 MHz): δ 7.96 (s, 1H), 7.51-7.49 (m, 3H), 7.37-7.34 (m, 4H), 7.19-7.13 (m, 3H), 7.11 (br, 1H), 7.02 (d, $J = 8.0$ Hz, 2H), 6.83 (d, $J = 8.0$ Hz, 2H), 3.78 (s, 3H). $^{13}\text{C}\{^1\text{H}\}$ NMR (CDCl_3 , 100 MHz): δ 165.2, 156.8, 138.2, 136.2, 135.2, 134.9, 131.3, 130.7, 130.3, 130.2, 129.2, 129.0, 128.5, 122.0, 114.4, 55.8. IR (KBr, cm^{-1}): 3134, 1670, 1401. HRMS (ESI) m/z : $[\text{M}+\text{Na}]^+$ Calcd for $\text{C}_{22}\text{H}_{19}\text{NO}_2\text{Na}$: 352.1308; Found 352.1322.



(E)-2,3-diphenyl-N-(p-tolyl)acrylamide (5ac):^{23d}

Physical State: pale-yellow liquid (20 mg, 62%), R_f = 0.4 (10% EtOAc/hexane). ^1H NMR (CDCl_3 , 400 MHz): δ 7.96 (s, 1H), 7.53-7.48 (m, 3H), 7.36-7.32 (m, 4H), 7.20-7.13 (m,

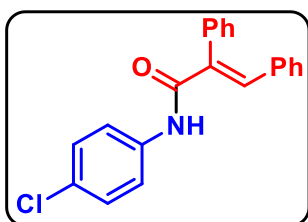
4H), 7.09 (d, J = 8.0 Hz, 2H), 7.02 (d, J = 8.0 Hz, 2H), 2.30 (s, 3H). $^{13}\text{C}\{^1\text{H}\}$ NMR (CDCl_3 , 100 MHz): δ 165.2, 138.4, 136.2, 135.6, 135.2, 135.0, 134.4, 130.8, 130.3, 130.2, 129.7, 129.2, 129.1, 128.5, 120.2, 21.2. IR (KBr, cm^{-1}): 3131, 1667, 1401. HRMS (ESI) m/z : $[\text{M}+\text{H}]^+$ Calcd for $\text{C}_{22}\text{H}_{20}\text{NO}$: 314.1539; Found 314.1526.



(E)-N-(4-fluorophenyl)-2,3-diphenylacrylamide (5ad):

Physical State: white solid (19 mg, 60%), R_f = 0.5 (10% EtOAc/hexane), mp = 182-183 °C. ^1H NMR (CDCl_3 , 400 MHz): δ 7.97 (s, 1H), 7.52-7.49 (m, 3H), 7.43-7.39 (m, 2H),

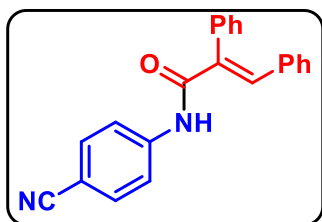
7.36-7.34 (m, 2H), 7.20-7.13 (m, 4H), 7.03-6.96 (m, 4H). $^{13}\text{C}\{^1\text{H}\}$ NMR (CDCl_3 , 100 MHz): δ 165.3, 159.7 (d, $J_{\text{C-F}}$ = 243.0 Hz), 138.7, 136.0, 135.0, 134.6, 134.2, 134.1, 130.8, 130.3 (2C), 129.2 (d, $J_{\text{C-F}}$ = 11.0 Hz), 128.5, 122.0 (d, $J_{\text{C-F}}$ = 7.0 Hz), 115.9 (d, $J_{\text{C-F}}$ = 22.0 Hz). ^{19}F NMR (CDCl_3 , 376 MHz): δ -117.7. IR (KBr, cm^{-1}): 3140, 1643, 1403. HRMS (ESI) m/z : $[\text{M}+\text{Na}]^+$ Calcd for $\text{C}_{21}\text{H}_{16}\text{FNONa}$: 340.1108; Found 340.1123.



(E)-N-(4-chlorophenyl)-2,3-diphenylacrylamide (5ae):

Physical State: yellow solid (22 mg, 67%), R_f = 0.6 (10% EtOAc/hexane), mp = 145-147 °C. ^1H NMR (CDCl_3 , 400 MHz): δ 7.97 (s, 1H), 7.53-7.51 (m, 3H), 7.43-7.40 (m, 2H),

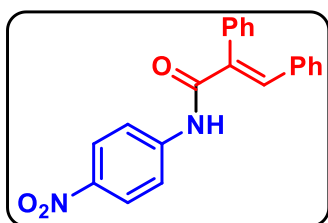
7.36-7.34 (m, 2H), 7.27-7.24 (m, 2H), 7.19-7.16 (m, 4H), 7.04-7.01 (m, 2H). $^{13}\text{C}\{^1\text{H}\}$ NMR (CDCl_3 , 100 MHz): δ 165.3, 138.9, 136.7, 135.9, 135.0, 134.5, 130.8, 130.3 (2C), 129.7, 129.4, 129.3, 129.2, 128.6, 121.4. IR (KBr, cm^{-1}): 3122, 1649, 1397. HRMS (ESI) m/z : $[\text{M}+\text{H}]^+$ Calcd for $\text{C}_{21}\text{H}_{17}\text{ClNO}$: 334.0993; Found 334.0998.



(E)-N-(4-cyanophenyl)-2,3-diphenylacrylamide (5af):

Physical State: white solid (26 mg, 80%), R_f = 0.5 (20% EtOAc/hexane), **mp** = 175-177 °C. ^1H NMR (CDCl_3 , 400 MHz): δ 7.99 (s, 1H), 7.58-7.53 (m, 7H), 7.36-7.34 (m, 3H),

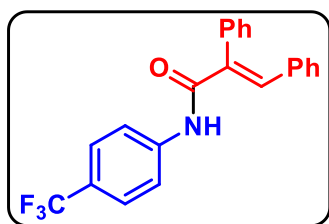
7.23-7.15 (m, 3H), 7.03 (d, J = 8.0 Hz, 2H). $^{13}\text{C}\{^1\text{H}\}$ NMR (CDCl_3 , 100 MHz): δ 165.5, 142.1, 139.9, 135.6, 134.7, 134.0, 133.5, 130.9, 130.5, 130.2, 129.6 (2C), 128.6, 119.9, 119.1, 107.5. IR (KBr, cm^{-1}): 3106, 2224, 1643, 1534. HRMS (ESI) m/z : $[\text{M}+\text{Na}]^+$ Calcd for $\text{C}_{22}\text{H}_{16}\text{N}_2\text{ONa}$: 347.1155; Found 347.1129.



(E)-N-(4-nitrophenyl)-2,3-diphenylacrylamide (5ag):

Physical State: yellow solid (28 mg, 81%), R_f = 0.6 (20% EtOAc/hexane), **mp** = 140-142 °C. ^1H NMR (CDCl_3 , 400 MHz): δ 8.17 (d, J = 8.0 Hz, 2H), 8.01 (s, 1H), 7.62 (d, J = 8.0

Hz, 2H), 7.56-7.54 (m, 3H), 7.47 (br, 1H), 7.38-7.35 (m, 2H), 7.24-7.16 (m, 3H), 7.03 (d, J = 8.0 Hz, 2H). $^{13}\text{C}\{^1\text{H}\}$ NMR (CDCl_3 , 100 MHz): δ 165.5, 143.9, 140.2, 135.5, 134.6, 133.9, 131.0, 130.5, 130.3, 129.7 (2C), 128.7, 125.3, 119.5. IR (KBr, cm^{-1}): 3121, 1682, 1405. HRMS (ESI) m/z : $[\text{M}+\text{Na}]^+$ Calcd for $\text{C}_{21}\text{H}_{16}\text{N}_2\text{O}_3\text{Na}$: 367.1053; Found 367.1054.

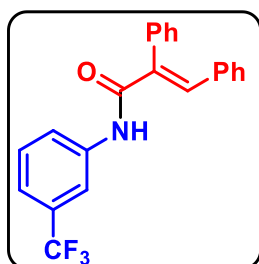


(E)-2,3-diphenyl-*N*-(4-(trifluoromethyl)phenyl)acrylamide

(5ah).^{23c}

was prepared according to general procedure 4 with a modified temperature 80 °C. **Physical State:** colorless liquid (31 mg,

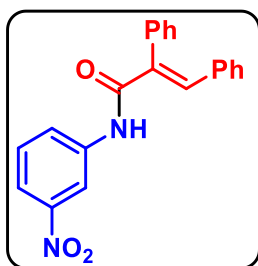
85%), R_f = 0.6 (20% EtOAc/hexane). ^1H NMR (CDCl_3 , 400 MHz): δ 7.99 (s, 1H), 7.59-7.51 (m, 7H), 7.37-7.35 (m, 2H), 7.33 (br, 1H), 7.22-7.15 (m, 3H), 7.03 (d, J = 8.0 Hz, 2H). $^{13}\text{C}\{^1\text{H}\}$ NMR (CDCl_3 , 100 MHz): δ 165.5, 141.2, 139.4, 135.8, 134.8, 134.3, 130.9, 130.4, 130.3, 129.5, 129.4, 128.6, 126.5 (q, $J_{\text{C-F}}$ = 4.0 Hz), 126.3, 124.4 (q, $J_{\text{C-F}}$ = 269.0 Hz), 119.7. ^{19}F NMR (CDCl_3 , 376 MHz): δ -62.1. IR (KBr, cm^{-1}): 3131, 1642, 1401. HRMS (ESI) m/z : $[\text{M}+\text{Na}]^+$ Calcd for $\text{C}_{22}\text{H}_{16}\text{F}_3\text{NONa}$: 390.1076; Found 390.1080.



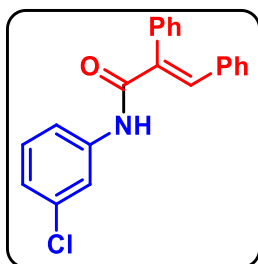
(E)-2,3-diphenyl-*N*-(3-(trifluoromethyl)phenyl)acrylamide (5ai):

was prepared according to general procedure 4 with a modified temperature 80 °C. **Physical State:** colorless liquid (22 mg, 60%),

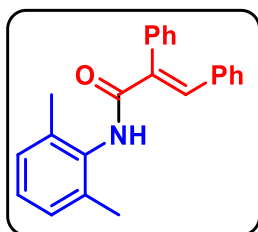
R_f = 0.6 (10% EtOAc/hexane). ^1H NMR (CDCl_3 , 400 MHz): δ 7.99 (s, 1H), 7.74 (s, 1H), 7.65 (d, J = 8.0 Hz, 1H), 7.54-7.53 (m, 3H), 7.42-7.33 (m, 4H), 7.30 (br, 1H), 7.22-7.15 (m, 3H), 7.03 (d, J = 8.0 Hz, 2H). $^{13}\text{C}\{^1\text{H}\}$ NMR (CDCl_3 , 100 MHz): δ 165.5, 139.3, 138.6, 135.8, 134.9, 134.3, 131.5, 130.9, 130.4, 130.3, 130.1 (q, $J_{\text{C-F}}$ = 231.0 Hz), 129.8, 129.5, 129.4, 128.6, 123.3, 121.2 (q, $J_{\text{C-F}}$ = 4.0 Hz), 116.9 (q, $J_{\text{C-F}}$ = 4.0 Hz). ^{19}F NMR (CDCl_3 , 376 MHz): δ -62.7. IR (KBr, cm^{-1}): 3140, 1666, 1400. HRMS (ESI) m/z : $[\text{M}+\text{Na}]^+$ Calcd for $\text{C}_{22}\text{H}_{16}\text{F}_3\text{NONa}$: 390.1076; Found 390.1067.



(E)-N-(3-nitrophenyl)-2,3-diphenylacrylamide (5aj): was prepared according to general procedure **4** with a modified temperature 80 °C. **Physical State:** yellow solid (26 mg, 76%), $R_f = 0.5$ (20% EtOAc/hexane), **mp** = 136-138 °C. ^1H NMR (CDCl_3 , 400 MHz): δ 8.24 (s, 1H), 8.01 (s, 1H), 7.93 (d, $J = 8.0$ Hz, 2H), 7.57-7.54 (m, 3H), 7.49-7.44 (m, 1H), 7.38-7.36 (m, 3H), 7.23-7.15 (m, 3H), 7.03 (d, $J = 8.0$ Hz, 2H). $^{13}\text{C}\{^1\text{H}\}$ NMR (CDCl_3 , 100 MHz): δ 165.6, 148.8, 139.8, 139.3, 135.5, 134.7, 134.0, 130.9, 130.5, 130.2, 130.1, 129.6, 129.5, 128.6, 125.9, 119.3, 114.9. IR (KBr, cm^{-1}): 3139, 1670, 1401. HRMS (ESI) m/z : $[\text{M}+\text{H}]^+$ Calcd for $\text{C}_{21}\text{H}_{17}\text{N}_2\text{O}_3$: 345.1234; Found 345.1220.

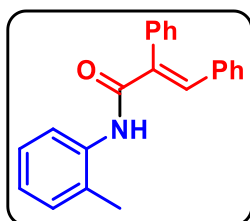


(E)-N-(3-chlorophenyl)-2,3-diphenylacrylamide (5ak): was prepared according to general procedure **4** with a modified temperature 80 °C. **Physical State:** yellow liquid (17 mg, 51%), $R_f = 0.8$ (10% EtOAc/hexane). ^1H NMR (CDCl_3 , 400 MHz): δ 7.97 (s, 1H), 7.55-7.50 (m, 4H), 7.35-7.30 (m, 3H), 7.22-7.14 (m, 5H), 7.07-7.01 (m, 3H). $^{13}\text{C}\{^1\text{H}\}$ NMR (CDCl_3 , 100 MHz): δ 165.3, 139.3, 139.1, 135.8, 134.9 (2C), 134.4, 130.8, 130.3 (2C), 130.2, 129.4, 129.3, 128.6, 124.7, 120.2, 118.1. IR (KBr, cm^{-1}): 3123, 1665, 1401. HRMS (ESI) m/z : $[\text{M}+\text{Na}]^+$ Calcd for $\text{C}_{21}\text{H}_{16}\text{ClN}\text{ONa}$: 356.0813; Found 356.0799.



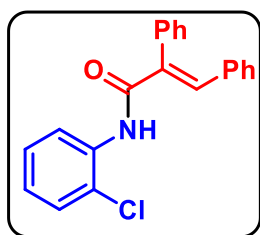
(E)-N-(2,6-dimethylphenyl)-2,3-diphenylacrylamide (5al): was prepared according to general procedure **4** with a modified temperature 80 °C. **Physical State:** colorless liquid (15 mg, 46%), $R_f = 0.5$ (10% EtOAc/hexane). ^1H NMR (CDCl_3 , 400 MHz): δ 7.96 (s, 1H), 7.53-7.46 (m, 3H), 7.43-7.41 (m, 2H), 7.20-7.13 (m, 3H), 7.09-7.05 (m, 5H), 6.70 (br, 1H), 2.18 (s, 6H). $^{13}\text{C}\{^1\text{H}\}$ NMR (CDCl_3 , 100 MHz): δ 165.6, 138.1, 136.9, 135.5,

135.1, 134.4 (2C), 130.8, 130.2, 130.1, 129.1 (2C), 128.5, 128.4, 127.6, 18.8. **IR (KBr, cm⁻¹):** 3131, 1670, 1401. **HRMS (ESI) m/z:** [M+H]⁺ Calcd for C₂₃H₂₂NO: 328.1696; Found 328.1681.



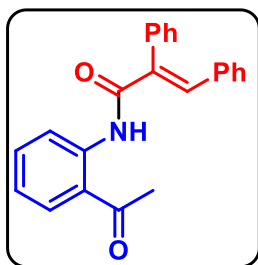
(E)-2,3-diphenyl-N-(o-tolyl)acrylamide (5am):^{23e}

Physical State: yellow solid (21 mg, 67%), **R_f** = 0.6 (10% EtOAc/hexane), **mp** = 92-94 °C; **¹H NMR (CDCl₃, 400 MHz):** δ 8.16 (d, *J* = 8.0 Hz, 1H), 7.99 (s, 1H), 7.55-7.48 (m, 3H), 7.40-7.38 (m, 2H), 7.24-7.15 (m, 5H), 7.08-7.06 (m, 3H), 7.01 (t, *J* = 8.0 Hz, 1H), 1.81 (s, 3H). **¹³C{¹H} NMR (CDCl₃, 100 MHz):** δ 165.1, 138.2, 136.5, 136.4, 135.1, 135.0, 130.8, 130.5, 130.3, 130.2, 129.2, 129.1, 128.5, 127.7, 127.2, 124.9, 121.6, 17.3. **IR (KBr, cm⁻¹):** 3125, 1666, 1401. **HRMS (ESI) m/z:** [M+H]⁺ Calcd for C₂₂H₂₀NO: 314.1539; Found 314.1525.



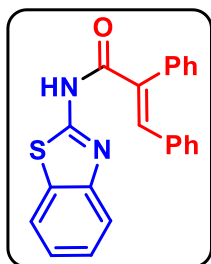
(E)-N-(2-chlorophenyl)-2,3-diphenylacrylamide (5an):

Physical State: pale-yellow solid (23 mg, 70%), **R_f** = 0.6 (10% EtOAc/hexane), **mp** = 107-109 °C. **¹H NMR (CDCl₃, 400 MHz):** δ 8.56 (dd, *J* = 8.0, 1.6 Hz, 1H), 8.00 (s, 1H), 7.92 (br, 1H), 7.54-7.48 (m, 3H), 7.38 (dd, *J* = 8.0, 1.6 Hz, 2H), 7.30-7.25 (m, 2H), 7.21-7.14 (m, 3H), 7.08-7.06 (m, 2H), 6.99 (dt, *J* = 7.6, 1.2 Hz, 1H). **¹³C{¹H} NMR (CDCl₃, 100 MHz):** δ 165.3, 138.8, 135.8, 135.2, 135.0 (2C), 134.9, 130.9, 130.3, 130.2, 129.3, 129.2, 128.6, 128.0, 124.8, 123.2, 121.4. **IR (KBr, cm⁻¹):** 3141, 1687, 1401. **HRMS (ESI) m/z:** [M+Na]⁺ Calcd for C₂₁H₁₆ClN ONa: 356.0813; Found 356.0805.



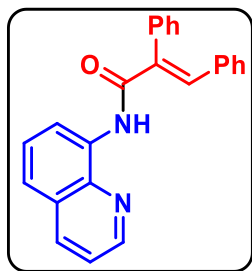
(E)-N-(2-acetylphenyl)-2,3-diphenylacrylamide (5ao):

Physical State: pale-yellow solid (22 mg, 65%), $R_f = 0.4$ (10% EtOAc/hexane), **mp** = 141-143 °C. **^1H NMR (CDCl_3 , 400 MHz):** δ 11.4 (s, 1H), 8.92 (d, $J = 8.0$ Hz, 1H), 7.91 (s, 1H), 7.80 (dd, $J = 8.0, 1.2$ Hz, 1H), 7.58-7.51 (m, 4H), 7.36-7.33 (m, 2H), 7.19-7.13 (m, 3H), 7.11-7.03 (m, 3H), 2.48 (s, 3H). **$^{13}\text{C}\{^1\text{H}\}$ NMR (CDCl_3 , 100 MHz):** δ 202.0, 167.4, 141.0, 138.5, 136.4, 135.5, 135.3, 135.0, 131.7, 130.8, 130.5, 129.8, 129.0, 128.5 (2C), 123.0, 122.8, 121.5, 28.7. **IR (KBr, cm^{-1}):** 3152, 1673, 1653, 1401. **HRMS (ESI) m/z :** $[\text{M}+\text{Na}]^+$ Calcd for $\text{C}_{23}\text{H}_{19}\text{NO}_2\text{Na}$: 364.1308; Found 364.1325.



(E)-N-(benzo[d]thiazol-2-yl)-2,3-diphenylacrylamide (5ap).^{23b}

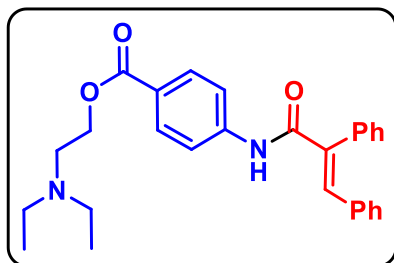
Physical State: pale-yellow solid (23 mg, 65%), $R_f = 0.5$ (10% EtOAc/hexane), **mp** = 198-200 °C. **^1H NMR (CDCl_3 , 400 MHz):** δ 8.74 (br, 1H), 8.10 (s, 1H), 7.84 (d, $J = 8.0$ Hz, 1H), 7.69 (d, $J = 8.0$ Hz, 1H), 7.54-7.53 (m, 3H), 7.42 (t, $J = 7.6$ Hz, 1H), 7.37-7.34 (m, 2H), 7.31 (t, $J = 8.0$ Hz, 1H), 7.25-7.23 (m, 1H), 7.18 (t, $J = 8.0$ Hz, 2H), 7.04 (d, $J = 7.6$ Hz, 2H). **$^{13}\text{C}\{^1\text{H}\}$ NMR (CDCl_3 , 100 MHz):** δ 165.2, 158.3, 148.8, 141.5, 134.5, 134.4, 132.7, 132.3, 131.2, 130.7, 130.3, 130.0, 129.9, 128.7, 126.6, 124.3, 121.7, 121.2. **IR (KBr, cm^{-1}):** 3140, 1666, 1401. **HRMS (ESI) m/z :** $[\text{M}+\text{H}]^+$ Calcd for $\text{C}_{22}\text{H}_{17}\text{N}_2\text{OS}$: 357.1056; Found 357.1041.



(E)-2,3-diphenyl-N-(quinolin-8-yl)acrylamide (5aq): was prepared according to general procedure 4 with a modified temperature 100 °C and reaction time 7 h (as monitored by TLC). **Physical State:** brownish solid (18 mg, 50%), $R_f = 0.5$ (10% EtOAc/hexane), **mp** = 168-170 °C. **^1H NMR (CDCl₃, 400 MHz):** δ 10.12 (br, 1H), 8.90

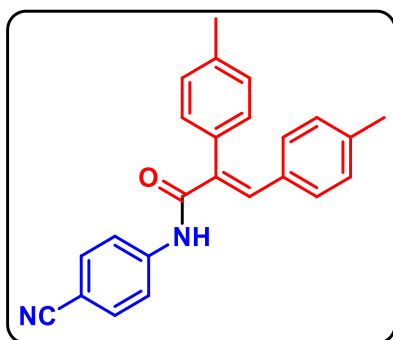
(d, $J = 8.0$ Hz, 1H), 8.47 (br, $J = 4.0$ Hz, 1H), 8.06 (d, $J = 8.0$ Hz, 1H), 8.02 (s, 1H), 7.56-7.53 (m, 4H), 7.47-7.43 (m, 3H), 7.31 (dd, $J = 8.0, 4.0$ Hz, 1H), 7.21-7.18 (m, 3H), 7.12 (d, $J = 8.0$ Hz, 2H). **$^{13}\text{C}\{^1\text{H}\}$ NMR (CDCl₃, 100 MHz):** δ 165.8, 148.3, 139.1, 137.9, 136.3, 136.2, 136.1, 135.3, 135.0, 130.9, 130.4, 130.0, 129.0, 128.8, 128.5, 128.1, 127.7, 121.9, 121.7, 116.6. **IR (KBr, cm⁻¹):** 3140, 1671, 1401. **HRMS (ESI) m/z:** [M+H]⁺ Calcd for C₂₄H₁₉N₂O: 351.1492; Found 351.1480.

(E)-2-(diethylamino)ethyl 4-(2,3-diphenylacrylamido)benzoate (5au):



Physical State: pale-yellow liquid (33 mg, 75%), $R_f = 0.3$ (100% EtOAc). **^1H NMR (CDCl₃, 400 MHz):** δ 7.93 (d, $J = 8.4$ Hz, 3H), 7.52-7.49 (m, 5H), 7.36-7.34 (m, 2H), 7.30 (br, 1H), 7.18-7.12 (m, 3H), 7.99 (d, $J =$

7.6 Hz, 2H), 4.34 (t, $J = 6.4$ Hz, 2H), 2.82 (t, $J = 6.4$ Hz, 2H), 2.62 (q, $J = 7.2$ Hz, 4H), 1.05 (t, $J = 7.2$ Hz, 6H). **$^{13}\text{C}\{^1\text{H}\}$ NMR (CDCl₃, 100 MHz):** δ 166.0, 165.0, 142.4, 139.4, 136.1, 135.0, 134.5, 131.1, 130.9, 130.4, 129.4 (2C), 128.6, 126.2, 119.1, 96.5, 63.4, 51.4, 48.1, 12.4. **IR (KBr, cm⁻¹):** 3132, 1717, 1675, 1402. **HRMS (ESI) m/z:** [M+H]⁺ Calcd for C₂₈H₃₁N₂O₃: 443.2329; Found 443.2338.

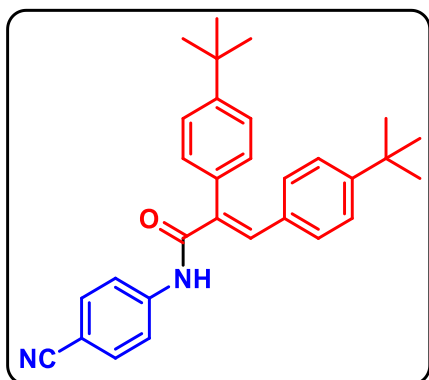


(E)-N-(4-cyanophenyl)-2,3-di-p-tolylacrylamide (5cf):

was prepared according to general procedure 4 with a modified temperature 80 °C. **Physical State:** yellow solid (26 mg, 72%), R_f = 0.2 (10% EtOAc/Hexane), **mp** = 194-195 °C. ^1H NMR (CDCl_3 , 400 MHz): δ 7.93 (s, 1H), 7.59-7.54 (m, 4H), 7.40 (br, 1H), 7.33 (d, J = 8.0

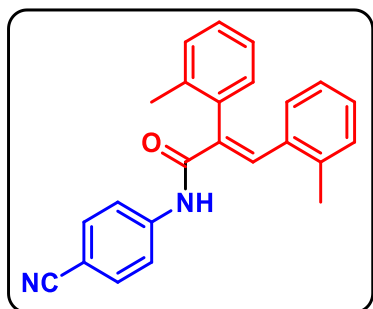
Hz, 2H), 7.22 (d, J = 8.0 Hz, 2H), 6.99 (d, J = 8.0 Hz, 2H), 6.93 (d, J = 8.0 Hz, 2H), 2.46 (s, 3H), 2.28 (s, 3H). $^{13}\text{C}\{^1\text{H}\}$ NMR (CDCl_3 , 100 MHz): δ 165.9, 142.2, 139.9, 139.7, 139.5, 133.4, 132.9, 132.6, 132.0, 131.2, 130.9, 130.1, 129.4, 119.9, 119.2, 107.3, 21.7, 21.6. **IR (KBr, cm^{-1}):** 3288, 2222, 1643, 1406. **HRMS (ESI) m/z :** $[\text{M}+\text{H}]^+$ Calcd for $\text{C}_{24}\text{H}_{21}\text{N}_2\text{O}$: 353.1648; Found 353.1660.

(E)-2,3-bis(4-(tert-butyl)phenyl)-N-(4-cyanophenyl)acrylamide (5df):



Physical State: yellowish liquid (20 mg, 54%), R_f = 0.4 (10% EtOAc/Hexane). ^1H NMR (CDCl_3 , 400 MHz): δ 7.94 (s, 1H), 7.57-7.55 (m, 6H), 7.39 (br, 1H), 7.28-7.26 (m, 2H), 7.18 (d, J = 8.8 Hz, 2H), 6.96 (d, J = 8.4 Hz, 2H), 1.42 (s, 9H), 1.25 (s, 9H). $^{13}\text{C}\{^1\text{H}\}$

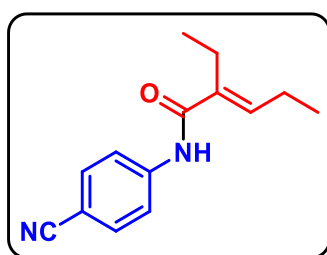
NMR (CDCl_3 , 100 MHz): δ 165.9, 153.1, 152.8, 142.3, 139.6, 133.4, 132.9, 132.6, 131.9, 130.9, 129.8, 127.4, 125.6, 120.0, 119.2, 107.4, 35.2, 35.0, 31.6, 31.4. **IR (KBr, cm^{-1}):** 3384, 3130, 2962, 2218, 1692, 1404. **HRMS (ESI) m/z :** $[\text{M}+\text{H}]^+$ Calcd for $\text{C}_{30}\text{H}_{33}\text{N}_2\text{O}$: 437.2587; Found 437.2578.



(E)-N-(4-cyanophenyl)-2,3-di-o-tolylacrylamide (5ef):

was prepared according to general procedure 4 with a modified temperature 80 °C. **Physical State:** yellowish liquid (16 mg, 46%), $R_f = 0.5$ (10% EtOAc/Hexane). ^1H NMR (CDCl_3 , 400 MHz): δ 8.24 (s, 1H), 7.57 (s, 4H),

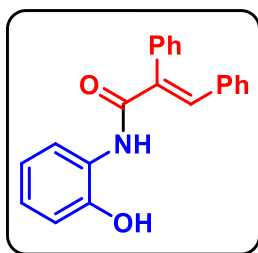
7.38-7.34 (m, 1H), 7.32-7.26 (m, 3H), 7.20-7.15 (m, 2H), 7.12-7.08 (m, 1H), 6.81 (t, $J = 7.6$ Hz, 1H), 6.59 (d, $J = 7.6$ Hz, 1H), 2.47 (s, 3H), 2.16 (s, 3H). $^{13}\text{C}\{^1\text{H}\}$ NMR (CDCl_3 , 100 MHz): δ 165.6, 142.1, 138.6, 138.2, 137.9, 134.5, 134.0, 133.8, 133.5, 131.6, 130.8, 130.6, 129.7, 129.3, 128.7, 127.5, 125.8, 120.0, 119.1, 107.6, 20.5, 19.9. **IR (KBr, cm^{-1}):** 3130, 2224, 1678, 1404. **HRMS (ESI) m/z :** $[\text{M}+\text{H}]^+$ Calcd for $\text{C}_{24}\text{H}_{21}\text{N}_2\text{O}$: 353.1648; Found 353.1643.



(E)-N-(4-cyanophenyl)-2-ethylpent-2-enamide (5hf): was

prepared according to general procedure 4 with a modified temperature 100 °C. **Physical State:** yellowish liquid (12 mg, 55%), $R_f = 0.7$ (30% EtOAc/Hexane). ^1H NMR (CDCl_3 , 400

MHz): δ 7.71-7.69 (m, 3H), 7.61 (d, $J = 8.8$ Hz, 2H), 6.28 (t, $J = 7.6$ Hz, 1H), 2.41 (q, $J = 7.6$ Hz, 2H), 2.24 (pent, $J = 7.6$ Hz, 2H), 1.08 (m, 6H). $^{13}\text{C}\{^1\text{H}\}$ NMR (CDCl_3 , 100 MHz): δ 168.1, 142.6, 138.6, 138.2, 133.5, 119.9, 119.2, 107.1, 21.8, 20.7, 14.0, 13.9. **IR (KBr, cm^{-1}):** 3135, 2223, 1659, 1401. **HRMS (ESI) m/z :** $[\text{M}+\text{Na}]^+$ Calcd for $\text{C}_{14}\text{H}_{16}\text{N}_2\text{ONa}$: 251.1155; Found 251.1153.



(E)-N-(2-hydroxyphenyl)-2,3-diphenylacrylamide (5av):

Physical State: brown solid (20 mg, 63% yield) in both condition **A** and condition **B**, R_f = 0.5 (20% EtOAc/Hexane), **mp** = 175-177

°C. ^1H NMR (CDCl_3 , 400 MHz): δ 9.26 (br, 1H), 8.03 (s, 1H),

7.54-7.51 (m, 3H), 7.43 (br, 1H), 7.38-7.36 (m, 2H), 7.23-7.21 (m, 1H), 7.17 (t, J = 8.0 Hz,

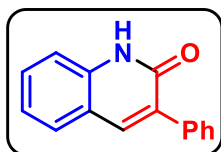
2H), 7.11 (dt, J = 8.4, 1.6 Hz, 1H), 7.03 (dd, J = 7.2, 1.6 Hz, 3H), 6.80-6.76 (m, 1H), 6.67

(d, J = 8.0 Hz, 1H). $^{13}\text{C}\{^1\text{H}\}$ NMR (CDCl_3 , 100 MHz): δ 167.2, 149.5, 140.3, 135.5, 134.6,

132.9 (2C), 131.0, 130.5, 130.3, 129.6, 128.6, 127.8, 125.7, 122.6, 120.5 (2C). **IR (KBr,**

cm^{-1}): 3139, 1653, 1401. **HRMS (ESI) m/z:** $[\text{M}+\text{H}]^+$ Calcd for $\text{C}_{21}\text{H}_{18}\text{NO}_2$: 316.1332;

Found 316.1311.



3-phenylquinolin-2(1H)-one (5aa').^{20g}

Physical State: pink solid (19 mg, 86%), R_f = 0.2 (20% EtOAc/Hexane), **mp** = 275-276 °C. ^1H NMR ($\text{DMSO}-d_6$, 400 MHz):

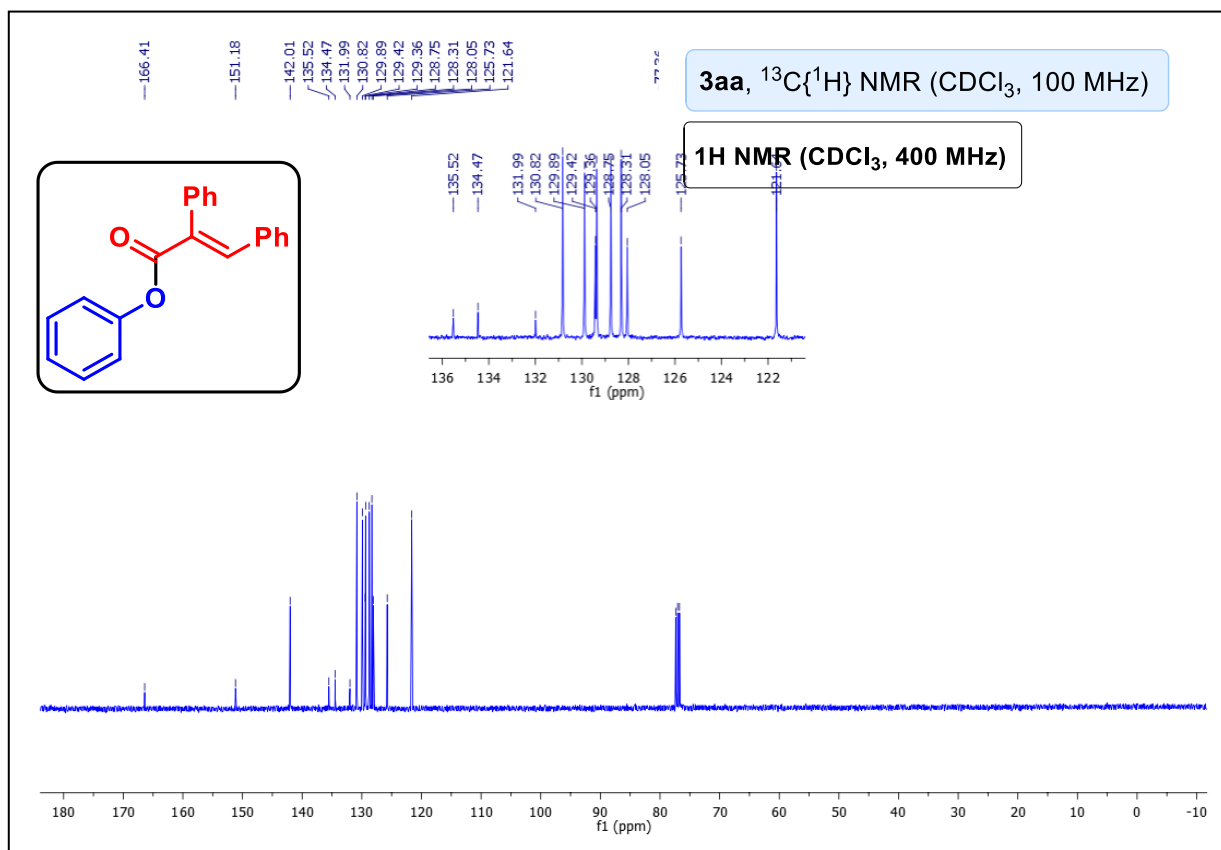
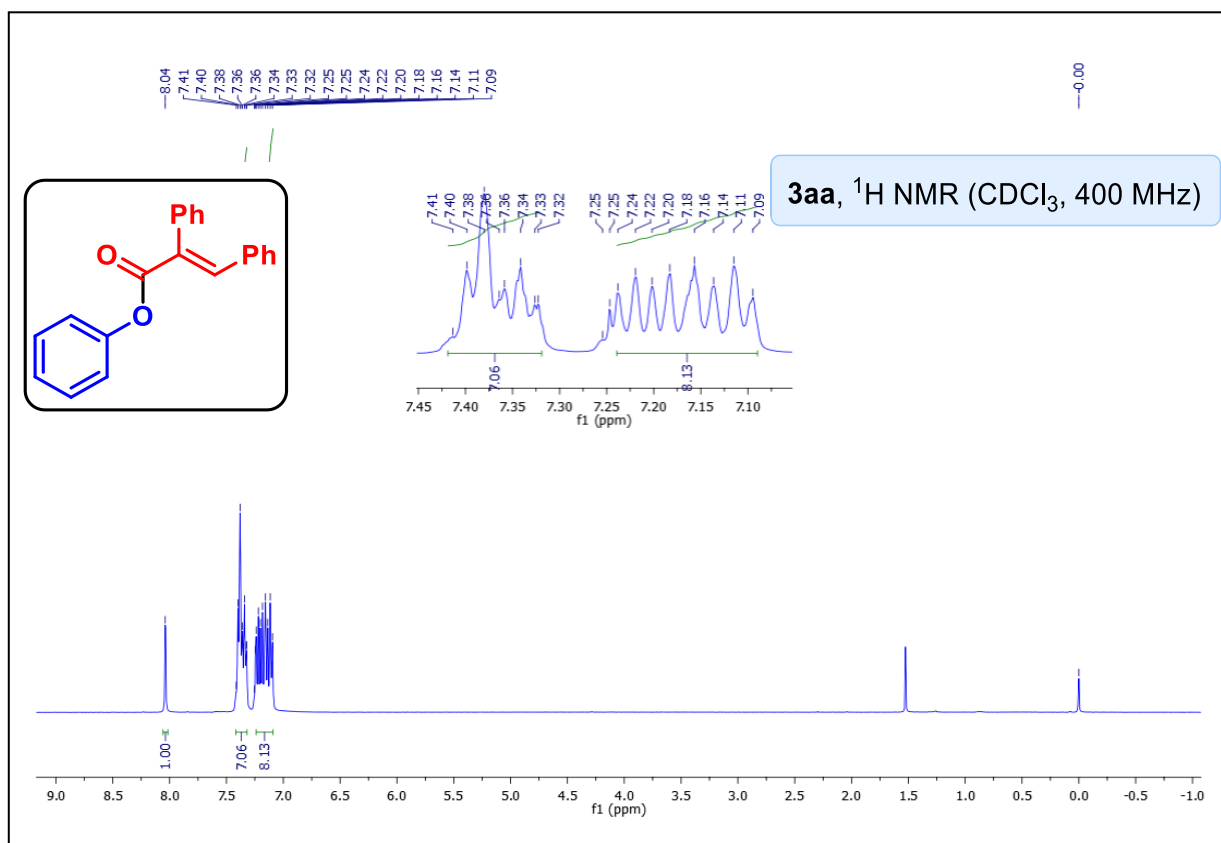
δ 11.98 (s, 1H), 8.13 (s, 1H), 7.80-7.75 (m, 3H), 7.55-7.51 (m, 1H), 7.48-7.45 (m, 2H),

7.42-7.36 (m, 2H), 7.23 (t, J = 7.2 Hz, 1H). $^{13}\text{C}\{^1\text{H}\}$ NMR ($\text{DMSO}-d_6$, 100 MHz): δ 161.9,

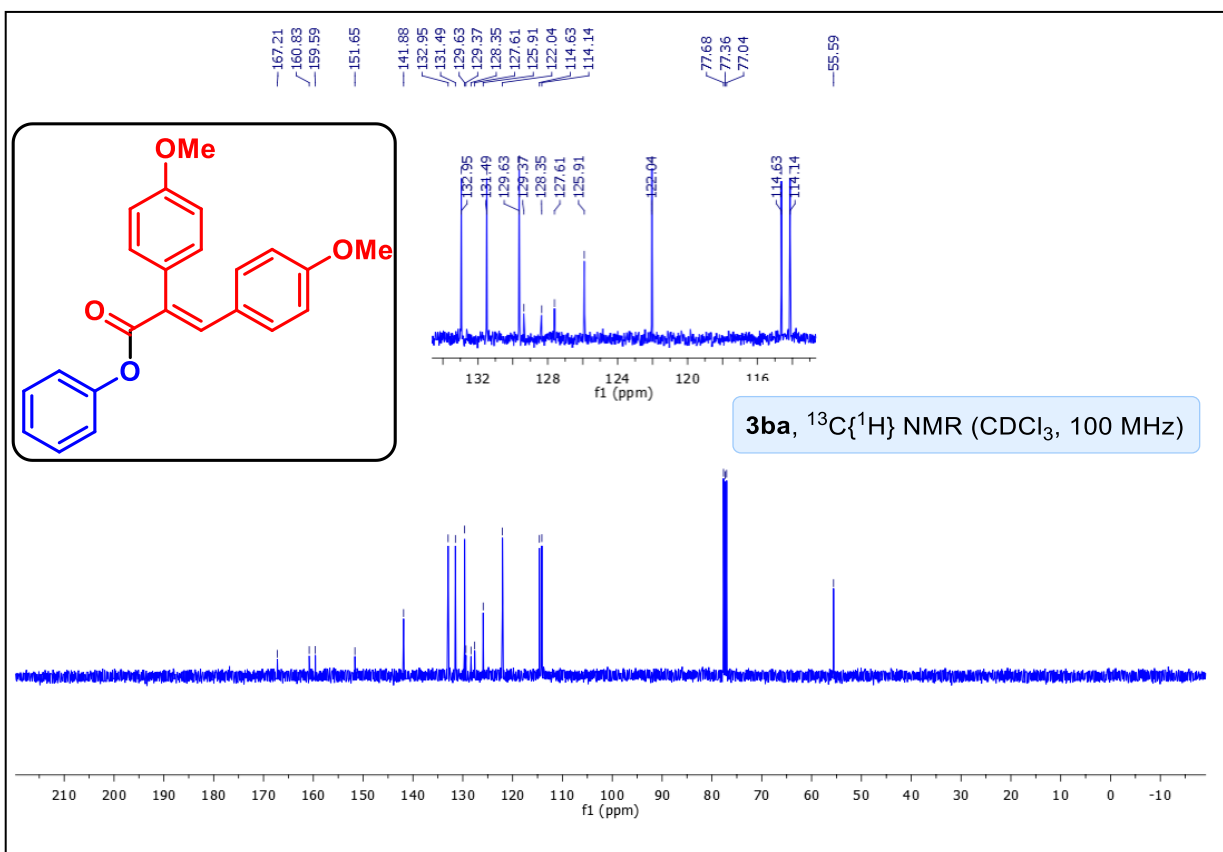
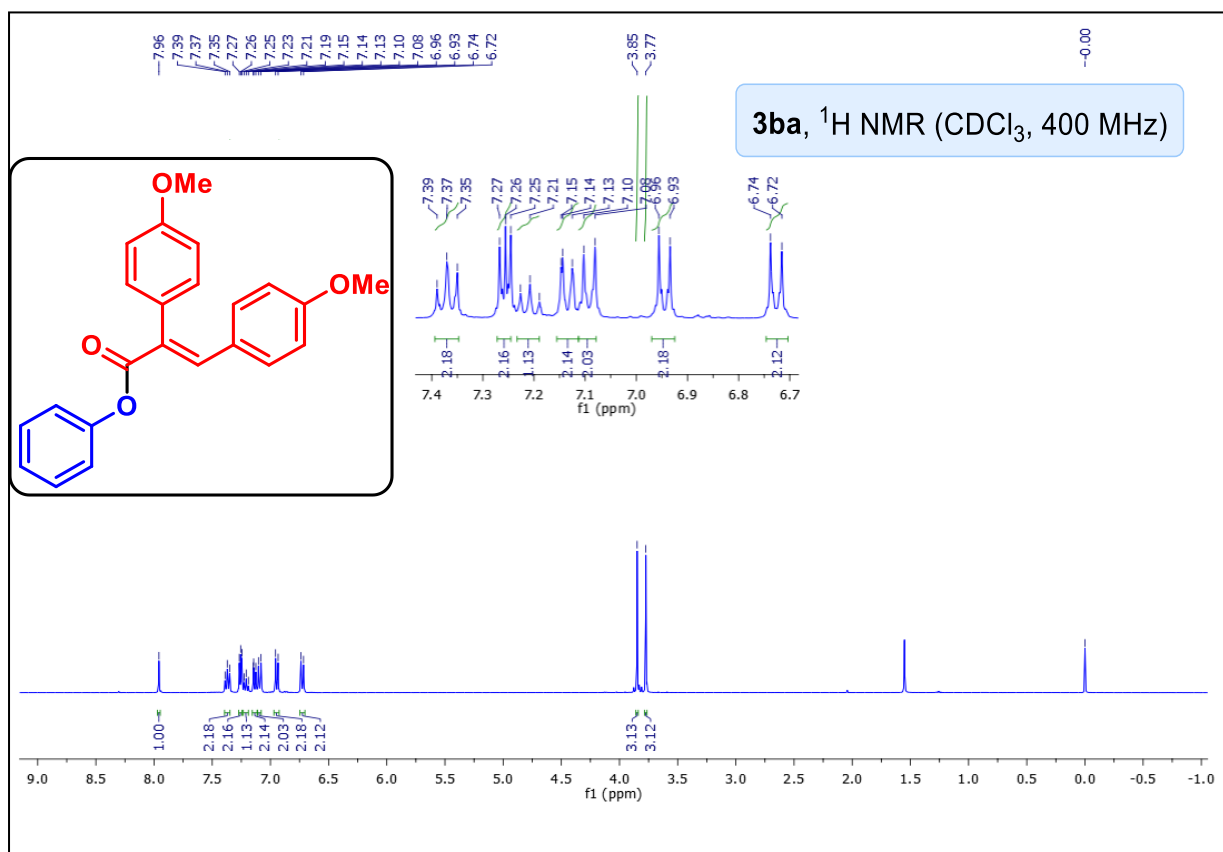
139.3, 138.5, 137.2, 132.4, 131.1, 129.6, 129.0, 128.8, 128.7, 122.8, 120.5, 115.6. **IR (KBr,**

cm^{-1}): 3305, 1652, 1567 1400.

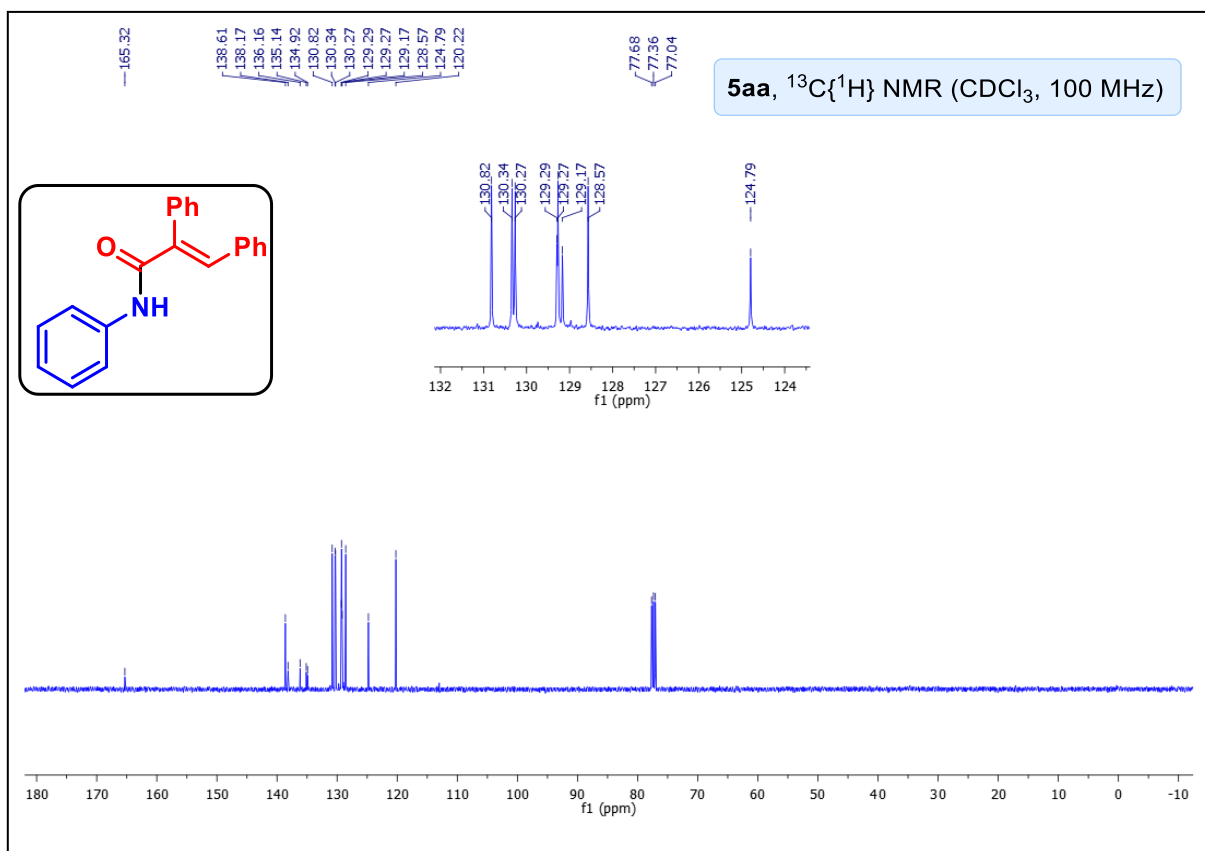
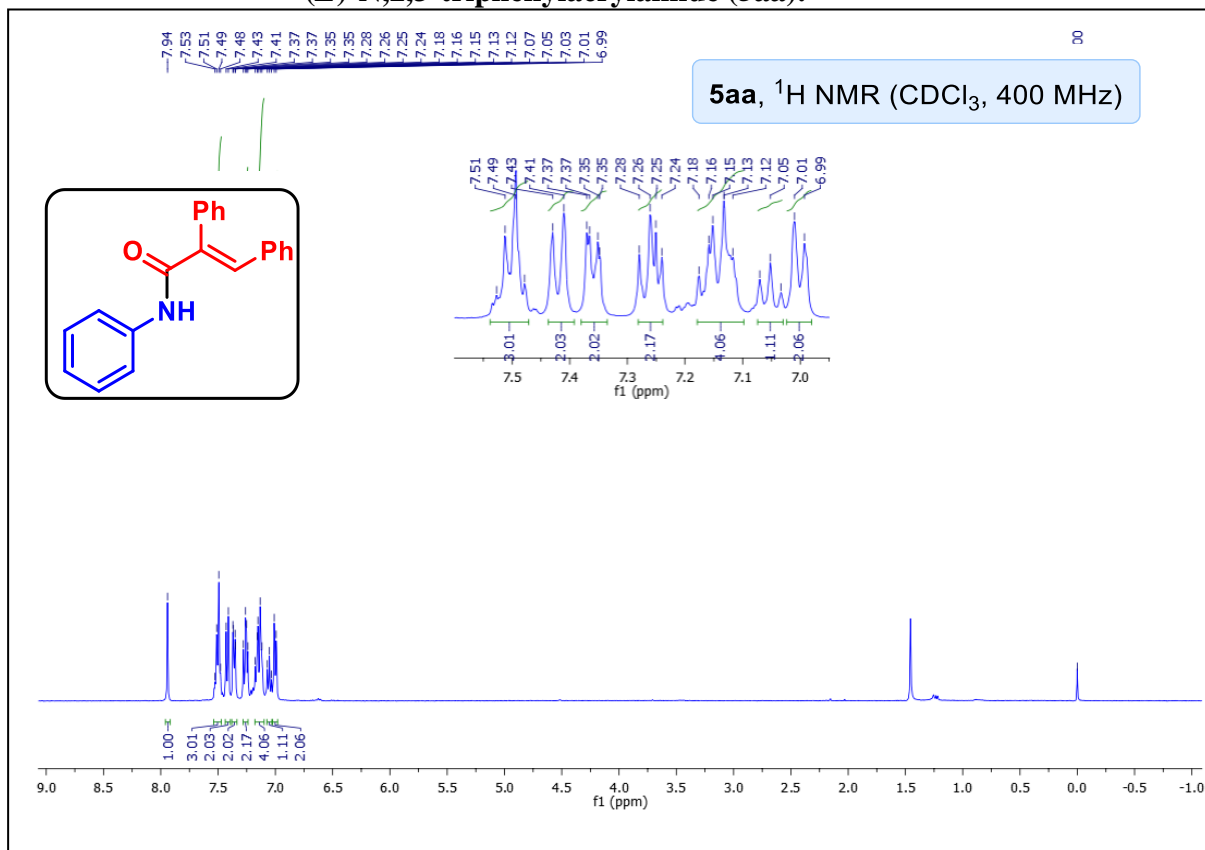
NMR spectra of (*E*)-phenyl 2,3-diphenylacrylate (3aa):



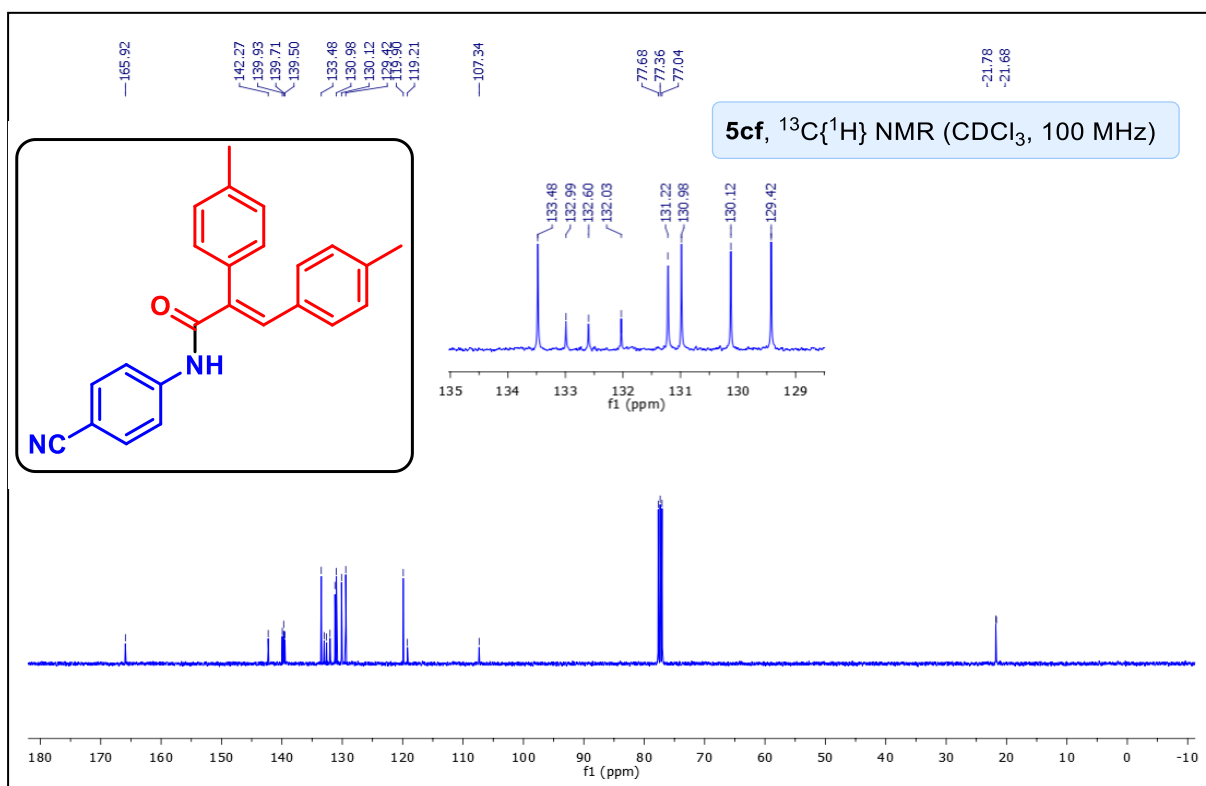
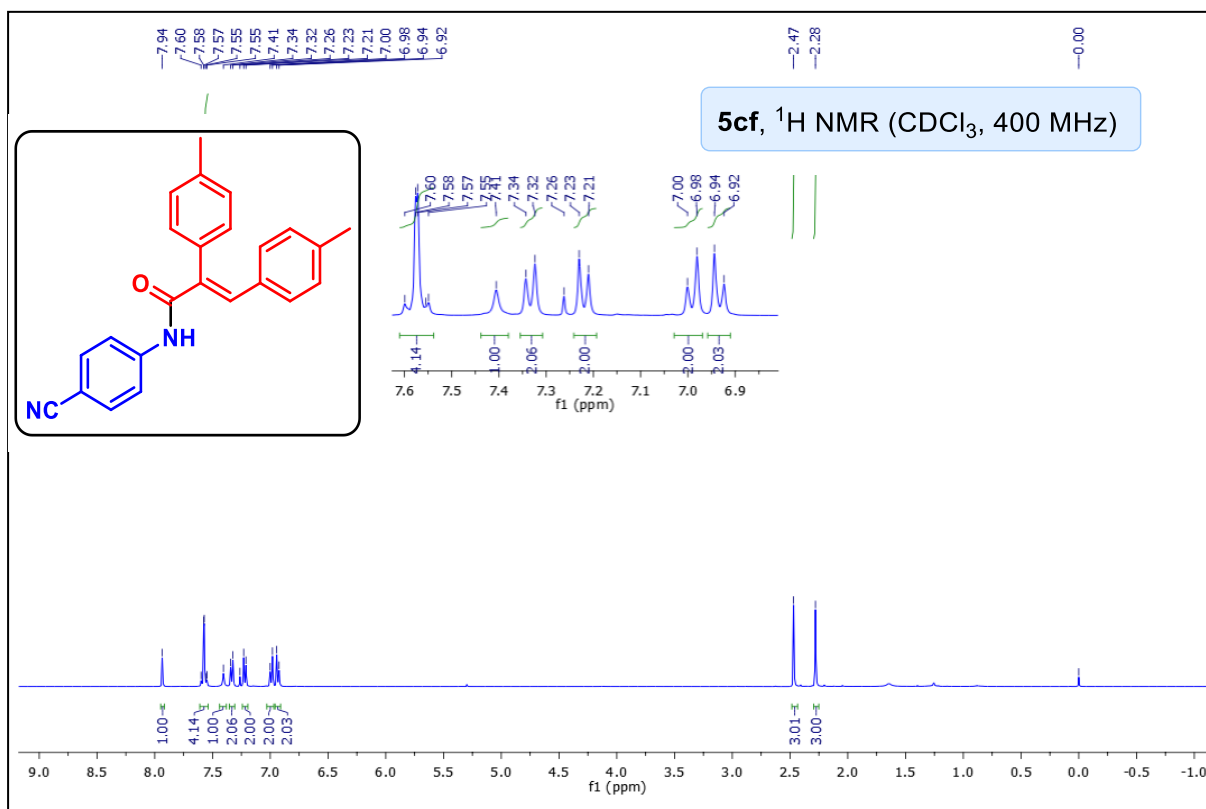
(*E*)-phenyl 2,3-bis(4-methoxyphenyl)acrylate (**3ba**):



(E)-N,2,3-triphenylacrylamide (5aa):



(*E*)-N-(4-cyanophenyl)-2,3-di-*p*-tolylacrylamide (5cf):



(a) X-ray data of (*E*)-benzo[d][1,3]dioxol-5-yl 2,3-diphenylacrylate (3aw**):**

Crystals of the compound (*E*)-benzo[d][1,3]dioxol-5-yl 2,3-diphenylacrylate (**3aw**) were obtained after slow evaporation of methylenedichloride. Crystals suited for single crystal X-Ray diffraction measurements were mounted on a glass fiber. Geometry and intensity data were collected with a Rigaku Smartlab X-ray diffractometer equipped with graphite-monochromated Mo-K α radiation ($\lambda = 0.71073$ Å, multilayer optics). Temperature was controlled using an Oxford Cryostream 700 instrument. Intensities were integrated with SAINT and SMART software packages and corrected for absorption with SADABS. The structure was solved by direct methods and refined on F² with SHELXL-97 using Olex-2 software.

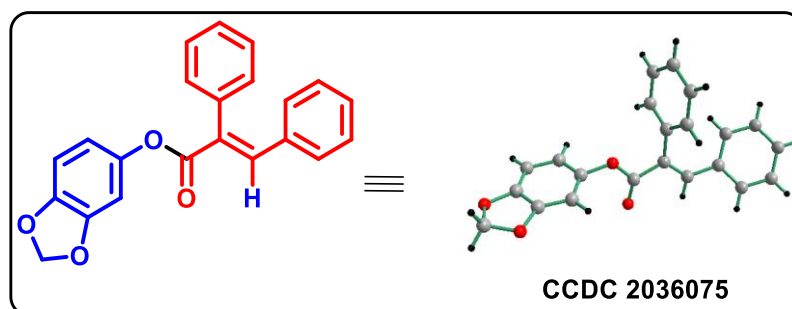
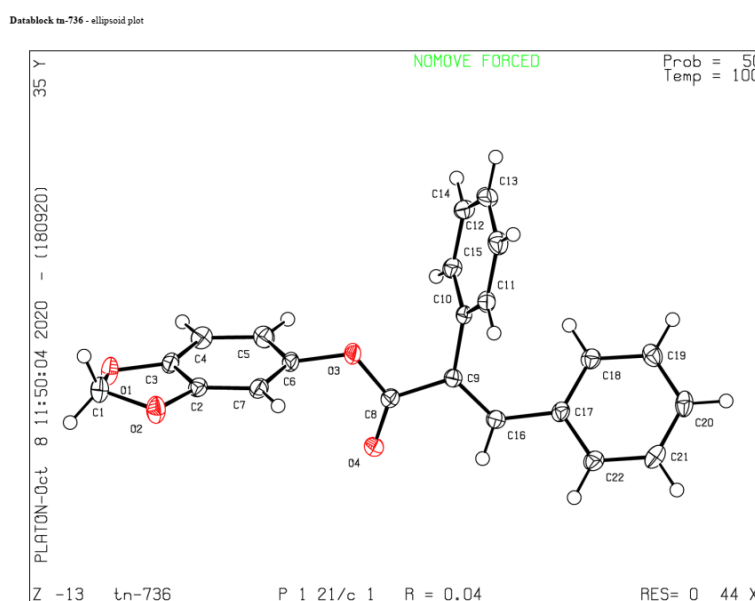


Figure 3.1 ORTEP diagram of **3aw** with 50% ellipsoid probability



(b) X-ray data of (*E*)-2, 3-diphenyl-*N*-(quinolin-8-yl)acrylamide (5aq**):**

Crystals of the compound (*E*)-2, 3-diphenyl-*N*-(quinolin-8-yl)acrylamide (**5aq**) were obtained after slow evaporation of methylenedichloride. Crystals suited for single crystal X-Ray diffraction measurements were mounted on a glass fiber. Geometry and intensity data were collected with a Rigaku Smartlab X-ray diffractometer equipped with graphite-monochromated Mo-K α radiation ($\lambda = 0.71073$ Å, multilayer optics). Temperature was controlled using an Oxford Cryostream 700 instrument. Intensities were integrated with SAINT and SMART software packages and corrected for absorption with SADABS. The structure was solved by direct methods and refined on F2 with SHELXL-97 using Olex-2 software.

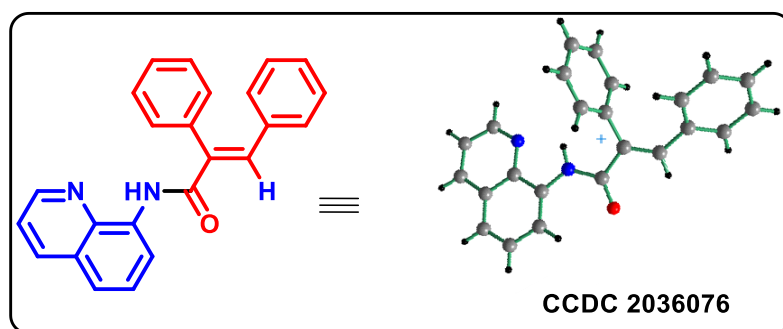
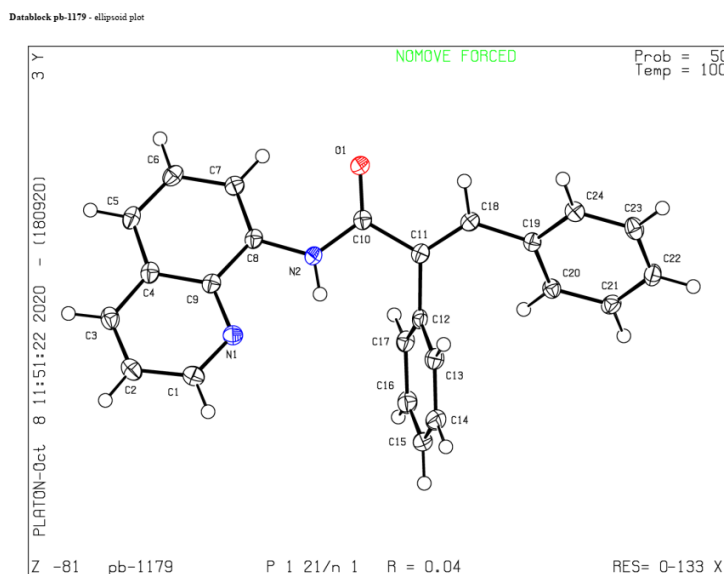


Figure 3.2 ORTEP diagram of **5aq** with 50% ellipsoid probability



3.6 REFERENCES

1. Crabtree, R. H. The Organometallic Chemistry of Alkanes. *Chem. Rev.* **1985**, *85*, 245-269. (b) Jones, W. D. The Fall of the C-C Bond. *Nature* **1993**, *364*, 676– 677. (c) Jun, C.-H.; Moon, C. W.; Lee, H.; Lee, D.Y. Chelation-Assisted Carbon–Carbon Bond Activation by Rh (I) Catalysts. *J. Mol. Catal. A: Chem.* **2002**, *189*, 145–156. (d) Jun, C.-H. Transition Metal-Catalyzed Carbon-Carbon Bond Activation. *Chem. Soc. Rev.* **2004**, *33*, 610–618. (e) Seiser, T.; Saget, T.; Tran, D. N.; Cramer, N. Cyclobutanes in Catalysis. *Angew. Chem., Int. Ed.* **2011**, *50*, 7740-7752. (f) Murakami, M.; Matsuda, T. Metal-Catalysed Cleavage of Carbon-Carbon Bonds. *Chem. Commun.* **2011**, *47*, 1100–1105. (g) Ruhland, K. Transition Metal-Mediated Cleavage and Activation of C–C Single Bonds. *Eur. J. Org. Chem.* **2012**, *14*, 2683–2706. (h) Chen, F.; Wang, T.; Jiao, N. Recent Advances in Transition Metal-Catalyzed Functionalization of Unstrained Carbon–Carbon Bonds. *Chem. Rev.* **2014**, *114*, 8613–8661. (i) Souillart, L.; Cramer, N. Catalytic C–C Bond Activations via Oxidative Addition to Transition Metals. *Chem. Rev.* **2015**, *115*, 9410– 9464.
2. Rybtchinski, B.; Milstein, D. Metal Insertion into C-C Bonds in Solution. *Angew. Chem., Int. Ed.* **1999**, *38*, 870–883.
3. (a) Murakami, M.; Matsuda, T. Metal-Catalysed Cleavage of Carbon-Carbon Bonds. *Chem. Commun.* **2011**, *47*, 1100–1105. (b) Ishida, N.; Sawano, S.; Murakami, M. Stereospecific Ring Expansion from Orthocyclophanes with Central Chirality to Metacyclophanes with Planar Chirality. *Nat. Commun.* **2014**, DOI: [10.1038/ncomms4111](https://doi.org/10.1038/ncomms4111). (c) Okumura, S.; Sun, F.; Ishida, N.; Murakami, M. Palladium Catalyzed Intermolecular Exchange between C-C and C-Si Sigma Bonds. *J. Am. Chem. Soc.* **2017**, *139*, 12414–12417.
4. (a) C-C Bond Activation; Dong, G., Ed.; Springer: Berlin, 2014; Topics in Current Chemistry 346. (b) Chen, P.; Billett, B. A.; Tsukamoto, T.; Dong, G. Cut and Sew” Transformations via Transition Metal-Catalyzed Carbon-Carbon Bond Activation. *ACS Catal.* **2017**, *7*, 1340–1360. (c) Deng, L.; Chen, M.; Dong, G. Concise Synthesis of (–)-Cycloclavine and (–)-5-epi-Cycloclavine via Asymmetric C–C Activation. *J. Am. Chem. Soc.* **2018**, *140*, 9652-9658.
5. (a) Wang, G.-W.; Bower, J. F. Modular Access to Azepines by Directed Carbonylative C–C Bond Activation of Aminocyclopropanes. *J. Am. Chem. Soc.* **2018**, *140*, 2743–2747. (b) Dalling, A. G.; Yamauchi, T.; McCreanor, N. G.; Cox, L.; Bower, J. F. Carbonylative C–C Bond Activation of Electron-Poor Cyclopropanes: Rhodium-Catalyzed (3 + 1 + 2) Cycloadditions of Cyclopropylamides. *Angew. Chem., Int. Ed.* **2019**, *58*, 221–225 (c) Ma, X. F.; Hazelden, I. R.; Langer, T.; Munday, R. H.; Bower, J. F. Enantioselective aza-Heck cyclizations of N-(tosyloxy)carbamates: Synthesis of pyrrolidines and piperidines. *J. Am. Chem. Soc.* **2019**, *141*, 3356 - 3360. (d) Wang, G.-W.; Boyd, O.; Young, T. A.; Bertrand, S. M.; Bower, J. F. Rhodacyclopentanones as Linchpins for the Atom Economical Assembly of Diverse Polyheterocycles. *J. Am. Chem. Soc.* **2020**, *142*, 1740–1745. (e) Sokolova, O. O.; Bower, J. F.; Selective Carbon–Carbon Bond Cleavage of Cyclopropylamine Derivatives *Chemical Reviews* DOI: [10.1021/acs.chemrev.0c00166](https://doi.org/10.1021/acs.chemrev.0c00166).
6. (a) Li, H.; Li, Y.; Zhang, X.-S.; Chen, K.; Wang, X.; Shi, Z.-J. Pyridinyl directed alkenylation with olefins via Rh(III)-catalyzed CC bond cleavage of secondary arylmethanols. *J. Am. Chem. Soc.* **2011**, *133*, 15244-15247. (b) Chen, K.; Li, H.; Lei, Z.-Q.; Li, Y.; Ye, W.-H.; Zhang, L.-S.; Sun, J.; Shi, Z.-J. Reductive cleavage of

- the Csp²-Csp³ bond of secondary benzyl alcohols: rhodium catalysis directed by N-containing groups. *Angew. Chem., Int. Ed.* **2012**, *51*, 9851-9855. (c) Souillart, L.; Parker, E.; Cramer, N. Highly Enantioselective Rhodium(I)-Catalyzed Activation of Enantiotopic Cyclobutanone C-C Bonds. *Angew. Chem., Int. Ed.* **2014**, *53*, 3001-3005. (d) Kumar, N. Y.; Bechtoldt, A.; Raghuvanshi, K.; Ackermann, L. Ruthenium (II)-Catalyzed Decarboxylative C-H Activation: Versatile Routes to meta-Alkenylated Arenes. *Angew. Chem., Int. Ed.* **2016**, *55*, 6929-6932. (e) Onodera, S.; Ishikawa, S.; Kochi, T.; Kakiuchi, F. Direct Alkenylation of Allylbenzenes via Chelation Assisted C-C Bond Cleavage. *J. Am. Chem. Soc.* **2018**, *140*, 9788-9792. (f) Qiu, Y.; Scheremetjew, A.; Ackermann, L. Electro-Oxidative C-C Alkenylation by Rhodium (III) Catalysis. *J. Am. Chem. Soc.* **2019**, *141*, 2731-2738.
7. (a) Chen, P.-H.; Dong, G. Cyclobutenones and Benzocyclobutenones: Versatile Synthons in Organic Synthesis. *Chem. - Eur. J.* **2016**, *22*, 18290-18315. (b) Deng, L.; Dong, G. Carbon-Carbon Bond Activation of Ketones. *Trends in Chemistry*. Cell Press **2020**. DOI: 10.1016/j.trechm.2019.12.002. (c) Wang, J.; Blaszczyk, S. A.; Li, X.; Tang, W. Transition Metal-Catalyzed Selective Carbon-Carbon Bond Cleavage of Vinylcyclopropanes in Cycloaddition Reactions. *Chem. Rev.* **2020**, DOI: 10.1021/acs.chemrev.0c00160. (d) Ishida, N.; Murakami, M.; Cleavage of Carbon-Carbon σ -Bonds of Four-Membered Rings. *Chem. Rev.* **2020**, DOI: 10.1021/acs.chemrev.0c00569.
 8. Pati, B. V.; Ghosh, A.; Ravikumar, P. C.; Rhodium-Catalyzed Room Temperature C-C Activation of Cyclopropanol for One-Step Access to Diverse 1,6-Diketones. *Org. Lett.* **2020**, *22*, 7, 2854-2860.
 9. (a) Baba, A.; Ohshiro, Y.; Agawa, T. Reactions of diphenylcyclopropenone with ketenes in the presence of nickel tetracarbonyl. *J. Organomet. Chem.* **1976**, *110*, 121-127. (b) Wender, P. A.; Paxton, T. J.; Williams, T. J. Cyclopentadienone Synthesis by Rhodium(I)-Catalyzed [3 + 2] Cycloaddition Reactions of Cyclopropenones and Alkynes. *J. Am. Chem. Soc.* **2006**, *128*, 14814-14815. (c) Matsuda, T.; Sakurai, Y. Palladium-Catalyzed Ring-Opening Alkynylation of Cyclopropenones. *Eur. J. Org. Chem.* **2013**, *2013*, 4219-4222. (d) Xu, J.; Cao, J.; Fang, C.; Lu, T.; Du, D. Organocatalytic C-C Bond Activation of Cyclopropenones for the Ring-Opening Formal [3+2] Cycloaddition with Isatins. *Org. Chem. Front.* **2017**, *4*, 560-564. (e) Kong, L. H.; Zhou, X.-K.; Xu, Y.-W.; Li, X.-W. Rhodium (III) Catalyzed Acylation of C (sp³)-H Bonds with Cyclopropenones. *Org. Lett.* **2017**, *19*, 3644-3647. (f) Ren, J.-T.; Wang, J.-X.; Tian, H.; Xu, J.-L.; Hu, H.; Aslam, M.; Sun, M. Ag(I)-Catalyzed [3 + 2]-Annulation of Cyclopropenones and Formamides via C-C Bond Cleavage. *Org. Lett.* **2018**, *20*, 6636-6639. (g) Zhao, W.-T.; Gao, F.; Zhao, D.; Intermolecular σ -Bond Cross Exchange Reaction between Cyclopropenones and (Benzo)silacyclobutanes: Straightforward Access towards Sila-(benzo)cycloheptenones. *Angew. Chem.* **2018**, *130*, 6437-6440. (h) Haito, A.; Chatani, N.; Rh (I)-Catalyzed [3+2] annulation reactions of cyclopropenones with amides. *Chem. Commun.*, **2019**, *55*, 5740-5742.
 10. (a) Tawata, S.; Taira, S.; Kobamoto, N.; Zhu, J.; Ishihara, M.; Toyama, S. Synthesis and antifungal activity of cinnamic acid esters. *Biosci. Biotechnol. Biochem.* **1996**, *60*, 909-910 (b) Natella, F.; Nardini, M.; Di Filici, M.; Scaccini, C. Benzoic and cinnamic acid derivatives as antioxidants: structure-activity. *J. Agric. Food Chem.* **1999**, *47*, 1453-1459. (c) Zhu, J.; Majikina, M.; Tawata, S. Syntheses and Biological Activities of Pyranyl substituted Cinnamates. *Biosci. Biotechnol. Biochem.* **2001**, *65*, 161-163. (d) Gobec, S.; Sova, M.; Kristan, K.; Rizner, T. L.

- Cinnamic acid esters as potent inhibitors of fungal 17-hydroxysteroid dehydrogenase - a model enzyme of the short-chain dehydrogenase/reductase superfamily. *Bioorg. Med. Chem. Lett.* **2004**, *14*, 3933–3936. (e) Narasimhan, B.; Belsare, D.; Pharande, D.; Mourya, V.; Dhake, A. Esters, amides and substituted derivatives of cinnamic acid: synthesis, antimicrobial activity and QSAR investigations. *Eur. J. Med. Chem.* **2004**, *39*, 827–834. (f) Sova, M.; Perdih, A.; Kotnik, M.; Kristan, K.; Rizner, T. L.; Solmajer, T.; Gobec, S. Flavonoids and cinnamic acid esters as inhibitors of fungal 17 β -hydroxysteroid dehydrogenase: A synthesis, QSAR and modelling study. *Bioorg. Med. Chem.* **2006**, *14*, 7404–7418. (g) Ruiz, D. M.; Romanelli, G. P.; Bennardi, D. O.; Baronetti, G. T.; Thomas, H. J.; Autinoa, J. C. Direct esterification of cinnamic acids with phenols and imidoalcohols: a simple, heteropolyacid-catalyzed procedure. *Arkivoc* **2008**, *8*, 269–276.
11. (a) *The Amide Linkage: Selected Structural Aspects in Chemistry, Biochemistry and Materials Science*; Greenberg, A., Breneman, C. M., Liebman, J. F., Eds.; Wiley-VCH: New York, 2000. (b) Caulfield, M. J.; Qiao, G. G.; Solomon, D. H. Some Aspects of the Properties and Degradation of Polyacrylamides. *Chem. Rev.* **2002**, *102*, 3067–3084. (c) Dugger, R. W.; Ragan, J. A.; Ripin, D. H. B. Development of a Pilot-Plant-Scale Synthesis of an Alkylated Dihydrobenzothiadiazole S,S-Dioxide: Incorporation of a Late-Stage Mitsunobu Reaction. *Org. Process Res. Dev.* **2005**, *9*, 253–258. (d) Hung, C.-C.; Tsai, W.-J.; Yang Kuo, L.-M.; Kuo, Y.-H. Evaluation of caffeic acid amide analogues as anti-platelet aggregation and anti-oxidative agents *Bioorg. Med. Chem.* **2005**, *13*, 1791–1797. (e) Buchanan, M. S.; Carroll, A. R.; Addepalli, R.; Avery, V. M.; Hooper, J. N. A.; Quinn, R. J. J. Psammaphysenes C and D, Cytotoxic Alkaloids from *Psammoclemma* sp. *Nat. Prod.* **2007**, *70*, 1827–1829. (f) Roughley, S. D.; Jordan, A. M. The Medicinal Chemist's Toolbox: An Analysis of Reactions Used in the Pursuit of Drug Candidates. *J. Med. Chem.* **2011**, *54*, 3451–3479.
 12. For selected books and reviews, see: (a) *Advanced Organic Chemistry*, 5th ed.; Smith, M. B., March, J., Eds.; Wiley-VCH: New York, 2001. (b) *Modern Aldol Reactions*; Mahrwald, R., Ed.; Wiley-VCH: Weinheim, Germany, 2004. (c) Nielsen, A. T.; Houlihan, W. J. The Aldol Condensation. *Org. React.* **2011**, *16*, 1–438
 13. (a) Maercker, A. The Wittig reaction. *Org. React.* **1965**, *14*, 270–490 (b) *Some Modern Methods of Organic Synthesis*; Carruthers, W., Ed.; Cambridge University Press: Cambridge, U.K., 1971. (c) Maryanoff, B. E.; Reitz, A. B. The Wittig olefination reaction and modifications involving phosphoryl-stabilised carbanions. Stereochemistry, mechanism and selected synthetic aspects. *Chem. Rev.* **1989**, *89*, 863–927.
 14. (a) Boutagy, J.; Thomas, R. Olefin Synthesis with Organic Phosphonate Carbanions. *Chem. Rev.* **1974**, *74*, 87–99. (b) Wadsworth, W. S., Jr. Synthetic applications of phosphoryl-stabilized anions. *Org. React.* **1977**, *25*, 73–253. (c) Kelly, S. E. In *Comprehensive Organic Synthesis*; Trost, B. M., Fleming, I., Eds.; Pergamon: Oxford, UK, 1991; Vol. 1, p 729.
 15. (a) *Handbook of Reagents for Organic Synthesis: Activating Agents and Protecting Groups*; Pearson, A. J., Roush, W. R., Eds.; Wiley-VCH: New York, 1999. (b) Montalbetti, C. A. G. N.; Falque, V. Amide bond formation and peptide coupling. *Tetrahedron* **2005**, *61*, 10827–10852. (c) Valeur, E.; Bradley, M. Amide Bond Formation: Beyond the Myth of Coupling Reagents. *Chem. Soc. Rev.* **2009**, *38*, 606–631. (d) Pattabiraman, V. J.; Bode, J. W. Rethinking amide bond synthesis. *Nature* **2011**, *480*, 471–479. (e) de Figueiredo, R. M.; Suppo, J.-S.; Campagne, J.-

- M. Nonclassical Routes for Amide Bond Formation. *Chem. Rev.* **2016**, *116*, 12029–12122.
16. Kuniyasu, H.; Yoshizawa, T.; Kambe, N. Palladium-catalyzed hydro phenoxy carbonylation of internal alkynes by phenol and CO: the use of Zn for the formation of active catalyst *Tetrahedron Lett.* **2010**, *51*, 6818-6821.
 17. (a) Park, J. H.; Kim, S. Y.; Kim, S. M.; Chung, Y. K. Cobalt–Rhodium Heterobimetallic Nanoparticle-Catalyzed Synthesis of α,β -Unsaturated Amides from Internal Alkynes, Amines, and Carbon Monoxide. *Org. Lett.* **2007**, *9*, 2465–2468. (b) Fujihara, T.; Katafuchi, Y.; Iwai, T.; Terao, J.; Tsuji, Y. Palladium-Catalyzed Intermolecular Addition of Formamides to Alkynes. *J. Am. Chem. Soc.* **2010**, *132*, 2094–2098.
 18. (a) Chenniappan, V. K.; Rahaim, R. J. Titanium-Promoted Cross Coupling for the Selective Synthesis of Polysubstituted, Conjugated Amides. *Org. Lett.* **2016**, *18*, 5090–5093. (b) Katafuchi, Y.; Fujihara, T.; Iwai, T.; Terao, J.; Tsuji, Y. Palladium-Catalyzed Hydroesterification of Alkynes Employing Aryl Formates without the Use of External Carbon Monoxide. *Adv. Synth. Catal.* **2011**, *353*, 475-482.
 19. Nanda, T.; Ravikumar, P. C. A Palladium-Catalyzed Cascade C–C Activation of Cyclopropenone and Carbonylative Amination: Easy Access to Highly Functionalized Maleimide Derivatives. *Org. Lett.* **2020**, *22*, 1368-1374.
 20. (a) Manimaran, T.; Natarajan, M.; Ramakrishnan, V. T.; Synthesis of 3-methylcoumarins, -thiacoumarins and-carbostyrils *Proc. - Indian Acad. Sci.*, **1979**, *88*, 125–130. (b) Grasa, G. A.; Viciu, M. S.; Huang, J.; Nolan, S. P. Amination Reactions of Aryl Halides with Nitrogen-Containing Reagents Mediated by Palladium/Imidazolium Salt Systems. *J. Org. Chem.* **2001**, *66*, 7729–7737. (c) Ito, N.; Watahiki, T.; Maesawa, T.; Maegawa, T.; Sajiki, H. Synergistic Effect of a Palladium-on-Carbon/Platinum-on-Carbon Mixed Catalyst in Hydrogen/Deuterium Exchange Reactions of Alkyl-Substituted Aromatic Compounds. *Adv. Synth. Catal.* **2006**, *348*, 1025–1028. (d) Molina de la Torre, J. A.; Espinet, P.; Albeniz, A. C. Solvent-Induced Reduction of Palladium-Aryls, a Potential Interference in Pd Catalysis. *Organometallics* **2013**, *32*, 5428-5434. (e) Shan, L.; Wu, G.; Liu, M.; Gao, W.; Ding, J.; Huang, X.; Wu, H. α . β -Diaryl Unsaturated Ketones via Palladium-Catalyzed Ring-Opening of Cyclopropenones with Organoboronic Acids. *Org. Chem. Front.* **2018**, *5*, 1651-1654. (f) Zhao, Q.; Meng, G.; Nolan, S. P.; Szostak, M. N-Heterocyclic Carbene Complexes in C-H Activation Reactions. *Chem. Rev.* **2020**, *120*, 1981–2048. (g) Reyes-Batlle, M.; Freijo, M. B.; López-Arencibia, A.; Lorenzo-Morales, J.; McNaughton-Smith, G.; Piñero, J.E.; Abad-Grillo, T. Identification of N-acyl quinolin-2(1H)-ones as new selective agents against clinical isolates of *Acanthamoeba keratitis*. *Bioorg. Chem.* **2020**, *99*, 103791.
 21. (a) Similar information was reported in Banjare, S. K.; Nanda, T.; Ravikumar, P. C. Cobalt-Catalyzed Regioselective Direct C-4 Alkenylation of 3-Acetyindole with Michael Acceptors Using a Weakly Coordinating Functional Group. *Org. Lett.* **2019**, *21*, 8138–8143. (b) Gottlieb, H. E.; Kotlyar, V.; Nudelman, A. NMR chemical shifts of common laboratory solvents as trace impurities. *J. Org. Chem.* **1997**, *62*, 7512. (b) Hintermann, L. *Beilstein J. Org. Chem.* **2007**, *3*, 22. (c) Tarrieu, R.; Dumas, A.; Thongpaen, J.; Vives, T.; Roisnel, T.; Dorcet, V.; Crevisy, C.; Basle, O.; Mauduit, M. *J. Org. Chem.* **2017**, *82*, 1880–1887.
 22. (a) Netland, K. A.; Gundersen, L.-L.; Rise, F. An improved synthesis of dialkylcyclopropenones *Synth. Commun.*, **2000**, *30*, 1767-1777. (b) Kuzmanich, G.; Gard, M.-N.; Garcia-Garibay, M. A. Photonic amplification by a singlet-state

- quantum chain reaction in the photodecarbonylation of crystalline diarylcyclopropenones. *J. Am. Chem. Soc.* **2009**, *131*, 11606–11614. (c) Poloukhine, A.; Popik, V. V. Highly efficient photochemical generation of a triple bond: Synthesis, properties, and photodecarbonylation of cyclopropenones. *J. Org. Chem.* **2003**, *68*, 7833–7840. (d) Vanos, C. M.; Lambert, T. H. Development of a Catalytic Platform for Nucleophilic Substitution: Cyclopropenone-Catalyzed Chlorodehydration of Alcohols. *Angew. Chem., Int. Ed.* **2011**, *50*, 12222–12226. (e) Shih, H.-W.; Prescher, J. A. A bioorthogonal ligation of cyclopropenones mediated by triarylphosphines. *J. Am. Chem. Soc.* **2015**, *137*, 10036–10039.
23. (a) Eicher, T.; Boehm, S.; Ehrhardt, H.; Harth, R.; Lerch, D. On the Reaction of Diphenylcyclopropenone, its Functional Derivatives and Imonium Salts with Amines. *Liebigs Ann. Chem.* **1981**, *5*, 765–787. (b) Albert Kascheres, Juan L. Reyes R., and Suzana M. Fonseca Reaction of Diphenylcyclopropenone with 2-Aminothiazoles and Related Compounds. Kascheres, A.; Reyes, J. -L.; Fonesca, S.-M. *Heterocycles*, **1984**, *22*, 2529–2540. (c) Nakaya, R.; Yasuda, S.; Yorimitsu, H.; Ohshima, K. Rhodium-Catalyzed Intermolecular [2 + 2] Cycloaddition of Terminal Alkynes with Electron-Deficient Alkenes. *Chem. Eur. J.* **2011**, *17*, 8559–8561. (d) Fan, T.; Wang, A.; Li, J.-Q.; Ye, J.-L.; Zheng, X.; Huang, P.-Q. Versatile One-Pot Synthesis of Polysubstituted Cyclopent-2-enimines from α,β -Unsaturated Amides: Imino-Nazarov Reaction *Angew. Chem., Int. Ed.* **2018**, *57*, 10352–10356. (e) Peng, J.-B.; Geng, H.-Q.; Wu, F.-P.; Li, D.; Wu, X.-F. Selectivity Controllable Divergent Synthesis of α,β -Unsaturated Amides and Maleimides from Alkynes and Nitroarenes via Palladium-Catalyzed Carbonylation. *J. Catal.* **2019**, *375*, 519–523.

Chapter 4

Breaking The Monotony: Cobalt and Maleimide as an Entrant to the Olefin Mediated *ortho* C-H Functionalization

4.1 Abstract

4.2 Introduction

4.3 Results and Discussions

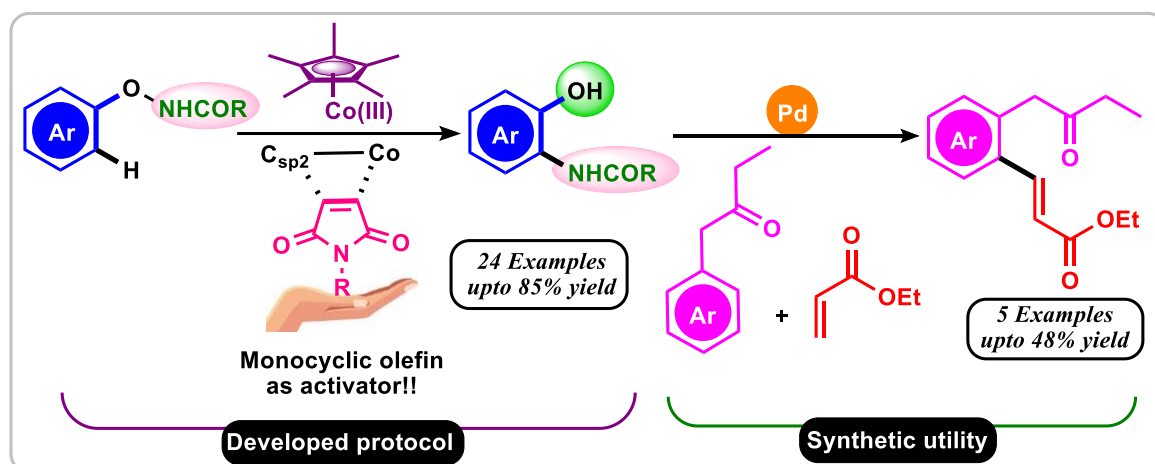
4.4 Conclusions

4.5 Experimental Section

4.6 References

Chapter 4

Breaking The Monotony: Cobalt and Maleimide as an Entrant to the Olefin Mediated *ortho* C-H Functionalization



4.1 ABSTRACT

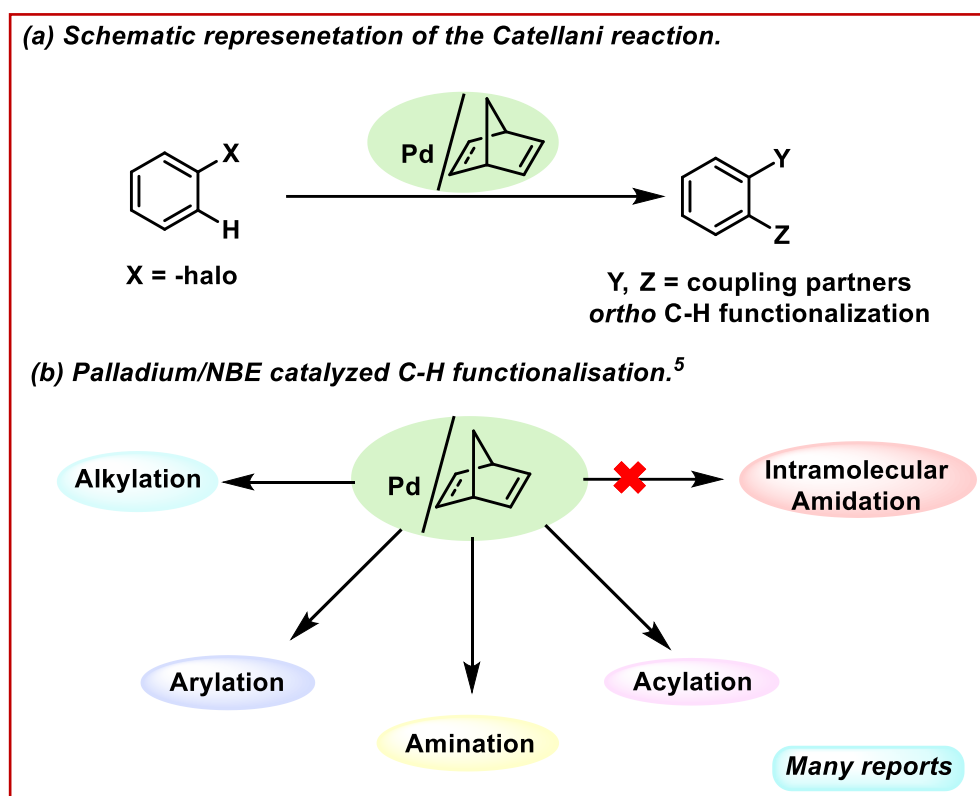
A new catalytic system is discovered for the intramolecular C-H amidation of *N*-phenoxy acetamide derivatives. Herein, a cobalt catalyst has been employed for the olefin-mediated *ortho* C-H functionalization. Moreover, a monocyclic olefin, maleimide, has been used as a transient mediator instead of well-established bicyclic norbornenes. Maleimide promotes a Co(III) intermediate to undergo oxidative addition into the O–N bond to form a Co(V) nitrene species and subsequently directs nitrene addition to the *ortho* position. Mechanistic study and density functional theory (DFT) study support the proposed mechanism. The products derived from this methodology have been demonstrated as a ligand in the C-H olefination reaction. Further, the synthetic utility of this methodology was demonstrated via the *ortho*-amidation of estrone.

4.2 INTRODUCTION

Since the dawn of the 21st century, transition metal-catalyzed C-H bond activation has been employed as a key strategy for the synthesis of biologically active scaffolds, functional

organic materials, and pharmaceuticals.¹ Due to the ubiquitous nature of C-H bonds in organic molecules, selective functionalization of C-H bonds is a challenging task. However, directing groups have enabled solutions to this problem by allowing the metal to activate proximal C-H bonds.² The nature of the substrate and coupling partner also control the threshold for the C-H bond activation process.³

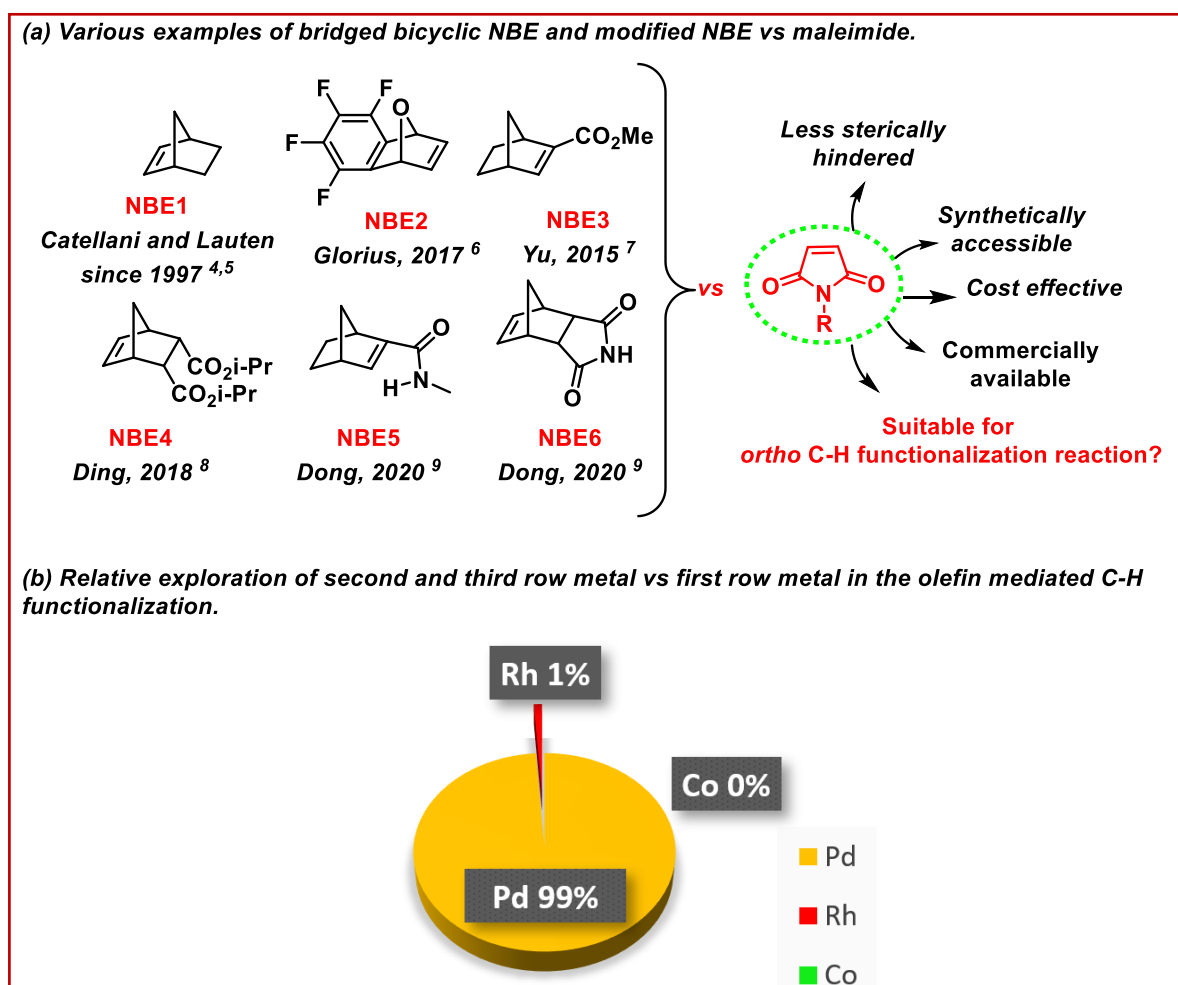
Scheme 4.1 Palladium/NBE catalyzed Catellani reaction



Among the various transformations involving C-H bond activation, the Catellani reaction is one of the earliest examples and occupies a unique space in organometallic chemistry. The Catellani reaction was first discovered by Marta Catellani in 1997 and later on developed by Lauten's group.⁴ This reaction uses a palladium catalyst and norbornene (NBE) as the transient directing group/mediator for the synthesis of *ortho* bi-functional aromatic molecules (Scheme 4.1a). This Pd/NBE combination has been declared as a winning combination after hundreds of successful attempts (Scheme 4.1b).⁵ Bicyclic olefins have been the gold standard for driving Catellani reactions^{4,5} and *ortho* C-H

functionalizations^{5b, 6} for the last 24 years – primarily limited to NBE and its derivatives. Pioneering research groups like those of Glorius,⁶ Yu,⁷ Ding,⁸ and Dong⁹ have used modified NBEs, which exhibited high reactivity and better selectivity than NBE1 (Scheme 4.2a).

Scheme 4.2 Traditional olefin-mediator and metal used in C-H functionalization reaction

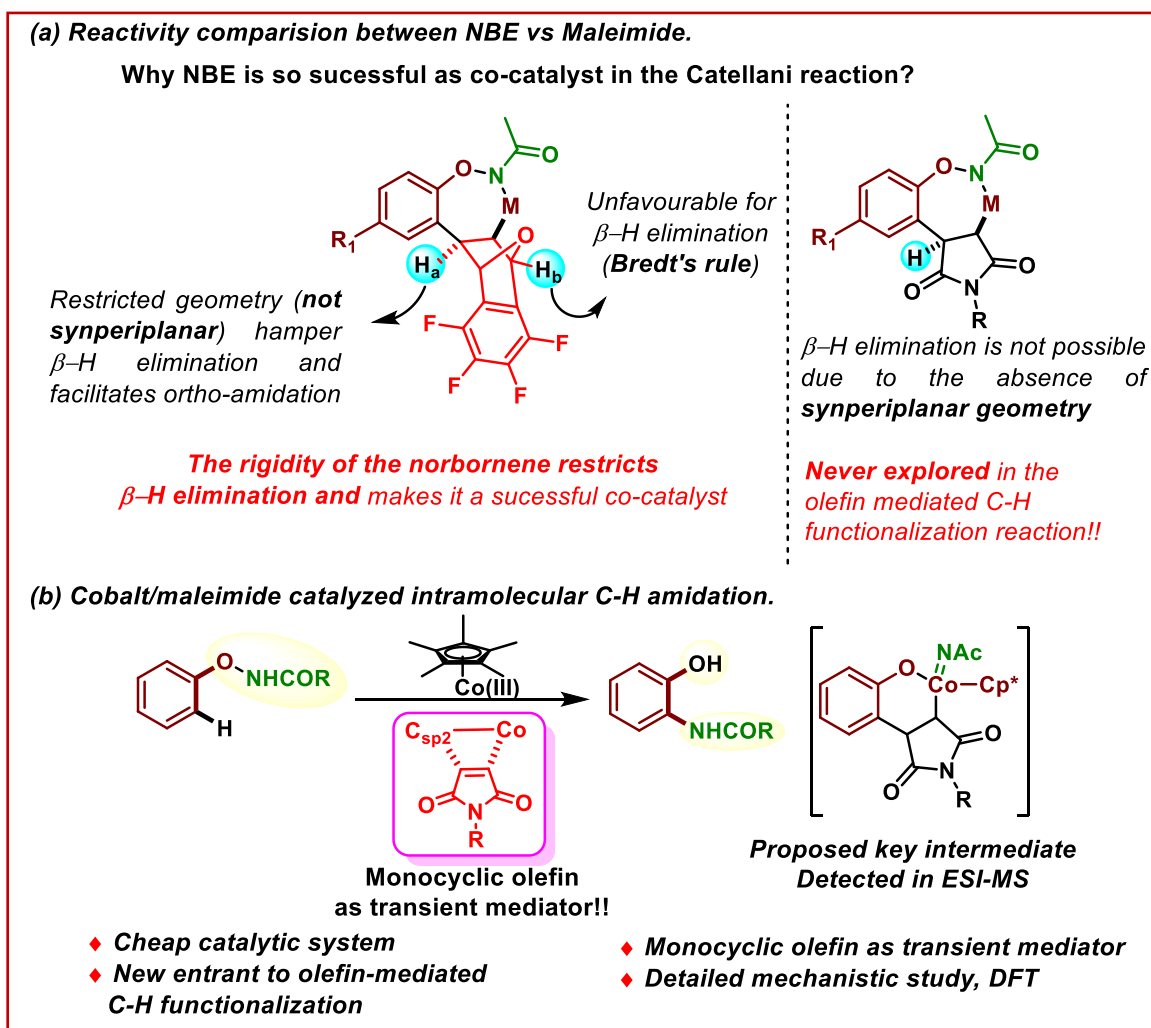


However, until now, the scope of the olefin mediator has not been expanded beyond bicyclic-bridged NBEs. In addition, only noble metal palladium has been employed in the olefin-mediated C-H functionalization reaction, barring a couple of reports with rhodium (Scheme 4.2b). This landscape provides an excellent opportunity to explore the reactivity

of earth-abundant, eco-friendly and less expensive first-row transition metals such as cobalt for olefin-mediated C-H functionalization reactions.

In 2017, the Glorius group reported an elegant approach for *o*-amidation of phenols, using a rhodium catalyst and a new oxanorbornene (NBE2) as the bicyclic olefin mediator.⁶ The key feature of the NBE2 structure is its rigidity, which precludes β -hydride elimination and facilitates *ortho* functionalization (Scheme 4.3a).^{9,10} Protons H_a and H_b do not undergo β -hydride elimination due to a lack of the requisite syn-periplanar arrangement and geometric constraints (c.f., Bredt's rule) respectively.¹¹

Scheme 4.3 Reactivity comparison between NBE and maleimide and our approach



To date, the potential utility of a monocyclic olefin/maleimide as a transient mediator has not been recognized by the scientific community. Therefore, we intended to perform the

intramolecular C-H amidation reaction of phenol in the presence of cationic Cp*Co as catalyst and maleimide as transient mediator. In this report, we successfully demonstrate the *o*-amidation of phenols using this combination of reagents (Scheme 4.3b). Thus, this is the first time a monocyclic olefin-mediated *ortho* C-H functionalization reaction has been found to be successful with first-row metal cobalt.^{11c}

This protocol has been established with an oxidizing auto-cleavable directing group that also serves as an amidating agent and facilitates the formation of a C-N bond. The salient features of the developed protocol are: (i) intramolecular C(*sp*²)-H amidation, (ii) a less expensive catalytic system, (iii) use of a cobalt and monocyclic olefin combination, (iv) oxidative addition of Co(III) to O–N bond forming a Co(V) nitrene species, (v) detection of a key cobalt (V) nitrenoid intermediate through HRMS, (vi) support for the proposed mechanism through DFT calculation, (vii) product derived from this methodology has been employed as a ligand in C-H alkenylation reaction, and (viii) application of the method to late-stage diversification of a natural product.

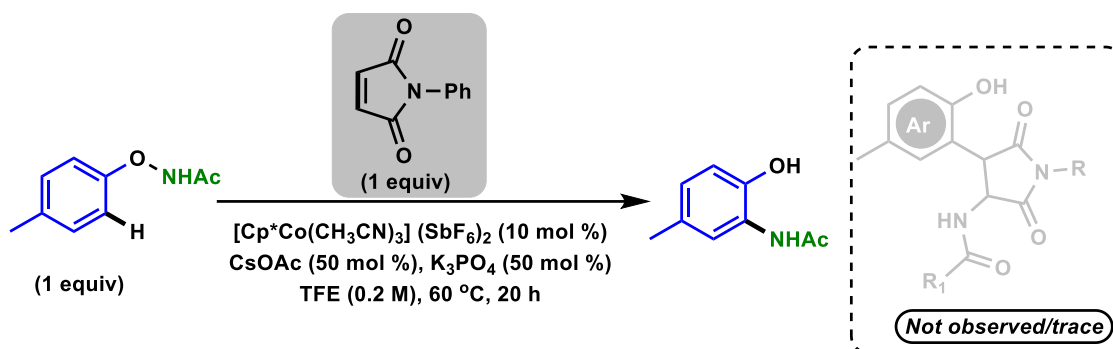
4.3 RESULTS AND DISCUSSIONS

We began our investigation by choosing *N*-(*p*-tolylloxy)acetamide **2b** as the model substrate. A stoichiometric amount of *N*-phenyl maleimide **1f** was used as the olefin mediator (Table 4.1). After several sets of optimizations, 10 mol % of cationic Cp*Co complex, 50 mol % of CsOAc, and 50 mol % of K₃PO₄ in the presence of 0.2 M of TFE solvent at 60 °C were found to deliver the desired *o*-amidation product **3b** in 70% yield (Table 4.1, entry 1).

Instead of a cationic cobalt complex, when we employed Cp*CoCOI₂ it produced lower yields (Table 4.1, entries 2-3). Product yield decreased to 53% when catalyst loading was reduced to 5 mol % (Table 4.1, entry 4). A lower yield was observed upon lowering the amount of maleimide from 1 equivalent to 20 mol % and 50 mol % (Table 4.1, entries 5-6). Changing the acetate base to NaOAc or KOAc did not result in much variation in the

product yield (Table 4.1, entries 7-8). CsOPiv was not efficient for the transformation; it gave only 50% yield of desired product **3b** (Table 4.1, entry 9). Varying the temperature from 60 °C to 40 °C or rt

Table 4.1 Optimization of Reaction Conditions^{a,b}



entry	deviation from standard conditions	yield of 3aa (%) ^b
1	none	70
2	$\text{Cp}^*\text{CoCOI}_2$	38
3	$\text{Cp}^*\text{CoCOI}_2 + \text{AgSbF}_6$	30
4	$[\text{Cp}^*\text{Co}(\text{CH}_3\text{CN})_3](\text{SbF}_6)_2$ (5 mol %)	53
5	maleimide (20 mol %)	40
6	maleimide (50 mol %)	64
7	NaOAc instead of CsOAc	68
8	KOAc instead of CsOAc	67
9	CsOPiv instead of CsOAc	50
10	RT instead of 60 °C	32
11	40 °C instead of 60 °C	60
12	without CsOAc	40
13	without K_3PO_4	65
14	without maleimide	nr
15	without catalyst	nd

^aConditions: **1f** (1 equiv.), **2b** (1 equiv.), $[\text{Cp}^*\text{Co}(\text{CH}_3\text{CN})_3](\text{SbF}_6)_2$ (10 mol%), CsOAc (50 mol%), K_3PO_4 (50 mol%), TFE (0.2 M), temperature (60 °C). ^bNMR yield (1,3,5-trimethoxybenzene was taken as an internal standard for crude NMR).

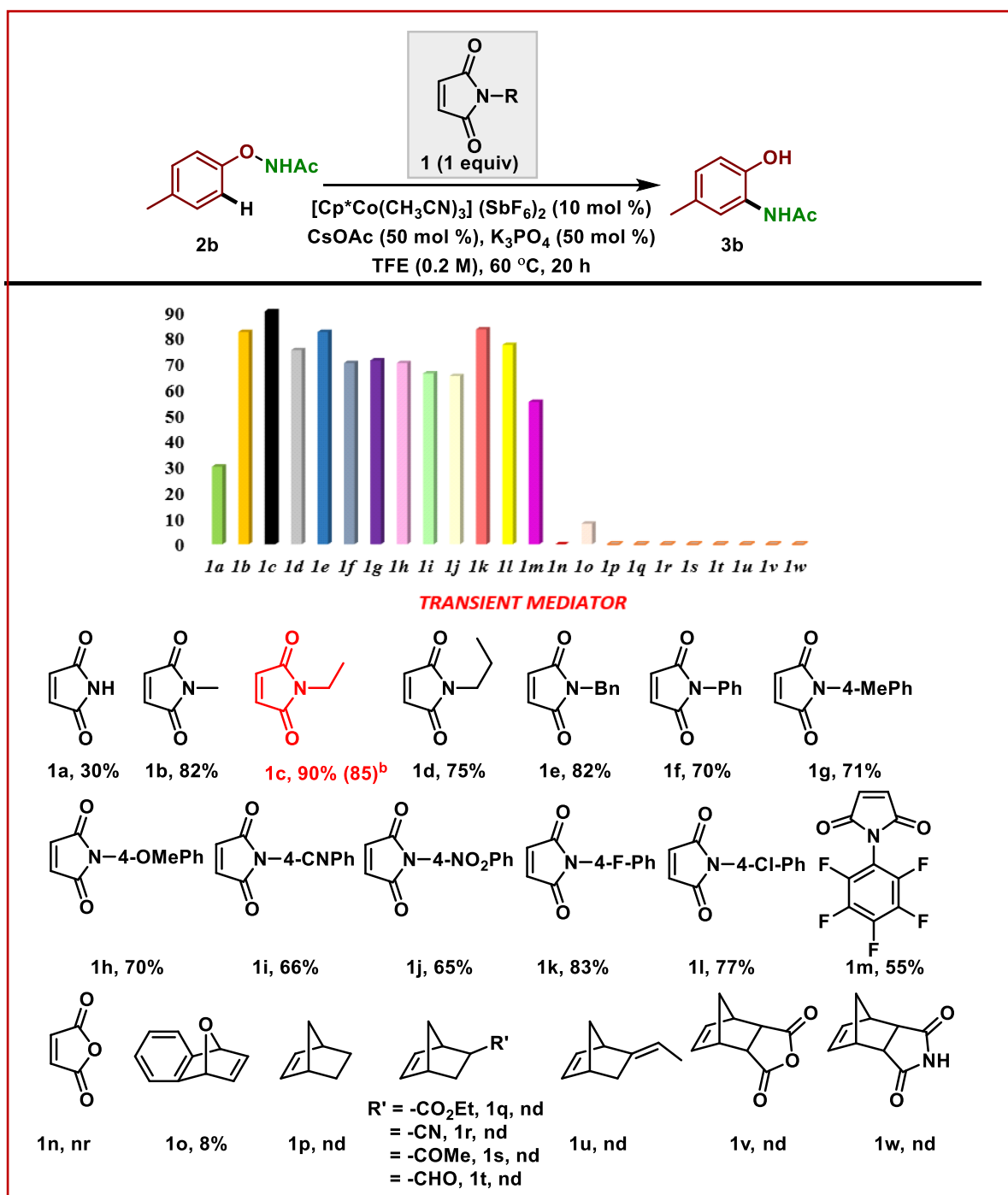
resulted in lower yields (Table 4.1, entries 10-11). The reaction without CsOAc and K_3PO_4 led to decreased product yield (Table 4.1, entries 12-13). Control experiments indicated that

Cp*Co catalyst and maleimide were indispensable for the transformation (Table 4.1, entries 14-15). The migration of the amide group to one of the olefin termini was the most common pathway that has been observed in transition metal-catalyzed C-H activation of phenoxy acetamide.¹² However, during optimization, the hydro arylated maleimide product was either not observed or observed only in trace amounts.

We also examined an array of maleimide derivatives for cobalt catalyzed C(*sp*²)-H amidation (Table 4.2). Simple maleimide **1a** showed poor reactivity, providing only 30% yield of the desired product. Enhancement in the reaction yield was observed when *N*-Me **1b** and *N*-Et **1c** maleimide were employed as co-catalysts. In addition, *N*-propyl maleimide **1d** resulted in 75% yield and *N*-benzyl maleimide **1e** gave 82% yield of the product. As *N*-Ph maleimide **1f** resulted in 70% yield of the desired product, various electron-rich and electron-poor *N*-phenyl substituted maleimides were explored. The variation in substituents on the phenyl ring did not lead to much difference in reactivity, resulting in 71%-65% yield of the desired product (Table 4.2, **1g-1j**). 4-Halo substituted *N*-phenyl maleimide was also tested under standard conditions, which resulted in a good yield (Table 4.2, **1k,1l**). However, *N*-pentafluorophenyl maleimide decreased the product yield to 55%, showing that electron deficiency on *N*-substitution negatively affects the reaction. The oxygen equivalent of maleimide, maleic anhydride **1n** was also tested, however it did not show any reactivity. The most commonly used oxanorbornene **1o** was also employed as a transient mediator and 8% product yield was observed. However, we have tried the reaction with some of the commercially available bicyclic NBEs and found it ineffective as an olefin-mediator. This observation implies that traditional NBEs are not effective as an olefin mediator, and we must synthesize some fancy NBEs to carry out the above transformation. In this context, we have provided a better alternative to use maleimide as an olefin mediator, which is cheap

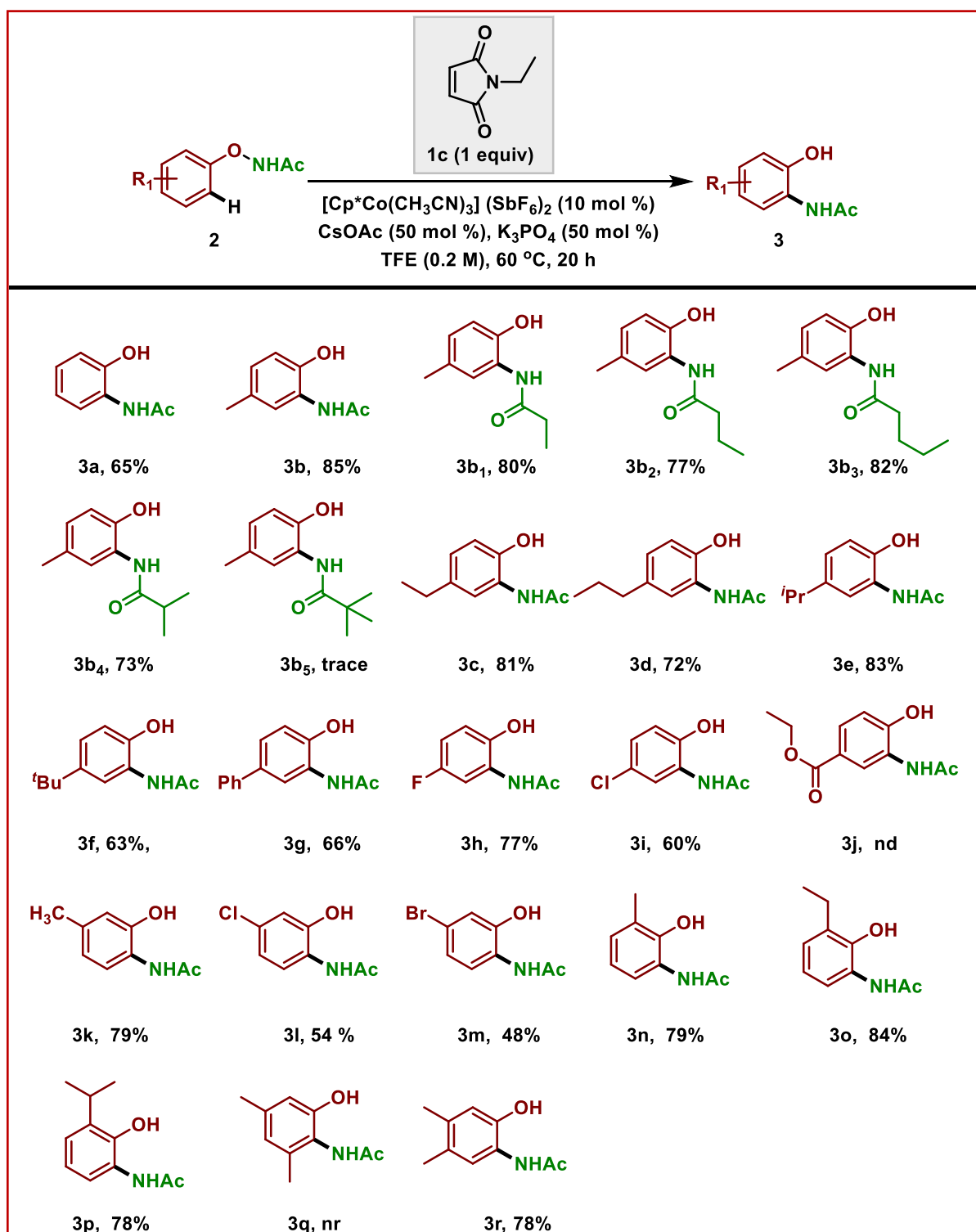
and easy to synthesize. In summary, *N*-Et maleimide was found to be the optimal transient mediator, delivering an 85% isolated yield of the desired product.

Table 4.2. Investigation of Monocyclic Maleimides in the Cp*Co Catalyzed C(*sp*²)-H *o*-Amination^{a,b}



^aConditions: **1** (1 equiv.), **2b** (1 equiv.), [Cp*Co(CH₃CN)₃] (SbF₆)₂ (10 mol %), CsOAc (50 mol %), K₃PO₄ (50 mol %), TFE (0.2 M), temperature (60 °C). ¹H NMR yield is shown (trimethoxybenzene was taken as an internal standard for crude NMR). ^bResult in parentheses is the isolated yield.

Scheme 4.4 Substrate Scope^{a,b}



^aConditions: **1** (1 equiv.), **2b** (1 equiv.), $[\text{Cp}^*\text{Co}(\text{CH}_3\text{CN})_3] (\text{SbF}_6)_2$ (10 mol %), CsOAc (50 mol %), K_3PO_4 (50 mol %), TFE (0.2 M), temperature (60 °C), ^bisolated yield.

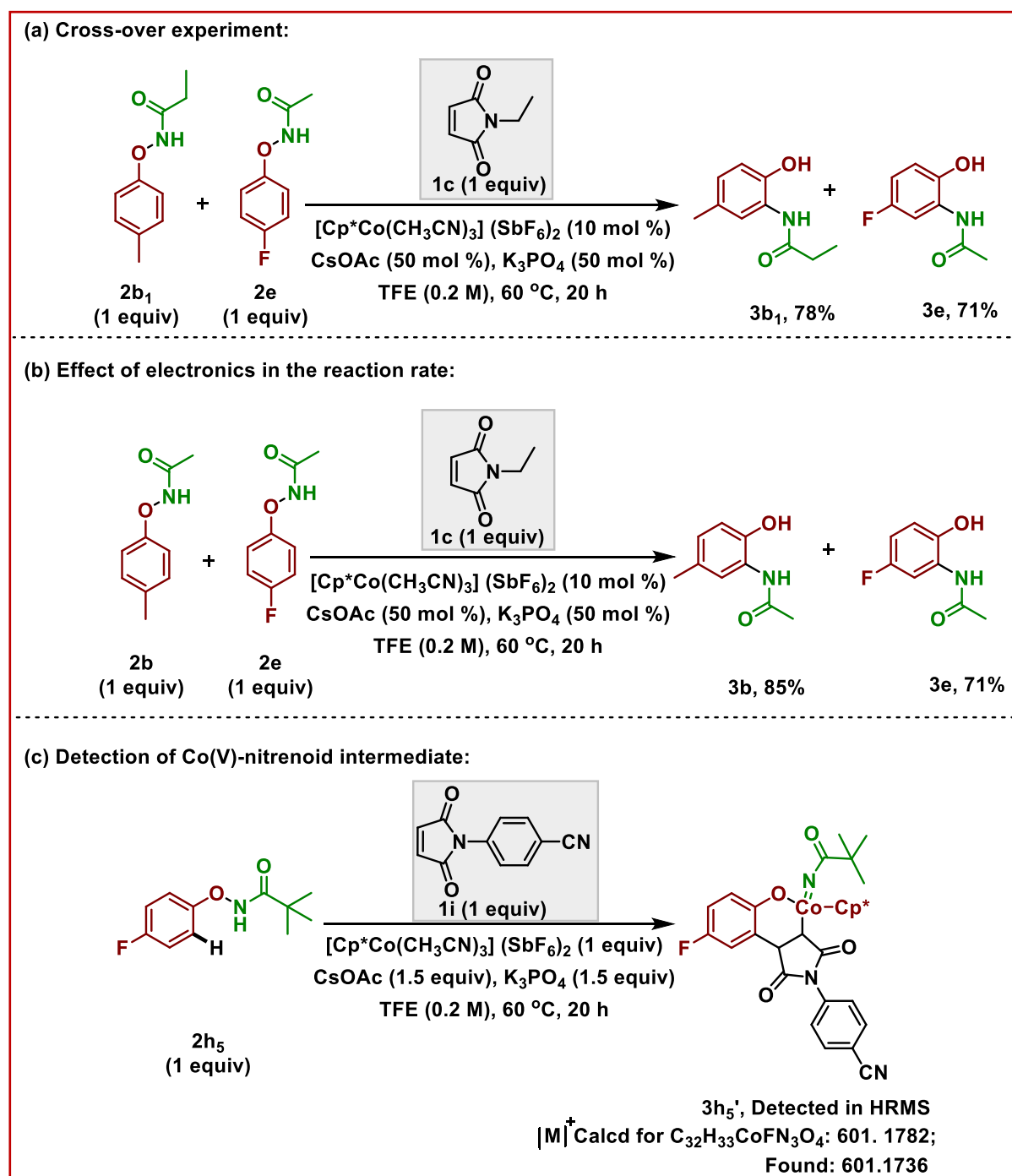
With the optimized conditions in hand, the substrate scope was studied (Scheme 4.4).

Unsubstituted phenoxy acetamide underwent intramolecular *ortho*-C-H amidation under

standard conditions to deliver 65% yield of the desired product **3a**. As, *p*-methyl phenoxy acetamide **2b** was found to deliver 85% yield of the product during optimization, various *N*-substituents were tested. Amide-directing group-containing alkyl chains up to four carbons in length were found compatible, delivering 77%-82% yields of the desired products (Scheme 4.4, **3b₁**-**3b₃**). In addition, branched alkyl substitution also led to good yields (Scheme 4.4, **3b₄**). However, further increases in bulkiness on the directing group resulted in only a trace amount of the product **3b₅**, which can be attributed to steric repulsion during the electrophilic attack (see mechanism).

Further, the effectiveness of the standard conditions was tested with other *p*-substituted phenoxy acetamides. Alkyl (linear and branched), aryl, and halo-substituted phenoxy acetamides were successfully converted to their respective products in good to very good yields (Scheme 4.4, **3c**-**3i**). However, phenoxy acetamides containing electron-withdrawing groups did not result in the desired product, instead delivering carbo-amidated product **3j*** in 86% yield. This finding was supported by the DFT study, which indicates a high energy barrier for the electrophilic attack of nitrogen to the aryl *ortho* C-center. Furthermore, *meta*-substituted substrates worked well, delivering the desired products with excellent selectivity (Scheme 4.4, **3k**-**3m**). *Ortho*-substituted substrates gave their respective products in very high yields, perhaps due to a steric-induced rate enhancement of the olefin extrusion step (Scheme 4.4, **3n**-**3p**). However, an increase in the steric effect *ortho* to the reacting center (C-H bond) shuts down the reactivity. Thus, no product was detected in the case of **2q**. Interestingly, *meta*-*para* disubstituted substrate **2r** gave the desired product **3r** in 78% yield, with the amide group transferred to the less sterically hindered site.

Scheme 4.5 Mechanistic studies

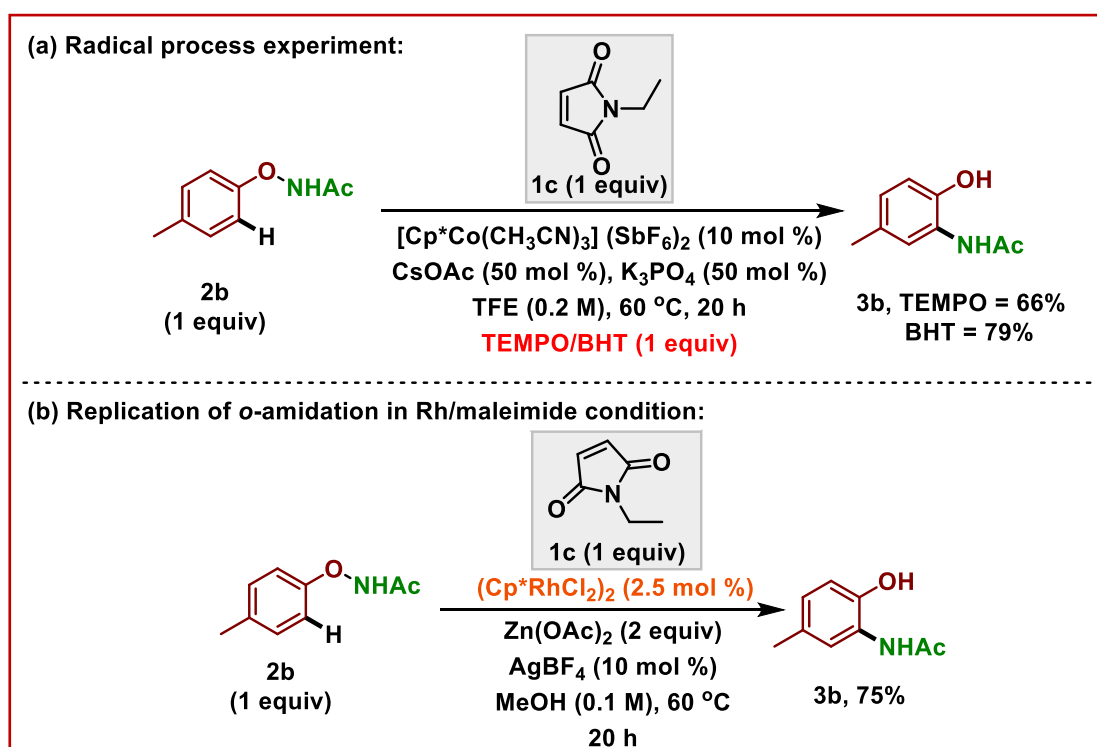


Mechanistic Studies

To understand the mechanism of the reaction, various mechanistic studies have been performed (Scheme 4.5 and 4.6). When a cross-over experiment was performed by reacting **2b₁** and **2e** together, we observed exclusive products **3b₁** and **3e**; this observation indicates that the *ortho*-amidation proceeded *via* an intramolecular pathway (Scheme 4.5a). The

effect of electronics on the reaction rate has been tested and substrate with electron-donating substituent works better than an electron-withdrawing substituent (Scheme 4.5b). An ESI-HRMS study led to the detection of a mass peak that corresponds to the mass of bulky cobalt-nitrenoid intermediate **3h₅'** (Scheme 4.5c). The addition of TEMPO or BHT as a radical scavenger did not impact the product yield, suggesting a non-radical pathway (Scheme 4.6a). The role of maleimide as an olefin mediator has been established by replicating the same reaction in Rh/maleimide condition, giving the desired product **3b** in 75% yield (Scheme 4.6b). It is worth mentioning here that a control experiment in the absence of maleimide failed to give any product.

Scheme 4.6 Mechanistic studies



To gain additional insight into the reaction mechanism, we performed DFT calculations at the PBE0-D4/Def2-TZVPP//SMD(TFE)-PBE0-D3(BJ)/Def2-SVP level of theory (Figure 4.1). We examined the rearrangement of **2b** mediated by **1c** as a representative reaction. We started our modelling from $[\text{Cp}^*\text{Co}(N\text{-(}p\text{-tolylloxy)acetamide})(\text{OAc})_2]$ (**IM1**), which could be generated from reacting $[\text{Cp}^*\text{Co}(\text{CH}_3\text{CN})_3] (\text{SbF}_6)_2$ with CsOAc and **2b**. Both open-shell

singlet and triplet cases were considered and, as shown below, the key steps of the reaction are predicted to proceed on the singlet surface due to high barriers on the triplet surface.

The predicted mechanism is summarized as follows: consecutive N–H activation and C–H activation of the substrate, olefin insertion, oxidative addition, electrophilic addition, and olefin elimination. The corresponding free energy profile for this transformation is shown in Figure 4.1. The reaction is predicted to begin on the triplet surface, since this is the computed ground state of $[\text{Cp}^*\text{Co}(\text{OAc})_2]$. After the substrate is coordinated to $[\text{Cp}^*\text{Co}(\text{OAc})_2]$, it is deprotonated by the acetate ligand and coordinates to the Co center through **TS1** (triplet). Subsequent *ortho* C–H bond activation can occur on either the triplet or singlet surface, with concerted metalation deprotonation (CMD; **IM3** \rightarrow **TS2** \rightarrow **IM4**)^{14,15} on the singlet surface predicted to involve a lower energy transition state.

The maleimide mediator can bind to **IM4** to form complex **IM5** and then undergo olefin insertion *via* **TS3**. This step, which forms a seven-membered cobaltacycle (**IM6**), is predicted to be quite exergonic, which leads to the next step having the highest predicted barrier. Oxidative addition of Co into the O–N bond of **IM6** has a predicted barrier of 26 kcal mol⁻¹ on the singlet surface and 36 kcal mol⁻¹ on the triplet surface. Which barrier is most relevant, however, depends on the efficiency of singlet-triplet interconversion, which is difficult to estimate. The resulting cobalt nitrene (**IM7**), however, has a very small, predicted singlet-triplet gap. Following O–N cleavage, nitrene addition to the *ortho* carbon is predicted to proceed with a low barrier on either surface (*via* **TS5**). This step leads to dearomatized complex **IM8**, which can then undergo maleimide dissociation *via* **TS6**. The formation of the final product would then be accomplished by two consecutive protodemetalation steps (not modeled here).

We conclude from our predicted free energy profile that this reaction likely involves two-state reactivity¹⁶, but with the key chemical transformations (from **TS2** to **TS4**) likely

occurring on the open shell singlet surface. For triplets, spin densities were primarily localized on the cobalt, while for open shell singlets a small amount of spin density is delocalized onto ligands. We suspect that the lack of a significant effect from the radical inhibitor used experimentally is due in large part to this localization of spin density on the metal, which is not very accessible due to its surrounding ligands.

Figure 4.1 Computed (PBE0-D4/Def2-TZVPP//SMD(TFE)-PBE0-D3(BJ)/Def2-SVP) reaction profiles for $\text{Cp}^*\text{Co}(\text{OAc})_2$ -catalyzed rearrangement of *N*-(*p*-tolylloxy)acetamide mediated by *N*-ethylmaleimide. Relative free energies are shown in kcal/mol. Selected distances are shown in Å. Note that the **IM3**, which is a conformer of **IM2**, is not present on the triplet surface. Maleimide is also unbound from Co in **IM5** on triplet surface and hence is not shown here.

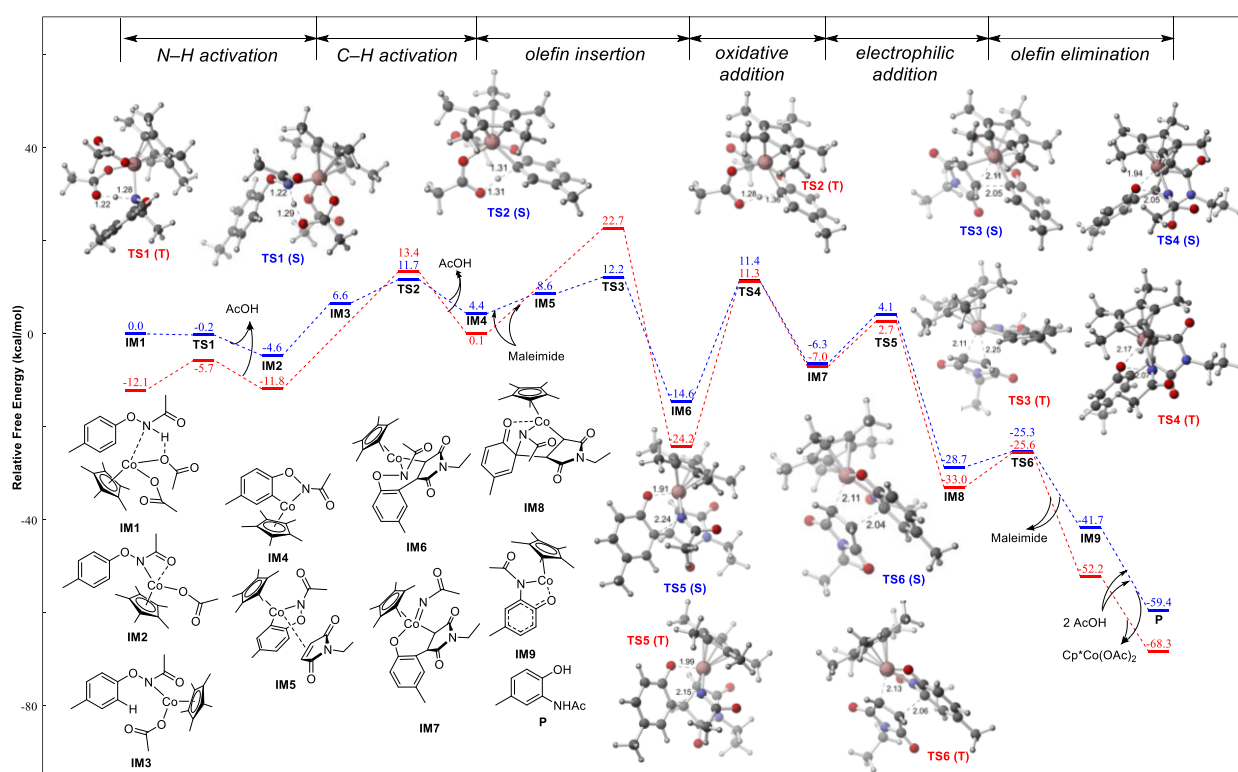
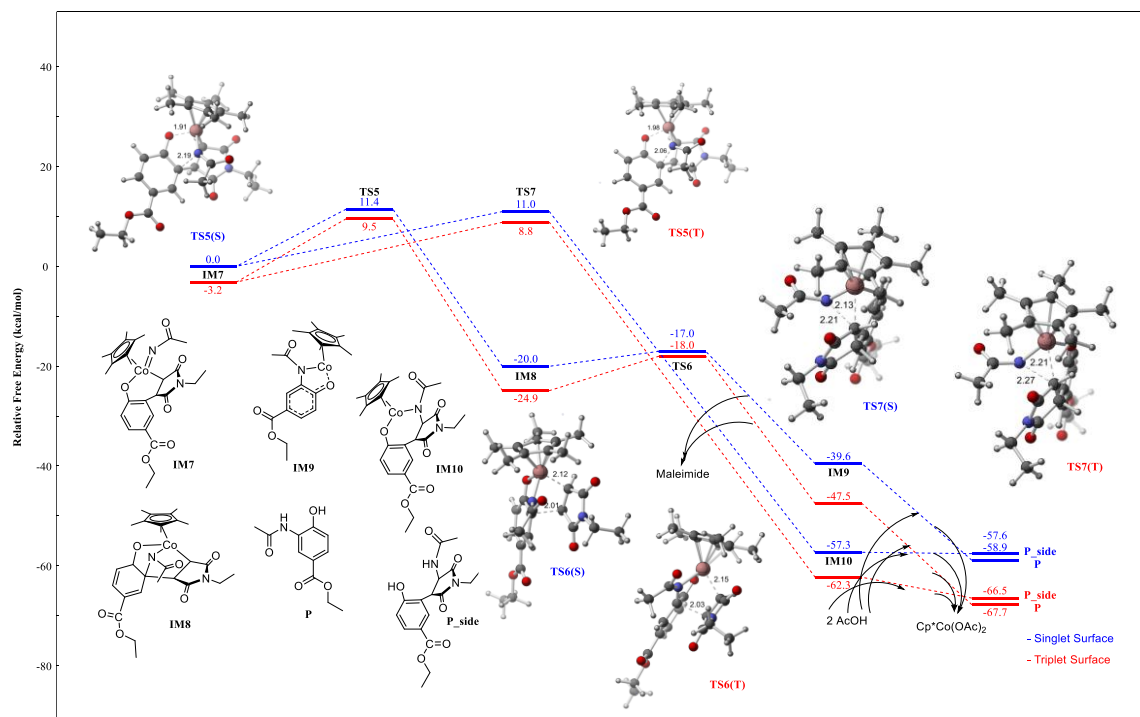


Figure 4.2 Computed (PBE0-D4/Def2-TZVPP//SMD(TFE)-PBE0-D3(BJ)/Def2-SVP) reaction profiles for Cp*Co(OAc)₂-catalyzed rearrangement of **2j** mediated by *N*-ethylmaleimide. Relative free energies are shown in kcal/mol. Selected distances are shown in Å.



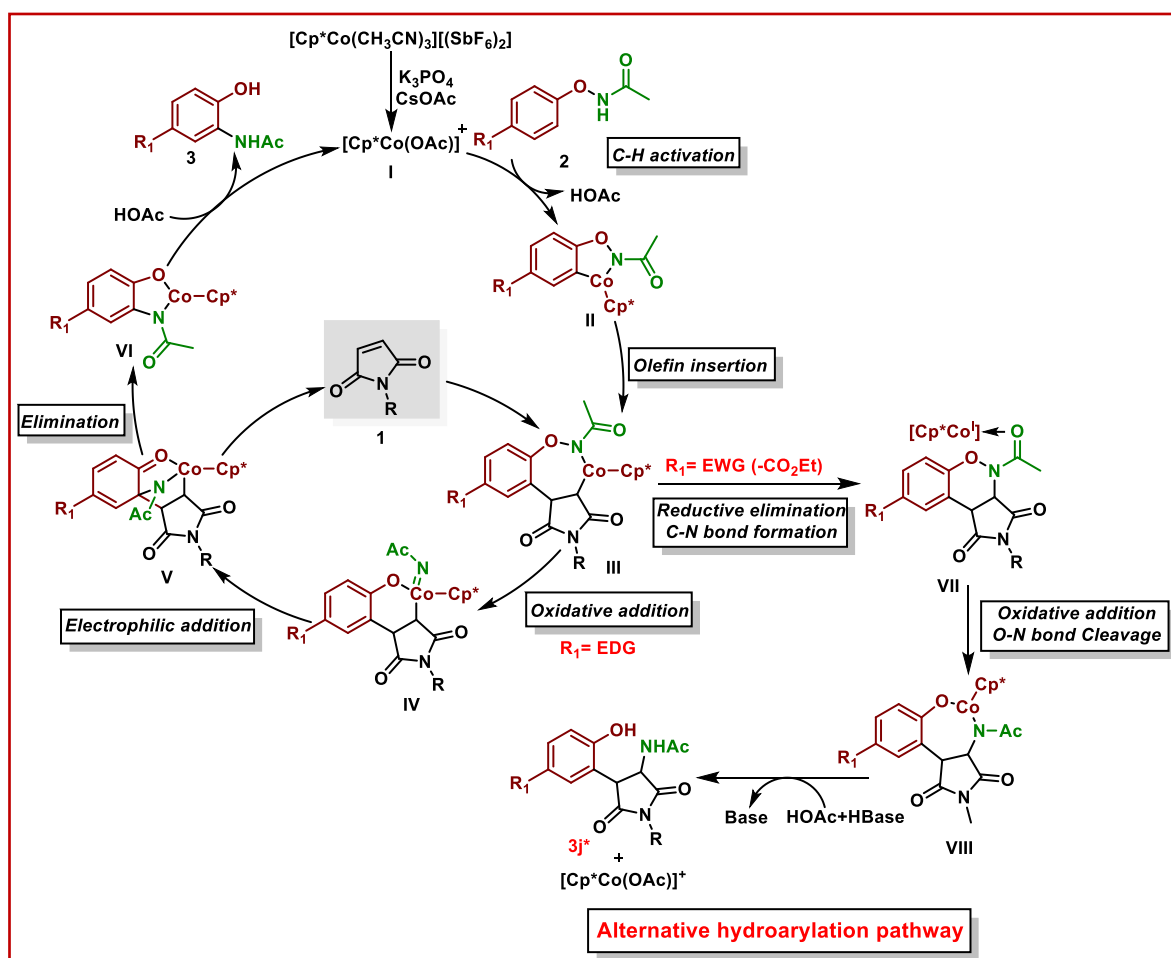
The reason behind the formation of carbo-amidation product in case of strong electron withdrawing group such as -CO₂Et has been understood from the computational data (Figure 4.2). The result shows that overall carbo-amidation of the *N*-ethylmaleimide is more favorable (by 0.4 kcal/mol on the singlet surface and 0.7 kcal/mol on the triplet surface) for this substituent, consistent with the formation of carbo-amidation product **3j*** when **2j** is subjected to the reaction.

Proposed Mechanism

Based on our experimental and computational studies, a plausible catalytic cycle is proposed as shown in scheme 4.7. Active cationic cobalt complex **I** generated *in situ* in the presence of CsOAc and K₃PO₄. The cobaltacycle intermediate **II** is generated *via* a C-H activation step. Olefin insertion leads to 7-membered cobaltacycle **III**. β -H elimination from

intermediate **III** has been restricted due to the absence of a syn-periplanar arrangement of the β -H and metal. Thus, the rigidity of maleimide allows intermediate **III** to persist and undergo oxidative addition of Co(III) to the O–N bond, leading to the formation of Co(V) nitrene intermediate **IV**.¹⁷ At this stage, the electrophilic addition of nitrogen to the *ortho* C–H bond generates a dearomatized spirocyclic intermediate **V** and reduces Co(V) to Co(III).

Scheme 4.7 Catalytic cycle



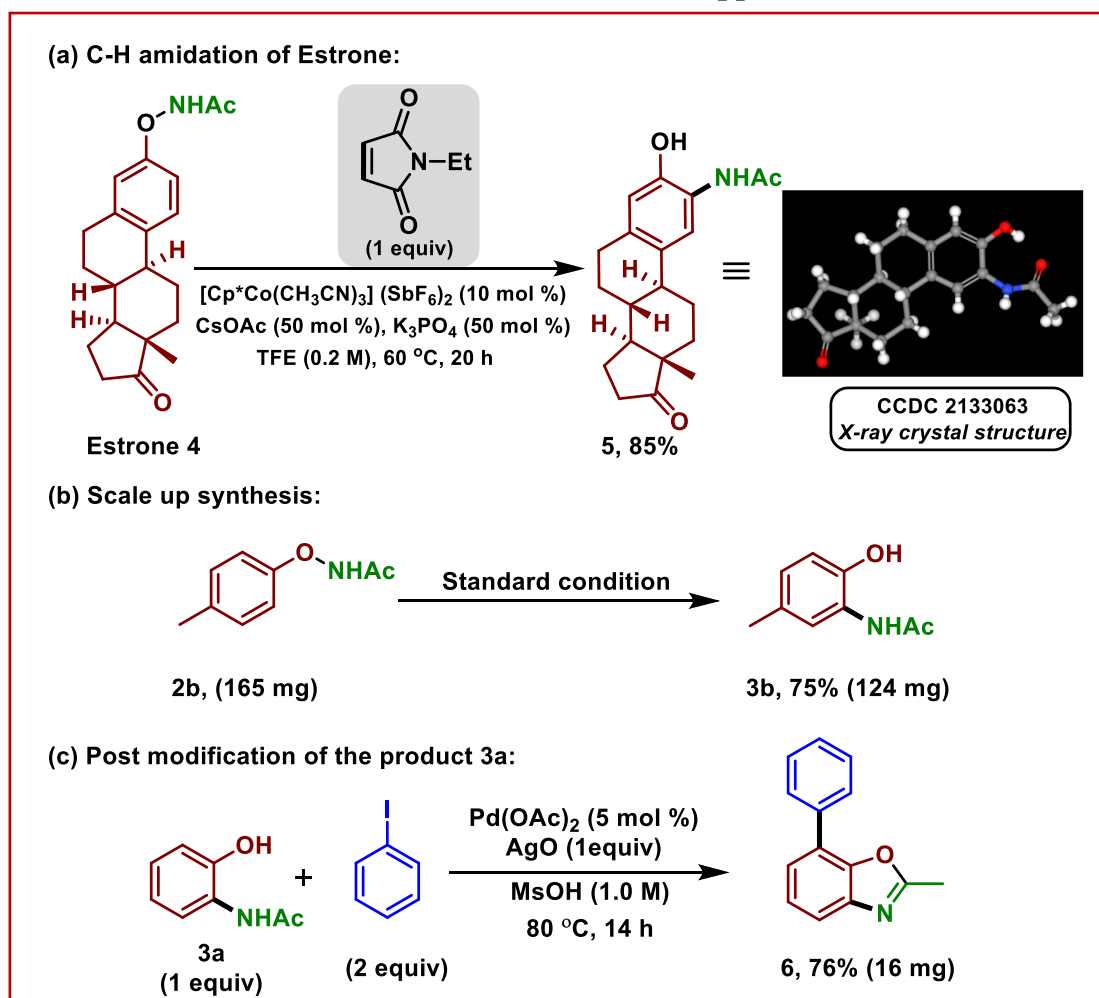
Rearomatization and steric repulsion favors the release of maleimide, resulting in intermediate **VI**. Further, protonation by acetic acid gives rise to product **3** and regenerates the active cationic cobalt catalyst for the next cycle. The formation of hydro arylated product **3j*** could be explained in another pathway, wherein intermediate **III** underwent reductive elimination followed by C–N bond formation to deliver intermediate **VII**. Then,

the oxidative addition of O-N bond to cobalt, followed by protonation in the presence of acetic acid delivered the desired hydro arylated product **3j*** along with the regeneration of the cationic cobalt catalyst.

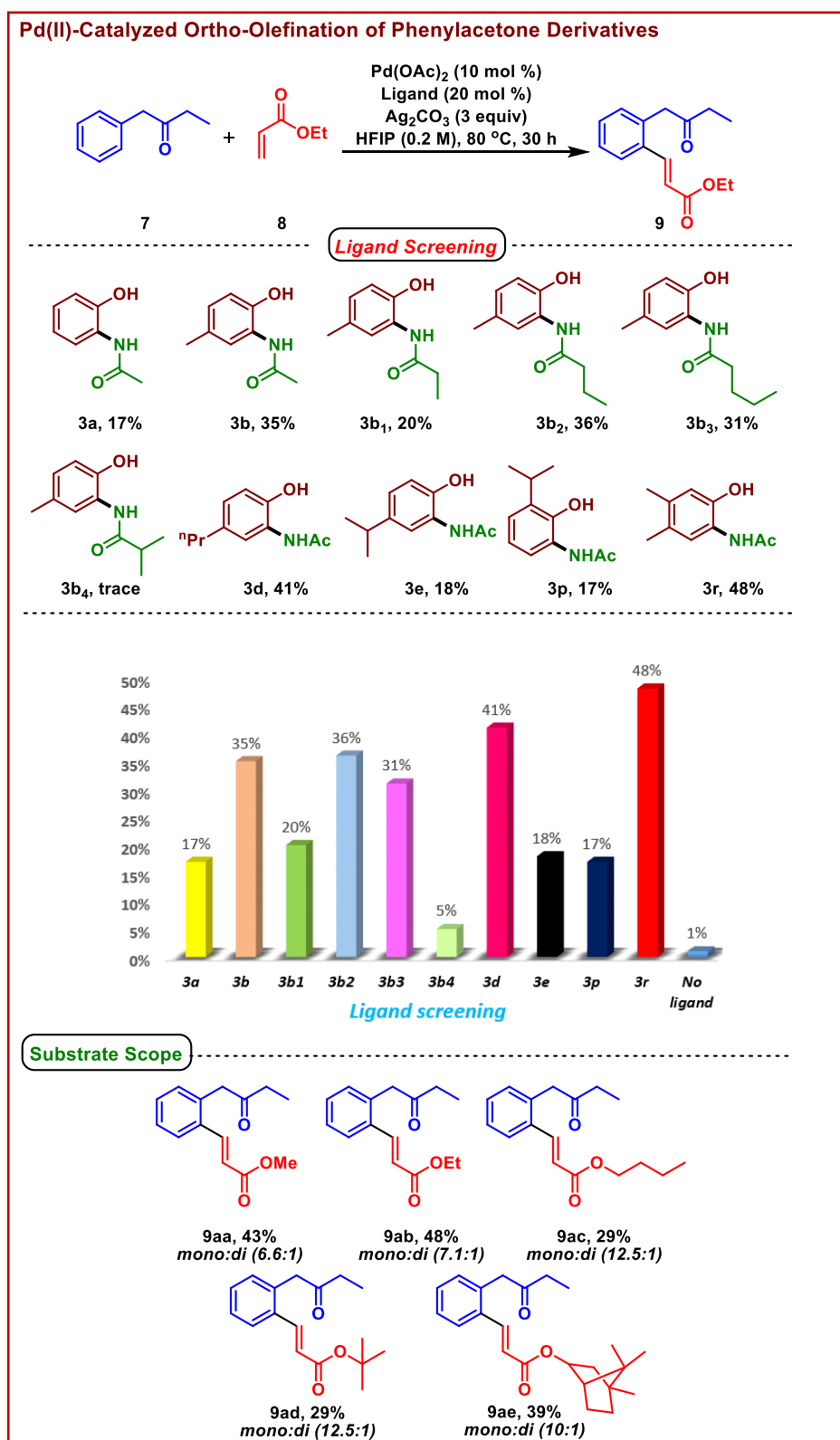
Synthetic Utility

The synthetic applicability of the developed protocol was demonstrated in scheme 4.8. Owing to the wide availability of phenol motifs in valuable drugs and pharmaceuticals,¹⁸ achieving site-selective amidation has significant potential utility. In this context, estrone **4** was subjected to our standard conditions (Scheme 4.8a), and the catalytic system worked efficiently, giving 85% yield of the desired product **5** (which is superior to the rhodium/NBE condition).⁶

Scheme 4.8 Diversification of Natural Products and Applications



Scheme 4.9 Application *o*-hydroxy acetamides as ligand^{a,b}



^aConditions: **7** (1 equiv.), **8** (1.25 equiv.), Pd(OAc)₂ (10 mol %), ligand (20 mol %), Ag₂CO₃ (3 equiv), HFIP (0.2 M), temperature (80 °C), ^bisolated yield. ^cRatio was calculated based on NMR.

Further, the reproducibility of the reaction has been checked at 1 mmol scale and found 75% product yield (Scheme 4.8b). Benzoxazole core is an important pharmacophore in drug discovery. The product *ortho*-acetamido phenol **3a** was subjected to palladium catalyzed condition¹⁹ in the presence of aryl iodide delivered benzoxazole derivative **6** in 76% yield (Scheme 4.8c).

To demonstrate the practical application of the products derived from this methodology, we explored its use as a potential ligand in the palladium-catalyzed C-H olefination reaction.²⁰ Chiral mono-protected amino acids (MPAA) ligand has been employed in various achiral transformations. Thus, we envisaged using *o*-hydroxy phenyl acetamidate as a ligand in a palladium-catalyzed C-H olefination reaction (Scheme 4.9). We have demonstrated the *o*-alkenylation of phenylacetone **7** with acrylates **8**. A good range of *o*-hydroxy acetamidate successfully acts as a ligand, among them 4,5-dimethyl-2-hydroxy phenyl acetamidate **3r** was found to deliver a better yield of the desired product.

As it is a very preliminary finding on *o*-hydroxy phenyl acetamidate as a ligand, further detailed studies need to be done in the future. With this condition, we have synthesized a few *o*-alkenylated benzyl ketone derivatives. With methyl acrylate, it delivers a 43% yield of the desired product, whereas ethyl acrylate furnishes 48% of the *o*-alkenylated product. While *n*-butyl and ^tBu acrylate were found to show equal reactivity to give the product in 29% yield, norbornyl acrylate show little superior reactivity to furnish the product in 39% yield. In all these cases mono alkenylated product was observed as the major product along with the di-alkenylated product.

4.4 CONCLUSION

The olefin-mediated Catellani reaction occupies a unique space in enabling numerous valuable organic transformations. In the last 24 years, Pd/NBE has been considered as a gold standard for conducting the olefin mediated *ortho* C-H

functionalizations. However, in this report we disclose a cobalt-catalyzed *ortho* C-H functionalizations reaction, which employed a simple monocyclic olefin that is maleimide as the transient mediator instead of complex bicyclic olefin, for the first time. The reaction followed an analogous Catellani reaction-type pathway. This catalytic system is compatible with a wide range of phenoxy acetamide derivatives, delivering the desired *o*-amidated products in good yields. The synthetic utility of the developed protocol has been demonstrated on estrone derivatives, and many additional applications can be envisioned. For example, the *o*-amidated phenol could act as a potential ligand in the C-H activation reaction that needs to be thoroughly examined in the future.

4.5 EXPERIMENTAL SECTION

General Information:^{21a}

Reactions were performed using borosil schlenk tube vial under N₂ atmosphere. Column chromatography was done by using 100-200 & 230-400 mesh size silica gel of Acme Chemicals. A gradient elution was performed by using distilled petroleum ether and ethyl acetate. TLC plates detected under UV light at 254 nm. ¹H NMR and ¹³C NMR were recorded on Bruker AV 400, 700 MHz spectrometer using CDCl₃ and DMSO-*d*₆ as NMR solvents. The residual CHCl₃ and DMSO-*H*₆ for ¹H NMR (δ = 7.26 ppm and 2.54 ppm respectively) were used as reference. The deuterated solvent signal for ¹³C NMR (δ = 77.36 ppm 40.45 ppm) is used as reference.^{21b} Multiplicity (s = single, d = doublet, t = triplet, q = quartet, m = multiplet, dd = double doublet), integration, and coupling constants (*J*) in hertz (Hz). HRMS signal analysis was performed using micro TOF Q-II mass spectrometer. X-ray analysis was conducted using Rigaku Smartlab X-ray diffractometer at SCS, NISER. Reagents and starting materials were purchased from Sigma Aldrich, Alfa Aesar, TCI, Avra, Spectrochem and other commercially available sources and used without further

purification unless otherwise noted. Structurally diverse maleimide were synthesized according to literature procedure.²²

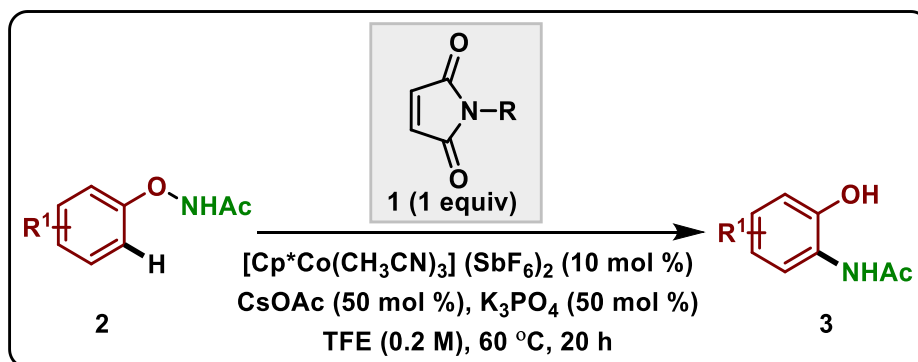
(a) General procedure for the synthesis of *N*-phenoxyacetamides 2:²³

Method A: *O*-mesitylsulfonylhydroxylamine (MSH) was prepared according to the literature.²⁴ Phenols (1.5 equiv) was dissolved in methanol (0.7 M), and then potassium tert-butoxide (1.5 equiv) was added. The mixture was allowed to stir for 0.5 h under argon atmosphere. Then methanol was removed under vacuum, and DMF was added into the residue (1.3 M). Then the freshly prepared *O*-mesitylsulfonylhydroxylamine (1.0 equiv, 0.9 M in DMF) was added under ice cooling bath. The mixture was allowed to stir for 2 h, diluted with ethylacetate, and washed with brine. The aqueous layer was extracted with EtOAc, which was then removed under reduce pressure to afford the corresponding *N*-aryloxyamine. Na₂CO₃ (1.5 equiv) and H₂O/EtOAc (v/v 1/2, 1.0 M) was next added to the reaction flask. The resulting solution was kept under ice bath followed by dropwise addition of acyl chloride (1.2 equiv). After stirring at 0 °C for 2 h, the reaction was quenched with saturated NaHCO₃ and diluted with EtOAc. The organic phase was washed twice with saturated NaHCO₃, dried over anhydrous Na₂SO₄, filtered, and evaporated under reduced pressure. The residue was purified by flash column chromatography on silica gel to provide the desired product.

Method B:²⁵ A mixture of *N*-hydroxyphthalimide (1.0 equiv), arylboronic acid (2.0 equiv), CuCl (1.0 equiv), freshly activated 4Å molecular sieves (250mg/mmol) and pyridine (1.1 equiv.) were dissolved in 1,2-dichloroethane (0.25 M) and stirred at room temperature under air. After 48-120 hours, the reaction mixture turned green. Silica gel was added to the flask and the solvent was evaporated under reduced pressure. The purification was performed by flash column chromatography on silica gel to afford desired *N*-aryloxyphthalimides. The product was directly used for the next step.

Hydrazine monohydrate (4.00 equiv., 51- 64%) was added to the solution of *N*-aryloxyphthalimide (1.0 equiv) in DCM (0.25 M). The reaction was stirred at room temperature overnight. MgSO₄ was added to the mixture and the suspension was stirred for additional 10 minutes. The precipitate was filtered off and washed with DCM followed by EtOAc. The filtrate was concentrated and the resulting oil was directly used without further purification. *N*-aryloxyamine (1.0 equiv.) was dissolved in DCM (0.2 M). The resulting solution was cooled to 0 °C and acetic anhydride (1.10 equiv.) was added dropwise to the mixture. After stirring at room temperature for 3 h the reaction was quenched with saturated NaHCO₃ and extracted with DCM. The organic phase was washed three times with saturated NaHCO₃ and dried over anhydrous Na₂SO₄, followed by filtration. The solvent was evaporated under reduced pressure. The crude product was purified by recrystallization from EtOAc/pentane to afford the desired *N*-aryloxyacetamide **2**.

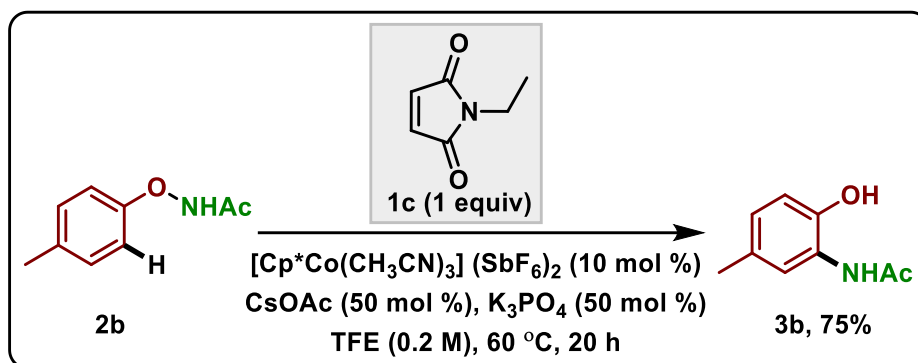
(b) General procedure for the Cp*Co(III)/Maleimide co-catalyzed *ortho*-C-H amidation of aryloxyacetamide :



To an oven dried Schlenk tube charged with a stir bar, maleimide **1** (0.1 mmol, 1 equiv), aryloxy acetamide **2** (0.1 mmol, 1 equiv), [Cp*Co(CH₃CN)₃](SbF₆)₂ (0.01 mmol, 10 mol %), CsOAc (0.05 mmol, 50 mol %), K₃PO₄ (0.05 mmol, 50 mol %) and TFE (0.5 mL, 0.2 M) were added under nitrogen atmosphere. The reaction mixture was stirred (700 rpm) in a preheated aluminum block at 60 °C for 20 h. After completion of the reaction (monitored by TLC), the solvent was evaporated under reduced pressure, and the crude was purified by

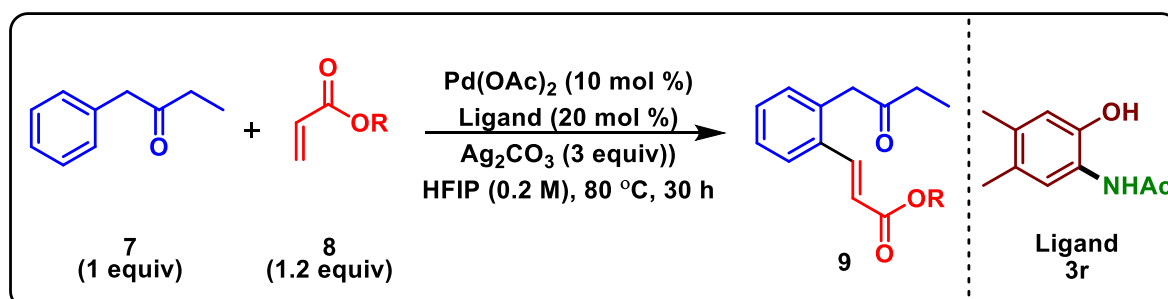
column chromatography using EtOAc/hexane as eluent to get corresponding *o*-amidated product **3**.

(c) General procedure for the Cp*Co(III)/Maleimide co-catalyzed *ortho*-C-H amidation of aryloxyacetamide in 1 mmol scale:



To an oven dried Schlenk tube charged with a stir bar, maleimide **1c** (1 mmol, 1 equiv), aryloxy acetamide **2** (0.1 mmol, 1 equiv), $[\text{Cp}^*\text{Co}(\text{CH}_3\text{CN})_3](\text{SbF}_6)_2$ (0.01 mmol, 10 mol %), CsOAc (0.05 mmol, 50 mol %), K_3PO_4 (0.05 mmol, 50 mol %) and TFE (5.0 mL, 0.2 M) were added under nitrogen atmosphere. The reaction mixture was stirred (700 rpm) in a preheated aluminum block at 60 °C for 20 h. After completion of the reaction (monitored by TLC), the solvent was evaporated under reduced pressure, and the crude was purified by column chromatography using EtOAc/hexane as eluent to get corresponding *o*-amidated product **3b** (124 mg, 75%).

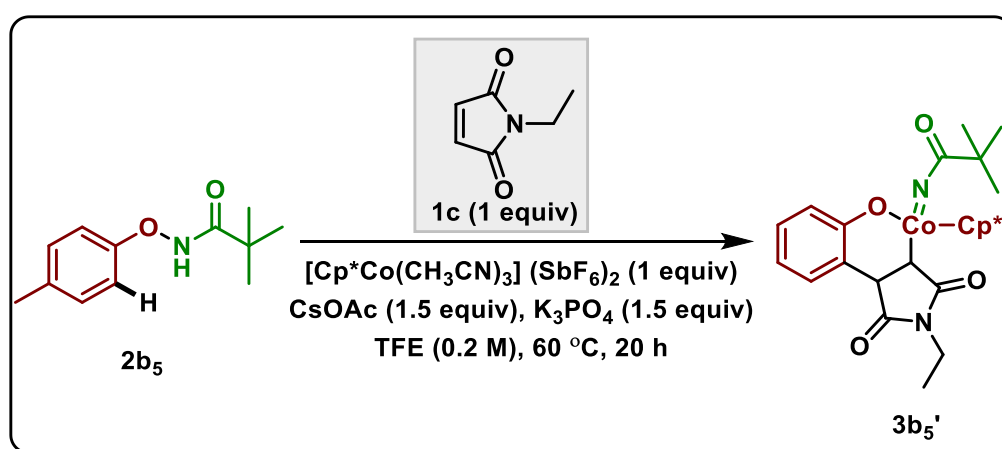
(d) General procedure for the palladium catalyzed C-H olefination reaction:



To an oven dried Schlenk tube charged with a stir bar, phenyl acetone **7** (0.1 mmol, 1 equiv), acrylate **8** (0.125 mmol, 1.25 equiv), $\text{Pd}(\text{OAc})_2$ (0.01 mmol, 10 mol %), ligand **3r** (0.02

mmol, 20 mol %), Ag_2CO_3 (0.3 mmol, 3 equiv) and HFIP (0.5 mL, 0.2 M) were added under nitrogen atmosphere. The reaction mixture was stirred (700 rpm) in a preheated aluminum block at 80 °C for 30 h. After completion of the reaction (monitored by TLC), the solvent was evaporated under reduced pressure, and the crude was purified by column chromatography using EtOAc/hexane as eluent to get corresponding *o*-alkenylated product **9**. The ratio of mono and dialkenylated product was determined from ^1H NMR.

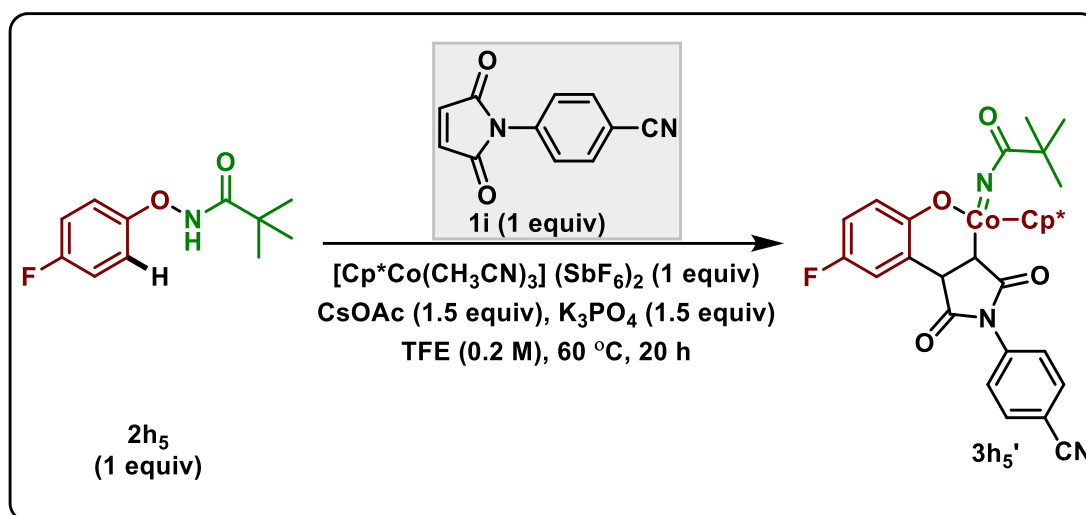
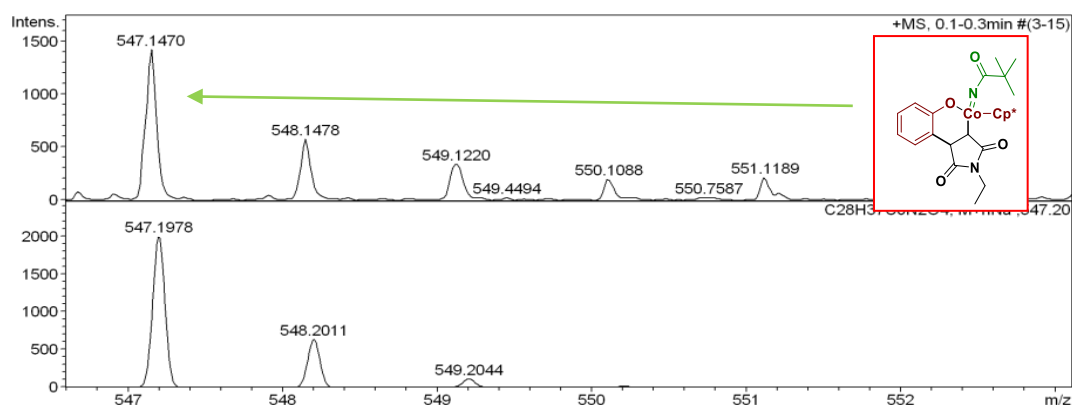
(e) Detection of intermediate in ESI-MS.



To an oven dried Schlenk tube charged with a stir bar, maleimide **1c** (0.1 mmol, 1 equiv), *N*-(*p*-tolylloxy)pivalamide **2b₅** (0.1 mmol, 1 equiv), $[\text{Cp}^*\text{Co}(\text{CH}_3\text{CN})_3](\text{SbF}_6)_2$ (0.1 mmol, 1 equiv), CsOAc (0.15 mmol, 1.5 equiv), K_3PO_4 (0.15 mmol, 1.5 equiv), and TFE (0.5 mL, 0.2 M) were added under nitrogen atmosphere. The reaction mixture was stirred (700 rpm) in a preheated aluminum block at 60 °C for 20 h. After completion of the reaction, the reaction mixture was filtered and mass was recorded, **3b₅'** was detected in LCMS.

Figure 4.3: ESI-MS spectra of intermediate **3h₅'**

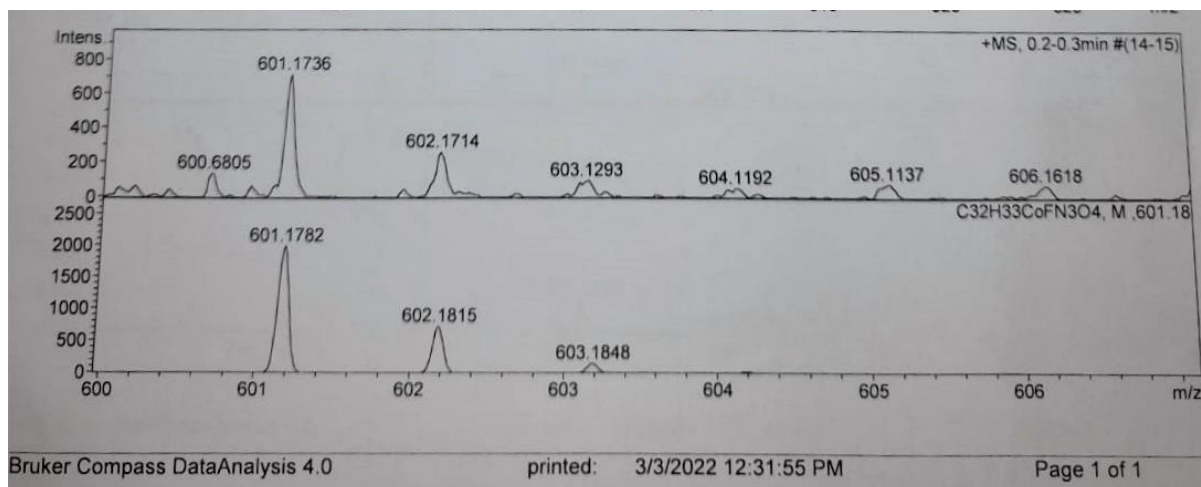
LCMS (ESI) m/z of **3h₅'**: [M+Na]⁺ Calcd for C₂₈H₃₇CoN₂O₄: 547.1; Found: 547.1



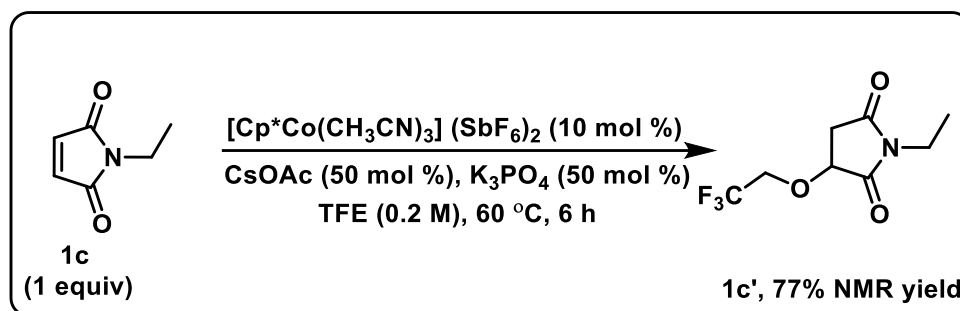
To an oven dried Schlenk tube charged with a stir bar, maleimide **1i** (0.1 mmol, 1 equiv), N-(4-fluorophenoxy)pivalamide **2h₅** (0.1 mmol, 1 equiv), [Cp*Co(CH₃CN)₃](SbF₆)₂ (0.1 mmol, 1 equiv), CsOAc (0.15 mmol, 1.5 equiv), K₃PO₄ (0.15 mmol, 1.5 equiv), and TFE (0.5 mL, 0.2 M) were added under nitrogen atmosphere. The reaction mixture was stirred (700 rpm) in a preheated aluminum block at 60 °C for 20 h. After completion of the reaction, the reaction mixture was filtered and mass was recorded, **3h₅'** was detected in HRMS.

Figure 4.4: ESI-MS spectra of intermediate **3h₅'**

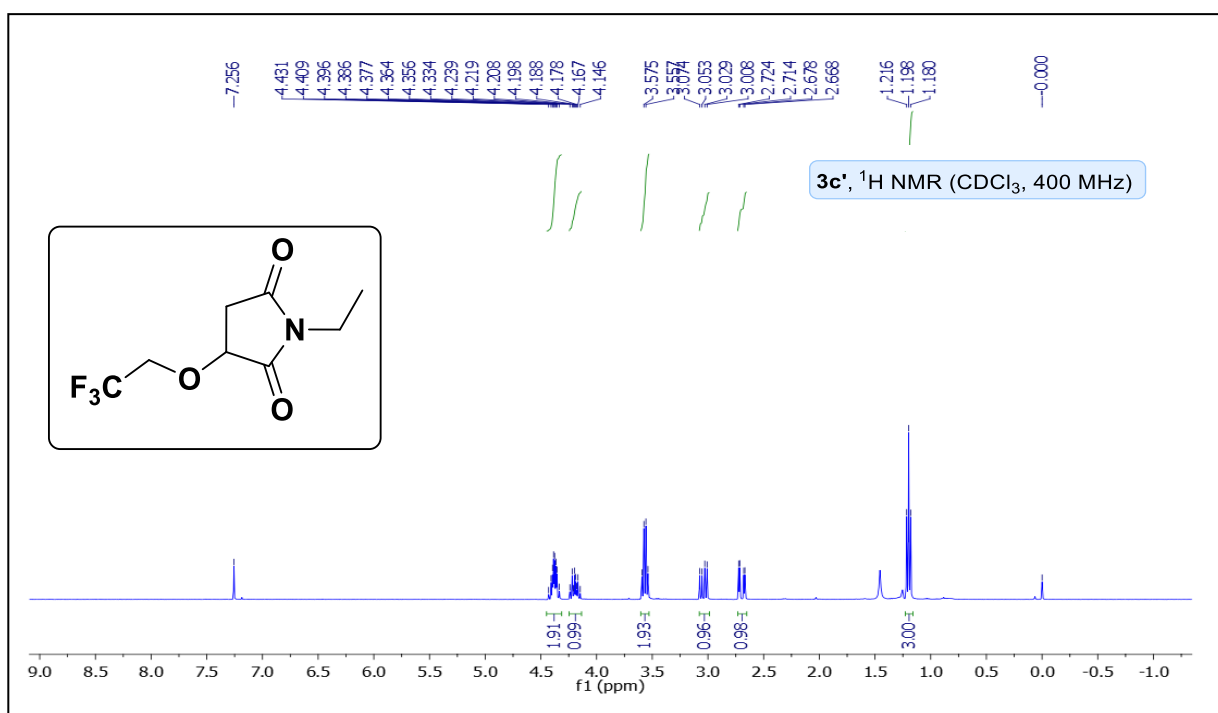
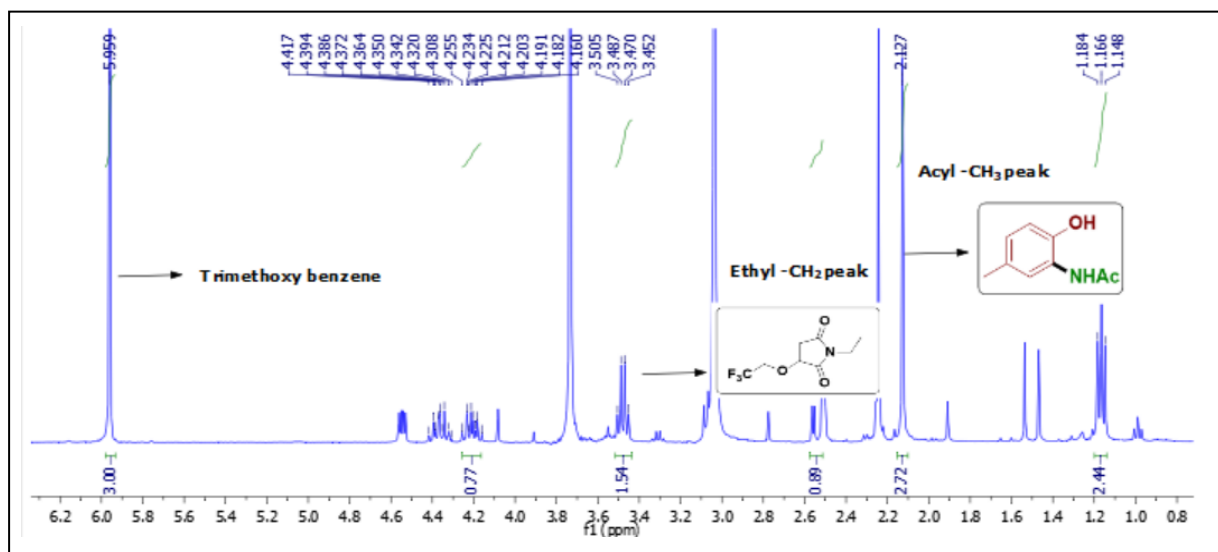
HRMS (ESI) m/z of **3h₅'**: [M]⁺ Calcd for C₃₂H₃₃CoFN₃O₄: 601.1782; Found: 601.1736.

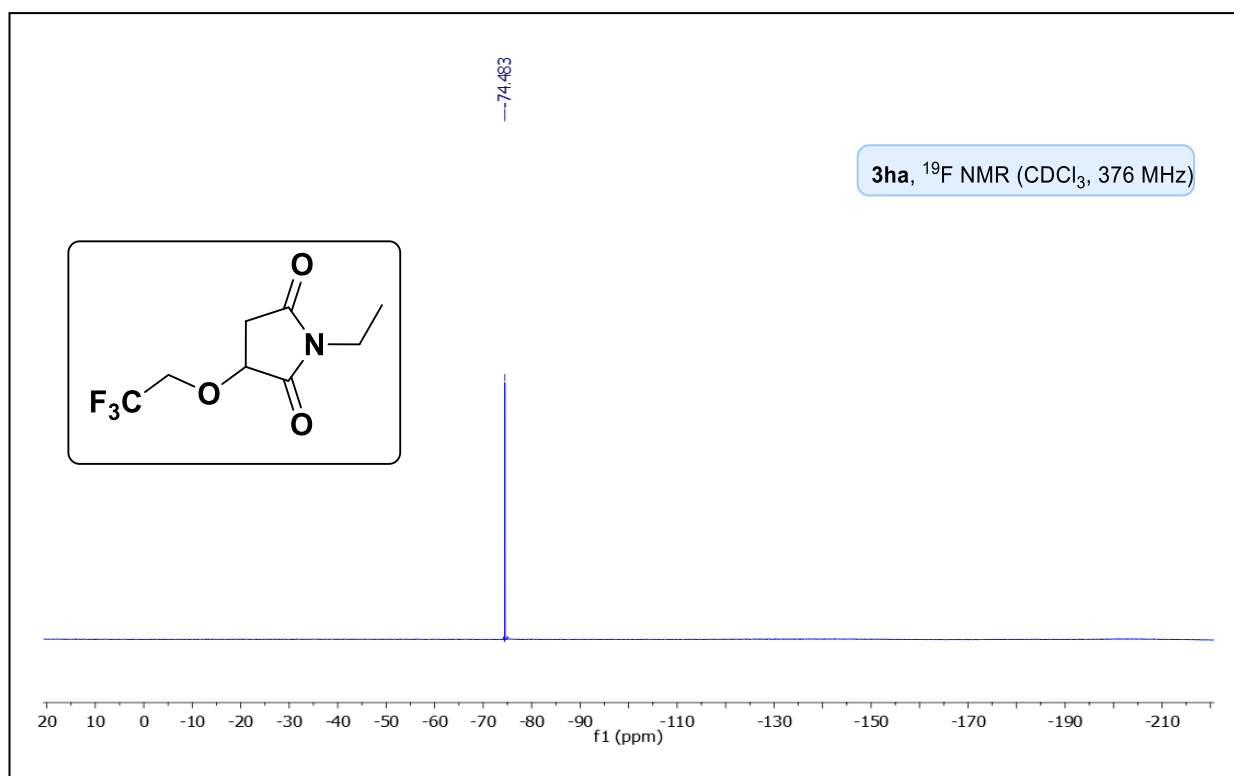
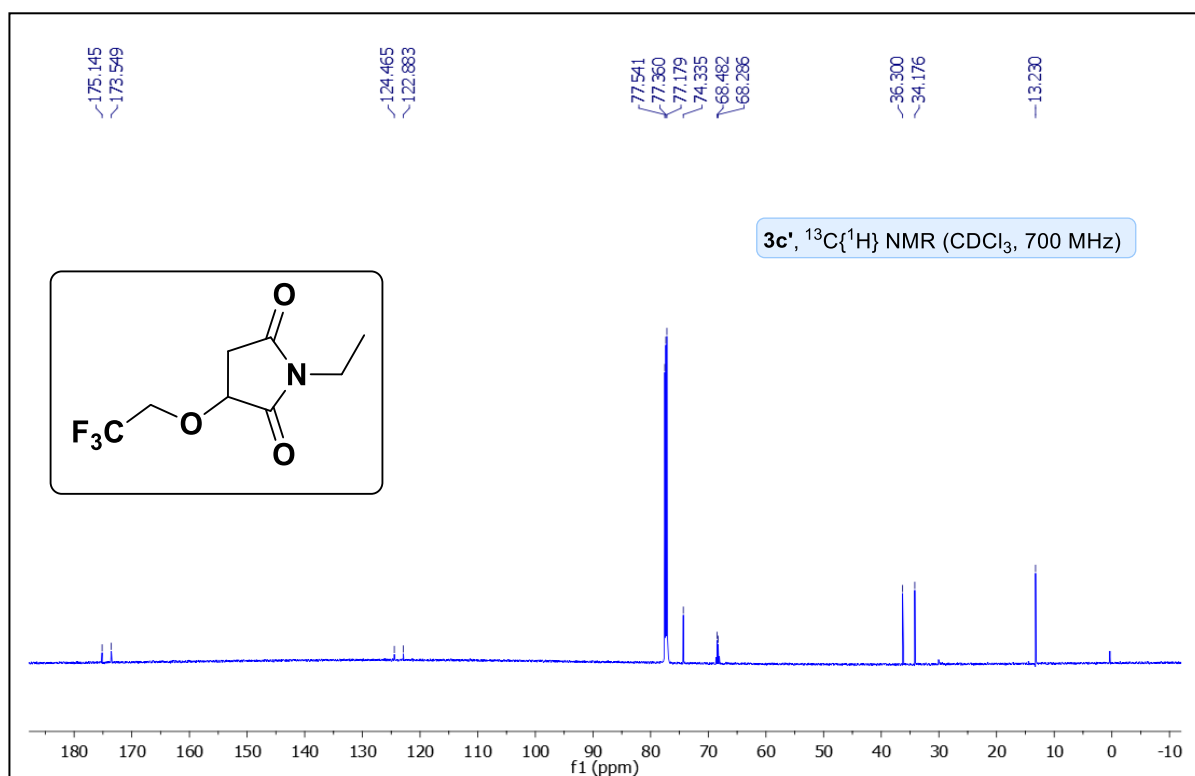


(f) Effect of reaction condition on the maleimide **1c:**

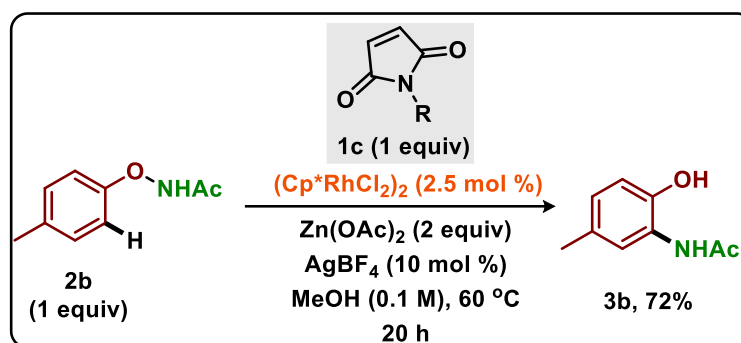


To an oven dried Schlenk tube charged with a stir bar, maleimide **1c** (0.1 mmol, 1 equiv), [Cp*Co(CH₃CN)₃](SbF₆)₂ (0.01 mmol, 10 mol %), CsOAc (0.05 mmol, 50 mol %), K₃PO₄ (0.05 mmol, 50 mol %), and TFE (0.5 mL, 0.2 M) were added under nitrogen atmosphere. The reaction mixture was stirred (700 rpm) in a preheated aluminum block at 60 °C for 20 h. After completion of the reaction (monitored by TLC), the solvent was evaporated under reduced pressure, and the crude NMR was recorded.



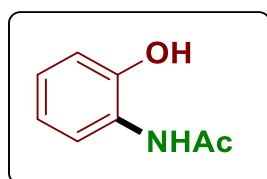


(g) Replication of *o*-amidation in Rh/maleimide condition:



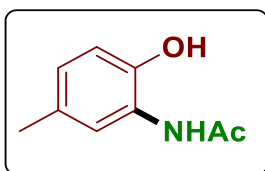
To an oven dried Schlenk tube charged with a stir bar, maleimide **1c** (0.1 mmol, 1 equiv), *N*-(*p*-tolylloxy)acetamide **2b** (0.1 mmol, 1 equiv), $[\text{Cp}^*\text{RhCl}_2]_2$ (0.0025 mmol, 2.5 mol %), $\text{Zn}(\text{OAc})_2$ (2 equiv), AgBF_4 (0.01 mmol, 10 mol %), and MeOH (1 mL, 0.1 M) were added under nitrogen atmosphere. The reaction mixture was stirred (700 rpm) in a preheated aluminum block at 60 °C for 20 h. After completion of the reaction (monitored by TLC), the solvent was evaporated under reduced pressure, and the crude was purified by column chromatography using EtOAc/hexane as eluent to get corresponding *o*-amidated product **3b**, 72% (12 mg) yield.

Experimental characterization data of products:



N-(2-hydroxyphenyl)acetamide (**3a**):⁶

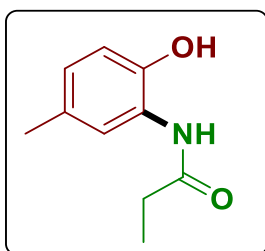
Physical State: pale white solid (10 mg, 65%), $R_f = 0.5$ (10% EtOAc/hexane). ^1H NMR ($\text{DMSO}-d_6$, 700 MHz): δ 9.76 (s, 1H), 9.32 (s, 1H), 7.69 (d, $J = 7.7$ Hz, 1H), 6.96 (t, $J = 7.7$ Hz, 1H), 6.88 (d, $J = 7.7$ Hz, 1H), 6.78 (t, $J = 7.7$ Hz, 1H), 2.12 (s, 3H). $^{13}\text{C}\{^1\text{H}\}$ NMR ($\text{DMSO}-d_6$, 175 MHz): δ 169.9, 148.8, 127.3, 125.5, 123.3, 119.9, 116.8, 24.5. IR (KBr, cm^{-1}): 3402, 1651.



N-(2-hydroxy-5-methylphenyl)acetamide (**3b**):⁶

Physical State: white solid (14 mg, 85%), $R_f = 0.4$ (30%

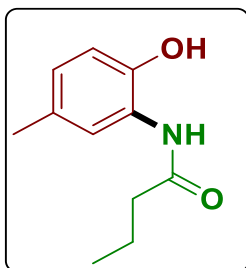
EtOAc/hexane). ^1H NMR (CDCl_3 , 700 MHz): δ 8.40 (s, 1H), 7.45 (s, 1H), 6.93-6.90 (m, 2H), 6.80 (s, 1H), 2.25 (s, 6H). $^{13}\text{C}\{^1\text{H}\}$ NMR (CDCl_3 , 175 MHz): δ 170.6, 146.7, 130.3, 128.2, 125.4, 122.7, 120.0, 24.0, 20.7. **IR** (KBr, cm^{-1}): 3437, 1634.



2-(ethylamino)-4-methylphenol (**3b₁**):

Physical State: white solid (14 mg, 80%), $R_f = 0.6$ (20%

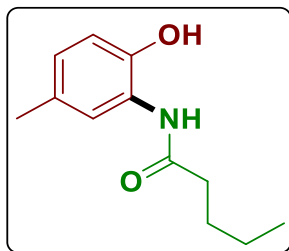
EtOAc/hexane). ^1H NMR ($\text{DMSO}-d_6$, 400 MHz): δ 9.52 (s, 1H), 9.21 (s, 1H), 7.53 (s, 1H), 6.76 (brs, 2H), 2.41 (q, $J = 7.6$ Hz, 2H), 2.21 (s, 3H), 1.10 (t, $J = 7.6$ Hz, 3H). $^{13}\text{C}\{^1\text{H}\}$ NMR ($\text{DMSO}-d_6$, 100 MHz): δ 173.5, 146.4, 128.4, 127.0, 125.8, 123.6, 116.7, 30.0, 21.3, 10.8. **IR** (KBr, cm^{-1}): 3412, 1644. **HRMS** (ESI) m/z : $[\text{M}+\text{H}]^+$ Calcd for $\text{C}_{10}\text{H}_{14}\text{NO}_2$: 180.1025; Found: 180.1015.



N-(2-hydroxy-5-methylphenyl)butyramide (**3b₂**):

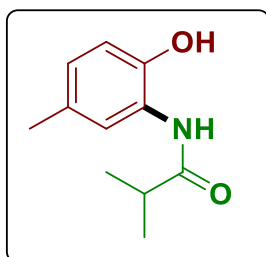
Physical State: white solid (15 mg, 77%), $R_f = 0.3$ (20%

EtOAc/hexane). ^1H NMR (CDCl_3 , 400 MHz): δ 8.58 (s, 1H), 7.53 (s, 1H), 6.90 (s, 2H), 6.82 (s, 1H), 2.41 (t, $J = 7.6$ Hz, 2H), 2.24 (s, 3H), 1.81-1.72 (m, 2H), 1.01 (t, $J = 7.6$ Hz, 3H). $^{13}\text{C}\{^1\text{H}\}$ NMR (CDCl_3 , 100 MHz): δ 173.6, 146.6, 130.2, 128.0, 125.5, 122.7, 119.9, 39.1, 20.6, 19.5, 13.9. **IR** (KBr, cm^{-1}): 3416, 2964, 1669. **HRMS** (ESI) m/z : $[\text{M}+\text{H}]^+$ Calcd for $\text{C}_{11}\text{H}_{16}\text{NO}_2$: 194.1181; Found: 194.1172.



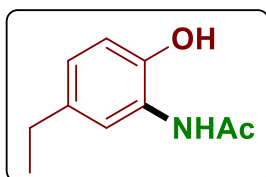
***N*-(2-hydroxy-5-methylphenyl)pentanamide (3b₃):**

Physical State: brown solid (17 mg, 82%), $R_f = 0.4$ (30% EtOAc/hexane). **¹H NMR (CDCl₃, 400 MHz):** δ 8.56 (s, 1H), 7.24 (brs, 1H), 6.93-6.89 (m, 2H), 6.79 (s, 1H), 2.44 (t, $J = 7.2$ Hz, 2H), 2.24 (s, 3H), 1.72 (pent, $J = 7.2$ Hz, 2H), 1.42 (sextet, $J = 7.2$ Hz, 2H), 0.95 (t, $J = 7.6$ Hz, 3H). **¹³C{¹H} NMR (CDCl₃, 100 MHz):** δ 173.8, 146.8, 130.2, 128.1, 125.5, 122.7, 120.0, 37.1, 28.1, 22.6, 20.6, 14.0. **IR (KBr, cm⁻¹):** 3414, 2959, 1639. **HRMS (ESI) m/z:** [M+H]⁺ Calcd for C₁₂H₁₈NO₂: 208.1338; Found: 208.1327.



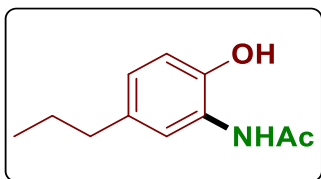
***N*-(2-hydroxy-5-methylphenyl)isobutyramide (3b₄):**

Physical State: white solid (14 mg, 73%), $R_f = 0.7$ (20% EtOAc/hexane). **¹H NMR (CDCl₃, 400 MHz):** δ 8.61 (s, 1H), 7.36 (s, 1H), 6.95-6.90 (m, 2H), 6.79 (s, 1H), 2.68-2.58 (m, 1H), 2.25 (s, 3H), 1.29 (d, $J = 6.8$ Hz, 6H). **¹³C{¹H} NMR (CDCl₃, 175 MHz):** δ 177.5, 146.8, 130.1, 128.1, 125.4, 122.7, 120.1, 36.5, 20.6, 20.0. **IR (KBr, cm⁻¹):** 3437, 1652. **HRMS (ESI) m/z:** [M+H]⁺ Calcd for C₁₁H₁₆NO₂: 194.1181; Found: 194.1172.



***N*-(5-ethyl-2-hydroxyphenyl)acetamide (3c):**

Physical State: yellow solid (14 mg, 81%), $R_f = 0.2$ (10% EtOAc/hexane). **¹H NMR (DMSO-*d*₆, 400 MHz):** δ 9.46 (s, 1H), 9.30 (s, 1H), 7.50 (s, 1H), 6.83-6.78 (m, 2H), 2.51 (q, $J = 7.6$ Hz, 2H), 2.12 (s, 3H), 1.16 (t, $J = 7.6$ Hz, 3H). **¹³C{¹H} NMR (DMSO-*d*₆, 100 MHz):** δ 169.9, 146.7, 135.0, 127.0, 124.7, 122.4, 116.8, 28.3, 24.3, 16.6. **IR (KBr, cm⁻¹):** 3414, 1652. **HRMS (ESI) m/z:** [M+H]⁺ Calcd for C₁₀H₁₄NO₂: 180.1025; Found: 180.1015.



***N*-(2-hydroxy-5-propylphenyl)acetamide (3d):**

Physical State: white solid (14 mg, 72%), $R_f = 0.4$ (30%

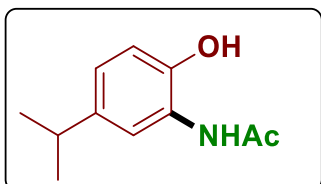
EtOAc/hexane). ^1H NMR (DMSO- d_6 , 700 MHz): δ 9.52 (s,

1H), 9.32 (s, 1H), 7.50 (s, 1H), 6.78 (s, 2H), 2.45 (t, $J = 7.7$ Hz, 2H), 2.11 (s, 3H), 1.55 (q,

$J = 7.0$ Hz, 2H), 0.90 (t, $J = 7.7$ Hz, 3H). $^{13}\text{C}\{^1\text{H}\}$ NMR (DMSO- d_6 , 175 MHz): δ 170.0,

146.7, 133.4, 127.0, 125.4, 123.1, 116.7, 37.6, 25.2, 24.5, 14.5. IR (KBr, cm^{-1}): 3420, 1651.

HRMS (ESI) m/z : $[\text{M}+\text{H}]^+$ Calcd for $\text{C}_{11}\text{H}_{16}\text{NO}_2$: 194.1176; Found: 194.1184.



***N*-(2-hydroxy-5-isopropylphenyl)acetamide (3e):**

Physical State: white solid (16 mg, 83%), $R_f = 0.6$ (10%

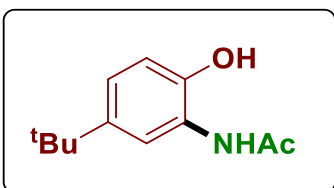
EtOAc/hexane). ^1H NMR (CDCl_3 , 400 MHz): δ 8.61 (s, 1H),

7.81 (s, 1H), 6.99-6.89 (m, 3H), 2.85-2.75 (m, 1H), 2.23 (s, 3H), 1.18 (d, $J = 6.8$ Hz, 6H).

$^{13}\text{C}\{^1\text{H}\}$ NMR (CDCl_3 , 100 MHz): δ 170.8, 146.7, 141.5, 125.5 (2C), 120.2, 119.8, 33.4,

24.4, 23.9. IR (KBr, cm^{-1}): 3418, 2953, 1655. HRMS (ESI) m/z : $[\text{M}+\text{Na}]^+$ Calcd for

$\text{C}_{11}\text{H}_{15}\text{NO}_2\text{Na}$: 216.0995; Found: 216.1003.



***N*-(5-(tert-butyl)-2-hydroxyphenyl)acetamide (3f):**

Physical State: brown solid (13 mg, 63%), $R_f = 0.5$ (30%

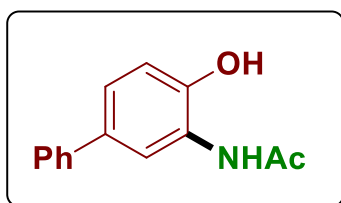
EtOAc/hexane). ^1H NMR (DMSO- d_6 , 700 MHz): δ 9.52 (s,

1H), 9.45 (s, 1H), 7.63 (s, 1H), 7.01 (d, $J = 8.4$ Hz, 1H), 6.80 (d, $J = 8.4$ Hz, 1H), 2.12 (s,

3H), 1.25 (s, 9H). $^{13}\text{C}\{^1\text{H}\}$ NMR (DMSO- d_6 , 175 MHz): δ 170.1, 146.6, 142.2, 126.6,

122.5, 120.4, 116.8, 34.6, 32.2, 24.4. IR (KBr, cm^{-1}): 3421, 2951, 1652. HRMS (ESI) m/z :

$[\text{M}+\text{H}]^+$ Calcd for $\text{C}_{12}\text{H}_{18}\text{NO}_2$: 208.1338; Found: 208.1327.



N-(4-hydroxy-[1,1'-biphenyl]-3-yl)acetamide (3g):⁶

Physical State: brown solid (15 mg, 66%), $R_f = 0.3$ (30%

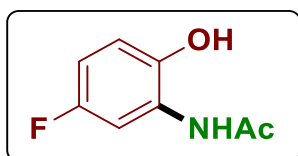
EtOAc/hexane). ^1H NMR (DMSO- d_6 , 400 MHz): δ 9.99 (s,

1H), 9.40 (s, 1H), 8.08 (d, $J = 1.6$ Hz, 1H), 7.56 (d, $J = 7.6$ Hz, 2H), 7.45 (t, $J = 7.6$ Hz, 2H),

7.34-7.27 (m, 2H), 6.97 (d, $J = 8.4$ Hz, 1H), 2.16 (s, 3H). $^{13}\text{C}\{^1\text{H}\}$ NMR (DMSO- d_6 , 100

MHz): δ 170.0, 148.5, 141.1, 132.0, 129.7, 127.7, 127.4, 126.9, 123.7, 121.5, 117.1, 24.6.

IR (KBr, cm^{-1}): 3413, 2963, 1652.



N-(5-fluoro-2-hydroxyphenyl)acetamide (3h):²⁶

Physical State: white solid (13 mg, 77%), $R_f = 0.5$ (20%

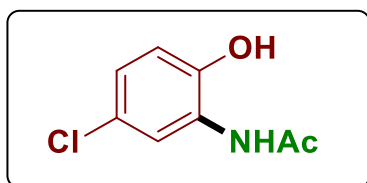
EtOAc/hexane). ^1H NMR (DMSO- d_6 , 700 MHz): δ 9.82 (s, 1H),

9.29 (s, 1H), 7.79 (dd, $J = 10.5$ Hz, 2.8 Hz, 1H), 6.86-6.84 (m, 1H), 6.77-6.74 (m, 1H), 2.14

(s, 3H). $^{13}\text{C}\{^1\text{H}\}$ NMR (DMSO- d_6 , 175 MHz): δ 169.9, 155.7 (d, $J_{\text{C-F}} = 230.6$ Hz), 144.2,

128.2 (d, $J_{\text{C-F}} = 11.2$ Hz), 116.2 (d, $J_{\text{C-F}} = 8.9$ Hz), 110.4 (d, $J_{\text{C-F}} = 22.4$ Hz), 108.9 (d, $J_{\text{C-F}}$

$= 27.8$ Hz), 24.7. ^{19}F NMR (CDCl_3 , 376 MHz): δ -74.4. IR (KBr, cm^{-1}): 3421, 2951, 1645.



N-(5-chloro-2-hydroxyphenyl)acetamide (3i):⁶

Physical State: white solid (11 mg, 60%), $R_f = 0.6$ (30%

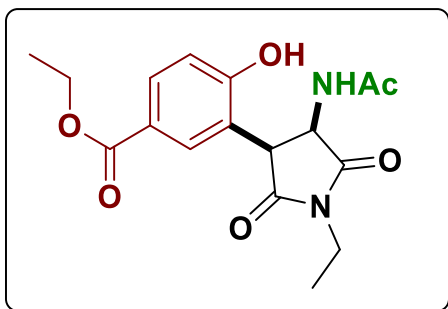
EtOAc/hexane). ^1H NMR (DMSO- d_6 , 700 MHz): δ 10.14

(s, 1H), 9.29 (s, 1H), 7.97 (s, 1H), 6.98 (d, $J = 8.4$ Hz, 1H), 6.88 (d, $J = 8.4$ Hz, 1H), 2.13

(s, 3H). $^{13}\text{C}\{^1\text{H}\}$ NMR (DMSO- d_6 , 175 MHz): δ 169.9, 147.1, 128.7, 124.3, 122.9, 121.9,

117.2, 24.7. IR (KBr, cm^{-1}): 3413, 1651.

Ethyl 3-(4-acetamido-1-ethyl-2,5-dioxopyrrolidin-3-yl)-4-hydroxybenzoate (3j*):

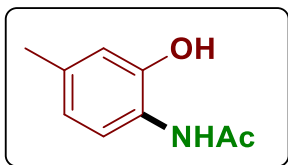


Physical State: yellow solid (30 mg, 86%), $R_f = 0.3$

(60% EtOAc/hexane), ^1H NMR (DMSO- d_6 , 700 MHz): δ 10.91 (s, 1H), 8.55 (d, $J = 7.0$ Hz, 1H), 7.85-7.83 (m, 2H), 6.94 (d, $J = 7.7$ Hz, 1H), 4.47-4.45 (m, 1H), 4.33-4.28 (m, 2H), 4.05-4.04 (m, 1H),

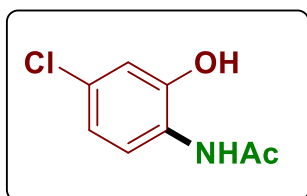
3.57-3.51 (m, 2H), 1.90 (s, 3H), 133 (t, $J = 7.0$ Hz, 3H), 1.14 (t, $J = 7.0$ Hz, 3H). $^{13}\text{C}\{^1\text{H}\}$ NMR (DMSO- d_6 , 175 MHz): δ 179.9, 179.1, 174.7, 170.3, 164.4, 138.0, 135.8, 128.3, 125.7, 120.1, 65.1, 59.7, 54.5, 38.1, 27.2, 19.2, 17.3. IR (KBr, cm^{-1}): 3421, 1674. HRMS (ESI) m/z : $[\text{M}-\text{H}]^+$ Calcd for $\text{C}_{17}\text{H}_{19}\text{N}_2\text{O}_6$: 347.1245; Found: 347.1245.

***N*-(2-hydroxy-4-methylphenyl)acetamide (3k):⁶**



Physical State: brown solid (13 mg, 79%), $R_f = 0.4$ (30% EtOAc/hexane). ^1H NMR (DMSO- d_6 , 400 MHz): δ 9.68 (s, 1H),

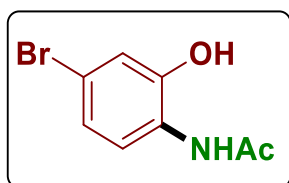
9.32 (s, 1H), 7.50 (d, $J = 8.0$ Hz, 1H), 6.69 (s, 1H), 6.60 (d, $J = 8.0$ Hz, 1H), 2.22 (s, 3H), 2.10 (s, 3H). $^{13}\text{C}\{^1\text{H}\}$ NMR (DMSO- d_6 , 100 MHz): δ 173.8, 152.8, 139.0, 128.7, 127.3, 124.5, 121.5, 28.4, 25.5. IR (KBr, cm^{-1}): 3414, 2960, 1652, 1575.



***N*-(4-chloro-2-hydroxyphenyl)acetamide (3l):²⁶**

Physical State: brown solid (10 mg, 54%), $R_f = 0.4$ (40% EtOAc/hexane). ^1H NMR (DMSO- d_6 , 700 MHz): δ 10.33 (s,

1H), 9.30 (s, 1H), 7.80 (d, $J = 8.4$ Hz, 1H), 6.90 (d, $J = 2.1$ Hz, 1H), 6.84 (d, $J = 9.0$ Hz, 1H), 2.11 (s, 3H). $^{13}\text{C}\{^1\text{H}\}$ NMR (DMSO- d_6 , 175 MHz): δ 173.8, 153.7, 132.5, 130.5, 128.2, 123.5, 120.1, 28.5. IR (KBr, cm^{-1}): 3414, 2953, 1652.



N-(4-Bromo-2-hydroxyphenyl)acetamide (**3m**):²⁶

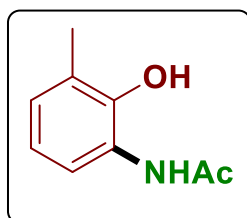
Physical State: white solid (11 mg, 48%), $R_f = 0.5$ (30%

EtOAc/hexane). ^1H NMR (DMSO- d_6 , 400 MHz): δ 10.34 (s, 1H),

9.29 (s, 1H), 7.77 (d, $J = 8.4$ Hz, 1H), 7.03 (d, $J = 2.0$ Hz, 1H), 6.96 (dd, $J = 8.8$ Hz, 2.4 Hz,

1H), 2.11 (s, 3H). $^{13}\text{C}\{^1\text{H}\}$ NMR (DMSO- d_6 , 175 MHz): δ 169.8, 149.8, 127.0, 124.5,

122.4, 118.8, 116.3, 24.6. IR (KBr, cm^{-1}): 3416, 2956, 1653.



N-(2-hydroxy-3-methylphenyl)acetamide (**3n**):⁶

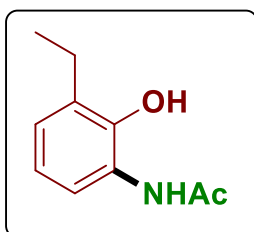
Physical State: brown solid (13 mg, 79%), $R_f = 0.4$ (20%

EtOAc/hexane). ^1H NMR (CDCl_3 , 400 MHz): δ 8.62 (s, 1H), 7.58

(s, 1H), 7.02 (d, $J = 7.2$ Hz, 1H), 6.81-6.73 (m, 2H), 2.29 (s, 3H),

2.24 (s, 3H). $^{13}\text{C}\{^1\text{H}\}$ NMR (CDCl_3 , 100 MHz): δ 170.9, 147.6, 129.4, 128.8, 125.5, 120.2,

120.2, 24.0, 16.8. IR (KBr, cm^{-1}): 3420, 1635.



N-(3-ethyl-2-hydroxyphenyl)acetamide (**3o**):

Physical State: brown solid (15 mg, 84%), $R_f = 0.4$ (30%

EtOAc/hexane). ^1H NMR (CDCl_3 , 400 MHz): δ 9.96 (s, 1H), 9.29

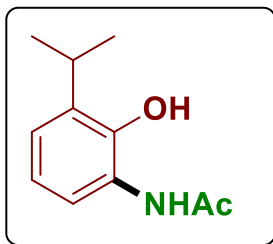
(s, 1H), 7.11 (d, $J = 8.0$ Hz, 1H), 6.98 (d, $J = 7.2$ Hz, 1H), 6.78 (t, J

= 7.6 Hz, 1H), 2.62 (q, $J = 7.6$ Hz, 2H), 2.16 (s, 3H), 1.16 (t, $J = 7.6$ Hz, 3H). $^{13}\text{C}\{^1\text{H}\}$ NMR

(CDCl_3 , 100 MHz): δ 171.2, 147.5, 133.8, 127.2, 126.5, 121.8, 120.2, 24.0 (2C), 15.2. IR

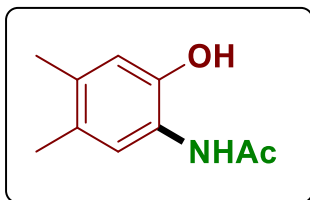
(KBr, cm^{-1}): 3419, 1651. HRMS (ESI) m/z : $[\text{M}+\text{H}]^+$ Calcd for $\text{C}_{10}\text{H}_{14}\text{NO}_2$: 180.1025;

Found: 180.1015.



***N*-(2-hydroxy-3-isopropylphenyl)acetamide (3p):**

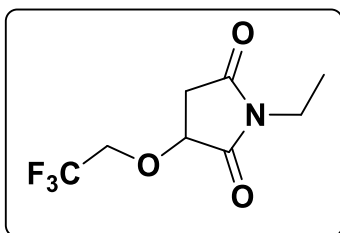
Physical State: dark yellow solid (15 mg, 78%), $R_f = 0.3$ (20% EtOAc/hexane). **^1H NMR (DMSO- d_6 , 700 MHz):** δ 9.98 (s, 1H), 9.26 (s, 1H), 7.07 (d, $J = 7.7$ Hz, 1H), 7.03 (d, $J = 7.7$ Hz, 1H), 6.82 (t, $J = 7.7$ Hz, 1H), 3.34-3.31 (m, 1H), 2.16 (s, 3H), 1.19 (d, $J = 7.0$ Hz, 6H). **$^{13}\text{C}\{^1\text{H}\}$ NMR (DMSO- d_6 , 175 MHz):** δ 171.1, 147.0, 138.2, 127.2, 123.5, 121.7, 120.3, 27.4, 24.0, 23.5. **IR (KBr, cm^{-1}):** 3421, 2956, 1636. **HRMS (ESI) m/z :** $[\text{M}+\text{H}]^+$ Calcd for $\text{C}_{11}\text{H}_{16}\text{NO}_2$: 194.1172; Found: 194.1172.



***N*-(2-hydroxy-4,5-dimethylphenyl)acetamide (3r):⁶**

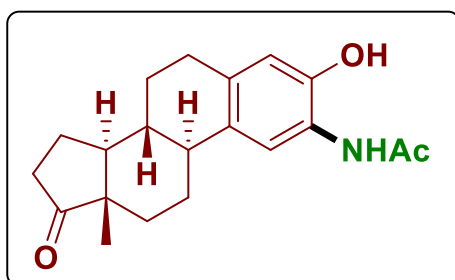
Physical State: brown solid (14 mg, 78%), $R_f = 0.3$ (30% EtOAc/hexane). **^1H NMR (DMSO- d_6 , 400 MHz):** δ 9.38 (s, 1H), 9.35 (s, 1H), 7.33 (s, 1H), 6.67 (s, 1H), 2.13 (s, 3H), 2.11 (s, 3H), 2.10 (s, 3H). **$^{13}\text{C}\{^1\text{H}\}$ NMR (DMSO- d_6 , 100 MHz):** δ 169.9, 146.8, 133.5, 127.0, 124.6, 124.5, 118.5, 24.3, 19.9, 19.5. **IR (KBr, cm^{-1}):** 3414, 2963, 1654.

***1*-ethyl-3-(2,2,2-trifluoroethoxy)pyrrolidine-2,5-dione (1c'):**



Physical State: colorless liquid (17 mg, 76% isolated yield), $R_f = 0.6$ (20% EtOAc/hexane). **^1H NMR (CDCl_3 , 400 MHz):** δ 4.43-4.33 (m, 2H), 4.23-4.14 (m, 1H), 3.56 (q, $J = 7.2$ Hz, 2H), 3.07-3.00 (m, 1H), 2.69 (dd, $J = 18.4$ Hz, 4.0 Hz, 1H), 1.19 (t, $J = 7.2$ Hz, 3H). **$^{13}\text{C}\{^1\text{H}\}$ NMR (CDCl_3 , 175 MHz):** δ 175.1, 173.5, 123.6 (d, $J_{\text{C-F}} = 276.5$ Hz), 74.3, 68.3 (q, $J_{\text{C-F}} = 34.3$ Hz), 36.3, 34.1, 13.2. **^{19}F NMR (CDCl_3 , 376 MHz):** δ -74.4. **IR (KBr, cm^{-1}):** 3437, 1634. **LC-MS (ESI) m/z :** $[\text{M}+\text{HCOOH}]^+$ Calcd for $\text{C}_9\text{H}_{12}\text{F}_3\text{NO}_5$: 271.0; Found: 271.0.

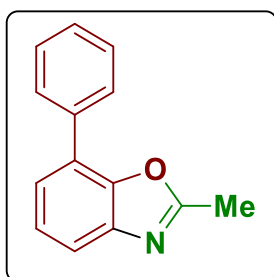
N-((8R,9S,13S,14S)-3-hydroxy-13-methyl-17-oxo-7,8,9,11,12,13,14,15,16,17-



*decahydro-6H-cyclopenta[a]phenanthren-2-yl)acetamide (5):*²²

Physical State: white solid (14 mg, 85%), R_f = 0.3 (2% EtOAc/DCM). ^1H NMR (DMSO- d_6 , 700

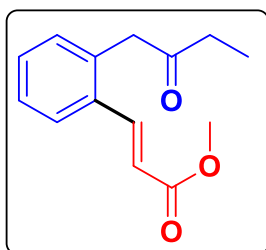
MHz): δ 9.49 (s, 1H), 9.35 (s, 1H), 7.52 (s, 1H), 6.57 (s, 1H), 2.78-2.75 (m, 2H), 2.48-2.44 (dd, J = 9.1 Hz, 1H), 2.24-2.18 (m, 2H), 2.12-2.07 (m, 3H), 2.00-1.94 (m, 2H), 1.79 (d, J = 8.4 Hz, 1H), 1.62-1.56 (m, 1H), 1.52-1.48 (m, 3H), 1.44-1.34 (m, 3H), 0.86 (m, 3H). $^{13}\text{C}\{^1\text{H}\}$ NMR (DMSO- d_6 , 175 MHz): δ 169.9, 146.9, 133.7, 131.0, 124.9, 120.4, 116.9, 50.5, 48.2, 44.3, 38.7, 36.3, 32.2, 29.4, 27.0, 26.6, 24.4, 22.0, 14.4. **IR (KBr, cm^{-1}):** 3416, 1644, 1538.



*2-methyl-7-phenylbenzo[d]oxazole (6):*¹⁹

Physical State: brown solid (16 mg, 76%), R_f = 0.6 (30% EtOAc/hexane). ^1H NMR (CDCl_3 , 400 MHz): δ 7.90 (d, J = 8.0 Hz, 2H), 7.51-7.43 (m, 4H), 7.36 (q, J = 8.0 Hz, 2H), 2.66 (s, 3H).

$^{13}\text{C}\{^1\text{H}\}$ NMR (CDCl_3 , 100 MHz): δ 164.0, 151.8, 139.6, 137.7, 133.1, 129.1, 128.9, 128.0, 124.8, 123.6, 109.4, 14.9.

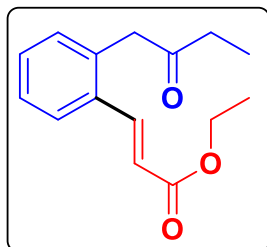


methyl (E)-3-(2-(2-oxobutyl)phenyl)acrylate (9aa):

Physical State: yellow liquid (10 mg, 43%), R_f = 0.3 (10% EtOAc/hexane). ^1H NMR (CDCl_3 , 700 MHz): δ 7.83 (d, J = 15.4 Hz, 1H), 7.60 (d, J = 7.7 Hz, 1H), 7.35 (t, J = 7.0 Hz, 1H), 7.30 (t,

J = 7.7 Hz, 1H), 7.18 (d, J = 7.7 Hz, 1H), 6.37 (d, J = 16.1 Hz, 1H), 3.86 (s, 2H), 3.80 (s, 3H), 2.50 (q, J = 7.0 Hz, 2H), 1.06 (t, J = 7.0 Hz, 3H). $^{13}\text{C}\{^1\text{H}\}$ NMR (175 MHz, CDCl_3): δ 208.3, 167.5, 142.2, 134.5, 134.2, 131.5, 130.5, 128.0, 127.2, 120.3, 52.1, 47.3, 36.0, 8.1.

IR (KBr, cm⁻¹): 2976, 1713, 1633. **HRMS (ESI) m/z:** [M+Na]⁺ Calcd for C₁₄H₁₆NaO₃: 255.0992; Found: 255.0991.



ethyl (E)-3-(2-(2-oxobutyl)phenyl)acrylate (9ab):²⁰

Physical State: yellow liquid (12 mg, 48%), **R_f** = 0.3 (10%

EtOAc/hexane). **¹H NMR (CDCl₃, 400 MHz):** δ 7.81 (d, *J* = 15.6

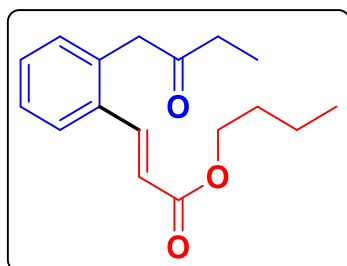
Hz, 1H), 7.60 (d, *J* = 7.6 Hz, 1H), 7.36-7.28 (m, 2H), 7.18 (d, *J* =

7.6 Hz, 1H), 6.36 (d, *J* = 15.6 Hz, 1H), 4.27 (q, *J* = 7.2 Hz, 2H), 3.86 (s, 2H), 2.50 (q, *J* =

7.2 Hz, 2H), 1.33 (t, *J* = 7.2 Hz, 3H), 1.06 (t, *J* = 7.2 Hz, 3H). **¹³C{¹H} NMR (CDCl₃, 100**

MHz): δ 208.2, 167.0, 141.9, 134.5, 134.3, 131.5, 130.4, 128.0, 127.2, 120.7, 60.9, 47.3,

36.0, 14.6, 8.1. **IR (KBr, cm⁻¹):** 2979, 1713, 1633.



butyl (E)-3-(2-(2-oxobutyl)phenyl)acrylate (9ac):

Physical State: yellow liquid (8 mg, 29%), **R_f** = 0.5 (10%

EtOAc/hexane). **¹H NMR (CDCl₃, 700 MHz):** δ 7.81 (d, *J*

= 16.1 Hz, 1H), 7.61 (d, *J* = 7.7 Hz, 1H), 7.34 (t, *J* = 7.7 Hz,

1H), 7.30 (t, *J* = 7.7 Hz, 1H), 7.18 (d, *J* = 7.7 Hz, 1H), 6.36 (d, *J* = 16.1 Hz, 1H), 4.20 (t, *J*

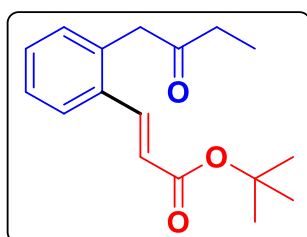
= 7.0 Hz, 2H), 3.86 (s, 2H), 2.50 (q, *J* = 7.7 Hz, 2H), 1.71-1.66 (m, 2H), 1.45-1.42 (m, 2H),

1.06 (t, *J* = 7.0 Hz, 3H), 0.96 (t, *J* = 7.7 Hz, 3H). **¹³C{¹H} NMR (175 MHz, CDCl₃):** δ

208.2, 167.1, 141.8, 134.5, 134.3, 131.5, 130.5, 128.0, 127.2, 120.7, 64.8, 47.3, 36.0, 31.0,

19.5, 14.0, 8.1. **IR (KBr, cm⁻¹):** 2959, 1713, 1633. **HRMS (ESI) m/z:** [M+Na]⁺ Calcd for

C₁₇H₂₂NaO₃: 297.1461; Found: 297.1457.



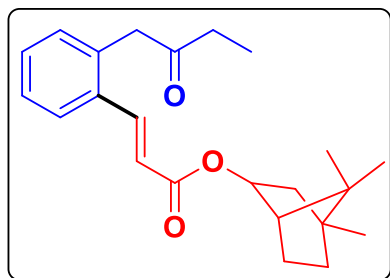
tert-butyl (E)-3-(2-(2-oxobutyl)phenyl)acrylate (9ad):

Physical State: yellow liquid (8 mg, 29%), **R_f** = 0.4 (10%

EtOAc/hexane). **¹H NMR (CDCl₃, 700 MHz):** δ 7.72 (d, *J* =

16.1 Hz, 1H), 7.59 (d, *J* = 7.0 Hz, 1H), 7.33 (t, *J* = 7.0 Hz, 1H),

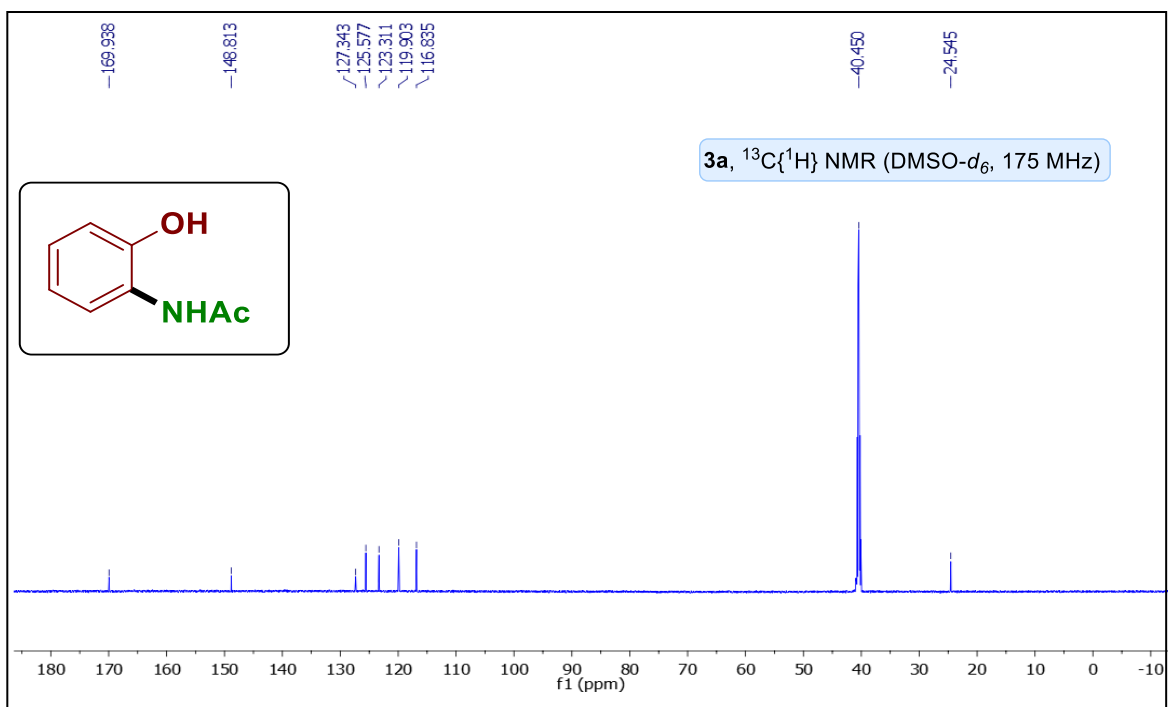
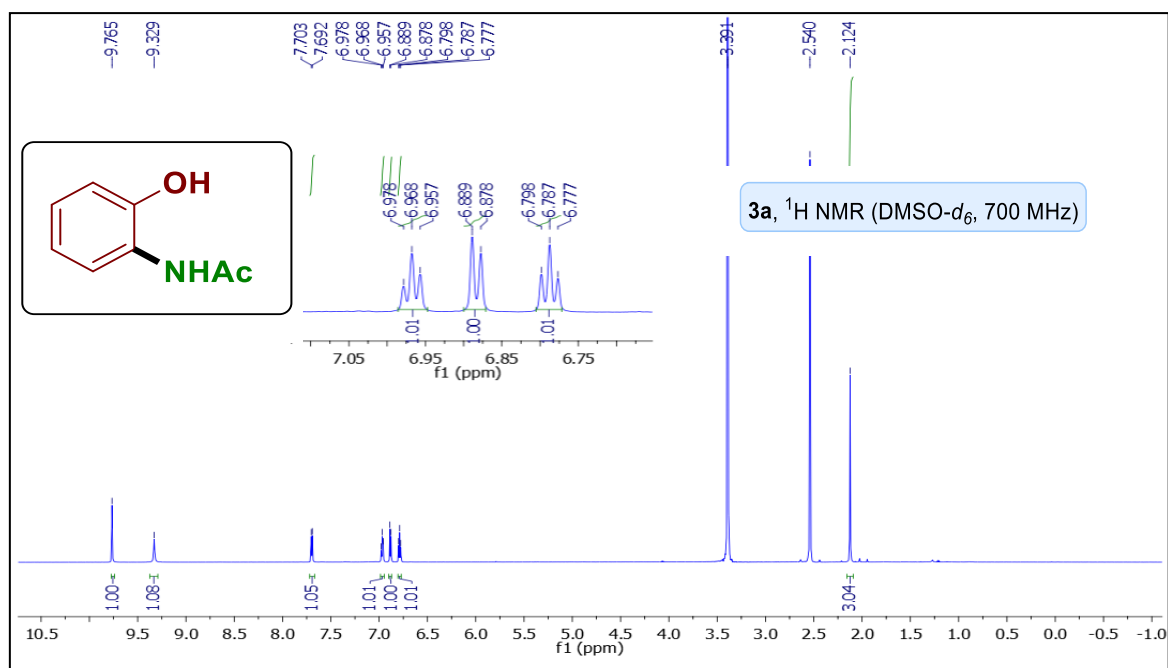
7.28 (t, $J = 7.7$ Hz, 1H), 7.17 (d, $J = 7.7$ Hz, 1H), 6.29 (d, $J = 16.1$ Hz, 1H), 3.85 (s, 2H), 2.50 (q, $J = 7.0$ Hz, 2H), 1.52 (s, 9H), 1.06 (t, $J = 7.0$ Hz, 3H). $^{13}\text{C}\{^1\text{H}\}$ NMR (175 MHz, CDCl_3): δ 208.3, 166.4, 140.8, 134.4, 134.4, 131.5, 130.2, 127.9, 127.1, 122.6, 80.9, 47.3, 36.0, 28.5, 8.1. IR (KBr, cm^{-1}): 2976, 1708, 1633. HRMS (ESI) m/z : $[\text{M}+\text{Na}]^+$ Calcd for $\text{C}_{17}\text{H}_{22}\text{NaO}_3$: 297.1461; Found: 297.1466.



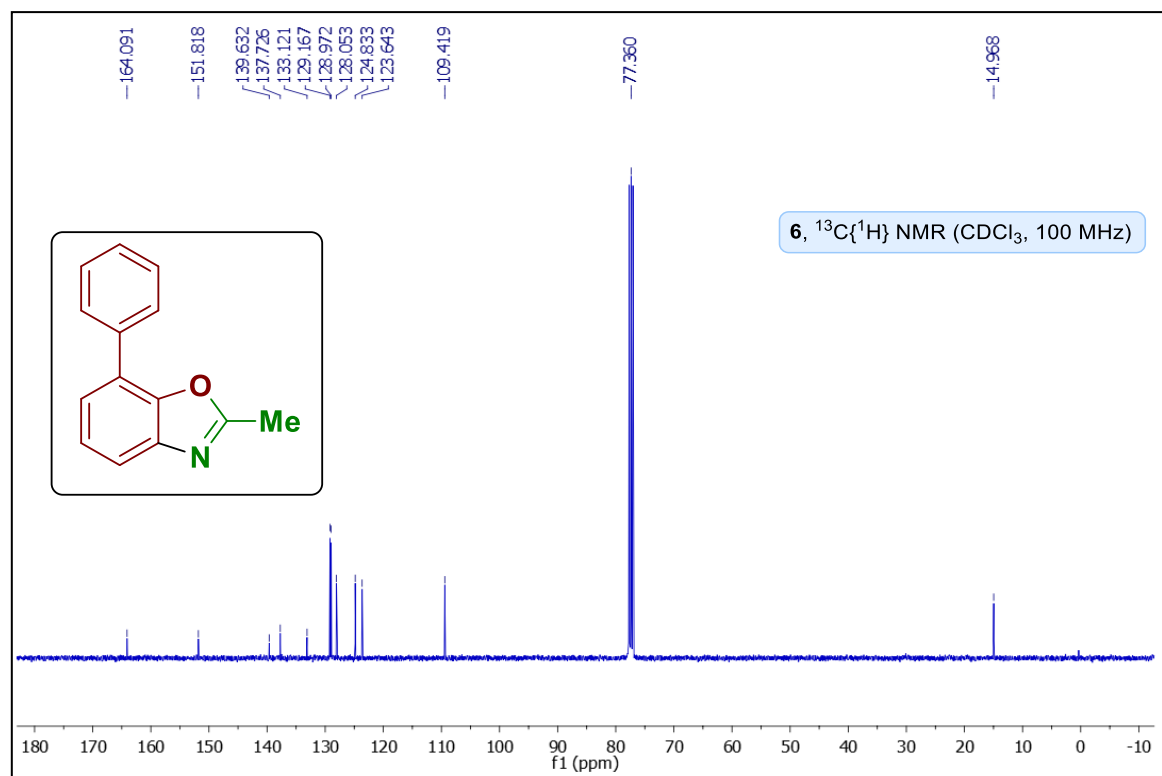
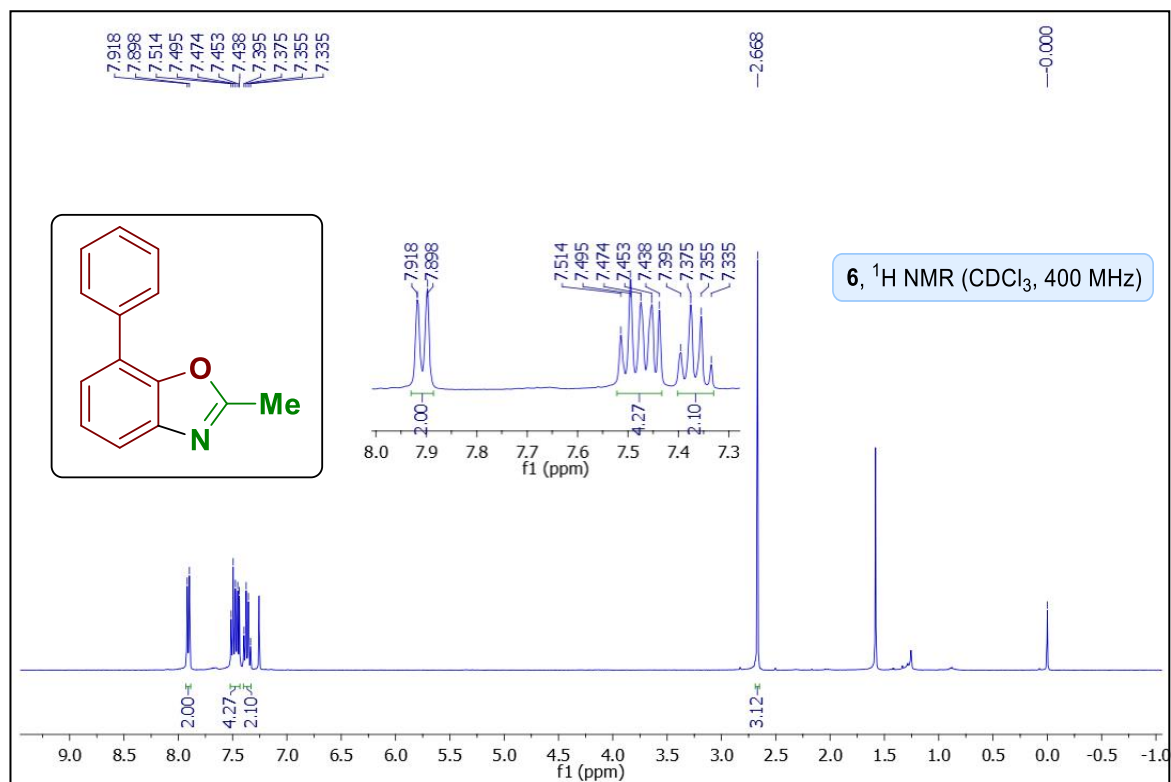
(1*R*,4*R*)-4,7,7-trimethylbicyclo[2.2.1]heptan-2-yl (*E*)-3-(2-(2-oxobutyl)phenyl)acrylate (**9ae**):

Physical State: yellow liquid (14 mg, 39%), $R_f = 0.4$ (10% EtOAc/hexane). ^1H NMR (CDCl_3 , 700 MHz): δ 7.77 (d, $J = 16.1$ Hz, 1H), 7.62 (d, $J = 7.7$ Hz, 1H), 7.34 (t, $J = 7.0$ Hz, 1H), 7.29 (t, $J = 7.0$ Hz, 1H), 7.18 (d, $J = 7.0$ Hz, 1H), 6.33 (d, $J = 16.1$ Hz, 1H), 4.79-4.78 (m, 1H), 3.84 (s, 2H), 2.50-2.47 (m, 2H), 1.88-1.85 (m, 1H), 1.84-1.83 (m, 1H), 1.77 (t, $J = 4.2$ Hz, 1H), 1.73-1.71 (m, 1H), 1.58 (d, $J = 4.2$ Hz, 1H), 1.22-1.18 (m, 1H), 1.13-1.10 (m, 1H), 1.05 (s, 6H), 0.89 (s, 3H), 0.86 (s, 3H). $^{13}\text{C}\{^1\text{H}\}$ NMR (175 MHz, CDCl_3): δ 208.0, 166.5, 141.4, 134.4, 134.3, 131.5, 130.4, 128.0, 127.1, 121.3, 81.5, 49.2, 47.3, 45.4, 39.2, 35.9, 34.0, 27.4, 20.4, 20.3, 11.8, 8.1. IR (KBr, cm^{-1}): 2953, 1712, 1633. HRMS (ESI) m/z : $[\text{M}+\text{Na}]^+$ Calcd for $\text{C}_{23}\text{H}_{30}\text{NaO}_3$: 377.2087; Found: 377.2105.

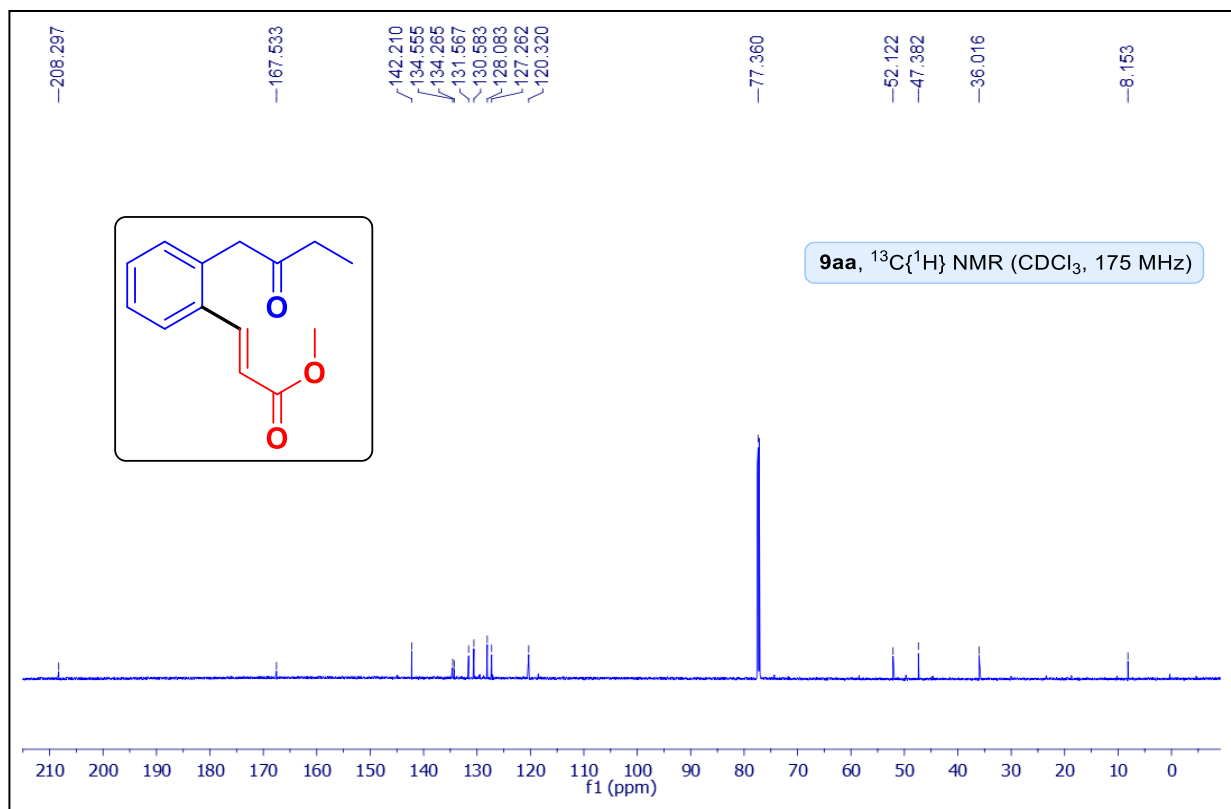
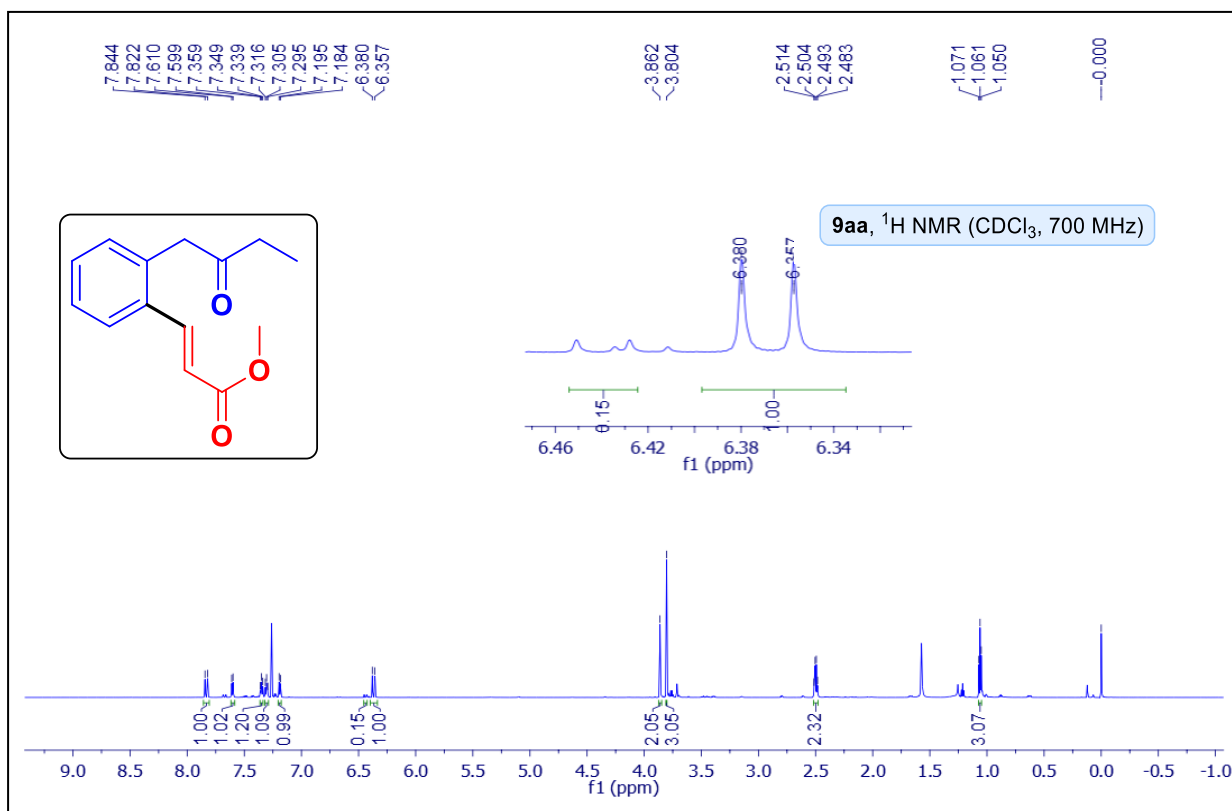
NMR spectra of *N*-(2-hydroxyphenyl)acetamide (3a):



NMR spectra of 2-methyl-7-phenylbenzo[d]oxazole (6):



NMR spectra of methyl (*E*)-3-(2-(2-oxobutyl)phenyl)acrylate (9aa**):**



X-ray data of *N*-((8*R*,9*S*,13*S*,14*S*)-3-hydroxy-13-methyl-17-oxo-7,8,9,11,12,13,14,15,16,17-decahydro-6*H*-cyclopenta[*a*]phenanthren-2-yl)acetamide

(5): Crystals of the compound *N*-((8*R*,9*S*,13*S*,14*S*)-3-hydroxy-13-methyl-17-oxo-7,8,9,11,12,13,14,15,16,17-decahydro-6*H*-cyclopenta[*a*]phenanthren-2-yl)acetamide **(5)** were obtained after slow evaporation of DMSO. Crystals suited for single crystal X-Ray diffraction measurements were mounted on a glass fiber. Geometry and intensity data were collected with a Rigaku Smartlab X-ray diffractometer equipped with graphite-monochromated Mo-K α radiation ($\lambda = 0.71073$ Å, multilayer optics). Temperature was controlled using an Oxford Cryostream 700 instrument. Intensities were integrated with SAINT and SMART software packages and corrected for absorption with SADABS. The structure was solved by direct methods and refined on F² with SHELXL-97 using Olex-2 software.

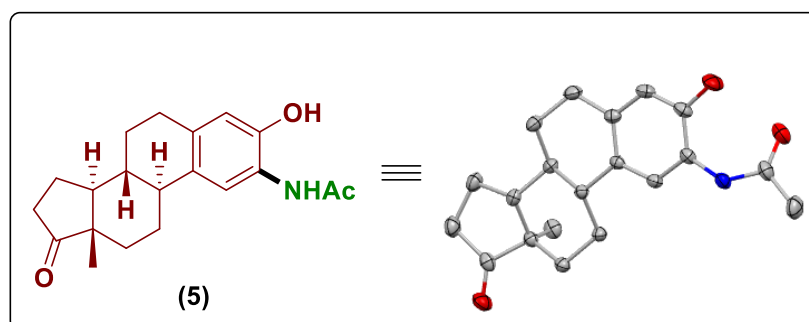
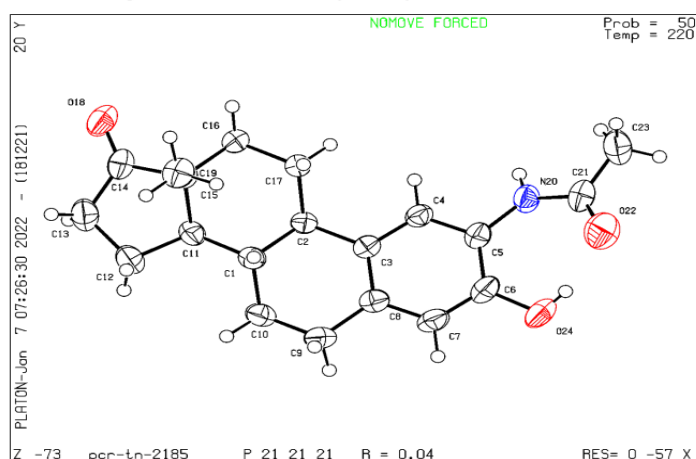


Figure 4.5 ORTEP diagram of **5** with 50% ellipsoid probability

Datablock pcr-tn-2185 - ellipsoid plot



4.6 REFERENCES

1. (a) Lyons, T. W.; Sanford, M. S. Palladium-Catalyzed Ligand Directed C–H Functionalization Reactions. *Chem. Rev.* **2010**, *110*, 1147–1169. (b) Gutekunst, W. R.; Baran, P. S. C–H Functionalization Logic in Total Synthesis. *Chem. Soc. Rev.* **2011**, *40*, 1976–1991. (c) Hartwig, J. F. Evolution of C–H Bond Functionalization from Methane to Methodology. *J. Am. Chem. Soc.* **2016**, *138*, 2–24. (d) Gensch, T.; Hopkinson, M. N.; Glorius, F.; Wencel-Delord, J. Mild Metal-Catalyzed C–H Activation: Examples and Concepts. *Chem. Soc. Rev.* **2016**, *45*, 2900–2936. (e) Rej, S.; Ano, Y.; Chatani, N. Bidentate Directing Groups: An Efficient Tool in C–H Bond Functionalization Chemistry for the Expedient Construction of C–C Bonds. *Chem. Rev.* **2020**, *120*, 1788–1887. (f) Lam, N. Y. S.; Wu, K.; Yu, J.-Q. Advancing the Logic of Chemical Synthesis: C–H Activation as Strategic and Tactical Disconnections for C–C Bond Construction. *Angew. Chem., Int. Ed.* **2021**, *60*, 15767–15790.
2. (a) Chen, F.-J.; Zhao, S.; Hu, F.; Chen, K.; Zhang, Q.; Zhang, S.-Q.; Shi, B.-F. Pd(II)-Catalyzed Alkoxylation of Unactivated C(sp³)–H and C(sp²)–H bonds Using a Removable Directing Group: Efficient Synthesis of Alkyl Ethers. *Chem. Sci.* **2013**, *4*, 4187–4192. (b) Sambriago, C.; Schönbauer, D.; Blicke, R.; Dao-Huy, T.; Pototschnig, G.; Schaaf, P.; Wiesinger, T.; Zia, M. F.; Wencel-Delord, J.; Besset, T.; Maes, B. U. W.; Schnürch, M. A Comprehensive Overview of Directing Groups Applied in Metal-Catalysed C-H Functionalisation Chemistry. *Chem. Soc. Rev.* **2018**, *47*, 6603–6743. (c) Biswal, P.; Pati, B. V.; Chebolu, R.; Ghosh, A.; Ravikumar, P. C. Hydroxylamine-O-Sulfonic Acid (HOSA) as a Redox-Neutral Directing Group: Rhodium Catalyzed, Additive Free, One-Pot Synthesis of Isoquinolines from Arylketones. *Eur. J. Org. Chem.* **2020**, *2020*, 1006–1014.
3. (a) Crabtree, R. H.; Lei, A. Introduction: C-H Activation. *Chem. Rev.* **2017**, *117*, 8481–8482. (b) Rej, S.; Das, A.; Chatani, N. Strategic evolution in transition metal-catalyzed directed C–H bond activation and future directions. *Coord. Chem. Rev.* **2021**, *431*, 213683.
4. (a) Catellani, M.; Frignani, F.; Rangoni, A. A Complex Catalytic Cycle Leading to a Regioselective Synthesis of o,o'-Disubstituted Vinylaromatics. *Angew. Chem., Int. Ed. Engl.* **1997**, *36*, 119–122. (b) Catellani, M.; Cugini, F. A Catalytic Process Based on Sequential ortho-Alkylation and Vinylation of ortho-Alkylaryl Iodides via Palladacycles. *Tetrahedron* **1999**, *55*, 6595–6602. (c) Lautens, M.; Piguel, S. A New Route to Fused Aromatic Compounds by Using a Palladium-Catalyzed Alkylation-Alkenylation Sequence. *Angew. Chem., Int. Ed.* **2000**, *39*, 1045–1046. (d) Ye, J.; Lautens, M. Palladium-Catalysed Norbornene-Mediated C–H Functionalization of Arenes. *Nat. Chem.* **2015**, *7*, 863–870.
5. (a) Dong, Z.; Wang, J.; Dong, G. Simple Amine-Directed Meta Selective C–H Arylation via Pd/Norbornene Catalysis. *J. Am. Chem. Soc.* **2015**, *137*, 5887–5890. (b) Della Ca', N.; Fontana, M.; Motti, E.; Catellani, M. Pd/ Norbornene: A Winning Combination for Selective Aromatic Functionalization via C–H Bond Activation. *Acc. Chem. Res.* **2016**, *49*, 1389–1400. (c) Wang, J.; Dong, G. Palladium/Norbornene Cooperative Catalysis. *Chem. Rev.* **2019**, *119*, 7478–7528.

6. Wang, X.; Gensch, T.; Lerchen, A.; Daniliuc, C. G.; Glorius, F. Cp*Rh(III)/Bicyclic Olefin Cocatalyzed C–H Bond Amidation by Intramolecular Amide Transfer. *J. Am. Chem. Soc.* **2017**, *139*, 6506–6512.
7. Shen, P.-X.; Wang, X.-C.; Wang, P.; Zhu, R.-Y.; Yu, J.-Q. Ligand-Enabled Meta-C–H Alkylation and Arylation using a Modified Norbornene. *J. Am. Chem. Soc.* **2015**, *137*, 11574–11577.
8. Liu, J.; Ding, Q.; Fang, W.; Wu, W.; Zhang, Y.; Peng, Y. Pd(II)/ Norbornene-Catalyzed Meta-C–H Alkylation of Nosyl-Protected Phenylalanines. *J. Org. Chem.* **2018**, *83*, 13211–13216.
9. Wang, J.; Dong, Z.; Yang, C.; Dong, G. Modular and Regioselective Synthesis of All Carbon Tetrasubstituted Olefins Enabled by an Alkenyl Catellani Reaction. *Nat. Chem.* **2019**, *11*, 1106–1112.
10. Maestri, G.; Derat, E. Alkenyl boost for Catellani. *Nat. Chem.* **2019**, *11*, 1082–1084.
11. (a) Buchanan, G. L.; Bredt's Rule. *Chem. Soc. Rev.*, **1974**, *3*, 41–63. (b) Elschenbroich, C. *Organometallics*, 3rd ed.; Wiley: Weinheim, 2006; p 817. (c) While our manuscript was under review, Jiao *et al.*, disclosed the use of olefin cyclopentene as olefin mediator for catellani type reaction which was published on 30th Jan 2022. However, we are the first to have published a preprint of our work in Chemrxiv (DOI: 10.26434/chemrxiv-2022-1355m) on 11th Jan 2022. Zheng, Y. X.; Jiao, L. Hybrid cycloolefin ligands for palladium–olefin cooperative catalysis. *Nature Synthesis*, **2022**, *1*, 180–187.
12. (a) Liu, G.; Shen, Y.; Zhou, Z.; Lu, X. Rhodium(III)-Catalyzed Redox-Neutral Coupling of *N*-Phenoxyacetamides and Alkynes with Tunable Selectivity. *Angew. Chem., Int. Ed.* **2013**, *52*, 6033–6037. (b) Zhou, Z.; Bian, M.; Zhao, L.; Gao, H.; Huang, J.; Liu, X.; Yu, X.; Li, X.; Yi, W. 2H-Chromene-3- carboxylic Acid Synthesis via Solvent-Controlled and Rhodium(III)- Catalyzed Redox-Neutral C-H Activation/[3 + 3] Annulation Cascade. *Org. Lett.* **2018**, *20*, 3892–3896. (c) Zhong, X.; Lin, S.; Gao, H.; Liu, F.-X.; Zhou, Z.; Yi, W. Rh(III)-Catalyzed Redox-Neutral C-H Activation/[3 + 2] Annulation of *N*-Phenoxy Amides with Propargylic Monofluoroalkynes. *Org. Lett.* **2021**, *23*, 2285–2291.
13. (a) Page, M.; McIver Jr., J. W. On evaluating the reaction path Hamiltonian. *J. Chem. Phys.*, **1988**, *88*, 922–35. (b) Adamo, C.; Barone, V. Toward Reliable Density Functional Methods without Adjustable Parameters: The PBE0 Model. *J. Chem. Phys.* **1999**, *110*, 6158–6170. (c) Weigend, F.; Ahlrichs, R. Balanced Basis Sets of Split Valence, Triple Zeta Valence and Quadruple Zeta Valence Quality for H to Rn: Design and Assessment of Accuracy. *Phys. Chem. Chem. Phys.* **2005**, *7*, 3297–3305. (d) Weigend, F. Accurate Coulomb-fitting basis sets for H to Rn. *Physical Chemistry Chemical Physics*, **2006**, *8*, 1057. (e) Marenich, A. V., Cramer, C. J., & Truhlar, D. G. *J. Phys. Chem. B.* **2009**, *113*, 6378–6396. (f) Neese, F.; Wennmohs, F.; Hansen, A.; Becker, U. Efficient, Approximate and Parallel Hartree–Fock and Hybrid DFT Calculations. A ‘Chain-of-Spheres’ Algorithm for the Hartree–Fock Exchange. *Chem. Phys.* **2009**, *356*, 98–109. (g) Grimme, S.; Antony, J.; Ehrlich, S.; Krieg, H. A Consistent and Accurate Ab Initio Parametrization of Density Functional Dispersion Correction (DFT-D) for the 94 Elements H–Pu. *J. Chem. Phys.* **2010**, *132*, 24103. (h) Grimme, S.; Ehrlich, S.; Goerigk, L. Effect of the Damping Function in Dispersion Corrected Density Functional Theory. *J. Comput. Chem.*

2011, 32, 1456–1465. (i) Grimme, S. Supramolecular Binding Thermodynamics by Dispersion-Corrected Density Functional Theory. *Chem. Eur. J.* **2012**, 18, 9955–9964. (j) Guo, X. K.; Zhang, L. B.; Wei, D.; Niu, J. L. Mechanistic Insights into Cobalt(II/III)-Catalyzed C-H Oxidation: A Combined Theoretical and Experimental Study. *Chem. Sci.* **2015**, 6, 7059–7071. (k) Mardirossian, N.; Head-Gordon, M. How Accurate Are the Minnesota Density Functionals for Noncovalent Interactions, Isomerization Energies, Thermochemistry, and Barrier Heights Involving Molecules Composed of Main-Group Elements? *J. Chem. Theory Comput.* **2016**, 12, 4303–4325. (l) Gaussian 16, Revision C.01, M. J. Frisch, G. W. Trucks, H. B. Schlegel, G. E. Scuseria, M. A. Robb, J. R. Cheeseman, G. Scalmani, V. Barone, G. A. Petersson, H. Nakatsuji, X. Li, M. Caricato, A. V. Marenich, J. Bloino, B. G. Janesko, R. Gomperts, B. Mennucci, H. P. Hratchian, J. V. Ortiz, A. F. Izmaylov, J. L. Sonnenberg, D. Williams-Young, F. Ding, F. Lipparini, F. Egidi, J. Goings, B. Peng, A. Petrone, T. Henderson, D. Ranasinghe, V. G. Zakrzewski, J. Gao, N. Rega, G. Zheng, W. Liang, M. Hada, M. Ehara, K. Toyota, R. Fukuda, J. Hasegawa, M. Ishida, T. Nakajima, Y. Honda, O. Kitao, H. Nakai, T. Vreven, K. Throssell, J. A. Montgomery, Jr., J. E. Peralta, F. Ogliaro, M. J. Bearpark, J. J. Heyd, E. N. Brothers, K. N. Kudin, V. N. Staroverov, T. A. Keith, R. Kobayashi, J. Normand, K. Raghavachari, A. P. Rendell, J. C. Burant, S. S. Iyengar, J. Tomasi, M. Cossi, J. M. Millam, M. Klene, C. Adamo, R. Cammi, J. W. Ochterski, R. L. Martin, K. Morokuma, O. Farkas, J. B. Foresman, and D. J. Fox, Gaussian, Inc., Wallingford CT, 2016. (m) Caldeweyher, E.; Ehlert, S.; Hansen, A.; Neugebauer, H.; Spicher, S.; Bannwarth, C.; Grimme, S. A Generally Applicable Atomic-Charge Dependent London Dispersion Correction. *J. Chem. Phys.* **2019**, 150, 154122. (n) Li, X.; Wu, H.; Wu, Z.; Huang, G. Mechanism and Origins of Regioselectivity of Copper-Catalyzed Borocyanation of 2-Aryl-Substituted 1,3-Dienes: A Computational Study. *J. Org. Chem.* **2019**, 84, 5514–5523. (o) Luchini, G.; Alegre-Requena, J. V.; Funes-Ardoiz, I.; Paton, R. S. GoodVibes: Automated Thermochemistry for Heterogeneous Computational Chemistry Data. *F1000Research*, **2020**, 9, 291. (p) Oliveira, J. C. A.; Dhawa, U.; Ackermann, L. Insights into the Mechanism of Low-Valent Cobalt-Catalyzed C-H Activation. *ACS Catal.* **2021**, 11, 1505–1515. (q) Neese, F. Software update: The ORCA program system—Version 5.0. *WIREs Comput. Mol. Sci.*, **2022**, e1606.

14. (a) Gorelsky, S. I.; Lapointe, D.; Fagnou, K. Analysis of the Concerted Metalation-Deprotonation Mechanism in Palladium-Catalyzed Direct Arylation across a Broad Range of Aromatic Substrates. *J. Am. Chem. Soc.* **2008**, 130, 10848–10849. (b) Lapointe, D.; Fagnou, K. Overview of the Mechanistic Work on the Concerted Metalation-Deprotonation Pathway. *Chem. Lett.* **2010**, 39, 11, 1118–1126. (c) R. Stuart, D.; Alsabeh, P.; Kuhn, M.; Fagnou, K. Rhodium(III)-Catalyzed Arene and Alkene C–H Bond Functionalization Leading to Indoles and Pyrroles. *J. Am. Chem. Soc.* **2010**, 132, 18326–18339. (d) Ackermann, L. Carboxylate-Assisted Transition-Metal-Catalyzed C-H Bond Functionalizations: Mechanism and Scope. *Chem. Rev.* **2011**, 111, 1315–1345. (e) Kapdi, A. R. Organometallic Aspects of Transition-Metal Catalysed Regioselective C-H Bond Functionalisation of Arenes and Heteroarenes. *Dalt. Trans.* **2014**, 43, 3021–3034. (f) Davies, D. L.; Macgregor, S. A.; McMullin, C. L. Computational Studies of Carboxylate-Assisted C-H Activation and Functionalization at Group 8-10 Transition Metal Centers. *Chem. Rev.* **2017**, 117, 8649–8709.

15. (a) Davies, D. L.; Donald, S. M. A.; Macgregor, S. A. Computational Study of the Mechanism of Cyclometalation by Palladium Acetate. *J. Am. Chem. Soc.* **2005**, *127*, 13754–13755. (b) Davies, D. L.; Donald, S. M. A.; Al-Duaij, O.; Macgregor, S. A.; Pölleth, M. Electrophilic C–H Activation at {Cp*Ir}: Ancillary-Ligand Control of the Mechanism of C–H Activation. *J. Am. Chem. Soc.* **2006**, *128*, 4210–4211. (c) Rousseaux, S.; Gorelsky, S. I.; Chung, B. K. W.; Fagnou, K. Investigation of the Mechanism of C(Sp³)–H Bond Cleavage in Pd(0)-Catalyzed Intramolecular Alkane Arylation Adjacent to Amides and Sulfonamides. *J. Am. Chem. Soc.* **2010**, *132*, 10692–10705. (d) Xiao, B.; Fu, Y.; Xu, J.; Gong, T.-J.; Dai, J.-J.; Yi, J.; Liu, L. Pd(II)-Catalyzed C–H Activation/Aryl–Aryl Coupling of Phenol Esters. *J. Am. Chem. Soc.* **2010**, *132*, 468–469. (e) Yamazaki, K., Kommagalla, Y., Ano, Y., & Chatani, N. A computational study of cobalt-catalyzed C–H iodination reactions using a bidentate directing group with molecular iodine. *Organic Chemistry Frontiers*. **2019**, *6*, 537–543.
16. Schröder, D., Shaik, S., & Schwarz, H. Two-State Reactivity as a New Concept in Organometallic Chemistry. *Acc. Chem. Res.* **2000**, *33*, 139–145.
17. (a) Patel, P.; Chang, S. Cobalt(III)-Catalyzed C-H Amidation of Arenes using Acetoxycarbamates as Convenient Amino Sources under Mild Conditions. *ACS Catal.* **2015**, *5*, 853–858. (b) Lee, J.; Kang, B.; Kim, D.; Lee, J.; Chang, S.; Cobalt–Nitrenoid Insertion-Mediated Amidative Carbon Rearrangement via Alkyl-Walking on Arenes. *J. Am. Chem. Soc.* **2021**, *143*, 18406–18412.
18. (a) Tyman, J. H. P. Synthetic and Natural Phenols. *Studies in Organic Chemistry*; Elsevier: 1996; Vol. 52, pp 1–700. (b) Rappoport, Z. *The Chemistry of Phenols*; John Wiley & Sons Ltd.: Chichester, U.K., 2003.
19. Sahoo, K.; Pradhan, P.; Panda, N. Access to C4-arylated benzoxazoles from 2-amido phenol through C–H activation. *Org. Biomol. Chem.*, 2020, *18*, 1820–1832.
20. Li, G.; Wan, L.; Zhang, G.; Leow, D.; Spangler, J.; Yu, J.-Q. Pd(II)-Catalyzed C–H Functionalizations Directed by Distal Weakly Coordinating Functional Groups. *J. Am. Chem. Soc.* 2015, *137*, 4391–4397.
21. (a) Similar information was reported in Banjare, S. K.; Nanda, T.; Ravikumar, P. C. Cobalt-Catalyzed Regioselective Direct C-4 Alkenylation of 3-Acetyldole with Michael Acceptors Using a Weakly Coordinating Functional Group. *Org. Lett.* **2019**, *21*, 8138–8143. (b) Gottlieb, H. E.; Kotlyar, V.; Nudelman, A. NMR chemical shifts of common laboratory solvents as trace impurities. *J. Org. Chem.* **1997**, *62*, 7512.
22. Yuan, Y. C.; Kamaraj, R.; Bruneau, C.; Labasque, T.; Roisnel, T.; Gramage-Doria, R. Unmasking Amides: Ruthenium-Catalyzed Protodecarbonylation of N-Substituted Phthalimide Derivatives. *Org. Lett.* **2017**, *19*, 6404–6407.
23. Li, B.; Lan, J.; Wu, D.; You, J. Rhodium(III)-Catalyzed orthoHeteroarylation of Phenols through Internal Oxidative C–H Activation: Rapid Screening of Single-Molecular White-Light-Emitting Materials. *Angew. Chem., Int. Ed.* **2015**, *54*, 14008–14012.

24. Bernardes, G. J. L.; Chalker, J. M.; Errey, J. C.; Davis, B. G. Facile Conversion of Cysteine and Alkyl Cysteines to Dehydroalanine on Protein Surfaces: Versatile and Switchable Access to Functionalized Proteins. *J. Am. Chem. Soc.* **2008**, *130*, 5052-5053.
25. Liu, G.; Shen, Y.; Zhou, Z.; Lu, X. Rhodium(III)-Catalyzed Redox-Neutral Coupling of N-Phenoxyacetamides and Alkynes with Tunable Selectivity. *Angew. Chem., Int. Ed.* **2013**, *52*, 6033-6037.
26. Chen, C.; Pan, Y.; Zhao, H.; Xu, X.; Luo, Z.; Cao, L.; Xi, S.; Li, H.; Xu, L. Ruthenium(II)-Catalyzed Regioselective C-8 Hydroxylation of 1,2,3,4-Tetrahydroquinolines. *Org. Lett.* **2018**, *20*, 6799–6803.

Chapter 5

Carboamination and Olefination: Revealing Two different Pathways in *ortho* C-H Functionalization of Phenoxyacetamide

5.1 Abstract

5.2 Introduction

5.3 Results and Discussions

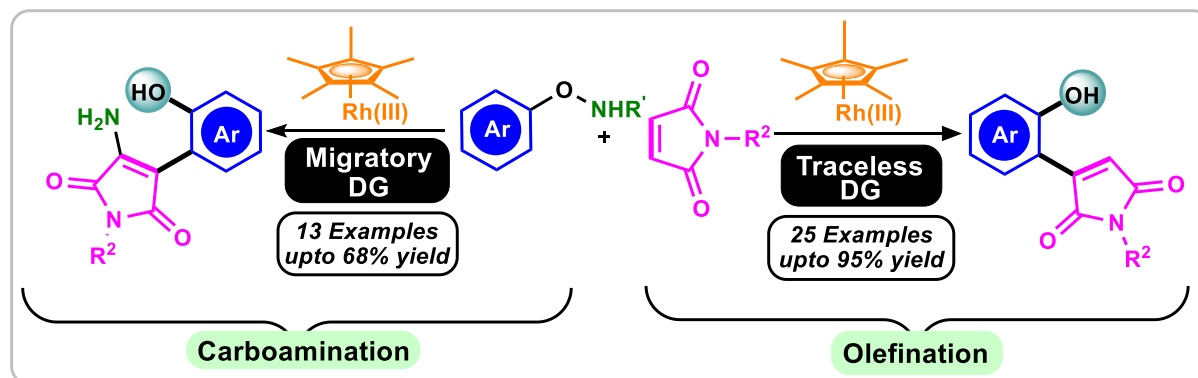
5.4 Conclusions

5.5 Experimental Section

5.6 References

Chapter 5

Carboamination and Olefination: Revealing Two different Pathways in *ortho* C-H Functionalization of Phenoxyacetamide



5.1 ABSTRACT

Herein, we have demonstrated a rhodium-catalyzed carboamination of olefin with the double bond intact. For the first time, deacylative carboamination of the maleimide has been achieved wherein phenoxyacetamide was behaved as the aminating source. The rhodium nitrenoid species adding to the double bond of maleimide to form aziridine is an interesting aspect of this methodology. In addition, the cleavage of amide C-N bond through hydrolysis by in situ generated water has been proved from ¹⁹F NMR analysis. The key intermediate involved has been well characterized through the HRMS study and validates the proposed catalytic cycle. In addition to carboamination, we have disclosed the C-H olefination protocol where the maleimide group has been installed successfully in the *ortho*-position of phenoxyacetamide. In this protocol, phenoxy acetamide behaved as a traceless directing group with the in-situ release of acetamide. The base-assisted E2-elimination is the key to the success of this reaction. A wide range of phenoxy acetamide and maleimide underwent reaction under our standard condition to deliver the desired product in good to excellent yield.

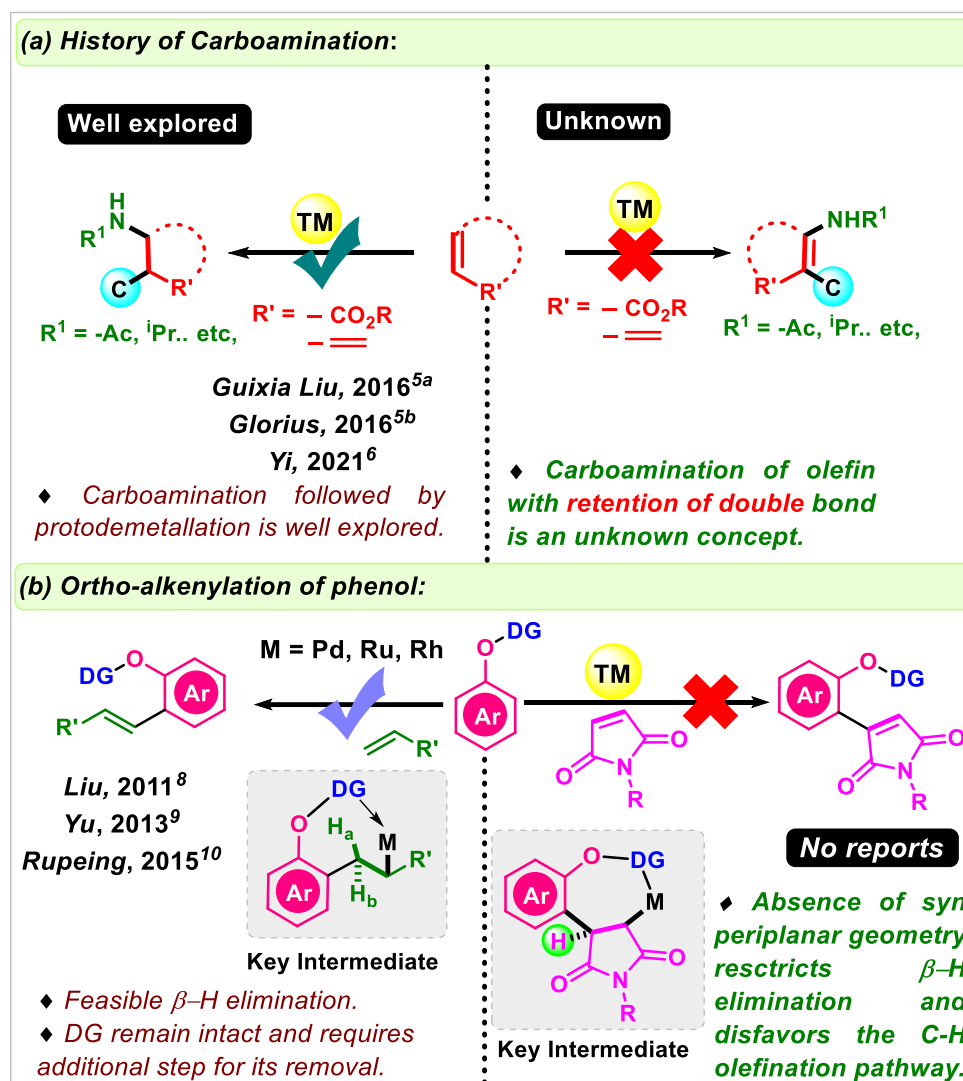
5.2 INTRODUCTION

The utilization of substrates that can bring diversification in the product found is an important aspect of transition-metal catalysis. With versatile starting material, one can synthesize various value-added scaffolds without recourse to many functional group modifications. In this regard, phenoxyacetamide is a versatile substrate which is first designed by Liu and Lu has become increasingly popular in recent years.¹ It has been heavily exploited in transition-metal catalyzed reactions.² It has been considered as a multitasking substrate that contains an oxy-acetamide functional group with an easily cleavable N-O bond, making it a good (i) directing group (ii) an oxidant, and (iii) electrophilic aminating reagent.^{1,2,3} Thus, working with such a versatile substrate could unfold and open a gateway towards a range of multiverse chemical reactivity.

Carboamination is an important class of reaction that results in the simultaneous formation of the C-C and C-N bonds across the π -system. This reaction resulted in an amine-containing scaffold that is present in various top-selling pharmaceuticals and drug molecules.⁴ In this context, phenoxyacetamide has been used as an amidating agent in carboamination reaction of olefins (Figure 5.1a). In 2016, Liu and Glorius's group independently reported the carboamination of acrylamides and acryl esters by taking phenoxy acetamide as an aminating agent.⁵ In 2021, Yi and co-workers successfully demonstrated the chiral carboamination of a diene to achieve the product in high enantioselectivity.⁶ In all these reports, carboamination of the π -systems has been achieved through protodemetalation that results in saturated amine product. However, there is no report on carboamination of olefin with the retention of double bond that can result in an enamine motif.

In addition to developing methodologies to synthesize scaffolds having medicinal importance, functionalization of naturally prevalent bioactive molecules is also equally important, as simple derivatization can also enhance its bioactive properties.

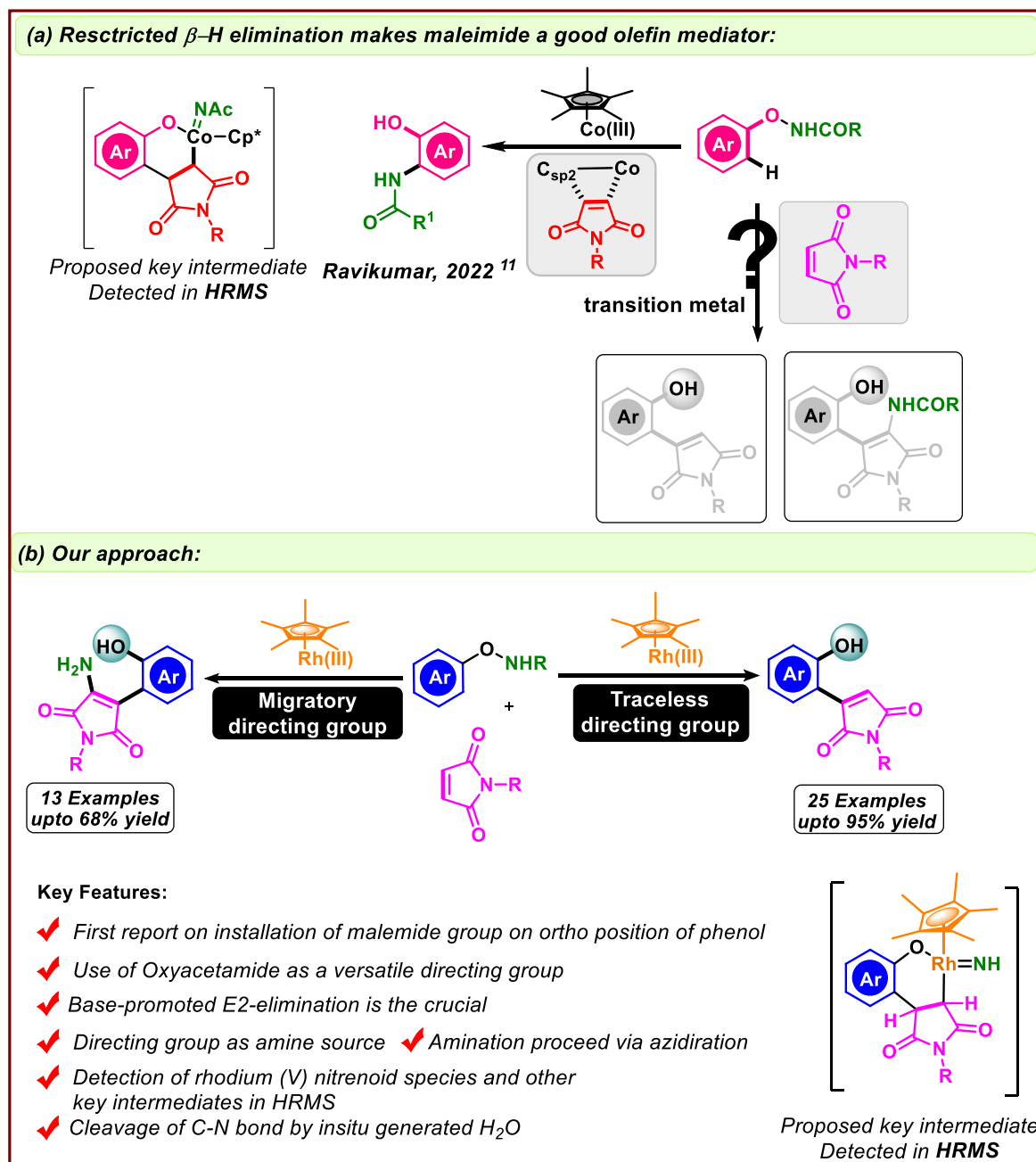
Figure 5.1 Overview on transition metal catalyzed carboamination and C-H olefination



Phenol derivatives are present in various value-added bioactive molecules and natural products.⁷ Thus, synthesizing the molecule containing functionalized phenol is considered very valuable from the medicinal chemistry point of view. Among all, transition metal-catalyzed *ortho* C-H functionalization reactions, olefination of phenol is one of the most pursued reactions.

In 2011, Liu and co-workers disclosed the rhodium-catalyzed *ortho*-olefination of phenol carbamates in high regioselectivity.⁸ Further, Yu and co-workers demonstrated palladium-catalyzed *ortho* and *meta* C-H olefination of α -phenoxy acetic acid derivatives.⁹

Figure 5.2 Previous challenges and our approach



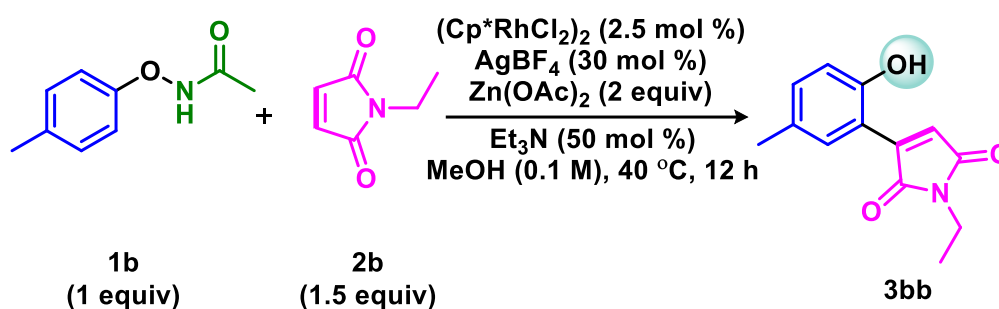
In the subsequent year, Rupeing and co-workers reported the *ortho*-olefination of phenol ether in the presence of combined ruthenium and photoredox catalysis.¹⁰ However, the prime limitation of these methodologies is that the resultant product will have the directing

group intact. Thus, an additional step was required to synthesize *ortho*-olefinated phenols, which is our prime target. Furthermore, the coupling partners employed in these reactions have β -hydrogen in synperiplanar geometry, thereby facilitating the β -hydride elimination to deliver the desired olefination product (Figure 5.1b). However, there is no report of olefination with maleimide due to the restricted β -hydride elimination. Moreover, to date, there is no synthetic procedure to install a maleimide group in the *ortho* position of phenol. Recently, our group has reported maleimide as an olefin mediator in intramolecular *ortho* amidation of phenol.¹¹ In this protocol, the restricted β -hydride elimination of the key intermediate makes maleimide a successful olefin mediator for *ortho* C-H amidation (Figure 5.2a). Hence, olefination using maleimide is a challenging task. Thus, the next question is how to overcome this limitation and demonstrate different methodologies to achieve the olefination of phenol and carboamination of maleimide. In continuation of our research on establishing other methods with phenoxyacetamide and maleimide, we have developed two different pathways. Herein, we have reported (a) the installation of the maleimide group in the *ortho* position of phenol, that is olefination pathway, and (b) carboamination of maleimide with retention of the double bond to deliver the enamine derivatives (Figure 5.2b). In this developed protocol, the base-mediated E2-elimination is crucial for the *ortho*-olefination of phenol. Phenoxyacetamide has been demonstrated to have a traceless and migratory directing group. The carboamination of maleimide proceeds through the formation of rhodium nitrenoid intermediate detected in HRMS. The olefination product is an intermediate in the carboamination reaction, to which nitrenoid insertion by *in situ* generated rhodium nitrenoid gives an aziridine intermediate.¹² The cleavage of the C-N bond by *in situ* generated H₂O from TFE has been proven from a ¹⁹F NMR study that shows a quantitative formation of fluorothyl (fluoro derivatives of diethyl ether).

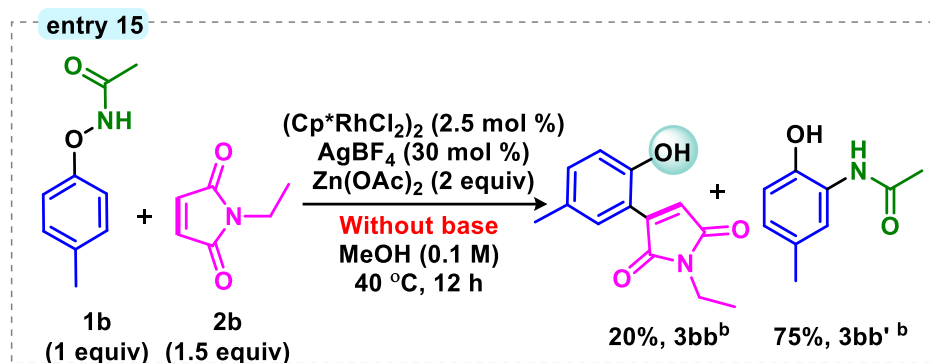
5.3 RESULTS AND DISCUSSION

We began our investigation by taking *p*-tolyl phenoxyacetamide **1b** as the model substrate and *N*-Et maleimide **2b** as the coupling partner. After an extensive screening of various parameters, a catalytic condition comprising of (Cp*RhCl₂)₂ (2.5 mol %), AgBF₄ (30 mol %), Zn(OAc)₂ (2 equiv), Et₃N (50 mol %), and MeOH solvent (0.1M) at 40 °C in 12 h provided the desired product **3bb** in 74 % yield (Table 5.1, entry 1).

Table 5.1 Optimization of reaction condition for *ortho* C-H olefination with maleimide.^a



entry	deviation from standard conditions	yield of 3bb (%) ^b
1	none	74 ^c
2	Room temperature	62
3	60 °C	45
4	80 °C	26
5	2c, 1 equiv	61
6	2c, 2 equiv	44
7	Ag ₂ SO ₄ instead of AgBF ₄	55
8	AgSbF ₆ instead of AgBF ₄	40
9	AgOAc instead of AgBF ₄	45
10	K ₂ CO ₃ instead of Et ₃ N	37
11	KOAc instead of Et ₃ N	29
12	(Cp*RhCl ₂) ₂ 5 mol %	50
13	without (Cp*RhCl ₂) ₂	0
14	without Zn(OAc) ₂	0

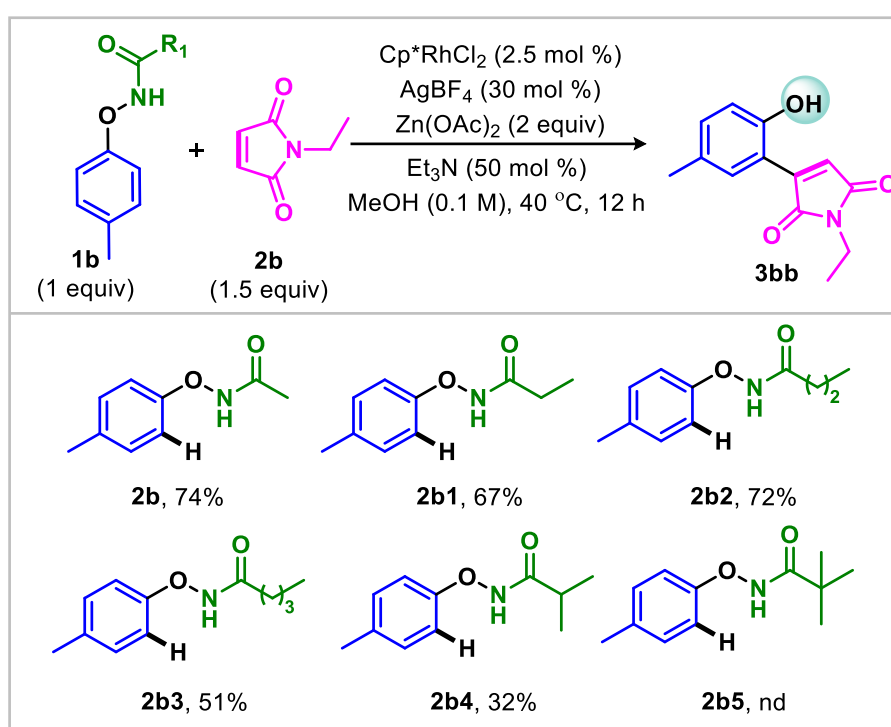


^aReaction conditions: **1a** (0.1 mmol), **2a** (0.15 mmol), $(\text{Cp}^*\text{RhCl}_2)_2$ (2.5 mol %), Ag salt (30 mol %), Base (50 mol %), $\text{Zn}(\text{OAc})_2$ (2 equiv), MeOH (1 mL), 40 °C, N_2 , ^bNMR yield (1,3,5-trimethoxy benzene was used as internal standard), ^cIsolated yield.

To ascertain the working limits of this condition, we varied different parameters. At first, the reaction temperature was changed to room temperature, 60 °C, and 80 °C (Table 5.1, entry 2-4). However, all these temperatures failed to increase the yield of the desired product. The variation in equivalence of the maleimide (coupling partner) also did not result in an improved yield (Table 5.1, entries 5-6). The effect of various silver salt in the reaction has been tested, and sulphate was found to be a suitable counter anion to stabilize the active catalyst after tetrafluoroborate (Table 5.1, entries 7-9). As the base plays a very crucial role, carbonate and acetate bases have been employed; however, we have not observed any superior results (Table 5.1, entries 10-11). Next, the catalyst loading was increased from 2.5 mol % to 5 mol %, and in this case, only a 50% yield of the desired product was observed (Table 5.1, entry 12). May be the availability of excess rhodium catalyst is consuming the substrate by undergoing oxidative addition between the O-N bond leading to the deactivation of the directing group. The control experiment without Rh catalyst and $\text{Zn}(\text{OAc})_2$ suggested that they play a very crucial role (Table 5.1, entry 13-14). While Cp^*RhCl_2 acts as a catalyst to activate the C-H bond, $\text{Zn}(\text{OAc})_2$ may serve as a Lewis acid¹³ to activate the maleimide double bond to undergo effective olefin insertion. The role of the base can be explained from the control experiment (Table 5.1, entry

15). It shows that without a base (Et₃N), only 20% of the olefination product and 75% of the *ortho*-amidated product were formed, which means without an adequate base, the restricted β -hydride elimination makes maleimide an effective olefin mediator rather a coupling partner. In the absence of Et₃N, acetate might be helping in the E2-elimination, albeit inefficiently, leading to a 20% yield of olefination product **3bb**.

Table 5.2. Screening of Various Direction Groups^a



^aReaction **Conditions:** **1a** (0.1 mmol), **2a** (0.15 mmol), [Cp^{*}RhCl₂] (2.5 mol %), AgBF₄ (30 mol %), Et₃N (50 mol %), Zn(OAc)₂ (2 equiv), MeOH (1 mL), 40 °C, N₂, Isolated yield were mentioned.

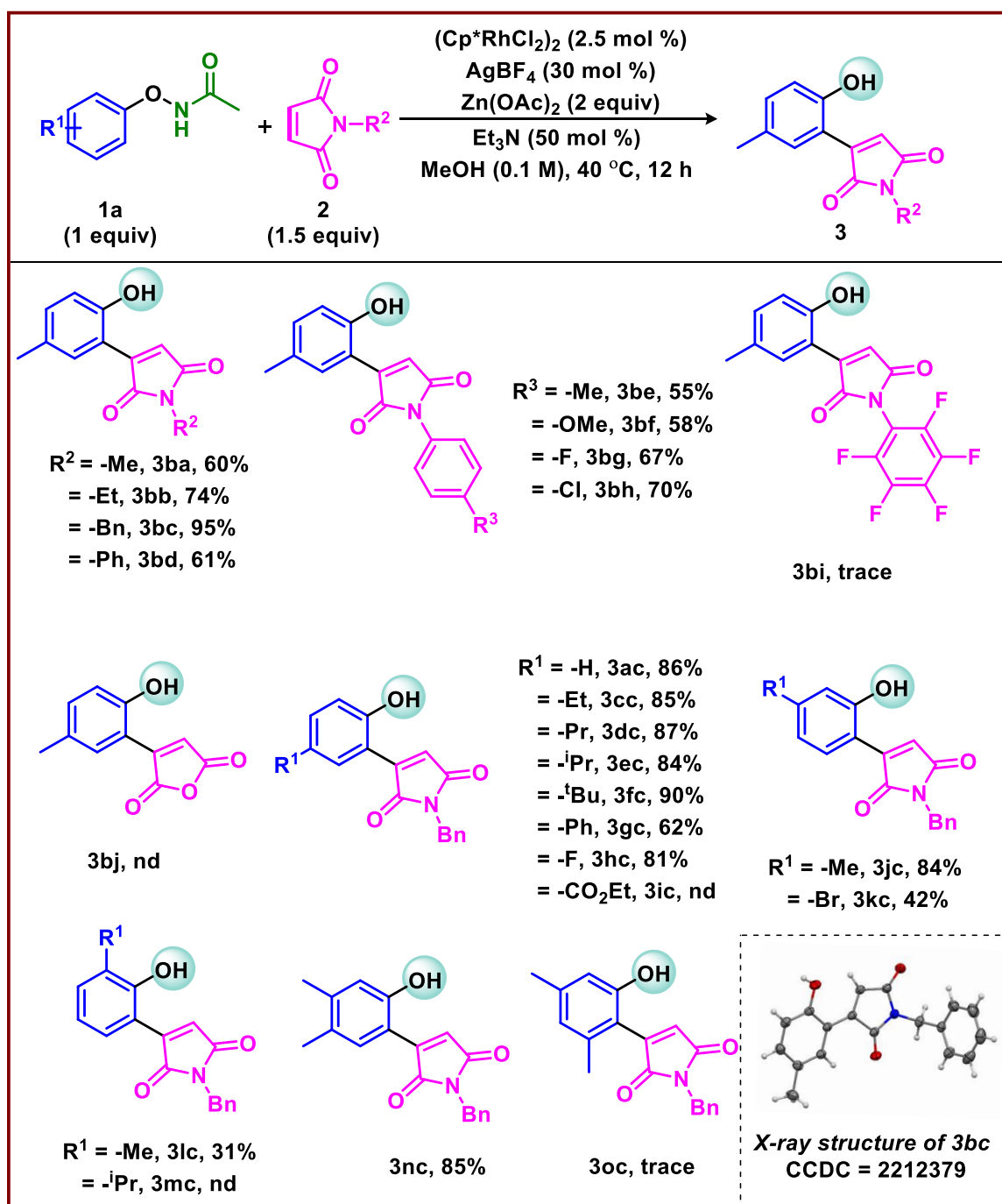
After screening the reaction parameters, we varied the substituent in the directing group. We found a good range *N*-substitution with an alkyl chain of up to four carbons working efficiently under the reaction condition giving 74%-51% yield of the desired product **3bb** (Table 5.2, **2b-2b3**). However, with an increase in the steric around the directing group, the reactivity decreases and further ceases when the *N*-pivaloyl group has been employed (Table 5.2, **2b4-2b5**). Thus, we stuck to *N*-

acetamide as our directing group as it is delivering 74% yield of the desired product **3bb**.

To demonstrate the generality of the condition developed, we screened different substrates. At first, we varied the *N*-substitution pattern in the maleimide coupling partner. A variety of *N*-alkyl substituted maleimide reacts with phenoxyacetamide to deliver the product in good to excellent yields (Scheme 5.1, **3ba-3bc**). Further, *N*-Ph substituted maleimide having substituents in the phenyl rings has also been screened. Electron-donating and withdrawing substituents in the phenyl ring work under the reaction condition to deliver the desired *ortho*-olefinated products (Scheme 5.1, **3bd-3bh**). However, a phenyl ring with a strong electron-withdrawing group failed to give the desired product in quantitative yield (Scheme 5.1, **3bi**). Succinic anhydride is also employed as a coupling partner but failed to provide the product (Scheme 5.1, **3bj**). It may be due to the high electronegativity of the oxygen atom that decreases the electron density around the olefin, inhibiting the olefin insertion step.

Next, the effect of electronics and steric has been tested by subjecting a variety of phenoxyacetamide to the standard reaction condition. Among various maleimides, *N*-benzyl maleimide works better. Thus, we proceed with this coupling partner. The unsubstituted phenoxyacetamide gave the desired product an 86% yield (Scheme 5.1, **3ac**). The substrates with a substituent in the *para* position with electron-donating and withdrawing groups reacted well, delivering the desired product in excellent yields (Scheme 5.1, **3cc-3hc**). However, a strong electron-withdrawing group, such as *p*-CO₂Et, deactivated the ring and failed to give the desired product (Scheme 5.1, **3ic**). The substitution patterns in the *meta* and *ortho* positions also have been tested.

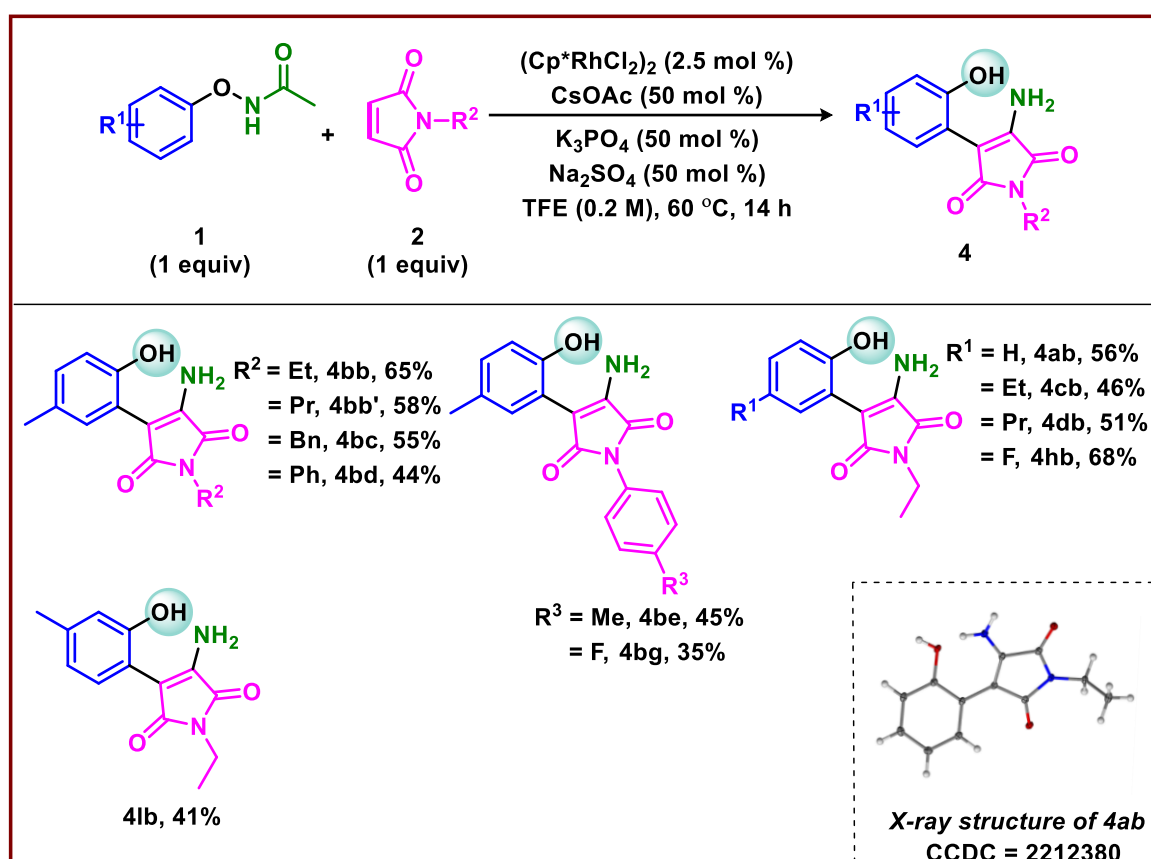
Scheme 5.1 Scope of various substrates and maleimide towards *ortho*-olefination



While *meta*-substituted substrate works under reaction conditions (Scheme 5.1, **3jc**-**3kc**), sterically bulky *ortho*-isopropyl substituted phenoxyacetamide failed to show any reactivity (Scheme 5.1, **3mc**). However, *ortho*-methyl substituted substrate worked moderately (Scheme 5.1, **3lc**). Further, the effect of steric in the reaction has been examined by taking 3,5-dimethyl, and 3,4-dimethyl substituted substrates.

While the latter worked efficiently to give the desired product **3nc** in 85% sterically hindered, 3,5-dimethyl substituted phenoxyacetamide resulted in a trace amount of the product **3oc**. The structure of the olefinated product **3be** has been confirmed by an X-ray crystallographic study.

Scheme 5.2 Scope of various substrates and maleimide towards carboamination product

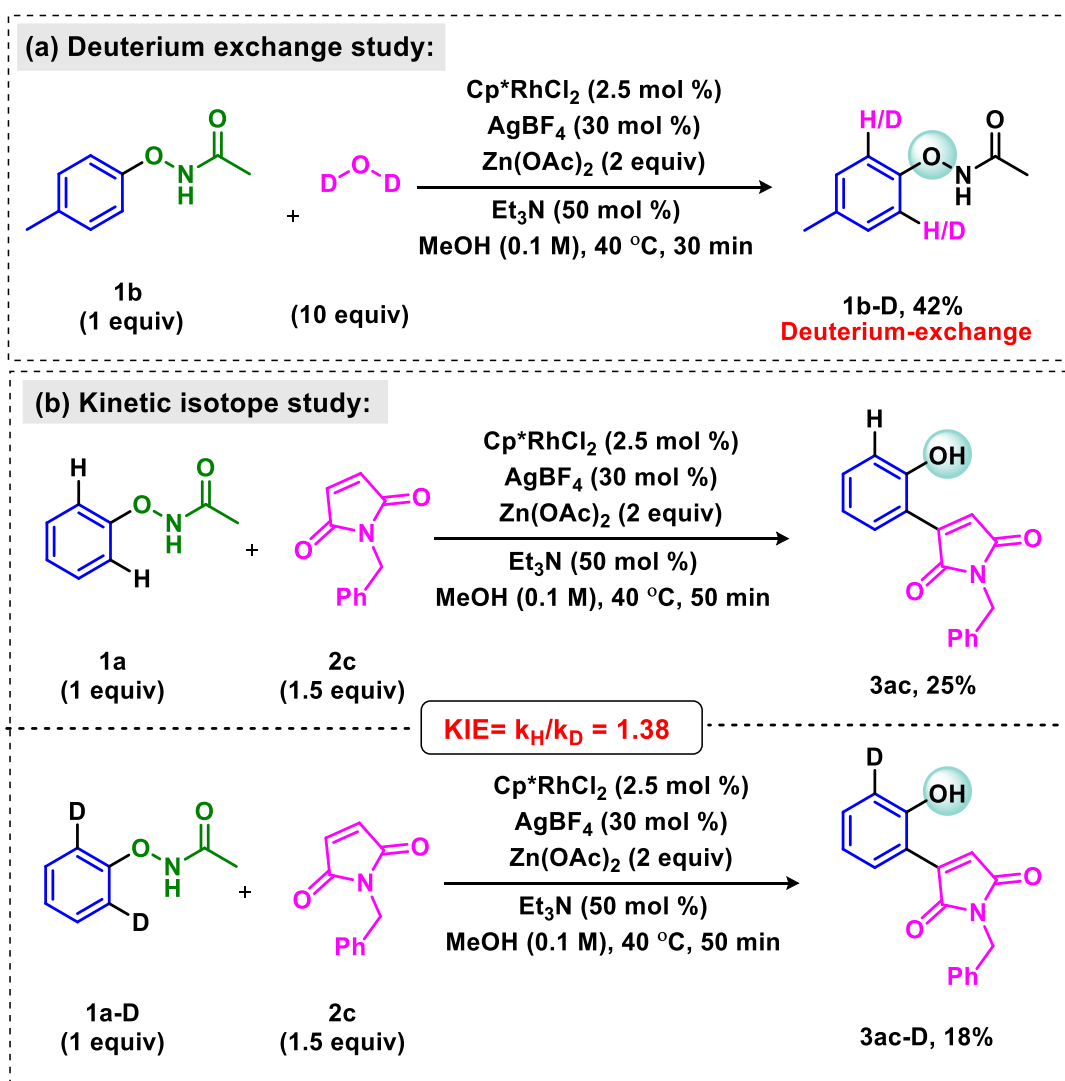


After successfully demonstrating the *ortho* olefination with maleimide, we have also demonstrated the carboamination of maleimide by utilizing the versatile nature of phenoxyacetamide. An optimized reaction condition has been obtained for the designed reaction (refer to Page 201). The generality of the reaction condition was explored with a wide range of substrates and coupling partners (Scheme 5.2). Maleimide having variation in *N*-substitution works under the developed condition delivering moderate to good product yields (Scheme 5.2, **4bb-4bg**). Moreover, the

substrate variations in the phenoxyacetamide ring also showed reactivity producing a good range of carboamination products with the double bond intact (Scheme 5.2, **4ab-4lb**). Further, the structure of the carboaminated product **4ab** has been confirmed by an X-ray crystallographic study.

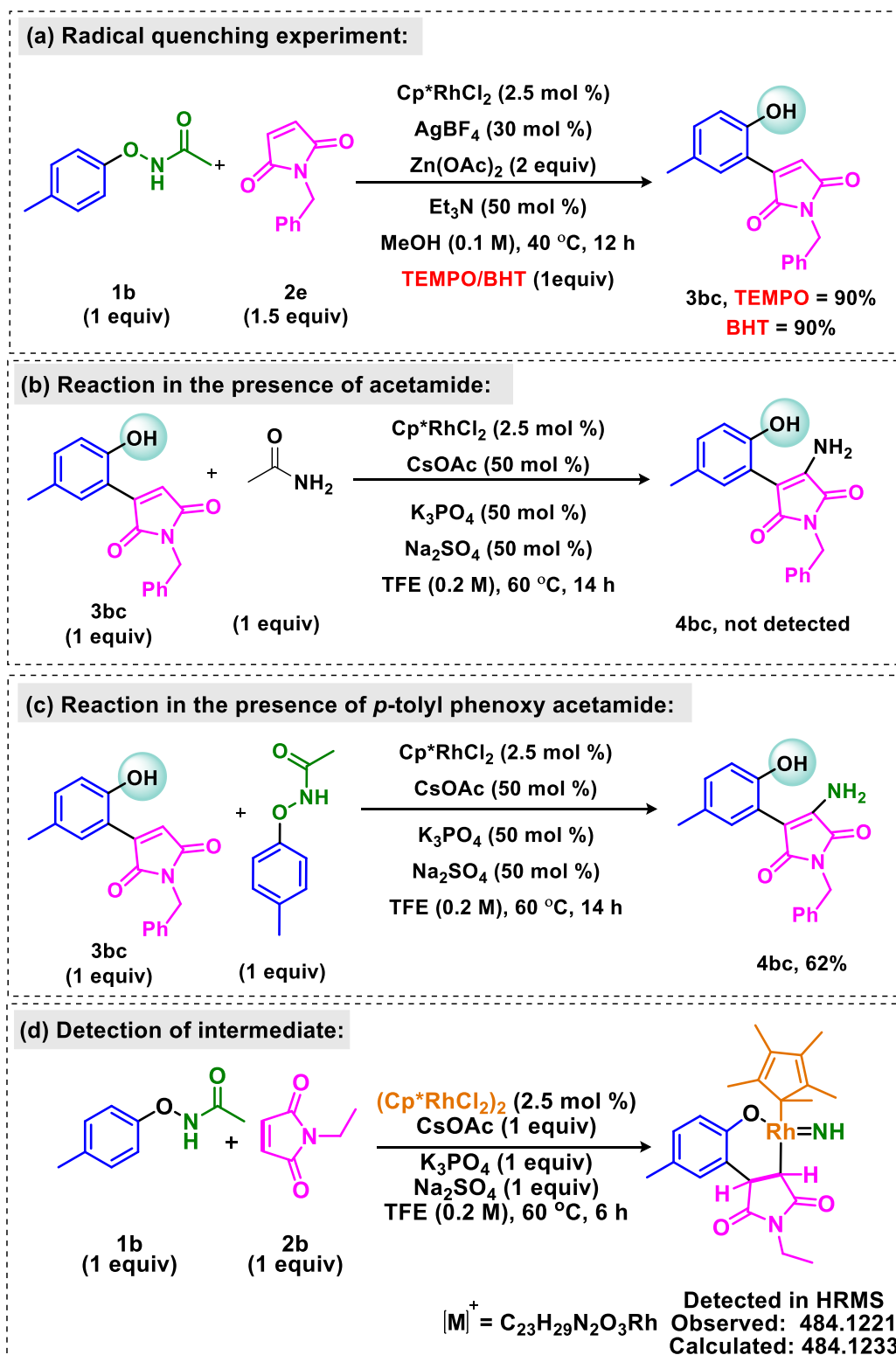
After synthesizing a wide range of *ortho*-olefination and carboamination products, we performed various mechanistic studies to understand the mechanism. We have done an H-D exchange that resulted in 42% deuterium exchanged in the *ortho* position (Scheme 5.3a).

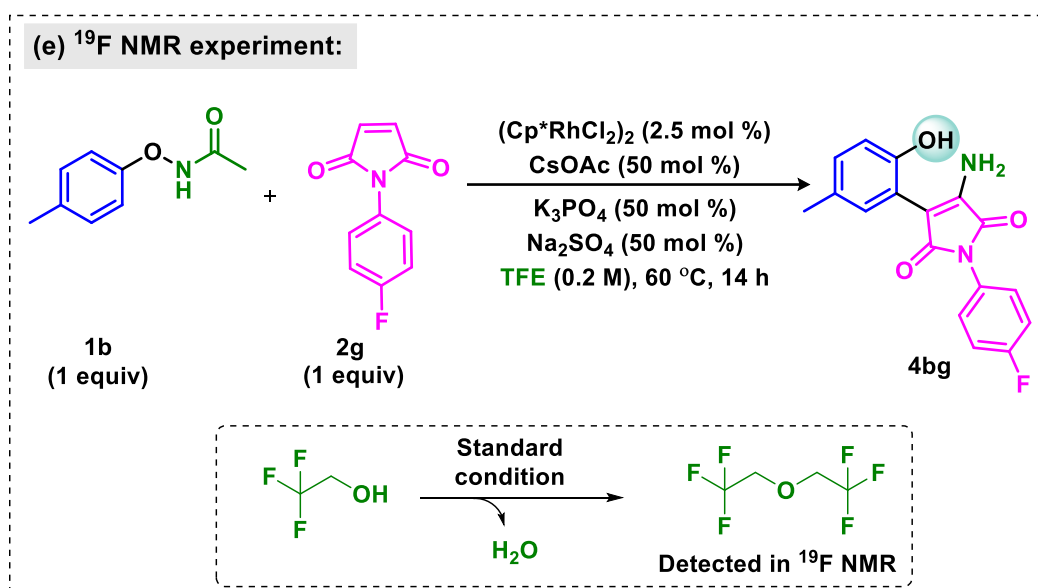
Scheme 5.3 Mechanistic studies



This implies cyclometallation step is reversible. A kinetic isotope study has been performed, which resulted in a KIE value of 1.38 (Scheme 5.3b). This result indicates that C-H bond cleavage is not involved in the rate-determining step.

Scheme 5.4 Mechanistic studies





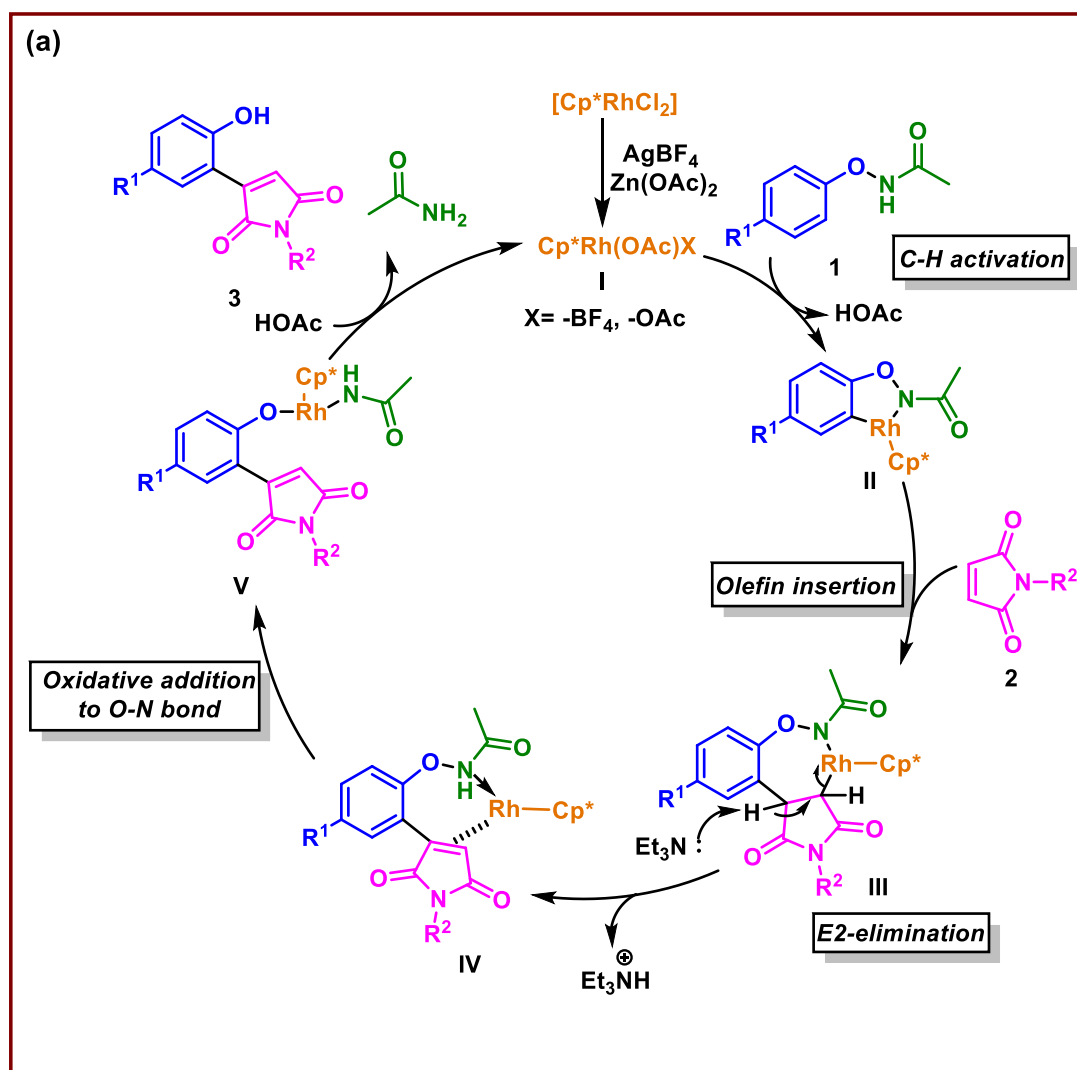
Furthermore, a mechanistic investigation has been done for the carboamination reaction. A reaction in the presence of a radical quencher such as TEMPO or BHT resulted in a 90% yield of the desired product **3bc** (Scheme 5.4a). This implies the non-involvement of the radical pathway in the reaction mechanism.

Further, a detailed mechanistic study has been done to understand the mechanism involved in the carboamination reaction. To find out the origin of the amine source and the intermediate involved in the carboamination reaction, we subjected the olefinated product **3bc** with acetamide under the standard reaction condition (Scheme 5.4b). However, product **4bc** is not forming in this case. Thus, we rationalized phenoxyacetamide as an aminating source and subjected it to the standard reaction condition; as expected, we observed the desired product in 62% yield (Scheme 5.4c). This experiment implies that the carboamination of maleimide goes through olefination followed by a nitrenoid insertion pathway.

A control experiment has been performed to get a clearer picture of the mechanism. The carboamination reaction was stopped before completion and subjected to high-resolution mass analysis (Scheme 5.4d). We have characterized many intermediates actively participating in the reaction (see Page 207). The nitrenoid intermediate was detected in

HRMS, which signifies that the reaction is going through a rhodium nitrenoid intermediate. To validate the *in-situ* formation of water from the solvent TFE, we have performed a ^{19}F NMR study (Scheme 5.4e).

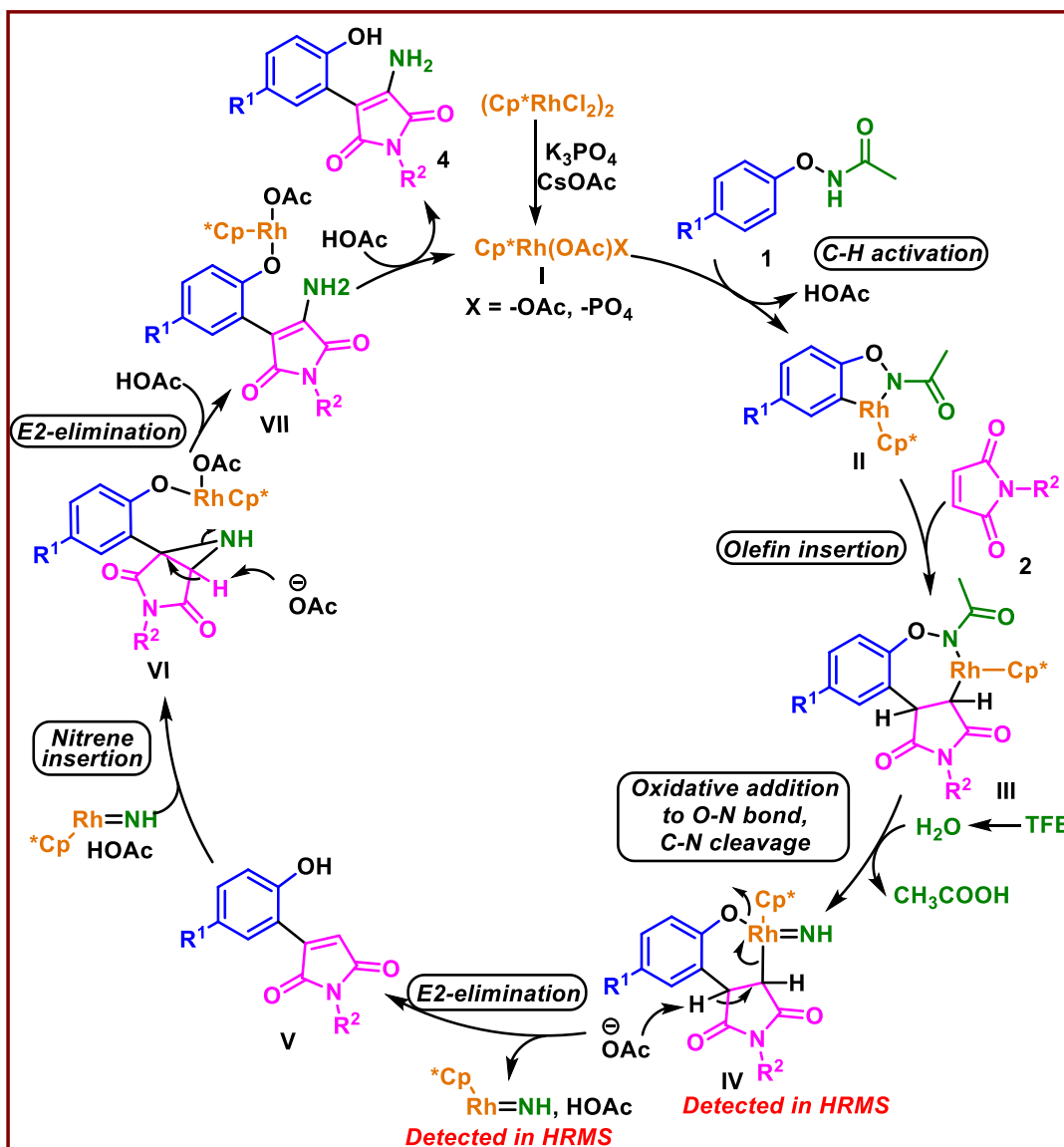
Scheme 5.5 Catalytic cycle for olefination reaction



The quantitative detection of fluoroethyl in ^{19}F NMR indicates the formation of optimal amount of water under the standard reaction condition. The optimal water generated is sufficient to cleave the amide C-N bond. To support this, when we increased the quantity of anhydrous sodium sulphate, the yield reduced to 30% from 65% (see page 202). This implies that a fine balance is required and an optimum amount of water is necessary for the C-N bond cleavage.

After performing a detailed mechanistic study and with literature precedence,¹⁴ we have proposed a plausible catalytic cycle for both the reaction. The olefination reaction proceeded after forming an active rhodium catalyst **I** (Scheme 5.5).

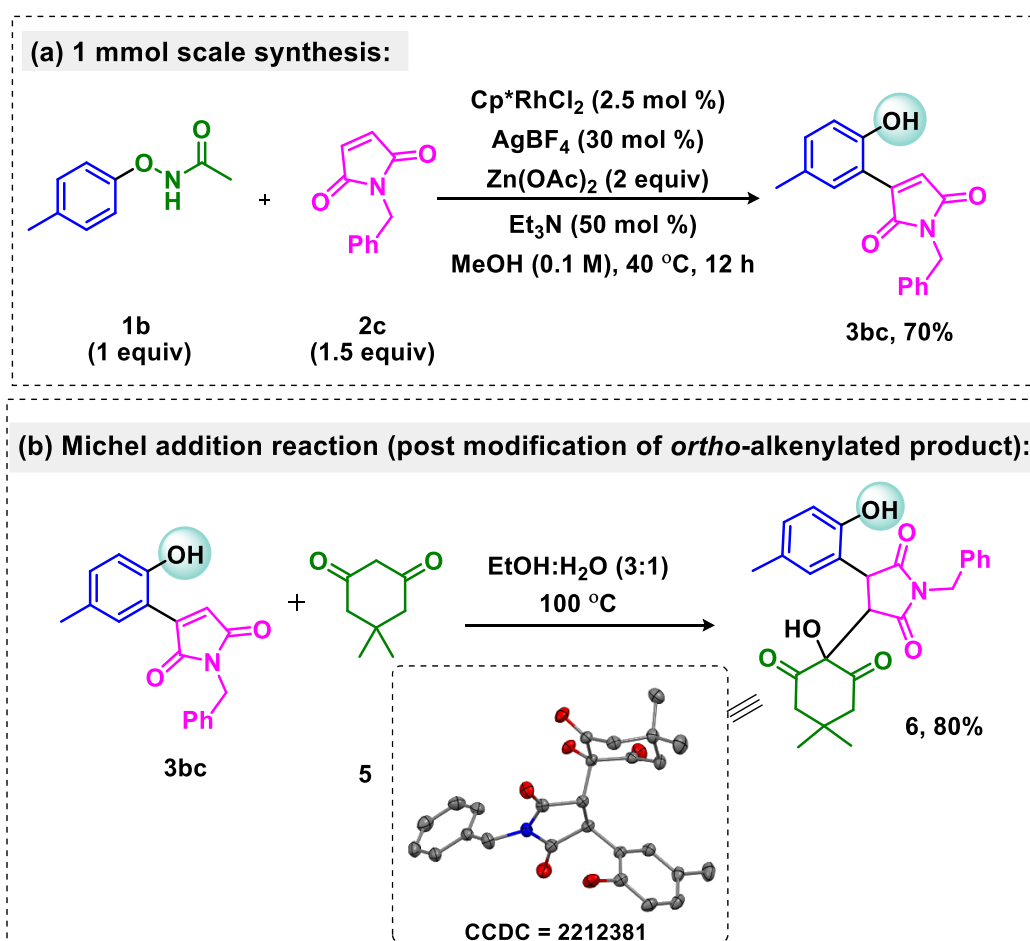
Scheme 5.6 Catalytic cycle for carboamination reaction



Rh(III) catalyst undergoes cyclometallation with phenoxyacetamide **2** to form the five-membered metallacycle **II**. Then, olefin insertion followed by base-mediated E2-elimination gives rise to intermediate **IV** with the generation of Rh(I) intermediate. Then, Rh(I) oxidatively inserts into the O-N bond to form Rh(III) intermediate **V**, which on protonation, delivered the desired product **3** with the formation of acetamide and

regenerated active Rh(III) catalyst. In another reaction condition (Scheme 5.6), the active Rh(III) catalyst generated undergoes cyclometallation followed by olefin insertion to deliver the intermediate **III**. Then, the in-situ generated water from TFE hydrolyses the amide C-N bond¹⁵ under the influence of Lewis acid Zn(OAc)₂ to generate the intermediate **IV** that is detected in HRMS (high-resolution mass spectrometry). Next, E2 elimination gave the olefinated product **V** and Rh(III) nitrenoid intermediate. Then, nitrenoid insertion into the olefin gives a strained aziridine skeleton **VI**, which further undergoes E2 elimination to give intermediate **VII**. The protonation of intermediate **VII** delivered the desired carboamination product **4** with the regeneration of the active catalyst.

Scheme 5.7 Synthetic utility



The synthetic utility of the demonstrated protocol has been further explored (Scheme 5.7).

A reaction was performed at a 1 mmol scale and successfully delivered the *ortho*-olefinated

product in 70% yield (Scheme 5.7a). The olefinated product generated through this protocol could be a suitable Michael acceptor.¹⁶ With this thought, we have treated the olefinated product **3bc** with dimedone **5** that delivered the desired Michael addition product **6** in 80% yield with a quaternary center having a hydroxy group (Scheme 5.7b). The product formed has been characterized by the X-ray crystallographic study. However, the origin of the hydroxy group and the mechanism involved in this reaction are yet to be studied.

5.4 CONCLUSION

In summary, we have disclosed two different pathways: the carboamination of maleimide and olefination of phenoxy acetamide by utilizing phenoxyacetamide as a versatile substrate. For the first time, deacylative carboamination of the maleimide has been disclosed with the double bond intact. An array of carboaminated products has been synthesized in moderate to good yield. The rhodium nitrenoid species adding to the double bond of maleimide to form aziridine is an interesting aspect of this methodology. In addition, the cleavage of amide C-N bond through hydrolysis by *in situ* generated water has been proved from ¹⁹F NMR analysis. The key intermediate involved has been well characterized through the HRMS study and validates the proposed catalytic cycle. In another case, phenoxy acetamide behaved as a traceless directing group with the *in-situ* release of acetamide. The base-assisted E2-elimination is the key to the success of this reaction.

5.5 EXPERIMENTAL SECTION

1. General Information:^{17a}

Reactions were performed using borosil seal tube vial under N₂ atmosphere. Column chromatography was done by using 100-200 & 230-400 mesh size silica gel of Acme Chemicals. A gradient elution was performed by using distilled petroleum ether and ethyl acetate. TLC plates detected under UV light at 254 nm. ¹H NMR and ¹³C NMR were

recorded on Bruker AV 400, 700 MHz spectrometer using CDCl_3 and $\text{DMSO}-d_6$ as NMR solvents. The residual CHCl_3 and $\text{DMSO}-H_6$ for ^1H NMR ($\delta = 7.26$ ppm and 2.54 ppm respectively) were used as reference. The deuterated solvent signal for ^{13}C NMR ($\delta = 77.36$ ppm 40.45 ppm) is used as reference.^{17b} Multiplicity (s = single, d = doublet, t = triplet, q = quartet, m = multiplet, dd = double doublet), integration, and coupling constants (J) in hertz (Hz). HRMS signal analysis was performed using micro TOF Q-II mass spectrometer. X-ray analysis was conducted using Rigaku Smartlab X-ray diffractometer at SCS, NISER. Reagents and starting materials were purchased from Sigma Aldrich, Alfa Aesar, TCI, Avra, Spectrochem and other commercially available sources and used without further purification unless otherwise noted. Structurally diverse maleimide were synthesized according to literature procedure.¹⁸

(2) Experimental procedure:

(2.1) General procedure for the synthesis of *N*-phenoxyacetamides 1:¹⁹

Method A: *O*-mesitylsulfonylhydroxylamine (MSH) was prepared according to the literature.²⁰ Phenol (1.5 equiv) was dissolved in methanol (0.7 M), and then potassium tert-butoxide (1.5 equiv) was added. The mixture was allowed to stir for 0.5 h under argon atmosphere. Then methanol was removed under vacuum, and DMF was added into the residue (1.3 M). Then the freshly prepared *O*-mesitylsulfonylhydroxylamine (1.0 equiv, 0.9 M in DMF) was added under ice cold bath. The mixture was allowed to stir for 2 h, diluted with ethylacetate, and washed with brine. The aqueous layer was extracted with EtOAc, which was then removed under reduced pressure to afford the corresponding *N*-aryloxyamine. Na_2CO_3 (1.5 equiv) and $\text{H}_2\text{O}/\text{EtOAc}$ (v/v 1/2, 1.0 M) was next added to the reaction flask. The resulting solution was kept under ice bath followed by dropwise addition of acyl chloride (1.2 equiv). After stirring at 0 °C for 2 h, the reaction was quenched with saturated NaHCO_3 and diluted with EtOAc. The organic phase was washed twice with

saturated NaHCO_3 , dried over anhydrous Na_2SO_4 , filtered, and evaporated under reduced pressure. The residue was purified by flash column chromatography on silica gel to provide the desired product.

Method B:¹ A mixture of *N*-hydroxyphthalimide (1.0 equiv), arylboronic acid (2.0 equiv), CuCl (1.0 equiv), freshly activated 4Å molecular sieves (250mg/mmol) and pyridine (1.1 equiv.) were dissolved in 1,2-dichloroethane (0.25 M) and stirred at room temperature under air. After 48-120 hours, the reaction mixture turned green. Silica gel was added to the flask and the solvent was evaporated under reduced pressure. The purification was performed by flash column chromatography on silica gel to afford desired *N*-aryloxyphthalimides. The product was directly used for the next step.

Hydrazine monohydrate (4.00 equiv., 51- 64%) was added to the solution of *N*-aryloxyphthalimide (1.0 equiv) in DCM (0.25 M). The reaction was stirred at room temperature overnight. MgSO_4 was added to the mixture and the suspension was stirred for additional 10 minutes. The precipitate was filtered off and washed with DCM followed by EtOAc. The filtrate was concentrated and the resulting oil was directly used without further purification. *N*-aryloxyamine (1.0 equiv.) was dissolved in DCM (0.2 M). The resulting solution was cooled to 0 °C and acetic anhydride (1.10 equiv.) was added dropwise to the mixture. After stirring at room temperature for 3 h the reaction was quenched with saturated NaHCO_3 and extracted with DCM. The organic phase was washed three times with saturated NaHCO_3 and dried over anhydrous Na_2SO_4 , followed by filtration. The solvent was evaporated under reduced pressure. The crude product was purified by recrystallization from EtOAc/pentane to afford the desired *N*-aryloxyacetamide **2**.

(3) Catalysis reactions:

(3.1) General procedure for the Cp*Rh catalyzed C-H olefination of aryloxy acetamide **1** with maleimide **2**:

To an oven-dried seal tube charged with a stir bar, aryloxy acetamide **1** (0.1 mmol, 1 equiv), maleimide **2** (0.15 mmol, 1.5 equiv), (Cp*RhCl₂)₂ (0.0025 mmol, 2.5 mol %), Zn(OAc)₂ (0.2 mmol, 2.0 equiv), Et₃N (0.05 mmol, 50 mol %) and MeOH (1.0 mL, 0.1 M with respect to **1**) were added under nitrogen atmosphere. The seal tube was taken inside the glove box and AgBF₄ (0.03 mmol, 30 mol %) was added. The reaction mixture was stirred (700 rpm) in a preheated aluminum block at 40 °C for 12 h. After completion of the reaction (monitored by TLC), the solvent was evaporated under reduced pressure, and the crude was purified by column chromatography using EtOAc/hexane as eluent to get the corresponding *ortho*-olefinated product **3**.

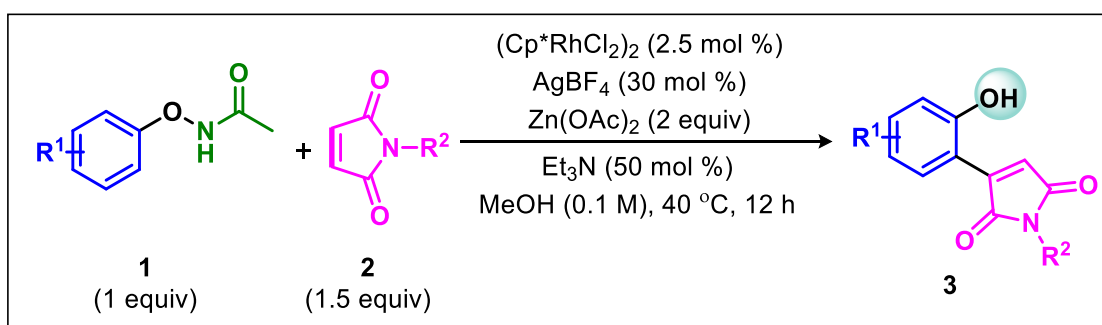


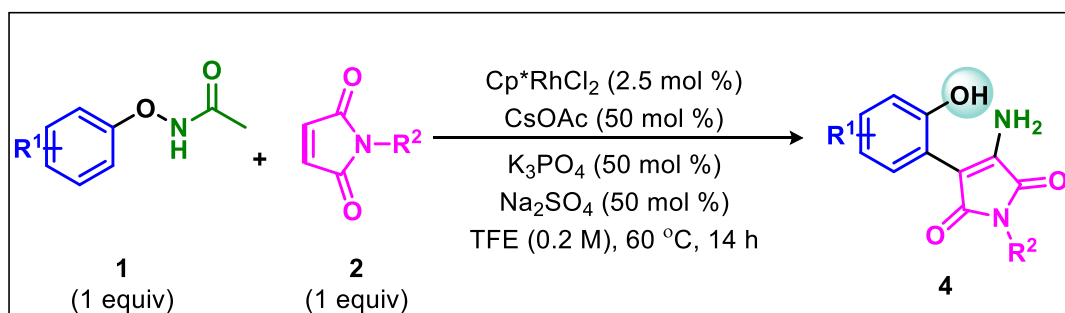
Table 5.3 Optimization Table for Cp*Rh Catalyzed Carboamination of Maleimide 2^a

	1b (1 equiv)	2b (1 equiv)		4bb
entry	catalyst	additive (50 mol %)	temp °C	yield of 4bb (%) ^b
1	Cp*[Rh] (5 mol %)	CsOAc + K ₃ PO ₄	60	11
2	Cp*[Rh] (5 mol %)	CsOAc + K ₃ PO ₄	rt	nd
3	Cp*[Rh] (5 mol %)	CsOAc + K ₃ PO ₄	40	6
4	Cp*[Rh] (5 mol %)	CsOAc + K ₃ PO ₄	80	30
5	Cp*[Rh] (2.5 mol %)	CsOAc + K ₃ PO ₄	60	36
6	Cp*RhCl ₂ (2.5 mol %)	CsOAc + K ₃ PO ₄	60	48
7	Cp*RhCl ₂ (2.5 mol %)	LiOAc + K ₃ PO ₄	60	28
8	Cp*RhCl ₂ (2.5 mol %)	NaOAc + K ₃ PO ₄	60	40
9	Cp*RhCl ₂ (2.5 mol %)	KOAc + K ₃ PO ₄	60	43
10	Cp*RhCl ₂ (2.5 mol %)	Cs ₂ CO ₃ + K ₃ PO ₄	60	19
11	Cp*RhCl ₂ (2.5 mol %)	CsOAc + K ₃ PO ₄ + Na ₂ SO ₄ (50 mol %)	60	65 ^c
12	Cp*RhCl ₂ (2.5 mol %)	CsOAc + K ₃ PO ₄ + Na ₂ SO ₄ (100 mol %)	60	30
13	--	CsOAc + K ₃ PO ₄ + Na ₂ SO ₄ (50 mol %)	60	nd

^aReaction conditions: **1b** (0.1 mmol), **2c** (0.15 mmol), Cp*[Rh] = [Cp*[Rh](CH₃CN)₃](SbF₆)₂, (Cp*RhCl₂)₂ (2.5 mol %), additives (50 mol %), EtOH (0.5 mL), temp °C, N₂.

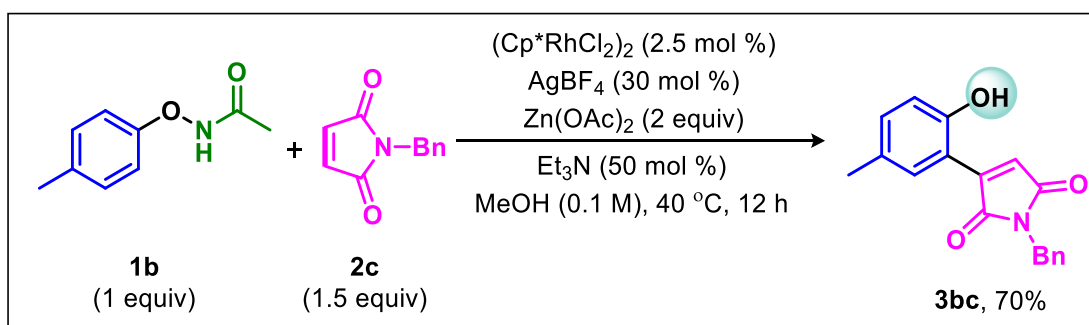
^bNMR yield (1,3,5-trimethoxy benzene was used as internal standard), ^cIsolated yield.

(3.2) General procedure for the Cp*Rh catalyzed C-H olefination of aryloxyacetamide **1** followed by intermolecular C-H amination of maleimide **2**.



To an oven-dried seal tube charged with a stir bar, aryloxy acetamide **1** (0.1 mmol, 1 equiv), maleimide **2** (0.1 mmol, 1.0 equiv), (Cp*RhCl₂)₂ (0.0025 mmol, 2.5 mol %), Na₂SO₄ (0.05 mmol, 50 mol %), and TFE (0.5 mL, 0.2 M with respect to **1**) were added under nitrogen atmosphere. The seal tube was taken inside the glove box and CsOAc (0.05 mmol, 50 mol %), and K₃PO₄ (0.05 mmol, 50 mol %), were added. The reaction mixture was stirred (700 rpm) in a preheated aluminum block at 60 °C for 14 h. After completion of the reaction (monitored by TLC), the solvent was evaporated under reduced pressure and the crude was purified by column chromatography using EtOAc/hexane as eluent to get the corresponding product **4**.

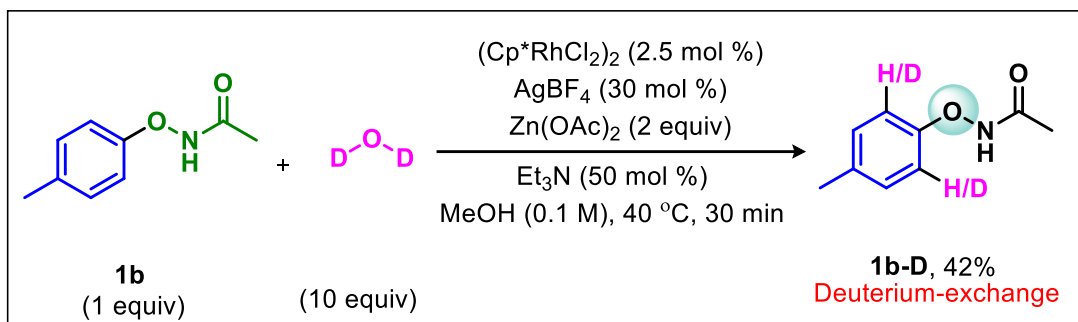
(3.3) General procedure for the Cp*Rh catalyzed olefination reaction of aryloxy acetamide **1b in 1 mmol scale:**



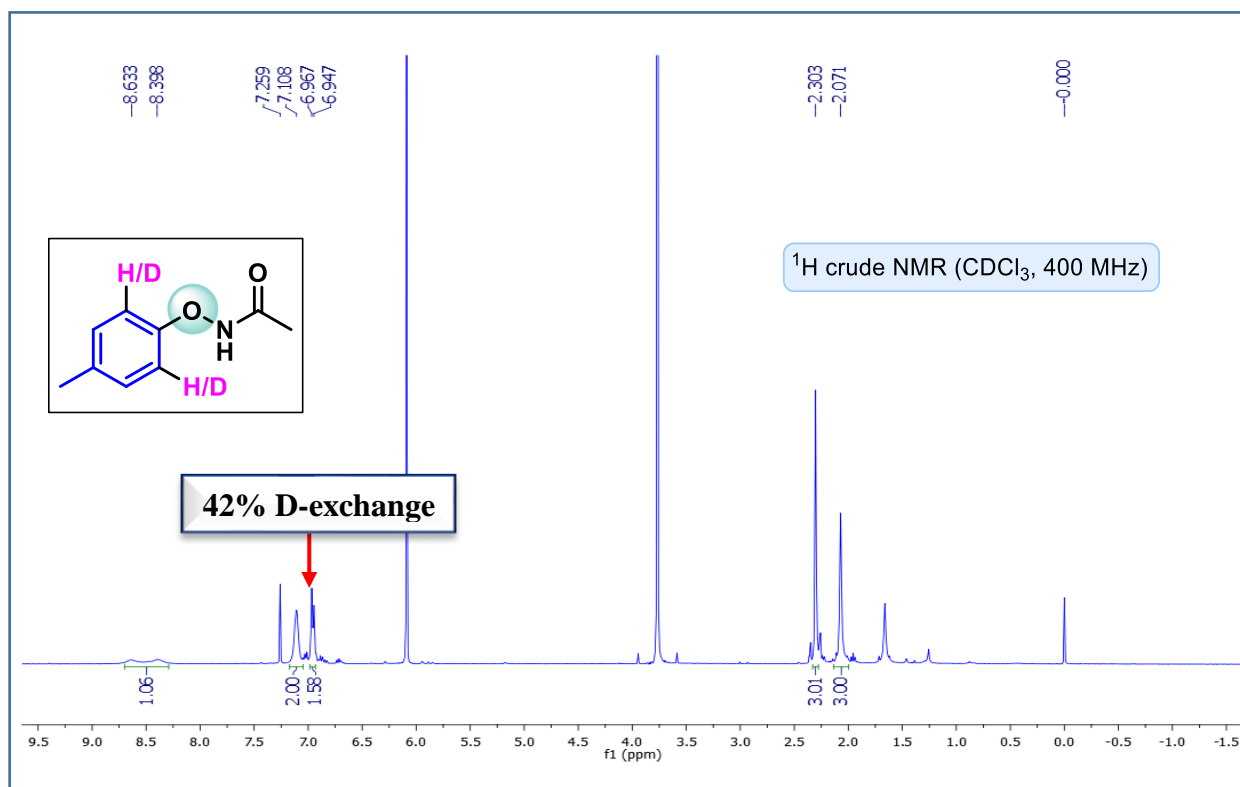
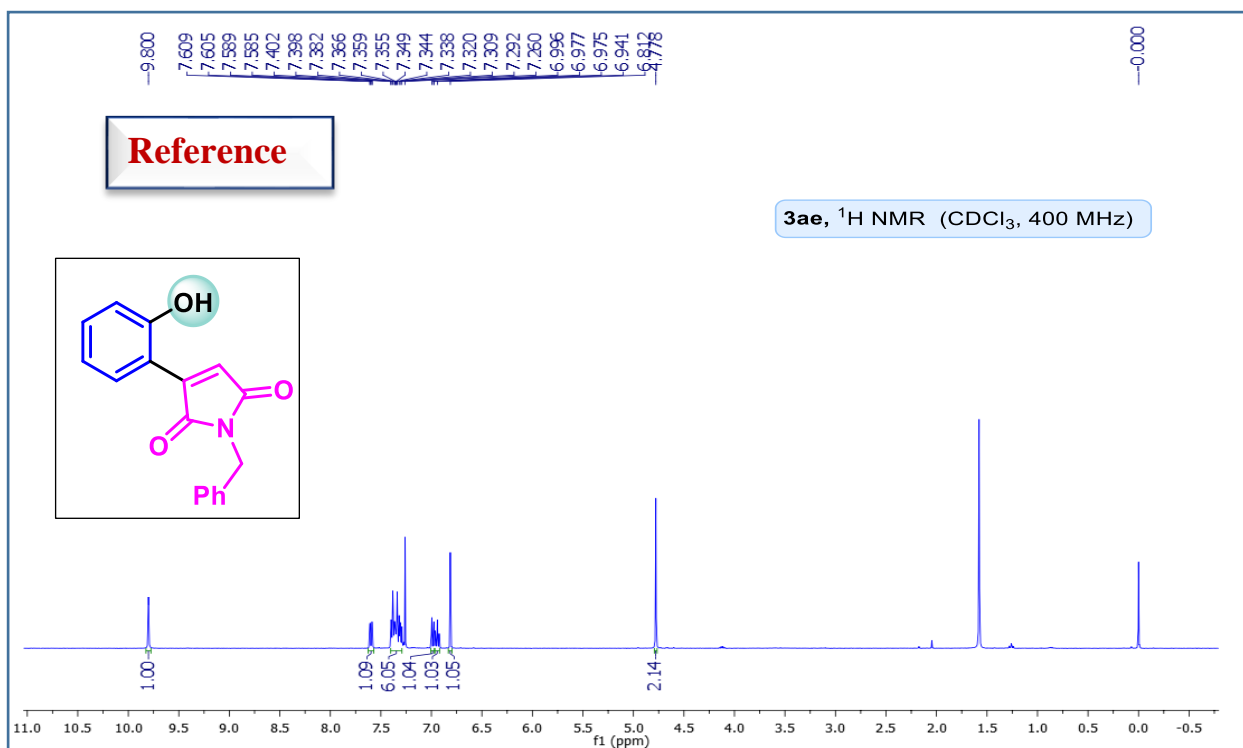
To an oven-dried seal tube charged with a stir bar, *N*-(*p*-tolylloxy)acetamide **1b** (1.0 mmol, 1 equiv), *N*-benzyl maleimide **2c** (1.5 mmol, 1.5 equiv), (Cp*RhCl₂)₂ (0.025 mmol, 2.5 mol %), Zn(OAc)₂ (2.0 mmol, 2.0 equiv), Et₃N (0.5 mmol, 50 mol %) and MeOH (10.0 mL, 0.1 M with respect to **1**) were added under nitrogen atmosphere. The seal tube was taken inside the glove box and AgBF₄ (0.3 mmol, 30 mol %) was added. The reaction mixture was stirred (700 rpm) in a preheated aluminum block at 40 °C for 12 h. After completion of the reaction (monitored by TLC), the solvent was evaporated under reduced pressure, and the crude was purified by column chromatography using EtOAc/hexane as eluent to get the corresponding *ortho*-olefinated product **3bc** in 70% (205 mg).

(4) Control and mechanistic experiments:

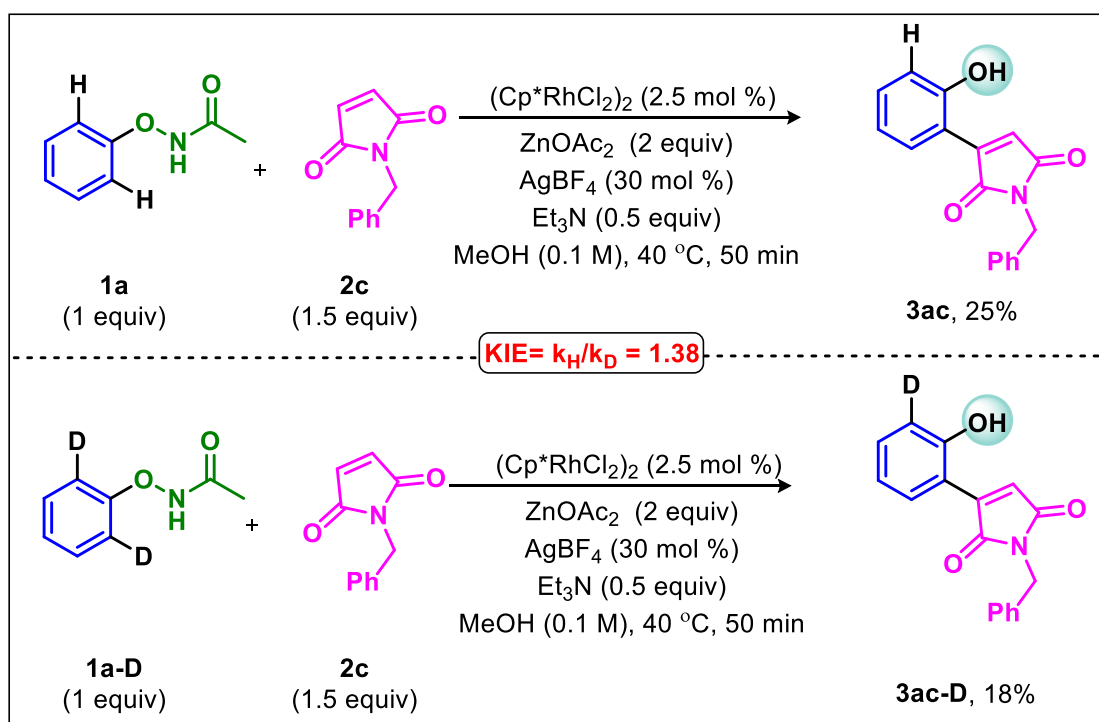
(4.1) Deuterium exchange study:



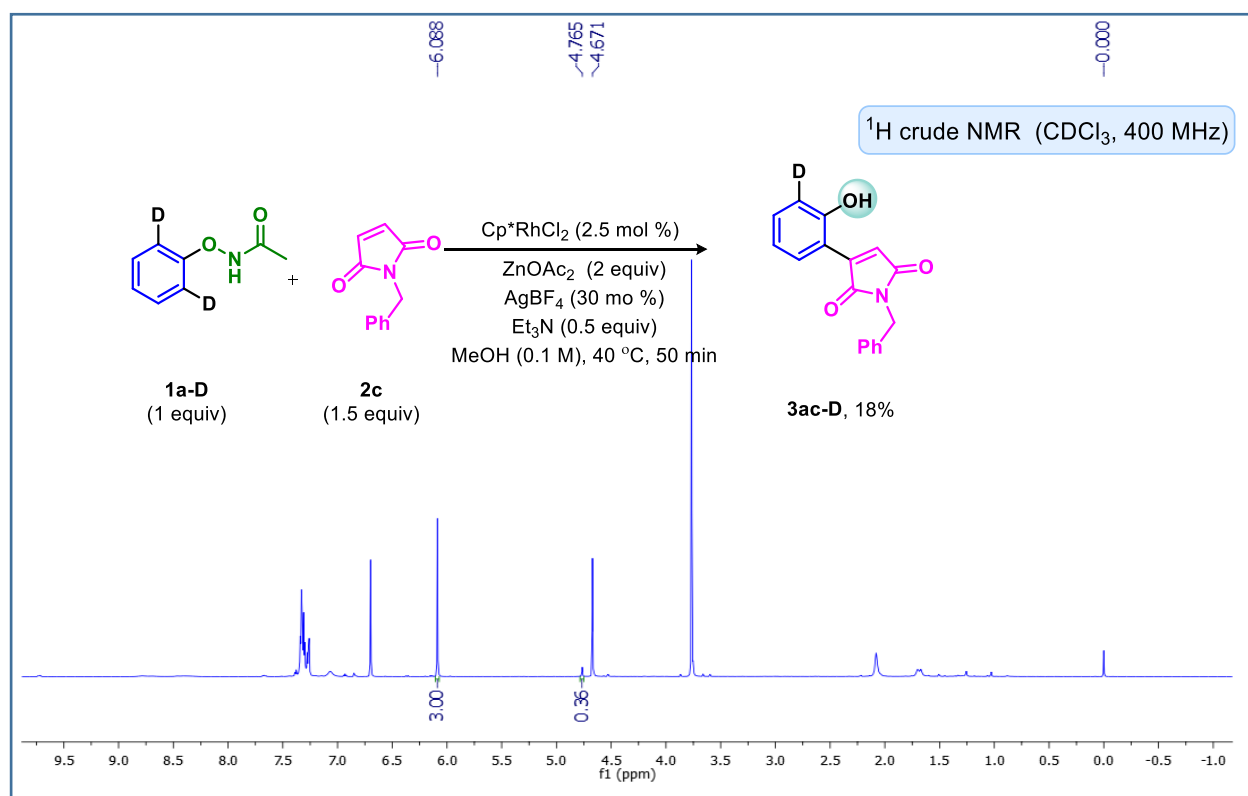
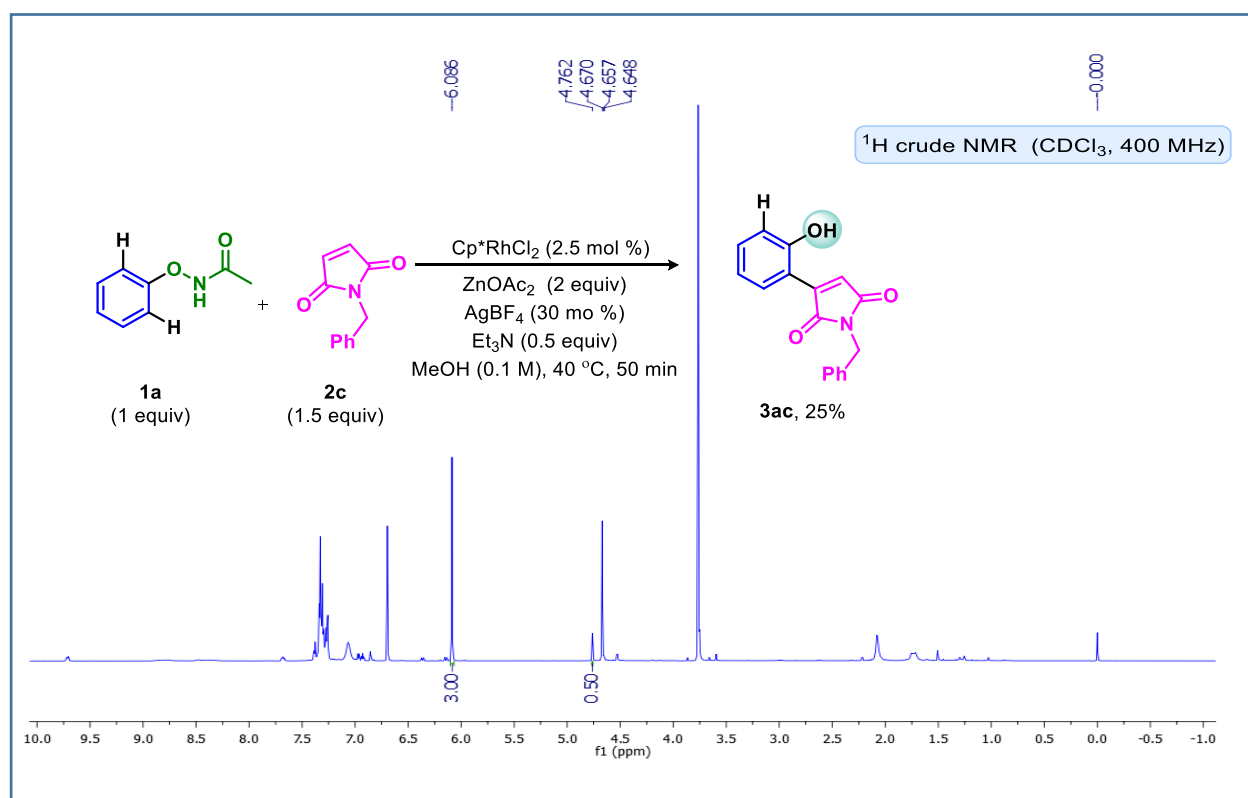
To an oven-dried seal tube charged with a stir bar, *N*-(*p*-tolylloxy)acetamide **1b** (0.1 mmol, 1 equiv), $(Cp^*RhCl_2)_2$ (0.0025 mmol, 2.5 mol %), $Zn(OAc)_2$ (0.2 mmol, 2.0 equiv), Et_3N (0.05 mmol, 50 mol %), and MeOH (1.0 mL, 0.1 M with respect to **1b**) were added under nitrogen atmosphere. The seal tube was taken inside the glove box, and $AgBF_4$ (0.03 mmol, 30 mol %) was added. Finally, D_2O (10 equiv) was added and the seal tube was sealed. The reaction mixture was stirred (700 rpm) in a preheated aluminum block at 40 °C for 30 min. Then, the reaction mixture was passed through a short silica pad washed with ethyl acetate, and evaporated under reduced pressure. The crude was submitted for NMR analysis. The percentage of H/D exchange was calculated from the crude 1H -NMR spectrum as shown below.



(4.2) Kinetic isotope effect (KIE):



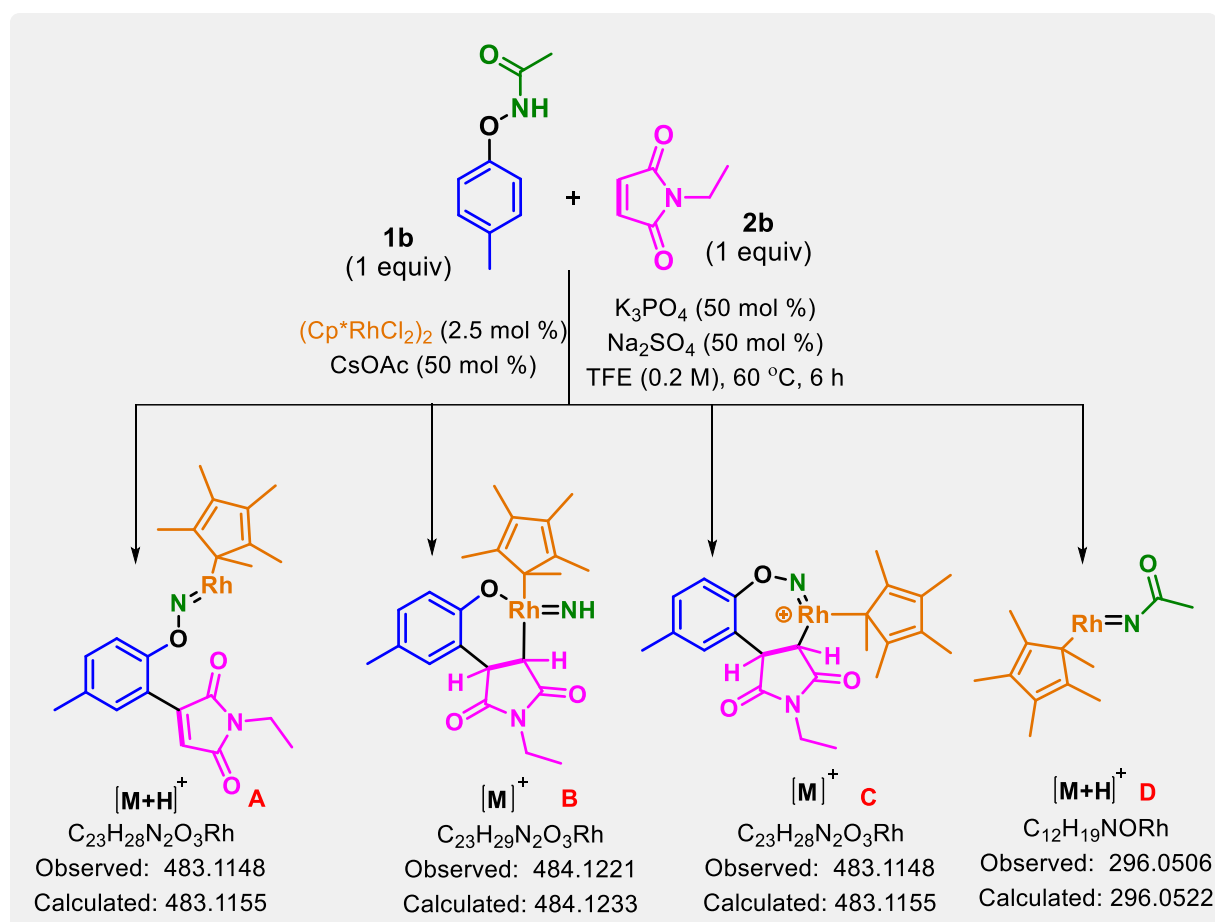
In a parallel set of reaction, to an oven-dried seal tube charged with a stir bar, *N*-phenoxy acetamide **1a/1a-D**¹⁹ (0.1 mmol, 1 equiv), *N*-benzyl maleimide **2c** (0.15 mmol, 1.5 equiv), $(\text{Cp}^*\text{RhCl}_2)_2$ (0.0025 mmol, 2.5 mol %), $\text{Zn}(\text{OAc})_2$ (0.2 mmol, 2.0 equiv), Et_3N (0.05 mmol, 50 mol %), and MeOH (1.0 mL, 0.1 M with respect to **1a**) were added under nitrogen atmosphere. The seal tube was taken inside the glove box, and AgBF_4 (0.03 mmol, 30 mol %) was added. The reaction mixture was stirred (700 rpm) in a preheated aluminum block at 40°C for 50 min. Then, the reaction mixture was passed through a short silica pad, washed with ethyl acetate, and evaporated under reduced pressure. The crude was submitted for NMR analysis. The percentage of H/D exchange was calculated from the crude ^1H -NMR spectrum as shown below.

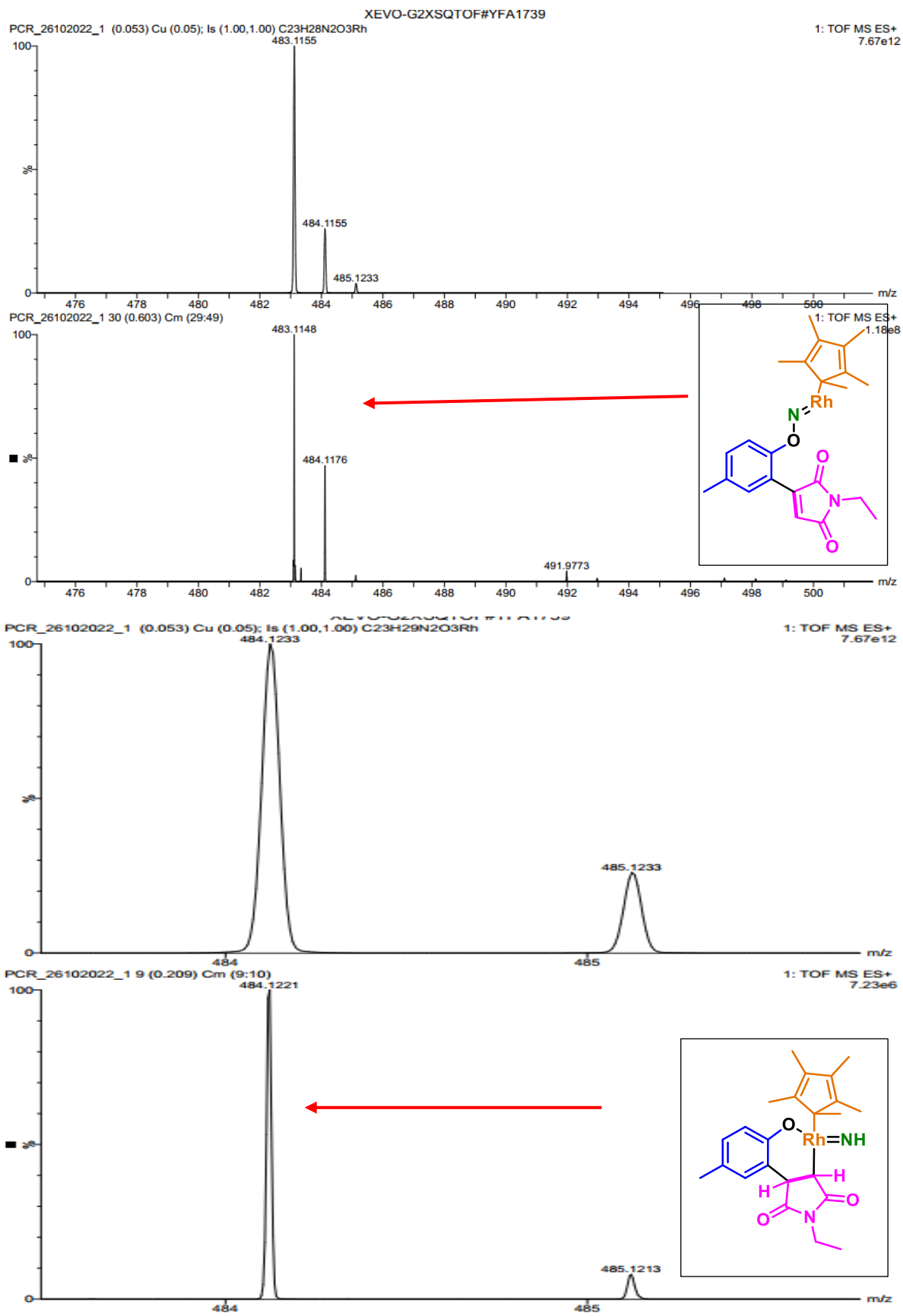


(4.3) Mass analysis of carboamination reaction:

To an oven-dried seal tube charged with a stir bar, 1-benzyl-3-(2-hydroxy-5-methylphenyl)-1*H*-pyrrole-2,5-dione **3bc** (0.1 mmol, 1 equiv), *N*-(*p*-tolxy)acetamide **1b** (0.1 mmol, 1 equiv), (Cp**Rh*Cl₂)₂ (0.0025 mmol, 2.5 mol %), Na₂SO₄ (0.05 mmol, 50 mol %), and TFE (0.5 mL, 0.2 M with respect to **1b**) were added under nitrogen atmosphere. The seal tube was taken inside the glove box, and CsOAc (0.05 mmol, 50 mol %), K₃PO₄ (0.05 mmol, 50 mol %), were added. The reaction mixture was stirred (700 rpm) in a preheated aluminum block at 60 °C for 6 h. After 6 h, the residue was filtered through a nylon filter and evaporated under reduced pressure. It was then submitted for mass analysis.

Figure 5.3 Mass analysis for reaction of **1b** with **2b**





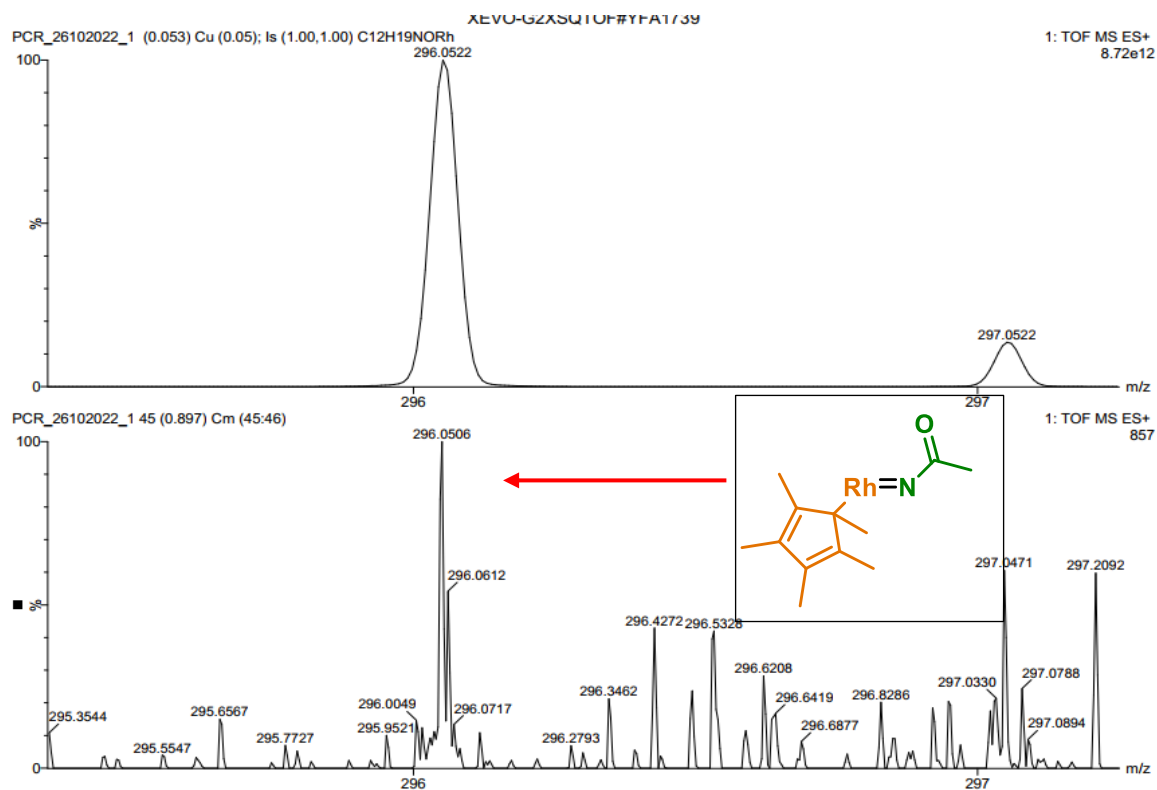
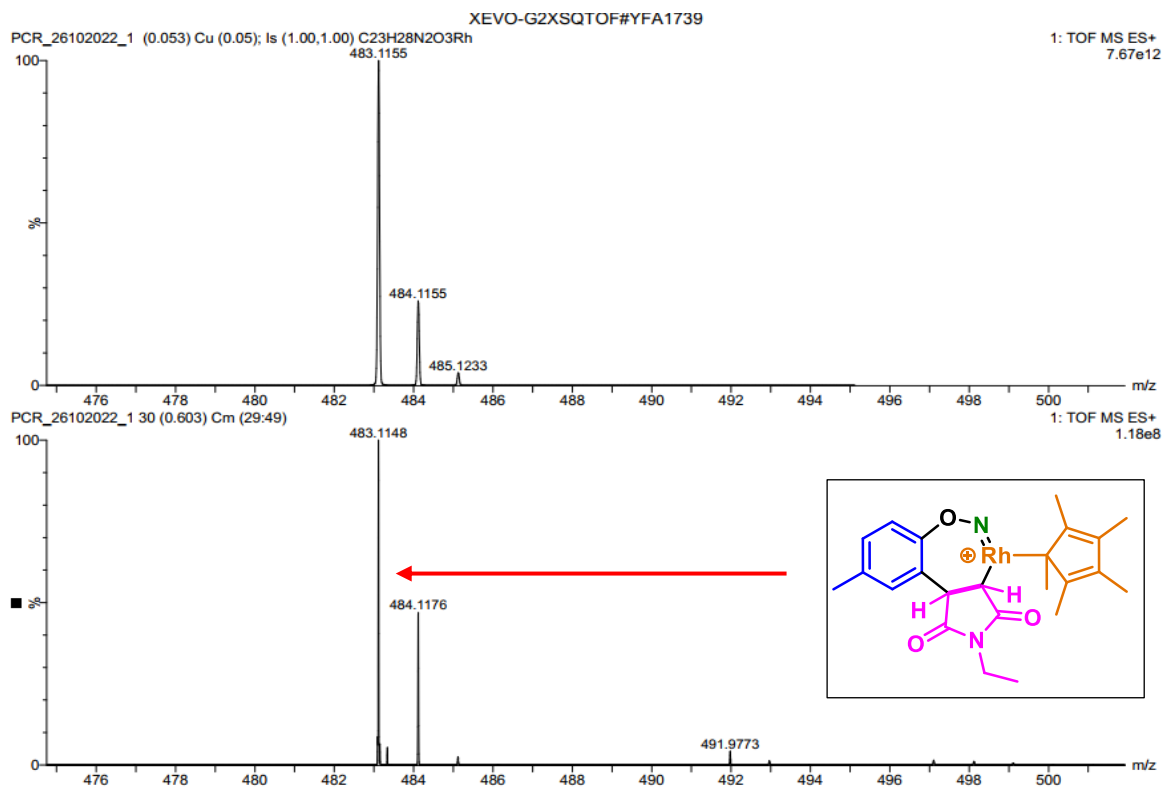
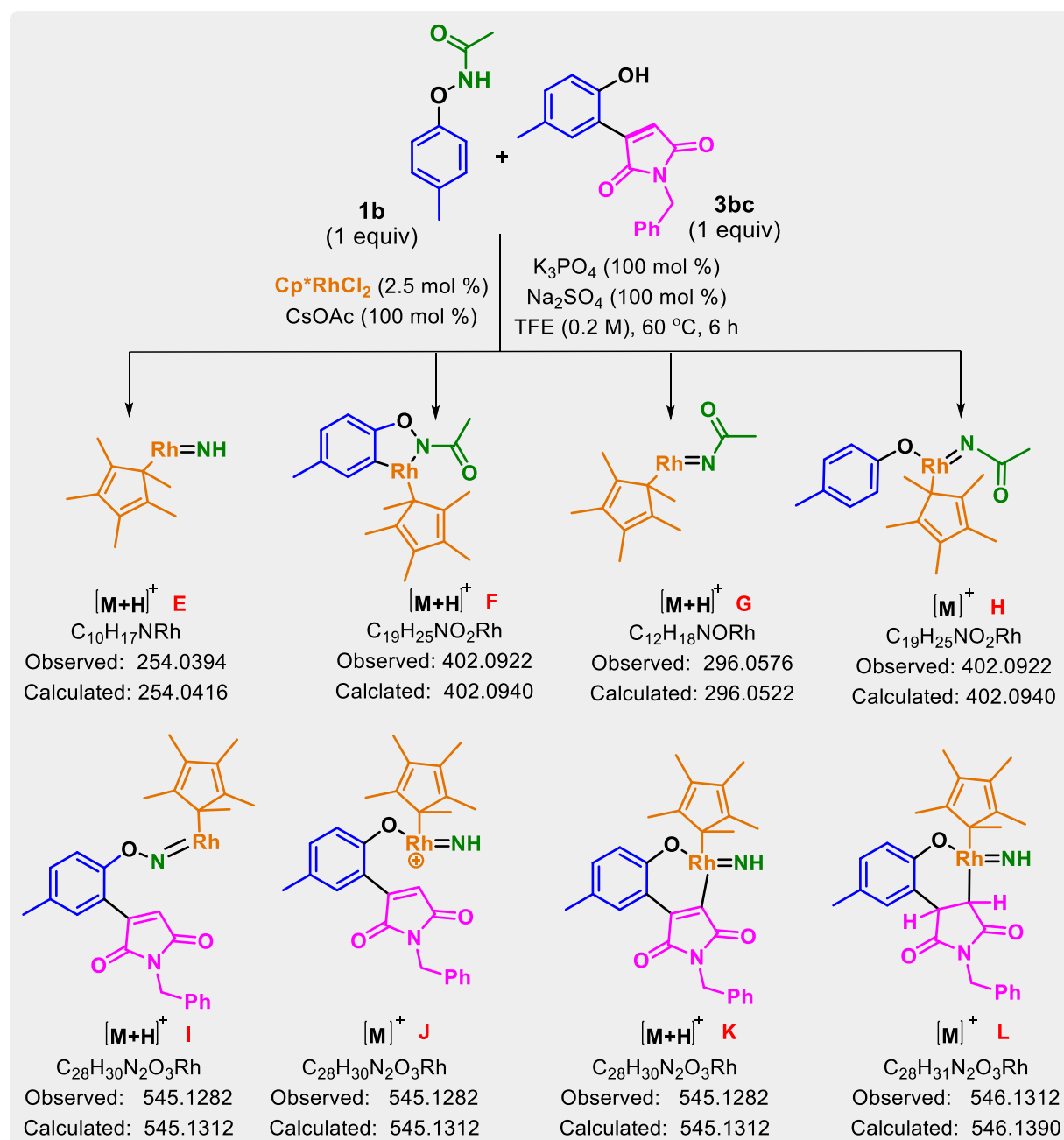
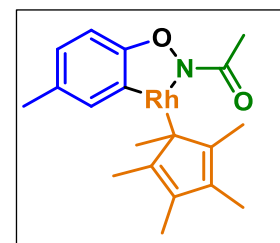
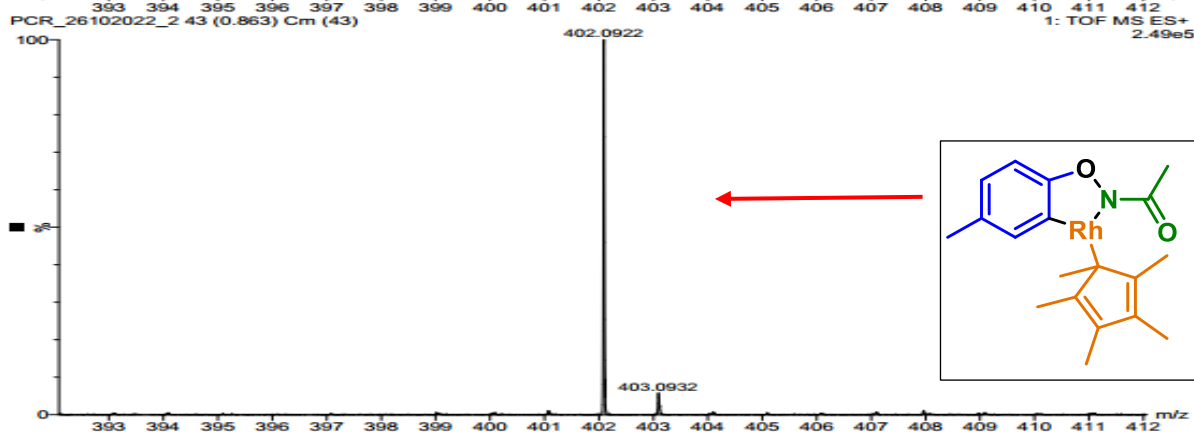
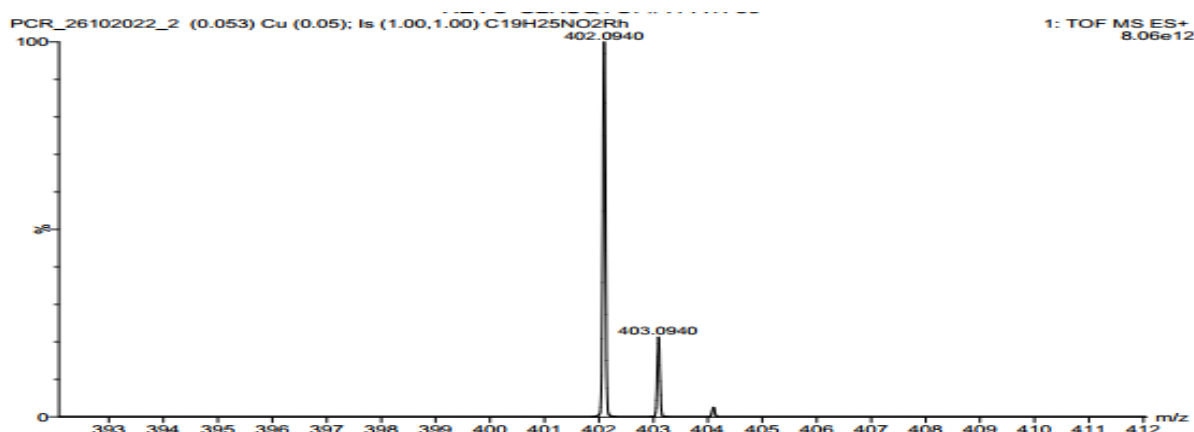
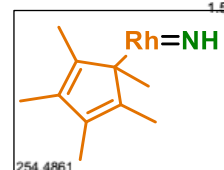
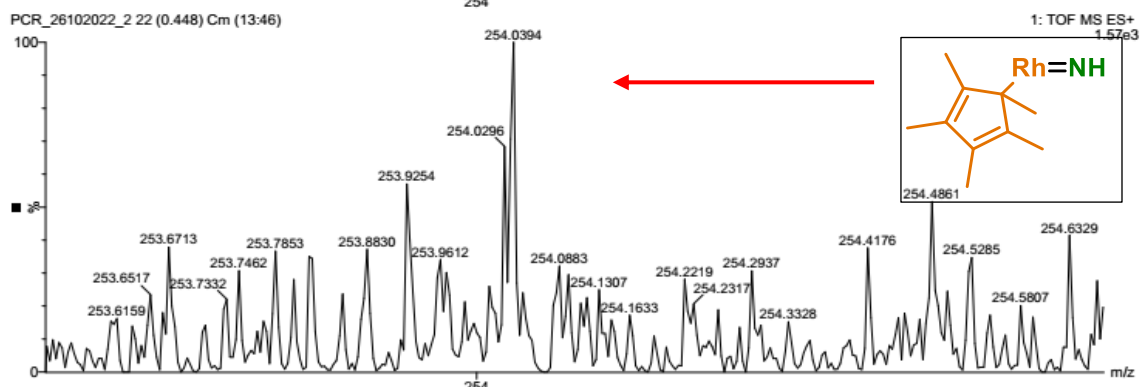
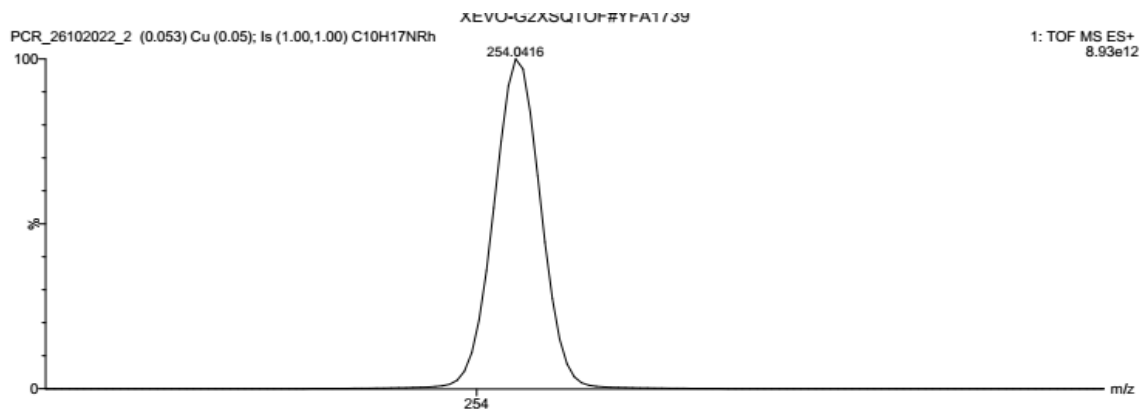
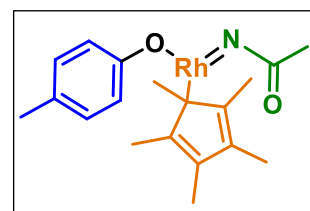
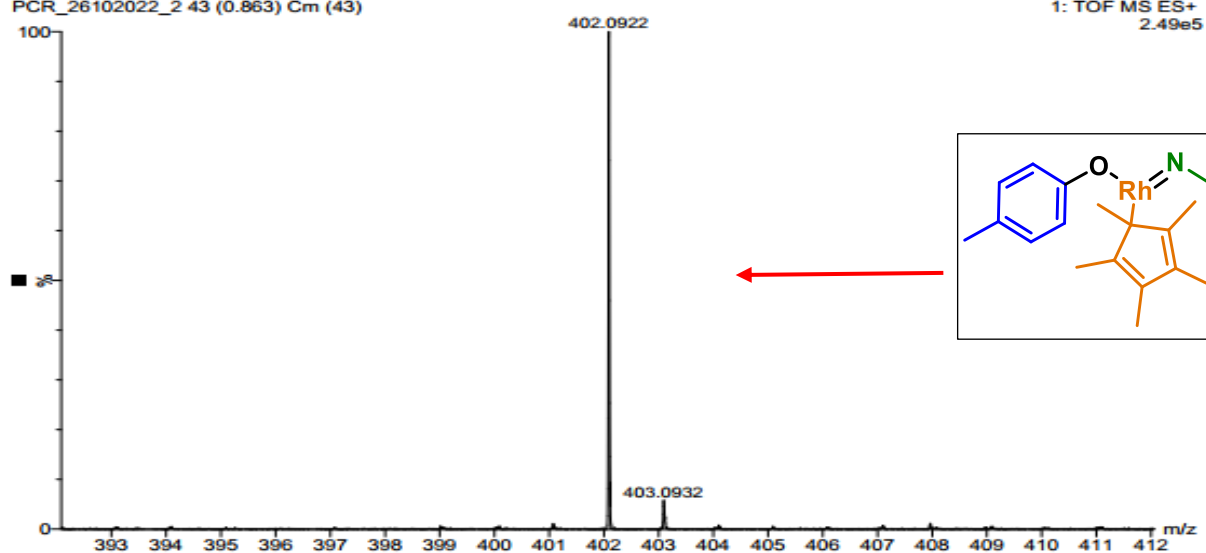
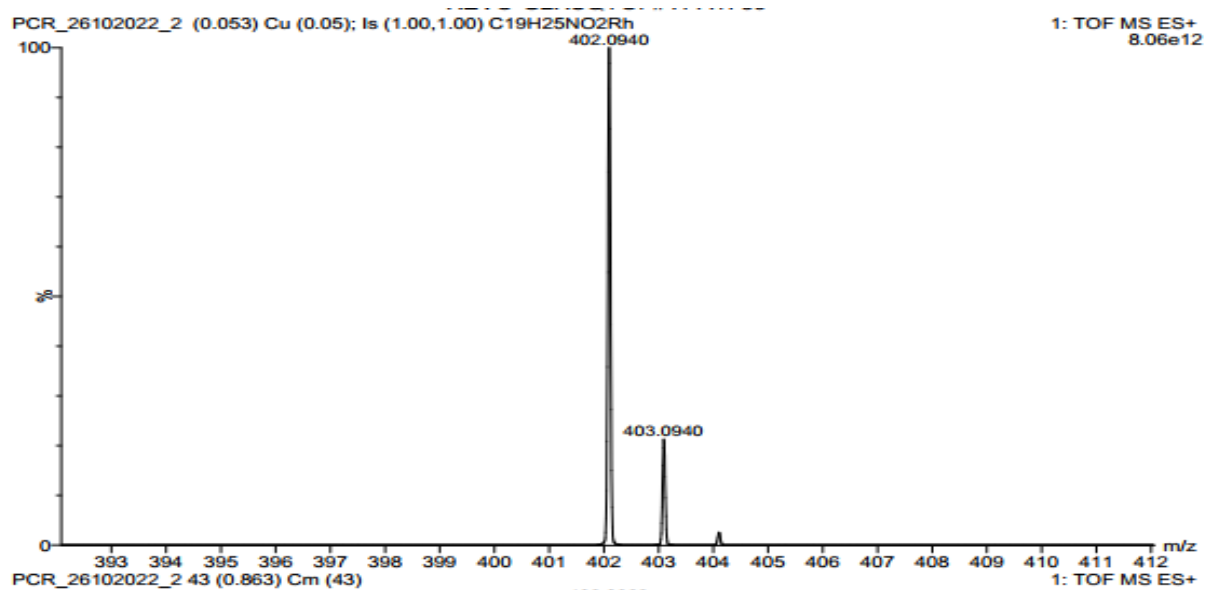
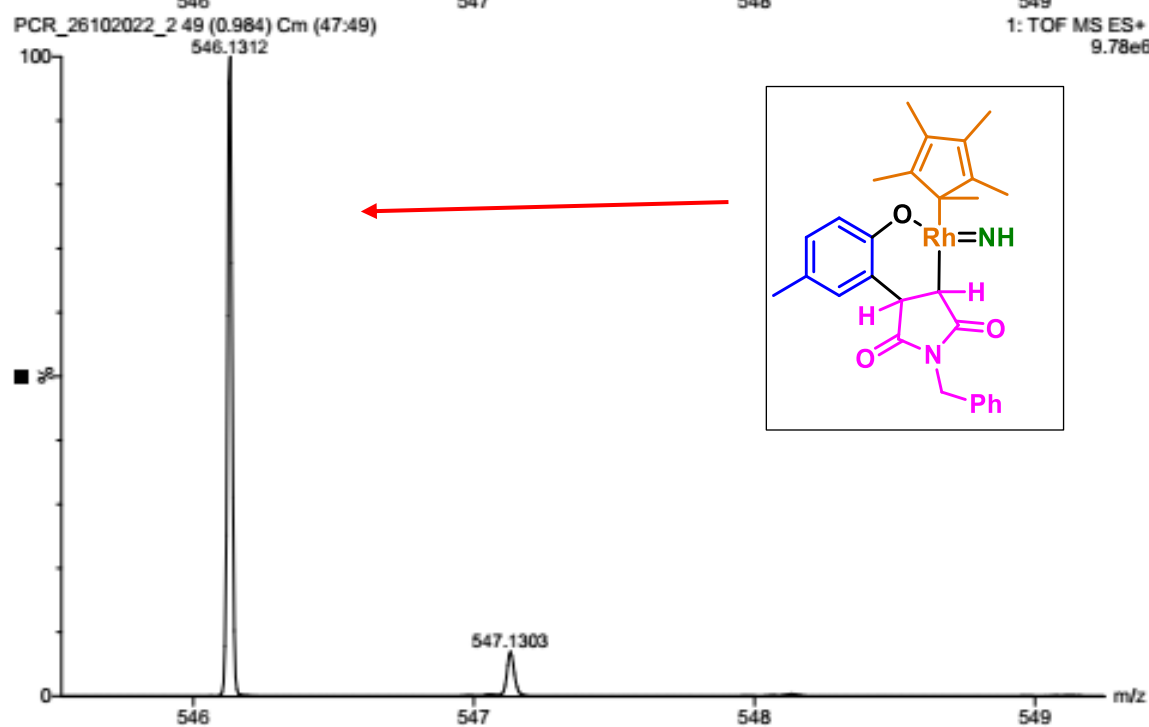
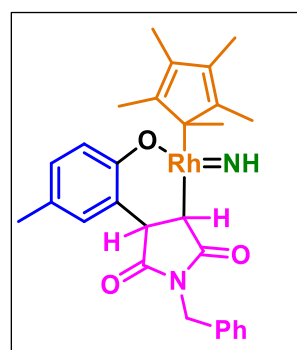
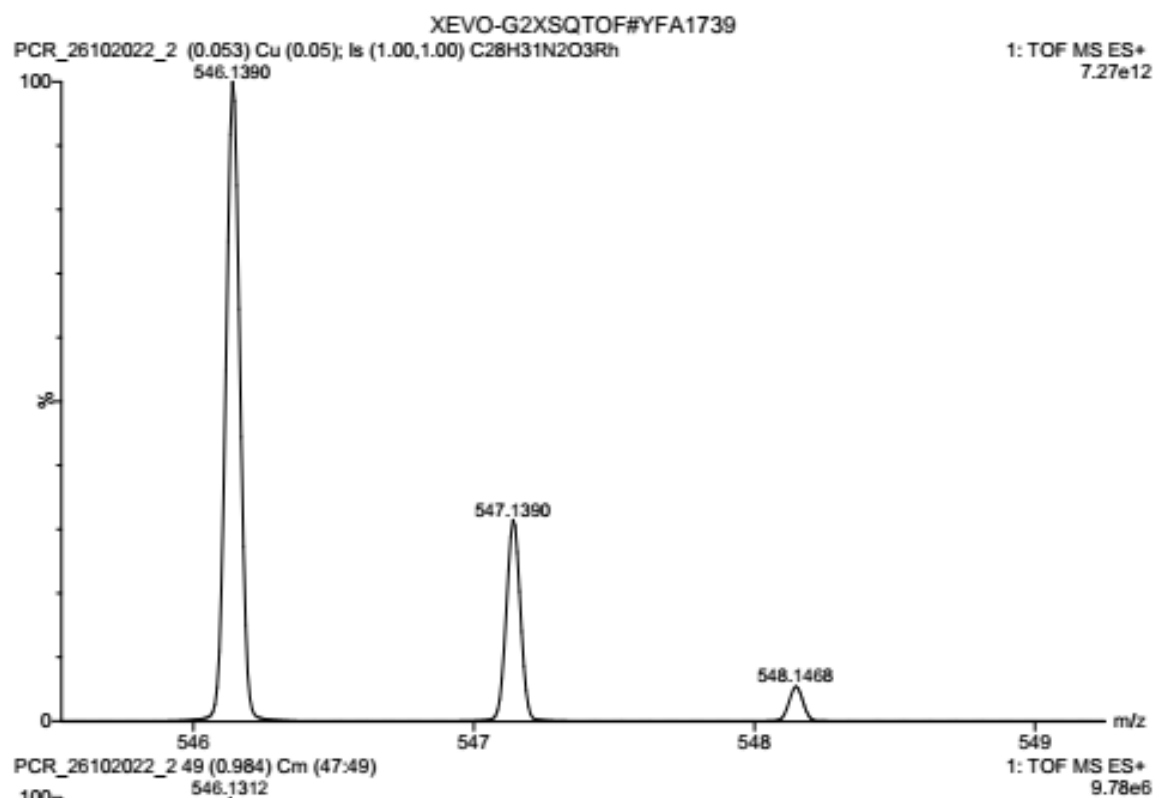


Figure 5.4 Mass analysis for reaction of **1b** with **3bc**



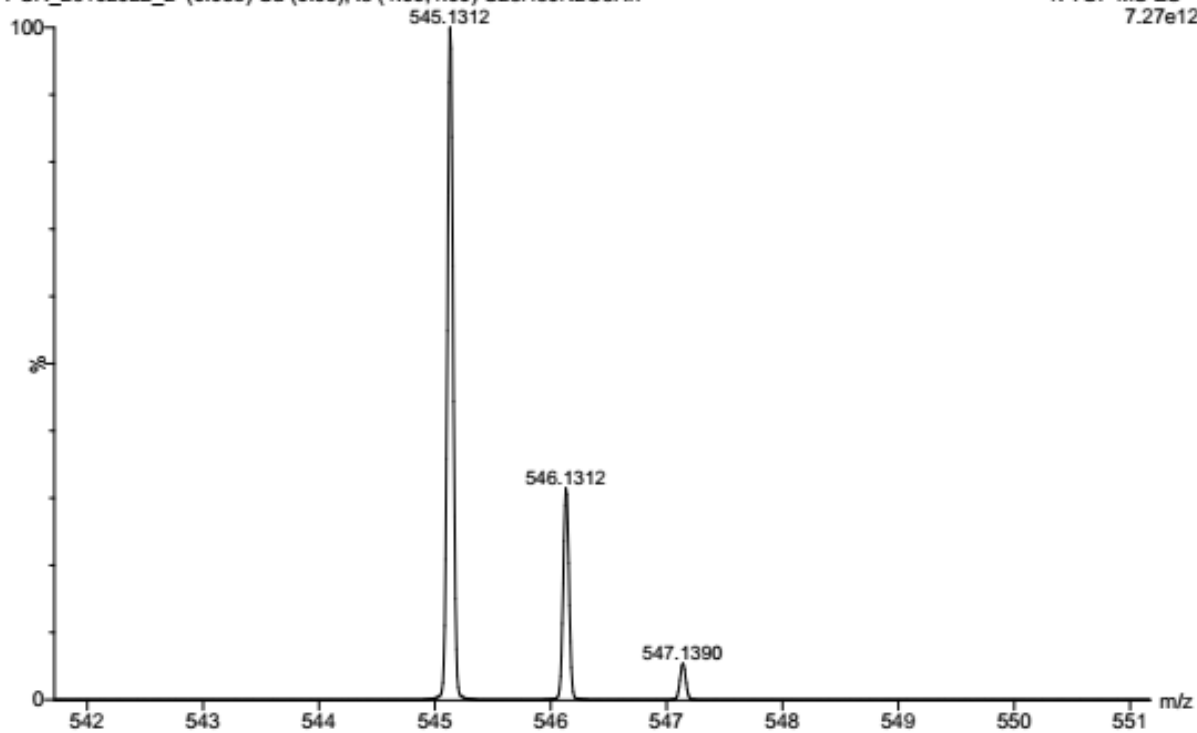






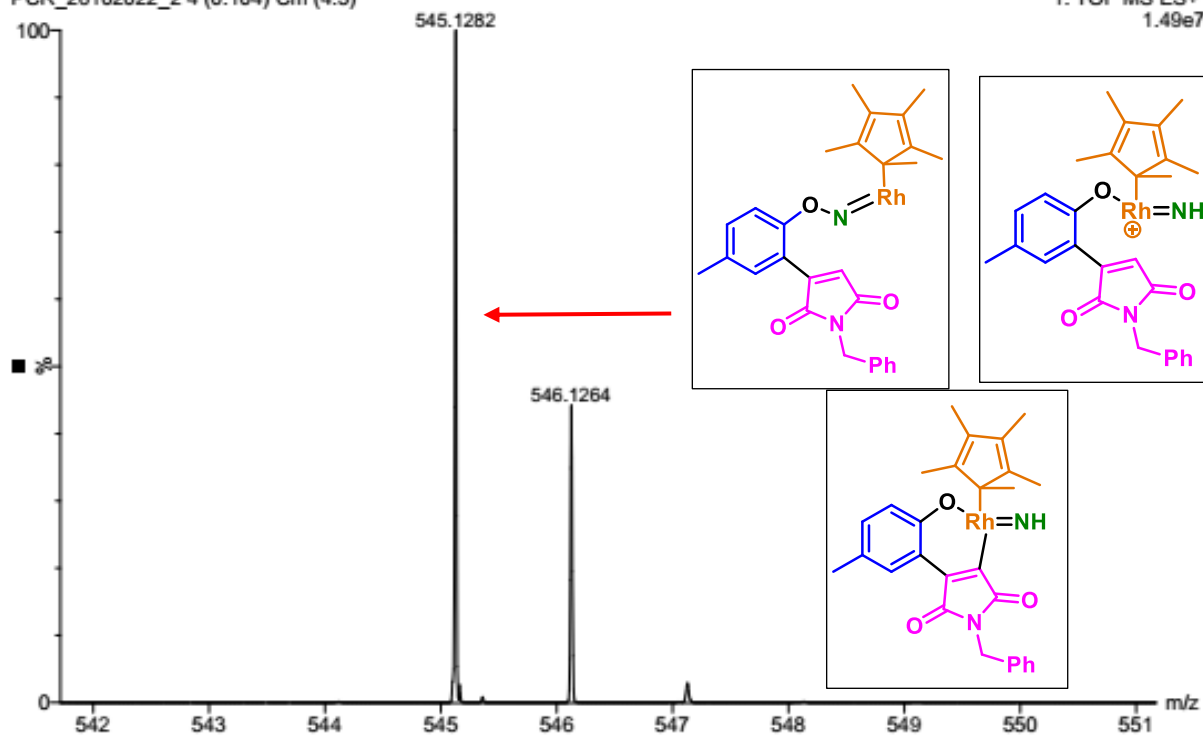
PCR_26102022_2 (0.053) Cu (0.05); Is (1.00,1.00) C₂₈H₃₀N₂O₃Rh

1: TOF MS ES+
7.27e12

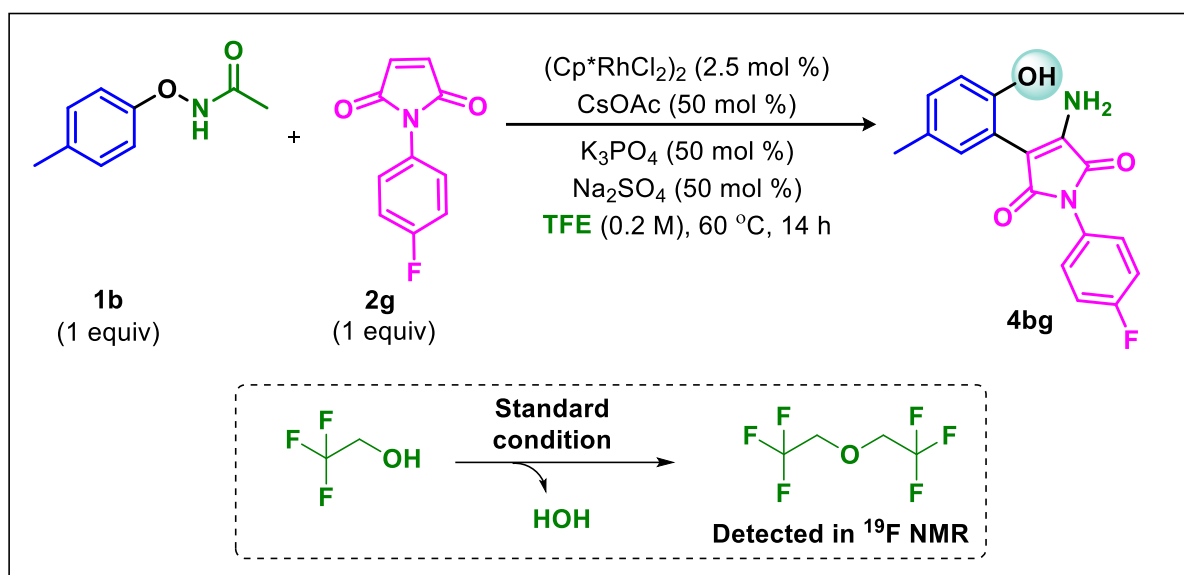


PCR_26102022_2 4 (0.104) Cm (4:5)

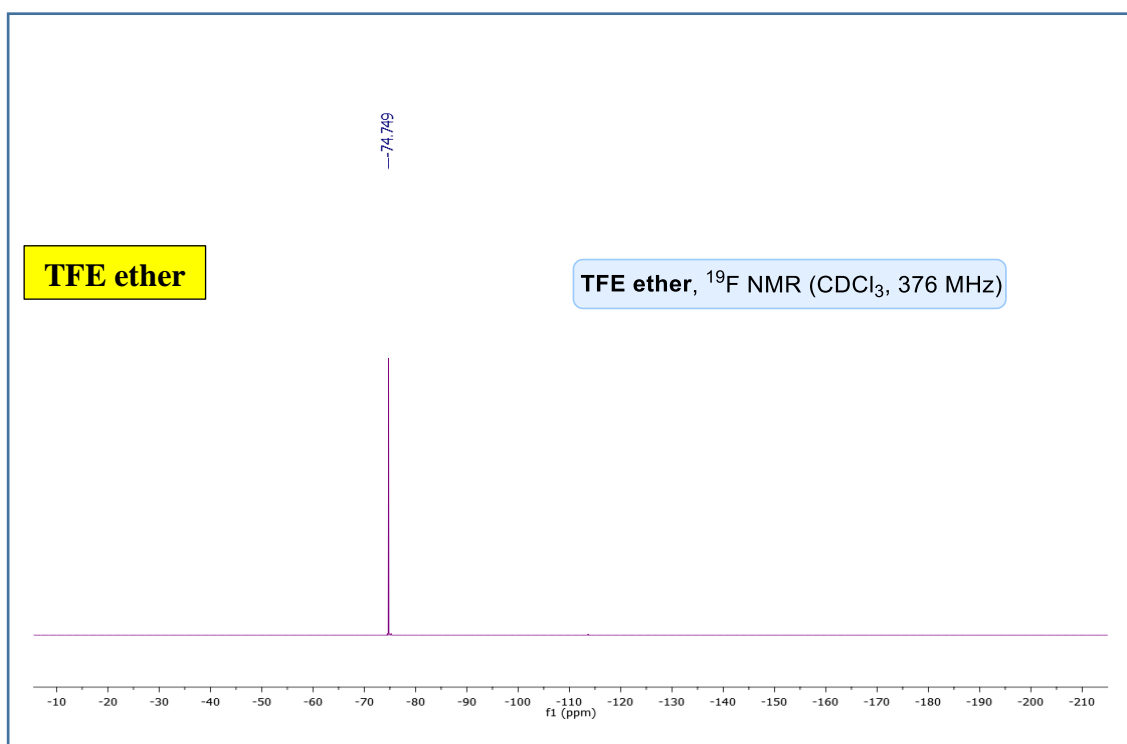
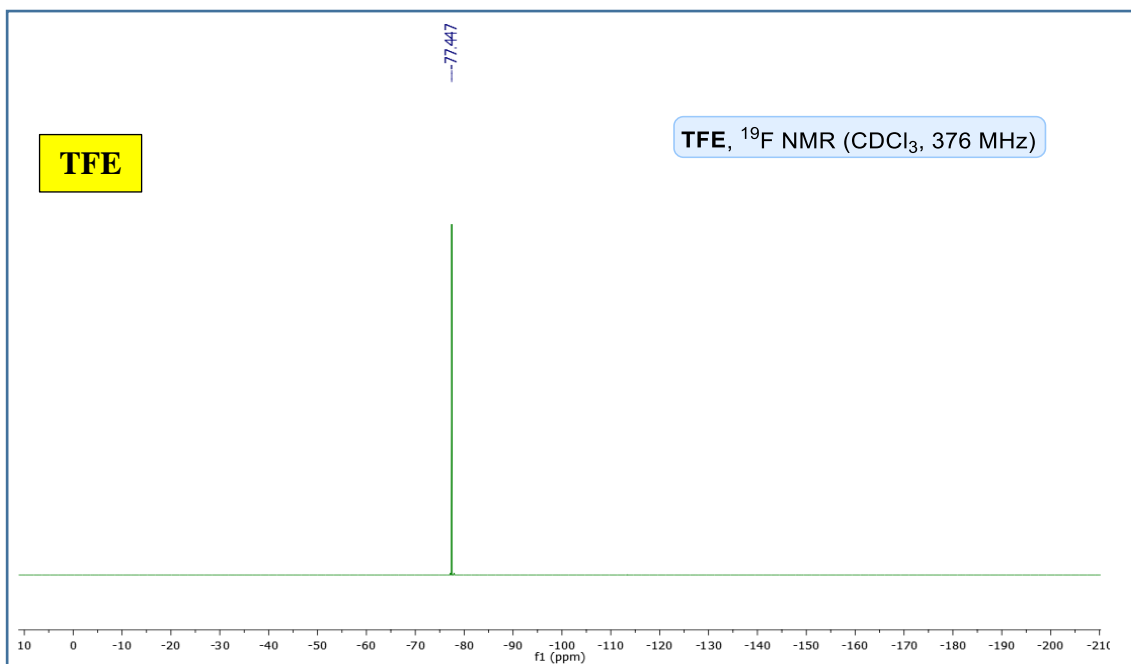
1: TOF MS ES+
1.49e7

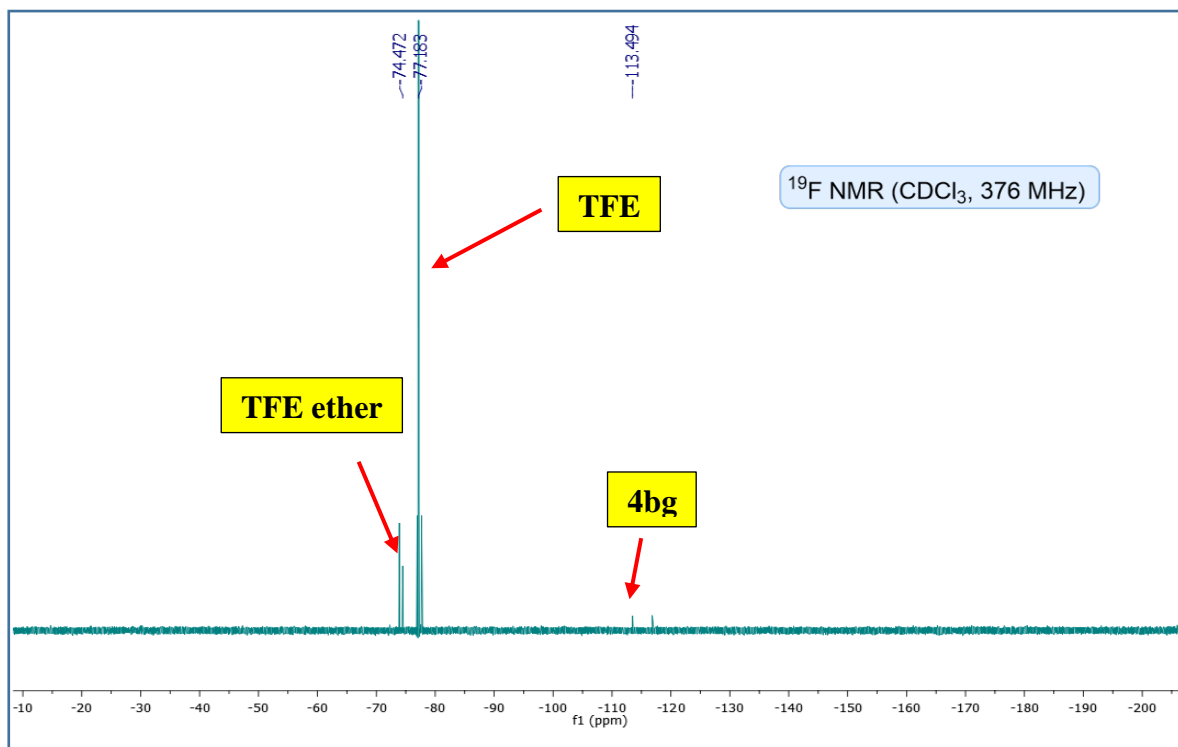


(4.4) ^{19}F NMR experiment:

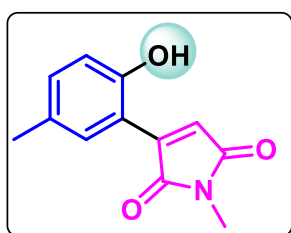


To an oven-dried seal tube charged with a stir bar, *N*-(*p*-tolyl)oxyacetamide **1b** (0.1 mmol, 1 equiv), 1-(4-fluorophenyl)-1H-pyrrole-2,5-dione **2g** (0.1 mmol, 1 equiv), $(\text{Cp}^*\text{RhCl}_2)_2$ (0.0025 mmol, 2.5 mol %), Na_2SO_4 (0.05 mmol, 50 mol %), and TFE (0.5 mL, 0.2 M with respect to **1b**) were added under nitrogen atmosphere. The seal tube was taken inside the glove box, and CsOAc (0.05 mmol, 50 mol %), K_3PO_4 (0.05 mmol, 50 mol %), were added. The reaction mixture was stirred (700 rpm) in a preheated aluminum block at 60 °C for 14 h. After 14 h, the residue was filtered through a nylon filter and submitted for ^{19}F NMR analysis with CDCl_3 as solvent.





Experimental characterization data of products:



3-(2-hydroxy-5-methylphenyl)-1-methyl-1H-pyrrole-2,5-dione

(*3ba*):

Physical State: yellow solid (13 mg, 60%), $R_f = 0.5$ (10%

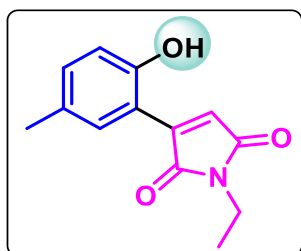
EtOAc/hexane), **mp** = 223-224 °C. ^1H NMR (CDCl_3 , 700 MHz):

δ 9.74 (s, 1H), 7.35 (s, 1H), 7.18 (dd, $J = 8.4$ Hz, 1.4 Hz, 1H), 6.90 (d, $J = 8.4$ Hz, 1H), 6.77

(s, 1H), 3.12 (s, 3H), 2.29 (s, 3H). $^{13}\text{C}\{^1\text{H}\}$ NMR (CDCl_3 , 175 MHz): δ 174.5, 170.2, 154.0,

146.0, 135.3, 130.3, 130.0, 124.0, 119.9, 115.1, 24.5, 20.7. **IR** (KBr, cm^{-1}): 3438, 1635.

HRMS (ESI) m/z: $[\text{M}+\text{H}]^+$ Calcd for $\text{C}_{12}\text{H}_{12}\text{NO}_3$: 218.0817; Found: 218.0833.



1-ethyl-3-(2-hydroxy-5-methylphenyl)-1H-pyrrole-2,5-dione

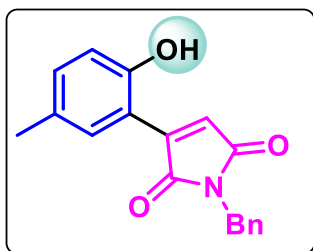
(*3bb*):

Physical State: yellow solid (17 mg, 74%), $R_f = 0.5$ (10%

EtOAc/hexane), **mp** = 147 -148 °C. ^1H NMR (CDCl_3 , 400

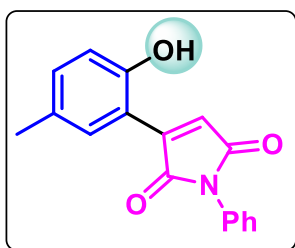
MHz): δ 9.85 (s, 1H), 7.34 (brs, 1H), 7.18 (dd, $J = 8.4$ Hz, 1.6 Hz, 1H), 6.90 (d, $J = 8.4\text{Hz}$,

1H), 6.75 (s, 1H), 3.67 (q, $J = 7.2$ Hz, 2H), 2.29 (s, 3H), 1.25 (t, $J = 7.2$ Hz, 3H). $^{13}\text{C}\{^1\text{H}\}$ NMR (CDCl_3 , 175 MHz): δ 174.3, 170.0, 154.8, 145.9, 135.3, 130.3, 130.0, 123.9, 119.9, 115.1, 33.7, 20.7, 14.1. IR (KBr, cm^{-1}): 3438, 1683, 1635. HRMS (ESI) m/z : $[\text{M}+\text{H}]^+$ Calcd for $\text{C}_{13}\text{H}_{14}\text{NO}_3$: 232.0974; Found: 232.0984.



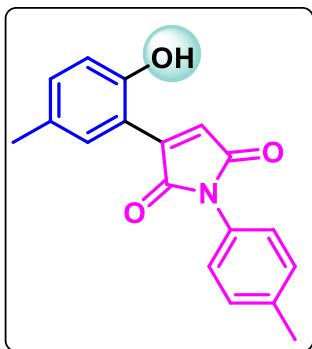
1-benzyl-3-(2-hydroxy-5-methylphenyl)-1H-pyrrole-2,5-dione
(3bc):

Physical State: yellow solid (28 mg, 95%), $R_f = 0.5$ (10% EtOAc/hexane), **mp** = 167-168 °C. ^1H NMR (CDCl_3 , 700 MHz): δ 9.56 (s, 1H), 7.38-7.36 (m, 3H), 7.33 (t, $J = 7.7$ Hz, 2H), 7.29 (d, $J = 7$ Hz, 1H), 7.16 (d, $J = 8.4$ Hz, 1H), 6.88 (d, $J = 8.4$ Hz, 1H), 6.79 (s, 1H), 4.76 (s, 2H), 2.28 (s, 3H). $^{13}\text{C}\{^1\text{H}\}$ NMR (CDCl_3 , 175 MHz): δ 174.1, 169.9, 154.0, 145.7, 136.0, 135.3, 130.3, 130.0, 129.1, 128.8, 128.4, 124.1, 119.8, 115.1, 42.2, 20.7. IR (KBr, cm^{-1}): 3438, 1682, 1634. HRMS (ESI) m/z : $[\text{M}+\text{H}]^+$ Calcd for $\text{C}_{18}\text{H}_{16}\text{NO}_3$: 294.1130; Found: 294.1147.



3-(2-hydroxy-5-methylphenyl)-1-phenyl-1H-pyrrole-2,5-dione
(3bd):

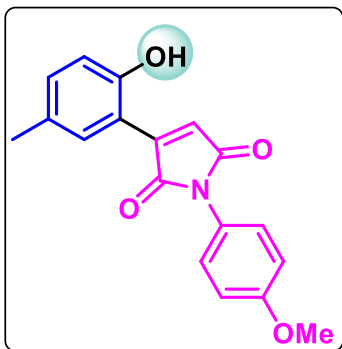
Physical State: yellow solid (17 mg, 61%), $R_f = 0.5$ (10% EtOAc/hexane), **mp** = 173 °C. ^1H NMR (CDCl_3 , 700 MHz): δ 9.27 (s, 1H), 7.50 (t, $J = 7$ Hz, 2H), 7.47 (s, 1H), 7.41 (t, $J = 7$ Hz, 1H), 7.38 (d, $J = 7$ Hz, 2H), 7.21 (d, $J = 8.4$ Hz, 1H), 6.95 (s, 1H), 6.91 (d, $J = 8.4$ Hz, 1H), 2.32 (s, 3H). $^{13}\text{C}\{^1\text{H}\}$ NMR (CDCl_3 , 175 MHz): δ 173.2, 169.2, 154.1, 145.3, 135.3, 131.2, 130.5, 130.4, 129.5, 128.7, 126.7, 124.6, 119.7, 115.2, 20.7. IR (KBr, cm^{-1}): 3423, 1700, 1617. HRMS (ESI) m/z : $[\text{M}+\text{H}]^+$ Calcd for $\text{C}_{17}\text{H}_{14}\text{NO}_3$: 280.0974; Found: 280.0958.



3-(2-hydroxy-5-methylphenyl)-1-(p-tolyl)-1H-pyrrole-2,5-dione (3be):

Physical State: yellow solid (16 mg, 55%), $R_f = 0.5$ (10% EtOAc/hexane), **mp** = 193-194 °C. **^1H NMR** (CDCl_3 , 400

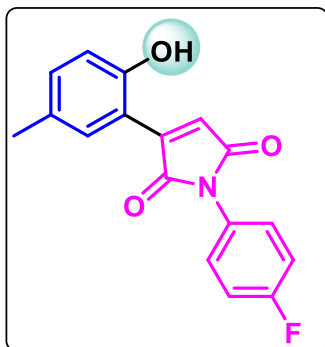
MHz): δ 9.38 (s, 1H), 7.45 (s, 1H), 7.30 (d, $J = 8.4$ Hz, 2H), 7.25-7.19 (m, 3H), 6.92-6.90 (m, 2H), 2.40 (s, 3H), 2.31 (s, 3H). **$^{13}\text{C}\{^1\text{H}\}$ NMR** (CDCl_3 , 175 MHz): δ 173.4, 169.3, 154.1, 145.4, 138.8, 135.4, 130.5, 130.3, 132.2, 128.5, 126.6, 124.4, 119.8, 115.2, 21.5, 20.7. **IR** (KBr, cm^{-1}): 3421, 1693, 1611. **HRMS** (ESI) **m/z:** $[\text{M}+\text{H}]^+$ Calcd for $\text{C}_{18}\text{H}_{16}\text{NO}_3$: 294.1130; Found: 294.1132.



3-(2-hydroxy-5-methylphenyl)-1-(4-methoxyphenyl)-1H-pyrrole-2,5-dione (3bf):

Physical State: yellow solid (18 mg, 58%), $R_f = 0.5$ (10% EtOAc/hexane), **mp** = 154-155 °C. **^1H NMR** (CDCl_3 , 700 MHz): δ 9.41 (s, 1H), 7.45 (s, 1H), 7.27 (d, $J = 8.4$ Hz, 2H), 7.20 (d, $J = 8.4$ Hz, 1H), 7.01 (d, $J = 9.1$ Hz, 2H) 6.92-6.90

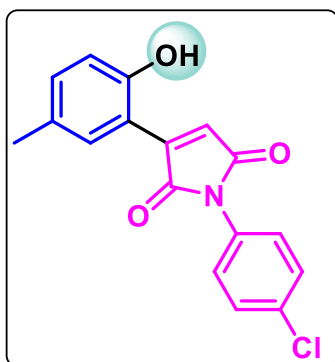
(m, 2H), 3.84 (s, 3H), 2.31 (s, 3H). **$^{13}\text{C}\{^1\text{H}\}$ NMR** (CDCl_3 , 175 MHz): δ 173.5, 169.5, 159.8, 154.1, 145.4, 135.4, 130.5, 130.3, 128.1, 124.3, 123.8, 119.8, 115.2, 114.9, 55.8, 20.7. **IR** (KBr, cm^{-1}): 3438, 1697, 1633. **HRMS** (ESI) **m/z:** $[\text{M}+\text{H}]^+$ Calcd for $\text{C}_{18}\text{H}_{16}\text{NO}_4$: 310.1079; Found: 310.1062.



1-(4-fluorophenyl)-3-(2-hydroxy-5-methylphenyl)-1H-pyrrole-2,5-dione (3bg):

Physical State: yellow solid (20 mg, 67%), $R_f = 0.5$ (10% EtOAc/hexane), **mp** = 189-190 °C. **^1H NMR (CDCl₃, 400 MHz):** δ 9.05 (s, 1H), 7.48 (brs, 1H), 7.39-7.35 (m, 2H), 7.22-7.19 (m, 3H), 6.96 (s, 1H), 6.91 (d, $J = 8.4$ Hz, 1H), 2.32 (s, 3H). **$^{13}\text{C}\{^1\text{H}\}$**

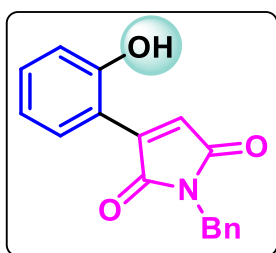
NMR (CDCl₃, 175 MHz): δ 173.0, 169.0, 162.4 (d, $J_{C-F} = 247.1$ Hz), 154.1, 145.2, 135.4, 130.6, 130.4, 128.5 (d, $J_{C-F} = 8.7$ Hz), 127.2 (d, $J_{C-F} = 2.6$ Hz), 124.6, 119.7, 116.6 (d, $J_{C-F} = 22.7$ Hz), 115.1, 20.7. **^{19}F NMR (CDCl₃, 376 MHz):** δ -112.5. **IR (KBr, cm⁻¹):** 3437, 1709, 1636. **HRMS (ESI) m/z:** [M+H]⁺ Calcd for C₁₇H₁₃NO₃F: 298.0879; Found: 298.0896.



1-(4-chlorophenyl)-3-(2-hydroxy-5-methylphenyl)-1H-pyrrole-2,5-dione (3bh):

Physical State: yellow solid (22 mg, 70%), $R_f = 0.5$ (30% EtOAc/hexane), **mp** = 210-211 °C. **^1H NMR (CDCl₃, 400 MHz):** δ 8.93 (s, 1H), 7.49-7.45 (m, 3H), 7.37-7.34 (m, 2H),

7.21 (dd, $J = 8.4$ Hz, 2 Hz, 1H), 6.97 (s, 1H), 6.91 (d, $J = 8.4$ Hz, 1H), 2.32 (s, 3H). **$^{13}\text{C}\{^1\text{H}\}$** NMR (CDCl₃, 175 MHz): δ 172.7, 168.9, 154.1, 145.1, 135.4, 134.4, 130.7, 130.4, 129.8, 129.7, 127.7, 124.7, 119.6, 115.1, 20.7. **IR (KBr, cm⁻¹):** 3420, 1684, 1635. **HRMS (ESI) m/z:** [M+H]⁺ Calcd for C₁₇H₁₃NO₃Cl: 314.0584; Found: 314.0578.

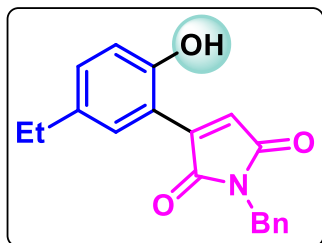


1-benzyl-3-(2-hydroxyphenyl)-1H-pyrrole-2,5-dione (3ac):

Physical State: yellow solid (24 mg, 86%), $R_f = 0.5$ (10% EtOAc/hexane), **mp** = 171-172 °C. **^1H NMR (CDCl₃, 400 MHz):** δ 9.80 (s, 1H), 7.59 (dd, $J = 8.0$ Hz, 1.6 Hz, 1H), 7.40-7.29 (m,

6H), 6.98 (dd, $J = 8.0$ Hz, 1.6 Hz, 1H), 6.94 (t, $J = 8.0$ Hz, 1H), 6.81 (s, 1H), 4.77 (s, 2H). **$^{13}\text{C}\{^1\text{H}\}$** NMR (CDCl₃, 175 MHz): δ 174.1, 169.8, 156.1, 145.7, 136.0, 134.3, 130.2, 129.1,

128.8, 128.4, 124.3, 121.1, 120.0, 115.4, 42.3. **IR (KBr, cm⁻¹):** 3438, 1698, 1606. **HRMS (ESI) m/z:** [M+Na]⁺ Calcd for C₁₇H₁₃NO₃Na: 302.0793; Found: 302.0803.

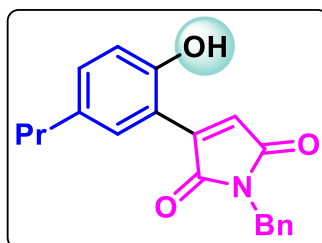


1-benzyl-3-(5-ethyl-2-hydroxyphenyl)-1H-pyrrole-2,5-dione

(3cc):

Physical State: yellow solid (26 mg, 85%), **R_f** = 0.5 (10% EtOAc/hexane), **mp** = 147-148 °C. **¹H NMR (CDCl₃, 400**

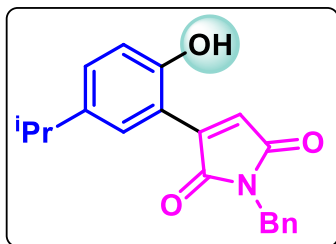
MHz): δ 9.59 (s, 1H), 7.38-7.37 (m, 3H), 7.33 (t, *J* = 7.0 Hz, 2H), 7.29 (t, *J* = 7.0 Hz, 1H), 7.20 (dd, *J* = 8.4 Hz, 2.1, Hz, 1H), 6.91 (d, *J* = 8.4 Hz, 1H), 6.80 (s, 1H), 4.77 (s, 2H), 2.58 (q, *J* = 7.7 Hz, 2H), 1.20 (t, *J* = 7.7 Hz, 3H). **¹³C{¹H} NMR (CDCl₃, 175 MHz):** δ 174.1, 169.9, 154.2, 145.8, 136.8, 136.0, 134.2, 129.1, 128.9, 128.8, 128.3, 124.0, 119.9, 115.1, 42.2, 28.2, 15.9. **IR (KBr, cm⁻¹):** 3437, 1684, 1635. **HRMS (ESI) m/z:** [M+H]⁺ Calcd for C₁₉H₁₈NO₃: 308.1287; Found: 308.1274.



1-benzyl-3-(2-hydroxy-5-propylphenyl)-1H-pyrrole-2,5-dione (3dc):

Physical State: yellow solid (28 mg, 87%), **R_f** = 0.5 (10% EtOAc/hexane), **mp** = 136-137 °C. **¹H NMR (CDCl₃, 400**

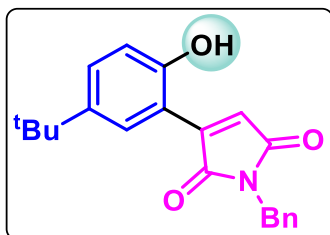
MHz): δ 9.59 (s, 1H), 7.39-7.28 (m, 6H), 7.17 (dd, *J* = 8.4 Hz, 2.0 Hz, 1H), 6.90 (d, *J* = 8.4 Hz, 1H), 6.80 (s, 1H), 4.76 (s, 2H), 2.51 (t, *J* = 7.2 Hz, 2H), 1.62-1.55 (m, 2H), 0.92 (t, *J* = 7.2 Hz, 3H). **¹³C{¹H} NMR (CDCl₃, 175 MHz):** δ 174.1, 169.9, 154.2, 145.7, 136.0, 135.3, 134.7, 129.6, 129.1, 128.8, 128.3, 124.0, 119.8, 115.1, 42.2, 37.2, 24.8, 13.9. **IR (KBr, cm⁻¹):** 3438, 1685, 1635. **HRMS (ESI) m/z:** [M+H]⁺ Calcd for C₂₀H₂₀NO₃: 322.1443; Found: 322.1429.



1-benzyl-3-(2-hydroxy-5-isopropylphenyl)-1H-pyrrole-2,5-dione (3ec):

Physical State: yellow solid (27 mg, 84%), $R_f = 0.5$ (10% EtOAc/hexane), **mp** = 136-137 °C. ^1H NMR (CDCl_3 , 400

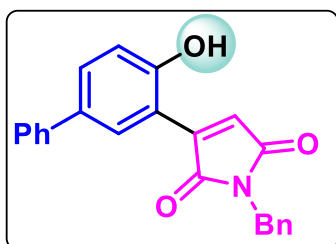
MHz): δ 9.58 (s, 1H), 7.40-7.28 (m, 6H), 7.25-7.23 (m, 1H), 6.92 (d, $J = 8.4$ Hz, 1H), 6.80 (s, 1H), 4.77 (s, 2H), 2.85 (sept, $J = 6.8$ Hz, 1H), 1.22 (d, $J = 7.2$ Hz, 6H). $^{13}\text{C}\{^1\text{H}\}$ NMR (CDCl_3 , 175 MHz): δ 174.1, 169.9, 154.2, 145.9, 141.5, 136.0, 132.7, 129.1, 128.8, 128.3, 127.6, 124.0, 119.9, 115.1, 42.2, 33.5, 24.3. **IR (KBr, cm^{-1}):** 3438, 1682, 1641. **HRMS (ESI) m/z:** $[\text{M}+\text{H}]^+$ Calcd for $\text{C}_{20}\text{H}_{20}\text{NO}_3$: 322.1443; Found: 322.1423.



1-benzyl-3-(5-(tert-butyl)-2-hydroxyphenyl)-1H-pyrrole-2,5-dione (3fc):

Physical State: yellow solid (30 mg, 90%), $R_f = 0.5$ (10% EtOAc/hexane), **mp** = 123-124 °C. ^1H NMR (CDCl_3 , 700

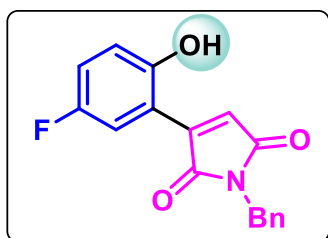
MHz): δ 9.57 (s, 1H), 7.54 (d, $J = 2.1$ Hz, 1H), 7.41 (dd, $J = 9.1$ Hz, 2.8 Hz, 1H), 7.37 (d, $J = 7.7$ Hz, 2H), 7.33 (t, $J = 7.7$ Hz, 2H), 7.29 (d, $J = 7.0$ Hz, 1H), 6.92 (d, $J = 9.1$ Hz, 1H), 6.80 (s, 1H), 4.77 (s, 2H), 1.29 (s, 9H). $^{13}\text{C}\{^1\text{H}\}$ NMR (CDCl_3 , 175 MHz): δ 174.1, 169.9, 153.9, 146.1, 143.8, 136.0, 132.0, 129.1, 128.8, 128.3, 126.4, 124.0, 119.6, 114.7, 42.2, 34.4, 31.6. **IR (KBr, cm^{-1}):** 3437, 1689, 1613. **HRMS (ESI) m/z:** $[\text{M}+\text{H}]^+$ Calcd for $\text{C}_{21}\text{H}_{22}\text{NO}_3$: 336.1600; Found: 336.1632.



1-benzyl-3-(4-hydroxy-[1,1'-biphenyl]-3-yl)-1H-pyrrole-2,5-dione (3gc):

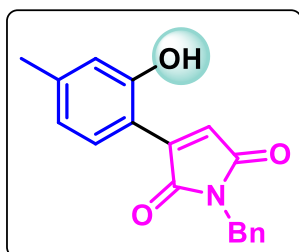
Physical State: yellow solid (22 mg, 62%), $R_f = 0.5$ (10% EtOAc/hexane), **mp** = 169-170 °C. ^1H NMR (CDCl_3 , 700

¹H NMR (CDCl₃, 400 MHz): δ 9.88 (s, 1H), 7.78 (d, J = 2.1 Hz, 1H), 7.60 (dd, J = 9.1 Hz, 2.8 Hz, 1H), 7.52 (d, J = 7.0 Hz, 2H), 7.43 (t, J = 7.7 Hz, 2H), 7.40 (d, J = 7.0 Hz, 2H), 7.35-7.34 (m, 3H), 7.30 (d, J = 7 Hz, 1H), 7.06 (d, J = 8.4 Hz, 1H), 6.88 (s, 1H), 4.79 (s, 2H). **¹³C{¹H} NMR (CDCl₃, 175 MHz):** δ 174.1, 169.7, 155.6, 149.5, 145.7, 140.1, 135.9, 134.4, 133.2, 129.2, 129.1, 128.9, 128.6, 127.6, 127.0, 124.5, 120.5, 115.7, 42.3. **IR (KBr, cm⁻¹):** 3438, 1683, 1639. **HRMS (ESI) m/z:** [M+H]⁺ Calcd for C₂₃H₁₈NO₃: 356.1287; Found: 356.1294.



1-benzyl-3-(5-fluoro-2-hydroxyphenyl)-1H-pyrrole-2,5-dione (3hc):

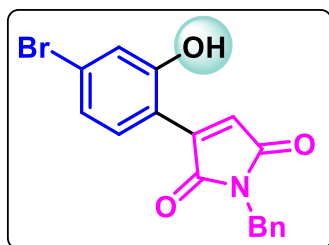
Physical State: yellow solid (24 mg, 81%), R_f = 0.4 (20% EtOAc/hexane), **mp** = 153-154 °C. **¹H NMR (CDCl₃, 400 MHz):** δ 9.49 (s, 1H), 7.39-7.29 (m, 6H), 7.08 (td, J = 10.0 Hz, 3.2 Hz, 1H), 6.95-6.91 (m, 1H), 6.83 (s, 1H), 4.77 (s, 2H). **¹³C{¹H} NMR (CDCl₃, 100 MHz):** δ 173.4, 169.4, 156.9 (d, J = 237.3 Hz) 152.5, 144.3, 135.8, 129.0 (d, J = 25.5 Hz), 128.5, 125.5, 121.5, 121.2 (d, J = 4.1 Hz), 121.1, 115.9 (d, J = 7.7 Hz), 115.3 (d, J = 24.2 Hz), 42.4. **¹⁹F NMR (CDCl₃, 376 MHz):** δ -123.37. **IR (KBr, cm⁻¹):** 3438, 1684, 1634. **HRMS (ESI) m/z:** [M+H]⁺ Calcd for C₁₇H₁₃NO₃F: 298.0879; Found: 298.0884.



1-benzyl-3-(2-hydroxy-4-methylphenyl)-1H-pyrrole-2,5-dione (3jc):

Physical State: yellow solid (25 mg, 84%), R_f = 0.5 (10% EtOAc/hexane), **mp** = 168-169 °C. **¹H NMR (CDCl₃, 700 MHz):** δ 9.96 (s, 1H), 7.47 (d, J = 7.0 Hz, 1H), 7.36 (d, J = 7.0 Hz, 2H), 7.33 (t, J = 7.0 Hz, 2H), 7.28 (t, J = 7.0 Hz, 1H), 6.79 (s, 1H), 6.75 (d, J = 8.4 Hz, 1H), 6.73 (s, 1H), 4.76 (s, 2H), 2.32 (s, 3H). **¹³C{¹H} NMR (CDCl₃, 175 MHz):** δ 174.2, 170.0, 156.1, 145.8, 145.6, 136.0,

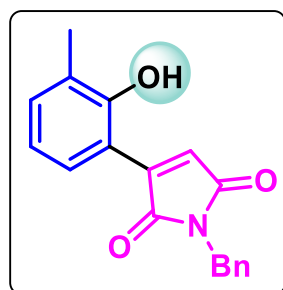
130.0, 129.1, 128.8, 128.4, 122.7, 122.5, 120.2, 112.7, 42.2, 21.7. **IR (KBr, cm⁻¹):** 3438, 1682, 1634. **HRMS (ESI) m/z:** [M+H]⁺ Calcd for C₁₈H₁₆NO₃: 294.1130; Found: 294.0930.



3-(4-bromo-2-hydroxyphenyl)-1-ethyl-1H-pyrrole-2,5-dione (3kc):

Physical State: yellow solid (15 mg, 42%), **R_f** = 0.4 (20% EtOAc/hexane), **mp** = 190-191 °C. **¹H NMR (CDCl₃, 400**

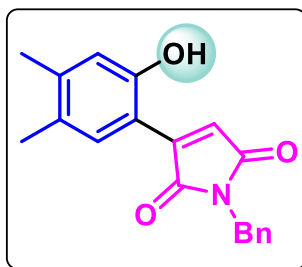
MHz): δ 10.23 (s, 1H), 7.43 (d, *J* = 8.4 Hz, 1H), 7.39-7.29 (m, 5H), 7.18 (d, *J* = 2.0 Hz, 1H), 7.06 (dd, *J* = 8.8 Hz, 2.0 Hz, 1H), 6.80 (s, 1H), 4.77 (s, 2H). **¹³C{¹H} NMR (CDCl₃, 175 MHz):** δ 174.0, 169.5, 156.7, 145.1, 135.8, 131.1, 129.1, 128.9, 128.5, 128.29, 124.5, 124.2, 123.2, 114.5, 42.4. **IR (KBr, cm⁻¹):** 3438, 1634. **HRMS (ESI) m/z:** [M+H]⁺ Calcd for C₁₇H₁₃NO₃Br: 358.0079; Found: 358.0072.



1-benzyl-3-(2-hydroxy-3-methylphenyl)-1H-pyrrole-2,5-dione (3lc):

Physical State: yellow solid (9 mg, 31%), **R_f** = 0.5 (10% EtOAc/hexane) **mp** = 153-154 °C. **¹H NMR (CDCl₃, 400 MHz):**

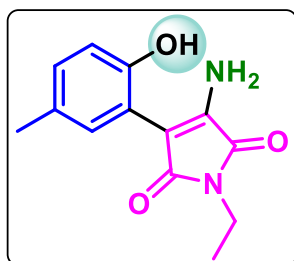
δ 10.03 (s, 1H), 7.39-7.28 (m, 6H), 7.26-7.24 (m, 1H), 6.84 (t, *J* = 7.6 Hz, 1H), 6.75 (s, 1H), 4.77 (s, 2H), 2.27 (s, 3H). **¹³C{¹H} NMR (CDCl₃, 175 MHz):** δ 174.3, 169.7, 154.3, 146.5, 136.0, 135.2, 129.1, 128.9, 128.4, 127.9, 124.2, 120.8, 115.3, 115.1, 42.3, 17.0. **IR (KBr, cm⁻¹):** 3422, 1684. **HRMS (ESI) m/z:** [M+H]⁺ Calcd for C₁₈H₁₆NO₃: 294.1130; Found: 294.1132.



1-benzyl-3-(2-hydroxy-4,5-dimethylphenyl)-1H-pyrrole-2,5-dione (3nc):

Physical State: yellow solid (26 mg, 85%), $R_f = 0.5$ (10%

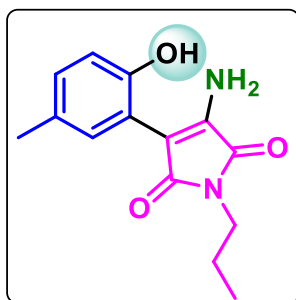
EtOAc/hexane), $mp = 174-175\text{ }^\circ\text{C}$. $^1\text{H NMR}$ (CDCl_3 , 700 MHz): δ 9.86 (s, 1H), 7.38 (d, $J = 7.0$ Hz, 2H), 7.33 (t, $J = 7.0$ Hz, 2H), 7.29-7.27 (m, 2H), 6.78 (s, 1H), 6.71 (s, 1H), 4.76 (s, 2H), 2.23 (s, 3H), 2.19 (s, 3H). $^{13}\text{C}\{^1\text{H}\}$ NMR (CDCl_3 , 175 MHz): δ 174.3, 170.0, 154.3, 145.9, 144.6, 136.1, 130.3, 129.5, 129.1, 128.8, 128.3, 122.3, 120.2, 112.7, 42.2, 20.3, 19.1. **IR** (KBr, cm^{-1}): 3438, 1680, 1634. **HRMS** (ESI) m/z : $[\text{M}+\text{H}]^+$ Calcd for $\text{C}_{19}\text{H}_{18}\text{NO}_3$: 308.1287; Found: 308.1300.



3-amino-1-ethyl-4-(2-hydroxy-5-methylphenyl)-1H-pyrrole-2,5-dione (4bb):

Physical State: yellow solid (16 mg, 65%), $R_f = 0.3$ (20%

EtOAc/hexane), $mp = 179-180\text{ }^\circ\text{C}$. $^1\text{H NMR}$ (CDCl_3 , 700 MHz): δ 7.38 (s, 1H), 7.16 (s, 1H), 7.04 (d, $J = 8.4$ Hz, 1H), 6.91 (d, $J = 7.7$ Hz, 1H), 5.37 (s, 2H), 3.64 (q, $J = 7.7$ Hz, 2H), 2.31 (s, 3H), 1.26 (t, $J = 7.0$ Hz, 3H). $^{13}\text{C}\{^1\text{H}\}$ NMR (CDCl_3 175 MHz): δ 174.5, 167.5, 151.3, 142.9, 130.7, 130.5, 129.1, 118.8, 117.5, 100.1, 33.4, 20.9, 14.3. **IR** (KBr, cm^{-1}): 3429, 1642. **HRMS** (ESI) m/z : $[\text{M}+\text{H}]^+$ Calcd for $\text{C}_{13}\text{H}_{15}\text{N}_2\text{O}_3$: 247.1083; Found: 247.1092.

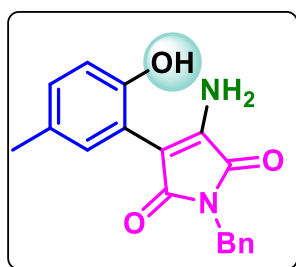


3-amino-4-(2-hydroxy-5-methylphenyl)-1-propyl-1H-pyrrole-2,5-dione (4bb'):

Physical State: orange liquid (15 mg, 58%), $R_f = 0.3$ (20%

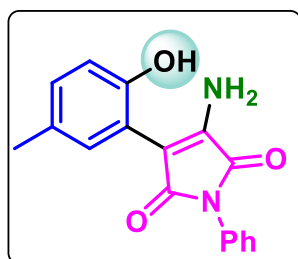
EtOAc/Hexane). $^1\text{H NMR}$ (CDCl_3 , 400 MHz): δ 7.39 (s, 1H), 7.14 (s, 1H), 7.02 (d, $J = 8.0$ Hz, 1H), 6.89 (d, $J = 8.0$ Hz, 1H),

5.36 (s, 2H), 3.52 (t, $J = 8.0$ Hz, 2H), 2.29 (s, 3H), 1.70-1.63 (m, 2H), 0.93 (t, $J = 8.0$ Hz, 3H). $^{13}\text{C}\{^1\text{H}\}$ NMR (CDCl_3 , 175 MHz): δ 174.8, 167.7, 151.3, 142.8, 130.6, 130.5, 129.1, 118.9, 117.5, 100.0, 40.1, 22.3, 20.9, 11.6. IR (KBr, cm^{-1}): 3438, 1649. HRMS (ESI) m/z : $[\text{M}+\text{H}]^+$ Calcd for $\text{C}_{14}\text{H}_{17}\text{N}_2\text{O}_3$: 261.1239; Found: 261.1225.



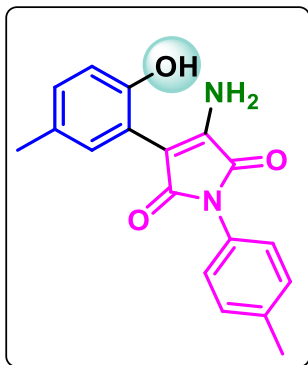
3-amino-1-benzyl-4-(2-hydroxy-5-methylphenyl)-1H-pyrrole-2,5-dione (4bc):

Physical State: orange liquid (17 mg, 55%), $R_f = 0.3$ (20% EtOAc/hexane). ^1H NMR (CDCl_3 , 400 MHz): δ 7.39-7.37 (m, 2H), 7.34-7.27 (m, 3H), 7.15 (d, $J = 1.6$ Hz, 2H), 7.01 (dd, $J = 8.0$ Hz, 1.6 Hz, 1H), 6.86 (d, $J = 8.4$ Hz, 1H), 5.36 (s, 2H), 4.71 (s, 2H), 2.28 (s, 3H). $^{13}\text{C}\{^1\text{H}\}$ NMR (CDCl_3 , 176 MHz): δ 174.0, 167.3, 151.2, 143.0, 136.6, 130.7, 130.5, 129.3, 129.0, 128.8, 128.1, 118.6, 117.3, 100.1, 42.0, 20.9. IR (KBr, cm^{-1}): 3438, 1643. HRMS (ESI) m/z : $[\text{M}+\text{H}]^+$ Calcd for $\text{C}_{18}\text{H}_{17}\text{N}_2\text{O}_3$: 309.1239; Found: 309.1252.



3-amino-1-benzyl-4-(2-hydroxy-5-methylphenyl)-1H-pyrrole-2,5-dione (4bd):

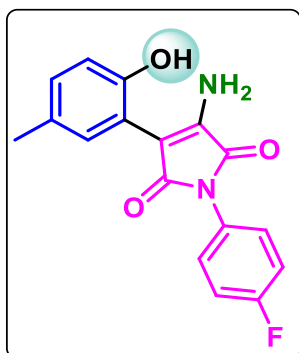
Physical State: orange liquid (13 mg, 44%), $R_f = 0.3$ (20% EtOAc/hexane). ^1H NMR (CDCl_3 , 400 MHz): δ 7.49- 7.40 (m, 4H), 7.38-7.34 (m, 1H), 7.24 (s, 1H), 7.05 (dd, $J = 8.0$ Hz, 1.6 Hz, 1H), 7.00 (s, 1H), 6.90 (d, $J = 8.0$ Hz, 1H), 5.50 (s, 2H), 2.31 (s, 3H). $^{13}\text{C}\{^1\text{H}\}$ NMR (CDCl_3 , 175 MHz): δ 172.9, 166.5, 151.3, 142.9, 131.8, 130.9, 130.7, 129.6, 129.4, 128.0, 126.2, 118.7, 117.2, 100.1, 20.9. IR (KBr, cm^{-1}): 3439, 1702, 1649. HRMS (ESI) m/z : $[\text{M}+\text{H}]^+$ Calcd for $\text{C}_{17}\text{H}_{15}\text{N}_2\text{O}_3$: 295.1083; Found: 295.1099.



3-amino-4-(2-hydroxy-5-methylphenyl)-1-(p-tolyl)-1H-pyrrole-2,5-dione (4be):

Physical State: orange liquid (14 mg, 45%), $R_f = 0.3$ (10% EtOAc/hexane). **^1H NMR (CDCl_3 , 400 MHz):** δ 7.27-7.24 (m, 4H), 7.22 (d, $J = 1.6$ Hz, 1H), 7.11 (s, 1H), 7.04 (dd, $J = 8.4$ Hz, 2.0 Hz, 1H), 6.90 (d, $J = 8.4$ Hz, 1H), 5.49 (s, 2H), 2.38 (s, 3H),

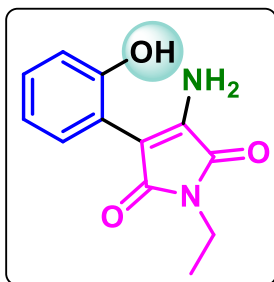
2.31 (s, 3H). **$^{13}\text{C}\{^1\text{H}\}$ NMR (CDCl_3 , 175 MHz):** δ 173.2, 166.6, 151.3, 143.0, 138.1, 130.8, 130.7, 130.0, 129.5, 129.0, 126.2, 118.7, 117.3, 100.1, 21.5, 20.9. **IR (KBr, cm^{-1}):** 3439, 1701, 1653. **HRMS (ESI) m/z:** $[\text{M}+\text{H}]^+$ Calcd for $\text{C}_{18}\text{H}_{17}\text{N}_2\text{O}_3$: 309.1239; Found: 309.1245.



3-amino-1-(4-fluorophenyl)-4-(2-hydroxy-5-methylphenyl)-1H-pyrrole-2,5-dione (4bg):

Physical State: orange solid (11 mg, 35%), $R_f = 0.3$ (10% EtOAc/hexane), **mp** = 166-167 °C. **^1H NMR (CDCl_3 , 400 MHz):** δ 7.41-7.37 (m, 2H), 7.24 (d, $J = 1.6$ Hz, 1H), 7.18-7.12 (m, 2H), 7.05 (dd, $J = 8.0$ Hz, 1.6 Hz, 1H), 6.89 (d, $J = 8.0$ Hz, 1H), 6.86

(s, 1H), 5.51 (s, 2H), 2.31 (s, 3H). **$^{13}\text{C}\{^1\text{H}\}$ NMR (CDCl_3 , 175 MHz):** δ 172.6, 166.4, 161.9 (d, $J_{\text{C-F}} = 246.4$ Hz), 151.2, 142.9, 131.0, 130.7, 129.8, 128.0 (d, $J_{\text{C-F}} = 8.7$ Hz), 127.7 (d, $J_{\text{C-F}} = 3.1$ Hz), 118.5, 117.0, 116.3 (d, $J_{\text{C-F}} = 22.5$ Hz), 100.0, 20.9. **^{19}F NMR (CDCl_3 , 376 MHz):** δ -113.5. **IR (KBr, cm^{-1}):** 3438, 1652. **HRMS (ESI) m/z:** $[\text{M}+\text{Na}]^+$ Calcd for $\text{C}_{17}\text{H}_{13}\text{FN}_2\text{O}_3$: 313.0988; Found: 313.1009.

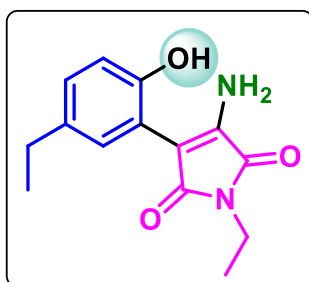


3-amino-1-ethyl-4-(2-hydroxyphenyl)-1H-pyrrole-2,5-dione

(4ab):

Physical State: yellow solid (13 mg, 56%), $R_f = 0.3$ (10% EtOAc/hexane), **mp** = 190-191 °C. **^1H NMR (CDCl_3 , 700 MHz):**

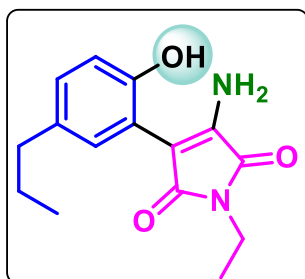
δ 7.74 (s, 1H), 7.33 (dd, $J = 7.7$ Hz, 1.4 Hz, 1H), 7.22 (td, $J = 8.4$ Hz, 1.4 Hz, 1H), 7.00 (d, $J = 7.7$ Hz, 1H), 6.98 (td, $J = 7.7$ Hz, 1.4 Hz, 1H), 5.37 (s, 2H), 3.62 (q, $J = 7$ Hz, 2H), 1.24 (t, $J = 7.0$ Hz, 3H). **$^{13}\text{C}\{^1\text{H}\}$ NMR (CDCl_3 , 175 MHz):** δ 174.7, 167.4, 153.6, 143.1, 129.8, 128.9, 121.4, 119.1, 117.8, 100.0, 33.4, 14.3. **IR (KBr, cm^{-1}):** 3440, 1645. **HRMS (ESI) m/z :** $[\text{M}+\text{H}]^+$ Calcd for $\text{C}_{12}\text{H}_{13}\text{N}_2\text{O}_3$: 233.0926; Found: 233.0914.



3-amino-1-ethyl-4-(5-ethyl-2-hydroxyphenyl)-1H-pyrrole-2,5-dione (4cb):

Physical State: orange liquid (12 mg, 46%), $R_f = 0.3$ (20% EtOAc/hexane). **^1H NMR (CDCl_3 , 700 MHz):** δ 7.37 (s, 1H),

7.16 (d, $J = 2.1$ Hz, 1H), 7.05 (dd, $J = 4.2$ Hz, 2.1 Hz, 1H), 6.91 (d, $J = 7.7$ Hz, 1H), 5.34 (s, 2H), 3.62 (q, $J = 7.0$ Hz, 2H), 2.59 (q, $J = 7.7$ Hz, 2H), 1.25-1.20 (m, 6H). **$^{13}\text{C}\{^1\text{H}\}$ NMR (CDCl_3 , 175 MHz):** δ 174.5, 167.5, 151.5, 142.9, 137.2, 129.3, 128.1, 118.8, 117.5, 100.2, 33.4, 28.3, 16.1, 14.3. **IR (KBr, cm^{-1}):** 3438, 1645. **HRMS (ESI) m/z :** $[\text{M}+\text{H}]^+$ Calcd for $\text{C}_{14}\text{H}_{17}\text{N}_2\text{O}_3$: 261.1239; Found: 261.1246.

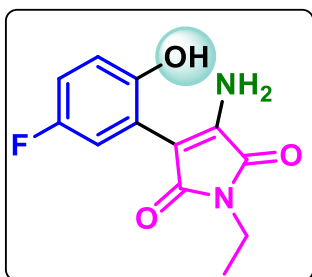


3-amino-1-ethyl-4-(2-hydroxy-5-propylphenyl)-1H-pyrrole-2,5-dione (4db):

Physical State: orange liquid (14 mg, 51%), $R_f = 0.3$ (20% EtOAc/hexane). **^1H NMR (CDCl_3 , 400 MHz):** δ 7.36 (s, 1H),

7.14 (d, $J = 2.0$ Hz, 1H), 7.03 (dd, $J = 8.0$ Hz, 2.0 Hz, 1H), 6.91 (d, $J = 8.0$ Hz, 1H), 5.33

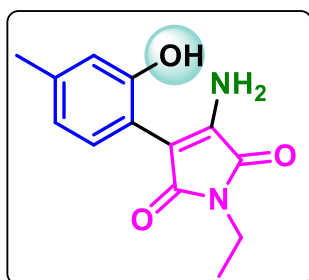
(s, 2H), 3.63 (q, $J = 7.2$ Hz, 2H), 2.53 (t, $J = 7.6$ Hz, 2H) 1.62 (q, $J = 7.6$ Hz, 2H), 1.24 (t, $J = 7.2$ Hz, 3H), 0.93 (t, $J = 7.2$ Hz, 3H). $^{13}\text{C}\{^1\text{H}\}$ NMR (CDCl_3 , 175 MHz): δ 174.5, 167.5, 151.5, 142.9, 135.6, 129.8, 128.7, 118.8, 117.4, 100.2, 37.5, 33.4, 25.1, 14.3, 14.1. IR (KBr, cm^{-1}): 3439, 2958, 1699, 1649. HRMS (ESI) m/z : $[\text{M}+\text{H}]^+$ Calcd for $\text{C}_{15}\text{H}_{19}\text{N}_2\text{O}_3$: 275.1396; Found: 275.1409.



3-amino-1-ethyl-4-(5-fluoro-2-hydroxyphenyl)-1H-pyrrole-2,5-dione (4hb):

Physical State: orange liquid (17 mg, 68%), $R_f = 0.3$ (20% EtOAc/hexane). ^1H NMR ($\text{DMSO}-d_6$, 700 MHz): δ 9.77 (s, 1H), 7.12 (dd, $J = 10.5$ Hz, 3.5 Hz, 1H), 6.99-6.96 (m, 3H),

6.90-6.88 (m, 1H), 3.48 (q, $J = 7.0$ Hz, 2H), 1.13 (t, $J = 7.0$ Hz, 3H). $^{13}\text{C}\{^1\text{H}\}$ NMR ($\text{DMSO}-d_6$, 175 MHz): δ 172.1, 167.7, 155.9 (d, $J_{\text{C-F}} = 231.5$ Hz), 151.7, 145.6, 119.5 (d, $J_{\text{C-F}} = 8.7$ Hz), 117.2 (d, $J_{\text{C-F}} = 8.4$ Hz), 117.04 (d, $J_{\text{C-F}} = 23.2$ Hz), 115.0 (d, $J_{\text{C-F}} = 22.5$ Hz), 95.2, 32.9, 14.8. ^{19}F NMR ($\text{DMSO}-d_6$, 376 MHz): δ -121.4. IR (KBr, cm^{-1}): 3437, 1647. HRMS (ESI) m/z : $[\text{M}+\text{H}]^+$ Calcd for $\text{C}_{12}\text{H}_{12}\text{FN}_2\text{O}_3$: 309.1239; Found: 309.1246.

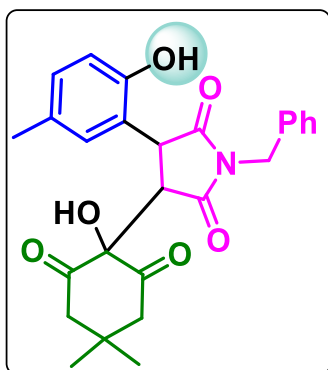


3-amino-1-ethyl-4-(2-hydroxy-4-methylphenyl)-1H-pyrrole-2,5-dione (4lb):

Physical State: orange liquid (10 mg, 41%), $R_f = 0.3$ (20% EtOAc/hexane). ^1H NMR (CDCl_3 , 700 MHz): δ 7.75 (s, 1H), 7.23(d, $J = 7.7$ Hz, 1H), 6.84 (s, 1H), 6.81 (d, $J = 7.7$ Hz, 1H),

5.33 (s, 2H), 3.63 (q, $J = 7.0$ Hz, 2H), 2.34 (s, 3H), 1.25 (t, $J = 7.0$ Hz, 3H). $^{13}\text{C}\{^1\text{H}\}$ NMR (CDCl_3 , 175 MHz): δ 174.8, 167.6, 153.5, 142.6, 140.3, 129.2, 122.3, 119.6, 114.8, 100.3,

33.4, 21.5, 14.3. **IR (KBr, cm⁻¹):** 3443, 1760, 1650. **HRMS (ESI) m/z:** [M+H]⁺ Calcd for C₁₃H₁₅N₂O₃: 247.1083; Found: 247.1092.



1-benzyl-3-(1-hydroxy-4,4-dimethyl-2,6-dioxocyclohexyl)-4-

(2-hydroxy-5-methylphenyl)pyrrolidine-2,5-dione (6):

Physical State: pale yellow liquid (36 mg, 80%), **R_f** = 0.3 (50%

EtOAc/hexane). **¹H NMR (CDCl₃, 400 MHz):** δ 9.64 (s, 1H),

7.38-7.31 (m, 5H), 6.96 (d, *J* = 8.0 Hz, 1H), 6.73 (d, *J* = 8.0

Hz, 1H), 6.65 (s, 1H), 4.71 (d, *J* = 15.2 Hz, 1H), 4.55 (d, *J* =

15.2 Hz, 1H), 4.12 (d, *J* = 4.0 Hz, 1H), 4.06 (d, *J* = 4.0 Hz, 1H), 3.82 (d, *J* = 3.6 Hz, 1H),

3.35-3.31 (m, 1H), 2.47-2.39 (m, 2H), 2.18-2.14 (m, 4H), 1.07 (s, 3H), 0.70 (s, 3H). **¹³C{¹H}**

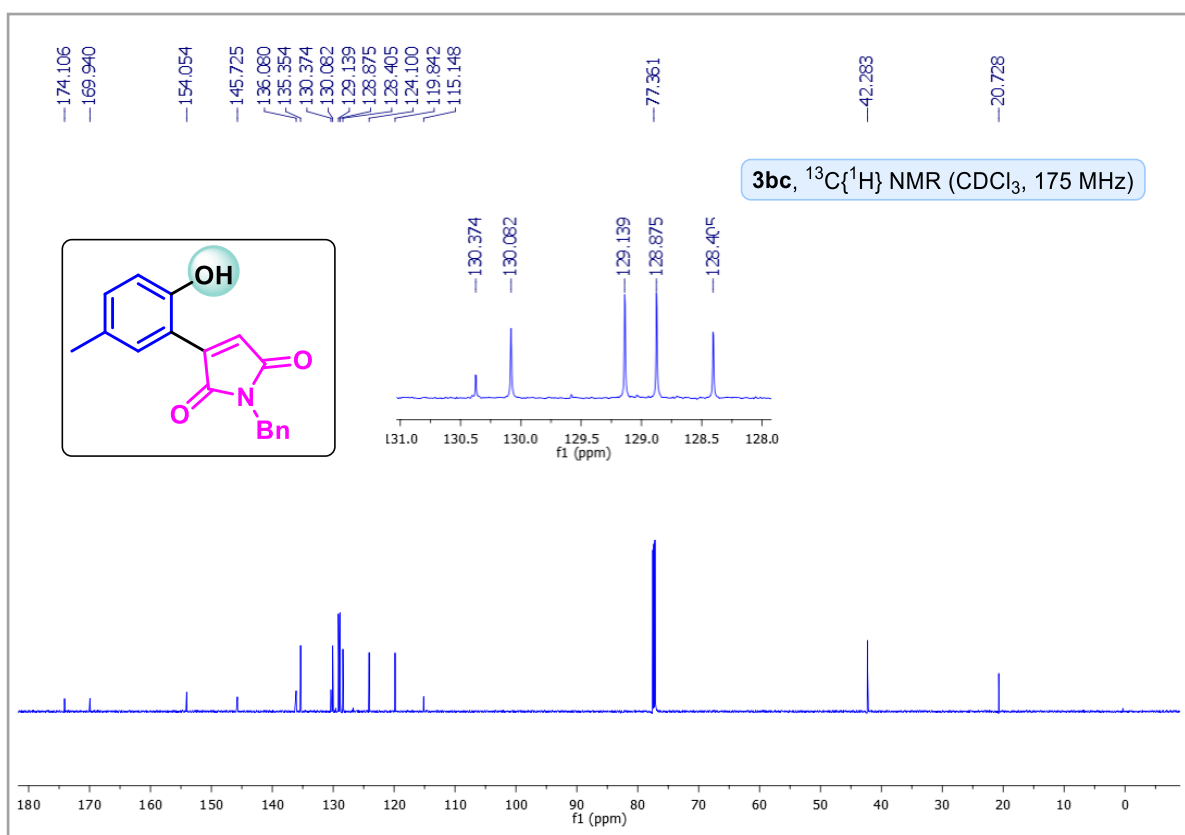
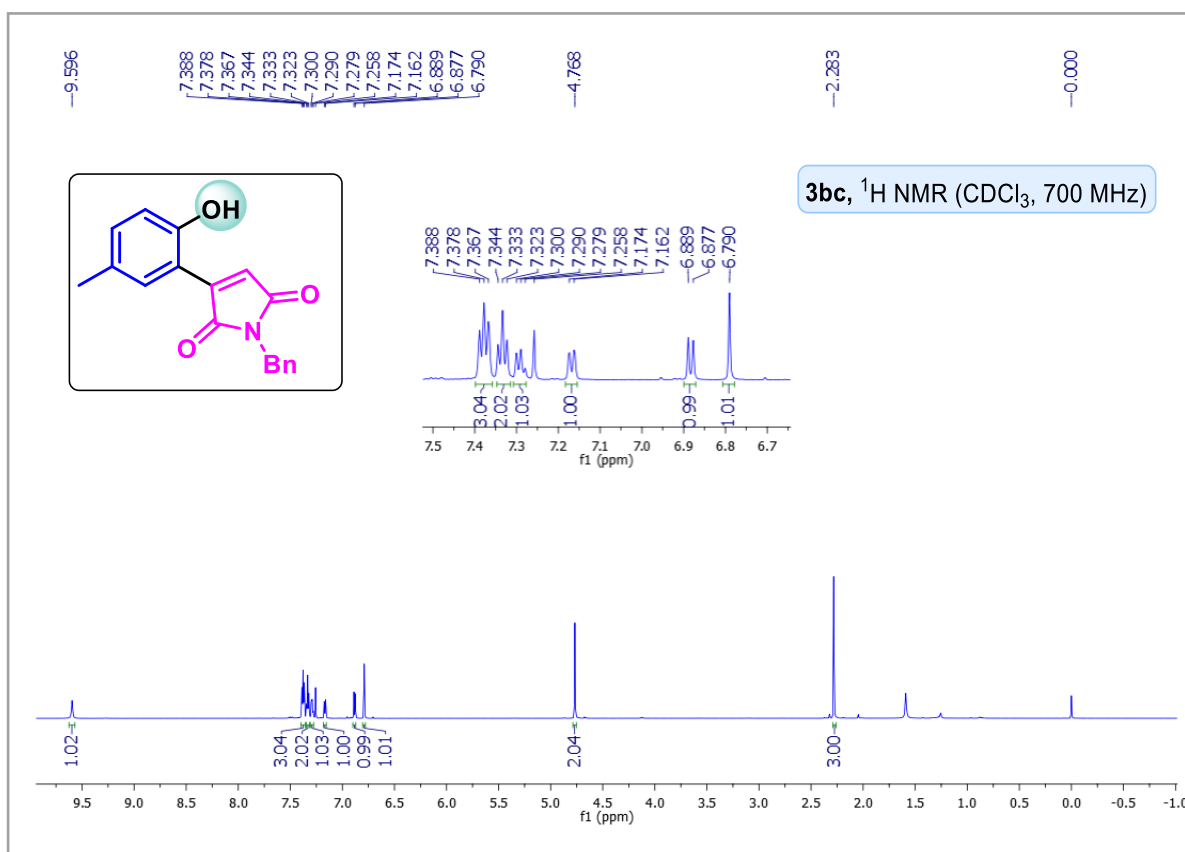
NMR (CDCl₃, 100 MHz): δ 205.3, 204.2, 177.8, 175.2, 153.5, 136.7, 132.5, 130.2, 129.2,

128.2, 128.1, 128.0, 123.7, 116.1, 89.3, 52.9, 51.6 (2C), 45.5, 42.6, 32.0, 29.7, 27.0, 20.9.

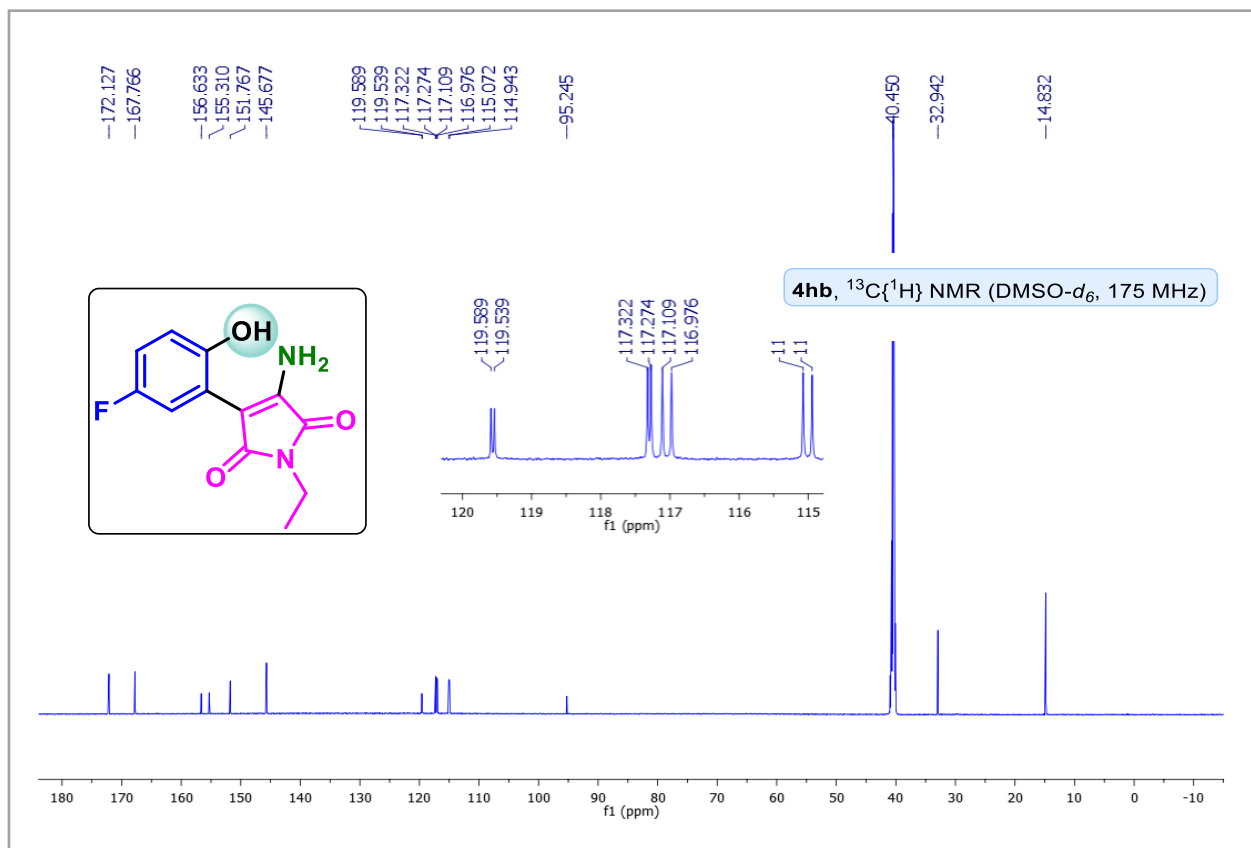
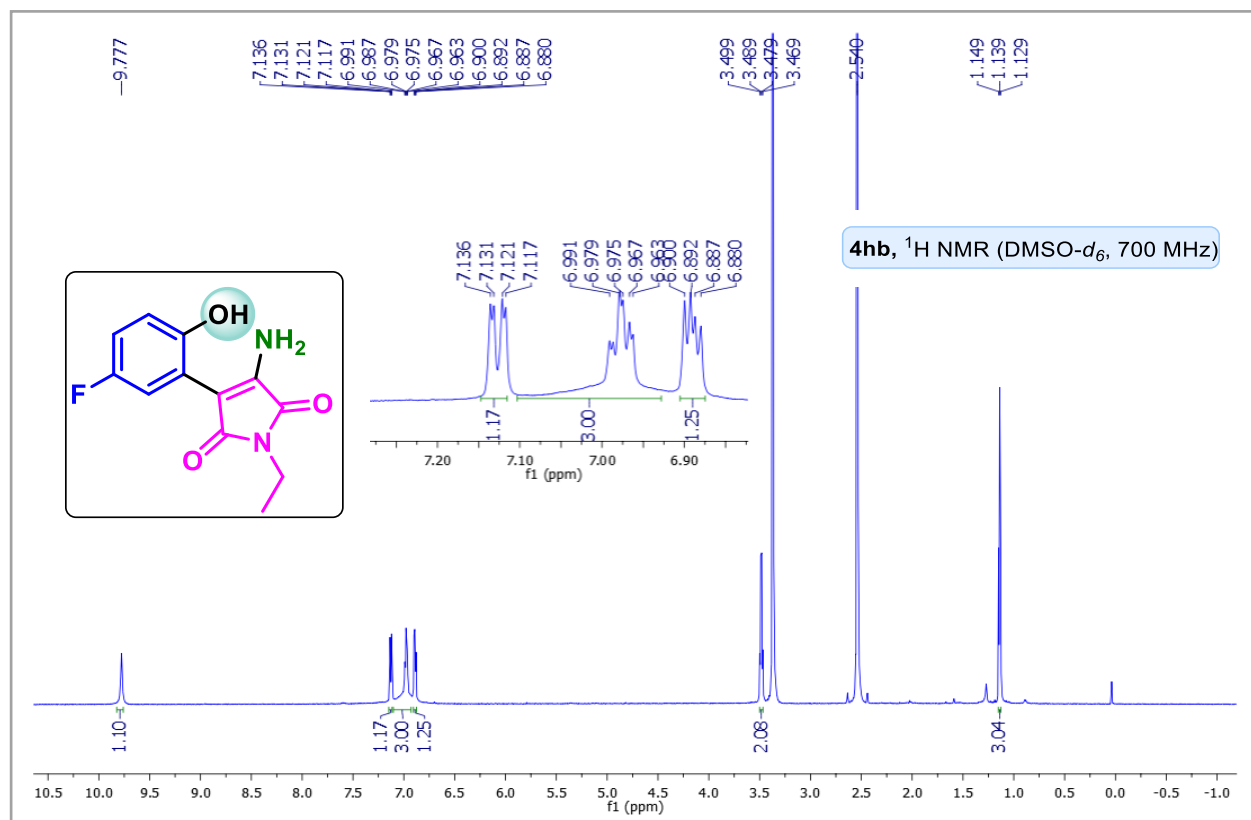
IR (KBr, cm⁻¹): 3422, 2922, 2852, 1700, 1635. **HRMS (ESI) m/z:** [M+Na]⁺ Calcd for

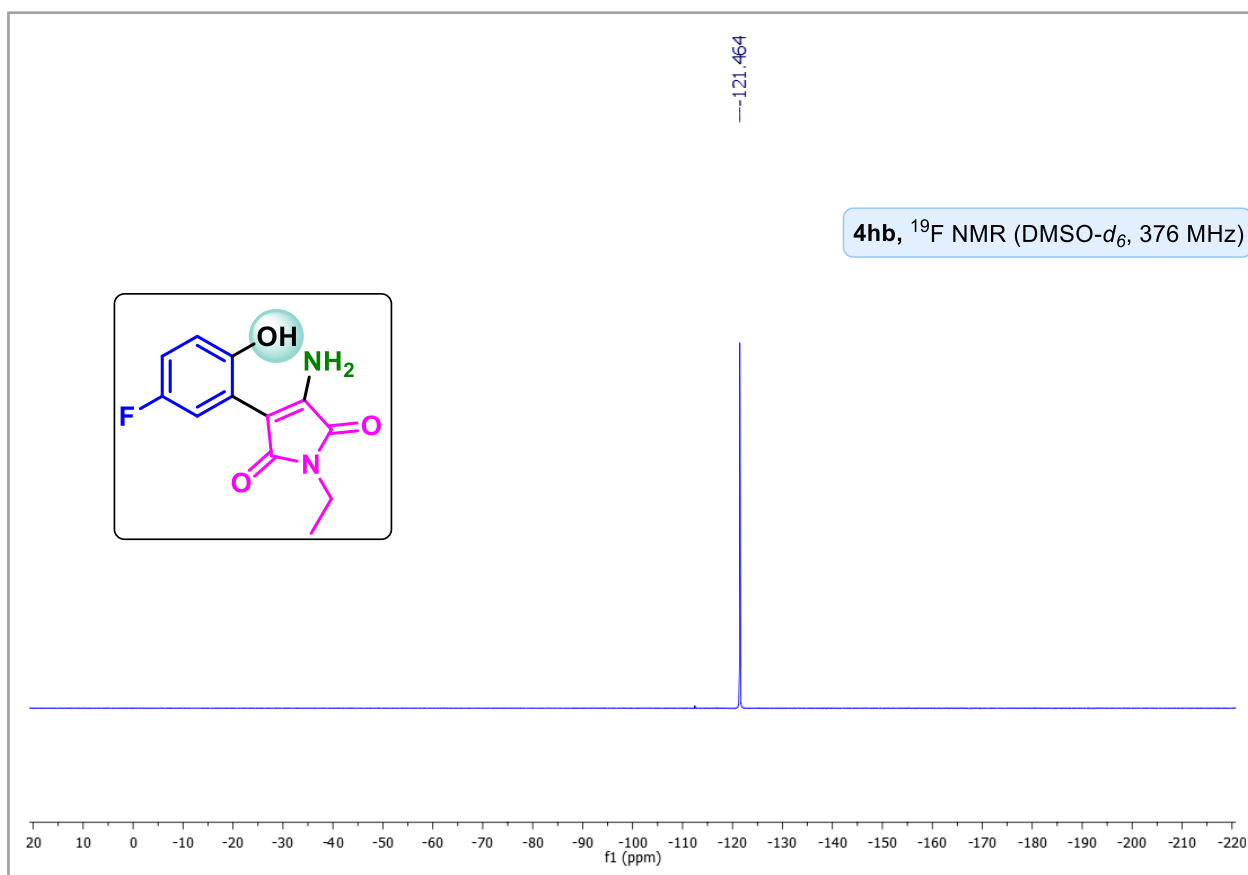
C₂₆H₂₇NO₆Na: 472.1736; Found: 472.1743.

NMR spectra of 1-benzyl-3-(2-hydroxy-5-methylphenyl)-1H-pyrrole-2,5-dione (3bc)

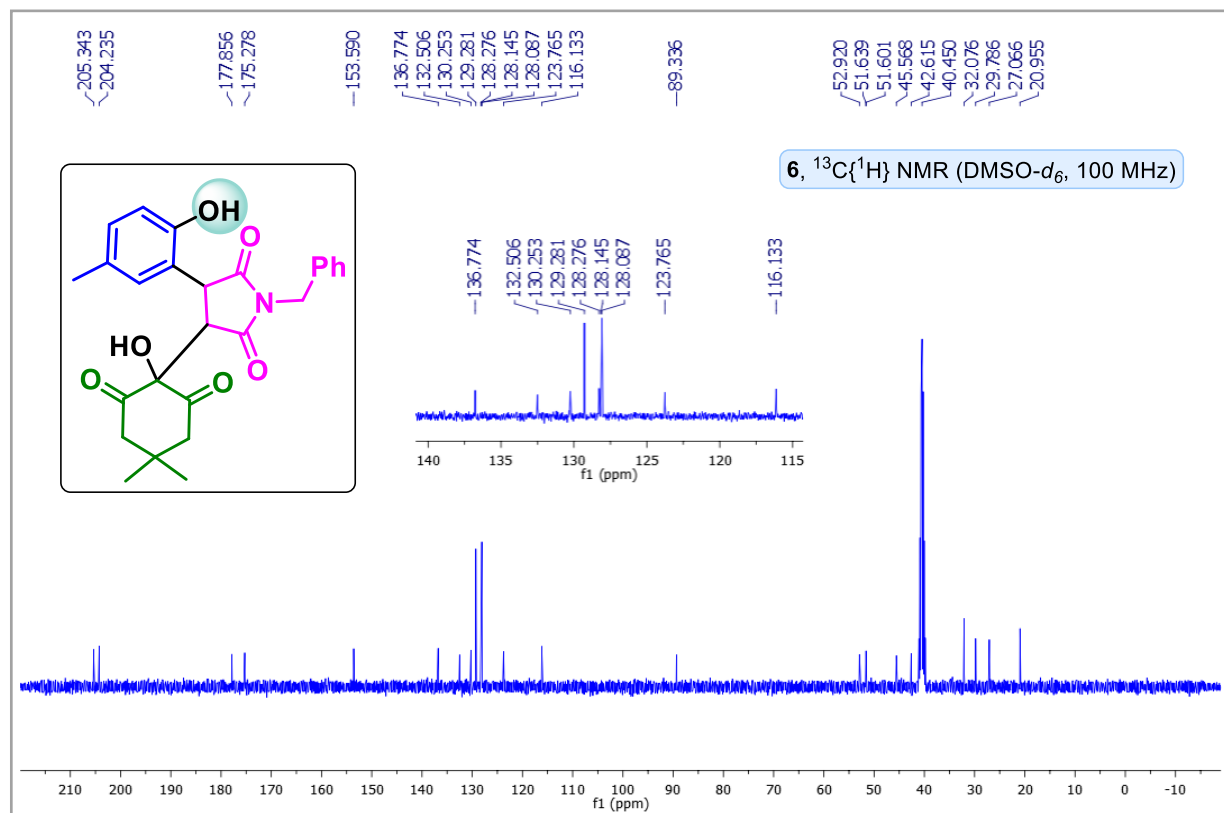
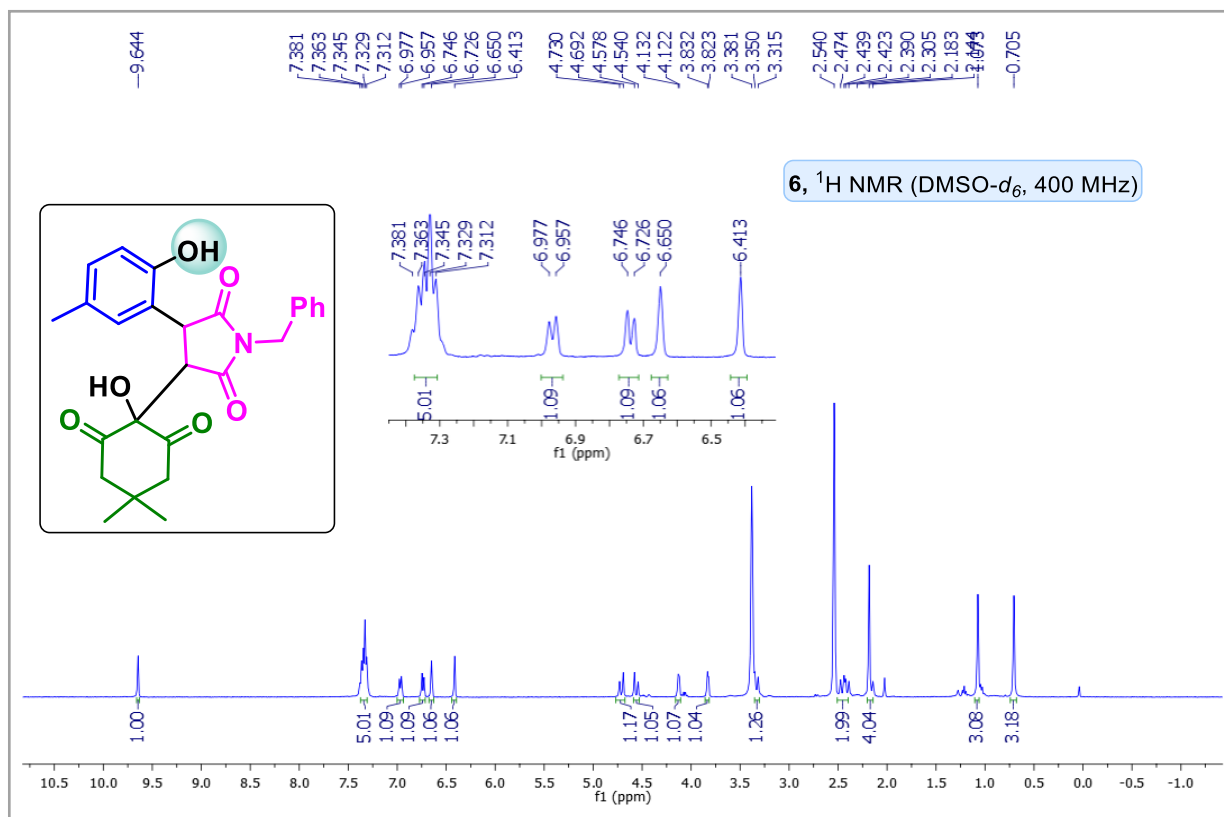


NMR spectra of 3-amino-1-ethyl-4-(5-fluoro-2-hydroxyphenyl)-1H-pyrrole-2,5-dione (4hb)





NMR spectra of 1-benzyl-3-(1-hydroxy-4,4-dimethyl-2,6-dioxocyclohexyl)-4-(2-hydroxy-5-methylphenyl)pyrrolidine-2,5-dione (6)



(a) X-ray data of 1-benzyl-3-(2-hydroxy-5-methylphenyl)-1H-pyrrole-2,5-dione (3bc):

Crystals of the compound 1-benzyl-3-(2-hydroxy-5-methylphenyl)-1H-pyrrole-2,5-dione (**3bc**) were obtained after slow evaporation of ethyl acetate. Crystals suited for single crystal X-Ray diffraction measurements were mounted on a glass fiber. Geometry and intensity data were collected with a Rigaku Smartlab X-ray diffractometer equipped with graphite-monochromated Mo-K α radiation ($\lambda = 0.71073$ Å, multilayer optics). Temperature was controlled using an Oxford Cryostream 700 instrument. Intensities were integrated with SAINT and SMART software packages and corrected for absorption with SADABS. The structure was solved by direct methods and refined on F² with SHELXL-97 using Olex-2 software.

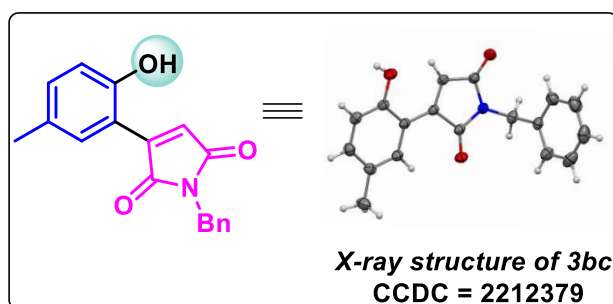
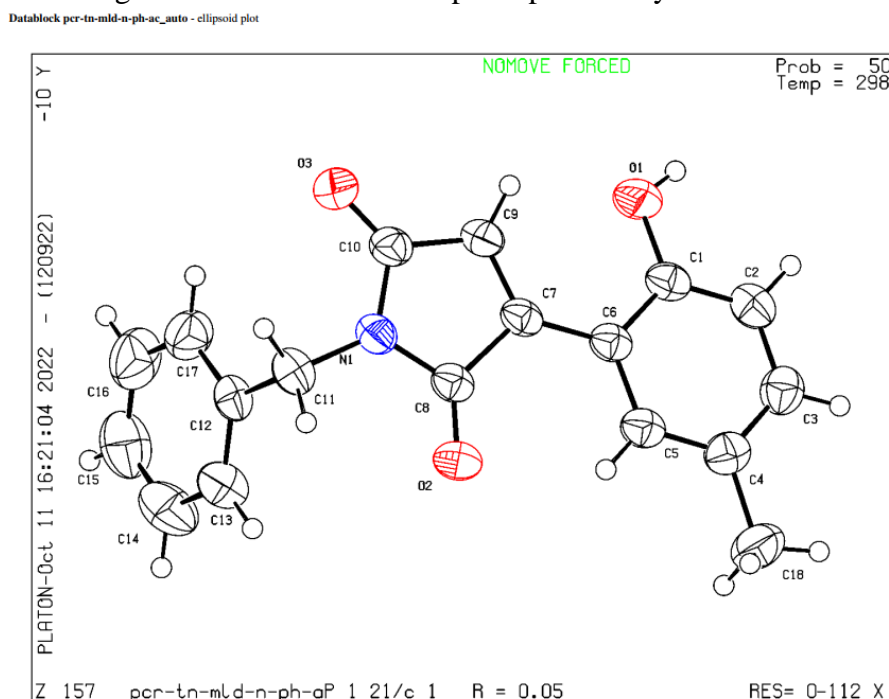


Figure 5.5 ORTEP diagram of **3bc** with 50% ellipsoid probability



(b) X-ray data of 3-amino-1-ethyl-4-(2-hydroxyphenyl)-1H-pyrrole-2,5-dione (4ab):

Crystals of the compound 3-amino-1-ethyl-4-(2-hydroxyphenyl)-1H-pyrrole-2,5-dione (**4ab**) were obtained after slow evaporation of ethyl acetate. Crystals suited for single crystal X-Ray diffraction measurements were mounted on a glass fiber. Geometry and intensity data were collected with a Rigaku Smartlab X-ray diffractometer equipped with graphite-monochromated Mo-K α radiation ($\lambda = 0.71073$ Å, multilayer optics). Temperature was controlled using an Oxford Cryostream 700 instrument. Intensities were integrated with SAINT and SMART software packages and corrected for absorption with SADABS. The structure was solved by direct methods and refined on F² with SHELXL-97 using Olex-2 software.

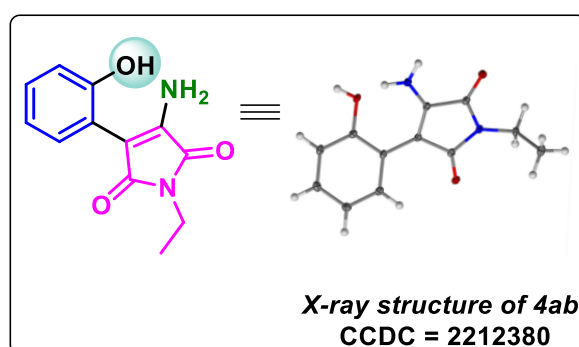
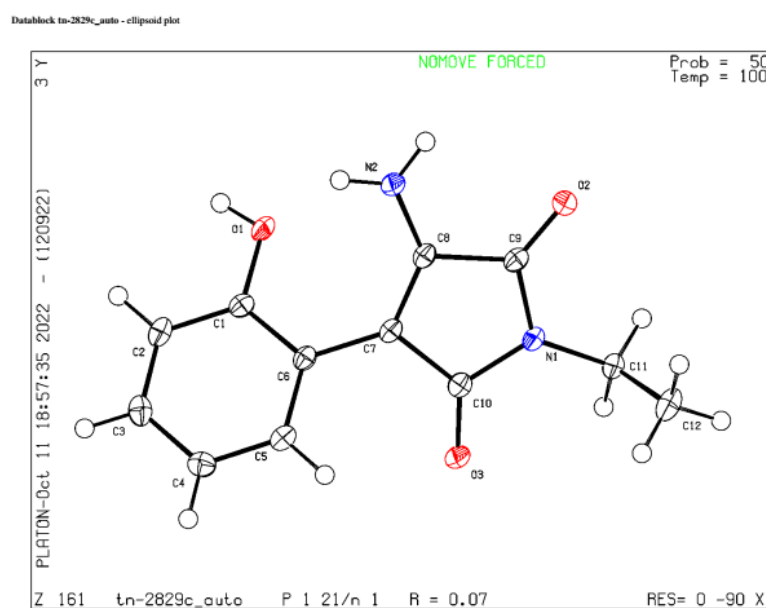


Figure 5.6 ORTEP diagram of **4ab** with 50% ellipsoid probability



(c) **X-ray data of 1-benzyl-3-(1-hydroxy-4,4-dimethyl-2,6-dioxocyclohexyl)-4-(2-hydroxy-5-methylphenyl)pyrrolidine-2,5-dione (6):** Crystals of the compound 1-benzyl-3-(1-hydroxy-4,4-dimethyl-2,6-dioxocyclohexyl)-4-(2-hydroxy-5-methylphenyl)pyrrolidine-2,5-dione (**4ac**) were obtained after slow evaporation of ethyl acetate. Crystals suited for single crystal X-Ray diffraction measurements were mounted on a glass fiber. Geometry and intensity data were collected with a Rigaku Smartlab X-ray diffractometer equipped with graphite-monochromated Mo-K α radiation ($\lambda = 0.71073$ Å, multilayer optics). Temperature was controlled using an Oxford Cryostream 700 instrument. Intensities were integrated with SAINT and SMART software packages and corrected for absorption with SADABS. The structure was solved by direct methods and refined on F² with SHELXL-97 using Olex-2 software.

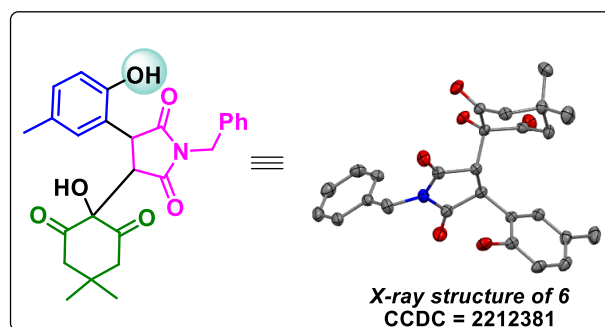
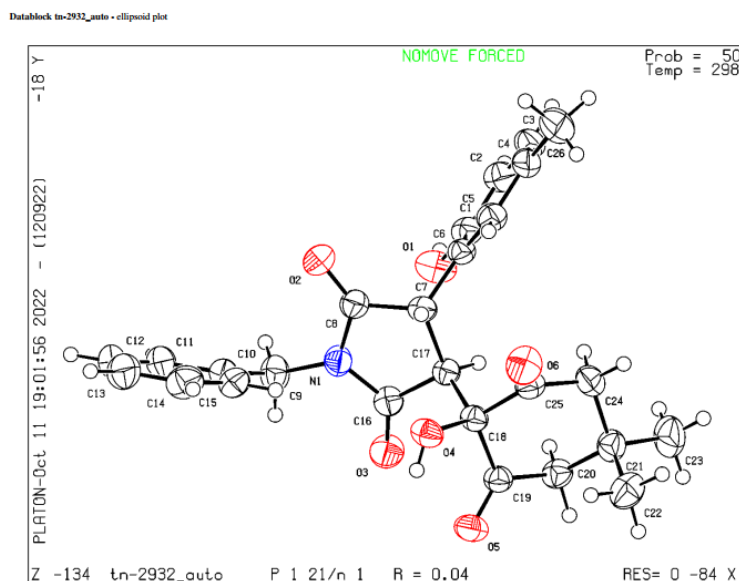


Figure 5.7 ORTEP diagram of **6** with 50% ellipsoid probability

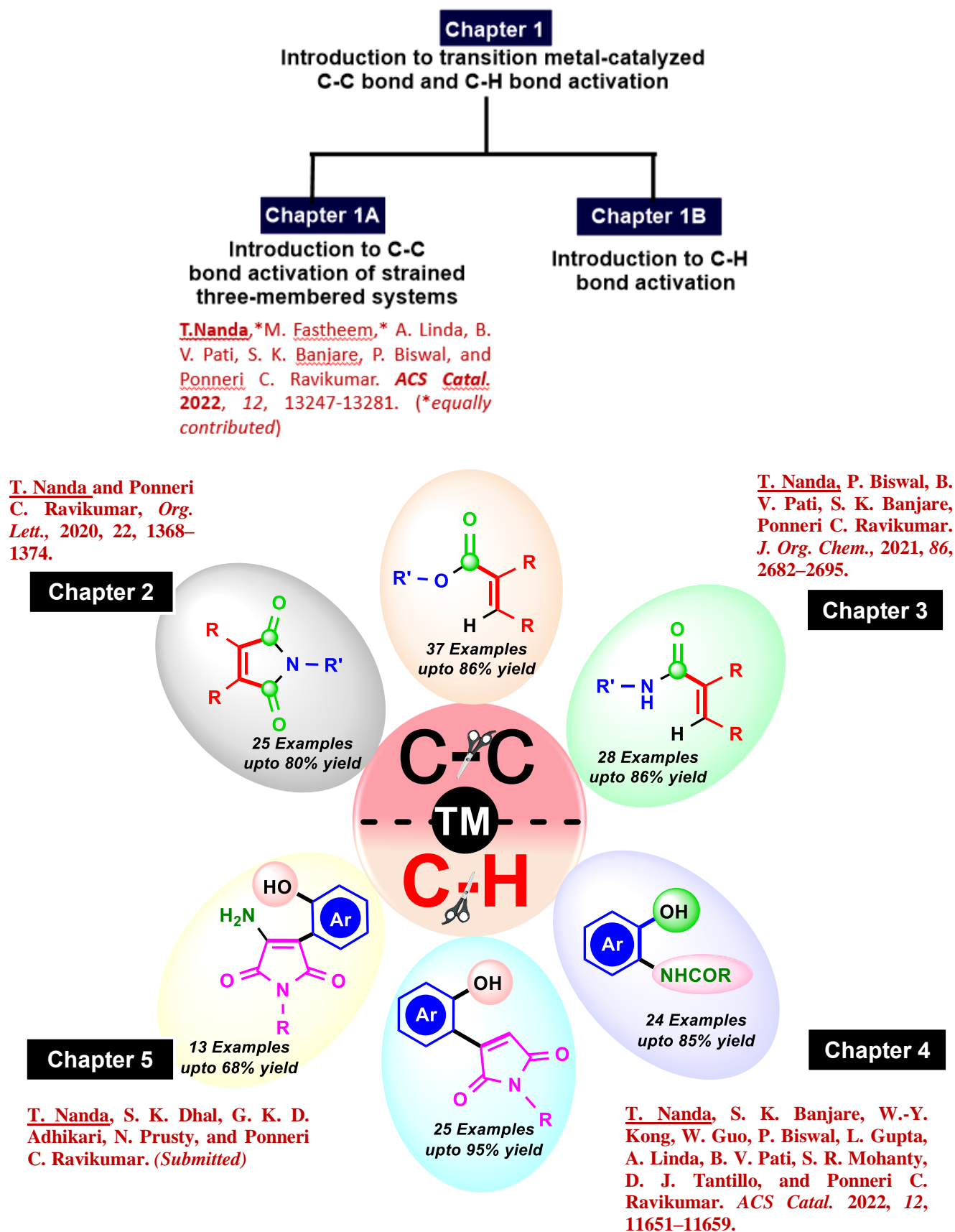


5.6 REFERENCES

1. Liu, G.; Shen, Y.; Zhou, Z.; Lu, X. Rhodium(III) - Catalyzed Redox - Neutral Coupling of N - Phenoxyacetamides and Alkynes with Tunable Selectivity. *Angew. Chem., Int. Ed.*, **2013**, *52*, 6033–6037.
2. For selected reviews check: (a) Zhang, F.; Spring, D. R. Arene C–H Functionalisation Using a Removable/modifiable or a Traceless Directing Group Strategy. *Chem. Soc. Rev.* **2014**, *43*, 6906–6919. (b) Chen, Z.; Wang, B.; Zhang, J.; Yu, W.; Liu, Z.; Zhang, Y. Transition Metal-Catalyzed C–H Bond Functionalizations by the Use of Diverse Directing Groups. *Org. Chem. Front.* **2015**, *2*, 1107–1295. (c) Gensch, T.; Hopkinson, M. N.; Glorius, F.; Wencel-Delord, J. Mild Metal-Catalyzed C–H Activation: Examples and Concepts. *Chem. Soc. Rev.* **2016**, *45*, 2900–2936. (d) Wu, Y.; Pi, C.; Wu, Y.; Cui, X. Directing Group Migration Strategy in Transition-Metal-Catalysed Direct C–H Functionalization. *Chem. Soc. Rev.* **2021**, *50*, 3677–3689.
3. Zeng, Z.; Gao, H.; Zhou, Z.; Yi, Wei. Intermolecular Redox-Neutral Carboamination of C–C Multiple Bonds Initiated by Transition-Metal-Catalyzed C–H Activation *ACS Catal.* **2022**, *12*, 14754–14772.
4. (a) Carey, J. S.; Laffan, D.; Thomson, C.; Williams, M. T. Analysis of the Reactions used for the Preparation of Drug Candidate Molecules. *Org. Biomol. Chem.* **2006**, *4*, 2337–2347. (b) Roughley, S. D.; Jordan, A. M. The Medicinal Chemist's Toolbox: An Analysis of Reactions Used in the Pursuit of Drug Candidates. *J. Med. Chem.* **2011**, *54*, 3451–3479. (c) Vitaku, E.; Smith, D. T.; Njardarson, J. T. Analysis of the Structural Diversity, Substitution Patterns, and Frequency of Nitrogen Heterocycles among U.S. FDA Approved Pharmaceuticals. *J. Med. Chem.* **2014**, *57*, 10257–10274.
5. (a) Hu, Z.; Tong, X.; Liu, G. Rhodium(III) Catalyzed Carboamination of Alkenes Triggered by C–H Activation of N-Phenoxyacetamides under Redox-Neutral Conditions. *Org. Lett.* **2016**, *18*, 1702–1705. (b) Lerchen, A.; Knecht, T.; Daniliuc, C. G.; Glorius, F. Unnatural Amino Acid Synthesis Enabled by the Regioselective Cobalt(III)-Catalyzed Intermolecular Carboamination of Alkenes. *Angew. Chem. Int. Ed.* **2016**, *55*, 15166–15170.
6. Wu, L.; Xu, H.; Gao, H.; Li, L.; Chen, W.; Zhou, Z.; Yi, W. Chiral Allylic Amine Synthesis Enabled by the Enantioselective CpXRh(III)-Catalyzed Carboaminations of 1,3-Dienes. *ACS Catal.* **2021**, *11*, 2279–2287.
7. (a) Tyman, J. H. P. Synthetic and Natural Phenols. *Studies in Organic Chemistry*; Elsevier: 1996; Vol. 52, pp 1–700. (b) Rappoport, Z. *The Chemistry of Phenols*; John Wiley & Sons Ltd.: Chichester, U.K., 2003. (c) Alonso, D. A.; Najera, C.; Pastor, I. M.; Yus, M. Transition - Metal - Catalyzed Synthesis of Hydroxylated Arenes *Chem. Eur. J.* **2010**, *16*, 5274–5284.
8. Gong, T.-J.; Xiao, B.; Liu, Z.-J.; Wan, J.; Xu, J.; Luo, D.-F.; Fu, Y.; Liu, L. Rhodium-Catalyzed Selective C–H Activation/ Olefination of Phenol Carbamates. *Org. Lett.* **2011**, *13*, 3235–3237.
9. Dai, H.-X.; Li, G.; Zhang, X.-G.; Stepan, A. F.; Yu, J.-Q. Pd(II)-Catalyzed ortho- or meta-C–H Olefination of Phenol Derivatives. *J. Am. Chem. Soc.* **2013**, *135*, 7567–7571.
10. Fabry, D. C.; Ronge, M. A.; Zoller, J.; Rueping, M. C–H Functionalization of Phenols Using Combined Ruthenium and Photoredox Catalysis: In Situ Generation of the Oxidant. *Angew. Chem., Int. Ed.* **2015**, *54*, 2801–2805.

11. Nanda, T.; Banjare, S. K.; Kong, W.-Y.; Guo, W.; Biswal, P.; Gupta, L.; Linda, A.; Pati, B. V.; Mohanty, S. R.; Tantillo, D. J.; Ravikumar, P. C. *ACS Catal.* **2022**, *12*, 11651–11659.
12. (a) Müller, P.; Baud, C.; Jacquier, Y.; Moran, M.; Nageli, I. "Rhodium(II)-Catalyzed Aziridinations and C–H Insertions with [N-(p-Nitrobenzenesulfonyl)imino]phenyliodinane. *J. Phys. Org. Chem.* **1996**, *9*, 341–347. (b) Jat, J. L.; Paudyal, M. P.; Gao, H.; Xu, Q.-L.; Yousufuddin, M.; Devarajan, D.; Ess, D. H.; Kürti, L.; Falck, J. R. Direct Stereospecific Synthesis of Unprotected N-H and N-Me Aziridines from Olefins. *Science* **2014**, *343*, 61–65. (c) Degennaro, L.; Trinchera, P.; Luisi, R. Recent Advances in the Stereoselective Synthesis of Aziridines. *Chem. Rev.* **2014**, *114*, 7881–7929.
13. (a) Calvin, J. R.; Frederick, M. O.; Laird, D. L. T.; Remacle, J. R.; May, S. A. Rhodium-Catalyzed and Zinc(II)-Triflate-Promoted Asymmetric Hydrogenation of Tetrasubstituted α,β -Unsaturated Ketones. *Org. Lett.* **2012**, *14*, 1038–1041. (b) Zhang, G.-Y.; Zhang, P.; Li, B.-W.; Liu, K.; Li, J.; Yu, Z.-X. Dual Activation Strategy to Achieve C–C Cleavage of Cyclobutanes: Development and Mechanism of Rh and Zn Co catalyzed [4 + 2] Cycloaddition of Yne-Vinylcyclobutanones. *J. Am. Chem. Soc.* **2022**, *144*, 21457–21469.
14. Shen, Y.; Liu, G.; Zhou, Z.; Lu, X. Rhodium(III)-Catalyzed C–H Olefination for the Synthesis of ortho-Alkenyl Phenols Using an Oxidizing Directing Group. *Org. Lett.* **2013**, *15*, 3366–3369.
15. Pan, J.-L.; Liu, T.-Q.; Chen, C.; Li, Q.-Z.; Jiang, W.; Ding, T.-M.; Yan, Z.-Q.; Zhu, G.-D. Rhodium(III)-Catalysed Cascade [3 + 2] Annulation of N-Aryloxyacetamides with 3-(Hetero)Arylpropionic Acids: Synthesis of Benzofuran-2(3H)-Ones. *Org. Biomol. Chem.* **2019**, *17*, 8589–8600.
16. Wang, S.; Lin, J.-J.; Cui, X.; Li, J.-P.; Huang, C. Controllable Synthesis of Two Isomers 4H-Chromene and 2,8-Dioxabicyclo[3.3.1]nonane Derivatives under Catalyst-Free Conditions. *J. Org. Chem.* **2021**, *86*, 16396–16408.
17. (a) Similar information was reported in Banjare, S. K.; Nanda, T.; Ravikumar, P. C. Cobalt-Catalyzed Regioselective Direct C-4 Alkenylation of 3-Acetylindole with Michael Acceptors Using a Weakly Coordinating Functional Group. *Org. Lett.* **2019**, *21*, 8138–8143. (b) Gottlieb, H. E.; Kotlyar, V.; Nudelman, A. NMR chemical shifts of common laboratory solvents as trace impurities. *J. Org. Chem.* **1997**, *62*, 7512.
18. Yuan, Y. C.; Kamaraj, R.; Bruneau, C.; Labasque, T.; Roisnel, T.; Gramage-Doria, R. Unmasking Amides: Ruthenium-Catalyzed Protodecarbonylation of N-Substituted Phthalimide Derivatives. *Org. Lett.* **2017**, *19*, 6404–6407.
19. Li, B.; Lan, J.; Wu, D.; You, J. Rhodium(III)-Catalyzed orthoHeteroarylation of Phenols through Internal Oxidative C–H Activation: Rapid Screening of Single-Molecular White-Light-Emitting Materials. *Angew. Chem., Int. Ed.* **2015**, *54*, 14008–14012.
20. Bernardes, G. J. L.; Chalker, J. M.; Errey, J. C.; Davis, B. G. Facile Conversion of Cysteine and Alkyl Cysteines to Dehydroalanine on Protein Surfaces: Versatile and Switchable Access to Functionalized Proteins. *J. Am. Chem. Soc.* **2008**, *130*, 5052–5053.

SUMMARY OF THE THESIS



About The Author



Tanmayee Nanda completed her B.Sc. (Chemistry Honours) in 2014 from Rajendra University, Bolangir, and her M.Sc. degree in 2016 from Ravenshaw University, Cuttack. She has completed her M.Phil. in 2017 from Utkal University, Bhubaneswar. She joined as a junior research fellow in July 2017 under the supervision of Prof. Ponneri Chandrababu Ravikumar (NISER, Bhubaneswar). Then, she worked as a senior research scholar from January 2019 onwards. She has submitted her thesis on 19th December, 2022. Her research focuses on the “Transition metal-catalysed C-H bond functionalization of phenoxy acetamide and C-C bond activation of the smallest Huckel aromatic cyclopropenone motif”.